

KINETIC, SPECTROSCOPIC AND X-RAY DIFFRACTION
STUDIES OF d^6 TRANSITION METAL COMPLEXES

A thesis presented for the Degree of
Doctor of Philosophy, in the Faculty
of Science, University of Leicester,
by R. I. Haines.

September 1977

UMI Number: U556604

All rights reserved

INFORMATION TO ALL USERS

The quality of this reproduction is dependent upon the quality of the copy submitted.

In the unlikely event that the author did not send a complete manuscript and there are missing pages, these will be noted. Also, if material had to be removed, a note will indicate the deletion.



UMI U556604

Published by ProQuest LLC 2015. Copyright in the Dissertation held by the Author.
Microform Edition © ProQuest LLC.

All rights reserved. This work is protected against
unauthorized copying under Title 17, United States Code.



ProQuest LLC
789 East Eisenhower Parkway
P.O. Box 1346
Ann Arbor, MI 48106-1346

THESIS

538 429

28 " 77



x753009209

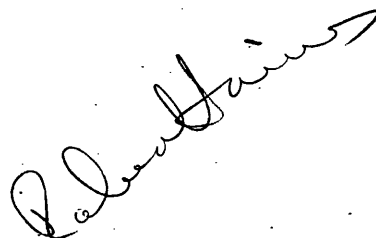
For Mo
and Richard.

STATEMENT

The work described in this thesis was carried out by the author in the Department of Chemistry of the University of Leicester between October 1974 and August 1977.

No part of this work has been submitted or is concurrently being submitted for any other degree.

Signed

A handwritten signature in cursive script, appearing to read 'R. I. Haines', written diagonally across the page.

September 1977

R. I. Haines

ACKNOWLEDGEMENTS

I wish to express my thanks to my supervisor, Dr. J. Burgess, for his continual guidance and encouragement throughout this work, and for his aid during any difficulties which arose.

I also wish to thank Dr. M. J. Blandamer, for his provision and discussion of certain thermodynamic functions used in this work; and Dr. J. G. Chambers, who wrote the computer programs used for many calculations. I am indebted to Dr. D. R. Russell and Mr. W. Scutcher for their invaluable help in the single-crystal structure determination.

I should like to thank Miss V. Orson-Wright for the production of this typescript, and her remarkable deciphering ability.

Finally, I am indebted to the Science Research Council for supporting my work with a Research Studentship Grant.

SUMMARY

The work in this thesis is concerned in the main with solvent effects on the kinetic, thermodynamic and spectroscopic properties of several d^6 transition metal complexes, and their reactions with various species.

Several reactions, which proceed via known mechanisms, have been analysed in terms of the solvation trends of the participant species in the various solvent mixtures studied. For example, the solvent effects on (i) the nucleophilic substitution reactions of the pentacyanoferrate(II) anions, $[\text{Fe}(\text{CN})_5\text{L}]^{n-}$ (D mechanism), (ii) the acid aquation of the $[\text{Fe}(\text{5-NO}_2\text{phen})_3]^{2+}$ cation (I_d), and (iii) mercury(II)-catalysed aquation of the ReCl_6^{2-} anion, and related complexes ($\text{S}_\text{E}2$ at Hg^{2+} , dissociative with respect to Re(IV) centre). (iv) The peroxo-disulphate oxidation of the $[\text{Fe}(\text{phen})_3]^{2+}$ and related cations has also been studied, in binary aqueous mixtures, together with the acid aquation of the $[\text{Fe}(\text{phen})_3]^{3+}$ cation, and its ligand-substituted derivatives, the latter study being in aqueous solution only.

In order to quantify such thermodynamic analyses, the solubilities of several pertinent compounds in ranges of binary aqueous mixtures have been measured, and the free energies of transfer of these compounds, and the appropriate single-ion values have been determined.

Changes in solvent have a profound effect on the UV/visible spectra of certain inorganic complexes, and a study of such solvatochromism has been undertaken (a) to provide greater understanding of the phenomenon, and (b) to qualitatively analyse selected compounds in terms of their solvatochromic properties, relative to those of compounds of known structure. In this vein, the X-ray crystal structure of trans-di-iso-

thiocyanato(cyclam)cobalt(III) thiocyanate (see chapter 7) has been determined, in an attempt to correlate its solvatochromic behaviour with its absolute stereochemistry.

Finally, nucleophilic substitution reactions at low-spin iron(II) complexes have been studied, to try to clarify some mechanistic complications which have arisen in such systems.

| CONTENTS | | Page |
|------------|--|------|
| CHAPTER 1 | Introduction. | 1. |
| CHAPTER 2 | Kinetic and Equilibrium Properties of Penta- cyano(3,5-dimethylpyridine)iron(II) and Related Anions in Binary Aqueous Mixtures. | 10. |
| CHAPTER 3 | Aquation of Tris(5-nitro 1,10-phenanthroline)- iron(II) in Binary Aqueous Mixtures; Comparison of Kinetic Parameters for Reaction and Thermo- dynamic Properties of the Mixture. | 56. |
| CHAPTER 4 | Solubilities and Solvation Characteristics of Selected Inorganic and Organic Compounds in Binary Aqueous Mixtures. | 72. |
| CHAPTER 5 | Mercury(II)-Catalysed Aquation of Transition Metal-Halo Complexes in Binary Aqueous Mixtures. | 89. |
| CHAPTER 6 | Solvent Effects on the Peroxodisulphate Oxidation of the $[\text{Fe}(\text{phen})_3]^{2+}$ and Related Cations. | 114. |
| CHAPTER 7 | X-Ray Diffraction Studies on Selected d^6 Transition Metal Complexes; Single-Crystal and Powder Diffraction Methods. | 135. |
| CHAPTER 8 | Solvatochromic Behaviour of a Series of Inorganic Complexes. | 157. |
| CHAPTER 9 | Nucleophilic Substitution Reactions at Ternary Iron(II), and Related Complexes. | 181. |
| | CONCLUSION | 222. |
| APPENDIX | 1 General Solvent Parameters. 2 BASIC Computer Programs. 3 The Arrhenius Law. 4 Structure Factors of the $\text{trans}[\text{Co}(\text{cyclam})-(\text{NCS})_2]$ SCN Crystal Structure. | |
| REFERENCES | | |

CHAPTER I

Introduction

It is possible to discuss Kinetic and Thermodynamic phenomena together by application of the transition-state theory [1.01]. According to this theory, the rate constant, k , of a reaction may be expressed in terms of the free energy of activation, ΔG^\ddagger , by the relation:-

$$k = \frac{\kappa T}{h} \exp. \left(\frac{-\Delta G^\ddagger}{RT} \right) \quad (1.01)$$

In general, high thermodynamic stability is not necessarily correlated with kinetic inertness, for metal complexes [1.02]. However, correlations may be expected between ΔG^\ddagger and the standard free energy change for the reaction, ΔG^\ominus , for a series of reactions proceeding via a common mechanism [1.03]. Indeed, for reactions proceeding via an I_a mechanism, Swaddle [1.04] has shown that the plot of ΔG^\ddagger versus ΔG^\ominus is linear with a slope of unity. Also, for reactions having an I_a mechanism, the analogous plot should have a slope less than unity, and where $\Delta G^\ddagger \gg \Delta G^\ominus$, the slope is expected to be ca. 0.5. Such behaviour has been observed [1.05] for the aquation of $[(H_2O)_5CrX]^{(3-n)+}$, where the slope of the ΔG^\ddagger vs. ΔG^\ominus plot is 0.56 at 298.2 K, at an ionic strength of 1.0 mol dm^{-3} ; where $X = Cl, Br, I, F, \underline{NCS}$ and \underline{SCN} .

When reactions are studied in mixed aqueous solvents, complicated patterns are often observed when the measured kinetic parameters are plotted against the solvent composition, which have aroused interest [1.06]. In aqueous solution at least, the re-organisation of the solvent which surrounds the reacting solutes is known to be an important aspect of the activation process [1.07-09]. It is not surprising that addition of a co-solvent to such aqueous solutions will profoundly affect such re-organisations of solvent. Indeed, it is clearly recognised that the action of the non-aqueous component of a

mixture is more than a simple diluent of water, or a modifier of its dielectric properties. Thus it is necessary to investigate the effects on the reactants and transition states of added co-solvent.

The kinetics of a number of substitution reactions of transition metal complexes have already been investigated in a variety of mixed aqueous solvents [1.10,11]. Often the subject of such studies has been to diagnose the nature of the mechanism from the variation of reactivity with solvent composition, using correlation of rates with, for example functions of the bulk dielectric constant [1.12] or empirical parameters such as Grunwald-Winstein solvent Y values [1.13]. Less often, attempts are made to interpret reactivity trends in terms of known physical properties of the solvent mixtures. The effect of solvent structure on reactivity has been described and discussed, in terms of viscosities and enthalpies of vapourisation, for reactions of metal(II) cations with 2,2'-bipyridyl [1.14]; the overriding importance of viscosity in determining reactivity has been illustrated for reactions of metal(II) cations with pyridine-2-azo-4'-dimethylaniline [1.15].

(i) BINARY AQUEOUS MIXTURES

These have been conveniently classified [1.16] on the basis of their thermodynamic properties; particularly their molar excess Gibbs function, G^E . This parameter expresses the extent to which the properties of a given mixture differ from those of the corresponding ideal mixture at the same temperature, pressure and mole fraction. An ideal mixture is defined as a mixture for which the chemical potential of each component can be described [1.17] by the equation:-

$$\mu_i(P,T,\underline{x}) = \mu_i^\ominus(P,T) + RT \ln \underline{x}_i \quad (1.02)$$

where μ_i^\ominus is the chemical potential of pure i , and x_i is the mole fraction of component i . For a real solution, the chemical potential is given by

$$\mu_i(P, T, x) = \mu_i^\ominus(P, T) + RT \ln a \quad (1.03)$$

where a = activity of i , $= x_i f_i$; f_i is the activity coefficient, such that $f_i \rightarrow 1$ as $x_i \rightarrow 1$.

Then the excess thermodynamic function, G^E is calculated as the difference between the real and ideal mixtures. Thus, for example, in the mixing of n_1 moles of component 1 with n_2 moles of component 2,

$$G(\text{ideal}) = n_1(\mu_1^\ominus + RT \ln x_1) + n_2(\mu_2^\ominus + RT \ln x_2) \quad (1.04)$$

$$\text{and } G(\text{real}) = n_1(\mu_1^\ominus + RT \ln x_1 f_1) + n_2(\mu_2^\ominus + RT \ln x_2 f_2) \quad (1.05)$$

then

$$\begin{aligned} G^E &= G(\text{real}) - G(\text{ideal}), \\ &= RT (-\ln x_1 - \ln x_2 + \ln x_1 f_1 + \ln x_2 f_2) \\ &= +RT \ln f_1 f_2 \end{aligned} \quad (1.06)$$

These mixtures fall into two main classes, (a) 'Typically Aqueous', T.A., and (b) 'Typically Non-Aqueous', T.N.A.

(a) Typically Aqueous

These mixtures are characterised by having positive G^E values, where the sign and magnitude of G^E are determined by the entropy term rather than the enthalpy, i.e.

$$|T S^E| > |H^E| \quad (1.07)$$

where

$$G^E = H^E - T S^E \quad (1.08)$$

Examples of co-solvents in T.A. mixtures include methanol, ethanol, t-

butyl alcohol, 1,4-dioxan and tetrahydrofuran.

(b) Typically Non-Aqueous

These mixtures are characterised [1.16(a)] by:-

$$|H^E| > |T S^E| \quad (1.09)$$

but G^E can either be positive, i.e. a T.N.A.P. mixture, or negative, T.N.A.N. For example aqueous acetonitrile is a T.N.A.P. mixture, but aqueous hydrogen peroxide and dimethylsulphoxide are T.N.A.N. ones.

In the ensuing chapters of this thesis, kinetic data have been collected in binary aqueous mixtures which embrace all three of the above types of solvent.

Values of G^E used in this work for a wide range of binary aqueous mixtures are those calculated by Dr. M. J. Blandamer. The dependence of G^E on solvent composition can be calculated from vapour pressure data [1.17]. Because the kinetic data and the G^E values available were not for coincident solvent compositions, interpolated values of G^E were estimated using the Guggenheim-Scatchard equation [1.18,19]:-

$$G^E = x_1 (1 - x_1) \sum_{i=1}^n A_i (1 - 2x_1)^{i-1} \quad (1.10)$$

Here, the dependence of G^E on mole fraction is expressed in a general algebraic form, where x_1 is the mole fraction of water in the binary aqueous mixture. The coefficients $A_1 - A_n$ were calculated by fitting G^E values to equation (1.05) using a least-squares technique [1.20]. The values of G^E for the wide range of binary aqueous mixtures which have been used in this work are listed in Appendix 1.

ACTIVATION FREE ENERGIES OF TRANSFER, $\delta_m \Delta G^\ddagger$

The difference between the chemical potentials of the transition state (μ^\ddagger) and of the reactants (μ^\ominus) in a reaction is defined as ΔG^\ddagger , the Gibbs free energy of activation of the reaction, i.e.

$$\Delta G^\ddagger = \mu^\ddagger - \mu^\ominus_{(\text{reactant})} \quad (1.11)$$

The changes in each term of equation (1.11) on going from aqueous solution to a binary aqueous mixture of co-solvent mole fraction \underline{x}_2 may be represented by the medium operator [1.21] δ_m (equation (1.12)).

$$\delta_m \Delta G^\ddagger = \delta_m \mu^\ddagger - \delta_m \mu^\ominus_{(\text{reactant})} \quad (1.12)$$

More conveniently, $\delta_m \mu^\ddagger$ may be called $\delta_m \mu^\ominus(\text{T.S.})$ and $\delta_m \mu^\ominus_{(\text{reactant})} = \delta_m \mu^\ominus(\text{I.S.})$ for the respective transition-state and initial-state of the reaction.

In equation (1.12), the parameters are defined as:-

$$\left. \begin{aligned} \delta_m \Delta G^\ddagger &= \Delta G^\ddagger(\underline{x}_2) - \Delta G^\ddagger(\underline{x}_2=0) \\ \delta_m \mu^\ominus(\text{T.S.}) &= \mu^\ominus(\text{T.S.})(\underline{x}_2) - \mu^\ominus(\text{T.S.})(\underline{x}_2=0) \\ \text{and } \delta_m \mu^\ominus(\text{I.S.}) &= \mu^\ominus(\text{I.S.})(\underline{x}_2) - \mu^\ominus(\text{I.S.})(\underline{x}_2=0) \end{aligned} \right\} \quad (1.13)$$

The $\delta_m \Delta G^\ddagger$ parameter is readily measurable from rate constant measurements in water and in binary aqueous mixtures. By combining equations (1.01) and (1.13),

$$\delta_m \Delta G^\ddagger = -RT \ln \left(k(\underline{x}_2) / k(\underline{x}_2=0) \right) \quad (1.14)$$

where $k(\underline{x}_2)$ is the rate constant in the binary aqueous mixture, of mole fraction \underline{x}_2 of co-solvent; and $k(\underline{x}_2=0)$ is the rate constant in water.

In this work, correlations have been drawn between $\delta_m \Delta G^\ddagger$ for some

reactions and the G^E values of the mixtures in which the reactions were studied. Attempts have been made to deduce any mechanistic implications of the results.

Initial State Free Energy of Transfer, $\delta_{m\mu}^\ominus(\text{I.S.})$

This parameter may be easily measured for a neutral species from solubility measurements. Here, there is no complication due to activity uncertainties, and the chemical potential of the species is given by:-

$$\mu_i^\ominus = -RT \ln K_s \quad (1.15)$$

where K_s is the solubility of the species, i , whence:-

$$\delta_{m\mu}^\ominus = -RT \ln K_s(x_2) / K_s(x_2=0) \quad (1.16)$$

Similarly, for a sparingly soluble salt, MX , where the activity coefficient is close to unity,

$$\delta_{m\mu}^\ominus(\text{MX}) = -RT \ln \frac{K_s(\text{MX})(x_2)}{K_s(\text{MX})(x_2=0)} \quad (1.17)$$

However a complication arises in the attempt to split this parameter into single-ion values, $\delta_{m\mu}^\ominus(\text{M}^+)$ and $\delta_{m\mu}^\ominus(\text{X}^-)$. Several methods have been used to effect such a single-ion split. Feakins *et al.* [1.22] adapted an extrapolation procedure, based on equations (1.18 and 1.19)

$$\delta_{m\mu}^\ominus(\text{HX}) = \delta_{m\mu}^\ominus(\text{H}^+) + a r_a^{-1} \quad (1.18)$$

$$\delta_{m\mu}^\ominus(\text{MCl}) = \delta_{m\mu}^\ominus(\text{Cl}^-) + b r_c^{-1} \quad (1.19)$$

where r_a and r_c are the crystallographic radii of the anions (X) and cations (M) respectively. In a different approach, Case & Parsons have

measured [1.23] the free energy change in transferring an individual ion from the gas phase into bulk solution. They then combined these results with similar ones for pure water [1.24] to obtain values for $\delta_{\text{m}}^{\ominus}(\text{ion})$ from water to mixed solvents. Wells [1.25] has considered the free energy of transfer of the proton, $\delta_{\text{m}}^{\ominus}(\text{H}^+)$, to be the sum of two processes; the transfer of a tetrahedral aquo-proton from water into the mixture (obtained using the Born expression), and the subsequent replacement of a water molecule in the tetrahedron by, in the case of methanol-water mixtures, a methanol molecule. The values of $\delta_{\text{m}}^{\ominus}(\text{H}^+)$ thus derived were then used to estimate $\delta_{\text{m}}^{\ominus}(\text{halide ion})$ for the appropriate hydrogen halides. Values for other cations (M^+) were then deduced for simple MX salts. De Ligny et al. have developed a method for calculating single-ion free energies of transfer in a range of binary aqueous mixtures, for a variety of ions [1.26]. They assume that the transfer function is composed of two components, $\delta_{\text{m}}^{\ominus}_{\text{el}}$ which accounts for the interaction of the charge of the ion with the solvent, and $\delta_{\text{m}}^{\ominus}_{\text{neutr}}$ for its Van der Waal's interaction with the solvent.

Parker et al. [1.27] made the assumption $\delta_{\text{m}}^{\ominus}(\text{Ph}_4\text{As}^+) = \delta_{\text{m}}^{\ominus}(\text{BPh}_4^-)$ in attempting to estimate single-ion transfer functions. This assumption is most reasonable, since the peripheries, magnitude of charges and ionic radii of these ions are very similar to one another. Abraham [1.28] however, made the arbitrary assumption that $\delta_{\text{m}}^{\ominus}(\text{Me}_4\text{N}^+) = 0$. From this he calculated relative transfer parameters for a variety of ions from water to several non-aqueous solvents. Although these results are internally consistent, they cannot be correlated satisfactorily with other workers' assumptions. For example, Parker's value of $\delta_{\text{m}}^{\ominus}(\text{Cl}^-)$ into methanol is $+12.6 \text{ kJ mol}^{-1}$, whereas Abraham's value is 20.3 kJ mol^{-1} .

In this thesis, single-ion values from Wells [1.25] and from

de Ligny *et al.* [1.26], which are fairly consistent with each other, have been employed. Using these values single-ion values for other salts, for which solubility data are available (or have been collected), have been estimated.[†]

Transition State Free Energy of Transfer, $\delta_{\text{m}\mu}^{\ominus}(\text{T.S.})$

We have seen that it is possible to estimate both $\delta_{\text{m}}\Delta G^{\ddagger}$ and $\delta_{\text{m}\mu}^{\ominus}$ (I.S.) by experiment. Obviously, such procedures are not possible in estimating $\delta_{\text{m}\mu}^{\ominus}(\text{T.S.})$, although we can intuitively guess at the approximate trends in this function with solvent composition, by relating the known transition state to a tangible compound of similar chemical and physical properties, where possible.

However, from equation (1.12), we can calculate $\delta_{\text{m}\mu}^{\ominus}(\text{T.S.})$, since we can measure experimentally the other variables of the equation. In this work, such an analysis of solvent effects on several inorganic reactions has been performed. For reactions of known mechanism, for example the mercury(II)-catalysed aquation of transition metal-halo complexes (chapter 5), the trends of the various transition state solvations (for different metal complexes) have been determined from the kinetic behaviours of the reactions, and the solvation characteristics of the initial states, and have been used to explain the differences in the kinetic behaviours of the reactions of the various metal complexes.

Note:-

In all the ensuing studies, the solvent compositions are expressed

[†] [For example, see chapters 5 and 6.]

as % by volume before mixing; all general properties (such as mole fraction, etc.) of these mixtures are tabulated in Appendix 1.

CHAPTER 2

Kinetic and Equilibrium Properties of Pentacyano-
(3,5-dimethylpyridine)iron(II) and Related Anions
in Binary Aqueous Mixtures.

2.1 INTRODUCTION

Substitution reactions of octahedral complexes generally occur by a predominantly bond breaking mechanism. In the case of extensive ion-pair formation, distinction between the limiting S_N1 (or D) [2.01] mechanism and a dissociative-interchange [2.01] (or I_d) mechanism is extremely difficult, since the empirical form of the rate law will be the same for both mechanisms [2.02]. To avoid such complications, anionic aquopentacyanocobaltate(III) has been used [2.03] and it has been found that replacement of water by azide and thiocyanate anions occurs by a limiting D mechanism. Another very clear example of the D mechanism with no ion-pairing involves activation by sulphite ions in the systems $\text{trans-}[\text{Co}(\text{CN})_4\text{SO}_3\text{X}]^{n-}$ (where $\text{X} = \text{CN}^-$, NCS^- , NH_3 , OH^- , N_3^- , NO_2^- and SO_3^{2-}) [2.04]. Work in this area has been recently reviewed [2.05].

Kinetic studies of ligand replacements in a number of pentacyanoferrate(II) complexes of pyridine, pyrazine and related nitrogen heterocycles have been recently reported, and the data interpreted in terms of a limiting dissociative mechanism [2.06]. Although the bulk of data collected on reactions of the pentacyano(ligand)ferrate(II) complexes with incoming nucleophiles supports the operation of a D mechanism [2.06-2.11], the question remains whether the data enable one to distinguish between D and I_d mechanisms or not, since studies of substitution at the $[\text{Fe}(\text{CN})_5(\text{OH}_2)]^{3-}$ anion in aqueous solution [2.11] and in ethylene glycol [2.12] tend to support the operation of an I_d mechanism.

In this work data have been accumulated to support a D mechanism for substitution at a complex of the type $[\text{Fe}(\text{CN})_5\text{L}]^{n-}$, and also conclu-

sive evidence proving the operation of such a mechanism is reported in the form of Volumes of Activation for several substituted complexes. Having proved conclusively the type of mechanism, a study has been made of the effects of varying solvent composition on the kinetic and thermodynamic properties of the system, the kinetic data being interpreted in the form of activation free energies of transfer, $\delta_m \Delta G^\ddagger$ (see text); the thermodynamic properties of the system in the form of standard free energies, ΔG^\ominus , and solvent composition in terms of the excess free energy of mixing, G^E (see text). The kinetics of the reaction have also been correlated with the Grunwald-Winstein Y parameter. The discriminatory power of the $[\text{Fe}(\text{CN})_5]^{3-}$ moiety has been investigated both in aqueous solution and in binary aqueous mixtures, and has been compared and contrasted with the equilibrium properties of the system described by equation (2.01) (see section 2.3(iii)).

A study of the solvatochromic behaviour of the $[\text{Fe}(\text{CN})_5(\text{mpz})]^{2-}$ anion both in pure solvents and in a range of binary aqueous mixtures has been made, and correlated with Reichardt's E_T parameter [2.14]. This study is discussed in Chapter 8.

Finally, it should be noted that (i) all solvent mixture compositions listed are in percentage by volume before mixing, and (ii) all rate constants reported are the mean values of at least two determinations, having a standard deviation of less than $\pm 1\%$, all kinetic runs having been performed at least in duplicate.

2.2 EXPERIMENTAL

(i) REAGENTS

Preparations

The trisodium salts of the pentacyano(ligand)ferrate(II) anions, $[\text{Fe}(\text{CN})_5\text{L}]^{3-}$, for the ligands 3,5-dimethylpyridine, 3-cyanopyridine, 3-chloropyridine and 4-cyanopyridine, and the corresponding disodium salt of the N-methylpyrazinium complex anion were prepared by published methods [2.06] from trisodium pentacyanoammineferrate(II) and the appropriate nitrogen heterocycle. The tetraphenylarsonium salt of the $[\text{Fe}(\text{CN})_5(\text{mpz})]^{2-}$ anion was prepared by precipitation from aqueous solution by addition of an excess of aqueous tetraphenylarsonium chloride to a solution of the complex anion, the insoluble product being filtered, washed with much water and dried at room temperature over phosphorus pentoxide in vacuo. The precursor pentacyanoammineferrate(II) was prepared by the method of Kenney [2.14], from sodium nitroprusside and ammonia. N-Methylpyrazinium iodide was prepared by direct methylation of pyrazine by methyl iodide according to Bahⁿer [2.15].

Characterisation

Carbon, hydrogen, nitrogen and in some cases oxygen analyses were performed on the sodium salts of $[\text{Fe}(\text{CN})_5(3,5\text{-Me}_2\text{py})]^{3-}$, $[\text{Fe}(\text{CN})_5(3\text{-CNpy})]^{3-}$, $[\text{Fe}(\text{CN})_5(3\text{-Clpy})]^{3-}$ and $[\text{Fe}(\text{CN})_5(4\text{-CNpy})]^{3-}$ by the "Butterworth Micro Analytical Company". These analyses proved to be difficult, and were found to require extended combustion times at elevated temperatures (1273 K) in order to obtain satisfactory results. Iron analyses were performed by the author on a Perkin Elmer 360 Atomic

Absorption Spectrophotometer. The microanalysis of the 3-chloropyridine complex proved to be repeatedly unsatisfactory, and samples were found to deteriorate over a period of several days. However, solutions made up from freshly prepared samples of the complex exhibited reproducible kinetic results. The analysis results for these complexes are given in Table 2.01. The complexes were found to contain varying amounts of water of crystallisation, as determined from oxygen analyses, which is not inconsistent with previously reported analogous complexes, examples of which are listed below:-

| Complex anion ^{a,b} | No. molecules water/ molecule of complex | Reference |
|--|---|-----------|
| [Fe(CN) ₅ (dmna)] ³⁻ | 2 | [2.11] |
| [Fe(CN) ₅ (PhNO)] ³⁻ | 4.5 | [2.16] |
| [Fe(CN) ₅ (pz)] ³⁻ | 4 | [2.06] |
| [Fe(CN) ₅ (mpz)] ²⁻ | 4 | [2.06] |
| [Fe(CN) ₅ (int)] ³⁻ | 5 | [2.06] |
| [Fe(CN) ₅ (1-(4pyr)py)] ³⁻ | 5 | [2.06] |

^a all results are for the sodium salts of these anions.

^b PhNO = nitrosobenzene; pz = pyrazine; mpz = N-methylpyrazinium; int = isonicotinamide; 1-(4pyr)py = 1-(4 pyridyl)-pyridine; dmna = N,N-dimethyl-p-nitrosoaniline.

The complexes do not melt below 593 K, but undergo gradual thermal decomposition above ca. 323 K. All samples were stored over phosphorus pentoxide in vacuo in the dark.

Trisodium pentacyanoammineferrate(II) was characterised by its UV/visible spectrum. Elemental analysis was not deemed necessary as the

TABLE 2.01 Micro-analysis results for complexes of the type $\text{Na}_3[\text{Fe}(\text{CN})_5(\text{L})]^{3-}$. Results are expressed in percentages by weight of the appropriate element.

| | Element | | | | |
|--------------------------------|---------|------|-------|-------|-------|
| | C | H | N | O | Fe |
| (a) L = 3,5-Me ₂ py | | | | | |
| % Calculated ^b | 33.9 | 3.79 | 19.8 | 13.2 | 13.13 |
| % Found | 33.5 | 3.63 | 19.8 | 13.0 | 13.08 |
| (b) L = 3-CNpy | | | | | |
| % Calculated ^b | 30.16 | 2.82 | 22.97 | 15.56 | 13.16 |
| % Found | 30.65 | 2.81 | 22.74 | 14.85 | 12.95 |
| (c) L = 4-CNpy | | | | | |
| % Calculated ^b | 29.4 | 2.63 | 21.8 | 17.8 | |
| % Found | 29.34 | 3.1 | 22.02 | 18.25 | |
| (d) L = 3-Clpy ^a | | | | | |
| % Calculated | 28.4 | 2.2 | 18.4 | | |
| % Found | 24.6 | 3.0 | 16.6 | | |

^a On repeating the analysis on the same batch of sample two days later, % Found for C and H had respectively decreased by one fifth and increased by one quarter of their original values.

^b These calculated percentages are for 3.5, 4.0 and 5.0 molecules of water per molecule of complex, for L = 3,5-Me₂py, 3-CNpy and 4-CNpy respectively.

compound was used solely for the preparation of the above substituted pentacyanoferrate(II) complexes, which themselves analysed satisfactorily. The N-methylpyrazinium complex salts prepared were also characterised by their UV/visible spectrum, data for which have been reported by Toma [2.06], as they were used for solvatochromic studies only (see Chapter 8).

Solvents and other Reagents

All solvents used were the best commercially available (usually AnalaR grade), and were used as received, except for (i) Water - which was doubly distilled; (ii) Methanol - which was dried over magnesium and iodine followed by distillation [2.17]; and (iii) Dioxan and Tetrahydrofuran - which were both dried and simultaneously freed from peroxides by passage down a column of alumina, followed by distillation [2.17]. A list of other reagents used, together with their source and purity is given in Table 2.02. All these reagents were used as received except where otherwise indicated.

(ii) KINETICS

Stock solutions of the appropriate $\text{Na}_3[\text{Fe}(\text{CN})_5(\text{X-py})]$ complex were prepared freshly each day in water, as the solutions are prone to decay with time when dilute [2.18]. The concentrations of these stock solutions were such that dilution by a factor of 3.75 (i.e. 0.8 cm³ stock solution diluted to 3 cm³) produced UV/visible spectra which possessed convenient absorptions at the respective wavelengths of maximum absorptions. The concentrations of the stock solutions used, together with the wavelengths of maximum absorption, λ_{max} , at which kinetics were monitored are listed below:-

TABLE 2.02 Reagents used in this work without further purification together with their source and purity.

| Reagent | Source | Purity |
|--|------------|----------------------|
| Potassium Cyanide | B.D.H. | AnalaR |
| Potassium Thiocyanate | B.D.H. | AnalaR |
| Potassium Nitrate | B.D.H. | AnalaR |
| Methyl Iodide | B.D.H. | Tech. |
| Thiourea | B.D.H. | AnalaR |
| Sodium Borate | B.D.H. | AnalaR |
| Pyrazine | Koch-Light | Gold label (99.9+ %) |
| 3-Chloropyridine | Koch-Light | Puris |
| 3-Cyanopyridine | Koch-Light | Puris |
| 4-Cyanopyridine | Koch-Light | Puris |
| 3,5-Dimethylpyridine | Koch-Light | Puris |
| N,N'-Dimethyl-p-nitroso- ^a aniline | Koch-Light | Tech. |

^a This reagent was recrystallised twice from absolute ethanol.

| Complex | Concentration/mol dm ⁻³ of Stock Solution | λ_{\max} /n.m. |
|--|---|------------------------|
| Na ₃ [Fe(CN) ₅ (3,5-Me ₂ py)] | 6.0 x 10 ⁻⁴ | 368 |
| Na ₃ [Fe(CN) ₅ (3-CNpy)] | | 406 |
| Na ₃ [Fe(CN) ₅ (3-Clpy)] | | 382 |
| Na ₃ [Fe(CN) ₅ (4-CNpy)] | | 478 |

Aqueous volumetric solutions of potassium cyanide and potassium nitrate were prepared by direct weighing of the materials. These stock solutions were 0.072 mol dm⁻³ for the studies in binary aqueous mixtures, the resulting constant ionic strength of the reaction solution having been 0.024 mol dm⁻³. For studies of activation parameters for the 3,5-dimethylpyridine and 3-cyanopyridine complexes, stock solutions of these reagents were 0.90 mol dm⁻³, as were the stock solutions for the studies on the discriminatory power of the [Fe(CN)₅]³⁻ moiety.

The kinetics of cyanide attack at [Fe(CN)₅(3-CNpy)]³⁻ in the presence of added 3-cyanopyridine were performed at 298.6 K at an ionic strength of 0.12 mol dm⁻³, maintained with potassium nitrate. The concentrations of added 3-cyanopyridine ranged from 0.001 to 0.009 mol dm⁻³, for a variety of cyanide concentrations in a range of binary aqueous mixtures. Plots of reciprocal observed rate constants versus (i) reciprocal cyanide concentration at constant 3-cyanopyridine concentration; and (ii) 3-cyanopyridine concentration at constant cyanide concentration were computed on a PDP11 computer using a BASIC least-mean-squares program (Program No. 3, Appendix 2). An analogous study was performed for the 4-cyanopyridine complex at 298.2 K and ionic strength 0.10 mol dm⁻³.

Suitable aliquots of the required reaction components were mixed in 1 cm path length silica cells of 3 cm³ capacity, the aliquot of the stock complex solution being the final addition. A typical cell mixture is

given below:-

1.0 cm³ of 'Potassium Cyanide/Potassium Nitrate' mixture.

1.2 cm³ of 'Water/Co-solvent' mixture.

0.8 cm³ of Iron(II) complex solution.

Thus varying the volume of potassium cyanide added, but maintaining the total volume of the 'cyanide/nitrate' mixture constant, a variety of cyanide concentrations were employed, the ionic strength being maintained at a constant value. Similarly, the solvent composition was varied by varying the co-solvent portion of the 'water/co-solvent mixture' and compensating for the change by altering the volume of water in the mixture.

The purpose of maintaining a constant ionic strength was to ensure the prevention of any rate variations with ionic strength which, as was discovered, were absent from the reaction of $[\text{Fe}(\text{CN})_5\text{L}]^{n-}$ anions with cyanide ion.

All kinetic runs were carried out in the thermostatted cell compartment of a Pye Unicam SP800 Recording Spectrophotometer fitted with an S.P. 825 clock attachment. The thermostatted cell compartment was calibrated in the range 288-333 K within an error of $\pm 0.05^\circ$. Optical density values were monitored at or near the wavelengths of maximum absorption of the appropriate complexes. Neither potassium cyanide, potassium nitrate nor any of the solvent mixtures employed showed any absorption at these wavelengths. All runs were performed in duplicate, the reported results being mean values of at least two measurements. The temperature of all runs was maintained at 298.6 K, except where otherwise indicated.

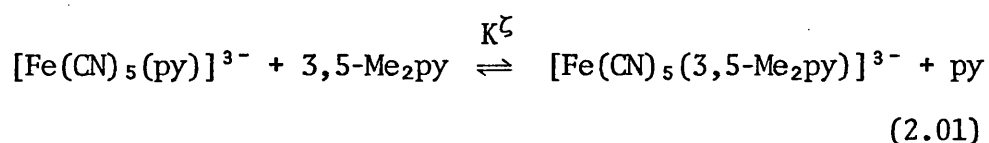
Observed rate constants, k_{obs} , were derived from changes in optical density measurements of the UV/visible spectra of the pertinent complexes

with time. The rates of change of such measurements were computed by means of a least-mean-squares BASIC program on a PDP11 computer (Appendix 2, Program No. 1), or by a similar BASIC program on a Cyber 72 computer (Appendix 2, Program No. 2).

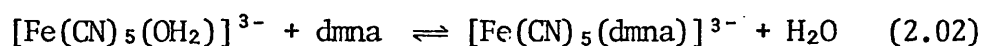
The kinetic study of the reactions of the $[\text{Fe}(\text{CN})_5(3,5\text{-Me}_2\text{py})]^{3-}$ and $[\text{Fe}(\text{CN})_5(3\text{-CNpy})]^{3-}$ anions with various nucleophiles at 298 K in aqueous solution, over a range of pressures was carried out at Melbourne University, by Prof. D. R. Stranks and Mr. T.R. Sullivan.

(iii) EQUILIBRIUM STUDIES

- on the system:-



The method of determination of the equilibrium constant, K^{ζ} , for the reaction illustrated in equation (2.01) is fully described in section 2.3. The method requires a study of the equilibria:-



where dmna = N,N'-dimethyl-p-nitrosoaniline and B is a substituted pyridine base.

In order to study these equilibria, it was necessary to prepare the following volumetric solutions:-

| Reagent | Concentration/mol dm ⁻³ | Solvent |
|--|------------------------------------|------------------------|
| Sodium Borate | 0.050 | Water |
| Pyridine base (B) | 0.020 | Water |
| dmna | 0.001 | Appropriate co-solvent |
| Na ₃ [Fe(CN) ₅ (NH ₃)] | 0.020 | Water |

In practice trisodium pentacyanoammineferrate(II) was employed rather than the aquo complex, the former being more easily prepared in a pure state, and as very dilute solutions were used, the complex anion in solution which was involved in the equilibria under study was in fact $[\text{Fe}(\text{CN})_5(\text{OH}_2)]^{3-}$ [2.18].

Reaction solutions consisting of the above components were prepared according to the table below, such that each solution mixture was composed of specific solvent compositions of increments of 10% by volume of co-solvent, from zero to 40% inclusive, and such that they exhibited a convenient optical density at 650 nm. (i.e. contained a convenient concentration of $[\text{Fe}(\text{CN})_5(\text{dmna})]^{3-}$ anion).

Equilibrium Mixture Components:-

- 1.0 cm³ of Sodium Borate stock solution,
- 0.8 cm³ of dmna stock solution,
- 1.0 cm³ of pyridine base stock solution,
- 6.4 cm³ of 'water/co-solvent' mixture,
- 0.8 cm³ of trisodium pentacyanoammineferrate(II) stock solution.

Values for the equilibrium constant, K^{ζ} , were also measured in aqueous solution for the equilibria between pyridine and (a) 3-cyanopyridine and (b) 3-chloropyridine.

For each equilibrium mixture the components were placed in a clean dry flask and thoroughly mixed, the pentacyanoammineferrate(II) solution

being the final addition. Each mixture was then thermostatted at 298 K in the dark. The complex solution was freshly prepared for each set of reaction solutions. The stock solution of dmna was made up in the appropriate co-solvent because (a) aqueous solutions are unstable [2.18] and (b) solubility problems were encountered in aqueous solution.

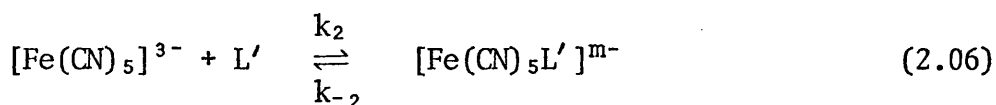
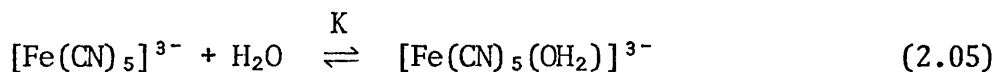
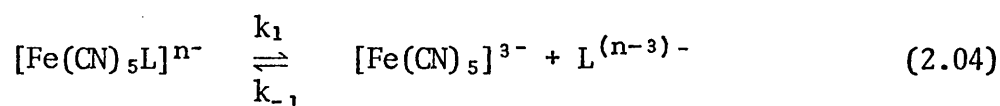
For measurements in aqueous solution a more dilute stock solution of dmna was employed, the component volumes of the mixtures being adjusted accordingly. Thus in aqueous solution, a fresh stock solution concentration $2.22 \times 10^{-3} \text{ mol dm}^{-3}$ was used. Sodium borate was included in the reaction mixtures as a buffer to minimise any disturbing effects of variation in pH.

Optical density measurements were recorded at 650 nm periodically to determine a suitable equilibration time (i.e. full colour development). An arbitrary period of three hours was allowed for attainment of equilibrium, which proved to be short enough so that negligible decomposition of the $[\text{Fe}(\text{CN})_5(\text{dmna})]^{3-}$ anion was detectable.

2.3 RESULTS AND DISCUSSION

(i) KINETICS IN AQUEOUS SOLUTION

There have been many kinetic studies in recent years of substitution at complexes of the pentacyanoferrate(II) type, $[\text{Fe}(\text{CN})_5\text{L}]^{n-}$, in aqueous solution. For example, Mitra et al. have studied the aquation of the $[\text{Fe}(\text{CN})_5\text{NO}]^{2-}$ anion [2.19]; and reactions of this anion with ammonia, hydroxylamine and hydrazine have been investigated by Dozsa [2.20]. The reactions of cyanide ion with the complex anions $[\text{Fe}(\text{CN})_5\text{L}]^{n-}$, for L = nitrosobenzene [2.09]; sulphite ion [2.10]; pyridine [2.21]; 3-cyanopyridine [2.11]; and dimethylsulphoxide [2.08] have also been studied, together with the reaction of the N-methylpyrazinium cation with a range of complex anions $[\text{Fe}(\text{CN})_5\text{L}]^{n-}$ where L is an aromatic nitrogen heterocycle [2.06]. In all these reactions, the kinetic evidence points to the operation of a limiting dissociative (or D) mechanism (equations (2.04 - 2.06)). Such a mechanism has been postulated by Toma [2.06] for these reactions which is consistent with the kinetic results. The mechanism is represented by the equations (2.04 - 2.06)



where L is the outgoing ligand, e.g. a substituted pyridine in this work, and L' is the incoming nucleophile, e.g. cyanide ion.

The equilibrium involving water, expressed by equation (2.05) is

written in the mechanism because it is a likely though non-productive step. It has been shown [2.07] that the assumption that the equilibrium expressed by equation (2.06) is labile compared with the rate-determining k_1 step shown in equation (2.04) is justified, since the specific rates of formation of L-substituted complexes from aqueous pentacyanoammineferrate(II) are more rapid than the specific rates of dissociation by a factor of approximately 10^6 . This suggests that the rate of loss of the ammine ligand and the exchange of inner-sphere water should be rapid compared to the k_1 step in equation (2.04).

In such a reaction proceeding via a D mechanism, the forward (k_2) step in equation (2.06) is assumed to be irreversible, e.g. for $L' = \text{CN}^-$, as is evidenced by the stability of aqueous $[\text{Fe}(\text{CN})_6]^{4-}$ in the absence of light [2.16]. The intermediate, $[\text{Fe}(\text{CN})_5]^{3-}$ is considered to persist as a species of reduced coordination number which exhibits distinctive reactivities towards different nucleophiles.

For the reactions of the $[\text{Fe}(\text{CN})_5(3,5\text{-Me}_2\text{py})]^{3-}$ anion with thiocyanate, thiourea, pyrazine and N-methylpyrazinium cation, clean isosbestic points were observed at 431, 515, 393 and 456 nm respectively in aqueous solution, and at 390 nm for reaction with 4,4'-bipyridyl in 33% by volume methanol.[†] For the reaction of the 3-cyanopyridine complex with cyanide ion, clean isosbestic points were observable at 216, 219, 222 and 252 nm in aqueous solution. Thus in all cases, the occurrence of such isosbestic points indicates that the rate of formation of product of the reaction equals the rate of disappearance of starting material, i.e.

[†] Due to the low solubility of 4,4'-bipyridyl in water, it was necessary to dissolve the nucleophile in methanol to ensure a large enough excess of nucleophile over complex concentration to satisfy pseudo first-order conditions.

$$-\frac{d[\{\text{Fe}(\text{CN})_5\text{L}\}^{n-}]}{dt} = + \frac{d[\{\text{Fe}(\text{CN})_5\text{L}'\}^{n-}]}{dt} \quad (2.07)$$

for L = outgoing ligand; L' = incoming nucleophile.

Such occurrences also indicate the lack of any significant build-up of concentration of the $[\text{Fe}(\text{CN})_5]^{3-}$ intermediate, i.e. the intermediate is very short-lived, and we can assume that the steady-state approximation holds, i.e.

$$\frac{d[\{\text{Fe}(\text{CN})_5\}^{3-}]}{dt} = 0 \quad (2.08)$$

All kinetic runs were performed in the presence of an excess of incoming nucleophile. Under these conditions all runs were first-order in iron(II) complex concentration up to at least three half-lives, i.e. the rate law for the reaction is given by equation (2.09).

$$\text{rate} = \frac{-d[\text{complex}]}{dt} = k_{\text{obs}}[\text{complex}] \quad (2.09)$$

where k_{obs} is the observed first-order rate constant.

Now,

$$-\frac{d[\text{complex}]}{dt} = k_1[\text{Fe}(\text{CN})_5\text{L}] - k_{-1}[\text{Fe}(\text{CN})_5][\text{L}]^\dagger \quad (2.10)$$

And,

$$\begin{aligned} -\frac{d[\text{Fe}(\text{CN})_5]}{dt} &= k_2[\text{Fe}(\text{CN})_5][\text{L}'] + k_{-1}[\text{Fe}(\text{CN})_5][\text{L}] - k_1[\text{Fe}(\text{CN})_5\text{L}] \\ &= 0 \quad \text{at steady state (equation (2.08))} \end{aligned} \quad (2.11)$$

[†] electrical charges on ions are omitted for simplicity.

Combining equations (2.10) and (2.11) we find the rate law is:-

$$\text{rate} = \frac{k_1 k_2 [L'] [\text{Fe}(\text{CN})_5 \text{L}]}{k_{-1} [\text{L}] + k_2 [L']} \quad (2.12)$$

Hence

$$k_{\text{obs}} = \frac{k_1 k_2 [L']}{k_{-1} [\text{L}] + k_2 [L']} \quad (2.13)$$

Equation (2.13) provides a set of kinetic criteria which has been applied in this work to the substitution reactions of the $[\text{Fe}(\text{CN})_5 \text{L}]^{n-}$ type anion to test the operation of a limiting dissociative mechanism.

First-order rate constants, k_{obs} , for the reaction of the $[\text{Fe}(\text{CN})_5(4\text{-CNpy})]^{3-}$ anion with cyanide ion in aqueous solution at 298.6 K and an ionic strength of 0.10 mol dm^{-3} are listed in Table 2.03. From a plot of k_{obs} against cyanide ion concentration, Figure 2.01(a), we see clearly that the rate depends initially upon the cyanide ion concentration, but soon reaches a constant value which is independent of the concentration of cyanide ion. This type of saturation behaviour is understood in terms of rate-determining loss of 4-CNpy ligand from the complex anion, with subsequent rapid attack by the incoming cyanide nucleophile. From equation (2.13) we see that at low cyanide ion (i.e. L') concentration, k_{obs} is a linear function of it. At high cyanide ion concentration, $k_2 [\text{CN}^-] \gg k_{-1} [\text{L}]$ in equation (2.13), which approximates to $k_{\text{obs}} = k_1$ (or $k_{1\text{im}}$).

Thus at high cyanide ion concentration, the observed first-order rate constant is equal to the rate of dissociation of the $[\text{Fe}(\text{CN})_5 \text{L}]^{n-}$ anion to $[\text{Fe}(\text{CN})_5]^{3-}$ and $\text{L}^{(n-3)-}$. By inverting equation (2.13) we obtain:-

$$\frac{1}{k_{\text{obs}}} = \frac{1}{k_1} + \frac{k_{-1} [\text{L}]}{k_1 k_2 [L']} \quad (2.14)$$

Thus the intercept of a plot of $1/k_{\text{obs}}$ versus $1/[L']$ (i.e. $1/[\text{CN}^-]$) for the reaction of cyanide ion with, for example, the $[\text{Fe}(\text{CN})_5(4\text{-CNpy})]^{3-}$ anion is the reciprocal of k_1 (or $k_{1\text{im}}$). For this case at 298.6 K in aqueous solution, the intercept was found to be 894 ± 31 s, hence $k_1 = 1.12 \times 10^{-3} \pm 0.04 \times 10^{-3} \text{ s}^{-1}$. This plot is depicted in Figure 2.01(b). We may also see that from the reciprocal plot in Figure 2.01(b), the slope of the line is directly proportional to the ratio k_{-1}/k_2 . This ratio is a direct measure of the relative reactivity of the $[\text{Fe}(\text{CN})_5]^{3-}$ moiety to the outgoing ligand and the incoming nucleophile. This aspect of the mechanism is dealt with in detail in section 2.3(ii) of this chapter. (However, a dissociative interchange (I_d) mechanism also exhibits the same functional dependence upon the incoming nucleophile concentration if the fraction of ML_5X which forms an encounter complex, $\{\text{L}_5\text{MX}, \text{Y}\}$, becomes large at large concentrations of Y, for the reaction of ML_5X with Y. So this saturation behaviour may not be deemed 'conclusive' evidence for a D mechanism.)

TABLE 2.03 First-order rate constants, $10^4 k_{\text{obs}}/\text{s}^{-1}$, for reaction of the $[\text{Fe}(\text{CN})_5(\text{X-py})]^{3-}$ anions with a range of cyanide ion concentrations at constant ionic strength (as indicated for different X), over a range of temperatures in aqueous solution.

| X | T/K | $10 [\text{CN}^-]/\text{mol dm}^{-3}$ | | | | | | | | |
|-------------------|-------|---------------------------------------|------|------|------|------|------|------|-------|-------|
| | | 0.03 | 0.04 | 0.05 | 0.10 | 0.15 | 0.20 | 0.25 | 0.50 | 0.75 |
| 4-CN ^a | 298.6 | 4.63 | 5.48 | 6.15 | 7.75 | 8.08 | 9.46 | 9.52 | 10.53 | 11.11 |

| | T/K | $[\text{CN}^-]/\text{mol dm}^{-3}$ | | | |
|----------------------------------|-------|------------------------------------|-------------------|-------------------|-------------------|
| | | 0.10 | 0.20 | 0.40 | 0.60 |
| 3-CN ^b | 295.4 | 15.2 ₉ | 15.5 ₁ | 15.2 ₂ | 15.3 ₄ |
| | 297.7 | 20.5 ₆ | 20.0 ₉ | 20.2 ₁ | 20.2 ₃ |
| | 302.7 | 40.1 ₁ | 38.2 ₂ | 39.8 ₅ | 38.7 ₀ |
| | 306.4 | 62.1 | 60.1 | 59.6 | 59.2 |
| | 309.2 | 89.5 | 86.1 | 87.9 | 88.9 |
| | 314.2 | 153.0 | 148.2 | 157.2 | 154.1 |
| 3,5-Me ₂ ^b | 298.6 | 13.1 ₀ | 13.4 ₄ | 13.2 ₆ | 13.5 ₈ |
| | 302.2 | 21.9 ₁ | 21.0 ₁ | 20.2 ₆ | 21.0 ₆ |
| | 305.0 | 34.5 ₃ | 33.5 ₉ | 34.6 ₄ | 33.5 ₅ |
| | 309.2 | 56.9 | 57.8 | 57.6 | 57.4 |
| | 311.0 | 80.0 | 78.6 | 81.2 | 77.8 |

^a Ionic strength = 0.10 mol dm^{-3} (maintained with potassium nitrate).

^b Ionic strength = 0.60 mol dm^{-3} (maintained with potassium nitrate).

Figure 2.01(a) Dependence of the observed first-order rate constant, k_{obs} , on the cyanide ion concentration, $[\text{CN}^-]$, for the reaction of cyanide ion with the $[\text{Fe}(\text{CN})_5(4\text{-CNpy})]^{3-}$ anion in aqueous solution, at 298.2K; ionic strength = 0.10 mol dm^{-3} .

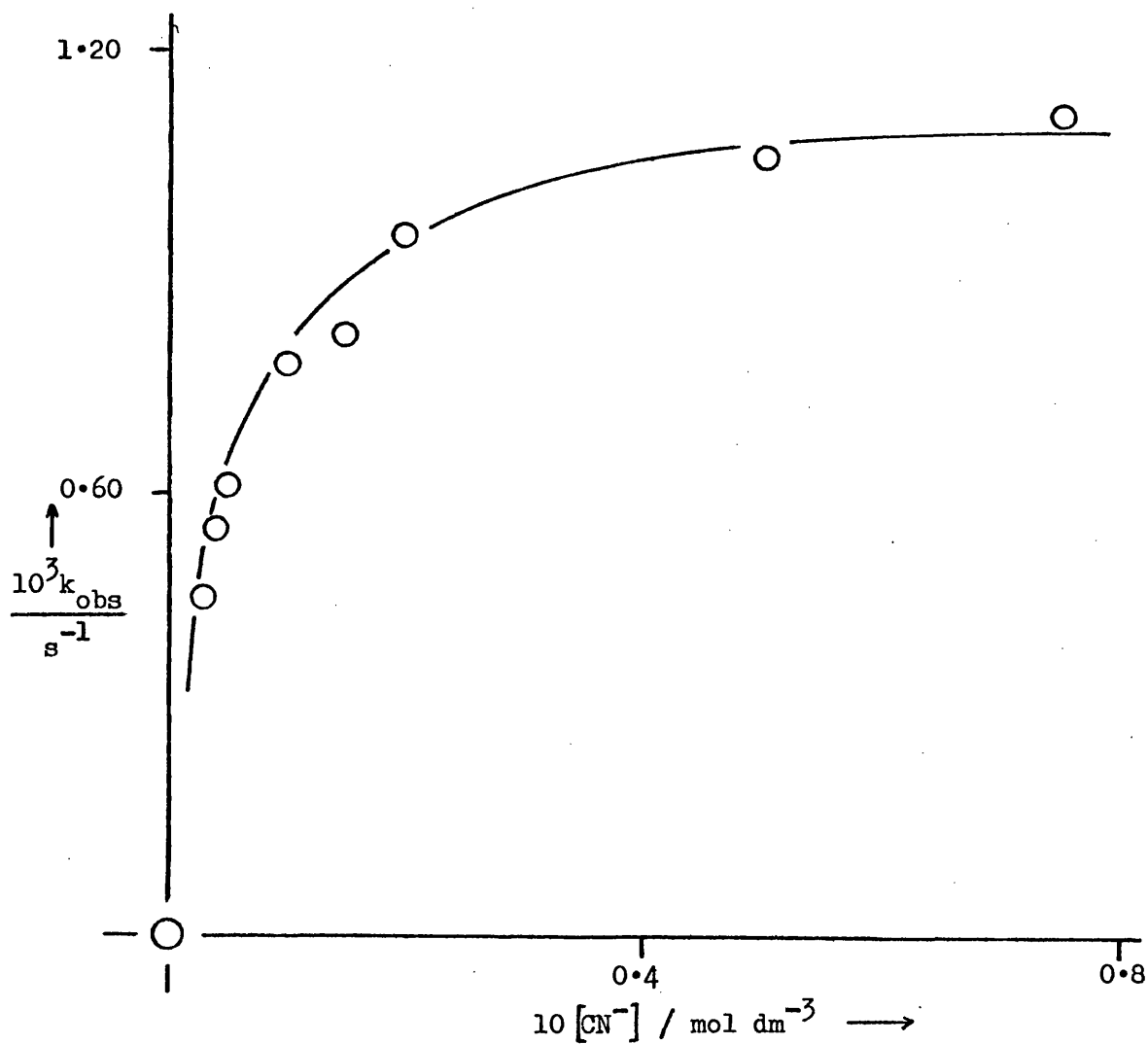
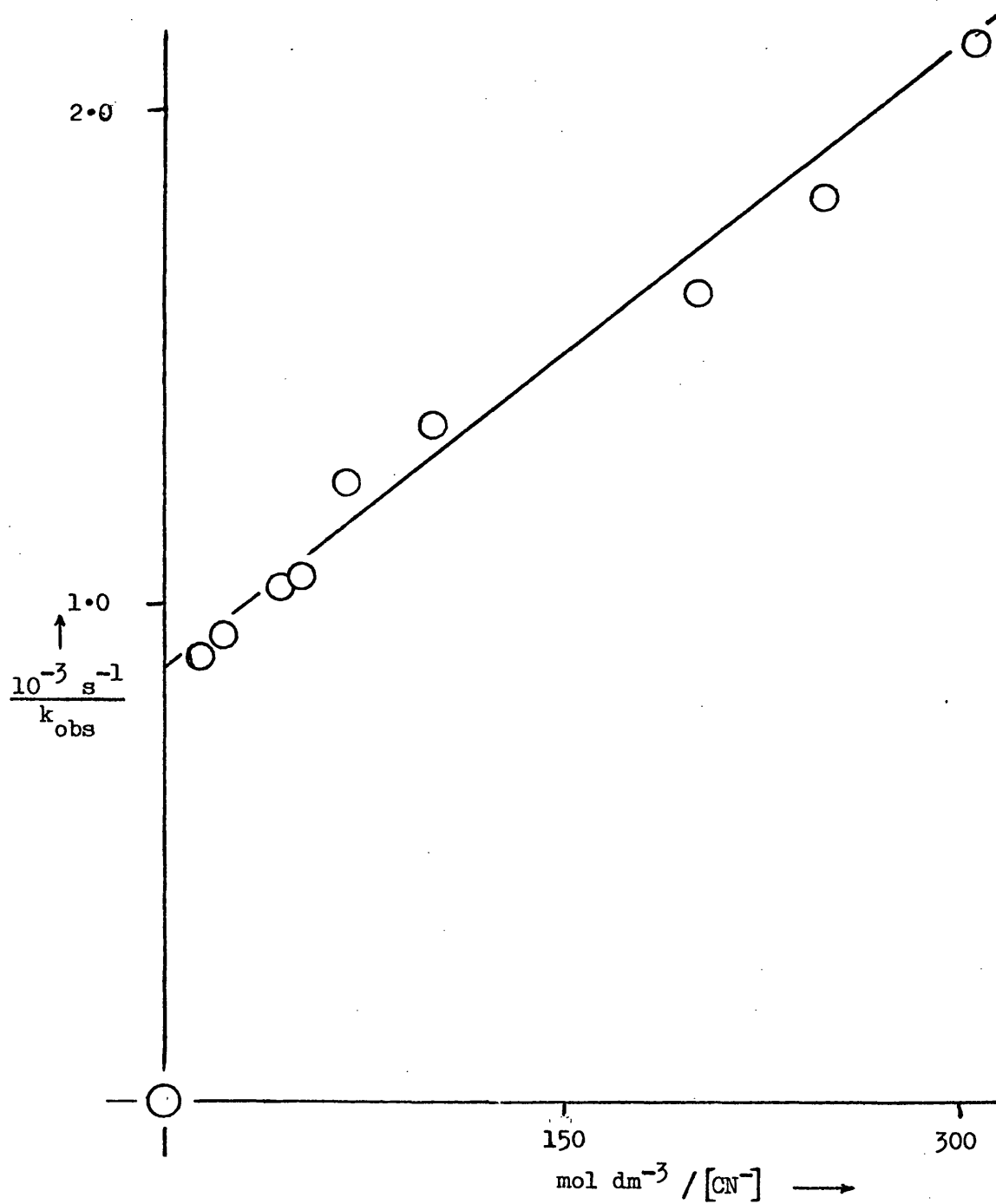


Figure 2.01(b) Reciprocal plot ($1/k_{\text{obs}}$ vs. $1/[\text{CN}^-]$) of Figure 2.01(a).



We have seen that at high cyanide ion concentration the observed rate constant is equivalent to k_1 . We see from equation (2.04) that the dissociative step of the reaction does not involve the incoming nucleophile, L' (i.e. CN^-). Hence the value of k_{lim} , i.e. k_{obs} at high $[L']$, should be independent of the nature of the incoming nucleophile L' . Table 2.04 lists observed first-order rate constants for the reaction of a variety of incoming nucleophiles with the $[Fe(CN)_5(3,5-Me_2py)]^{3-}$ and the $[Fe(CN)_5(3-CNpy)]^{3-}$ anions in aqueous solution at 298.6 K. From this table and from Figure 2.02, which is a graphical representation of the results, we see that the hypothesis holds true for the reactions in question, k_1 being ca. $1.3 \times 10^{-3} \text{ s}^{-1}$ for the 3,5- Me_2py complex, and ca. $2.4 \times 10^{-3} \text{ s}^{-1}$ for the 3-CNpy analogue. The slight increase in k_1 when the incoming nucleophile is the N-methylpyrazinium cation (for the 3,5- Me_2py complex) is consistent with a similar observation for the reaction of mpz^+ with the analogous 3-CNpy complex [2.11]. In this case the irregularity may be ascribed to the consequences of electrostatic interaction between the negatively charged complex or intermediate and the positively charged incoming nucleophile. Thus this fact can be encompassed by a D mechanism if we consider the outgoing ligand to first dissociate itself from the $[Fe(CN)_5]^{3-}$ moiety, then we get electrostatic interaction between the intermediate and mpz^+ , which would increase the value of k_2 . However, k_1 is the limiting rate constant, and if mpz^+ increases (as we see it does) the value of k_1 by way of its electrical charge, then there must be some electrostatic interaction between the $[Fe(CN)_5L]^{n-}$ anion and the mpz^+ cation.

TABLE 2.04 First-order rate constants, $10^3 k_{\text{obs}}/\text{s}^{-1}$, for reactions of the $[\text{Fe}(\text{CN})_5(\text{X-py})]^{3-}$ anions with a range of incoming nucleophiles (L) in aqueous solution at 298.6 K; initial $[\text{complex}] \leq 10^{-3} \text{ mol dm}^{-3}$ and ionic strength = 0.20 mol dm^{-3} (maintained with potassium nitrate) except where otherwise indicated.

| $\frac{[\text{L}]}{\text{mol dm}^{-3}}$ | incoming nucleophile (L) ^a | | | | | | |
|---|---------------------------------------|----------------|-----------------------------|------------------|------|-----------------------------|-----------------------------|
| | CN^- | SCN^- | tu | 4,4'- bipy | imid | pz | mpz ⁺ |
| X = 3,5-Me₂^b | | | | | | | |
| 0.024 | 1.32 | 0.30 | 1.22 (1.30) ^c | | | 1.39 (1.42) ^c | 1.82 (1.72) ^c |
| X = 3-CN | | | | | | | |
| 0.024 | 2.5 ^b | | | 2.5 ^d | | | |
| 0.04 | | | | | 2.1 | | |
| 0.05 | | | | | | 2.4 | |
| 0.06 | | | | | | 2.0 | |
| 0.10 | | | 2.41 | | | | |
| 0.14 | | | 2.38 | | 2.1 | 2.6 | |
| 0.15 | | | | | | 2.4 | |
| 0.16 | | | 2.42 | | | | |
| 0.20 | | | 2.39 | | 2.0 | 2.5 | |

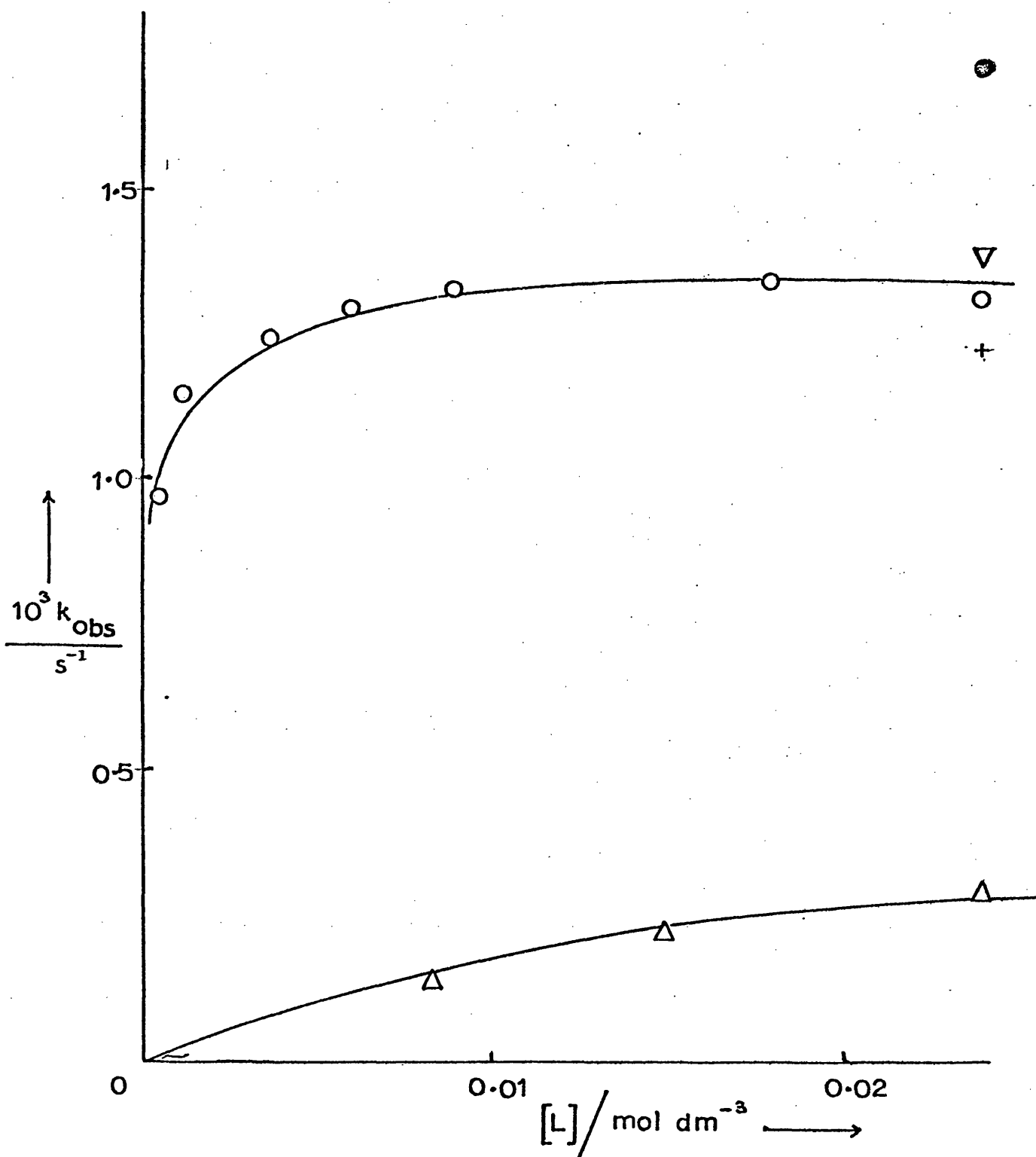
^a tu = thiourea, 4,4'-bipy = 4,4'-bipyridyl, imid = imidazole, pz = pyrazine and mpz = N-methylpyrazinium.

^b Results for X = 3,5-Me₂ were measured at an ionic strength of $0.024 \text{ mol dm}^{-3}$ (maintained with potassium nitrate).

^c Results in parentheses were calculated from $+d[\text{product}]/dt$.

^d Results measured at an ionic strength of $10^{-3} \text{ mol dm}^{-3}$.

Figure 2.02 Dependence of the first-order rate constant for nucleophilic substitution reactions of the $[\text{Fe}(\text{CN})_5(3,5\text{-Me}_2\text{py})]^{3-}$ anion on the nature and concentration of the incoming nucleophile, in aqueous solution at 298.6 K; (O) = CN^- , (∇) = pz, (\odot) = Mpz^+ , (+) = tu, (Δ) = SCN^- . (Abbreviations as in Table 2.04).



Thus we have the beginnings of an I_d mechanism for these two oppositely charged reactants. Such an occurrence is impossible for two similarly charged species, e.g. the anions $[\text{Fe}(\text{CN})_5\text{L}]^{n-}$ and the nucleophile CN^- , the reaction on which this work is based.

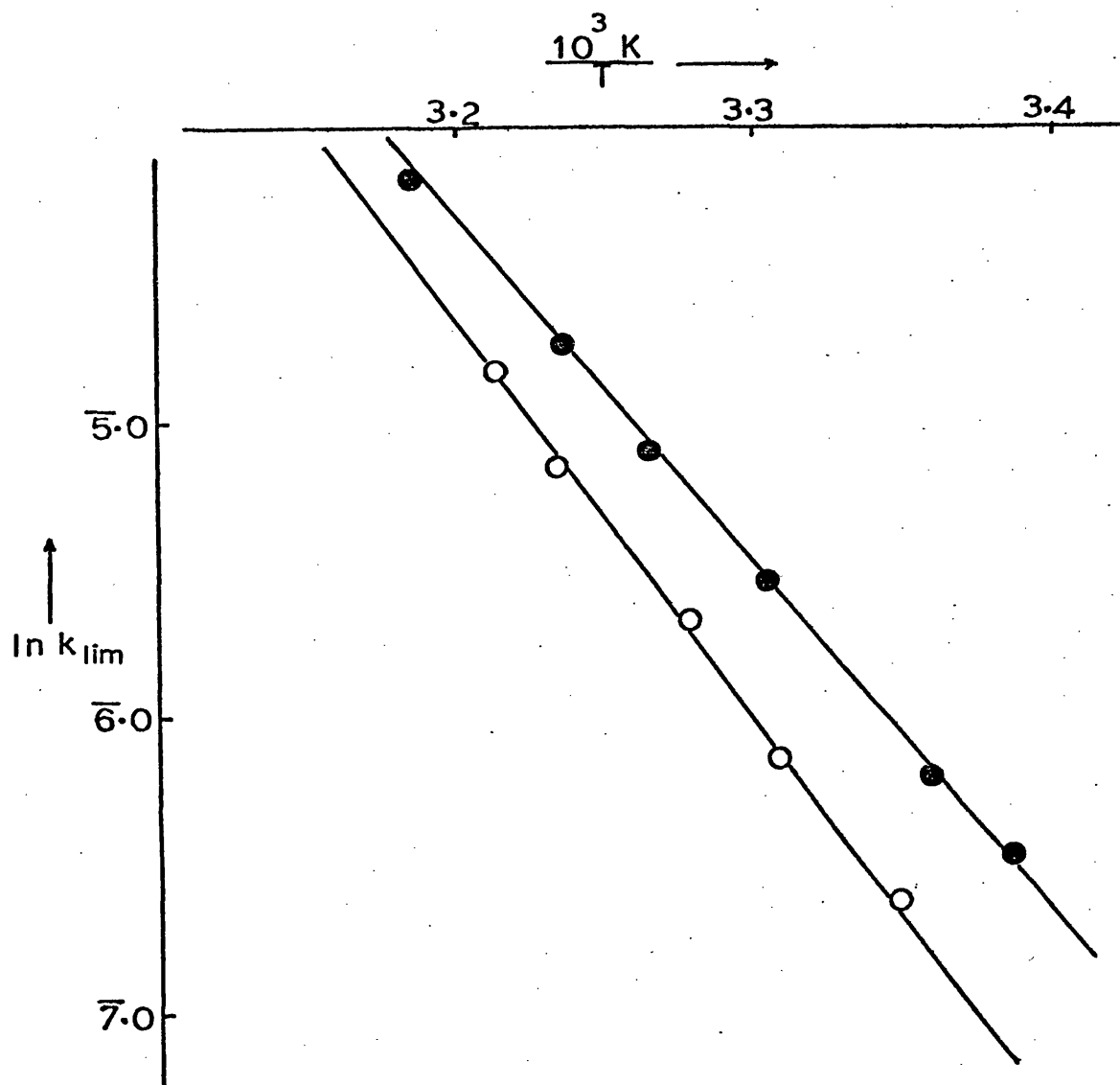
The very different behaviour of thiocyanate as incoming nucleophile (see Figure 2.02) indicates that it competes only feebly with the leaving 3,5- Me_2py for the $[\text{Fe}(\text{CN})_5]^{3-}$ intermediate. Indeed, the reaction with thiocyanate was found to go only to equilibrium.

The rate constants listed in Table 2.04 were, except where otherwise indicated, determined by monitoring the disappearance of the starting complex. The close approximation of the rate constants in parentheses in Table 2.04 to the corresponding values determined as stated above supports the conclusion that the rate of formation of products equals the rate of disappearance of starting material in this reaction, drawn from the observation of the clean isosbestic points mentioned earlier.

It must be pointed out that from a theoretical point of view, the equality of k_{lim} values for different incoming nucleophiles could arise because the reaction temperature happened to be an isokinetic one. As will be seen below, the interdependence of activation enthalpies and entropies for reactions of the $[\text{Fe}(\text{CN})_5\text{L}]^{n-}$ type anions has been studied, and the possibility of the reaction temperature of 298.6 K being an isokinetic one dismissed.

A further criterion for the establishment of a limiting dissociative mechanism is the sign and magnitude of the activation parameters. First-order rate constants for reaction of cyanide ion with the 3,5- Me_2py and 3-CNpy complexes of pentacyanoferrate(II) have been measured over a range of temperatures in aqueous solution at an ionic strength of 0.60 mol dm^{-3} for different cyanide concentrations. The results are listed in Table 2.03.

Figure 2.03 Arrhenius plot ($\ln(k_{\text{lim}})$ vs. $1/T$) for the reaction of cyanide ion with the $[\text{Fe}(\text{CN})_5\text{L}]^{3-}$ anions in aqueous solution at an ionic strength of 0.60 mol dm^{-3} , for $\text{L} = 3,5\text{-Me}_2\text{py}$ (O) and 3-CNpy (\bullet).



Hence activation parameters, E_a , ΔH^\ddagger and ΔS^\ddagger have been calculated from the Arrhenius equation:-

$$k = A \cdot e^{\frac{-E_a}{RT}} \quad (2.15)$$

(see Appendix 3). Figure 2.03 is a plot of Napierian logarithm of the rate constants versus the reciprocal absolute temperature, for the reactions indicated in Table 2.03, the slopes being directly proportional to the activation energies, E_a , and the intercept being the logarithm of the "A" factor of equation (2.13). These parameters were computed via a least-mean-squares BASIC program (Program No. 4, Appendix 2), the results of which are:-

| Complex | $\frac{E_a}{\text{kJ mol}^{-1}}$ | $\log_{10} A$ |
|---|----------------------------------|------------------|
| $[\text{Fe}(\text{CN})_5(3,5\text{-Me}_2\text{py})]^{3-}$ | 110.7 ± 2.3 | 16.47 ± 0.39 |
| $[\text{Fe}(\text{CN})_5(3\text{-CNpy})]^{3-}$ | 95.5 ± 1.3 | 14.07 ± 0.22 |

The enthalpies and entropies of activation for these complexes are listed in Table 2.05 together with similar data for differently substituted pentacyanoferrate(II) complexes, collected from the references noted in the table. Large positive entropies of activation are seen to occur for these complexes, which is consistent with a dissociative mechanism [2.22]. Figure 2.04 displays the relationship between ΔH^\ddagger and ΔS^\ddagger for the ligand replacement reaction (incoming ligand being cyanide anion or N-methylpyrazinium cation) of the $[\text{Fe}(\text{CN})_5\text{L}]^{n-}$ anions in aqueous solution. Such a linear relationship between the activation enthalpy and entropy of a reaction, of the form:-

$$\delta \Delta H^\ddagger = \beta \delta \Delta S^\ddagger \quad (2.16)$$

with $\beta \geq 0$

TABLE 2.05 Activation parameters at 298K for ligand exchange reactions of substituted pentacyanoferrate(II) complexes, for a variety of outgoing substituents.

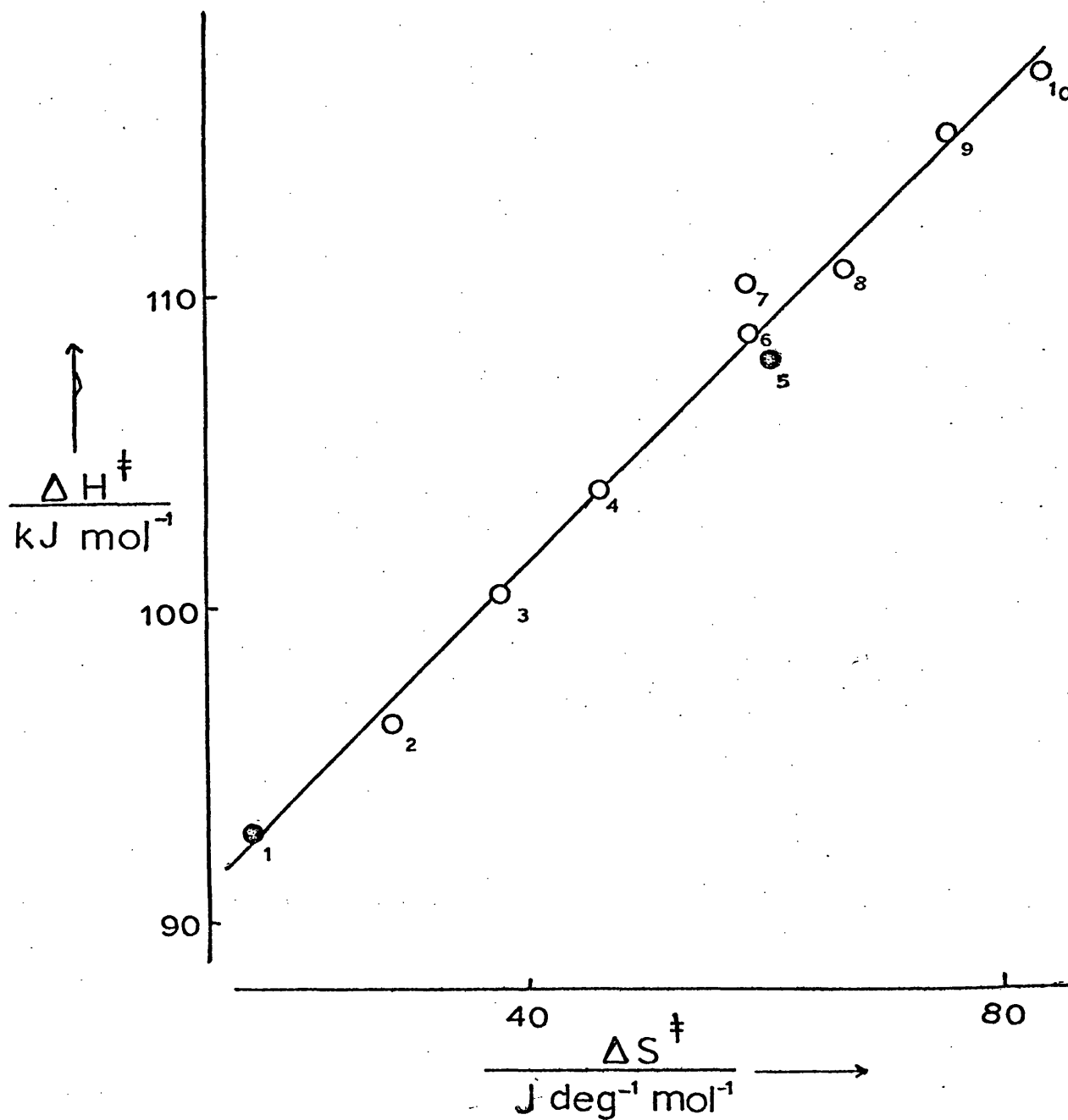
| Substituent | $\Delta H^\ddagger/\text{kJ mol}^{-1}$ | $\Delta S^\ddagger/\text{J K}^{-1} \text{ mol}^{-1}$ | Reference |
|-------------------------------------|--|--|------------------------|
| 3-CNpy | 93.0 ± 1.3 | 16.3 ± 4.3 | This work ^b |
| 4-Mepy | 100.4 ± 2.1 | 37.6 ± 8.4 | 2.06 ^c |
| py | 103.7 ± 2.1 | 46.0 ± 8.4 | 2.06 ^c |
| 3,5-Me ₂ py | 108.0 ± 2.5 | 58.5 ± 8.4 | This work ^b |
| 4-CONH ₂ py ^a | 108.8 ± 2.1 | 58.6 ± 8.4 | 2.06 ^c |
| pz | 110.8 ± 2.1 | 66.9 ± 8.4 | 2.06 ^c |
| 4,4'-bipy | 110.4 ± 2.1 | 58.6 ± 8.4 | 2.06 ^c |
| mpz ⁺ | 115.0 ± 2.1 | 75.3 ± 8.4 | 2.06 ^b |

^a 4-CONH₂py = isonicotinamide(4-amidopyridine)

^b Incoming nucleophile = CN⁻

^c Incoming nucleophile = mpz⁺

Figure 2.04 Dependence of the activation enthalpy (ΔH^\ddagger) on the entropy (ΔS^\ddagger) for the reaction of cyanide ion with a range of anions $[\text{Fe}(\text{CN})_5\text{L}]^{n-}$, for L = 1. 3-CNpy; 2. 4-Mepy; 3. py; 4. 3,5-Me₂py; 5. 4-CONH₂py; 6. pz; 7. 4,4'-bipy; 8. mpz⁺: Temperature = 298.2K.



is called an Isokinetic Relationship [2.23]. The parameter β has the dimensions of absolute temperature, and is identified as an actual temperature at which all the differences in the rate constants will vanish. There have been many studies of isokinetic temperatures of organic reactions [2.24], values of β varying greatly, from 70 K for the dimerisation of cyclopentadiene in the absence of solvent at varying pressures [2.25], to 1400 K for the dehydrogenation of 1,4-dihydronaphthalene by a series of alkyl-substituted p-benzo quinones in phenetole [2.26]. Although the great majority of studies are organic ones, several inorganic reactions have been studied, which include the reaction of iron(II) with hydrogen peroxide and a series of hydroperoxides [2.27], having a value for β of 380 K; and electron-transfer between aqueous chromium(II) and complexes of the type $[\text{Co}^{\text{III}}(\text{NH}_3)_5\text{L}]^{n+}$, where L is p-sulphobenzoate, methylterephthalate, or cis- or trans-1,2 chloropropanedicarboxylate, with $\beta = 296$ K [2.28].

From Figure 2.04, we find the slope of the best line through the points (computed via the BASIC least-mean-squares program No. 3, Appendix 2), i.e. β , or the isokinetic temperature for the reaction is 373 ± 18 K. Thus, as mentioned earlier, there is no practically attainable isokinetic temperature for the nucleophilic substitution reaction at $[\text{Fe}(\text{CN})_5\text{L}]^{n-}$ type anions, so such a temperature cannot account for the independence of the limiting rate constant, k_{lim} , of the nature of the incoming nucleophile. By definition, reactions proceeding via the same reaction mechanism have identical isokinetic temperatures [2.24]. Hence it would be interesting to investigate possible isokinetic relationships for other inorganic reactions proceeding via similar dissociative mechanisms, and compare their β values with that of this work. The above criteria for a D mechanism were first applied [2.03], [2.29] in aqueous systems to the substitution of

$[\text{Co}(\text{CN})_5\text{OH}_2]^{2-}$ by a variety of anionic and nitrogen nucleophiles. Subsequently D mechanisms have been proposed for substitutions of both sulphito complexes of cobalt(III) [2.30-2.31] and [2.04] and of $[\text{RhCl}_5(\text{OH}_2)]^{2-}$ [2.32], and the evidence has been reviewed [2.02].

All of the above results constitute good evidence for a dissociative mechanism, although it has been argued [2.10] that an I_d mechanism can equally well account for the experimental results. However, by far the most conclusive evidence for the operation of a pure D mechanism in the reactions in question is provided by high pressure studies of the reaction of the pentacyanoferrate(II) complexes of the 3,5-Me₂py and 3-CNpy ligands, with a range of incoming nucleophiles in aqueous solution [2.33], leading to measurements of Volumes of Activation.

High Pressure Studies

The effect of pressure upon the rate of a chemical reaction in solution is attributed to a volume change which occurs in the activation step of the reaction. If the change in volume on activation is negative, then the reaction is accelerated by an increase in pressure; if the volume change is positive, then the reaction is retarded by an increase in pressure. The interpretation of a volume change is based in principle on inferred changes in nuclear positions. This involves a structural concept which is intrinsically easier to handle than the more conventionally studied, but intangible concept of an entropy change, which depends on inferred changes in both nuclear positions and energy.

The volume of activation, ΔV^\ddagger of a reaction is defined as the excess of the partial molar volume of the transition state over the combined partial molar volumes of the initial reactant species, i.e:-

$$\Delta V^\ddagger = \bar{V}_{T.S} - a \bar{V}_A - b \bar{V}_B \dots\dots\dots = \bar{V}_{T.S} - \sum_A a \bar{V}_A \quad (2.17)$$

where $V_{T.S}$ is the partial molar volume of the transition state, and V_A is the partial molar volume of the initial reactant, A [2.34]. ΔV^\ddagger is derived from the rate constant of a reaction by the expression:-

$$\left(\frac{\partial \ln k}{\partial P} \right)_T = \frac{-\Delta V^\ddagger}{RT} \quad (2.18)$$

A limitation on the accuracy of evaluating ΔV^\ddagger is that frequently, but not always, ΔV^\ddagger itself exhibits a pressure dependence. An analysis [2.35] of the pressure dependence of the rate constant for a reaction has shown that the quadratic expression

$$\ln k_p = \ln k_0 + bP + cP^2, \quad (2.19)$$

most accurately describes a variety of reactions. Hence, the volume of activation at any pressure P , ΔV^\ddagger_p , is then given by:-

$$\Delta V^\ddagger_p = -bRT - 2RTcP, \quad (2.20)$$

and the volume of activation at zero pressure is:-

$$\Delta V^\ddagger_0 = -bRT, \quad (2.21)$$

(see ref. [2.34]).

Hence the quantity representing the pressure dependence of ΔV^\ddagger_p , called the compressibility coefficient of activation, $\Delta\beta^\ddagger$, is defined by:-

$$\Delta\beta^\ddagger = - \left(\frac{\partial \Delta V^\ddagger}{\partial P} \right)_T = 2RTc \quad (2.22)$$

The determination of ΔV^\ddagger is a well established approach to the diagnosis of substitution reaction mechanisms in organic chemistry [2.36]. This method is particularly useful for uncharged leaving (or entering)

groups, where no complications due to solvent electrostriction effects arise in the interpretation of ΔV^\ddagger . Recently the determination of volumes of activation for some substitution reactions of transition metal complexes has proved informative, in particular the demonstration of negative volumes of activation for water exchange at the $[\text{Cr}(\text{OH}_2)_6]^{3+}$ cation [2.37], and at the $[\text{Cr}(\text{NH}_3)_5(\text{OH}_2)]^{3+}$ cation [2.38], but of a positive volume of activation for water exchange at the $[\text{Co}(\text{NH}_3)_5(\text{OH}_2)]^{3+}$ cation [2.39]. These findings have indicated considerable associative character in the substitutions mentioned at chromium(III), in contrast to the established dissociative mode at cobalt(III).

Despite the large number of kinetic studies on substitution reactions of low spin iron(II) complexes (especially those of 1,10-phenanthroline and its derivatives) [2.40-2.43], the mechanism of aquation of these complexes is not unequivocally established. However, high pressure studies on the aquation of tris-(1,10-phenanthroline)iron(II) cation and several substituted analogues in aqueous acidic media have led to the conclusion that the reactions proceed with volumes of activation consistent with a dissociative mechanism [2.44].

The kinetics of the reaction of the $[\text{Fe}(\text{CN})_5(3,5\text{-Me}_2\text{py})]^{3-}$ and the $[\text{Fe}(\text{CN})_5(3\text{-CNpy})]^{3-}$ anions with various nucleophiles have been studied at 298 K in aqueous solution, over a range of pressures, varying from atmospheric pressure to 1379 bar.[†] In Table 2.06(a), values of k_{obs} for the reaction of the $[\text{Fe}(\text{CN})_5(3,5\text{-Me}_2\text{py})]^{3-}$ anion with cyanide ion, pyrazine and imidazole are recorded over a range of five pressures, at 298 K in aqueous solution; and for the reaction of the $[\text{Fe}(\text{CN})_5(3\text{-CNpy})]^{3-}$ anion with

[†] [1 bar = 10^5 Pa, 1 atm = 101325 Pa]

TABLE 2.06(a) First-order rate constants, $10^3 k_{\text{obs}}/\text{s}^{-1}$, for the reactions of the $[\text{Fe}(\text{CN})_5\text{L}]^{3-}$ anions with various nucleophiles, Y, over a range of pressures at 298 K, in aqueous solution. Y = 0.05 mol dm^{-3} , and ionic strength = 0.50 mol dm^{-3} (maintained with sodium perchlorate).

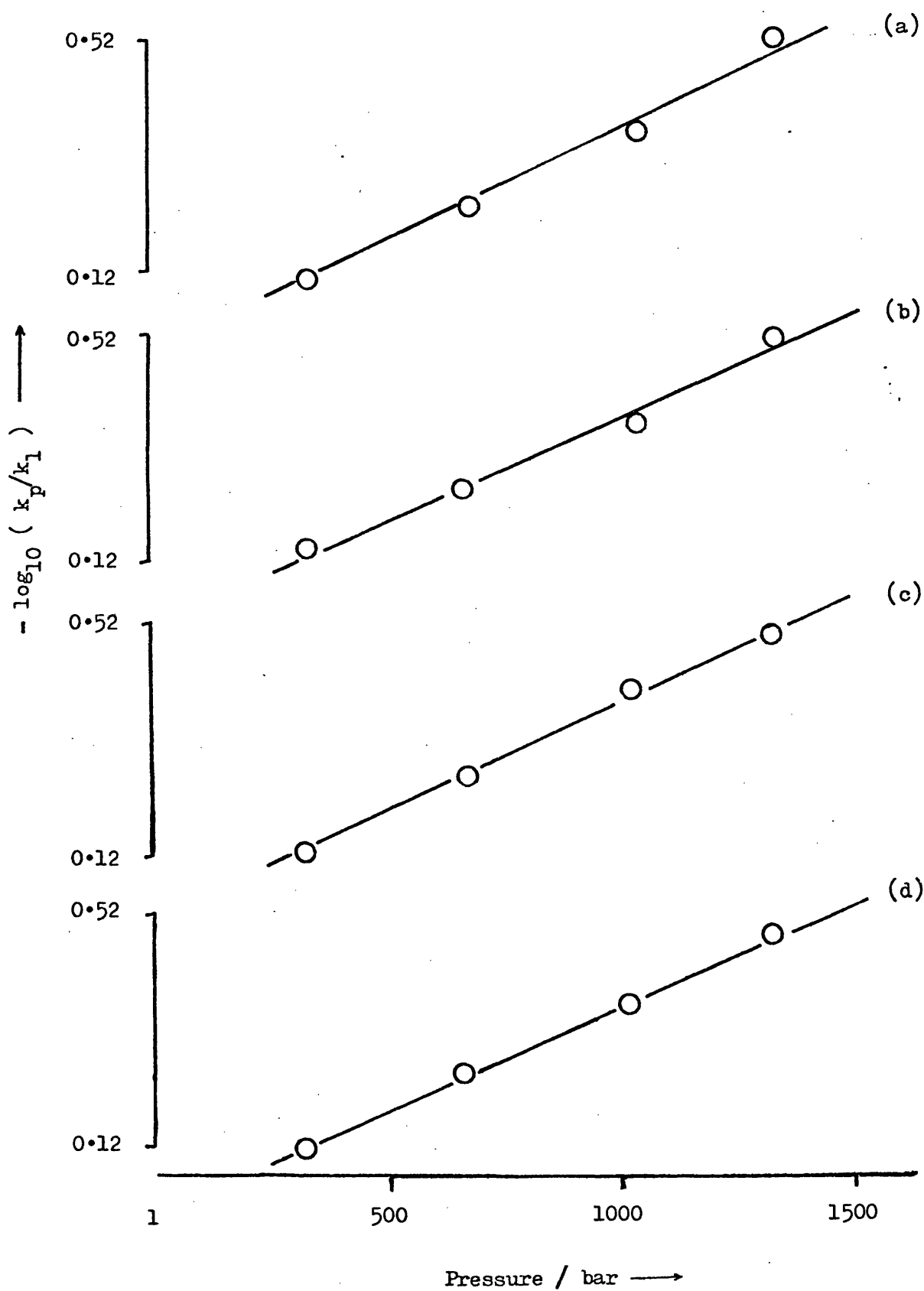
| Y | Pressure/bar | | | | | $10^3 k_{\text{obs}}/\text{s}^{-1} \text{ }^a$ | | | | |
|----------------------------|--------------|-------------|-------------|---------------|-------------|--|------|------|------|------|
| | 1 | 345 | 690 | 1034 | 1379 | | | | | |
| L = 3-CNpy | | | | | | | | | | |
| CN ⁻ | 2.06 | 0.06 | 1.53 | 0.05 | 1.13 | 0.04 | 0.87 | 0.03 | 0.65 | 0.03 |
| L = 3,5-Me ₂ py | | | | | | | | | | |
| CN ⁻ | 1.33 ± 0.04 | 0.96 ± 0.02 | 0.71 ± 0.02 | 0.515 ± 0.015 | 0.41 ± 0.02 | | | | | |
| pz | 1.27 ± 0.03 | 0.90 ± 0.03 | 0.70 ± 0.02 | 0.515 ± 0.02 | 0.39 ± 0.01 | | | | | |
| imid | 1.25 ± 0.03 | 0.94 ± 0.03 | 0.71 ± 0.02 | 0.52 ± 0.25 | 0.40 ± 0.02 | | | | | |

^a Errors quoted are standard deviations of mean values of several measurements of k_{obs} .

TABLE 2.06(b) Volumes of Activation, $\Delta V^\ddagger/\text{cm}^3 \text{ mol}^{-1}$, for the reactions of the $[\text{Fe}(\text{CN})_5\text{L}]^{3-}$ anions with various nucleophiles at 298 K, and at an ionic strength of 0.50 mol dm^{-3} (maintained with sodium perchlorate).

| Reactants | $\Delta V^\ddagger/\text{cm}^3 \text{ mol}^{-1}$ |
|--|--|
| $[\text{Fe}(\text{CN})_5(3\text{-CNpy})]^{3-} + \text{CN}^-$ | 20.6 ± 0.5 |
| $[\text{Fe}(\text{CN})_5(3,5\text{-Me}_2\text{py})]^{3-} \left\{ \begin{array}{l} + \text{CN}^- \\ + \text{pz} \\ + \text{imid} \end{array} \right.$ | 20.5 ± 0.8 21.2 ± 1.0 20.3 ± 1.0 |

Figure 2.05 Variation of the term $-\log_{10}(k_p/k_1)$ with pressure, at 298 K; for the reactions of (a) cyanide ion with the 3-CNpy complex, (b) cyanide ion (c) pyrazine and (d) imidazole with the 3,5-Me₂py complex.



cyanide ion under the same conditions, are recorded. These k_{obs} values are the mean of several determinations at various concentrations of incoming nucleophile, the number being shown in parentheses in Table 2.06(a). The volumes of activation, ΔV^\ddagger , for these substitutions were evaluated from the relation shown in equation (2.18), and are shown in Table 2.06(b). As explained above, the relation in equation (2.18) assumes that ΔV^\ddagger is itself independent of pressure, i.e. that the compressibility coefficient of activation, $\Delta\beta^\ddagger$, is zero. Figure 2.05 illustrates the pressure variation of the term $-\log_{10}(k_p/k_1)$ for the three nucleophiles used in Table 2.06. Each of the plots shows a high degree of linearity, indicating that $\Delta\beta^\ddagger$ is in fact zero within experimental error for this reaction. This is to be expected for a neutral leaving group, since finite values of $\Delta\beta^\ddagger$ usually arise in reactions involving solvent electrostriction by newly generated ions [2.34]. The slopes of these plots are virtually identical, and the corresponding ΔV^\ddagger values, which are listed in Table 2.06(b), all fall close to a mean value of $+20.7 \pm 0.9 \text{ cm}^3 \text{ mol}^{-1}$.

The corresponding plot for the 3-CNpy analogue is also displayed in Figure 2.05, which also has $\Delta\beta^\ddagger = \text{zero}$. The ΔV^\ddagger value calculated for this latter reaction was found to be $+20.6 \pm 0.5 \text{ cm}^3 \text{ mol}^{-1}$, which is identical to the mean value recorded for the reaction of the 3,5-Me₂py complex anion above.

The finding that ΔV^\ddagger_1 , the volume of activation for the limiting dissociative step (see equation (2.04)) is independent of the nature of the incoming nucleophile constitutes very strong evidence for the operation of a D mechanism, indicating that the incoming nucleophile takes no part in the rate-determining activation step (the k_1 step in equation (2.04)) of the reaction, i.e. the rate determining step is purely the dissociation of the complex $[\text{Fe}(\text{CN})_5\text{L}]^{n-}$ into its components $[\text{Fe}(\text{CN})_5]^{3-}$ and $\text{L}^{(n-3)-}$.

The volume of activation for the k_1 step, ΔV_1^\ddagger , may be visualised as arising from the stretching of the Fe—N bond to form the transition state with the leaving nitrogen heterocycle sweeping out a consequential volume in the surrounding solvent. The remaining $[\text{Fe}(\text{CN})_5]^{3-}$ moiety may contemporaneously rearrange to a distorted square-pyramid, but it is assumed that this involves changes in bond angles, and not bond lengths, and hence there is no consequential volume change [2.34]. This is illustrated diagrammatically in Diagram 2.01, below:-

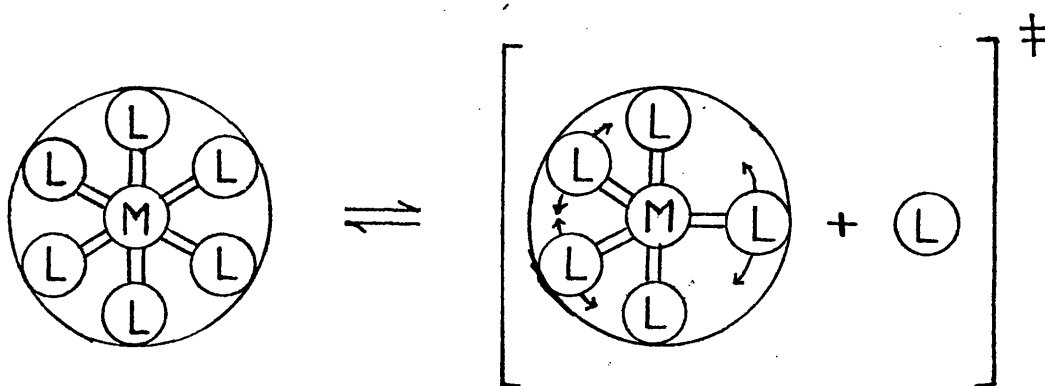


Diagram 2.01

Diagrams 2.02 and 2.03 present scale diagrammatic representations of the proposed activated complexes for the reactions of the 3,5-Me₂py and 3-CNpy complex anions respectively, in which the component atoms have been assigned their usual covalent and Van der Waal radii [2.45]. For the 3,5-Me₂py complex, substituents in the 3, 4 and 5 positions of the aromatic ring should be in contact with solvent in the ground state, and the two methyl groups will also be surrounded by solvent molecules. In the transition state, when the Fe—N bond becomes elongated, the 3,5-Me₂py ligand moves out, and the solvent should be able to adapt to the motion of the two methyl groups; the volume vacated by these groups should then be occupied by solvent molecules, and no net volume change should occur from the motion

of these groups. Hence the volume swept out by the 3,5-Me₂py ligand should be due to the motion of substituents in the 1, 2 and 6 positions out into the solvent. The thickness of the 3,5-Me₂py ligand may be assigned a value of 370 pm [2.45], and the width is defined effectively by the extremities of the 2, 6 hydrogen atoms, namely 670 pm (distance b in Diagram 2.02). If the Fe—N bond extension in the transition state is Δl(pm), then

$$\Delta V^\ddagger = 10^{-30} \text{ N} \times \left(\frac{\text{cross-sectional area of 3,5-Me}_2\text{py}}{\text{area of 3,5-Me}_2\text{py}} \right) \times \Delta l \quad (2.23)$$

$$\begin{aligned} \text{i.e. } \Delta V^\ddagger &= 10^{-30} \text{ N} \times 370 \times 670 \times \Delta l \\ &= 20.7 \text{ cm}^3 \text{ mol}^{-1} \end{aligned}$$

Hence Δl = 139 pm, and so the Fe—N bond is stretched from 197 pm in the ground state to 336 pm in the transition state. Complete dissociation of the 3,5-Me₂py ligand from the pentacyanoferrate(II) complex may be taken to be reached when the Fe—N bond is stretched until it equals the sum of their respective Van der Waal radii, i.e. 205 pm (Fe) + 150 pm (N) = 355 pm. Hence this simplified structural model suggests that in the transition state, the Fe—N bond is elongated to 139/158, or about 88% of the distance required to effect complete dissociation of the N-heterocycle from the Fe atom. If however the effective width of the outgoing ligand is taken to be the distance apart of the 3- and 5- methyl groups (910 pm, distance a in Diagram 2.02) then Δl = 102 pm, and hence the percentage Fe—N bond extension would be 65% of that required for complete bond rupture.

Thus we see that for the k₁ step of this reaction, the leaving group is almost completely free in the activated complex. This may be compared with the study of the aquation of the tris-(1,10-phenanthroline)iron(II) complex [2.44], the mechanism of which was found to be dissociative in character, but is probably best described as reacting through an I_a mechanism,

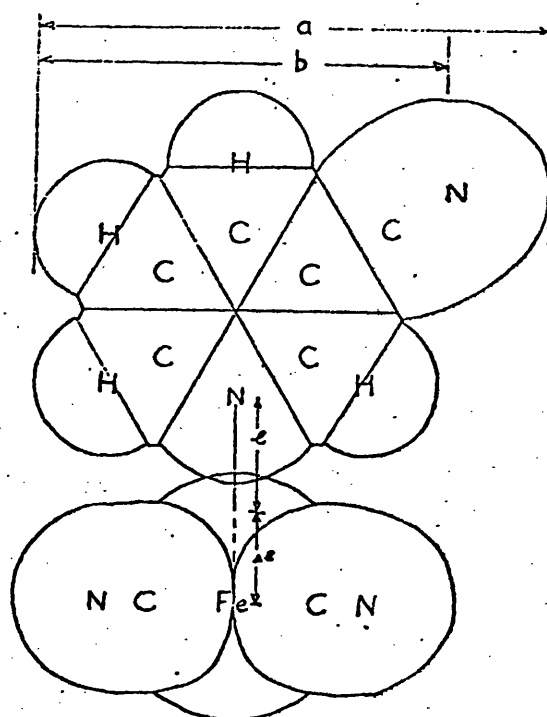


DIAGRAM 2.03

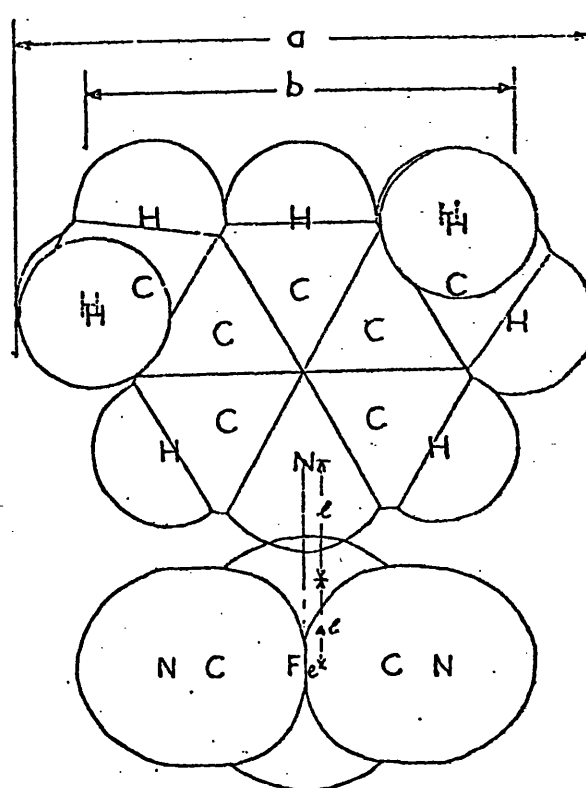


DIAGRAM 2.02

since no intermediate is kinetically recognisable. The Fe—N bond in this case was found to be extended by 39% of the distance required for complete dissociation.

Although the structural model used to interpret ΔV^\ddagger values is necessarily a very simplified one, it does enable a more incisive picture of the activated complex to be drawn than that possible with entropies of activation. We may compare the results with those of model dissociative reactions. For example, in the unimolecular elimination of trialkyl sulphonium halides [2.46], in which desolvation by dispersal of charge is believed to be unimportant, the C-S bond is calculated to undergo a bond elongation of 63% of the distance required for complete dissociation. The dissociative trialkylphosphite substitution of carbonyls of nickel, molybdenum and chromium is estimated [2.47] to involve bond elongations of 60%, 72% and 100% of the theoretical bond rupture distance. A corresponding estimation [2.48, 2.49] for solvolysis of t-butyl chloride is complicated by the charge separation in the activated complex, and consequent electrostriction changes. We may conclude from this study that knowledge of the volume of activation for the reaction in this study has provided firm proof of the operation of a D mechanism in aqueous solution.

2.3(ii) KINETICS IN BINARY AQUEOUS MIXTURES

Having conclusively assigned the operation of a limiting dissociative mechanism to the nucleophilic substitution reaction at the $[\text{Fe}(\text{CN})_5\text{L}]^{n-}$ centre, a study of the reaction in a range of binary aqueous mixtures was made. The kinetics of a number of substitution reactions of transition metal complexes have been investigated in a variety of mixed aqueous solvents [2.40]. Often, the object of such studies has been to diagnose the nature of the mechanism from the variation of reactivity with solvent composition, using correlation of rates with, for example, functions of the bulk dielectric constant, or, as has been done in this work, with empirical parameters such as Grunwald-Winstein solvent Y values [2.50]. Less often, attempts are made to interpret reactivity trends in terms of known physical properties of the solvent mixtures. The effect of solvent structure on reactivity has been described and discussed, in terms of viscosities and enthalpies of vapourisation, for reactions of metal(II) cations with 2,2'-bipyridyl [2.51]; the overriding importance of viscosity in determining reactivity has been illustrated for reactions of metal(II) cations with pyridine-2-azo-4'-dimethylaniline (pada) [2.52].

The reasons why the rate constant for a particular reaction in aqueous solution at a fixed temperature and pressure changes when a co-solvent is added are many and various [2.53]. Nevertheless, an important aspect of any discussion of these phenomena is the way in which the solvent, water, and the co-solvent interact. An indication of the magnitude of such interactions, and their dependence on solvent composition can be gained from the excess molar Gibbs function of mixing, G^E , for the mixture. A description of G^E , together with other thermodynamic functions used in

the analysis of the experimental results in this chapter has been given in chapter 1.

First-order rate constants for the reactions of $[\text{Fe}(\text{CN})_5(\text{X-py})]^{3-}$ (for $\text{X} = 3,5\text{-Me}_2$, 3-CN and 3-Cl^\dagger) with cyanide ion, in water and 40% by volume ethylene glycol and 40% by volume t-butyl alcohol at 298.6 K and constant ionic strength are reported in Table 2.07. In aqueous solution, the limiting rate constants, k_{lim} , for these reactions were found to be $1.33 \times 10^{-3} \text{ s}^{-1}$, $2.46 \times 10^{-3} \text{ s}^{-1}$ and $2.30 \times 10^{-3} \text{ s}^{-1}$ respectively. A plot of the observed first-order rate constants for the reaction of the 3-CNpy complex with cyanide ion, against cyanide ion concentration in the solvent mixtures indicated above is displayed in Figure 2.06. We can see from this plot that the first-order dependence of k_{obs} on $[\text{CN}^-]$ at low values of $[\text{CN}^-]$, which is just observable in aqueous solution, is unobservable in the t-butyl alcohol mixture, but is accentuated in the glycol one. Hence there appears to be a strong dependence of the discriminatory power of the $[\text{Fe}(\text{CN})_5]^{3-}$ moiety (see section 2.3(iv)) on solvent composition. Unfortunately, this solvent dependence is impossible to observe quantitatively under these conditions, but has been successfully studied in the presence of added outgoing X-py (for $\text{X} = 3\text{-CN}$ and 4-CN) and is described in section 2.3(iv) below.

The dependence of the limiting rates for cyanide substitution at relatively high cyanide concentrations, on the nature of the binary aqueous mixture is shown in Table 2.08 for the $3,5\text{-Me}_2\text{py}$ complex. For solvent mixtures for which the dependence of k_{obs} on cyanide concentration had been established over a range of cyanide concentrations (Table 2.07),

[†] [Due to the difficulties mentioned in section 2.2 concerning the handling of the 3-Cl py complex, no further studies were made with it.]

TABLE 2.07 First-order rate constants, $10^3 k_{\text{obs}}/\text{s}^{-1}$, for the reaction of cyanide ion with the $[\text{Fe}(\text{CN})_5(\text{X-py})]^{3-}$ anions, at 298.2 K and a constant ionic strength of $0.024 \text{ mol dm}^{-3}$ (maintained with potassium nitrate).

| X = | 3-CN | | | 3,5-Me ₂ | | 3-Cl | |
|--|------|------|------|---------------------|------|------|------|
| Solvent ^a Mixture | A | B | C | A | B | A | B |
| $\frac{10^3 [\text{KCN}]}{\text{mol dm}^{-3}}$ | | | | | | | |
| 0.6 | 1.74 | 2.40 | 0.22 | 0.97 | | 1.64 | 2.31 |
| 1.2 | 1.94 | 2.44 | 0.80 | 1.15 | 1.55 | 1.64 | 2.38 |
| 1.8 | 1.93 | 2.47 | | 1.23 | | 1.75 | |
| 2.4 | 2.12 | 2.41 | 1.11 | 1.26 | 1.71 | 1.76 | 2.40 |
| 3.0 | 2.09 | 2.44 | | 1.29 | | | |
| 3.6 | 2.00 | 2.42 | 1.32 | 1.24 | 1.76 | 1.93 | 2.55 |
| 4.2 | 2.15 | | | 1.35 | | | |
| 4.8 | 2.20 | 2.49 | 1.40 | 1.33 | 1.83 | 1.88 | 2.61 |
| 6.0 | | 2.46 | 1.23 | 1.30 | 1.58 | 2.05 | 2.45 |
| 7.2 | | | | | | 2.00 | 2.46 |
| 8.4 | | | 1.35 | | | | 2.57 |
| 9.0 | | 2.58 | | 1.33 | | | |
| 9.6 | | | | | | 2.15 | 2.56 |
| 12.0 | 2.25 | 2.61 | 1.43 | 1.24 | 1.67 | | 2.49 |
| 15.0 | | | 1.35 | | | | |
| 18.0 | 2.24 | 2.60 | 1.38 | 1.35 | 1.63 | 2.28 | 2.73 |
| 21.0 | | | 1.42 | | | 2.43 | |
| 24.0 | 2.54 | 2.76 | 1.39 | 1.32 | 1.94 | | 2.75 |

^a A = Water; B = 40 % t-Butyl alcohol; C = 40 % Ethylene glycol.

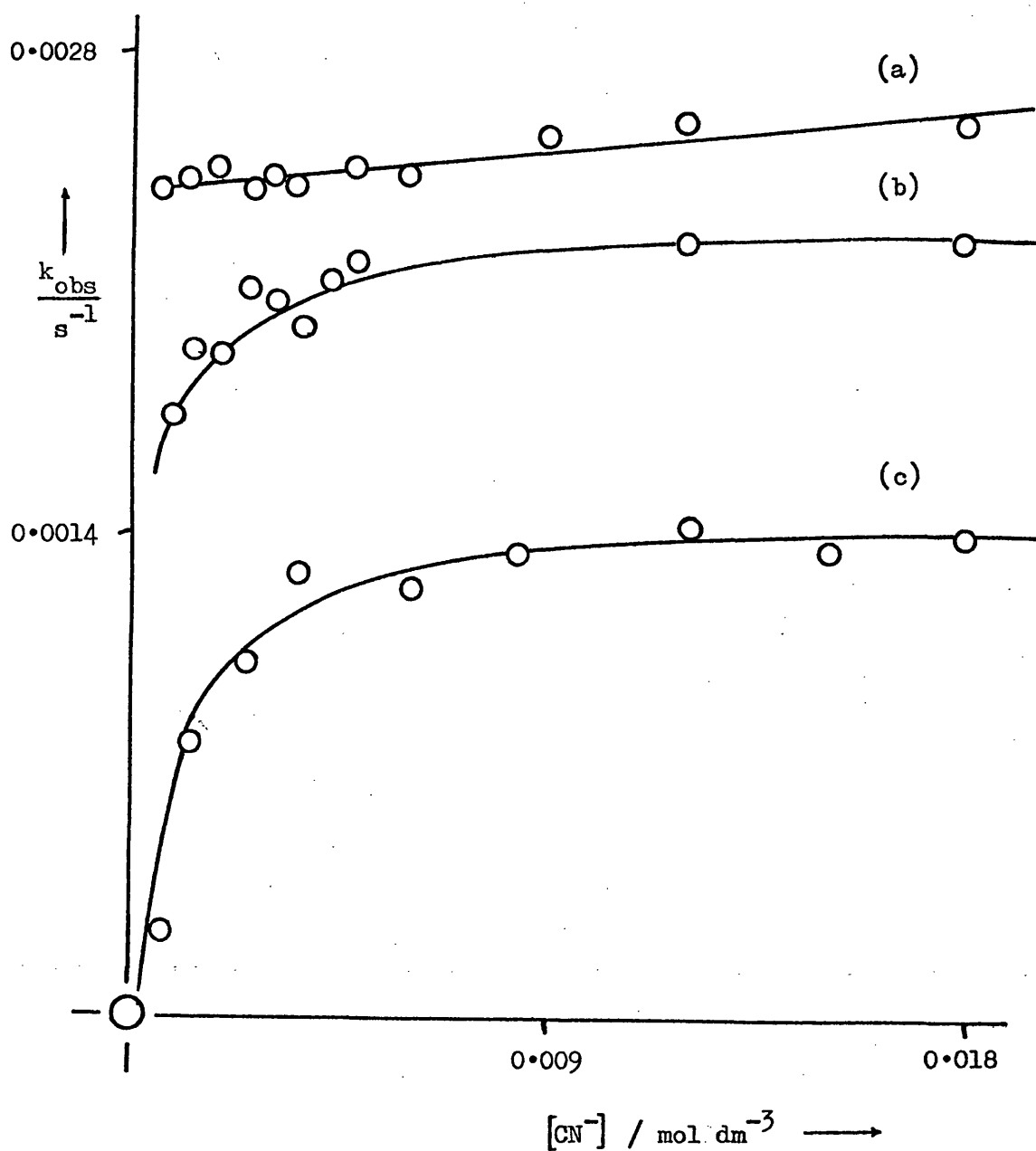
TABLE 2.08 First-order rate constants, k_{lim} , and activation free energies of transfer from water to a range of binary aqueous mixtures for the reaction of $[\text{Fe}(\text{CN})_5(3,5\text{-Me}_2\text{-py})]^{3-}$ with cyanide ion at 298.6 K in such mixtures.^a

| Solvent Mixture | $10^3 k_{lim}/\text{s}^{-1}$ | $-\delta_m \Delta G^\ddagger / \text{kJ mol}^{-1}$ |
|---------------------------------|------------------------------|--|
| 10 | 1.36 | 0.154 |
| 20 | 1.45 | 0.309 |
| 30 % Methanol | 1.49 | 0.377 |
| 40 | 1.61 | 0.571 |
| 10 | 1.45 | 0.309 |
| 20 | 1.65 | 0.634 |
| 30 % Ethanol | 1.84 | 0.903 |
| 40 | 2.10 | 1.228 |
| 10 | 1.41 | 0.240 |
| 20 | 1.60 | 0.554 |
| 30 % ^t Butyl alcohol | 1.85 | 0.914 |
| 40 | 2.21 | 1.354 |
| 10 | 1.28 | 0 |
| 20 | 1.28 | 0 |
| 30 % Glycol | 1.19 | -0.177 |
| 40 | 1.10 | -0.377 |
| 10 | 1.19 | -0.177 |
| 20 | 1.11 | -0.354 |
| 30 % Glycerol | 1.14 | -0.286 |
| 40 | 1.05 | -0.491 |
| 10 | (1.77) ^b | (0.806) ^b |
| 20 | 1.85 | 0.914 |
| 30 % Tetrahydrofuran | 2.28 | 1.434 |
| 40 | 2.55 | 1.714 |

^a In aqueous solution, $10^3 k_{lim} = 1.3 \text{ s}^{-1}$; $\delta_m \Delta G^\ddagger = \text{zero}$

^b k_{lim} and hence $\delta_m \Delta G^\ddagger$ in parentheses are unreliable.

Figure 2.06 Variation of the observed first-order rate constants, k_{obs} , for the reaction of cyanide ion with the $[\text{Fe}(\text{CN})_5(3\text{-CNpy})]^{3-}$ anion at 298.6 K, in (a) 40 % t-butyl alcohol, (b) water and (c) 40 % ethylene glycol; ionic strength = 0.024 mol dm⁻³.



k_{lim} values were estimated from plots of reciprocal rate constants versus reciprocal cyanide concentrations. For other solvent mixtures, k_{lim} values listed in Table 2.08 are mean rate constants determined at the maximum concentration of $0.024 \text{ mol dm}^{-3}$. These variations in k_{lim} with solvent composition have been illustrated in Figure 2.07(a), by plotting k_{lim} versus mole fraction of co-solvent; in Figure 2.07(b) by plotting k_{lim} versus the molar excess Gibbs function of mixing, G^E ; and in Figure 2.08 in terms of the activation free energy of transfer, $\delta_m \Delta G^\ddagger$, versus G^E . The parameters $\delta_m \Delta G^\ddagger$ and G^E have been described in chapter 1. Values for $\delta_m \Delta G^\ddagger$ for a particular k_{lim} value at the appropriate mole fraction, x_2 , were calculated from Transition State Theory [2.54], using:-

$$\Delta G^\ddagger_{(x_2 = 0)} = -RT \ln K^\ddagger_{(x_2 = 0)} \quad (2.24)$$

where

$$K^\ddagger = \frac{k T}{N h}$$

$$K = \frac{k T}{h} K^\ddagger$$

(N = Avogadro's Number; h = Planck's constant; T = Absolute temperature and $k = k_{lim}$)

Hence

$$\delta_m \Delta G^\ddagger = \Delta G^\ddagger_{(x_2)} - \Delta G^\ddagger_{(x_2 = 0)} \quad (2.25)$$

$$= -RT \ln \left(\frac{k_{lim}(x_2)}{k_{lim}(x_2 = 0)} \right) \quad (2.26)$$

The calculated values for $\delta_m \Delta G^\ddagger$ have been listed in Table 2.08. From Figures 2.07(a) and (b) it is apparent that rates of substitution at the $[\text{Fe}(\text{CN})_5\text{L}]^{n-}$ anion are remarkably insensitive to the composition of the mixed solvent. In this respect it resembles the behaviour of the reaction of the complex $\text{Fe}(\text{bipy})_2(\text{CN})_2$ with 1,10-phenanthroline in mixed aqueous

Figure 2.07(a) Variation of k_{lim} for the reaction of cyanide ion with the $[\text{Fe}(\text{CN})_5(3,5\text{-Me}_2\text{py})]^{3-}$ anion with solvent composition in a range of binary aqueous mixtures, at 298.6 K; cosolvents used are methanol(\circ), ethanol(Δ), t-butyl alcohol(\square), ethylene glycol(\blacktriangle), glycerol(\blacksquare) and tetrahydrofuran($*$); (\bullet) = water solvent.

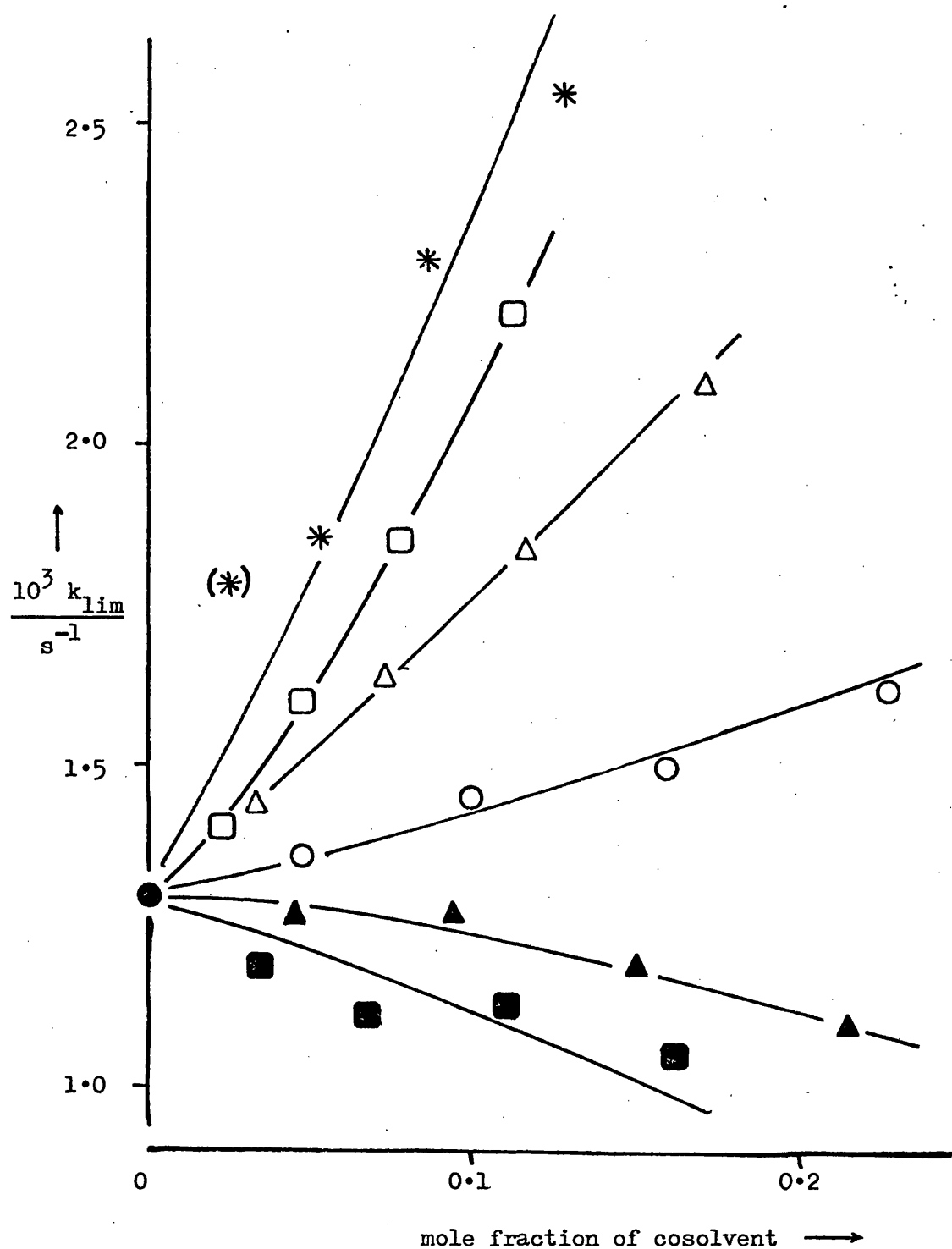
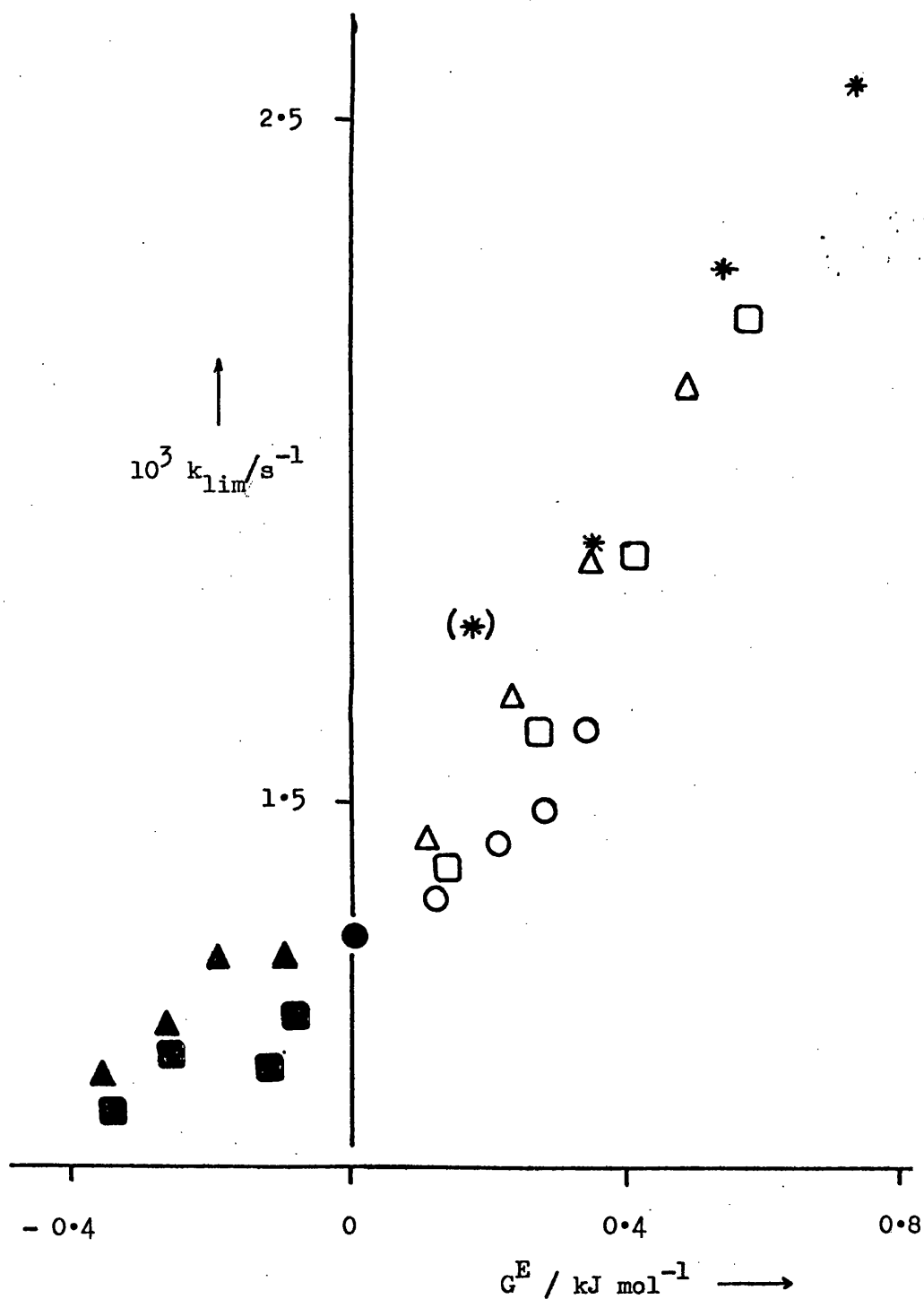


Figure 2.07(b) Correlation of k_{lim} (see Figure 2.07(a)) with the excess Gibbs function of mixing, G^E , in a range of binary aqueous mixtures. Symbols as in Figure 2.07(a).



solvents [2.55].

The low sensitivity of the rate constants for the reaction under study to composition of solvent strongly contrasts ^{with} the chemical potential of the cyanide ion in the appropriate solvent mixture relative to its value in water, $\delta_m \mu^\ominus(\text{CN}^-)$ [2.56]. This function is better known as the Gibbs free energy of transfer of the cyanide ion (see chapter 1). This observation is easily explained by the fact that the reaction proceeds via a D mechanism, the rate determining step, from which values of $\delta_m \Delta G^\ddagger$ are determined, being dissociation of the nitrogen heterocycle from the $[\text{Fe}(\text{CN})_5]^{3-}$ moiety, with no cyanide being involved. Thus the changes in $\delta_m \Delta G^\ddagger$ with varying solvent composition must arise from changes in the chemical potentials of the reactant; $\delta_m \mu^\ominus$ (reactant) and transition state, $\delta_m \mu^\ominus$ (T.S.). These changes are seen to be small, and must reflect relatively small changes in the differences between the solvation properties of the initial state and transition state of the reaction in various solvent mixtures. This follows from the knowledge that the difference between the I.S. and the T.S. is simply that the latter has a stretched Fe-N bond.

The dependence of kinetic parameters for reactions on the composition of mixed aqueous solvents often affords complicated patterns, e.g. for reaction between nickel(II) and 2,2'-bipyridyl in methanol-water mixtures [2.53]. In order to understand such patterns, it is necessary to investigate how reactants and transition states are affected when a co-solvent is added to the reacting system. Nevertheless, an important aspect of any discussion of these phenomena is the way in which the solvent water and the co-solvent interact. An indication of the magnitude and dependence on composition of such interactions can be gained from the molar excess Gibbs function of mixing, G^E , for the mixture. Hence it is of interest

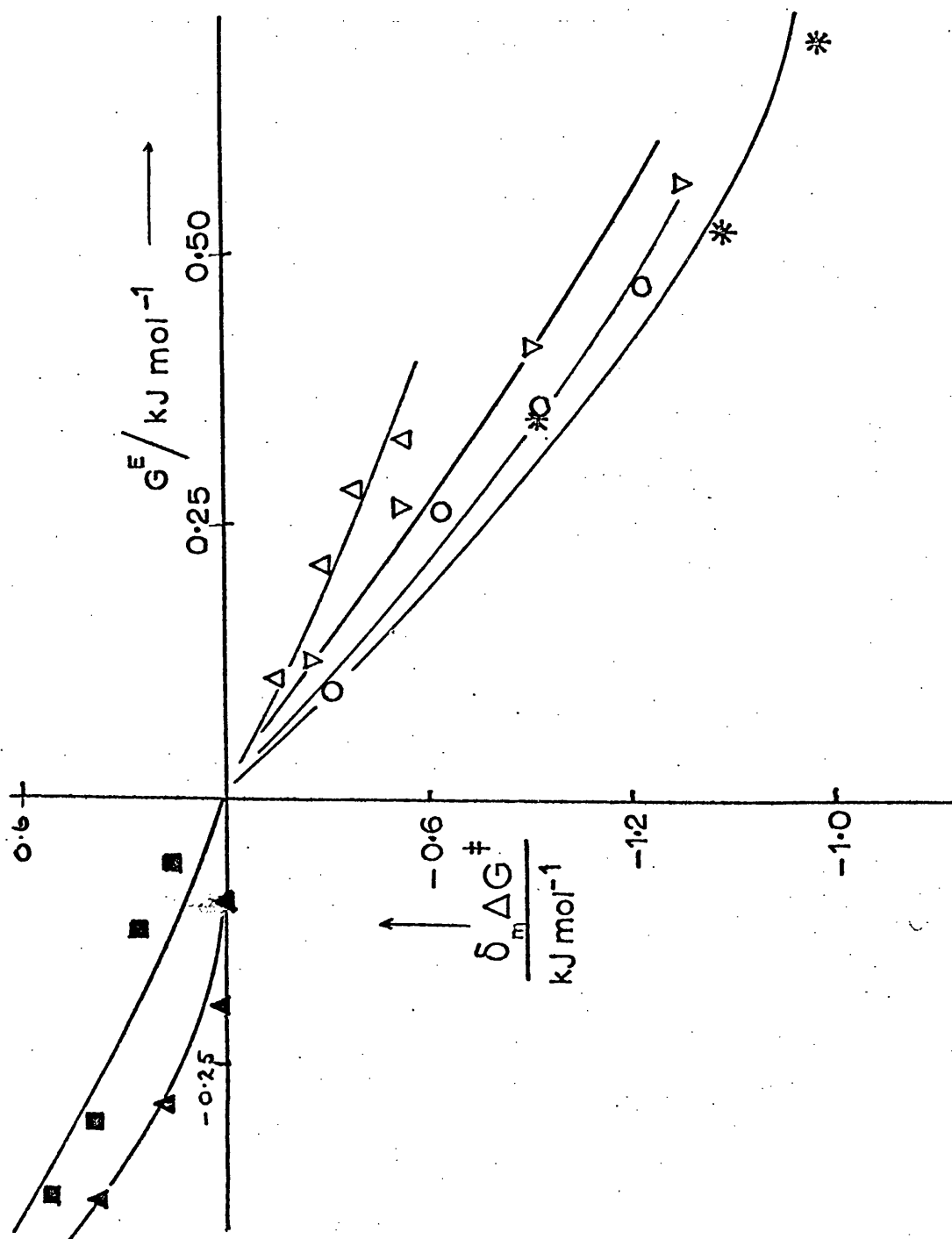


Figure 2.08 Variation of $\delta_m \Delta G^\ddagger$ for the reaction of cyanide ion with the $[\text{Fe}(\text{CN})_5(3,5\text{-Me}_2\text{py})]^{3-}$ anion at 298.6 K, in a range of binary aqueous mixtures. Solvents used are methanol (\blacksquare), ethanol (\circ), t-butyl alcohol (∇), ethylene glycol (\blacktriangle), glycerol (\blacksquare) and tetrahydrofuran (*).

to see whether the reactivities in substitution reactions in binary aqueous mixtures can be correlated with G^E for the respective mixtures.

Figure 2.08 indicates a well marked correlation between values of $\delta_m \Delta G^\ddagger$ calculated from measured rate constants and G^E values for the respective solvent mixtures. The immediately striking feature of this figure is the behaviour of the 'typically aqueous', T.A., mixtures used, i.e. mixtures of aqueous methanol, ethanol, t-butyl alcohol and tetrahydrofuran; the results for which all fall into one narrow sector. It could be argued that the results for ethylene glycol- and glycerol-water mixtures, which are both T.N.A.N. mixtures (see chapter 1) also lie along the same correlation line if one extends the line back through the origin.

In view of the similarity of mechanism between the substitution reaction studied in this work and the solvolysis of t-butyl chloride, it would be interesting to compare Figure 2.08 with an analogous plot for the latter reaction. This comparison is studied, together with a similar study for the acid aquation reaction of the tris-(5-nitro 1,10-phenanthroline)iron(II) cation in mixed aqueous solvents in chapter 3.

The classical approach to kinetic studies in mixed solvents was presented by Grunwald & Winstein [2.50]:-

Grunwald-Winstein Analysis

The study of the reaction of the $[\text{Fe}(\text{CN})_5(3,5\text{-Me}_2\text{py})]^{3-}$ anion with cyanide ion in binary aqueous mixtures has also been approached from a classical point of view, i.e. the Grunwald-Winstein analysis for the S_N1 solvolysis of an organic chloride. The background of this analysis has been described fully in chapter 1.

The dependence of reactivity on solvent composition for the 3,5-Me₂py

complex is illustrated in Figure 2.09 in the form of a Grunwald-Winstein $m.Y$ plot. Values for $k_{1,m}$ were taken from Table 2.08. The solvent Y parameter was calculated for each solvent mixture used from rate constants measured in the respective solvent mixture for the solvolysis of *t*-butyl chloride, the model S_N1 -type reaction used as standard in Grunwald and Winstein's original work. Y values were thus calculated from data available according to the equation:-

$$Y = \log_{10} \frac{k(^t\text{BuCl})}{k_o(^t\text{BuCl})} \quad (2.27)$$

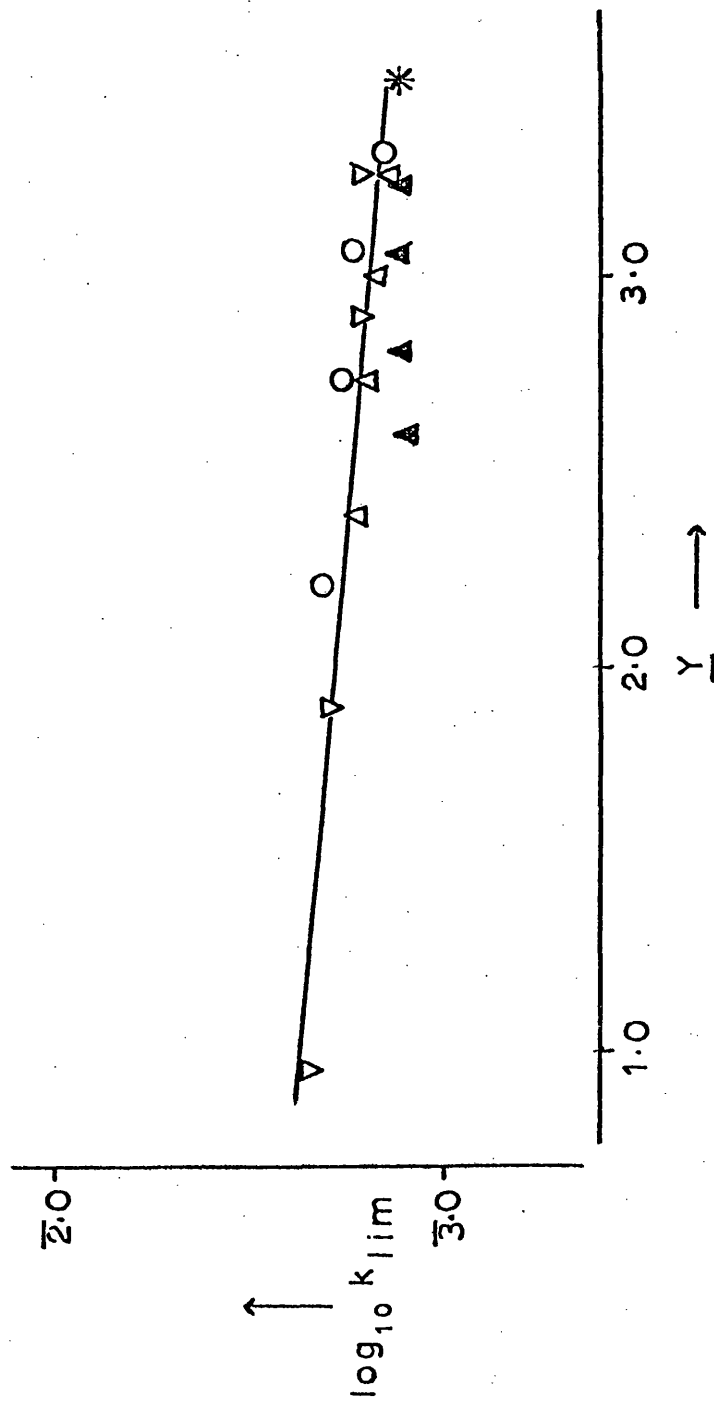
where k is the rate constant in the appropriate solvent mixture;
 k_o is the corresponding rate constant measured in 80% aqueous ethanol at 298 K.

These Y values have been listed, together with other physical data for binary aqueous mixtures, in Appendix 1.

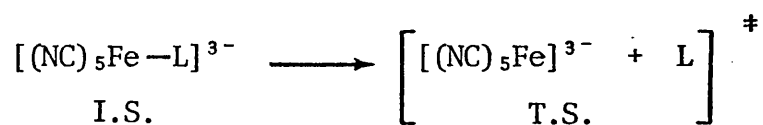
As we can see from Figure 2.09, the value of the slope (m) is -0.10 ± 0.01 .[†] The correlation lines corresponding to the three organic co-solvents do not quite coincide; such behaviour for dissociative inorganic reactions has been established for cobalt(III) complexes [2.57], where the Grunwald-Winstein m value is ca. 0.3. Negative m values have previously been reported for inorganic substitution reactions in which one of the separating moieties is a negatively charged species containing several hydrophilic groups, viz. bromide ligands in the aquation of the hexabromorhenate(IV) anion [2.58], where $m = -0.55$; and thiocyanate ligands in the

[†] [This value was estimated from results in T.A. mixtures, ignoring results in aqueous ethylene glycol (T.N.A.N.) mixtures.]

Figure 2.09 Grunwald-Winstein plot of $\log_{10}(k_{\text{lim}})$ against solvent Y value, for the reaction of cyanide ion with the $[\text{Fe}(\text{CN})_5(3,5\text{-Me}_2\text{py})]^{3-}$ anion in a range of binary aqueous mixtures, at 298.6 K. Cosolvents used are methanol (O), ethanol (○), t-butyl alcohol (▽) and ethylene glycol (▲); (*) = solvent water.



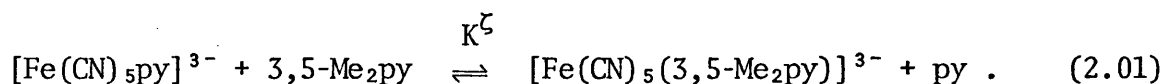
aquation of the hexathiocyanatochromium(III) anion [2.59]. Similarly, the negatively charged $[\text{Fe}(\text{CN})_5]^{3-}$ moiety may be regarded as separating from the nitrogen heterocycle in the transition state, having five hydrophilic cyanide ligands. Thus the negative m value obtained for this reaction is not unprecedented. The very low value of m obtained, i.e. -0.10, for the reaction of the $[\text{Fe}(\text{CN})_5(3,5\text{-Me}_2\text{py})]^{3-}$ anion with cyanide ion is understandable as there is no charge separation on forming the transition state, i.e.:-



The Grunwald-Winstein theory [2.50] requires that for a maximised m value, the extent of charge separation on going from I.S. to T.S. should be maximised (see chapter 1). If indeed it is the solvation of the $[\text{Fe}(\text{CN})_5]^{3-}$ moiety rather than that of the leaving 3,5-Me₂py which determines the solvent variation of reactivity in our system, then it is easy to understand how the ratio of substitution rates in, say water and 40% by volume aqueous *t*-butyl alcohol is very similar for the three complexes of 3,5-Me₂py, 3-CNpy and 3-Clpy (Table 2.07) despite the expected differences in solvation of these three species, as evidenced by their very different solubilities in water.

2.3(iii) EQUILIBRIUM STUDIES

- on the system:-



Calculation of K^ζ

Baudisch first observed that the violet colour due to the interaction of nitrosobenzene with trisodium pentacyanoammineferrate(II) was reduced by the addition of an α -unsubstituted pyridine base [2.60]. However, nitrosobenzene is unstable and so N,N'-dimethyl-p-nitrosoaniline, dmna, was used by Herington [2.18], which produced a strong absorption in the visible spectrum at 650 n.m., on interacting with the pentacyanoammineferrate(II) complex, which in turn is affected by an α -unsubstituted pyridine base in the same way that the nitrosobenzene analogue was.

Introduction of a pyridine base, B, into the system of $[\text{Fe}(\text{CN})_5(\text{OH}_2)]^{3-}$ + dmna (equation (2.02)) leads to the additional equilibrium shown in equation (2.03). It has been shown [2.18] that for the equilibrium constants K_1 and K_2 for the equilibria shown in equations (2.02) and (2.03) respectively, and for initial concentrations of dmna, of base B and of $[\text{Fe}(\text{CN})_5(\text{OH}_2)]^{3-}$ equal to a, b and c respectively, then:-

$$K_1 = \frac{\alpha_1}{[(1-\alpha_1 - \alpha_2)(a - \alpha_1 c)]} \quad (2.28)$$

and

$$K_2 = \frac{\alpha_2}{[(1-\alpha_1 - \alpha_2)(b - \alpha_2 c)]} \quad (2.29)$$

where α_1 is the fraction of initial $[\text{Fe}(\text{CN})_5(\text{OH}_2)]^{3-}$ converted into $[\text{Fe}(\text{CN})_5(\text{dmna})]^{3-}$;

and α_2 is the fraction of $[\text{Fe}(\text{CN})_5(\text{OH}_2)]^{3-}$ converted into $[\text{Fe}(\text{CN})_5\text{B}]^{3-}$, at equilibrium.

Conditions were chosen such that both the dmna and the base B were at much higher concentrations than the $[\text{Fe}(\text{CN})_5(\text{OH}_2)]^{3-}$, so that $a \gg \alpha_1 c$; and $b \gg \alpha_2 c$, whence equations (2.28) and (2.29) reduce, respectively to:-

$$K_1 = \frac{\alpha_1}{[(1-\alpha_1 - \alpha_2)a]} \quad (2.30)$$

and

$$K_2 = \frac{\alpha_2}{[(1-\alpha_1 - \alpha_2)b]} \quad (2.31)$$

If we consider two solutions, the first containing the complex $[\text{Fe}(\text{CN})_5(\text{dmna})]^{3-}$ at a concentration equal to $\alpha_1 c$, and a large excess of free dmna; and the second solution containing the same concentration of free dmna, but no iron(II) complex, then by Beer's Law, the concentration of complex in the first solution is proportional to the optical density difference, d , between the two solutions, i.e:-

$$\alpha_1 c = k d \quad (2.32)$$

where k is a constant.

Hence, from equations (2.30-32) it follows that in a series of experiments in which a and c are kept constant, and $a \gg c$, then b is given by the expression

$$b = \frac{k'}{\left(\frac{1}{d} - \frac{1}{d_0}\right)} \quad (2.33)$$

where $k' = \frac{acK_1}{kK_2}$; and d_0 is the optical density difference

as defined above when $b = 0$.

Hence,

$$K_2 = \frac{acK_1}{kb} \left(\frac{1}{d} - \frac{1}{d_0} \right) \quad (2.34)$$

where $kb = d$ from above.

We are now in a position to determine the equilibrium constant K^{ζ} ,

for the equilibrium shown in equation (2.01). We define this constant as

$$K^{\zeta} = \frac{K_{2B}}{K_{2P}} = \frac{d_p (d_o - d_B)}{d_B (d_o - d_p)} \quad (2.35)$$

where K_{2B} is the equilibrium constant K_2 for the pyridine base B;

and K_{2P} " " " " pyridine itself.

d_p is the optical density as defined for d , when B = pyridine,

and d_B " " " " " B = substituted pyridine.

Hence a study has been made of the equilibrium constant, K^{ζ} for the relative stabilities of pyridine and several substituted pyridines with respect to the $[\text{Fe}(\text{CN})_5]^{3-}$ moiety, as described by the equilibrium in equation (2.01), in aqueous solution at 298 K. The study has been extended, for the 3,5-Me₂py base and pyridine to a range of binary aqueous mixtures.

Table 2.09 lists the measured optical density values required for the calculation of K^{ζ} . These calculated K^{ζ} values have been listed in Table 2.10. K^{ζ} for B = 3,5-Me₂py, 3-CNpy and 3-Clpy were found to be 0.93, 0.83 and 0.65 respectively, indicating a trend of decreasing stability of the respective pentacyanoferrate(II) complex anions. Such a trend is consistent with the observed trend in the limiting rate constants for dissociation of these complexes (section 2.3(i), Table 2.07), which were $1.33 \times 10^{-3} \text{ s}^{-1}$ and $2.46 \times 10^{-3} \text{ s}^{-1}$ for the 3,5-Me₂py and 3-CNpy complexes respectively.

The relative stabilities of the $[\text{Fe}(\text{CN})_5(3,5\text{-Me}_2\text{py})]^{3-}$ and $[\text{Fe}(\text{CN})_5\text{py}]^{3-}$ anions have been studied in a range of binary aqueous mixtures at 298 K, in terms of K^{ζ} values. The trends in K^{ζ} for varying solvent composition has been illustrated in Figure 2.10(a), and in terms

TABLE 2.09 Optical density measurements, d_o , d_p and d_b , as defined in section 2.3(iii), together with calculated equilibrium constants, K_{2p} and K_{2b} , in water and in binary aqueous mixtures at 298 K.

| Solvent Mixture | | d _o | d _p | d _b | K _{2p} | K _{2b} |
|----------------------------|------------------------------|----------------|----------------|----------------|-----------------|-----------------|
| B = 3,5-Me ₂ py | | | | | | |
| Water | | 1.21 | 0.57 | 0.55 | 1.11 | 1.18 |
| 10 | % Methanol | 1.18 | 0.58 | 0.59 | 1.03 | 1.01 |
| 20 | | 1.14 | 0.58 | 0.60 | 0.98 | 0.90 |
| 30 | | 1.17 | 0.61 | 0.67 | 0.93 | 0.75 |
| 40 | | 1.11 | 0.64 | 0.70 | 0.73 | 0.58 |
| 10 | % Ethanol | 1.16 | 0.55 | 0.59 | 1.11 | 0.99 |
| 20 | | 1.14 | 0.54 | 0.60 | 1.10 | 0.90 |
| 30 | | 1.10 | 0.55 | 0.62 | 0.99 | 0.77 |
| 40 | | 1.06 | 0.57 | 0.67 | 0.86 | 0.59 |
| 10 | % ^t Butyl alcohol | 1.14 | 0.55 | 0.64 | 1.06 | 0.79 |
| 20 | | 1.11 | 0.50 | 0.70 | 1.23 | 0.59 |
| 30 | | 1.10 | 0.53 | 0.76 | 1.09 | 0.45 |
| 40 | | 1.07 | 0.41 | 0.68 | 1.64 | 0.58 |
| B | | | | | | |
| Aqueous Solution | | | | | | |
| 3-CNpy | | | | 0.64 | | 0.89 |
| 3-Clpy | | | | 0.71 | | 0.70 |

TABLE 2.10 Values for the equilibrium constant, K^{\pm} , (equation (2.01)) in several binary aqueous mixtures at 298 K. The derived values of ΔG^{\ominus} in these mixtures are also included.

| Solvent Mixture | K^{\pm} | $\Delta G^{\ominus} / \text{kJ mol}^{-1}$ |
|-----------------|-----------|---|
| Water | 1.06 | -0.14 |
| 10 | 0.98 | 0.050 |
| 20 | 0.92 | 0.21 |
| 30 % Methanol | 0.81 | 0.52 |
| 40 | 0.80 | 0.55 |
| 10 | 0.89 | 0.29 |
| 20 | 0.82 | 0.49 |
| 30 % Ethanol | 0.78 | 0.62 |
| 40 | 0.69 | 0.92 |
| 10 | 0.75 | 0.71 |
| 20 % t-Butyl | 0.48 | 1.8 ₂ |
| 30 alcohol | 0.41 | 2.2 ₁ |
| 40 | 0.35 | 2.6 ₀ |

Figure 2.10(a) Dependence of the equilibrium constant, K^s on solvent composition in a range of binary aqueous mixtures, at 298.6 K. Cosolvents used are methanol(\circ), ethanol(Δ) and t-butyl alcohol(∇); (\bullet) = solvent water.

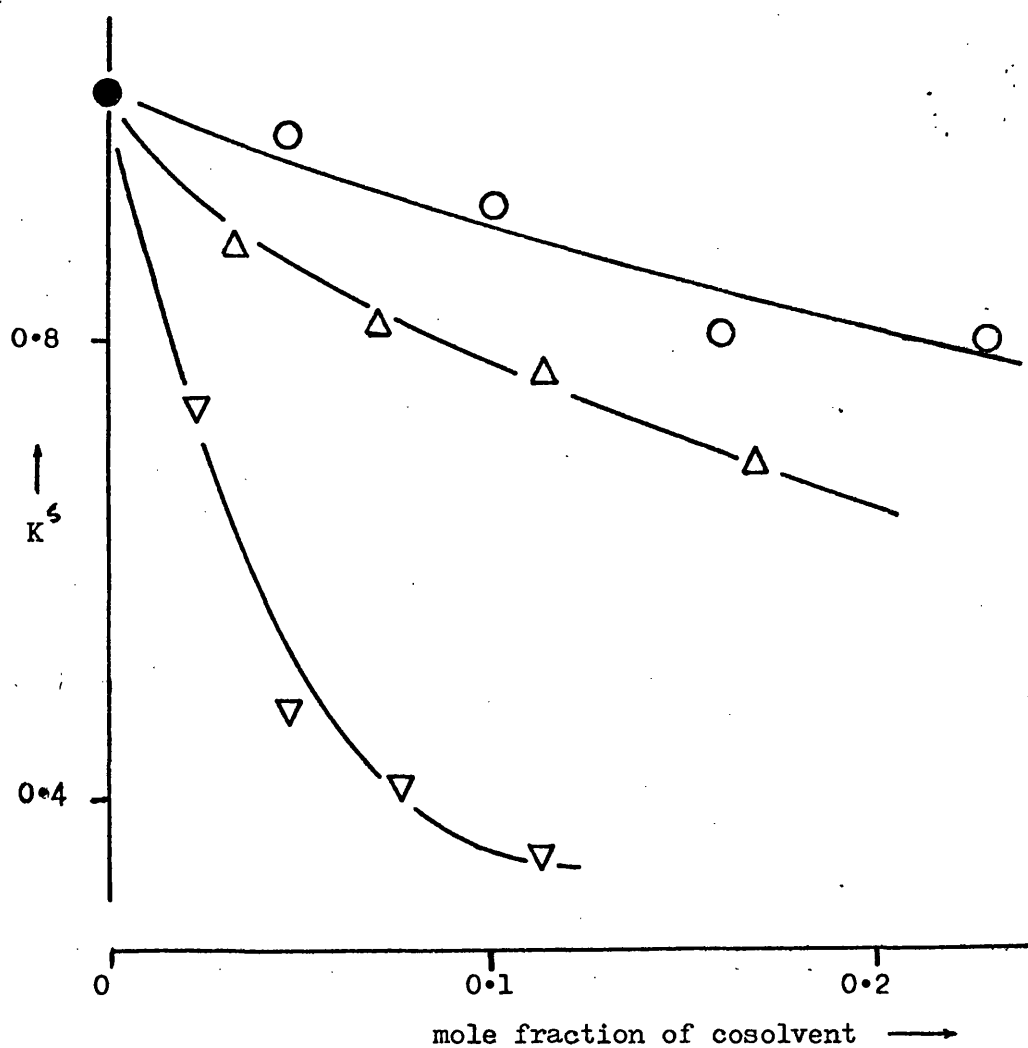
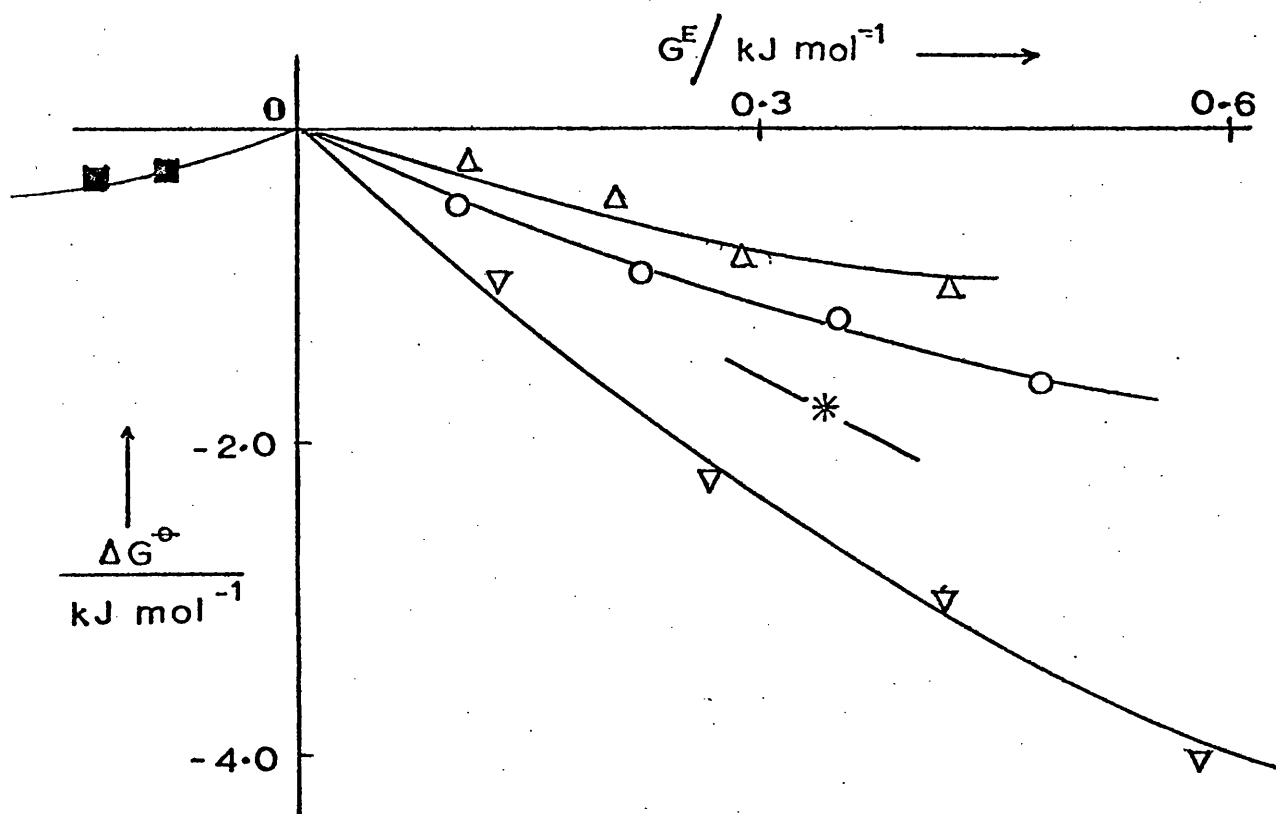


Figure 2.10(b) Correlation of ΔG^\ominus for the equilibrium shown in equation (2.01) with G^E , for a range of binary aqueous mixtures. Symbols as in Figure 2.08 for cosolvent type.



of the standard Gibbs free energy, $\Delta G^{\ominus \dagger}$ compared with G^E values for the appropriate solvent mixtures, in Figure 2.10(b).

From Figure 2.10(a) we see that K^{ζ} decreases in magnitude as we go from aqueous solution to mixed aqueous solutions. Qualitatively, this trend may be understood by considering that in aqueous solution, the 3,5-Me₂py base is less well solvated than pyridine itself (as is evidenced by the latter's complete miscibility with water) and so has a relatively unfavourable chemical potential in water. On adding co-solvent to the system, the chemical potential of the base becomes increasingly more negative, i.e. the base is stabilised in solution. Thus its tendency to stay in solution, and hence its tendency not to react with the iron(II) complex increases as the mole fraction of co-solvent does. A similar effect is expected for pyridine, but to a lesser extent. So the overall effect is that on increasing the mole fraction of co-solvent in the system, the equilibrium expressed by equation 2.01 moves to the left, thus decreasing the value of K^{ζ} .

In Figure 2.10(b) we see a good correlation of ΔG^{\ominus} with G^E for T.A. mixtures, the results falling into the same type of narrow sector as was observed for the analogous kinetic plot of $\delta_m \Delta G^{\ddagger}$ against G^E (Figure 2.08). The ΔG^{\ominus} results for the T.N.A.N. solvent mixture of aqueous glycerol do not fall on the correlation line for the T.A. mixtures. This pattern, as shall be seen in Chapter 3, repeats its consistent pattern for T.A. mixtures, and its consistent inconsistencies for T.N.A. ones.

[†] [ΔG^{\ominus} values calculated from the expression $\Delta G^{\ominus} = -RT \ln K^{\zeta}$.]

The above kinetic and thermodynamic aspects of the reactions and equilibria described by equations (2.01-03) for the $[\text{Fe}(\text{CN})_5\text{L}]^{n-}$ anions are obviously related. Trends in stability constants should be reflected in the discriminatory tendencies of the transient $[\text{Fe}(\text{CN})_5]^{3-}$ intermediate, in other words the curvatures of the plots of k_{obs} against the concentration of incoming nucleophile, of the type illustrated in Figures 2.01, 2.06(a). In practice, it has been shown (section 2.3(i)) that the curvature of such plots for reactions of $[\text{Fe}(\text{CN})_5\text{L}]^{n-}$ anions with cyanide ion, pyrazine or N-methylpyrazinium cation is too sharp for accurate intercomparisons between different solvent mixtures. At the other extreme, reaction with thiocyanate anion is unsuitable, as this ligand was found not to compete sufficiently strongly with substituted pyridines for the reaction to proceed far enough towards completion.

However, it has been shown that k_{obs} is inversely proportional to the concentration of outgoing ligand in these reactions. The effect of adding an amount of outgoing ligand is shown below to greatly reduce the curvature of the k_{obs} versus [incoming ligand] plot, and hence allow quantitative determinations of the discriminatory power, or 'reactivity ratio' of the $[\text{Fe}(\text{CN})_5]^{3-}$ moiety to be made.

2.3(iv) KINETICS IN PRESENCE OF ADDED OUTGOING LIGAND

For a dissociative (D) mechanism, it has been shown earlier (section 2.3(i), equation (2.11)) that for reaction of cyanide ion with the $[\text{Fe}(\text{CN})_5\text{L}]^{n-}$ anion in the presence of a constant concentration of outgoing ligand, the reciprocal of the observed first-order rate constant, $1/k_{\text{obs}}$ is directly proportional to the reciprocal of the cyanide ion concentration, $1/[\text{CN}^-]$. From equation (2.11), we see that for such a plot the

intercept is equal to the reciprocal of the limiting rate constant, $1/k_1$ (or $1/k_{lim}$), the slope being:-

$$\text{slope} = \frac{k_{-1} [L]}{k_1 k_2} \quad (2.36)$$

Hence we can calculate the 'reactivity ratio', $R (= k_{-1}/k_2)$ by adding a known concentration of L to the reaction system.

Conversely, at constant cyanide ion concentration, $1/k_{obs}$ is linearly dependent on $[L]$, again the intercept being equal to $1/k_1$, and in this case,

$$\text{slope} = \frac{k_{-1}}{k_1 k_2 [CN^-]} \quad (2.37)$$

Studies in Aqueous Solution

For the 3-cyanopyridine complex, first-order rate constants were measured for a range of added 3-cyanopyridine concentrations of zero, 0.001, 0.003, 0.004 and 0.009 mol dm⁻³, for four sets of constant cyanide ion concentrations, as indicated in Table 2.11. Hence R values in aqueous solution were calculated from four plots of $1/k_{obs}$ versus $1/[CN^-]$ at various constant concentrations of 3-cyanopyridine; and from four plots of $1/k_{obs}$ versus $[3-CNpy]$ at various constant concentrations of cyanide ion. An analogous study was performed for the 4-cyanopyridine analogue, with various concentrations of both cyanide ion and added 4-cyanopyridine, which are indicated in Table 2.12. The observed first-order rate constants measured in this study are also listed in Table 2.12. The consequent R values, together with those of the 3-CNpy case are reported in Table 2.13, together with k_1 values estimated from the appropriate reciprocal plots.

TABLE 2.11 First-order rate constants for the reaction of the $[\text{Fe}(\text{CN})_5(3\text{-CNpy})]^{3-}$ anion (10^{-4} mol dm $^{-3}$) with cyanide ion in the presence of various concentrations of added 3-cyanopyridine, at 298.6 K; ionic strength of 0.12 mol dm $^{-3}$ maintained with potassium nitrate.

| Solvent Mixture | | [KCN] / mol dm $^{-3}$ | | | |
|----------------------|--|---------------------------------------|-------|-------|-------|
| | | 0.03 | 0.06 | 0.09 | 0.12 |
| | | 10 3 k $_{\text{obs}}$ / s $^{-1}$ | | | |
| | | [3-CNpy] / mol dm $^{-3}$ | | | |
| | | 0 | 0.001 | 0.003 | 0.004 |
| | | 0.009 | | | |
| Water | | 0 | 0.001 | 0.003 | 0.004 |
| | | 0.009 | | | |
| | | 2.72 | 2.80 | 2.84 | 2.81 |
| | | 1.68 | 1.85 | 2.42 | 2.58 |
| | | 0.88 | 1.39 | 1.73 | 1.93 |
| | | 0.76 | 1.14 | 1.52 | 1.69 |
| | | 0.40 | 0.66 | 0.93 | 1.11 |
| 10 | | 0.32 | 0.40 | 0.51 | 0.62 |
| 20 | | 0.57 | 0.70 | 0.82 | 0.98 |
| 30 % Methanol | | 0.75 | 0.91 | 1.09 | 1.16 |
| 40 | | 0.92 | 1.08 | 1.21 | 1.51 |
| 10 | | 0.33 | 0.36 | 0.52 | 0.61 |
| 20 | | 0.56 | 0.63 | 0.82 | 0.96 |
| 30 % Ethanol | | 0.78 | 0.79 | 1.06 | 1.25 |
| 40 | | 0.90 | 0.99 | 1.21 | 1.42 |
| 10 | | 0.44 | 0.52 | 0.73 | 0.91 |
| 20 | | 0.74 | 0.84 | 1.16 | 1.49 |
| 30 % t-Butyl alcohol | | 0.99 | 1.07 | 1.43 | 1.77 |
| 40 | | 1.18 | 1.31 | 1.52 | 1.80 |

TABLE 2.12 First-order rate constants for the reaction of the $[\text{Fe}(\text{CN})_5(4\text{-CNpy})]^{3-}$ anion with cyanide ion in the presence of varying concentrations of added 4-cyanopyridine, at 298.6 K; ionic strength of 0.10 mol dm^{-3} maintained with potassium nitrate.

| Solvent Mixture | $\frac{[\text{KCN}]}{\text{mol dm}^{-3}}$ | $\frac{[4\text{-CNpy}]}{\text{mol dm}^{-3}}$ | | | |
|-----------------|---|--|-------|-------|-------|
| | | 0 | 0.001 | 0.002 | 0.004 |
| | | $\frac{10^4 k_{\text{obs}}}{\text{s}^{-1}}$ | | | |
| Water | 0.010 | 7.3 | 2.5 | 1.43 | 0.70 |
| | 0.020 | 9.0 | 4.2 | 2.5 | 1.41 |
| | 0.040 | 9.6 | 6.1 | 4.1 | 2.6 |
| | 0.060 | 9.8 | 6.8 | 5.0 | 3.2 |
| | 0.080 | 9.9 | 7.5 | 5.9 | 3.8 |
| | 0.100 | 9.9 | 8.2 | 6.7 | 4.8 |
| 40 % Methanol | 0.020 | 9.4 | 5.4 | 3.6 | 2.0 |
| | 0.040 | 9.6 | 7.1 | 5.3 | 3.3 |
| | 0.060 | 9.6 | 7.8 | 6.3 | 4.4 |
| | 0.080 | 9.8 | 8.7 | 7.1 | 5.4 |
| | 0.100 | 10.0 | 8.8 | 8.3 | 5.8 |
| 40 % Ethanol | 0.012 | 11.1 | 4.5 | 2.5 | 1.30 |
| | 0.020 | 14.4 | 5.7 | 3.9 | 2.0 |
| | 0.040 | 13.3 | 8.3 | 6.3 | 3.3 |
| | 0.060 | 14.3 | 10.0 | 7.4 | 5.6 |
| | 0.100 | 12.5 | 11.1 | 9.1 | 6.3 |

TABLE 2.13 Reactivity ratios, k_{-1} / k_2 , and limiting first-order rate constants, k_1 , for replacement of the substituted pyridine in $[\text{Fe}(\text{CN})_5(3\text{-CNpy})]^{3-}$ or $[\text{Fe}(\text{CN})_5(4\text{-CNpy})]^{3-}$ by cyanide ion in binary aqueous mixtures at 298.6 and 298.2 K respectively.

| Solvent Mixture | $[\text{Fe}(\text{CN})_5(3\text{-CNpy})]^{3-}$ | | $[\text{Fe}(\text{CN})_5(4\text{-CNpy})]^{3-}$ | |
|----------------------|--|----------------------------|--|----------------------------|
| | k_{-1} / k_2 | $10^3 k_1 / \text{s}^{-1}$ | k_{-1} / k_2 | $10^3 k_1 / \text{s}^{-1}$ |
| Water | 25.4 | 2.86 | 33.6 | 1.01 |
| 10 | 18.2 | 2.80 | | |
| 20 | 8.6 | 2.90 | | |
| 30 % Methanol | 6.0 | 2.88 | | |
| 40 | 4.8 | 2.99 | 21.3 | 1.41 |
| 10 | 21.7 | 2.90 | | |
| 20 | 11.8 | 3.02 | | |
| 30 % Ethanol | 7.4 | 3.21 | | |
| 40 | 5.8 | 3.54 | 30.3 | 1.55 |
| 10 | 13.8 | 2.98 | | |
| 20 | 8.0 | 3.23 | | |
| 30 % t-Butyl alcohol | 5.1 | 3.51 | | |
| 40 | 3.3 | 3.55 | | |

Figure 2.11 shows the dependence of k_{obs} on cyanide ion concentration, in aqueous solution in the presence of varying concentrations of added 4-CNpy, for the reaction of the $[\text{Fe}(\text{CN})_5(4\text{-CNpy})]^{3-}$ anion with cyanide ion at 298 K and a constant ionic strength of 0.10 mol dm^{-3} . From the expression for k_{obs} in equation (2.10) we see

$$k_{\text{obs}} = \frac{k_1 k_2 [\text{CN}^-]}{k_{-1} [4\text{-CNpy}] + k_2 [\text{CN}^-]} \quad (2.38)$$

Hence we see that at very low $[\text{CN}^-]$, the term $k_{-1} [4\text{-CNpy}] \gg k_2 [\text{CN}^-]$ in equation (2.38), and hence k_{obs} is linearly dependent on $[\text{CN}^-]$. When no 4-CNpy is added, this dependence is very difficult to observe. However, on addition of as little as $0.001 \text{ mol dm}^{-3}$ of 4-CNpy, we find that the slope of the dependence is greatly reduced, enabling relatively simple measurement of the R factor. Figure 2.12 is the reciprocal equivalent of Figure 2.11. It is clear that for a particular solvent mixture and temperature, the intercept and hence (from equation (2.37)) k_1 is independent of added outgoing ligand, in spite of large variations in k_{obs} with $[\text{L}]$. This is to be expected from equation (2.10), as at very high $[\text{CN}^-]$, $k_2 [\text{CN}^-] \gg k_{-1} [\text{L}]$, and k_{obs} approximates to:-

$$k_{\text{obs}} \approx \frac{k_1 k_2 [\text{CN}^-]}{k_2 [\text{CN}^-]} \approx k_1 \quad (2.39)$$

Figure 2.13 is a plot of $1/k_{\text{obs}}$ versus $[4\text{-CNpy}]$ from the same data used to compile Figures 2.13(a) and (b). Again, as expected k_1 is seen to be constant. We see remarkable linearity in Figures 2.12 and 2.13, as is expected from equations (2.36) and (2.37). We find that the computed values of R for the 3-CNpy and the 4-CNpy complexes in aqueous solution are 25.4 ± 1.0 and 33.6 ± 2.0 respectively. These are

Figure 2.11

Dependence of first-order rate constants, k_{obs} , on cyanide ion concentration for the reaction of the $[\text{Fe}(\text{CN})_5(4\text{-CNpy})]^{3-}$ anion with cyanide ion in aqueous solution, at 298.2 K. Curve (1) applies to runs with no added 4-CNpy; curves (2), (3) and (4) correspond to 0.001, 0.002 and 0.004 mol dm⁻³ of added 4-CNpy respectively.

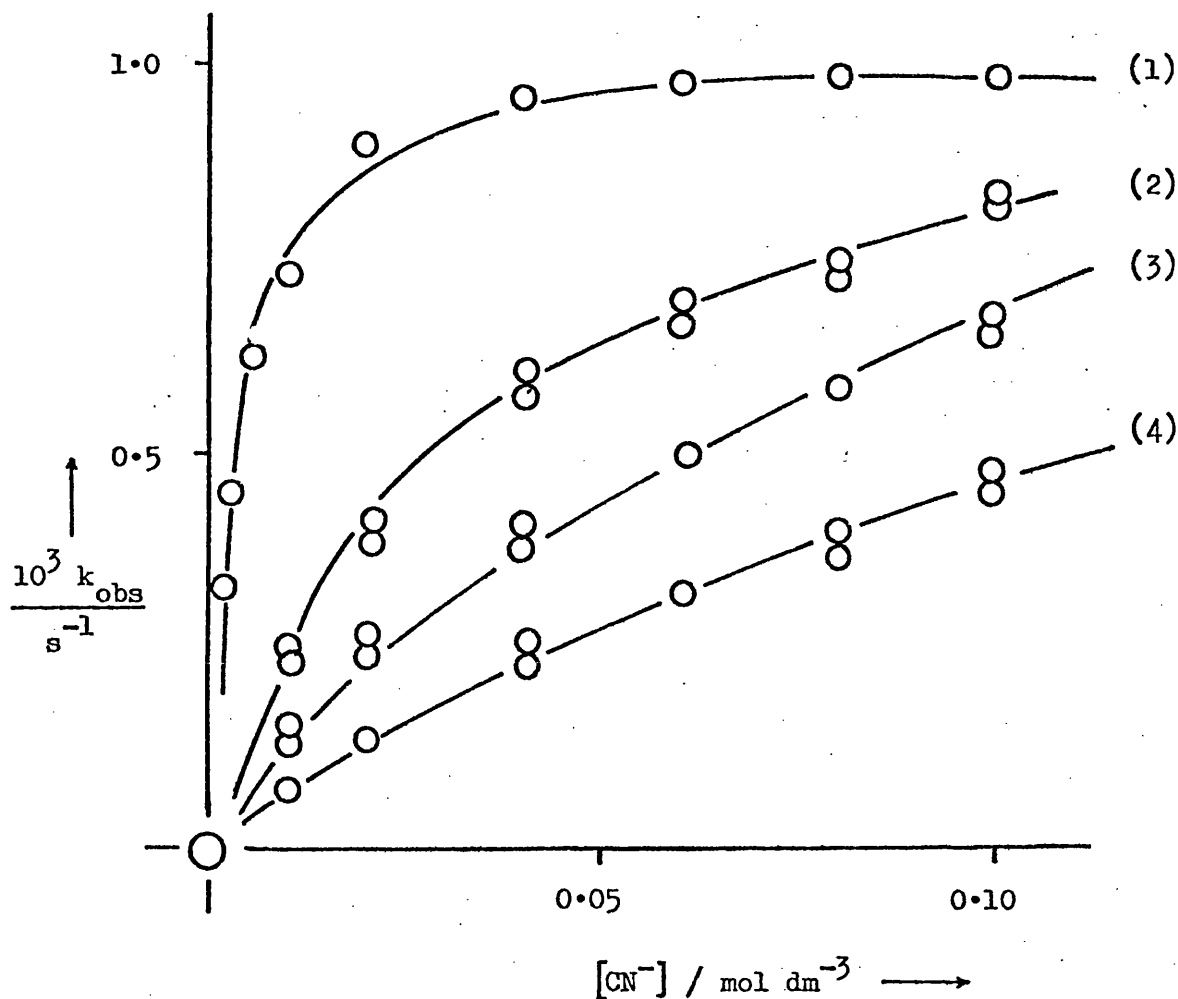
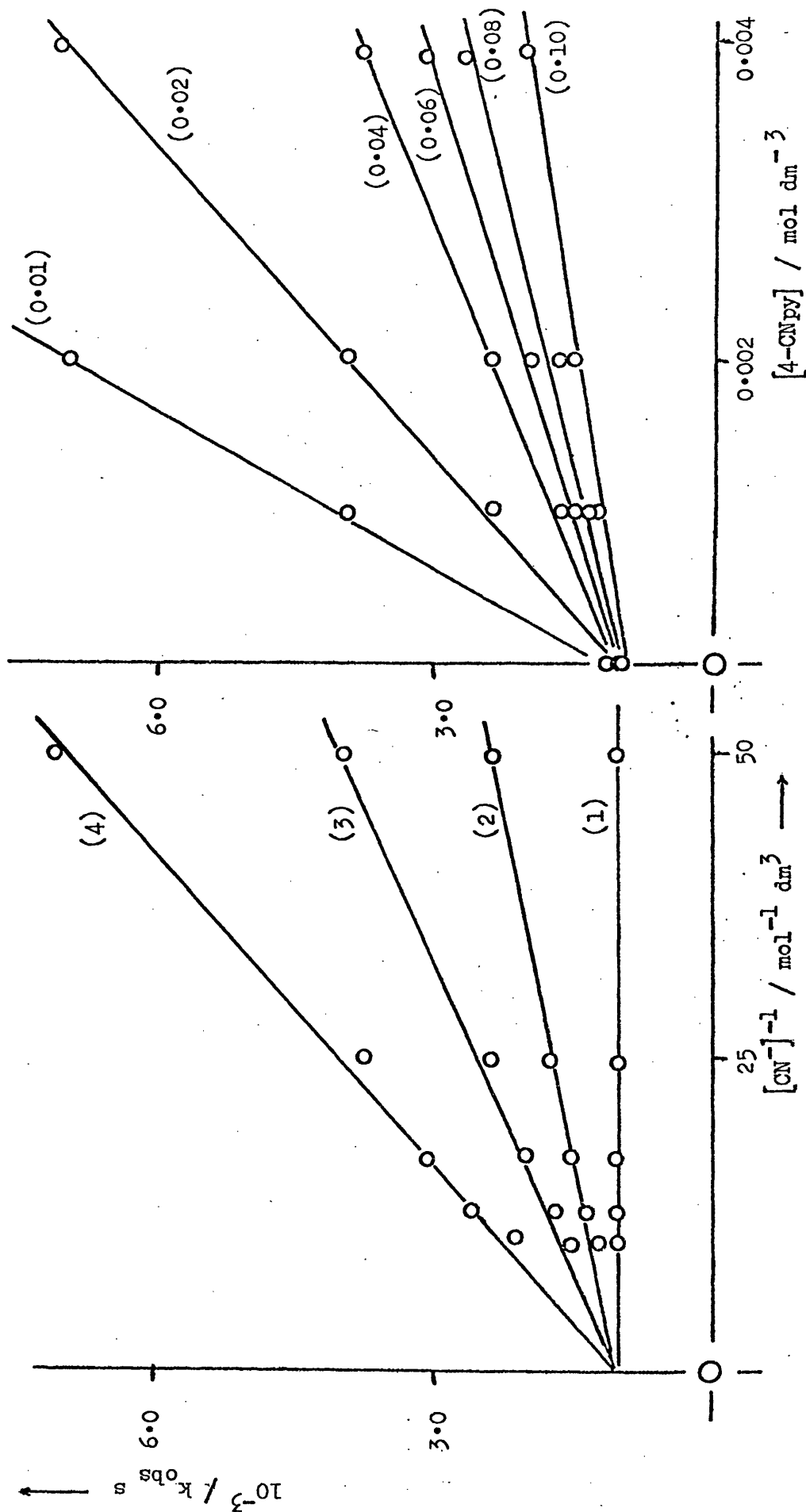


Figure 2.12 Dependence of the reciprocals of k_{obs} and $[\text{CN}^-]$ for the runs shown in Figure 2.11. Numbering as in Figure 2.11. Dependence of the reciprocal of k_{obs} on the concentration of added 4-CNpy for the runs shown in Figure 2.11. Numbers in parentheses indicate $[\text{CN}^-]$ (mol dm^{-3}).



mean values of the individual R values computed from the various plots of $1/k_{\text{obs}}$ vs $1/[\text{CN}^-]$ and $1/k_{\text{obs}}$ vs $[\text{L}]$. These R factors, which may be expressed as $k_{(\text{L})}/k_{(\text{CN}^-)}$, appear to have anomalous magnitudes. One might expect a very small value, i.e. $k_2 \gg k_{-1}$. The ratio k_{-1}/k_2 for the outgoing ligand dmna, with various incoming nucleophiles, e.g. 3-CNpy, SCN^- , NO_2^- , CN^- and SO_3^{2-} has been examined by Ašperger [2.11]. It was found that the R factor $k_{(\text{dmna})}/k_{(\text{CN}^-)}$ was 9.21, i.e. dmna is approximately nine times better as a competitor for the $[\text{Fe}(\text{CN})_5]^{3-}$ moiety than is cyanide ion. Great importance is attached to the electrical charge of the nucleophile in Ašperger's work. Thus it is shown that dmna is ca. nine times better than cyanide ion, but only 1.3 times better than the neutral nitrosobenzene. In a similar study on substitution at the $[\text{Fe}(\text{CN})_5(\text{SO}_3)]^{5-}$ anion by cyanide ion [2.12], the R factor $k_{(\text{SO}_3^{2-})}/k_{(\text{CN}^-)}$ = $1/8.8$, i.e. SO_3^{2-} is 8.8 times worse than CN^- as a nucleophile for the $[\text{Fe}(\text{CN})_5]^{3-}$ intermediate. This behaviour can be qualitatively understood on the basis that the $[\text{Fe}(\text{CN})_5]^{3-}$ intermediate, which is exerting a discriminatory power over the nucleophiles present, both incoming and outgoing, will naturally prefer to react with one of opposite charge, or one of charge as dissimilar as possible to that of itself.

In Ašperger's work on the kinetics of formation of complexes of the type $[\text{Fe}(\text{CN})_5\text{L}]^{n-}$ from the pentacyanoaquoferate(II) anion, second-order rate constants were measured for a variety of incoming nucleophiles [2.11]. He states that reactivity ratios (R factors) may be roughly obtained as a ratio of these second-order rate constants. Thus they estimate, from $k_{(\text{nu})}$ values ($\text{dm}^3 \text{ mol}^{-1} \text{ s}^{-1}$) for $\text{nu} = \text{CN}^-$, dmna and PhNO, of 38, 185 and 230 respectively, that R factors, $k_{\text{dmna}}/k_{\text{nu}}$ are 4.87 and 0.80 for $\text{nu} = \text{CN}^-$ and PhNO respectively. These compare with their measured R factors of 9.2 and 1.3 respectively. Similarly, $k_{(\text{SO}_3^{2-})}/k_{(\text{CN}^-)}$

may be estimated as 0.087, as compared with the measured 0.114.

Using Ašperger's value of $370 \text{ dm}^3 \text{ mol}^{-1} \text{ s}^{-1}$ for the second-order rate constant for formation of $[\text{Fe}(\text{CN})_5(3\text{-CNpy})]^{3-}$, we can estimate an R factor $k_{(3\text{-CNpy})}/k_{(\text{CN}^-)} = 9.7$, which compares with the R factor measured in this work of 20.4. Although the discrepancy is large, it is consistent with the very similar discrepancies found for the above estimations in Ašperger's work.

Toma [2.07] has measured similar second-order rate constants for the formation of a series of neutral substituted N-heterocyclic incoming nucleophiles reacting with the $[\text{Fe}(\text{CN})_5(\text{OH}_2)]^{3-}$ anion. It was found that in spite of the differing basicities of the heterocycles, the rate constants were all very similar, which led to the conclusion that the second-order rate constant was very close to the diffusion controlled limit. For reaction between two oppositely charged ions, the diffusion-controlled rate constant is increased [2.61] as compared with that of neutral species by a factor of up to about ten, depending on the 'reaction distance' (= diameter of the reacting particles treated as spheres). Analogously, this rate constant for similarly charged ions is decreased, so that the variations in the second-order rate constant ($\text{dm}^3 \text{ mol}^{-1} \text{ s}^{-1}$) from 3.3 for SO_3^{2-} through 38 for CN^- , 185 for dmna to 550 for mpz^+ [2.11] is roughly what one would expect.

An R factor $k_{(\text{CN}^-)}/k_{(\text{H}_2\text{O})} = 1.2 \times 10^4$ has been previously determined [2.09] at 298 K. Similarly a value for $k_{(\text{CN}^-)}/k_{\text{SO}_3^{2-}} = 8.8$ has been determined at 316 K [2.10]. Hence we can estimate the relative order of reactivity of these nucleophiles as:-

$$k_{\text{H}_2\text{O}} : k_{\text{SO}_3^{2-}} : k_{\text{CN}^-} = 1 : 7.6 \times 10^4 : 6.7 \times 10^5.$$

This indicates that water does not effectively compete as a nucleophile

for the intermediate, which is another fact favouring a D mechanism.

Similar reactivity ratios for these nucleophiles have been calculated for the intermediate $[\text{Co}(\text{CN})_4(\text{SO}_3)]^{3-}$ [2.02]. The R factor $k_{(\text{CN}^-)}/k_{(\text{SO}_3^{2-})} = 13.4$, which is remarkably close to that for the $[\text{Fe}(\text{CN})_5]^{3-}$ intermediate, bearing in mind the different temperatures at which the studies were made. Considering water as a competitor for this reaction, it has been shown [2.10] that the reactivity ratio is:-

$$k_{(\text{H}_2\text{O})} : k_{(\text{SO}_3^{2-})} : k_{(\text{CN}^-)} = 1 : 146 : 1960.$$

Water here exerts a much stronger influence than in the $[\text{Fe}(\text{CN})_5]^{3-}$ case, considering the similarities in the $\text{SO}_3^{2-} : \text{CN}^-$ ratios for both intermediates. It is possible that water behaves specially in the case of the $[\text{Co}(\text{CN})_4(\text{SO}_3)]^{3-}$ intermediate case due to hydrogen-bonding due to the sulphito-oxygen atoms which might help water to co-ordinate. Another possibility is that the $[\text{Co}(\text{CN})_4(\text{SO}_3)]^{3-}$ intermediate is especially reactive, and nucleophiles do not get a chance to exert their reactivity characteristics.

Reactivity Ratios in Binary Aqueous Mixtures

First-order rate constants for the reaction of cyanide ion with the $[\text{Fe}(\text{CN})_5(3\text{-CNpy})]^{3-}$ anion were measured at 298.2 K in a range of binary aqueous at various cyanide ion concentrations, for a fixed concentration of added 3-cyanopyridine of $0.009 \text{ mol dm}^{-3}$. These rate constants are listed in Table 2.11. R factors for the reaction in these mixtures were calculated from plots of $1/k_{\text{obs}}$ versus $1/[\text{CN}^-]$, as described for the analogous study in aqueous solution above. For the 4-CNpy complex, the reaction was studied for a range of cyanide ion concentrations over a

range of fixed concentrations of added 4-CNpy, in 40% by volume aqueous methanol and aqueous ethanol. These results are listed in Table 2.12. The consequent R factors and corresponding k_1 values are tabulated in Table 2.13. Figure 2.14 shows the variation of the observed first-order rate constants with cyanide ion concentration at a constant 3-CNpy concentration of $0.009 \text{ mol dm}^{-3}$ for a range of solvent mixtures. A striking feature of such plots is that the intercepts, i.e. $1/k_1$ do not vary greatly with solvent composition. This fact was also evident from direct measurements of k_{lim} values in section 2.3(ii). The trends shown in this graph are impossible to observe quantitatively in the absence of outgoing ligand (see section 2.3(ii)). The quantitative estimation of such variations is most conveniently expressed in terms of the variation of reactivity ratios with solvent composition. Figure 2.15 expresses the variation of the measured R factors in terms of reactivity in mixed solvents relative to that in aqueous solution, i.e. the ratio R_s/R_w (where R_s = R factor in solvent mixture s and R_w = R factor in water), with molefraction of co-solvent for the reaction of the 3-CNpy complex. The decrease in the R factor on going from aqueous solution to binary aqueous mixtures can be understood qualitatively in terms of the relative solvations of the components of the system. The R factor, k_{-1}/k_2 is obviously related to the reactions shown in equations (2.40) and (2.41). Now the $[\text{Fe}(\text{CN})_5]^{3-}$ intermediate, the $[\text{Fe}(\text{CN})_5(3\text{-CNpy})]^{3-}$ anion and the

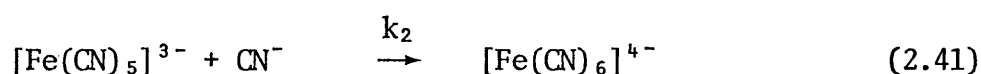
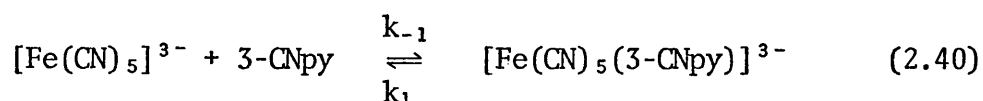


Figure 2.14 Variation of the first-order rate constant, for the reaction of the $[\text{Fe}(\text{CN})_5(4\text{-CNpy})]^{3-}$ anion with cyanide ion, with solvent composition over a range of cyanide ion concentrations, at 298.2 K. Concentration of added 4-CNpy in all runs = $0.009 \text{ mol dm}^{-3}$; curves numbered (a), (b), (c) and (d) represent solvent mixtures 10, 20, 30 and 40 % by volume aqueous t-butyl alcohol.

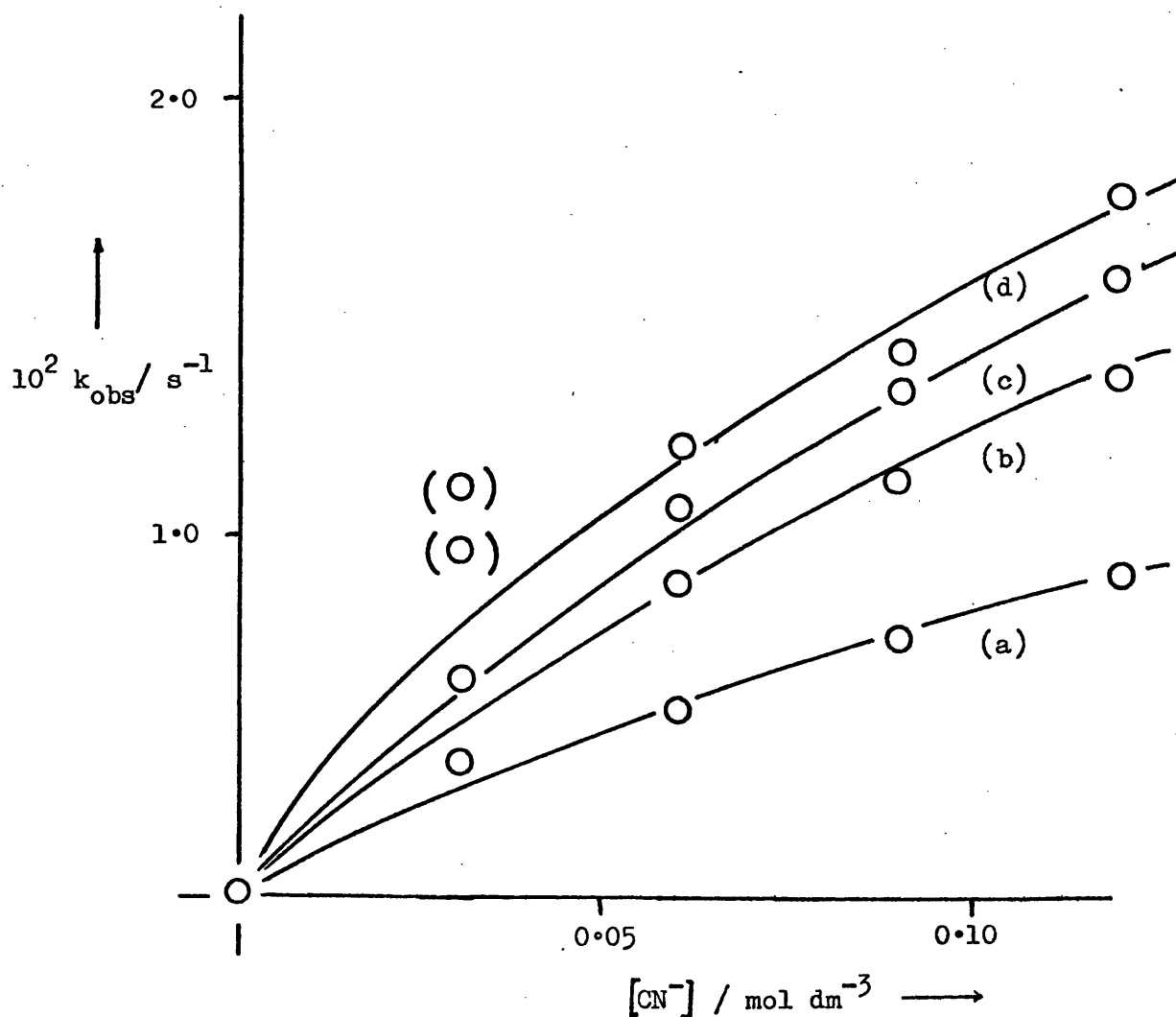
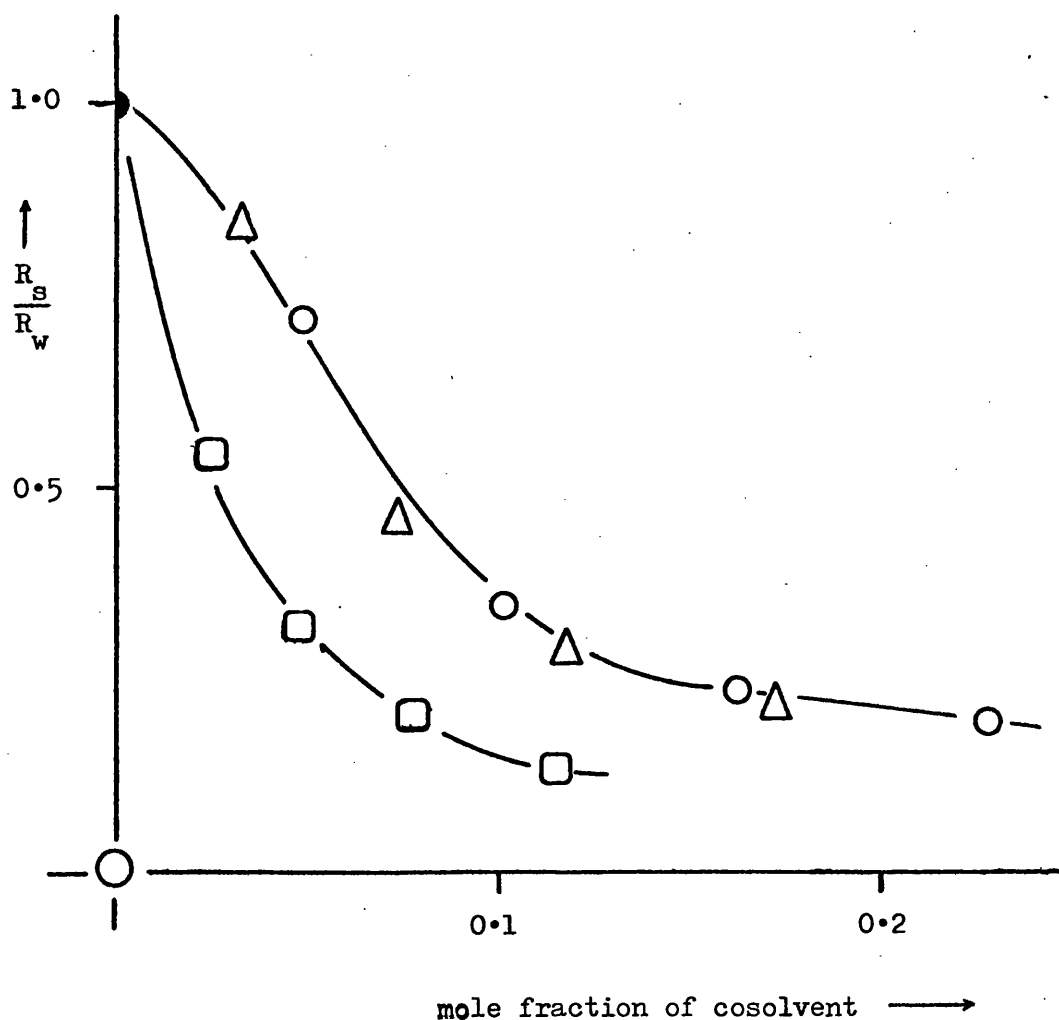


Figure 2.15 Variation of the reactivity ratio, $k_{-1}/k_2 (= R)$ with solvent composition in binary aqueous mixtures (R_s), relative to that in water (R_w), for the reaction of the $[\text{Fe}(\text{CN})_5(3\text{-CNpy})]^{3-}$ anion with cyanide ion. Temperature = 298.6 K; (●) = water; (○) = methanol, (Δ) = ethanol, (□) = t-butyl alcohol mixtures.



$[\text{Fe}(\text{CN})_6]^{4-}$ anion all have approximately the same size,[†] and have similar electrical charges, so we might expect their solvation characteristics to be very similar. This assumption is not unreasonable at least for comparisons of the first two species, the relative solvations of which have been discussed earlier (section 2.3(ii)). Estimations of the Gibbs free energy of transfer of cyanide ion, $\delta_{\text{ml}}^\ominus(\text{CN}^-)$ from water to binary aqueous mixtures have been made [2.56] in a study of the reaction of cyanide ion with the tris-(2,2'-bipyridyl)iron(II) cation in binary aqueous mixtures, and is found to become increasingly unfavourable with increasing mole fraction of co-solvent. Considering the reaction of cyanide ion with the $[\text{Fe}(\text{CN})_5]^{3-}$ species, addition of co-solvent to the system will tend to destabilise the cyanide and hence promote the reaction, assuming the solvation of the $[\text{Fe}(\text{CN})_6]^{4-}$ is similar to $[\text{Fe}(\text{CN})_5]^{3-}$. Thus k_2 should increase, which will produce a decrease in the R factor. Conversely, the solubility and hence free energy of transfer of 3-cyanopyridine increases rapidly with increasing mole fraction of co-solvent in binary aqueous mixtures. Thus the 3-cyanopyridine becomes 'happier' to exist uncoordinated in solution with increasing mole fraction of co-solvent. This trend in turn tends to decrease the value of k_{-1} , and so decrease the R factor. It is noteworthy that any decrease caused in k_{-1} will also be reflected in an equal but opposite change in k_1 . We have seen earlier (section 2.3(ii)) that k_1 values are remarkably insensitive to solvent composition, although they do increase slightly with increasing mole fraction of co-solvent. Hence it may be concluded that the changes in the R factors reflect changes in the free energy of transfer of the

[†] [From considerations made in the Volume of Activation study made in section 2.3(i).]

Figure 2.16 Correlation between the free energies of transfer of the cyanide ion and the reactivity ratios, R_s , (as shown in Figure 2.15), at 298.6 K in aqueous t-butyl alcohol mixtures. The correlation of these parameters is depicted as a plot of $\ln(R_s)$ vs. $\delta_m \mu^\ominus(\text{CN}^-)$.

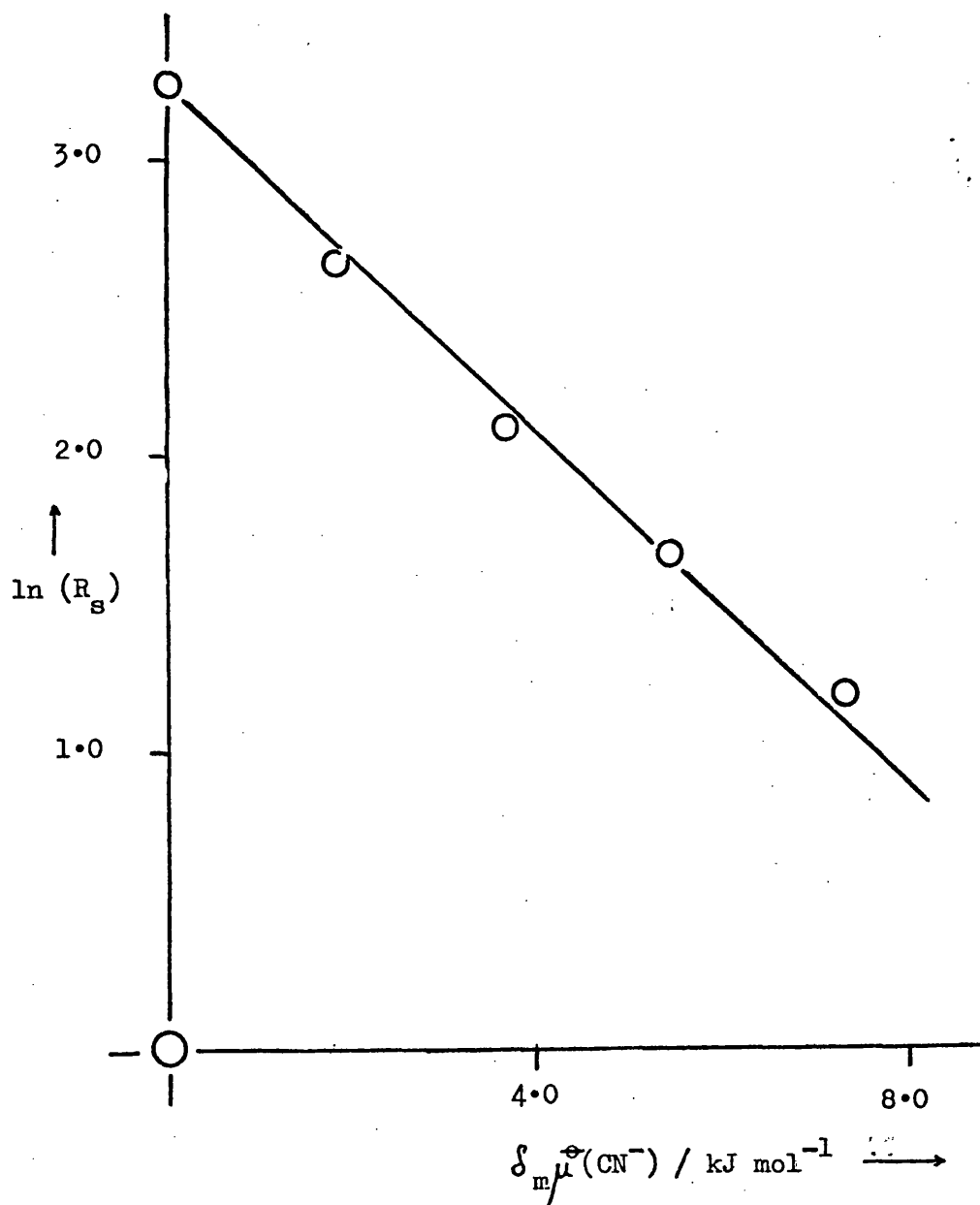
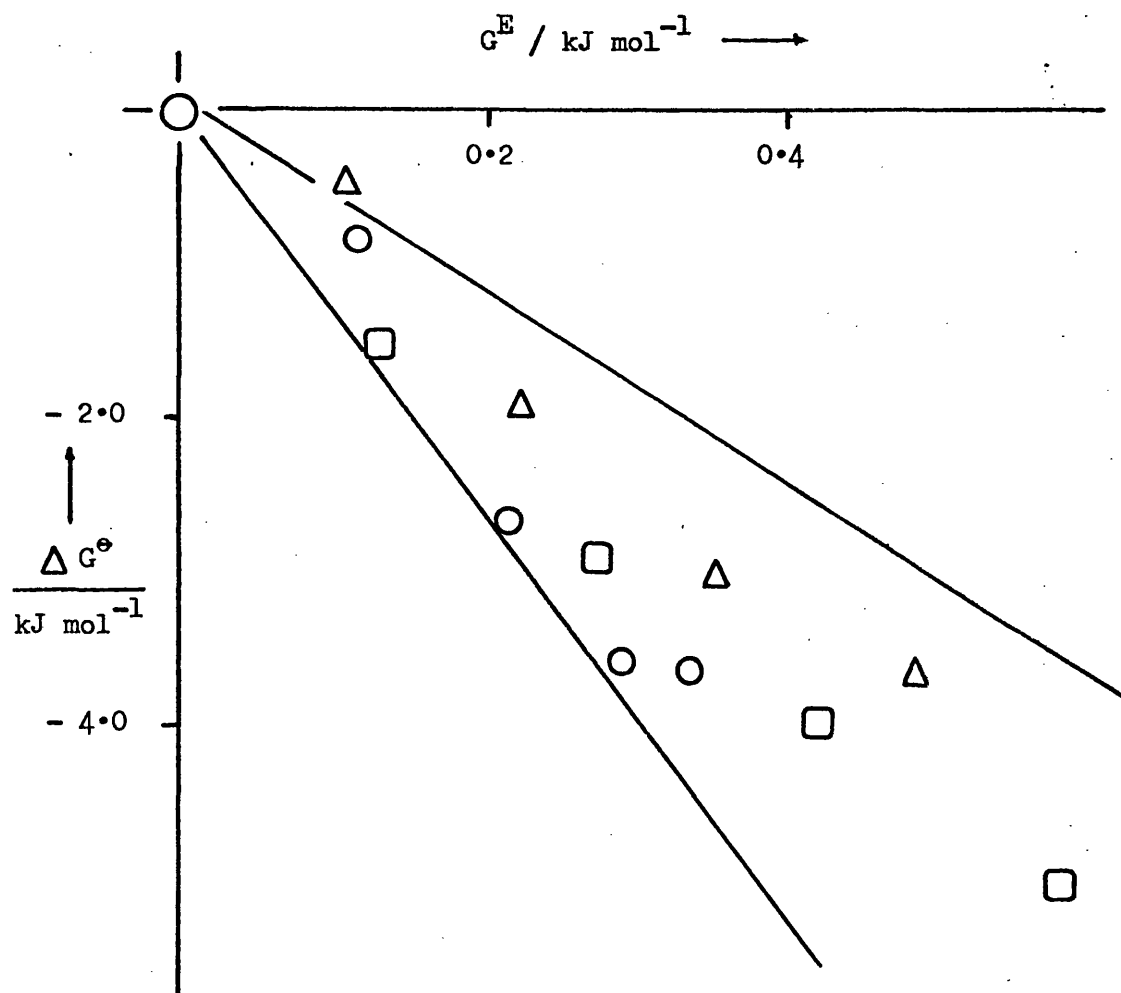


Figure 2.17 Correlation between ΔG^\ominus for the competition of 3-CNpy and CN^- for $[\text{Fe}(\text{CN})_5]^{3-}$ and G^E in binary aqueous mixtures, at 298.6 K. Symbols as in Figure 2.15.

ΔG^\ominus values used are relative to that in aqueous solution; i.e. here,

$$\Delta G^\ominus = -RT \ln (R_w / R_s)$$



incoming nucleophile, CN^- . Figure 2.16 shows graphically the correlation of our measured R factors with relevant $\delta_{\text{m}}\mu^{\ominus}(\text{CN}^-)$ values, which have been interpolated from published values [2.56], in aqueous t-butyl alcohol mixtures. Figure 2.16 thus supports the above discussion of the factors influencing the measured R values.

From equations (2.02-03) and (2.40-41) we can see that the R factor is related to the relative stabilities of the $[\text{Fe}(\text{CN})_5\text{L}]^{n-}$ anions for $\text{L} = 3\text{-CNpy}$ or CN^- . These stabilities can be related, in terms of their differences in standard Gibbs free energies, $\Delta G^{\ominus\dagger}$ to solvent composition in terms of the excess Gibbs function of mixing, G^{E} . Figure 2.17 illustrates this relation for the 3-CNpy versus CN^- reactivity ratio. The solvent mixtures used are all of the T.A. type, and we can again see the consistent relationship between ΔG^{\ominus} and G^{E} for this discrimination study, which correlates very well with both the equilibrium study of py versus 3,5-Me₂py (section 2.3(iii)) which is to be expected, considering the similarity of the systems, and also the kinetic study involving the correlations of $\delta_{\text{m}}\Delta G^{\ddagger}$ with G^{E} (section 2.3(ii)).

R factors calculated for the 4-CNpy analogue are listed in Table 2.13, and show the expected similar trends which have been fully discussed for the 3-CNpy case.

[†] [Here, $\Delta G^{\ominus} = -RT \ln K'$, where $K' \propto R$ factor. Hence $\Delta G^{\ominus} = -RT \ln n R$, or $\Delta G^{\ominus} = -(RT \ln R + RT \ln n)$, where n is a constant.]

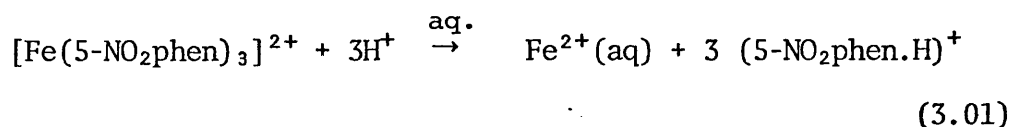
CHAPTER 3

Aquation of Tris(5-nitro 1,10-phenanthroline)iron(II)
in Binary Aqueous Mixtures; Comparison of Kinetic
Parameters for Reaction and Thermodynamic Properties
of the Mixture.

3.1 INTRODUCTION

In chapter 2 we saw the emergence of a striking correlation in binary aqueous mixtures of the kinetic and thermodynamic parameters of a reaction proceeding via a 'D' mechanism with the excess Gibbs function of mixing of the respective solvent mixtures. It would be interesting to examine whether such a correlation also occurs in reaction systems proceeding via similar mechanisms, with the possible aim of using such a correlation as a diagnostic tool for reactions where the mechanism is not clearly understood.

A reaction which has proved to be a useful probe for medium effects on reactivities is the acid aqutation of the tris(5-nitro 1,10-phenanthroline)iron(II) cation, $[\text{Fe}(\text{5-NO}_2\text{phen})_3]^{2+}$, which is represented by equation (3.01).



The rate determining step of this reaction is loss of the first ligand [3.01], which has been shown [3.02] from volume of activation measurements to be of a dissociative nature.[†] Thus this reaction is mechanistically similar to the previously studied (chapter 2) substitution at pentacyanoferrate(II) type anions, and should prove a useful test of the aforementioned correlation. The 5-nitro substituted complex has been chosen in preference to the unsubstituted one because of its

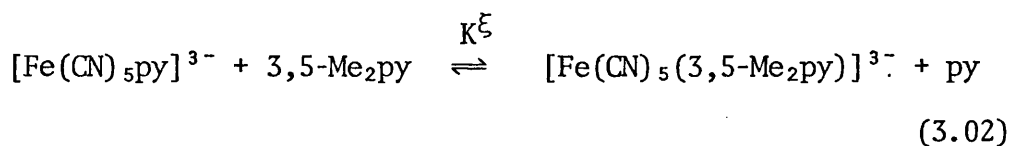
[†] [The mechanism is best described as I_d , the degree of Fe-N bond breaking in the transition state being 46%.]

higher sensitivity [3.03-05] to solvent effects. For examples, the ratio of the rates of acid aquation of the unsubstituted complexes in aqueous-acetonitrile, and in water, $k_1(x_2)/k_1(x_2=0)$, is 1.1 for $x_2 = 0.16$ at 25° , whereas $k_1(x_2)/k_1(x_2=0)$ for the 5-NO₂ substituted complex under the same conditions is 2.0.

There have already been several investigations [3.03-06] of the kinetics of this reaction in binary aqueous mixtures. In this work, the range of co-solvents has been extended to include the ~~TNAN~~ type solvent mixtures of aqueous-ethylene glycol and -glycerol. Combining these results with similar data on different solvent mixtures from the recent mixed solvent study of this reaction [3.07], correlations of the activation free energies of transfer, $\delta_m \Delta G^\ddagger$ for the reaction with the excess Gibbs function of mixing, G^E , for the respective solvent mixtures have been drawn. These correlations have been compared and contrasted with similar ones obtained in chapter 2, and also for the analogous correlations for the classical organic paradigm, the solvolysis of t-butyl chloride.

It was previously observed [3.07] that in weakly acidic media and solvent compositions of high molefraction of co-solvent, the acid aquation reaction of the $[\text{Fe}(\text{5-NO}_2\text{phen})_3]^{2+}$ cation fails to proceed to completion, an equilibrium mixture of reactants and aquation products being produced. Although this phenomenon was disadvantageous in studies of the reaction in high molefractions of solvent [3.07], it has been taken advantage of in this work in the form of a study of solvent effects on such an equilibrium.

The standard Gibbs free energies of transfer,[†] $\delta_m \Delta G^\ominus$ from water solvent into a range of binary aqueous mixtures have been measured, and correlations with G^E for the respective solvent mixtures have been drawn. These correlations have also been compared with similar ones which were observed (chapter 2) for the equilibrium represented by equation (3.02)



[†] [This seemingly eccentric function, $\delta_m \Delta G^\ominus$ is the difference between the values of ΔG^\ominus in a given solvent mixture and the value for solvent water. Thus it is defined as:

$$\begin{aligned} \delta_m \Delta G^\ominus &= \Delta G^\ominus_{(x_2)} - \Delta G^\ominus_{(x_2=0)} \\ &= -RT \ln \left(\frac{K_{(x_2)}}{K_{(x_2=0)}} \right) \end{aligned}$$

3.2 EXPERIMENTAL

(i) REAGENTS

A stock solution of $5 \times 10^{-4} \text{ mol dm}^{-3}$ of the iron(II) complex sulphate was prepared by adding 1.6×10^{-3} mole of ligand (B.D.H.) to 5×10^{-4} mole of AnalaR ammonium iron(II) sulphate (BDH) in 100 cm^3 of doubly distilled water, and stirring overnight. The solution of complex was then filtered to remove any excess of ligand and diluted to 1 dm^3 .

A stock solution of 4.10 mol dm^{-3} of sulphuric acid was standardised by titration with recrystallised sodium tetraborate, using methyl red as indicator [3.08]. This solution was subsequently diluted as required for the kinetic and equilibrium studies.

All solvents used in this work were of the same quality as those used in chapter 2.

(ii) KINETICS

The technique used to measure rate constants here and in all subsequent work in this thesis is the same as that used and fully described in chapter 2, details of which need not be repeated here. Kinetic runs were performed at 298.2 K , in a medium of 0.54 mol dm^{-3} sulphuric acid, in the thermostatted cell compartment of a Unicam SP800A recording spectrophotometer. The rates of change of optical density were measured at 508 nm , and all reactions were seen to go to completion, as evidenced by a final optical density of zero at 508 nm in the visible spectrum. In this kinetic study, the concentration of acid used was found to be sufficiently strong to effect complete dissociation of the iron(II) complex cation. First-order rate constants were measured in duplicate and calculated via a standard least-mean-squares program (Appendix 2, program no. 2).

(iii) EQUILIBRIUM STUDIES

All equilibrium solutions were prepared by adding 2 cm³ of stock iron(II) complex solution to a mixture of 4 cm³ of 0.50 mol dm⁻³ sulphuric acid (obtained by dilution of the standardised 4.1 mol dm⁻³ solution) and 4 cm³ of an appropriate mixture of water and co-solvent. By varying the composition of this last component, solvent mixtures of zero to 40% by volume of co-solvent were obtained, in an analogous manner to that described in chapter 2.

The resulting reaction mixtures, in clean stoppered flasks, were thoroughly agitated and suspended in a thermostatted water bath at 298.2 K overnight. The optical densities of the resulting equilibrium mixtures were measured at 508 nm on a Unicam SP800 recording spectrophotometer and were then measured periodically until constant values were observed. At the wavelength monitored, all components of the equilibrium mixtures except the $[\text{Fe}(\text{5-NO}_2\text{phen})_3]^{2+}$ cation gave no detectable visible absorption. All measurements were duplicated with fresh equilibrium mixtures using the original stock solutions of iron(II) complex and sulphuric acid.

The equilibrium constant K for the reaction (see equation 3.02) was measured as a function of the extent of reaction from optical density measurements of equilibrium mixtures and blank control solutions (containing no acid).

3.3 RESULTS AND DISCUSSION

(i) KINETICS

There have already been several investigations of the kinetics of aquation of the $[\text{Fe}(\text{5-NO}_2 \text{ phen})_3]^{2+}$ cation, equation (3.01), in binary aqueous mixtures. Organic co-solvents which have been used have included ethanol [3.03], t-butyl alcohol [3.04], 1,4-dioxan [3.05], acetonitrile [3.06] and formic acid [3.03]. In the solvent mixtures containing t-butyl alcohol and acetonitrile, detailed patterns of reactivity with solvent composition have been drawn, for various substituted derivatives of the $[\text{Fe}(\text{phen})_3]^{2+}$ cation. Detailed patterns for the dependence of the aquation rate constant on solvent composition for tetrahydrofuran-water and for dimethylsulphoxide-water solvent mixtures have also been studied [3.07]. These have been found to be very similar to those found earlier for t-butyl alcohol and acetonitrile.

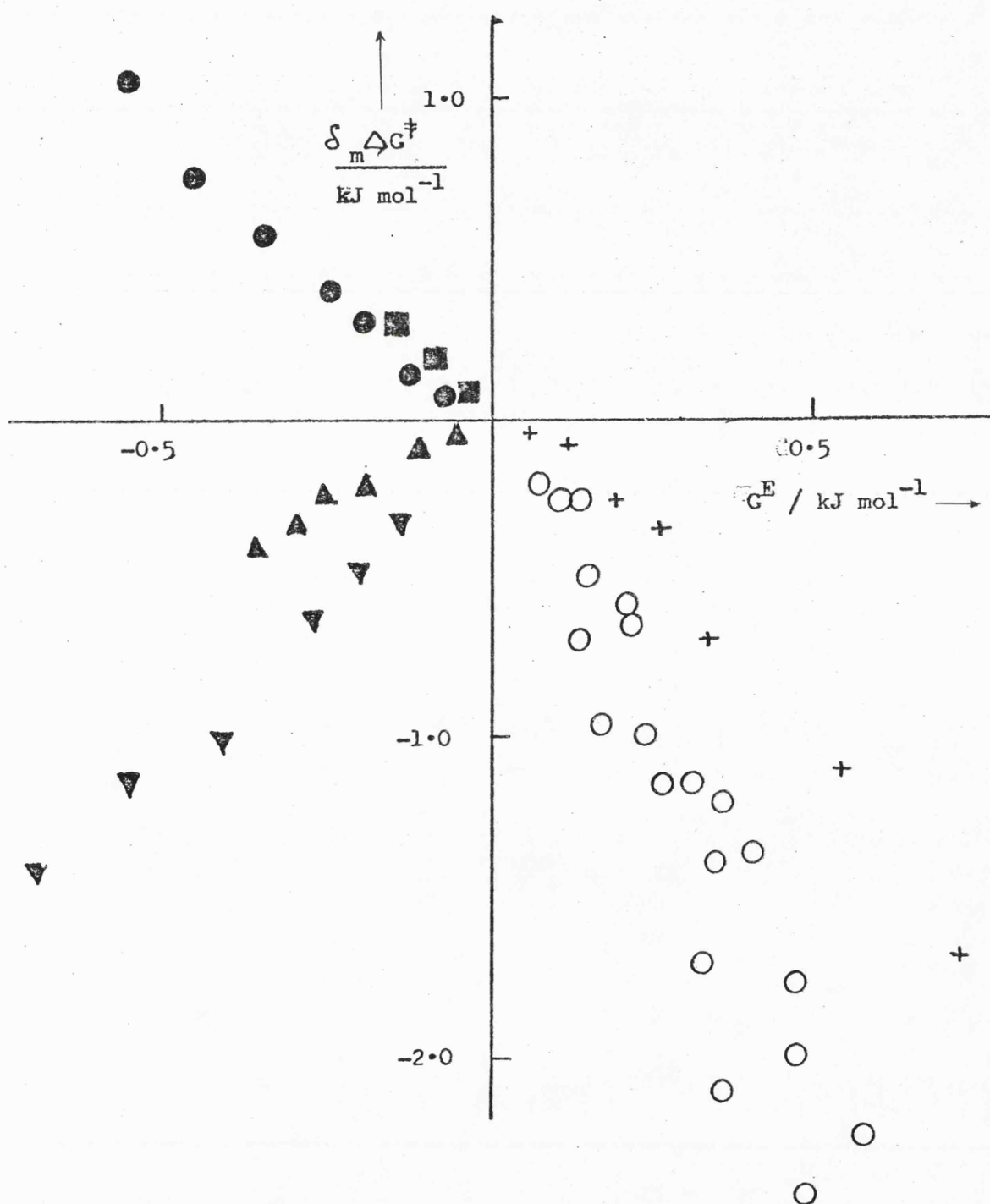
This work extends the range of co-solvents used to include aqueous-ethylene glycol and -glycerol mixtures, which are T.N.A.N. type solvent mixtures.

Observed first-order rate constants, k_{obs} for these solvent mixtures were measured at 298.2 K in 0.54 mol dm⁻³ sulphuric acid, and are reported in Table 3.01. It is seen that the rate constants increase slightly with molefraction of ethylene glycol, but decrease in aqueous glycerol solutions. Values of $\delta_m \Delta G^\ddagger$ have been calculated from these results (as described in chapter 1) and are also listed in Table 3.01. Figure 3.01 shows a plot of $\delta_m \Delta G^\ddagger$ versus G^E for the title reaction in a wide range of binary aqueous mixtures embracing the three groups, T.A., T.N.A.P. and T.N.A.N. of solvent mixtures. The results for solvent mixtures other than aqueous-ethylene glycol and -glycerol have been

TABLE 3.01 Observed first-order rate constants, $10^4 k_{\text{obs}}/\text{s}^{-1}$, for the acid aquation of the $[\text{Fe}(\text{5-NO}_2\text{phen})_3]^{2+}$ cation at 298.2 K, in a range of aqueous-ethylene glycol and -glycerol mixtures; $[\text{H}_2\text{SO}_4] = 0.54 \text{ mol dm}^{-3}$.

| Solvent Composition | mole fraction | $\frac{10^4 k_{\text{obs}}}{\text{s}^{-1}}$ | $\frac{\delta_m \Delta G^\ddagger}{\text{kJ mol}^{-1}}$ |
|------------------------|------------------|---|---|
| 5 | 0.023 | 4.9 | -0.04 |
| 10 | 0.047 | 5.0 | -0.08 |
| 20 % | 0.094 | 5.4 | -0.25 |
| 27 Ethylene | 0.139 | 5.4 | -0.25 |
| 30 glycol | 0.151 | 5.6 | -0.34 |
| 40 | 0.217 | 5.8 | -0.42 |
| 6 % | 0.017 | 4.7 | +0.09 |
| 12 Glycerol | 0.036 | 4.5 | +0.18 |
| 13 | 0.058 | 4.3 | +0.30 |

Figure 3.01 Dependence of $\delta_m \Delta G^\ddagger$ on G^E for the aquation of the $[\text{Fe}(\text{5-NO}_2\text{phen})_3]^{2+}$ cation. T.A. mixtures are represented by open circles, (O), T.N.A.P. mixtures by crosses, (+) and T.N.A.N. mixtures by solid symbols (●), hydrogen peroxide; (■), glycerol; (▲), ethylene glycol; (▼), dimethyl sulphoxide.



taken from ref. 3.07.

A clear feature of Figure 3.01 is the narrow sector occupied by the T.A. type solvent mixtures in the "+ ive G^E , - ive $\delta_m \Delta G^\ddagger$ " quadrant. This is analogous to the correlation found in the pentacyanoferrate(II) system studied in chapter 2. Further, the plot of $\delta_m \Delta G^\ddagger$ vs G^E for aqueous-acetonitrile mixtures (T.N.A.P. type) lies close to the T.A. results. Again the T.N.A.N. results do not fall on the T.A. correlation line. Although the aqueous-glycerol results here are found to behave in a similar manner to those in the study in chapter 2 (i.e. decreasing rate producing positive values of $\delta_m \Delta G^\ddagger$), those for aqueous-ethylene glycol mixtures are found to exhibit an increase in the rate constant (and hence a negative value of $\delta_m \Delta G^\ddagger$). Thus although we have mechanistically similar reactions in those of the acid aquation of the $[\text{Fe}(\text{5-NO}_2\text{phen})_3]^{2+}$ cation and substitution at $[\text{Fe}(\text{CN})_5\text{L}]^{n-}$ anions, the $\delta_m \Delta G^\ddagger / G^E$ correlations are not identical. One important feature however is the remarkable similarity in the behaviour of the T.A. type solvent mixtures.

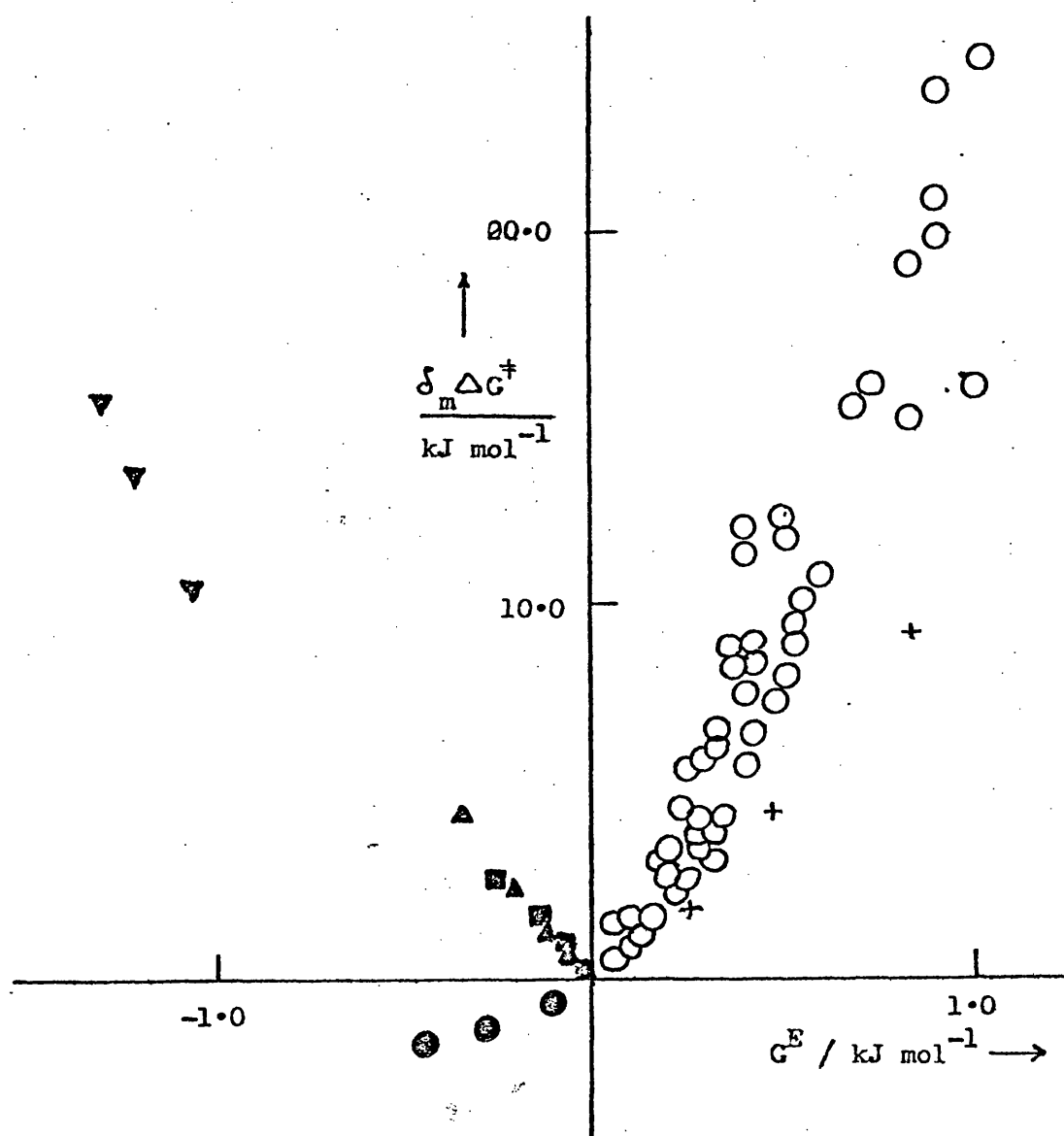
It is seen that the aquation reaction studied in this work is, like the substitution reaction of chapter 2, remarkably insensitive to solvent composition. This property may be explained in a similar fashion to the previous example. That is, the solvation properties of the initial state reactants must be similar to those of the transition state of the reaction. This is reasonable when one considers that the reaction proceeds by elongation of the iron-nitrogen bonds of the dissociating 5-NO₂phen ligand by 35% [3.02] to form the transition state. Thus the transition state solvation, and hence $\delta_m \mu^\oplus(\text{T.S.})^\dagger$ will be very similar

[†] [$\delta_m \mu^\oplus(\text{T.S.})$ is the free energy of transfer of the transition state - see chapter 1.]

to that of the initial state $[\text{Fe}(\text{5-NO}_2\text{phen})_3]^{2+}$ species, the proton having taken no part in this rate determining step. The elongation of the iron-nitrogen bonds mentioned above will expose more of the hydrophobic periphery of the 5-NO₂phen ligand, thus enhancing the stabilisation of the transition state relative to the initial state somewhat [3.09], hence producing a slightly more favourable transfer of the transition state from water into binary aqueous mixtures than that of the initial state. This leads to a slight rate enhancement on addition of co-solvent to the reaction solution.

In view of the similarity in mechanism of the above two inorganic reactions to that of the solvolysis of t-butyl chloride, $\delta_m\Delta G^\ddagger$ vs G^E plots for the last example in a range of binary aqueous mixtures have been compiled and compared with the former two examples. Kinetic data for this solvolysis reaction are available for binary aqueous mixtures containing the co-solvents methanol [3.10,3.11], ethanol [3.10,3.12], t-butyl alcohol [3.12], tetrahydrofuran [3.13], 1,4-dioxan [3.10,3.12], acetone [3.10,3.14], acetonitrile [3.13], dimethylsulphoxide [3.15], ethylene glycol [3.16], glycerol [3.16] and hydrogen peroxide [3.17]. Values of $\delta_m\Delta G^\ddagger$ and G^E for these systems have been calculated by Dr. M. J. Blandamer, and have been plotted in Figure 3.02. For the solvolysis of t-butyl chloride, the same clustering of points for T.A. mixtures in one narrow sector is observed, and again the results for T.N.A.P. mixtures containing acetonitrile are close to these. However, the T.A. sector is in a different quadrant from those of the inorganic examples above. This difference may be attributed to the different natures of the respective leaving groups. In the case of the $[\text{Fe}(\text{5-NO}_2\text{phen})_3]^{2+}/\text{H}^+$ system, exposure of the more hydrophobic periphery of the 5-NO₂phen ligand as it departs from the iron atom renders the transition state

Figure 3.02 Dependence of $\delta_m \Delta G^\ddagger$ on G^E for the solvolysis of t-butyl chloride; symbols as in Figure 3.01.



more hydrophobic than the initial state, as described in the previous paragraph. In contrast, the hydrophilic nature of the chloride ion which departs in the solvolysis of t-butyl chloride renders the transition state more hydrophilic than the initial state. Thus the initial state is stabilised relative to the transition state on adding co-solvent to the system, producing a retardation of the reaction relative to that in aqueous solution.

The solvolysis of t-butyl chloride is also more sensitive to added co-solvent than the reaction of the iron(II) complex. This is because of the charge separation produced in the transition state relative to the initial state, due to the separation of the Cl^- ion from the tBu^+ moiety. The consequent changes in chemical potentials of these species, and hence of $\delta_m \Delta G^\ddagger$ produce greater changes in observed rate constants for the reaction.

Hence it may be concluded that although the clustering of results for T.A. solvent mixtures (and to some extent T.N.A.P. ones) seems to occur for several reactions, this correlation pattern appears simply to be some function of the physical characteristics of the solvent mixtures, rather than a feature of the mechanism by which the reactions occur.

A further example of a $\delta_m \Delta G^\ddagger$ vs G^E correlation for an inorganic reaction is the very recent study [3.18] of solvent effects on the reaction portrayed by equation (3.03)



(Et_4dien = N,N,N'',N''-tetraethyldiethylenetriamine)

This reaction, unlike most substitutions at square-planar centres, is dissociative. This is due to drastic steric hindrance of the incoming nucleophile by the very bulky ethyl-substituted ligand. Thus the approach

of, in this case Br^- to the metal centre is prevented, thus precluding the formation of an associative transition state.

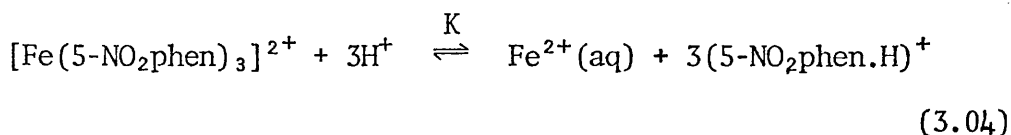
Here, a pattern emerged which was analogous to the solvolysis of t-butyl chloride, the rate of the reaction decreasing on addition of organic co-solvent for all solvent mixtures studied. The T.A. results all fell into one narrow sector, with the T.N.A.P. results being very similar. Again the T.N.A.N. results were found to be anomalous, as they were for the systems discussed in this work.

A detailed study of the solvation characteristics of the initial state species and the transition state for a series of bimolecular inorganic reactions[†] has been carried out in chapter 5. Although the mechanism operating in these systems is very different from the dissociative-type ones of this chapter and chapter 2, correlations between $\delta_m \Delta G^\ddagger$ and G^E have been drawn, and compared with the above dissociative-type systems above.

(ii) EQUILIBRIUM STUDIES

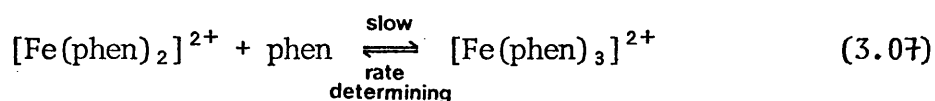
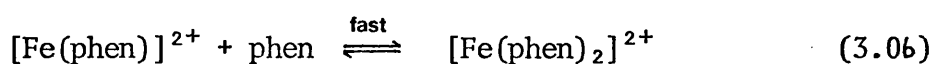
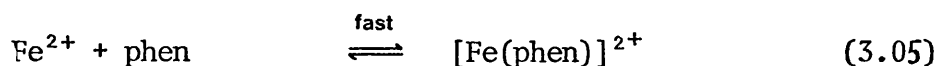
As was noted in the introduction to this chapter, the acid aquation of the $[\text{Fe}(\text{5-NO}_2\text{phen})_3]^{2+}$ cation has been observed to go to equilibrium rather than to complete dissociation in weakly acid solutions in binary aqueous mixtures [3.07]. In this work the equilibrium has been studied in a range of binary aqueous mixtures, and may be represented by equation (3.04)

[†] [These are in fact metal-ion catalysed aquations, where the mechanism is actually $S_E 2$ at the catalysing metal-centre.]



where K is the equilibrium constant. K can theoretically be determined from the ratio of the forward and reverse rate constants, $k_{\text{diss}}/k_{\text{form}}$, where k_{diss} is the rate constant for the acid aquation reaction of the $[\text{Fe}(\text{5-NO}_2\text{phen})_3]^{2+}$ cation, and k_{form} is that for the formation reaction of the complex cation from iron(II) ions and the 5-NO₂phen ligand.

Unfortunately, the kinetic nature of the formation reaction makes the measurement of k_{form} experimentally difficult. This reaction has been thoroughly studied for the analogous 1,10-phenanthroline complex [3.01]. It has been found that the reaction is fourth-order, being first-order in iron(II) and third-order in 1,10-phen, the mechanism being represented by equations (3.05-3.07)[†]



the rate law being:-

$$\text{rate} = k_{\text{form.}} [\text{Fe}^{2+}] [\text{phen}]^3 \quad (3.08)$$

In acid solution the equilibria shown in equations (3.05-3.07) are

[†] [co-ordinated water is ignored.]

all displaced to the left, as the ligand is removed from the system in the protonated form, $(\text{phen.H})^+$ which will not coordinate with iron(II) ions. In order to estimate $K = k_{\text{diss}}/k_{\text{form}}$, the dissociation and formation rate constants would have to be measured under similar conditions. Thus as the dissociation of the complex occurs in acidic solution, so the reverse reaction would have to be studied in a similar medium. This would produce protonated ligand which would not complex with the iron(II) ion present. Also the reaction is third-order in ligand, so to set up pseudo-first-order conditions, a vast excess of ligand would be required, which is not feasible owing to solubility problems.[†]

Fortunately, the equilibrium described by equation (3.04) can easily be studied, as K is a function of the concentration of $[\text{Fe}(\text{5-NO}_2\text{phen})_3]^{2+}$ cation present at equilibrium. This may be seen from the following simple calculation:-

Consider the equilibrium:-



Then the equilibrium constant K' is defined as

$$K' = \frac{[\text{C}][\text{D}]^3}{[\text{A}][\text{B}]^3} \text{ at equilibrium,} \quad (3.10)$$

assuming the activity coefficients are unity for all species, for simplicity. If we have an initial concentration of A, $[\text{A}]_0 = a$ moles, and at equilibrium, $[\text{A}]_e = (a-x)$ moles, then at equilibrium,

[†] [The solubility of 5-NO₂phen in water is measured in chapter 4 as $1.21 \times 10^{-4} \text{ mol dm}^{-3}$ at 298.2 K.]

$$[A]_e = (a-x); \quad [B]_e = 3x; \quad [C]_e = x; \quad \text{and } [D] = 3x \quad \text{moles}$$

and

$$K' = \frac{x \cdot (3x)^2}{(a-x) \cdot (3x)^2} = \frac{x}{(a-x)} \quad (3.11)$$

now

$$\Delta G^\ominus = -RT \ln K', \quad (3.12)$$

∴ from equation (3.11),

$$\Delta G^\ominus = +RT \ln \left(\frac{(a-x)}{x} \right) \quad (3.13)$$

Since the iron(II) complex obeys Beer's Law, i.e. the optical density in the visible spectrum is proportional to the concentration of complex present, then from equation (3.13),

$$\Delta G^\ominus = RT \ln \left(\frac{OD_o - \Delta OD}{\Delta OD} \right) \quad (3.14)$$

where OD_o is the optical density of a control solution,[†] and ΔOD is the difference between OD_o and the optical density of a reaction mixture at equilibrium.

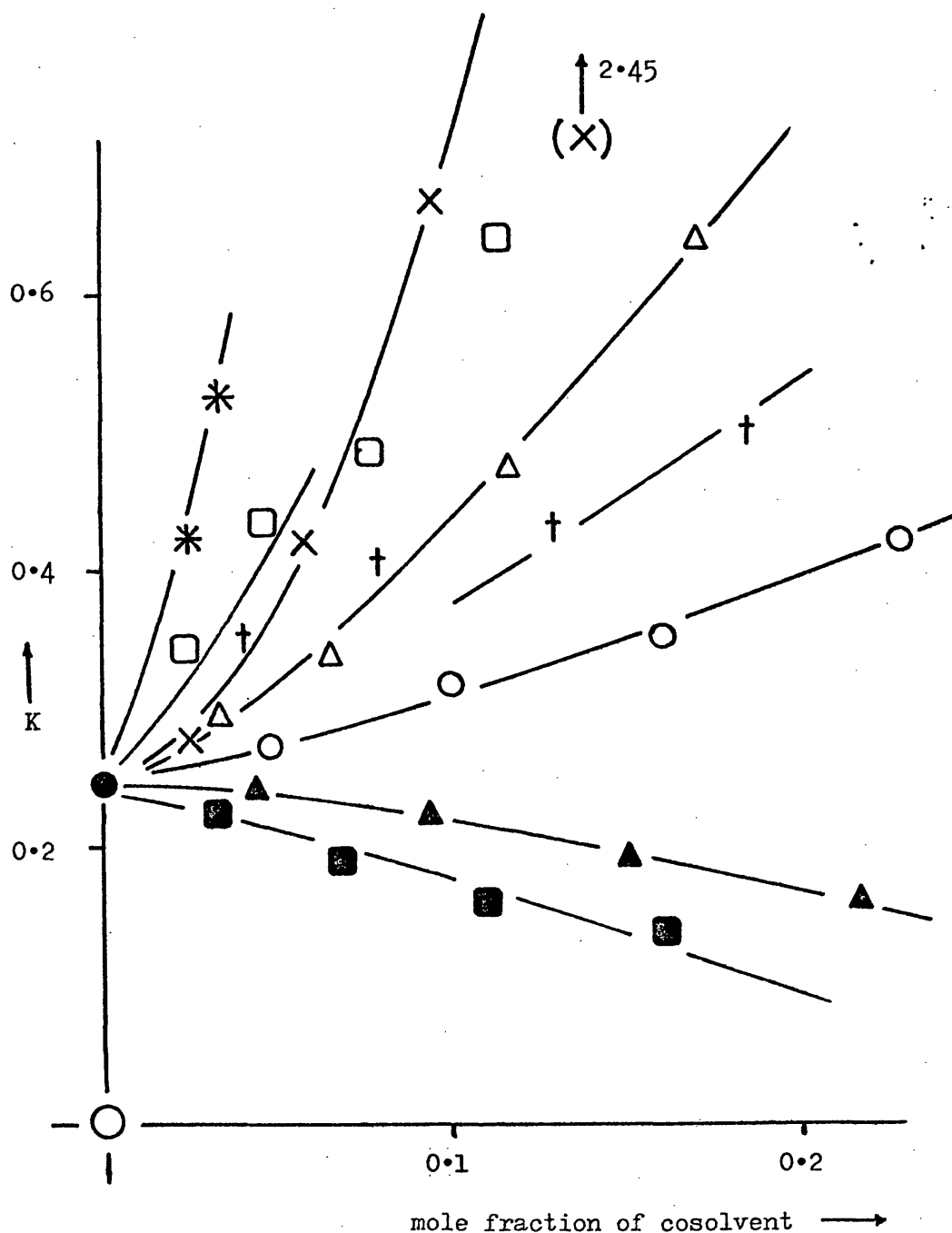
The optical density measurements required for calculation of ΔG^\ominus in a wide range of binary aqueous mixtures were made at 298.2 K, and have been listed in Table 3.02, together with the calculated values of the equilibrium constant (from equation (3.11)) and the consequent ΔG^\ominus . Figure 3.03 illustrates the variation of K with molefraction of co-solvent. This clearly shows the displacement of the equilibrium (equation 3.04) to the left on introduction of organic co-solvents to the system. This

[†] [i.e. a solution containing the same concentration of complex as the equilibrium mixtures on mixing, but no acid.]

TABLE 3.02 Optical density values of equilibrium mixtures in binary aqueous solutions for the $[\text{Fe}(\text{5-NO}_2\text{phen})_3]^{2+}/\text{H}^+$ system at 298.2 K; $[\text{H}_2\text{SO}_4] = 0.20 \text{ mol dm}^{-3}$; initial O.D. = 1.62 absorbance units. Calculated equilibrium constants, K, and standard Gibbs free energies, ΔG^\ominus , are also listed.

| Solvent Composition | O.D. | K | $\Delta G^\ominus/\text{kJ mol}^{-1}$ |
|---------------------|-------|-------|---------------------------------------|
| 10 | 0.345 | 0.271 | 3.24 |
| 20 % Methanol | 0.390 | 0.317 | 2.85 |
| 30 | 0.420 | 0.350 | 2.60 |
| 40 | 0.480 | 0.421 | 2.16 |
| 10 | 0.370 | 0.296 | 3.02 |
| 20 % Ethanol | 0.410 | 0.339 | 2.68 |
| 30 | 0.520 | 0.473 | 1.86 |
| 40 | 0.660 | 0.688 | 0.93 |
| 10 | 0.415 | 0.344 | 2.65 |
| 20 % | 0.490 | 0.434 | 2.07 |
| 30 t-Butyl alcohol | 0.530 | 0.486 | 1.79 |
| 40 | 0.660 | 0.688 | 0.93 |
| 10 | 0.320 | 0.246 | 3.48 |
| 20 % | 0.290 | 0.218 | 3.78 |
| 30 Ethylene glycol | 0.260 | 0.191 | 4.10 |
| 40 | 0.224 | 0.160 | 4.54 |
| 10 | 0.300 | 0.227 | 3.68 |
| 20 % Glycerol | 0.255 | 0.187 | 4.16 |
| 30 | 0.220 | 0.157 | 4.59 |
| 40 | 0.195 | 0.137 | 4.93 |
| 10 | 0.350 | 0.276 | 3.19 |
| 20 % Acetone | 0.480 | 0.421 | 2.16 |
| 30 | 0.650 | 0.670 | 0.99 |
| 40 | 1.15 | 2.45 | -2.22 |
| 10 | 0.350 | 0.276 | 3.19 |
| 20 % Dimethyl | 0.360 | 0.286 | 3.10 |
| 30 sulphoxide | 0.390 | 0.317 | 2.85 |
| 40 | 0.450 | 0.385 | 2.37 |
| 10 | 0.430 | 0.361 | 2.53 |
| 20 % Acetonitrile | 0.470 | 0.409 | 2.22 |
| 30 | 0.490 | 0.434 | 2.07 |
| 40 | 0.540 | 0.500 | 1.72 |
| 10 | 0.480 | 0.421 | 2.16 |
| 20 Tetrahydrofuran | 0.560 | 0.528 | 1.58 |
| Water | 0.320 | 0.246 | 3.48 |

Figure 3.03 Dependence of the equilibrium constant, K , on solvent composition for equilibrium mixtures of $[\text{Fe}(5\text{-NOphen})_3]^{2+}$ / sulphuric acid, in a range of binary aqueous mixtures at 298.2K. Cosolvents used are methanol(\circ), ethanol(Δ), t-butyl alcohol(\square), ethylene glycol(\blacktriangle), glycerol(\blacksquare), acetone(\times) and acetonitrile(\dagger); (\bullet) = solvent water; ($*$) = cosolvent tetrahydrofuran.



displacement may be explained in terms of the relative solvation characteristics of the participant species. Considering firstly the aquation products, $\text{Fe}^{2+}(\text{aq})$ and $(5\text{-NO}_2\text{phen.H})^+$; the former is most certainly hydrophilic, and will be greatly destabilised in binary aqueous mixtures, relative to water, i.e. it will have a positive free energy of transfer, $\delta_{\text{m}}^{\ominus}$. In the case of the protonated ligand, although the periphery of the ligand is strongly hydrophobic, it is still ionic, and may be expected to behave accordingly. This is not too unreasonable in the light of the solubility properties of some protonated amines, for example, ethylenediamine dihydrochloride [3.19], and cyclam.3.5 HCl [3.20], and hence hydrophilicity.

Secondly, although the reactants $[\text{Fe}(5\text{-NO}_2\text{phen})_3]^{2+}$ and H^+ are charged, there is evidence to indicate some hydrophobic nature. In the case of the proton, Wells [3.21] has calculated the single-ion free energy of transfer, $\delta_{\text{m}}^{\ominus}(\text{H}^+)$ from water into several binary aqueous mixtures. The results indicate a stabilisation in free energy for the transfer, for example $\delta_{\text{m}}^{\ominus}(\text{H}^+)$ for 50% by weight aqueous methanol has a value of $-6.75 \text{ kJ mol}^{-1}$ [3.21].

If we consider the $[\text{Fe}(\text{phen})_3]^{2+}$ cation, the solubilities of the perchlorate salt in a range of binary aqueous mixtures have been measured [3.22], from which single-ion free energies of transfer of the cation can be calculated (for the mixtures where values of $\delta_{\text{m}}^{\ominus}(\text{ClO}_4^-)$ are available - see chapter 4). The results indicate a very strong stabilisation of the cation in such mixtures relative to water. This is also supported by the observation that salts of $[\text{Fe}(\text{phen})_3]^{2+}$ will dissolve in pure organic solvents such as nitrobenzene, dimethyl

sulphoxide and N,N -dimethyl formamide[†] despite the unfavourable anion solvation in non-aqueous media.

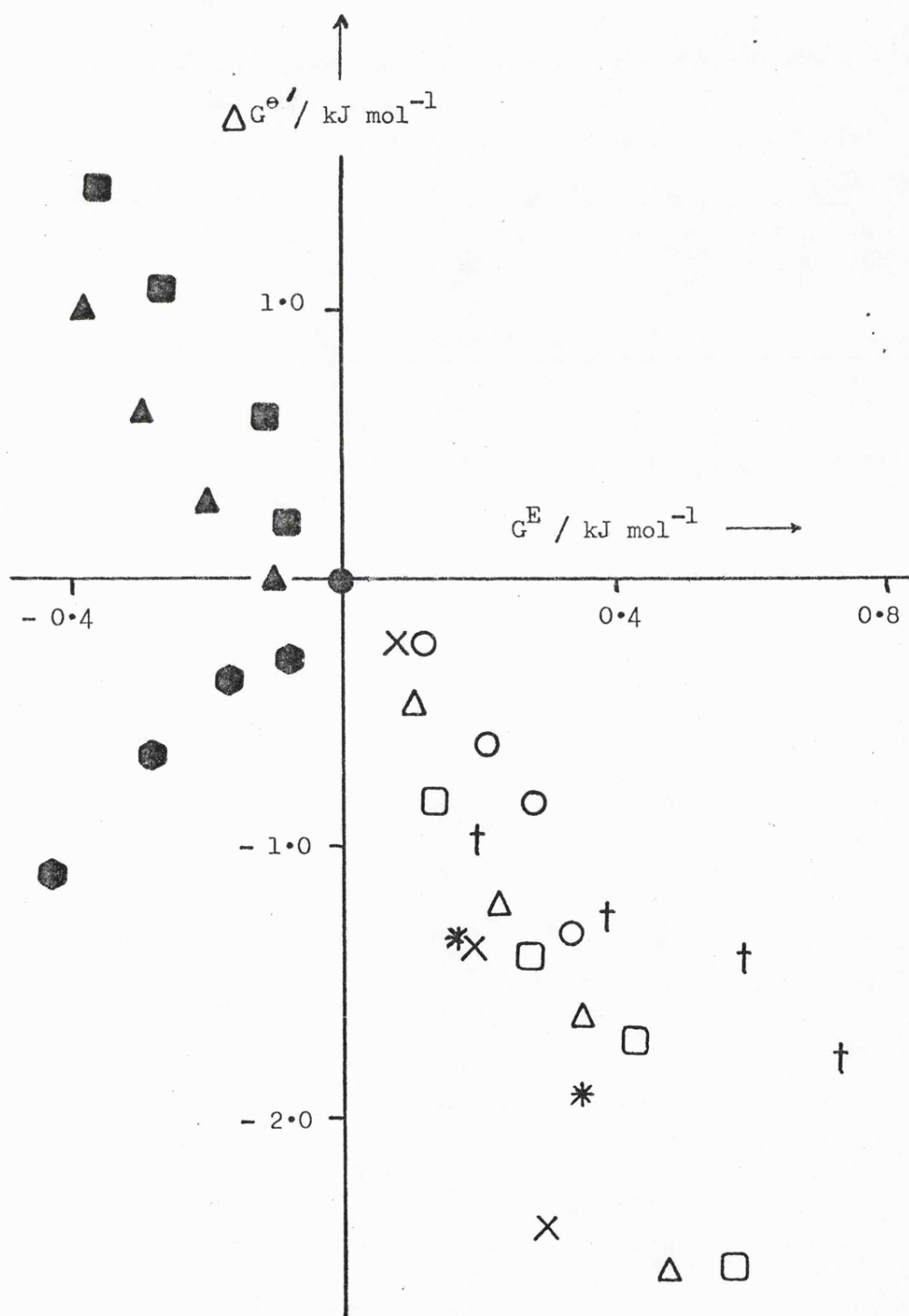
Hence by combining the properties of the participant species of the equilibrium (equation (3.04)) we can see that the introduction of an organic co-solvent to the system should tend to stabilise the reactants rather than the aquation products, and so displace the equilibrium to the left. We can see that this is so for all the co-solvents used except the T.N.A.N. solvent mixtures of aqueous-ethylene glycol and -glycerol.

The results may be presented in terms of ΔG^\ominus correlated with G^E for the respective solvent mixtures. Figure 3.04 is such a plot, in which we see the trend in T.A. results which was typical of the kinetic studies on the acid aquation reaction earlier in this chapter. Again the T.N.A.N. results are anomalous - a now not uncommon observation. Figure 3.04 may be directly compared with the analogous plot for the equilibrium, described by equation (3.02), which was studied in chapter 2 (Figure 2.08). We see a remarkable similarity between these two systems, not only the recognised T.A. correlation sector being common to both, but also the behaviour of anomalous T.N.A.N. results.

Thus we find that the effects of adding organic co-solvents to reacting systems appear to take on some consistent behaviours. That is, all 'typically aqueous' solvent mixtures appear to have the same general effect on reaction rates and equilibria regardless of the mechanisms operating, at least for those reactions mentioned above. The

[†][Indeed, the solubility of the hexachlororhenate salt has been measured in these solvents and in a range of binary aqueous mixtures, which is reported in chapter 4.]

Figure 3.04 Solvent dependence of $\Delta G^{\ominus'}$ ($= \Delta G^{\ominus}_{x_2} - \Delta G^{\ominus}_{x_2=0}$) for the $[\text{Fe}(\text{5-NO}_2\text{phen})_3]^{2+}/\text{H}^+$ equilibrium system as a function of G^{E} , at 298.2 K. Symbols as in Figure 3.03; (\bullet) = dimethyl sulphoxide cosolvent.



behaviour of the 'typically non-aqueous' mixtures appears somewhat more complicated, the T.N.A.P. type having a similar effect to the T.A. ones, but the T.N.A.N. type seem variable to an extent.

These behaviours seem to be a property of the physical nature of the solvent mixtures. The observed trends in changes of reaction parameters (both kinetic and thermodynamic) with solvent composition appear to be explicable in terms of the free energy changes of the participant species on transfer from water to the solvent mixtures, which are a function of the solvation characteristics of these species.

CHAPTER 4

Solubilities and Solvation Characteristics of
Selected Inorganic and Organic Compounds in
Binary Aqueous Mixtures.

4.1 INTRODUCTION

In later chapters of this thesis, solvent effects on the kinetic behaviour of several selected inorganic reactions have been studied, and discussed in terms of the solvation characteristics of the reacting species and of the transition states formed in these reactions. The thermodynamic parameters concerning the solvation characteristics of the initial state species, i.e. the Gibbs free energy of transfer from water into an appropriate binary aqueous mixture in this work, $\delta_{\text{m}\mu}^{\ominus}$ (I.S.), may be calculated from solubility data on the appropriate species. As has been pointed out in chapter 1, such a parameter is difficult to estimate when the initial state species are ionic. However, estimations of single-ion values have been made [4.01,02] by using various assumptions concerning the solvation properties of the constituent ions.

In this work, studies have been made on the solubility trends of selected compounds in binary aqueous mixtures or in aqueous salt solutions. The former study includes the mercury(II) and caesium tetraphenylborate salts, $\text{Hg}(\text{BPh}_4)_2$ and CsBPh_4 . Here, using literature single-ion values for $\delta_{\text{m}\mu}^{\ominus}(\text{Cs}^+)$, $\delta_{\text{m}\mu}^{\ominus}(\text{BPh}_4^-)$ and consequently $\delta_{\text{m}\mu}^{\ominus}(\text{Hg}^{2+})$ have been estimated for transfer from water into several binary aqueous mixtures. Similarly, from data available [4.03] on the solubilities of caesium hexachlororhenate, Cs_2ReCl_6 , estimates have been made for values of $\delta_{\text{m}\mu}^{\ominus}(\text{ReCl}_6^{2-})$. The solubilities of the salts $[\text{Fe}(\text{phen})_3](\text{ReCl}_6)$ and $\text{MgReCl}_6 \cdot 6\text{H}_2\text{O}$ have also been measured in binary aqueous mixtures, and attempts to split the free energies of transfer of the salts into single-ion values have been made. This has involved using both literature data on solubilities of $[\text{Fe}(\text{phen})_3](\text{ClO}_4)_2$ [4.04], and making new assumptions

concerning the relative solvation of the ions involved. The resulting values of $\delta_{\text{m}\mu}^{\ominus}(\text{Hg}^{2+})$ and $\delta_{\text{m}\mu}^{\ominus}(\text{ReCl}_6^{2-})$ have been utilised in chapter 5 in the discussion of solvent effects on the mercury(II)-catalysed aquation of the ReCl_6^{2-} anion.

In chapter 6, the peroxodisulphate oxidation of the $[\text{Fe}(\text{phen})_3]^{2+}$ cation is studied in binary aqueous mixtures. Determinations of $\delta_{\text{m}\mu}^{\ominus}$ (I.S.) for this reaction in these mixtures are made from estimated values of $\delta_{\text{m}\mu}^{\ominus}(\text{S}_2\text{O}_8^{2-})$ and $\delta_{\text{m}\mu}^{\ominus}([\text{Fe}(\text{phen})_3]^{2+})$. These parameters have been estimated in this chapter from solubility measurements of $\text{K}_2\text{S}_2\text{O}_8$ and literature data for $\delta_{\text{m}\mu}^{\ominus}(\text{K}^+)$ [4.01], and from solubilities of $[\text{Fe}(\text{phen})_3](\text{ClO}_4)_2$ in binary aqueous mixtures [4.04] and literature values of $\delta_{\text{m}\mu}^{\ominus}(\text{ClO}_4^-)$ [4.01].

Salt effects on the solubility of a compound having an ambiguous constitution have been investigated in order to determine the electrolytic (or otherwise) nature of the compound.

The solubility of the important and widely used ligand 2,2'-bipyridyl in aqueous solution has been established over the temperature range 273.2 to 333.2 K by Bennetto & Letcher [4.05]. Data on the solubility of the closely related, and equally important ligand, 1,10-phenanthroline, and of substituted 1,10-phenanthrolines, are sparse. In this work, a study of the solubility of 1,10-phenanthroline monohydrate in water at various temperatures has led to a value for the heat of solution of this material. Its solubility in several aqueous methanol mixtures has produced values of $\delta_{\text{m}\mu}^{\ominus}(\text{phen.H}_2\text{O})$, to compare with values of this parameter for the $\text{Fe}(\text{phen})_2(\text{CN})_2$ and $[\text{Fe}(\text{phen})_3]^{2+}$. Substituent effects on the solubilities of phenanthrolines have been studied, and discussed in terms of relative molecular volumes of the various substituted compounds.

4.2 EXPERIMENTAL

(i) REAGENTS

Preparations

Magnesium hexachlororhenate hexahydrate and tris-(1,10-phenanthroline)iron(II) hexachlororhenate were prepared as described in chapter 7. The complex of the form ' $\text{Fe}(5\text{-NO}_2\text{phen.CN})_2(5\text{-NO}_2\text{phen})$ ' was prepared as described in chapter 9.

Mercury(II) tetraphenylborate, $\text{Hg}(\text{BPh}_4)_2$ was prepared as follows:-

To 10 cm³ of a 0.1 mol dm⁻³ perchloric acid solution of 0.45 g(1 mmol) of mercury(II) perchlorate trihydrate (K & K Laboratories) was added with stirring a filtered aqueous solution (10 cm³) of 0.68 g(2 mmol) of sodium tetraphenylborate (B.D.H.) at room temperature. The precipitated white product was filtered, washed copiously with water, and recrystallised three times from water-rich ethanol-water mixtures. The long white needles produced were washed with water and dried in vacuo over phosphorus pentoxide for two days in the dark. This compound was analysed spectrophotometrically for BPh_4^- content ($\epsilon_{\text{max}} = 2970$ at 267 nm in ethanol [4.06]). The results of this analysis are, for $\text{Hg}(\text{BPh}_4)_2$, %(BPh_4^-) calc. = 76.1, % found = 76.6, 76.4.

Caesium tetraphenylborate, CsBPh_4 , was prepared in a similar manner to the mercury(II) salt, but using neutral conditions, from aqueous solutions of caesium chloride and sodium tetraphenylborate. Analysis:- %(BPh_4^-) calc. = 70.63, % found = 70.72, 70.70.

Solvents and Other Reagents

All solvents used were of the same quality as those mentioned in

chapter 2.

AnalaR grade potassium peroxodisulphate, which was supplied by B.D.H., was used as received. 1,10-Phenanthroline and its substituted derivatives were supplied by G. F. Smith and were recrystallised from ethanol-water mixtures prior to use. The alkali metal chlorides used in the study of salt effects on solubilities were AnalaR grade materials (B.D.H.), and were used without further purification.

(ii) SOLUBILITIES

Saturated Solutions

An excess of the solid sample to be studied was added to the appropriate solvent mixture (expressed as % by volume of co-solvent before mixing) or salt solution in a stoppered flask suspended in a thermostatted water bath at 298.2 K. The flasks were agitated periodically, and the solutions were allowed to equilibrate for sufficient periods of time. Such periods ranged from three weeks in the case of the phenanthrolines to four hours for the ReCl_6^{2-} salts. This latter short equilibration time was necessary due to the decomposition of ReCl_6^{2-} in aqueous solution (see chapter 5), and necessitated continuous agitation of the mixtures. These equilibration times were arrived at by periodic monitoring of the concentrations of solute by the methods mentioned below, until constant values were achieved.

Measurement

The solubilities of $\text{Hg}(\text{BPh}_4)_2$ and CsBPh_4 were measured spectrophotometrically on a Pye Unicam SP800A recording spectrophotometer,

using 1 cm path length silica cells. The wavelength of maximum absorption for the anion monitored was 267 nm ($\epsilon_{\max} = 2970$ in ethanol [4.06]). Aliquots of filtered, saturated solution of the compound in the appropriate mixture were diluted with ethanol until a suitably measurable absorbance at 267 nm was observed. The concentration of the saturated solution was then calculated using Beer's Law:-

$$c = \epsilon_{\max} A.l \quad (4.01)$$

where c = concentration of solute in mol dm^{-3} , ϵ_{\max} = extinction coefficient, A = absorbance and l = path length = 1 cm.

The solubilities of the substituted phenanthrolines were also measured by this method, the wavelength of maximum absorption monitored for these compounds, and their extinction coefficients at these wavelengths being listed below:-

| Compound | λ_{\max}/nm | ϵ_{\max} |
|------------------------------|----------------------------|-------------------|
| phen | 267 | 25060 |
| 5-NO ₂ phen | 260 | 28410 |
| 4,7-Me ₂ phen | 273 | 37490 |
| 4,7-Ph ₂ phen | 274 | 42560 |
| 3,4,7,8-Me ₄ phen | 278 | 41590 |

The solubilities of $[\text{Fe}(\text{phen})_3][\text{ReCl}_6]$ were measured spectrophotometrically, using the charge-transfer band at 510 nm due to the $[\text{Fe}(\text{phen})_3]^{2+}$ cation ($\epsilon_{\max} = 11100$ [4.07]). At this wavelength there is no observable absorption due to the $[\text{ReCl}_6]^{2-}$ cation.

The solubilities of the ' $\text{Fe}(5\text{-NO}_2\text{phen.CN})_2(5\text{-NO}_2\text{phen})$ ' type compound were measured by atomic absorption spectrophotometry. Suitably diluted

aliquots of the appropriate solutions were prepared in a similar manner to those for the $\text{Hg}(\text{BPh}_4)_2$ case, and analysed for iron content on a Perkin Elmer 360 atomic absorption spectrophotometer, using the 273.2 nm wavelength band. The spectrophotometer was calibrated using standard potassium hexacyanoferrate(II) solutions, having concentration ranging between 10 and 100 $\mu\text{g cm}^{-3}$ of iron.

The solubilities of potassium peroxodisulphate

were measured by means of flame photometry, using a potassium filter. The photometer (EEL Model) was calibrated using standard solutions of potassium sulphate, containing between 0.05 and 1.00 g dm^{-3} of potassium, at 0.05 g dm^{-3} intervals. This range was necessary due to the curvature in the plot of %age emission vs. [K] observed.

All solubility determinations were performed at least in duplicate using fresh solutions and reagents for each set of determinations.

4.3 RESULTS AND DISCUSSION

The kinetics of the oxidation of the $[\text{Fe}(\text{phen})_3]^{2+}$ cation by peroxodisulphate, $\text{S}_2\text{O}_8^{2-}$, in a wide range of binary aqueous mixtures are reported in chapter 6. An integral part of the discussion of such a study is a knowledge of the solvation characteristics of the initial state of the reaction, i.e. of the free energies of transfer of the reacting species, $\delta_{\text{m}\mu}^\ominus ([\text{Fe}(\text{phen})_3]^{2+})$ and $\delta_{\text{m}\mu}^\ominus (\text{S}_2\text{O}_8^{2-})$. These parameters may be calculated from solubility data on appropriate compounds, as was described in chapter 1.

Values of $\delta_{\text{m}\mu}^\ominus ([\text{Fe}(\text{phen})_3]^{2+})$ have been estimated from solubility

data on the perchlorate salt in some binary aqueous mixtures [4.04], using literature values of $\delta_{\text{m}\mu}^{\ominus}(\text{ClO}_4^-)$ [4.01], and are listed in Table 4.04(b). Values of $\delta_{\text{m}\mu}^{\ominus}(\text{S}_2\text{O}_8^{2-})$ have similarly been arrived at via solubilities of $\text{K}_2\text{S}_2\text{O}_8$ and literature values of $\delta_{\text{m}\mu}^{\ominus}(\text{K}^+)$ [4.01].

(i) Potassium Peroxodisulphate

The solubilities of this salt were measured at 298.2 K in aqueous solution and in a range of binary aqueous mixtures. The value in aqueous solution, measured by analysis of the saturated solution for content of potassium by flame photometry was found to be 5.78 or 5.90 g/100 cm³. These results compare very favourably with a literature value of 5.84 g/100 cm³ [4.08]. Table 4.01 lists these measured solubilities, together with the consequently calculated free energies of transfer of the salt from water into the binary aqueous mixtures employed, $\delta_{\text{m}\mu}^{\ominus}(\text{K}_2\text{S}_2\text{O}_8)$ at 298.2 K. From these results we see that, as expected for an electrolyte, the solubility decreases with increasing mole fraction of cosolvent, thus $\delta_{\text{m}\mu}^{\ominus}(\text{K}_2\text{S}_2\text{O}_8)$ becomes correspondingly more positive indicating destabilisation of the salt in more organic mixtures.

The single-ion free energy of transfer of the peroxodisulphate anion, $\delta_{\text{m}\mu}^{\ominus}(\text{S}_2\text{O}_8^{2-})$ can be calculated from the expression:

$$\delta_{\text{m}\mu}^{\ominus}(\text{K}_2\text{S}_2\text{O}_8) = 2 \delta_{\text{m}\mu}^{\ominus}(\text{K}^+) + \delta_{\text{m}\mu}^{\ominus}(\text{S}_2\text{O}_8^{2-}). \quad (4.02)$$

since values of $\delta_{\text{m}\mu}^{\ominus}(\text{K}^+)$ are available in the literature [4.01] for certain binary aqueous mixtures. Table 4.01 includes such values for the K^+ ion together with the calculated values of $\delta_{\text{m}\mu}^{\ominus}(\text{S}_2\text{O}_8^{2-})$ in the various aqueous-methanol and -acetone mixtures used.

TABLE 4.01 Solubility measurements and calculated free energies of transfer of $K_2S_2O_8$ in water and in several binary aqueous mixtures, together with calculated single-ion transfer functions in these mixtures at 298.2 K.

| Solvent Mixture | Solubility $\frac{\text{mol dm}^{-3}}$ | $\frac{\delta_m \mu(K_2S_2O_8)}{\text{kJ mol}^{-1}}$ | $\frac{\delta_m \mu(K^+)^a}{\text{kJ mol}^{-1}}$ | $\frac{\delta_m \mu(S_2O_8^{2-})}{\text{kJ mol}^{-1}}$ |
|--------------------|---|--|--|--|
| Water | 0.216 | 0.0 | 0 | 0 |
| 10 | 0.153 | + 2.57 | + 0.34 | + 1.89 |
| 20 | 0.105 | + 5.37 | + 0.63 | + 4.11 |
| 30 Methanol | 0.077 | + 7.67 | + 0.92 | + 5.83 |
| 40 | 0.045 | +11.67 | + 1.12 | + 9.43 |
| 10 | 0.192 | + 0.88 | - 0.15 | + 1.18 |
| 20 | 0.160 | + 2.23 | - 0.31 | + 2.84 |
| 30 Acetone | 0.115 | + 4.69 | - 0.44 | + 5.57 |
| 40 | 0.088 | + 6.68 | - 0.54 | + 7.76 |

^a Values obtained by interpolation of literature values taken from ref. 4.01

Many decades ago, Rothmund [4.09] showed that Setschenow's [4.10] treatment of the effects of added electrolytes on the solubility of non-electrolytes in water could also be applied to the complementary effect of added non-electrolytes on the solubility of inorganic salts in water. Rothmund's treatment has subsequently been refined and generalised by incorporating the characteristic volume \underline{V}^* , of the added non-electrolyte [4.11]. The solubilities of a salt in a series of binary aqueous mixtures; \underline{S}_x , were related to its solubility in pure water, \underline{S}_0 , and the concentration of non-electrolyte, \underline{C}_s , by the expression

$$\log_{10} \underline{S}_0 = \log_{10} \underline{S}_x + \underline{K}_s \underline{V}^* \underline{C}_s \quad (4.03)$$

where \underline{K}_s is a constant, characteristic of the electrolyte. Although this works well for electrolytes containing small ions, it has been found to break down for salts of large ions such as $[\text{Fe}(\text{phen})_3]^{2+}$ and BPh_4^- . Burgess *et al.* [4.03] have calculated values of \underline{K}_s for a series of 1:1, 1:2, 2:1 and 2:2 electrolytes. They obtained values for Cs_2ReCl_6 , CsReBr_6 and K_2PtCl_6 of 0.7, 0.6 and 1.0 respectively. The corresponding value of $\text{K}_2\text{S}_2\text{O}_8$ in methanol-water mixtures was calculated as 0.7, which is in good agreement with the aforementioned 2:1 electrolytes.

In chapter 5, the mercury(II)-catalysed aquation of several transition metal-chloro complexes has been studied in a range of binary aqueous mixtures. As for the peroxodisulphate oxidation reaction, the solvation properties of the initial state for this catalysed aquation are desired in order to discuss the solvent effects observed. Consequently, estimates of $\delta_{\text{m}\mu}^\ominus(\text{Hg}^{2+})$ and $\delta_{\text{m}\mu}^\ominus(\text{complex})$ have been made. For the complex cations $[\text{Co}(\text{NH}_3)_5\text{Cl}]^{2+}$ and $\text{trans-}[\text{Co}(\text{en})_2\text{Cl}_2]^+$, the

free energies of transfer from water into a series of binary aqueous mixtures at 298.2 K have been estimated from published data on the respective solubilities of the chloride [4.12] and perchlorate [4.13] salts, and literature values of $\delta_{\text{m}\mu}^{\ominus}(\text{Cl}^-)$ and $\delta_{\text{m}\mu}^{\ominus}(\text{ClO}_4^-)$ [4.01]. These estimates have been reported and discussed in chapter 5.

Estimates of $\delta_{\text{m}\mu}^{\ominus}(\text{Hg}^{2+})$ are attainable from solubility measurements of the tetraphenylborate salt, $\text{Hg}(\text{BPh}_4)_2$, whence $\delta_{\text{m}\mu}^{\ominus}(\text{Hg}(\text{BPh}_4)_2)$ is calculated. Some values of $\delta_{\text{m}\mu}^{\ominus}(\text{BPh}_4^-)$ are available [4.01], and this parameter has also been estimated (below) from solubility data on CsBPh_4 , using literature values [4.01] of $\delta_{\text{m}\mu}^{\ominus}(\text{Cs}^+)$. An estimate of $\delta_{\text{m}\mu}^{\ominus}(\text{BPh}_4^-)$ for aqueous ethanol mixtures may also be made using the assumption $\delta_{\text{m}\mu}^{\ominus}(\text{TAB}^+)^{\dagger} = \delta_{\text{m}\mu}^{\ominus}(\text{BPh}_4^-)$ (cf. $\delta_{\text{m}\mu}^{\ominus}(\text{Ph}_4\text{As}^+) = \delta_{\text{m}\mu}^{\ominus}(\text{BPh}_4^-)$ [4.14]), from data on the solubility of $(\text{TAB}^+)(\text{BPh}_4^-)$ [4.06].

(ii) Mercury(II) Tetraphenylborate

Table 4.02(a) lists the solubilities of the title compound in water and in a range of binary aqueous mixtures at 298.2 K. The solubility of $\text{Hg}(\text{BPh}_4)_2$ was found to increase rapidly with increase in the mole fraction of co-solvent. Hence it appears that the solvation of the hydrophobic anion dominates the solvation characteristics of the mercury(II) salt, which is observed to become more stable in binary aqueous mixtures relative to pure water. Also included in Table 4.02(a) are the free energies of transfer of the salt, $\delta_{\text{m}\mu}^{\ominus}(\text{Hg}(\text{BPh}_4)_2)$ from water into the binary aqueous mixtures used. The solubilities of

[†] [TAB = Triisoamyl n-butyl ammonium.]

TABLE 4.02(a) Solubilities of mercury(II) tetraphenylborate in water and in binary aqueous mixtures at 298.2 K, together with calculated free energies of transfer from water into these mixtures.

| Solvent Mixture | 10^5 Solubility mol dm ⁻³ | $\delta_m \mu^\circ(\text{Hg}(\text{BPh}_4)_2)$ kJ mol ⁻¹ |
|-------------------------|---|---|
| Water | 5.09 | 0. |
| 10 | 5.20 | - 0.145 |
| 20 % Methanol | 5.80 | - 0.972 |
| 30 | 6.65 | - 1.99 |
| 40 | 6.70 | - 2.05 |
| 10 | 5.25 | - 0.230 |
| 20 % Ethanol | 5.70 | - 0.842 |
| 30 | 7.25 | - 2.63 |
| 40 | 10.6 ₅ | - 5.49 |
| 10 | 5.35 | - 0.371 |
| 20 % ^t Butyl | 6.85 | - 2.21 |
| 30 alcohol | 10.5 ₀ | - 5.39 |
| 40 | 14.5 ₅ | - 7.81 |
| 10 | 7.00 | - 2.37 |
| 20 % Acetonitrile | 11.7 ₀ | - 6.19 |
| 30 | 15.5 ₀ | - 8.28 |
| 40 | 19.1 ₅ | - 9.86 |

TABLE 4.02(b) Solubilities of caesium tetraphenylborate in water and in binary aqueous mixtures, at 298.2 K. Also included are the free energies of transfer of the salt from water into these mixtures.

| Solvent Mixture | $\frac{10^4 \text{ Solubility}}{\text{mol dm}^{-3}}$ | $\frac{\delta_m \mu^\circ(\text{Salt})}{\text{kJ mol}^{-1}}$ |
|------------------|--|--|
| Water | 1.00 | 0 |
| 10 | 1.87 | - 3.10 |
| 20 | 2.17 | - 3.84 |
| 30 % Methanol | 3.33 | - 5.97 |
| 40 | 3.67 | - 6.44 |
| 10 | 2.10 | - 3.68 |
| 20 | 3.17 | - 5.72 |
| 30 % Ethanol | 4.50 | - 7.46 |
| 40 | 5.80 | - 8.72 |

CsBPh₄ in water and in aqueous methanol and ethanol mixtures have been measured at 298.2 K, and are reported in Table 4.02(b). Literature values of $\delta_{m\mu}^{\ominus}(\text{Cs}^+)$ [4.01] are included in Table 4.03, together with the consequent values of $\delta_{m\mu}^{\ominus}(\text{BPh}_4^-)$, calculated by the expression

$$\delta_{m\mu}^{\ominus}(\text{CsBPh}_4) = \delta_{m\mu}^{\ominus}(\text{Cs}^+) + \delta_{m\mu}^{\ominus}(\text{BPh}_4^-) \quad (4.04)$$

Using these estimated values of $\delta_{m\mu}^{\ominus}(\text{BPh}_4^-)$, values of $\delta_{m\mu}^{\ominus}(\text{Hg}^{2+})$ have been calculated from

$$\delta_{m\mu}^{\ominus}(\text{Hg}(\text{BPh}_4)_2) = \delta_{m\mu}^{\ominus}(\text{Hg}^{2+}) + 2\delta_{m\mu}^{\ominus}(\text{BPh}_4^-) \quad (4.05)$$

and are also listed in Table 4.03, together with estimates of $\delta_{m\mu}^{\ominus}(\text{Hg}^{2+})$ derived using different assumptions about the solvation of the BPh₄⁻ ion. Abraham [4.02] used the convention that $\delta_{m\mu}^{\ominus}(\text{Me}_4\text{N}^+) = 0$ in order to estimate single-ion values, $\delta_{m\mu}^{\ominus}(\text{X}^{n\pm})$. We can clearly see that an analogous assumption, i.e. $\delta_{m\mu}^{\ominus}(\text{BPh}_4^-) = 0$ is most unsatisfactory since here,

$$\delta_{m\mu}^{\ominus}(\text{Hg}(\text{BPh}_4)_2) = \delta_{m\mu}^{\ominus}(\text{Hg}^{2+}) \quad (4.06)$$

but we have suggested above that the solvation of the BPh₄⁻ anion dominates that of the mercury(II) salt. Table 4.03 also lists some literature values [4.01] of $\delta_{m\mu}^{\ominus}(\text{BPh}_4^-)$ in several aqueous methanol and acetone mixtures.

The estimates of $\delta_{m\mu}^{\ominus}(\text{Hg}^{2+})$ in Table 4.03 (omitting those derived from the $\delta_{m\mu}^{\ominus}(\text{BPh}_4^-) = 0$ assumption) follow the expected trend of increasing positive character with increasing mole fraction of co-solvent.

Estimations of $\delta_{m\mu}^{\ominus}(\text{ReCl}_6^{2-})$, to be used to calculate $\delta_{m\mu}^{\ominus}(\text{I.S.})$ in the mercury(II)-catalysed aquation of this anion, have been attempted

TABLE 4.02 Gibbs free energies of transfer, $\delta_m \mu^\circ$, of the Cs^+ , BPh_4^- and Hg^{2+} ions from water into several binary aqueous mixtures, at 298.2 K. Values of $\delta_m \mu^\circ(\text{Cs}^+)$ are taken from ref. 4.01; values of $\delta_m \mu^\circ(\text{BPh}_4^-)$ are calculated from eqn.(4.04), using data from Table 4.02(b), (b) literature values taken from ref. 4.01, and (c) estimated assuming $\delta_m \mu^\circ(\text{TAB}^+) = \delta_m \mu^\circ(\text{BPh}_4^-)$. Values of $\delta_m \mu^\circ(\text{Hg}^{2+})$ are (d) calculated from data from Table 4.02(a) using eqn.(4.05), (e) estimated assuming $\delta_m \mu^\circ(\text{BPh}_4^-) = 0$, and (f) calculated from eqn.(4.05) using values of $\delta_m \mu^\circ(\text{BPh}_4^-)$ estimated (i) as in (b) and (ii) as in (c).

| Solvent Mixture | $\delta_m \mu^\circ(\text{Cs}^+) / \text{kJ mol}^{-1}$ | $\delta_m \mu^\circ(\text{BPh}_4^-) / \text{kJ mol}^{-1}$ | $\delta_m \mu^\circ(\text{Hg}^{2+}) / \text{kJ mol}^{-1}$ | (d) | (e) | (f) |
|-----------------|--|---|---|-------|-------|--------------------|
| Water | 0 | 0 | 0 | 0 | 0 | 0 |
| 10 | -0.38 | -2.72 | | +3.24 | -0.15 | |
| 20 | -0.08 | -3.76 | | +3.94 | -0.97 | |
| 30 | +0.42 | -6.39 | | +6.57 | -1.99 | |
| 40 | +1.05 | -7.49 | | +6.94 | -2.05 | |
| 10 | +0.67 | -4.35 | -1.77 | +5.96 | -0.23 | (i) +3.2 (ii) +1.8 |
| 20 | +1.38 | -7.10 | -3.6 | +9.31 | -0.84 | +6.4 +3.6 |
| 30 | +2.09 | -9.55 | -6.9 | +11.4 | -2.63 | +11.2 +4.6 |
| 40 | +2.93 | -11.05 | -11.3 | +16.1 | -5.49 | +17.1 +4.5 |

from several routes. These involve attempting to make a 'single-ion split' using the assumptions:-

$$\delta_{\text{m}\mu}^{\ominus}([\text{Fe}(\text{phen})_3]^{2+}) = \delta_{\text{m}\mu}^{\ominus}(\text{ReCl}_6^{2-}) \quad (4.07)$$

and

$$\delta_{\text{m}\mu}^{\ominus}([\text{Mg}(\text{OH}_2)_6]^{2+}) = \delta_{\text{m}\mu}^{\ominus}(\text{ReCl}_6^{2-}) . \quad (4.08)$$

These assumptions having proved unsuccessful, estimates of $\delta_{\text{m}\mu}^{\ominus}(\text{ReCl}_6^{2-})$ have been made using more conventional methods (below).

(iii) Tris-(1,10-phenanthroline)iron(II) Hexachlororhenate

This compound was found to be very sparingly soluble in water, having a solubility of $5.13 \times 10^{-6} \text{ mol dm}^{-3}$ at 298.2 K. The solubilities of the compound in a range of binary aqueous mixtures were also measured at 298.2 K, the results of which are listed in Table 4.04, together with values of the solubility in several pure non-aqueous solvents. From these solubilities, $\delta_{\text{m}\mu}^{\ominus}([\text{Fe}(\text{phen})_3](\text{ReCl}_6))$ has been calculated (Table 4.04). These results, i.e. the free energies of transfer becoming more negative with increase in mole fraction of co-solvent, indicate that the hydrophobic nature of the $[\text{Fe}(\text{phen})_3]^{2+}$ cation dominates the solubility of the hexachlororhenate salt. This trend is analogous to the effect of the BPh_4^- anion in $\text{Hg}(\text{BPh}_4)_2$ above.

Clearly, the assumption

$$\delta_{\text{m}\mu}^{\ominus}([\text{Fe}(\text{phen})_3]^{2+}) = \delta_{\text{m}\mu}^{\ominus}(\text{ReCl}_6^{2-}) \quad (4.09)$$

is totally unsatisfactory. Although the magnitudes of the charges of the ions are identical, their peripheries are very different. Also, as we shall see in chapter 7, the sizes of these ions are very different, with $r(\text{ReCl}_6^{2-}) = 4.2 \text{ \AA}$ [4.15] and $r(\text{Fe}(\text{phen})_3^{2+}) = 7.0 \text{ \AA}$ [4.16].

TABLE 4.04 (a) Solubilities of the $[\text{Fe}(\text{phen})_3] (\text{ReCl}_6)$ salt in water and in a range of binary aqueous mixtures, together with the calculated free energies of transfer of the salt, $\delta_m \mu^\ominus(\text{salt})$ from water into these mixtures at 298.2 K. Also included are similar results for several pure non-aqueous solvents.

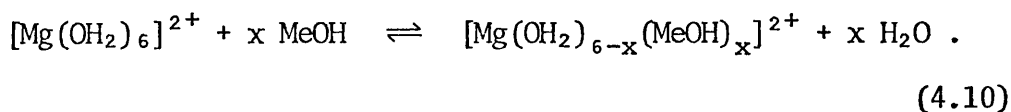
| Solvent Mixture | 10^6 Solubility mol dm ⁻³ | $\delta_m \mu^\ominus(\text{salt})$ kJ mol ⁻¹ |
|---------------------|---|---|
| Water | 5.13 | 0 |
| 10 | 8.00 | - 2.20 |
| 20 | 10.56 | - 3.58 |
| 30 | 17.95 | - 6.21 |
| 40 % Methanol | 25.95 | - 8.04 |
| 60 | 37.4 | - 9.85 |
| 80 | 33.7 | - 9.34 |
| 100 | 6.77 | - 1.38 |
| 10 | 8.92 | - 2.74 |
| 20 | 13.74 | - 4.89 |
| 30 % Ethanol | 24.20 | - 7.69 |
| 40 | 22.15 | - 7.25 |
| 100 | 4.41 | - 0.75 |
| 10 | 6.15 | - 0.90 |
| 20 % Ethylene | 9.02 | - 2.80 |
| 30 glycol | 16.41 | - 5.77 |
| 40 | 14.77 | - 5.24 |
| Acetonitrile | 55.9 | -11.8 |
| Dimethylformamide | 554 | -23 |
| Dimethyl sulphoxide | 1550 | -40 |
| Nitrobenzene | 50.5 | -11.3 |

TABLE 4.04(b) Gibbs free energies of transfer, $\delta_m \mu^\ominus$, of the ClO_4^- anion, taken from ref.4.01; and of the $[\text{Fe}(\text{phen})_3]^{2+}$ cation, (a) calculated using eqn.(4.05)(i.e for a 1:2 electrolyte) and data from ref.4.04, (b) estimated assuming $\delta_m \mu^\ominus ([\text{Fe}(\text{phen})_3]^{2+}) = \delta_m \mu^\ominus (\text{ReCl}_6^{2-})$. All values estimated at 298.2 K.

| Solvent Mixture | $\delta_m \mu^\ominus (\text{ClO}_4^-)$ | $\delta_m \mu^\ominus ([\text{Fe}(\text{phen})_3]^{2+})$ | |
|-----------------|---|--|--------|
| | kJ mol^{-1} | kJ mol^{-1} | |
| | | (a) | (b) |
| Water | 0 | 0 | 0 |
| 10 | + 0.55 | - 3.5 | - 1.10 |
| 20 | + 1.10 | - 7.6 | - 1.79 |
| 30 | + 1.80 | -11.8 | - 3.11 |
| 40 | + 2.65 | -16.3 | - 4.02 |
| 10 | + 1.3 | -14.0 | |
| 20 | + 2.2 | -24 | |
| 30 | + 3.1 | -30 | |
| 40 | + 3.7 | -34 | |

What is required to make a 'single-ion split' to estimate $\delta_{\text{ML}}^{\ominus}$ (ReCl_6^{2-}) is obviously a cation having very similar solvation characteristics. That is, a divalent cation having an ionic radius of ca. 4.2 \AA , and a hydrophilic periphery. Such a possible candidate is the hexa-aquomagnesium(II) cation, $[\text{Mg}(\text{OH}_2)_6]^{2+}$. The X-ray powder photograph of the $\text{MgReCl}_6 \cdot 6\text{H}_2\text{O}$ has been measured (chapter 7), wherein it was found that this compound crystallises in the cubic CsCl structure. From this photograph, the relative ionic radii were estimated to be almost equivalent, the mean value being $4.27 \pm 0.02 \text{ \AA}$.

Unfortunately, $\text{MgReCl}_6 \cdot 6\text{H}_2\text{O}$ was found to be very soluble in water and in low mole fractions of aqueous methanol. In such solutions, the activity coefficients will not approximate to unity. The solubility of the compound was measured in 60 and 80% by volume aqueous methanol, as 0.015 and 0.0041 mol dm^{-3} respectively. At such high mole fractions of co-solvent, the divergence of the activity coefficients from unity will be much increased, as calculated from the Davies equation [4.17]; also there will be the risk of one or more water molecules being replaced by methanol, i.e.



The equilibrium constant for such an equilibrium involving the $[\text{Mn}(\text{OH}_2)_6]^{2+}$ cation has been measured [4.18] as 4.5×10^{-2} .

Consequently, although $\text{MgReCl}_6 \cdot 6\text{H}_2\text{O}$ at first sight appears to be a fair model for a 'single-ion split', the experimental difficulties encountered render the system impractical.

Values of $\delta_{\text{ML}}^{\ominus}(\text{ReCl}_6^{2-})$ can be estimated from solubility data available [4.03] for Cs_2ReCl_6 , using literature [4.01] values for $\delta_{\text{ML}}^{\ominus}$

TABLE 4.05 Gibbs free energies of transfer of the ReCl_6^{2-} anion, $\delta_m \mu^\ominus(\text{ReCl}_6^{2-})$, from water into several binary aqueous mixtures, at 298.2 K. Values listed are (a) calculated from solubility data for Cs_2ReCl_6 (ref.4.03) and lit. values of $\delta_m \mu^\ominus(\text{Cs}^+)$ (see Table 4.03); (b) calculated using data from Table 4.04(a) and 4.04(b); (c) estimated using the assumption in eqn.(4.07).

| Solvent Mixture | $\delta_m \mu^\ominus(\text{ReCl}_6^{2-}) / \text{kJ mol}^{-1}$ | | |
|-----------------|---|-------|-------|
| | (a) | (b) | (c) |
| Water | 0 | 0 | 0 |
| 10 | + 2.8 | + 1.8 | - 1.1 |
| 20 | + 5.5 | + 3.7 | - 1.8 |
| 30 % Methanol | + 6.7 | + 5.0 | - 3.1 |
| 40 | + 8.6 | + 7.9 | - 4.0 |
| 10 | + 0.7 | | - 1.4 |
| 20 | + 2.8 | | - 2.4 |
| 30 % Ethanol | + 2.6 | | - 3.8 |
| 40 | + 5.2 | | - 3.6 |

(Cs⁺). Such estimates are reported in Table 4.05. There are some solubility data available for [Fe(phen)₃](ClO₄)₂ in some binary aqueous mixtures [4.04], whence, using literature values of $\delta_{\text{m}\mu}^{\ominus}(\text{ClO}_4^-)$, $\delta_{\text{m}\mu}^{\ominus}([\text{Fe}(\text{phen})_3]^{2+})$ can be estimated. Consequently, using the measured solubilities of the [Fe(phen)₃](ReCl₆) salt (Table 4.04), it is possible to estimate $\delta_{\text{m}\mu}^{\ominus}(\text{ReCl}_6^{2-})$ for these mixtures. Such estimates are listed in Table 4.05. We can see that the two reasonable methods of estimating $\delta_{\text{m}\mu}^{\ominus}(\text{ReCl}_6^{2-})$ compare quite well with each other.

Hence we have arrived at reasonable estimates of $\delta_{\text{m}\mu}^{\ominus}(\text{Hg}^{2+})$ and $\delta_{\text{m}\mu}^{\ominus}(\text{ReCl}_6^{2-})$ in several binary aqueous mixtures, which lead to an estimate of $\delta_{\text{m}\mu}^{\ominus}(\text{Initial State})$ for the reaction of these two species, which will be fully discussed in chapter 5.

(iv) [Fe(5-NO₂phen.CN)₂(5-NO₂phen)]

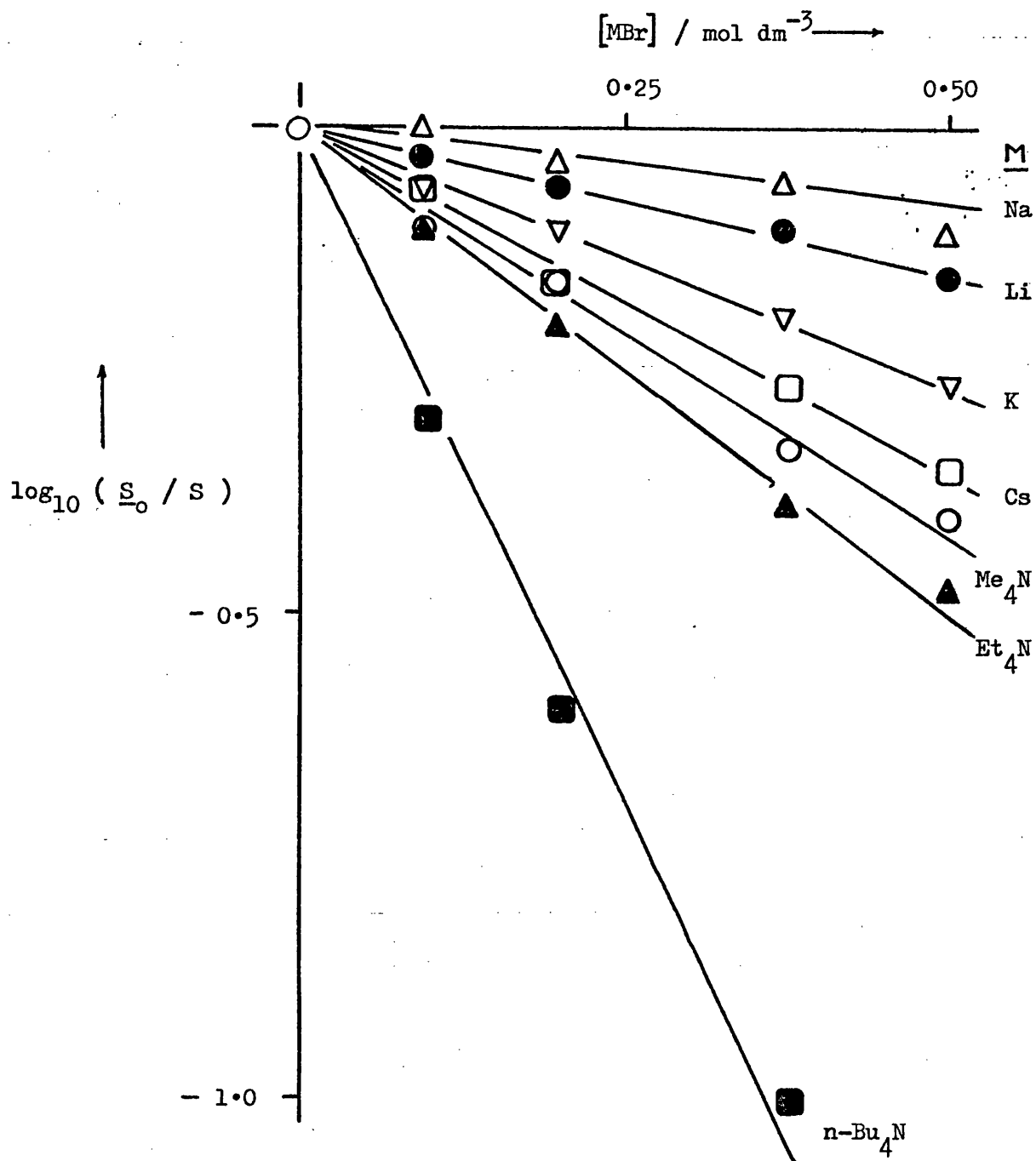
In the reaction of cyanide ion with the [Fe(5-NO₂phen)₃]²⁺ cation (chapter 9) a red compound was isolated which was sparingly soluble in water. Analogous reactions of differently substituted tris-phenanthroline complex cations of iron(II) yield a dicyano product, Fe(X-phen)₂(CN)₂ (for X = H, 5-Cl, 5-Me, 4,7-Me₂, etc.). The product in the 5-NO₂-substituted case did not behave like a dicyano complex, having negligible solvatochromic character (see chapter 8). Various qualitative methods of analysis of this compound have been employed in order to give insight into its structure (chapters 8 and 9).

The [Fe(phen)₃]²⁺ cation does not react with thiocyanate in aqueous solution, but rather is precipitated as the insoluble salt [Fe(phen)₃](SCN)₂. Hence the solubility properties of the 5-NO₂phen product in aqueous salt solutions were studied, to see if the compound behaved as the [Fe(5-NO₂phen)₃](CN)₂ salt, i.e. as an electrolyte, or as a non-

TABLE 4.06 Solubilities, S, of the $[\text{Fe}(5\text{-NO}_2\text{phen.CN})_2(5\text{-NO}_2\text{phen})]$ type compound in aqueous alkali metal and related bromide salt solutions, at 298.2 K. Also included are the corresponding Setschenow coefficients, K.

| Medium | | <u>M</u> | $10^5 \underline{S} / \text{mol dm}^{-3}$ | <u>K</u> |
|--------------|----------------------------|-------------------------|---|----------|
| <u>[MBr]</u> | <u>mol dm⁻³</u> | | | |
| zero | | | 2.51 | 0 |
| 0.100 | | Li | 2.69 | |
| 0.200 | | | 2.87 | |
| 0.375 | | | 3.22 | - 0.31 |
| 0.500 | | | 3.58 | |
| 0.100 | | Na | 2.51 | |
| 0.200 | | | 2.69 | |
| 0.375 | | | 2.87 | - 0.17 |
| 0.500 | | | 3.22 | |
| 0.100 | | K | 2.87 | |
| 0.200 | | | 3.22 | |
| 0.375 | | | 3.94 | - 0.54 |
| 0.500 | | | 4.66 | |
| 0.100 | | Cs | 2.87 | |
| 0.200 | | | 3.58 | |
| 0.375 | | | 4.67 | - 0.72 |
| 0.500 | | | 5.73 | |
| 0.100 | | Me_4N | 3.22 | |
| 0.200 | | | 3.58 | |
| 0.375 | | | 5.37 | - 0.85 |
| 0.500 | | | 6.45 | |
| 0.100 | | Et_4N | 3.22 | |
| 0.200 | | | 3.94 | |
| 0.375 | | | 6.09 | - 0.99 |
| 0.500 | | | 7.52 | |
| 0.100 | | $n\text{-Bu}_4\text{N}$ | 5.01 | |
| 0.200 | | | 10.03 | |
| 0.375 | | | 26.4 | - 2.9 |
| 0.500 | | | | |

Figure 4.01 Correlation of $\log_{10}(\underline{S}_0/S)$ with concentration of added salt ($[MBr]$), for the $[Fe(5-NO_2phen.CN)_2(5-NO_2phen)]$ type compound, at 298.2 K.



electrolyte, having no ionic cyanides.

The compound in question is deduced to be of the form $[\text{Fe}(\text{5-NO}_2\text{phen. CN})_2(\text{5-NO}_2\text{phen})]$ in chapter 9. Its solubility in water and in aqueous salt solutions containing various concentrations of the alkali metal bromides and tetraalkyl ammonium bromides at 298.2 K have been measured, and are reported in Table 4.06. Figure 4.01 shows a plot of $\log_{10}(\underline{S}_0/\underline{S})$ against $[\text{MBr}]$, where \underline{S}_0 is the solubility in water, and \underline{S} is that in a given salt solution. Table 4.06 also includes the Setschenow coefficients, K , which are equal to the slopes of the correlation lines in Figure 4.01, for these salt solutions. The behaviour of the solubility of the compound is analogous to that found for both polar and non-polar non-electrolytes [4.19], the trends in K for the alkali metal halides being in the same order as that for this study.

Hence the salt effects on the solubility of the compound in question tend to suggest a covalent rather than an ionic species. Thus the possibility of the compound being a sparingly soluble $[\text{Fe}(\text{5-NO}_2\text{phen})_3](\text{CN})_2$ salt is ruled out. As will be seen in chapters 8 and 9, the compound is not $\text{Fe}(\text{5-NO}_2\text{phen})_2(\text{CN})_2$. Moreover, from microanalysis, i.r. spectroscopy, kinetic behaviour, and comparison with an analogous ruthenium species [4.20], the true form of the compound will be shown to be $[\text{Fe}(\text{5-NO}_2\text{phen. CN})_2(\text{5-NO}_2\text{phen})]$.

(v) 1,10-Phenanthroline and Substituted Derivatives

The solubility of 1,10-phenanthroline monohydrate in water at 298.2 K was measured as $0.0149 \text{ mol dm}^{-3}$, which compares favourably with a literature value of $0.0161 \text{ mol dm}^{-3}$ [4.21]. The solubilities at various temperatures of phen. H_2O in aqueous solution are listed in Table 4.07. From the observed variation in solubility with temperature,

TABLE 4.07 Concentrations of 1,10-phenanthroline in saturated aqueous solutions as a function of absolute temperature.

| T / K | [phen]/mol dm ⁻³ | T / K | [phen]/mol dm ⁻³ |
|-------|-----------------------------|-------|-----------------------------|
| 298.2 | 0.0149 ^a | 313.2 | 0.0255 |
| 304.0 | 0.0185 | 318.6 | 0.0288 |
| 308.0 | 0.0209 | 323.2 | 0.0341 |

^a Compare lit. value of 0.0161 mol dm⁻³ in ref. 4.21.

TABLE 4.08 Concentrations of 1,10-phenanthroline in saturated methanol-water solutions, and Gibbs free energies of transfer ($\delta_m \mu^\circ$) of 1,10-phenanthroline from water into the solvent mixtures, at 298.2 K.

| % Methanol | [phen]/mol dm ⁻³ | $\delta_m \mu^\circ(\text{phen})/\text{kJ mol}^{-1}$ |
|------------|-----------------------------|--|
| 5.0 | 0.0173 | - 0.4 |
| 10.0 | 0.0207 | - 0.8 |
| 15.0 | 0.0247 | - 1.3 |
| 20.0 | 0.0280 | - 1.6 |
| 25.0 | 0.0339 | - 2.0 |

TABLE 4.09 Concentrations of saturated aqueous solutions of 1,10-phenanthroline and of related compounds at 298.2K. Included are the molecular volumes of the compounds, and certain of their extinction coefficients (ϵ) and wavelengths of maximum absorption (λ).

| Compound | λ_{max} nm | ϵ_{max} | [Compound] mol dm ⁻³ | Molecular volume $\times 10$ dm ³ mol ⁻¹ |
|------------------------------|------------------------------|-------------------------|---|--|
| phen | 265 | 29510 | 0.0149 | 0.1374 |
| 5-NO ₂ phen | 267 | 28410 | 0.000121 ^a | 0.1549 |
| 4,7-Me ₂ phen | 266 | 37490 | 0.000107 | 0.1656 |
| 3,4,7,8-Me ₄ phen | 278 | 41590 | 0.0000064 | 0.1938 |
| 4,7-Ph ₂ phen | | | < 10 ⁻⁶ | 0.2590 |
| 5-Br phen | | | 0.00099 ^b | 0.1549 |
| bipy | | | 0.038 ^c , 0.041 ^d | 0.1244 |

^a Compare value of 0.000119 in ref. 4.21; ^b ref. 4.21; ^c ref. 4.05; ^d ref. 4.28.

a value for the enthalpy of solution of $-2.6 \pm 0.02 \text{ kJ mol}^{-1}$ was calculated from the Van't Hoff Isochore:-

$$\ln \left(\frac{S_2}{S_1} \right) = - \frac{\Delta H_{\text{soln}}}{R} \left(\frac{1}{T_1} - \frac{1}{T_2} \right) \quad (4.11)$$

(where S_2 and S_1 are the solubilities of phen at the absolute temperatures T_2 and T_1) using a BASIC least-mean-squares program (Appendix 2, Program 4).

The standard deviation of 0.02 kJ mol^{-1} obtained does not account for possible systematic uncertainties, and the likely error must be considerably larger than this value, perhaps ten times so. The value of ΔH_{soln} obtained for 1,10-phenanthroline monohydrate is similar to that of -4.2 kJ mol^{-1} reported for anhydrous 2,2'-bipyridyl [4.05].

The solubility of 1,10-phenanthroline monohydrate has been measured in several aqueous methanol mixtures at 298.2 K, the results of which are listed in Table 4.08. The solubility increases as the proportion of methanol increases in these mixtures, which is the expected trend for such a hydrophobic non-electrolyte. This hydrophobicity outweighs the hydrophilic character of the heterocyclic nitrogen, which have a lone pair of electrons each, that are said [4.22] to be able to form hydrogen-bonds with water. This hydrophilicity can account for the greater solubilities of 2,2'-bipyridyl and 1,10-phenanthroline in aqueous solution compared with those of biphenyl [4.05] and phenanthrene[†] [4.23] respectively, where the hydrophobicities of the two sets of compounds are constant for each set. Thus, for example, the solubility

[†] [The lit. value for the solubility of phenanthrene is available in 59.8% by weight of methanol, as $0.0067 \text{ mol dm}^{-3}$ [4.23].]

of 1,10-phenanthroline in ethanol at 298.2 K is 2.78 mol dm^{-3} [4.22]. From the measured solubilities of the compound in these mixtures, the free energies of transfer, $\delta_{\text{m}\mu}^{\ominus}(\text{phen.H}_2\text{O})$ from water into the mixtures have been calculated, and are included in Table 4.08. Figure 4.02 is a plot of the free energies of transfer of phen.H₂O, Fe(phen)₂(CN)₂ [4.24] and of the [Fe(phen)₃]²⁺ cation (section 4.3(iii)) from water into aqueous methanol against mole fraction of methanol. We see that the relative free energies of transfer of these species are

$$\begin{aligned} \delta_{\text{m}\mu}^{\ominus}(\text{phen.H}_2\text{O}) &: \delta_{\text{m}\mu}^{\ominus}(\text{Fe(phen)}_2(\text{CN})_2) : \delta_{\text{m}\mu}^{\ominus}([\text{Fe(phen)}_3]^{2+}) \\ &= \quad 1 \quad : \quad 2 \quad : \quad 4.5 \text{ approx.} \end{aligned}$$

The large solvation of the cation is surprising in view of its positive charge, and must be dominated by the hydrophobicity of the ligands. For these iron(II)-phen complexes, the hydrophilic heterocyclic nitrogens are complexed to the iron(II) centre, and so their solvation characteristics will not influence the solubility properties of the complexes.

The solubilities of X-1,10-phenanthroline (where X = 5-nitro, 4,7-dimethyl and 3,4,7,8-tetramethyl) in water at 298.2 K have been measured, the results of which are listed in Table 4.09. These solubilities do not correlate with the hydrophilic or hydrophobic natures of the substituents, nor with their electron releasing or withdrawing effects. Rather, they depend on the size of the molecule [4.25], with solubility decreasing with increasing size. Indeed a plot of the logarithm of solubility against molecular volume [4.26] is linear for all the phenanthrolines and for 2,2'-bipyridyl (Figure 4.03), having a slope of $58 \pm 7 \text{ mol dm}^{-3}$. Grigg & Hall [4.27] found water of crystallisation

Figure 4.02 Dependence of the Gibbs free energies of transfer, $\delta_m \mu^\ominus(X)$, where $X =$ (a) phen. H_2O , (b) $\text{Fe}(\text{phen})_2(\text{CN})_2$ and (c) $[\text{Fe}(\text{phen})_3]^{2+}$ on solvent composition, at 298.2K.

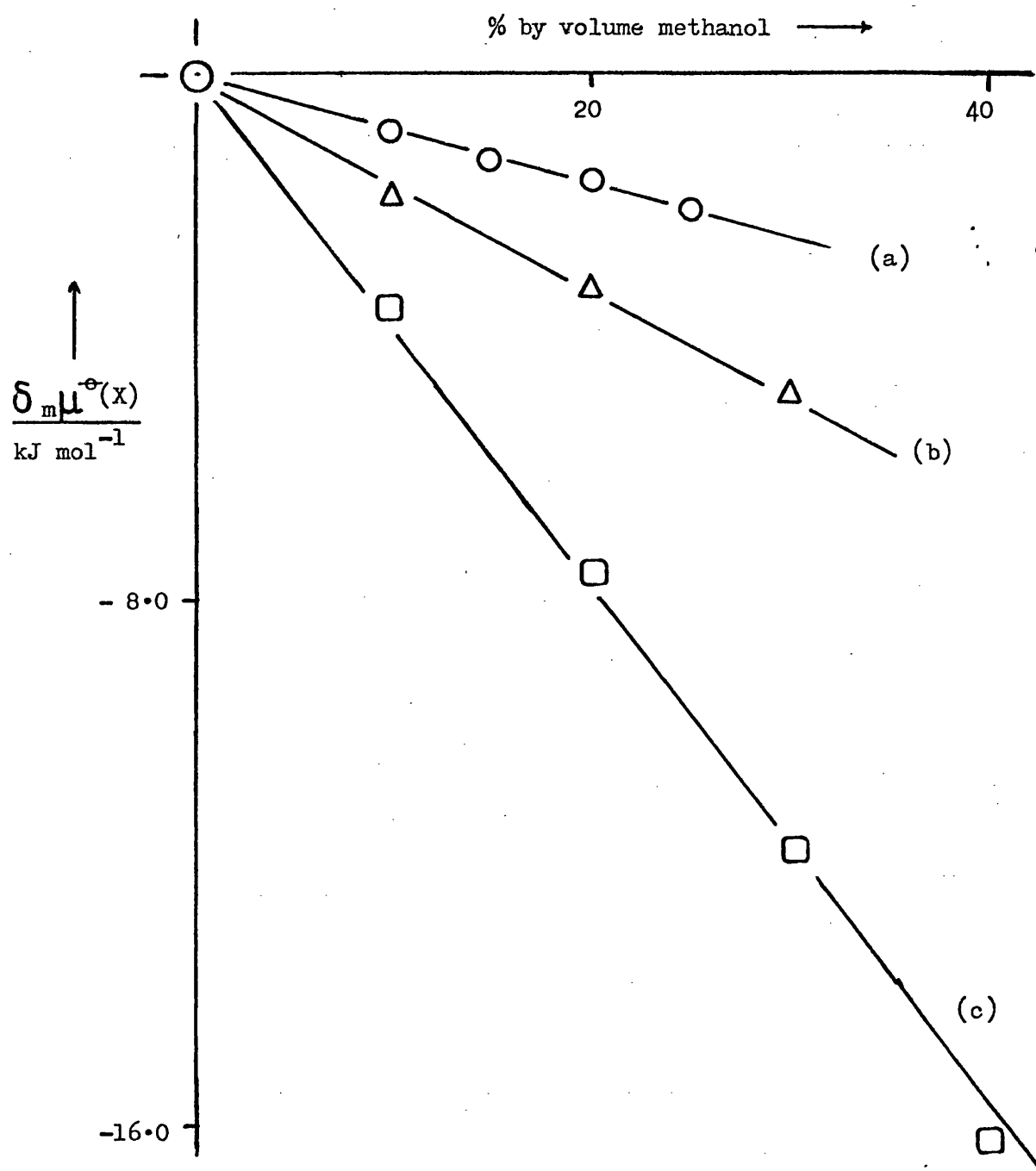
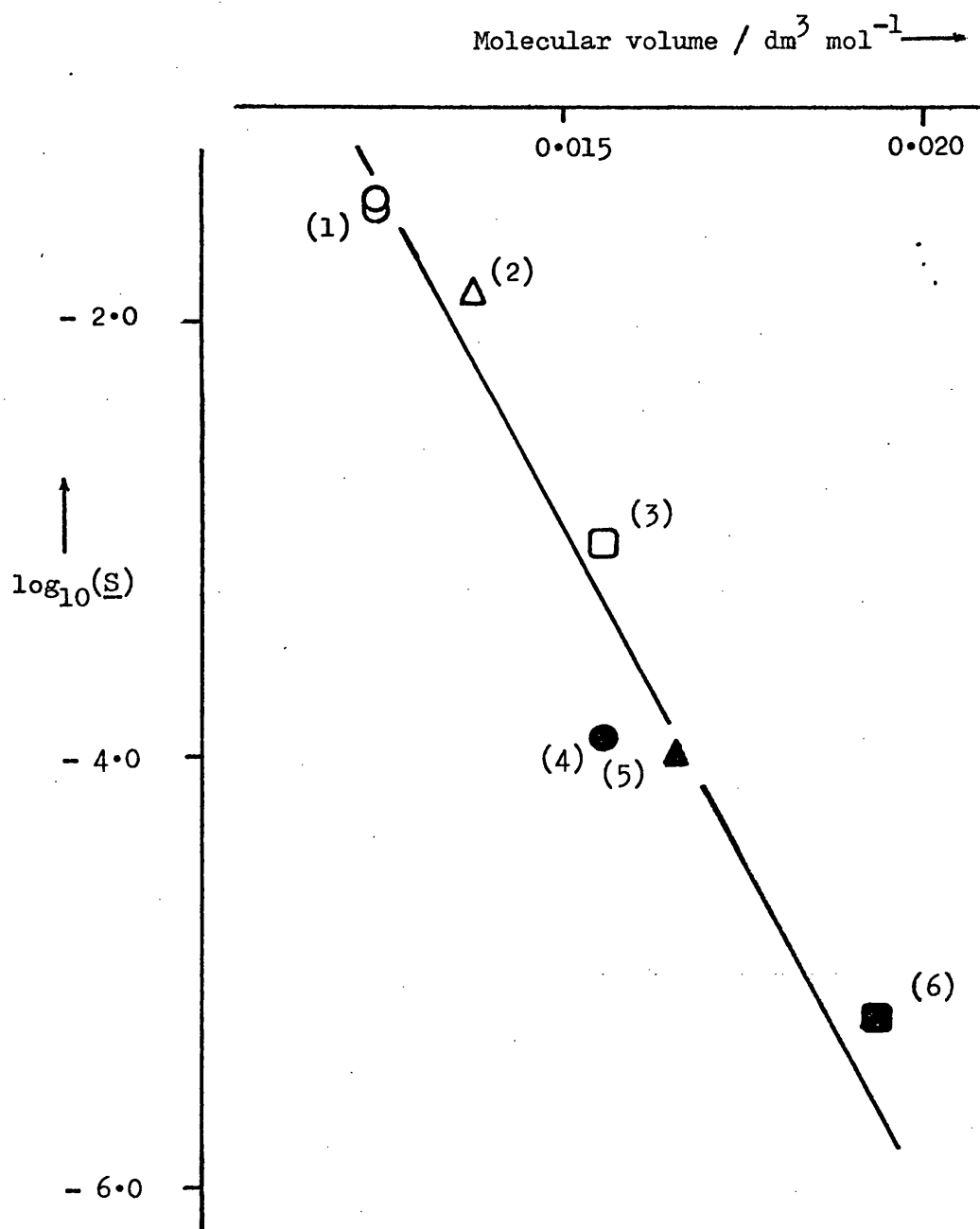
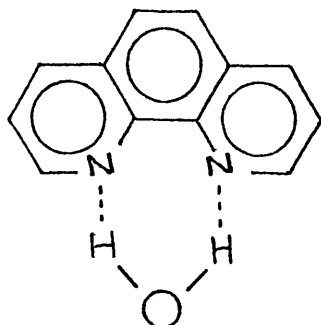


Figure 4.03 Relation between the logarithms of solubilities, $\log_{10}(\underline{S})$, of 1,10-phenanthroline and related compounds and their molecular volumes, at 298.2 K. Points (1) bipy; (2) phen; (3) 5-Br phen; (4) 5-NO₂ phen; (5) 4,7-Me₂phen; (6) 3,4,7,8-Me₄phen.



in the 4,7-Me₂- and 5-NO₂- substituted phenanthrolines (as well as the 3,8-Me₂- and 2,4,7,9-Me₄- ones). Such water molecules have been said to be hydrogen bonded to the nitrogens of the heterocycles, for 1,10-phenanthroline monohydrate at least, as shown below:-



In aqueous solution it would be expected that all the phenanthrolines would be so hydrogen-bonded, and so their relative molecular volumes would be the same in aqueous solution as in the anhydrous solid state.

The solubility of 3,4,7,8-tetramethyl 1,10-phenanthroline was measured in aqueous solution at 323.2 K as $3.9 \times 10^{-5} \text{ mol dm}^{-3}$. From this and the solubility at 298.2 K (Table 4.09), an estimate of ca. -2.6 kJ mol^{-1} can be made for its enthalpy of solution (using equation (4.11)). This value is very similar to those established for 1,10-phenanthroline monohydrate itself and for 2,2'-bipyridyl. The very different solubilities of these compounds therefore must reflect markedly different entropies of solution.

CHAPTER 5

Mercury(II)-Catalysed Aquation of Transition
Metal-Halo Complexes in Binary Aqueous Mixtures.

5.1 INTRODUCTION

In chapters 2 and 3, the solvent effects on the dissociative reactions of (i) nucleophilic substitution at pentacyano(ligand)ferrate (II) anions and (ii) the acid aquation of the tris-(5-nitro 1,10-phenanthroline)iron(II) cation were studied. These solvent effects having been found to be similar for these mechanistically similar reactions, interest was aroused in the solvent effects on a bimolecular reaction. Such effects have been studied in order to determine whether the conclusions drawn from the results of the studies on the dissociative reactions were limited to them, or whether they could be extended to encompass the other extreme type of reaction mechanism.

Unfortunately, there are very few purely bimolecular inorganic reactions of octahedral complexes which can be conveniently studied by the spectrophotometric technique readily available to this work.

One example of an octahedral substitution reaction which proceeds via a bimolecular rate-determining step is that of the reaction of the tris-(2,2'-bipyridyl)iron(II) cation with cyanide ion [5.01] and with hydroxide ion [5.02]. This has been studied in a wide range of binary aqueous mixtures [5.03,04], wherein it has been shown that reactivity trends in the reaction are predominantly determined by changes in the chemical potential of the attacking nucleophile. An organic reaction which has been successfully studied by a titration technique is the alkaline hydrolysis of sulphurtrioxide-trimethylamine, $\text{Me}_3\text{N}\cdot\text{SO}_3$, where associative attack by water at the sulphur atom is assumed [5.05-07]. A series of reactions in which the rate-determining step is bimolecular in nature is that of metal ion-catalysed aquations of certain ammine-halide complexes of d^3 and d^6 transition metal cations [5.08-11]. These

reactions are in fact bimolecular elimination reactions, S_E2 , with respect to the catalysing metal-ion centre. The mechanism operating within this series of reactions has been shown to depend upon the nature of the transition metal complex studied, for example, the mercury(II)-catalysed aquation of the cis-dichloro bis(ethylenediamine)cobalt(III) cation deviates from simple second-order kinetic behaviour [5.12].

In this work, complexes have been chosen which have been observed not to deviate from the simple second-order behaviour in aqueous solution, since the prime objective of this work is to study the behaviour of the second-order rate constants of the reactions when the solvent composition of the reaction media is altered. Thus the solvent effects on the apparent second-order rate constants for the metal-ion catalysed aquations of several transition metal complexes have been studied, and correlated with the thermodynamic parameter G^E of the solvent mixtures used, in the form of the activation free energy of transfer, $\delta_m \Delta G^\ddagger$, and with the standard free energy of transfer of the initial state of the reaction, $\delta_m \mu^\ominus$ (I.S.).

The range of complexes studied has been extended by observing the mercury(II)-catalysed aquation of the trans-dichloro bis(ethylenediamine)rhodium(III) cation in aqueous solution. This complex was chosen as it was expected to behave in a similar fashion to the analogous cobalt(III) complex cation.

5.2 EXPERIMENTAL

(i) REAGENTS

Preparations

A sample of the chloride salt of chloropenta-ammine cobalt(III) was prepared *via* aquo-penta-ammine cobalt(III) chloride according to Schlessinger [5.13]. *trans*-Dichloro bis(ethylenediamine) cobalt(III) chloride, [5.14] and the analogous rhodium(III) complex nitrate [5.15] were prepared from the metal(III) chlorides according to standard published methods.

A sample of the potassium salt of the hexachlororhenate anion, K_2ReCl_6 , was kindly donated by Dr. S. J. Cartwright.

Solvents and Other Reagents

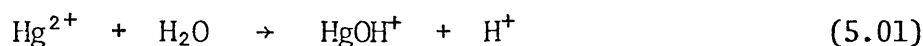
All solvents used were the best commercially available (usually AnalaR grade), and were used as received. 1,4-Dioxan was purified as described in chapter 2.

Mercury(II) perchlorate trihydrate (99.9% pure) was supplied by K & K Laboratories. Mercury(II) nitrate, magnesium nitrate and perchlorate, perchloric acid (specific gravity 1.54) and nitric acid (70% by wt.) were all supplied by British Drug Houses as AnalaR grade materials, and were used without further purification.

(ii) KINETICS

Fresh solutions of the appropriate mercury(II) salt were prepared daily to avoid possible formation of polynuclear mercury(II) species. These were made up using a solution of known concentration of the

appropriate acid, in order to prevent the hydrolysis reaction:-



Sze & Irish [5.16] have shown that in acid solution, the mercury(II)-ion catalyses the hydrolysis of acetonitrile. They showed this catalysis to be first-order in mercury(II)-ions, with a second-order rate constant of $1.9 \times 10^{-6} \text{ dm}^3 \text{ mol}^{-1} \text{ s}^{-1}$ at 298.2 K. As the reactions studied in this chapter are much faster than this, it is safe to assume that under the conditions used, there is no appreciable hydrolysis of acetonitrile in the relevant solvent mixtures.

For the mercury(II)-catalysed aquation of the hexachlororhenate(IV) anion, ReCl_6^{2-} , a stock solution of mercury(II) perchlorate of strength $6 \times 10^{-2} \text{ mol dm}^{-3}$ in 0.1 mol dm^{-3} perchloric acid was used. This produced a reaction medium of metal(II) perchlorate concentration $0.040 \text{ mol dm}^{-3}$ (maintained with magnesium perchlorate), and an acid strength of $0.025 \text{ mol dm}^{-3}$.

Fresh solutions of K_2ReCl_6 were prepared daily in degassed, doubly distilled water, and stored under nitrogen to prevent any decomposition which occurs in the presence of dissolved oxygen [5.17]. For kinetic measurements, aliquots of the complex solution were extracted from the stock solution via a 2 cc graduated syringe through a septum cap, and transferred to the silica cell. The concentration of complex in all kinetic runs was $1 \times 10^{-4} \text{ mol dm}^{-3}$.

In the study of the mercury(II)-catalysed aquation of the chloropenta-ammine cobalt(III) cation, $[\text{Co}(\text{NH}_3)_5\text{Cl}]^{2+}$, a stock solution of 0.08 mol dm^{-3} strength mercury(II) perchlorate in 0.80 mol dm^{-3} perchloric acid was used. The maximum concentration of $\text{Hg}^{2+}(\text{aq})$ ion used in the kinetic runs was 0.02 mol dm^{-3} . The concentration of complex used

throughout the study was $5 \times 10^{-4} \text{ mol dm}^{-3}$. The acid strength was kept constant at 0.20 mol dm^{-3} .

In the case of the mercury(II)-catalysed aquation of the trans-dichloro bis(ethylenediamine)cobalt(III) cation, $\text{trans-}[\text{Co(en)}_2\text{Cl}_2]^+$, the stock solution of mercury(II) perchlorate used was 0.6 mol dm^{-3} in 0.1 mol dm^{-3} perchloric acid. Due to the low extinction coefficient of the complex cation and the large second-order rate constant for the reaction with mercury(II) ion, only one concentration of mercury(II) ion was used for solvent mixtures other than 40% co-solvent ones. These runs were repeated at least three times, and apparent second-order rate constants were calculated from the expression:-

$$k_{\text{app}} = \frac{k_{\text{obs}}}{[\text{Hg}^{2+}]} \quad (5.02)$$

In this system the complex concentration for all runs was $1 \times 10^{-3} \text{ mol dm}^{-3}$, and $[\text{Hg}^{2+}] = 2 \times 10^{-2} \text{ mol dm}^{-3}$.

Thus all kinetic runs on the above systems were performed in the presence of an excess of mercury(II) ion so that first-order conditions were maintained. The method of generating suitable reaction mixtures of the required composition is analogous to that fully described earlier (see chapter 2). The temperature at which the above systems were studied was maintained at 298.2 K.

The mercury(II)-catalysed aquation of the $\text{trans-}[\text{Rh(en)}_2\text{Cl}_2]^+$ cation was studied in aqueous solution at 308.2 K, over a range of mercury(II)-ion concentrations up to $1.453 \text{ mol dm}^{-3}$, in 0.67 mol dm^{-3} nitric acid. The metal(II) nitrate concentration was maintained at a constant value of $1.453 \text{ mol dm}^{-3}$ with magnesium nitrate. The complex concentration used in the kinetic runs was $1.8 \times 10^{-3} \text{ mol dm}^{-3}$.

All kinetic runs for all complexes except the $\text{trans-}[\text{Rh}(\text{en})_2\text{Cl}_2]^+$ cation were performed in the thermostatted cell compartment of a Pye Unicam SP800A Recording Spectrophotometer, fitted with an S.P.825 clock attachment. The thermostatted cell compartment was calibrated in the range 288-333 K, to within an error of ± 0.05 deg. Rates of change of the optical densities of the complexes under observation were monitored at positions of maximum difference in optical densities between the starting materials and the final products of the reaction. The kinetic study on the rhodium complex was performed on a Pye Unicam SP1800A Spectrophotometer fitted with a data-logging interface. This was necessary due to the low extinction coefficient of the cation, with consequent small changes in optical density from starting complex to aquation products. The thermostating system here was identical to that used for the other kinetics studies.

The fixed wavelengths at which the kinetics of the above reactions were monitored were 282 nm, 270 nm, 461 nm and 420 nm for the ReCl_6^{2-} , $[\text{Co}(\text{NH}_3)_5\text{Cl}]^{2+}$, $\text{trans-}[\text{Co}(\text{en})_2\text{Cl}_2]^+$ and $\text{trans-}[\text{Rh}(\text{en})_2\text{Cl}_2]^+$ complex ions respectively. Good first-order kinetics were observed for at least three to four half-lives of all the reactions studied.

5.3 RESULTS AND DISCUSSION

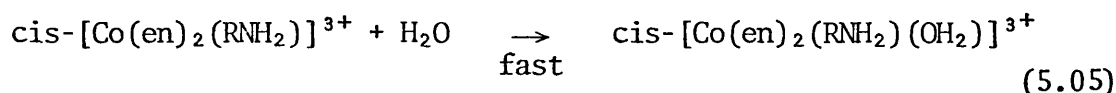
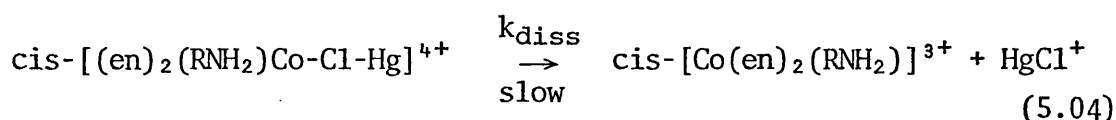
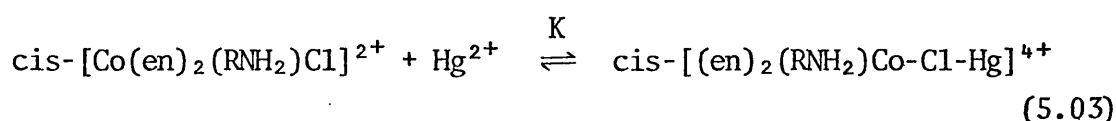
The reaction of metal-ion-catalysed aquation of transition metal complexes in acidic media has been fairly extensively studied for a variety of both transition metal complexes and of metal-ion catalysts. Examples include the reaction of the chloropentamminecobalt(III) cation with mercury(II) [5.08], thallium(III) [5.09] or silver(I) [5.09]; of the chloropentamminechromium(III) cation with mercury(II) [5.10]; and of the chloropentamminerhodium(III) cation with mercury(II) [5.11]. All these examples exhibit a first-order dependence of the rate of reaction on the catalyst concentration and on complex concentration, i.e. obey the simple second-order rate law:-

$$\text{rate} = \frac{-d[\text{complex}]}{dt} = k_2 [\text{complex}][\text{catalyst}] \quad (5.02)$$

The analogous reactions of the hexachloro- and hexabromo-complex anions of rhenium(IV), ReCl_6^{2-} and ReBr_6^{2-} have been shown [5.17] to follow a similar kinetic behaviour to the aforementioned complexes of other kinetically inert transition metal cations. Other examples of such second-order kinetic behaviour include the metal-ion-catalysed aquation of the trans-dichloro bis(ethylenediamine)cobalt(III) cation [5.12].

However, a complication in the kinetic behaviour of the reaction arises for several complexes, for example the cations $\text{cis}[\text{Co}(\text{en})_2\text{Cl}_2]^+$ [5.12] and $\text{cis}[\text{Co}(\text{en})_2(\text{RNH}_2)\text{Cl}]^{2+}$ [5.18] and some chloro-rhodium(III) complexes [5.11], where deviations from second-order kinetics occur. In these systems, the apparent second-order rate constants, $k_2 (= k_{\text{obs}}/[\text{catalyst}])$, decrease upon increase in concentration of the catalysing metal ion.

Both the straightforward (second-order) and the more unusual kinetic behaviours which are observed for the above systems are explained by the authors in terms of an equilibrium association of the $[\text{ML}_5\text{Cl}]^{n+}$ complex ions with the catalysing metal ion, e.g. Hg^{2+} , to form a binuclear intermediate, $[\text{L}_5\text{M}-\text{Cl}-\text{Hg}]^{(n+2)+}$. The subsequent step of the mechanism is 'unimolecular' dissociation of the binuclear intermediate to produce an aquated product, $[\text{ML}_5(\text{OH}_2)]^{(n+1)+}$ and HgCl^+ as the leaving group. For the case of the mercury(II)-catalysed aquation of the cation $\text{cis}[\text{Co}(\text{en})_2(\text{RNH}_2)\text{Cl}]^{2+}$ (from ref. [5.18])



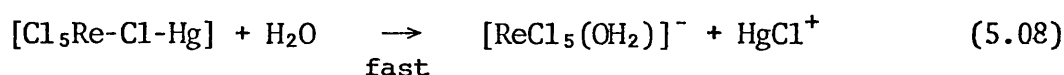
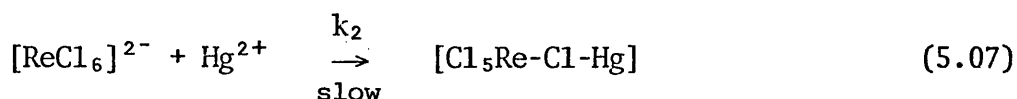
Under pseudo-first-order conditions, the observed first-order rate constant is related to the mechanistically derived rate constants by:-

$$k_{\text{obs}} = \frac{k_{\text{diss}} K [\text{Hg}^{2+}]}{1 + K [\text{Hg}^{2+}]} \quad (5.06)$$

For the simple second-order reaction mentioned above, a slow rate-determining pre-equilibrium is required, with subsequent rapid dissociation of the 'unstable' transition state. Alternatively, the reaction may be regarded as a simple bimolecular reaction between the reactants ML_6^{n-} and Hg^{2+} , forming the $[\text{L}_5\text{M}-\text{L}-\text{Hg}]^{(n-2)-}$ transition state. Here, the rate-determining step of the reaction is then bimolecular association of the reactants. Such a mechanism is more appealing than the other

possible reaction scheme outlined in equations (5.03-05) with regard to the application of extra complicating factors such as variable solvent composition. Hence in this work complexes have been chosen which have previously been shown to exhibit simple second-order kinetics in aqueous solution.

The kinetic behaviour of the mercury(II)-catalysed aquation of the hexachlororhenate(IV) anion is consistent with direct rate-determining association of the reactants. This reaction is in fact a bimolecular elimination reaction (S_E2) with respect to the mercury(II) ion.



In the analysis of the results of the study of this reaction it seems most reasonable to work on the simplest assumption, that the bimolecular associative attack of mercury(II) at the halide ligand is the rate-determining-step, i.e. k_2 of equation (5.07) is a simple bimolecular rate constant. It must be borne in mind, however, that this k_2 may be a composite quantity, with part of the reaction progressing via equilibrium formation of an intermediate.

Although there is the possibility of using several catalysing metal ions, mercury(II) has alone been chosen in this work. One practical reason is that mercury(II) perchlorate trihydrate is readily available commercially, and consequently easier to handle than, for example thallium(III) ion as a catalyst [5.19]. More importantly, the mercury(II) cation has been shown to have a higher catalytic activity than the thallium(III) cation with respect to various complexes, as is illustrated

below:-

| Complex Ion | $k_2(\text{Hg}^{2+})/k_2(\text{Tl}^{3+})$ | ref. |
|--|---|-------------------|
| ReCl_6^{2-} | 8.7 | [5.19] |
| $[\text{Co}(\text{NH}_3)_5\text{Cl}]^{2+}$ | 16.2 | [5.20] |
| $\text{trans-}[\text{Co}(\text{en})_2\text{Cl}_2]^+$ | 8.4 | [5.09, 12 and 21] |
| $\text{cis-}[\text{Co}(\text{en})_2\text{Cl}_2]^+$ | 11.8 | [5.09, 12 and 21] |

Hence, in this work the three complex ions, $[\text{ReCl}_6]^{2-}$, $[\text{Co}(\text{NH}_3)_5\text{Cl}]^{2+}$ and $\text{trans-}[\text{Co}(\text{en})_2\text{Cl}_2]^+$ have been chosen, and the mercury(II)-catalysed aquation of these ions in aqueous solution and in a range of binary aqueous mixtures has been studied.

(a) Mercury(II)-Catalysed Aquation of the Hexachlororhenate(IV) Anion

Although this reaction has been shown to exhibit second-order kinetics in aqueous solution, i.e:-

$$\text{rate} = - \frac{d[\text{ReCl}_6^{2-}]}{dt} = k_2 [\text{ReCl}_6^{2-}] [\text{Hg}^{2+}] \quad (5.09)$$

it is necessary to ensure that this behaviour is not deviated from on changing the solvent composition. It has been shown by Chan & Tan [5.22] that for the mercury(II)-catalysed aquation of $\text{trans-}[\text{Co}(\text{dmgH})(\text{NH}_3)\text{Cl}]$ in aqueous solution, there is significant formation of the binuclear intermediate $\text{trans-}[(\text{dmgH})(\text{NH}_3)\text{Co-Cl-Hg}]^{2+}$, as evidenced by a decrease in the apparent second-order rate constant with increase in the concentration of mercury(II)-ion (see ref. [5.12]). On adding ethanol to the system, they showed that the association constant, K (cf. equations (5.03,06)) increased rapidly with molefraction of ethanol. Hence, if the reaction concerning $[\text{ReCl}_6]^{2-}$ were proceeding with very slight, and

so unnoticed formation of a binuclear intermediate, we might expect the association constant to increase with increasing molefraction of co-solvent, and so increase any deviation from second-order kinetics.

Observed first-order rate constants for the mercury(II)-catalysed aquation of the $[\text{ReCl}_6]^{2-}$ anion have been measured at 298.2 K in water and in 10% to 40% by volume of organic co-solvent inclusive, for various mercury(II)-ion concentrations, $[\text{Hg}^{2+}]$. These rate constants, together with the consequent second-order rate constants, k_2 , are listed in Table 5.01. The results for the 40% co-solvent mixtures are illustrated in Figure 5.01, as a function of k_{obs} on $[\text{Hg}^{2+}]$, and clearly show that under these conditions, there is no deviation from second-order kinetics. This fact tends to support the assumption made earlier that the rate-determining step is the simple bimolecular association of the reactant species, and that the $[\text{Cl}_5\text{Re}-\text{Cl}-\text{Hg}]$ species is simply the transition state of the reaction. The lack of evidence for any recognisable intermediate in this reaction is also supported by the very clean isosbestic point which is observed for the reaction at 260 nm, when the UV spectrum of the reaction mixture is repeatedly scanned. Such spectra are shown in Figure 5.02.

The measured k_2 values in the range of solvent mixtures are expressed as a function of mole fraction of co-solvent in Figure 5.03, and show a remarkable sensitivity to solvent composition. From Table 5.01 we can see a 75 fold increase in k_2 on going from solvent water to 40% ethanol-water mixture. This may be contrasted with the very low solvent sensitivity of the previously studied (see chapter 2) limiting dissociative mechanism of nucleophilic substitution at pentacyanoferrate(II), where the rate enhancement on going from water to 40% ethanol was found to be only two-fold. One might at first sight ascribe this

TABLE 5.01 Observed first-order rate constants, k_{obs} , and derived second-order rate constants, k_2 , for the mercury(II)-catalysed reaction of the hexachloroantimonate(IV) anion in a range of binary aqueous mixtures, for various mercury(II) ion concentrations at 298.2 K; ionic strength = 0.04 mol dm⁻³ (maintained with magnesium perchlorate).

| Solvent Composition ^a | $\frac{[\text{Hg}^{2+}]}{\text{mol dm}^{-3}}$ | | | $10^3 k_{\text{obs}} / \text{s}^{-1}$ | $k_2 / \text{dm}^3 \text{mol}^{-1} \text{s}^{-1}$ | $-\delta_m \Delta G^\ddagger / \text{kJ mol}^{-1}$ |
|----------------------------------|---|-------|-------|---------------------------------------|---|--|
| | 0.003 | 0.005 | 0.010 | 0.015 | | |
| Water | 0.061 | 0.106 | 0.210 | 0.310 | 0.0207 ± 0.0003 | 0 |
| 10 | 0.108 | 0.190 | 0.385 | 0.577 | ± 0.0003 | 1.57 |
| 20 | 0.321 | 0.541 | 1.07 | 1.61 | ± 0.001 | 4.08 |
| 30 | 0.691 | 1.06 | 2.30 | 3.47 | ± 0.004 | 6.02 |
| 40 | 1.90 | 3.05 | 6.19 | 9.18 | ± 0.009 | 8.39 |
| 10 | 0.137 | 0.221 | 0.451 | 0.684 | ± 0.0005 | 1.96 |
| 20 | 0.401 | 0.669 | 1.35 | 2.02 | ± 0.003 | 4.65 |
| 30 | 1.07 | 1.86 | 3.61 | 5.46 | ± 0.004 | 7.10 |
| 40 | 4.44 | 7.32 | 14.8 | 22.3 | ± 0.02 | 10.6 |
| 10 | 0.191 | 0.314 | 0.622 | 0.932 | ± 0.0008 | 2.71 |
| 20 | 0.497 | 0.646 | 1.70 | 2.52 | ± 0.002 | 5.30 |
| 30 | 1.88 | 3.04 | 6.10 | 9.09 | ± 0.009 | 8.36 |
| 40 | 4.69 | 7.91 | 15.6 | 23.5 | ± 0.02 | 10.7 |
| 10 | 0.160 | 0.271 | 0.535 | 0.802 | ± 0.0009 | 2.35 |
| 20 | 0.213 | 0.359 | 0.719 | 1.08 | ± 0.0011 | 3.09 |
| 30 | 0.340 | 0.572 | 1.14 | 1.72 | ± 0.002 | 4.24 |
| 40 | 0.451 | 0.778 | 1.54 | 2.31 | ± 0.003 | 4.99 |
| 10 | 0.269 | 0.441 | 0.890 | 1.33 | ± 0.0011 | 3.60 |
| 20 | 1.41 | 2.20 | 4.62 | 6.82 | ± 0.007 | 7.67 |
| 30 | 3.20 | 5.51 | 11.0 | 16.6 | ± 0.03 | 9.89 |
| 40 | 5.01 | 6.53 | 17.0 | 25.6 | ± 0.11 | 11.0 |
| 10 | 0.181 | 0.399 | 0.596 | 0.872 | ± 0.0006 | 2.38 |
| 20 | 0.610 | 0.930 | 1.91 | 2.94 | ± 0.003 | 5.57 |
| 30 | 2.19 | 3.61 | 7.42 | 11.1 | ± 0.012 | 8.89 |
| 40 | 5.50 | 9.20 | 18.2 | 27.1 | ± 0.12 | 11.1 |

^a Solvent composition is expressed as % by volume before mixing.

Figure 5.01 Dependence of $k_{\text{obs}}(\text{s}^{-1})$ on $[\text{Hg}^{2+}]$ (mol dm^{-3}) in several binary aqueous mixtures (40 % cosolvent); o = methanol, Δ = ethanol, \square = t-butyl alcohol, \times = 1,4-dioxan, \dagger = acetonitrile, \blacktriangle = ethylene glycol cosolvent; at 298.2 K, for the mercury(II)-catalysed aquation of the ReCl_6^{2-} anion, at 298.2 K.

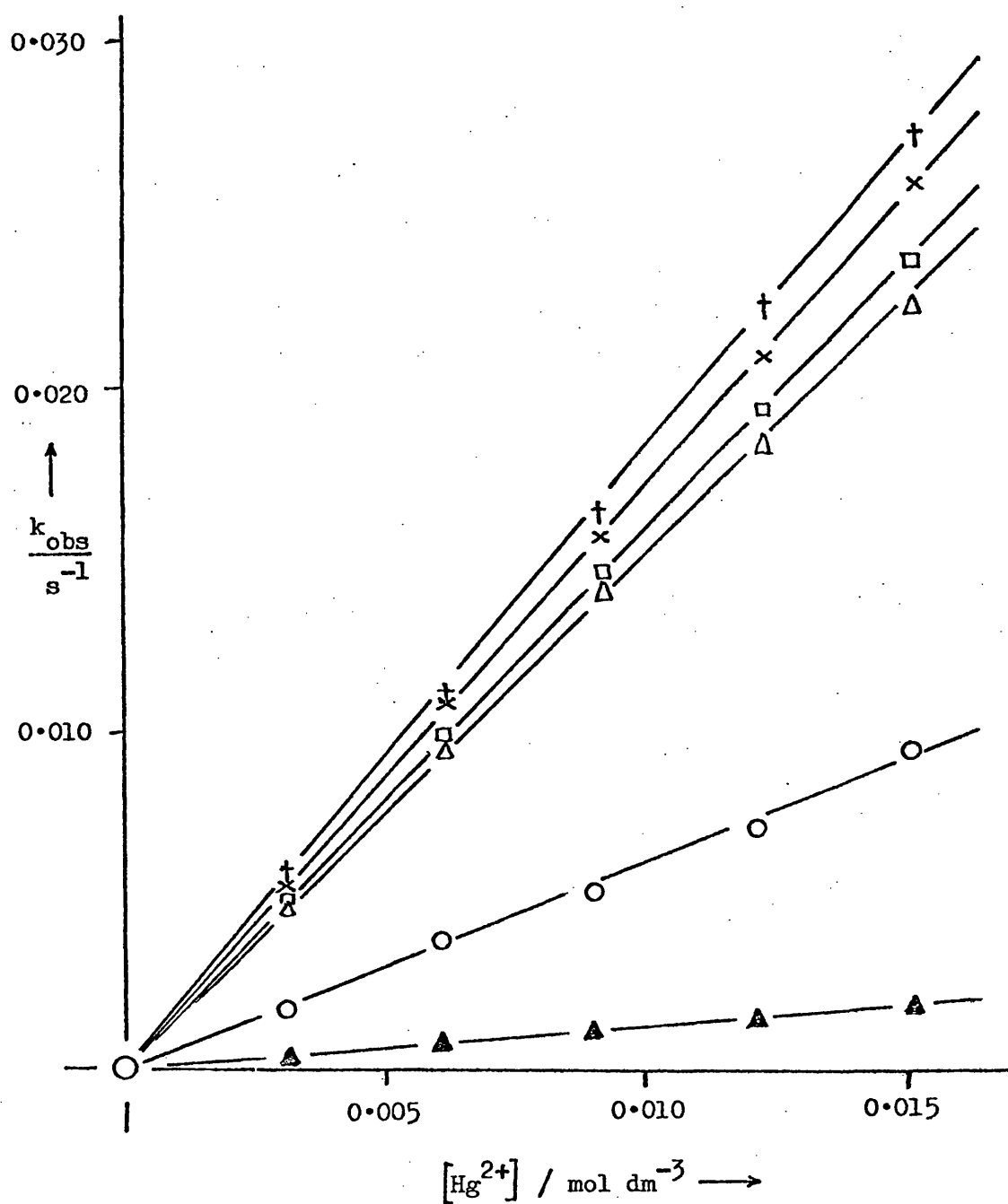


Figure 5.02 Variable wavelength repeat-scan of the UV spectrum of the reaction between Hg^{2+} and ReCl_6^{2-} in aqueous solution; initial $[\text{ReCl}_6^{2-}] = 1.5 \times 10^{-4} \text{ mol dm}^{-3}$; $[\text{Hg}^{2+}] = 0.015 \text{ mol dm}^{-3}$; temperature = 298.2 K.

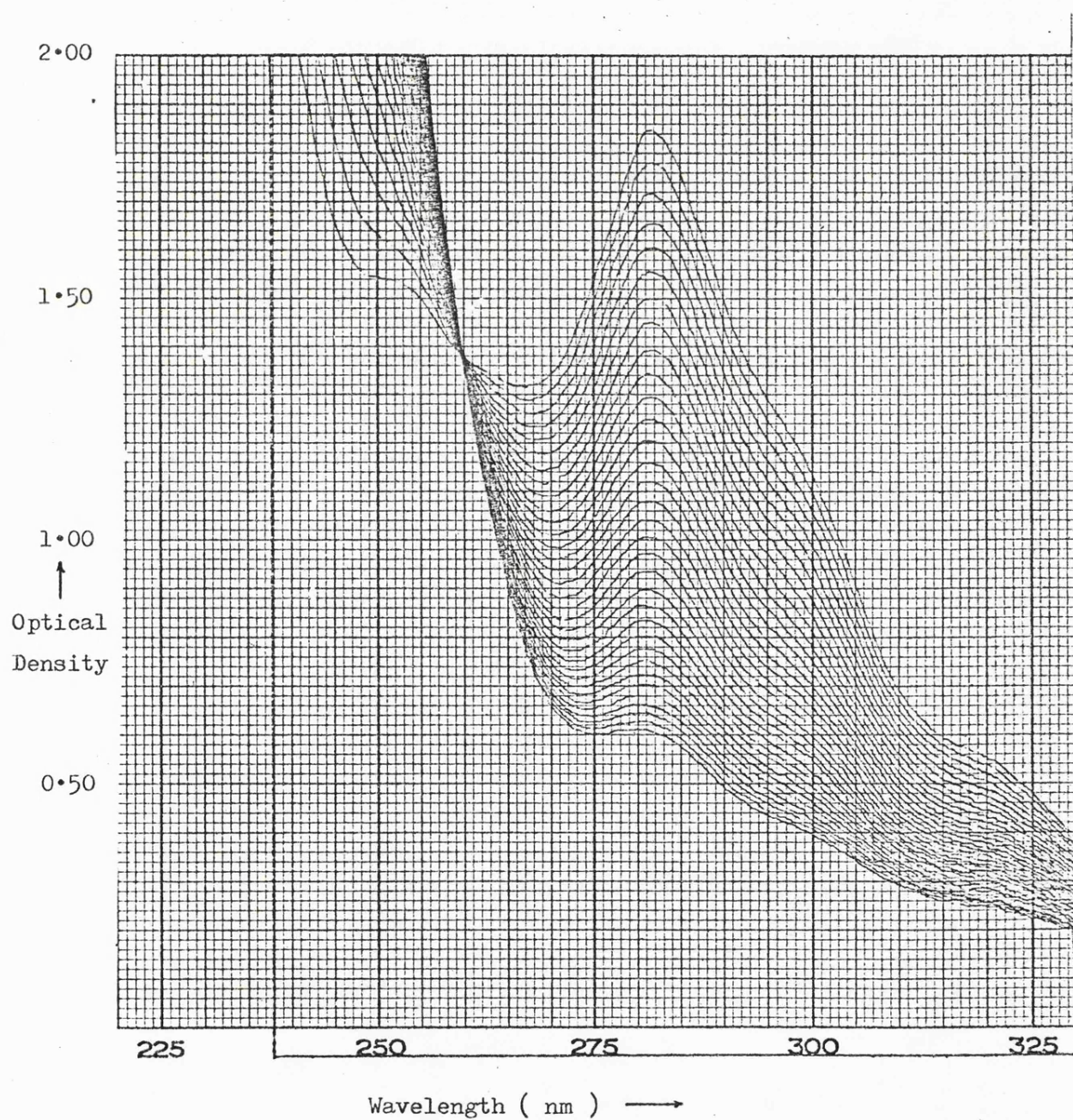
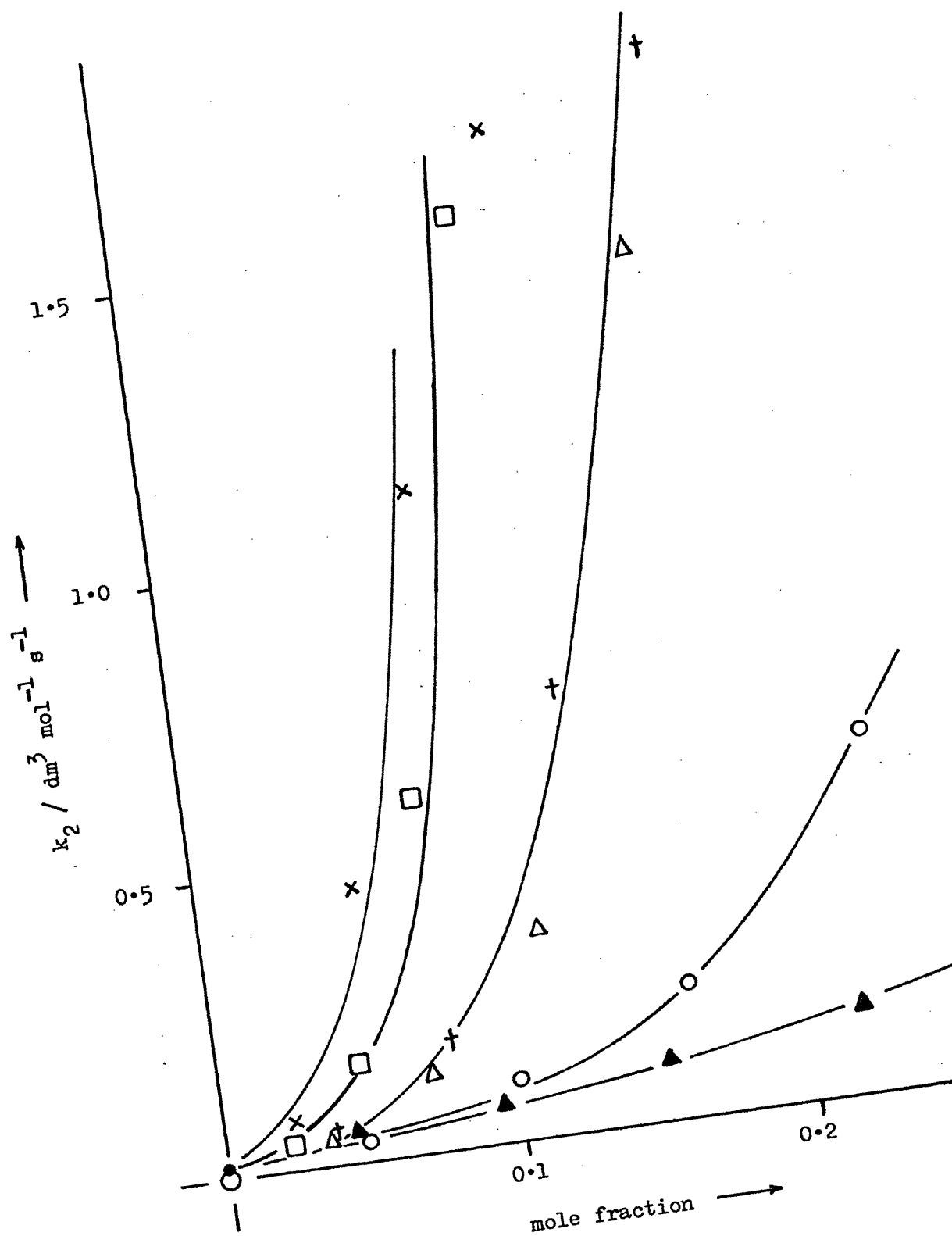


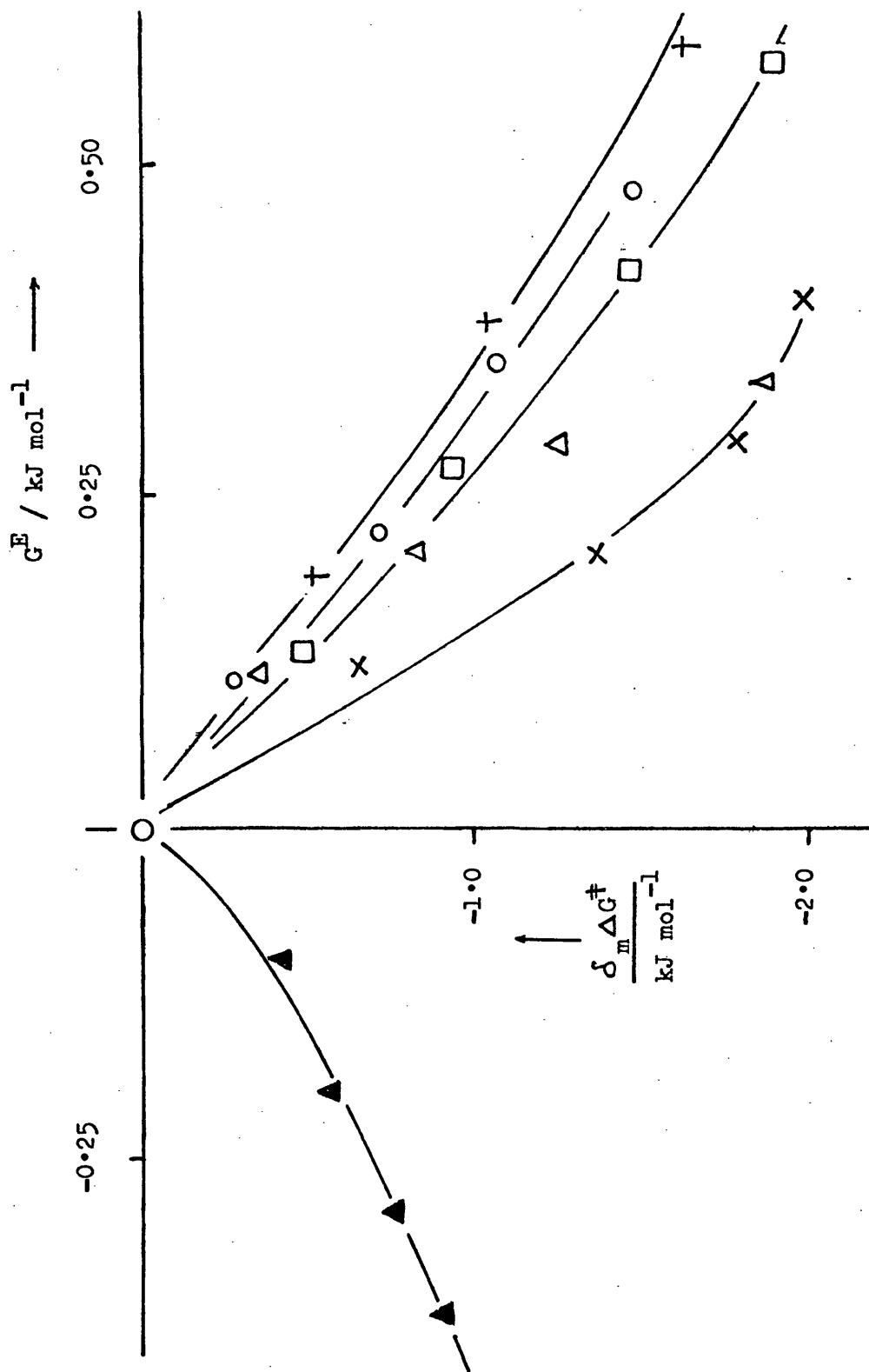
Figure 5.03 Variation of $k_2(\text{dm}^3 \text{mol}^{-1} \text{s}^{-1})$ with mole fraction of cosolvent, x_2 , for the $\text{Hg}^{2+}/\text{ReCl}_6^{2-}$ reaction at 298.2 K; symbols as in Figure 5.01.



difference in the behaviour of the two reactions to the different mechanisms operating for them. In chapter 2, the solvent effects were described by and discussed in terms of the variation of the free energy of transfer, $\delta_m \Delta G^\ddagger$ for the reaction with respect to G^E values for the relevant solvent mixtures. We can again examine the $\text{ReCl}_6^{2-}/\text{Hg}^{2+}$ system in terms of the dependence of $\delta_m \Delta G^\ddagger$ on G^E . Such a plot is illustrated in Figure 5.04. We can see from this plot that again the T.A.type solvent mixtures (see chapter 1) produce values of $\delta_m \Delta G^\ddagger$ for the reaction which become more negative with increase in molefraction of co-solvent, producing a correlation sector for these solvent mixtures in the $+G^E, -\delta_m \Delta G^\ddagger$ quadrant. We see also that T.N.A.type solvent mixtures do not correlate with the T.A. ones, an occurrence which was also observed for the dissociative mechanisms, for example the acid aquation of the tris-(5-nitro 1,10-phenanthroline)iron(II) cation in chapter 3. The steeper slope of the T.A.results sector in Figure 5.04 is again a function of the solvent sensitivity of this bimolecular reaction, and hence is much steeper than the analogous sector for the dissociative reactions studied in chapters 2 and 3.

From the knowledge of the very different mechanisms operating for the mercury(II)-catalysed aquation of the $[\text{ReCl}_6]^{2-}$ anion here and the nucleophilic substitution reactions at the $[\text{Fe}(\text{CN})_5\text{L}]^{n-}$ anions and the acid aquation of the $[\text{Fe}(5\text{-NO}_2\text{phen})_3]^{2+}$ cation studied previously, it is obvious that we cannot attribute the consistent pattern of the results in T.A. mixtures to mechanism type. This is further supported by the results of the study in binary aqueous mixtures of the reaction of the tris-(2,2'-bipyridyl)iron(II) cation with cyanide ion and with hydroxide ion [5.07 and 08], where the rate constant increases (and so $\delta_m \Delta G^\ddagger$ becomes more negative) on adding co-solvents to the system, regardless

Figure 5.04 Dependence of $\delta_m \Delta G^\ddagger$ on G^E for the $\text{Hg}^{2+}/\text{ReCl}_6^{2-}$ reaction in a range of binary aqueous mixtures at 298.2 K; symbols as in Figure 5.01.



of the nature (either T.A. or T.N.A.) of the resulting solvent mixture.

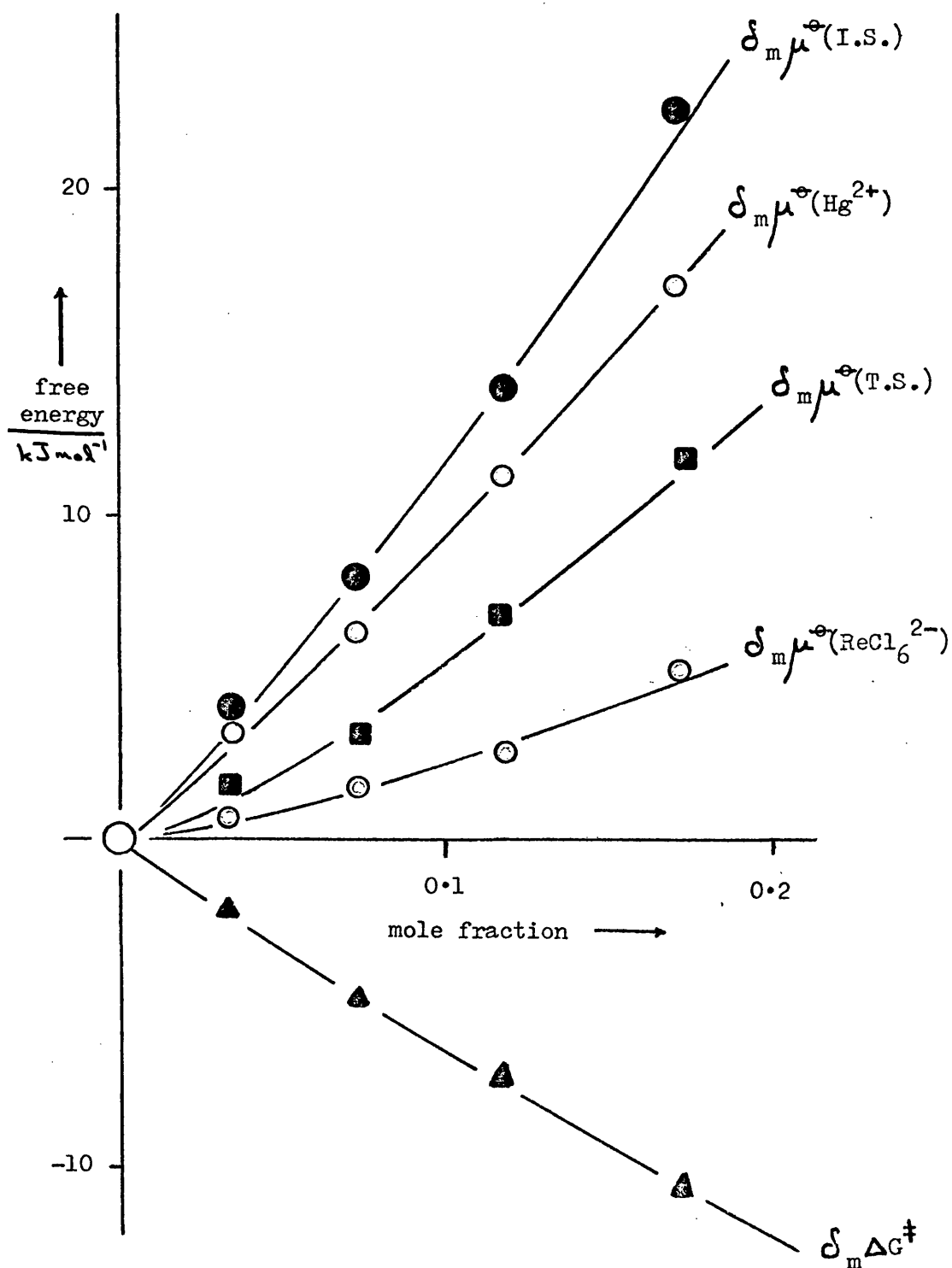
In order to account for the observed drastic changes in rate constants for the mercury(II)-catalysed aquation of $[\text{ReCl}_6]^{2-}$ with solvent composition, the relationship of the kinetic parameters of the reaction in terms of the activation free energy of transfer, $\delta_m \Delta G^\ddagger$ with the Gibbs free energy of transfer, $\delta_{\text{m}\mu}^\ominus$ of the initial state of the reaction, i.e. $\delta_{\text{m}\mu}^\ominus$ for the $[\text{ReCl}_6]^{2-}$ anion and for the Hg^{2+} cation has been investigated. The estimation of the $\delta_{\text{m}\mu}^\ominus$ (I.S.) parameter has been made from solubility measurements of suitable salts of the Hg^{2+} and $[\text{ReCl}_6]^{2-}$, and literature values for the single-ion free energies of transfer of the corresponding anion and cation from water into the appropriate solvent mixture. These measurements, together with the subsequent calculations have been fully described in chapter 4. Due to the unfortunate lack of data on the single-ion values in binary aqueous mixtures, $\delta_{\text{m}\mu}^\ominus$ (I.S.) can at present only be calculated in several aqueous-methanol or -ethanol mixtures, as shown in Table 5.02. Values of $\delta_m \Delta G^\ddagger$, which are listed in Table 5.01 were calculated as described earlier (see chapter 1). At present, we have data available through kinetic measurements on $\delta_m \Delta G^\ddagger$ for several systems (in this work), and through solubility measurements (chapter 4) on $\delta_{\text{m}\mu}^\ominus$ (salt) for a mercury(II) salt and for salts of the transition metal complexes studied in this chapter. If in the future more single-ion transfer data become available, or if new reasonable assumptions for estimating single ion values from salts, (e.g. see chapter 4, "magnesium hexachlororhenate"), then the present limited set of solvent mixtures in which $\delta_{\text{m}\mu}^\ominus$ (T.S.) has been estimated will be greatly expanded.

Figure 5.05 shows a comparison of the trends in $\delta_m \Delta G^\ddagger$ with solvent composition with those of $\delta_{\text{m}\mu}^\ominus$ (I.S.) for aqueous-ethanol solvent

TABLE 5.02 Gibbs free energies of transfer of the initial and transition states, and the Gibbs activation free energies of transfer for the mercury(II)-catalysed aquation reactions of the ReCl_6^{2-} , $[\text{Co}(\text{NH}_3)_5\text{Cl}]^{2+}$ and $\text{trans-}[\text{Co}(\text{en})_2\text{Cl}_2]^+$ ions, at 298.2 K. Parameters are for transfer from water into aqueous ethanol mixtures; units are of kJ mol^{-1} .

| | % by volume ethanol | | | |
|--|---------------------|-------|-------|--------|
| | 10 | 20 | 30 | 40 |
| $\delta_m \mu^\ominus(\text{Hg}^{2+})$ | + 3.2 | + 6.4 | +11.2 | +17.1 |
| $\delta_m \mu^\ominus(\text{ReCl}_6^{2-})$ | + 0.7 | + 1.6 | + 2.6 | + 5.2 |
| $\delta_m \mu^\ominus(\text{I.S.})$ | + 3.9 | + 8.0 | +13.8 | +22.3 |
| $\delta_m \Delta G^\ddagger$ | - 2.0 | - 4.7 | - 7.1 | -10.6 |
| $\delta_m \mu^\ominus(\text{T.S.})$ | + 1.9 | + 3.3 | + 6.7 | +11.7 |
| $\delta_m \mu^\ominus([\text{Co}(\text{NH}_3)_5\text{Cl}]^{2+})$ | + 2.0 | + 3.6 | + 7.0 | + 9.6 |
| $\delta_m \mu^\ominus(\text{I.S.})$ | + 5.2 | +10.0 | +18.2 | +26.7 |
| $\delta_m \Delta G^\ddagger$ | - 0.05 | - 0.4 | - 0.6 | - 0.7 |
| $\delta_m \mu^\ominus(\text{T.S.})$ | + 5.25 | +10.4 | +18.8 | +27.4 |
| $\delta_m \mu^\ominus(\text{t-}[\text{Co}(\text{en})_2\text{Cl}_2]^+)$ | + 0.1 | + 0.5 | + 0.7 | + 0.6 |
| $\delta_m \mu^\ominus(\text{I.S.})$ | + 3.3 | + 6.9 | +11.9 | +17.7 |
| $\delta_m \Delta G^\ddagger$ | - 0.4 | - 0.6 | - 0.3 | - 0.05 |
| $\delta_m \mu^\ominus(\text{T.S.})$ | + 3.7 | + 7.5 | +12.2 | +17.75 |

Figure 5.05 Correlation of the various transfer parameters of the $\text{ReCl}_6^{2-}/\text{Hg}^{2+}$ system with solvent composition, at 298.2 K.



mixtures. These trends do not coincide, and it may be concluded that the quantity $\delta_m \mu^\ominus$ (Transition State) has some importance in determining the solvent sensitivity of the reaction. Considering diagram 5.01,

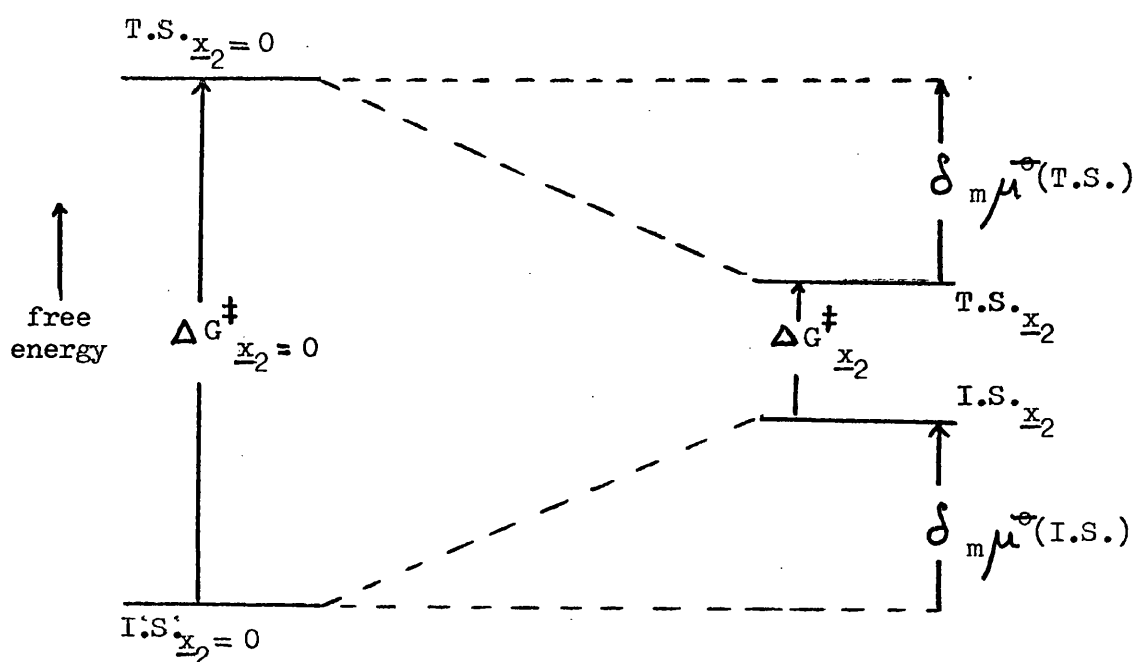


Diagram 5.01

we can see that

$$\delta_m \Delta G^\ddagger = \Delta G^\ddagger_{x_2} - \Delta G^\ddagger_{x_2=0} \quad (5.10)$$

where

$\Delta G^\ddagger_{x_2}$ is the Gibbs free energy of activation for the reaction in solvent of molefraction x_2 ,

and $\Delta G^\ddagger_{x_2=0}$ " " " " " " in solvent water.

This is in fact the general definition of $\delta_m \Delta G^\ddagger$ as laid out in chapter 1. Similarly, $\delta_m \mu^\ominus$ (I.S.) is defined as the difference in free energies of the initial state of the reaction between solvent of molefraction \underline{x}_2 and solvent water.

$$\text{i.e. } \delta_m \mu^\ominus \text{ (IS)} = \mu^\ominus \text{ (IS)}_{\underline{x}_2} - \mu^\ominus \text{ (IS)}_{\underline{x}_2=0} \quad (5.11)$$

Analogously,

$$\delta_m \mu^\ominus \text{ (TS)} = \mu^\ominus \text{ (TS)}_{\underline{x}_2} - \mu^\ominus \text{ (TS)}_{\underline{x}_2=0} \quad (5.12)$$

For the $\text{ReCl}_6^{2-}/\text{Hg}^{2+}$ system, we can see from the estimated values of $\delta_m \mu^\ominus$ (IS) in Table 5.02 in aqueous-methanol mixtures that this function becomes more positive with increase in the mole fraction of co-solvent. This trend is to be expected for ionic species such as are present in this system, as is evidenced by general solubility trends of ionic salts in binary aqueous mixtures [5.23] (see also chapter 4). The transition state in this system is the uncharged $[\text{Cl}_5\text{Re}-\text{Cl}-\text{Hg}]$ species, and would be expected to behave like a neutral covalent compound with respect to its solvation characteristics, i.e. the solubility of such a species would be expected to increase with increase in the mole fraction of co-solvent in a range of binary aqueous mixtures. This would appear to be a good assumption in the light of the measured transfer parameter for mercury(II) chloride, $\delta_m \mu^\ominus$ (HgCl_2) [5.24]. This has a very similar periphery to our proposed transition state, and it seems reasonable that the solvation characteristics of the two species would be similar. Obviously it is impossible to measure such transfer parameters of the transition state of a reaction directly. However, by combining the kinetic transfer function, $\delta_m \Delta G^\ddagger$, and the thermodynamic transfer function, $\delta_m \mu^\ominus$ (IS), both of which can be directly measured experimentally, we can gain insight into the otherwise elusive free energy of transfer of the

transition state, $\delta_m\mu^\ominus$ (TS). From Diagram 5.01 we find that

$$-\delta_m\mu^\ominus \text{ (TS)} = \delta_m\mu^\ominus \text{ (IS)} + \delta_m\Delta G^\ddagger. \quad (5.13)$$

The calculated values of $\delta_m\mu^\ominus$ (T.S.) are listed in Table 5.02, and as expected this function becomes more negative with increase in the mole fraction of co-solvent. Other neutral covalently bonded transition metal complexes include those of the type $\text{Fe}^{\text{II}}(\text{LL})_2(\text{CN})_2$ (where LL = 2,2'-bipyridyl or 1,10-phenanthroline), whose solubilities have been measured in a range of binary aqueous mixtures, whence the parameters $\delta_m\mu^\ominus$ ($\text{Fe}(\text{LL})_2(\text{CN})_2$) can be seen to become more negative with increase in mole fraction of co-solvent [5.25].

We have seen that on adding co-solvent to the $\text{ReCl}_6^{2-}/\text{Hg}^{2+}$ system, $\delta_m\mu^\ominus$ (I.S.) becomes more positive, thus destabilising the reactant species, and so providing some driving force for the reaction. On the other hand, the transition state is stabilised by adding a co-solvent to the system, as evidenced by an increasingly negative $\delta_m\mu^\ominus$ (TS) term. Thus the transfer parameters of both initial and transition states combine to produce a large rate enhancement on addition of a co-solvent to the system.

In order to determine the relative importance of the initial and transition state solvation effects on this type of reaction, a doubly charged cationic complex was studied. Here, using the chloropentammine-cobalt(III) cation, the solvation characteristics of the initial state should be somewhat similar to those of the $\text{ReCl}_6^{2-}/\text{Hg}^{2+}$ system in that both reactants are still doubly charged ions.

(b) Mercury(II)-Catalysed Aquation of the $[\text{Co}(\text{NH}_3)_5\text{Cl}]^{2+}$ Cation

This reaction has been shown [5.08 and 12] to obey simple second-

order kinetics in aqueous solution. As with the previous $\text{ReCl}_6^{2-}/\text{Hg}^{2+}$ system studied, it was necessary to ensure that the kinetic behaviour of this system did not deviate on addition of organic co-solvent to it. First-order rate constants, k_{obs} , were measured at 298.2 K over a range of mercury(II)-ion concentrations, for 10 to 40% by volume of each co-solvent used. These results are listed in Table 5.03, together with the derived second-order rate constants, k_2 . Figure 5.06 clearly shows the constancy of the second-order kinetics of this reaction regardless of solvent composition over the range of mole fractions studied.

An immediately striking feature of these results, which is graphically described by Figure 5.07 is the remarkable solvent insensitivity of this system relative to the $\text{ReCl}_6^{2-}/\text{Hg}^{2+}$ one. Here, the rate increase on going from water to 40% by volume ethanol is only ca. 1.25 fold. At first sight these results seem somewhat surprising when compared with those of the $\text{ReCl}_6^{2-}/\text{Hg}^{2+}$ system. However, applying an analogous analysis to the results as was done with the previous system, the situation becomes clearer. Values of $\delta_{\text{m}\mu}^{\ominus}$ ($[\text{Co}(\text{NH}_3)_5\text{Cl}]^{2+}$) were estimated from published solubilities of the chloride salt [5.26] and literature values of $\delta_{\text{m}\mu}^{\ominus}$ (Cl^-) in aqueous ethanol mixtures [5.27]. These values are listed in Table 5.02. $\delta_{\text{m}\mu}^{\ominus}$ ($[\text{Co}(\text{NH}_3)_5\text{Cl}]^{2+}$) is seen to increase positively in nature rapidly with increase in mole fraction of ethanol. Hence in aqueous mixtures, $\delta_{\text{m}\mu}^{\ominus}$ (I.S.) for the $[\text{Co}(\text{NH}_3)_5\text{Cl}]^{2+}/\text{Hg}^{2+}$ system strongly favours rate enhancement by virtue of the destabilisation of the initial state reactants on going from water to binary aqueous mixtures. However, the transition state in this system is $[(\text{NH}_3)_5\text{Co}-\text{Cl}-\text{Hg}]^{4+}$. Such a species is expected to have very different solvation characteristics from the previous neutral $[\text{Cl}_5\text{Re}-\text{Cl}-\text{Hg}]$ transition state. For a 4+ cation, we would expect a strongly increasing positive trend in $\delta_{\text{m}\mu}^{\ominus}$ (Y^{4+}) with mole

TABLE 5.03 Observed first-order rate constants, k_{obs} , and derived second-order rate constants, k_2 , for the mercury(II)-catalysed aquation of the $[\text{Co}(\text{NH}_3)_5\text{Cl}]^{2+}$ cation in a range of binary aqueous mixtures, for various $[\text{Hg}^{2+}]$ at 298.2 K. Ionic strength = 0.84 mol dm^{-3} (maintained with magnesium perchlorate); $[\text{HClO}_4] = 0.20 \text{ mol dm}^{-3}$.

| Solvent Mixture | $[\text{Hg}^{2+}] / \text{mol dm}^{-3}$ | | | | k_2 $\text{dm}^3 \text{ mol}^{-1} \text{ s}^{-1}$ |
|----------------------|---|-------|-------|-------|--|
| | 0.005 | 0.010 | 0.015 | 0.020 | |
| | $10^3 k_{\text{obs}} / \text{s}^{-1}$ | | | | |
| Water | 0.49 | 0.95 | 1.47 | 1.91 | 0.095 ± 0.002 |
| 10 % Methanol | 0.47 | 0.97 | 1.45 | 1.93 | 0.096 ± 0.005 |
| 20 % Methanol | 0.52 | 1.07 | 1.52 | 2.09 | 0.102 ± 0.004 |
| 30 % Methanol | 0.53 | 1.09 | 1.63 | 2.15 | 0.106 ± 0.003 |
| 40 % Methanol | 0.57 | 1.12 | 1.70 | 2.26 | 0.112 ± 0.005 |
| 10 % Ethanol | 0.49 | 0.98 | 1.50 | 1.95 | 0.097 ± 0.002 |
| 20 % Ethanol | 0.53 | 1.10 | 1.66 | 2.21 | 0.113 ± 0.003 |
| 30 % Ethanol | 0.57 | 1.18 | 1.71 | 2.32 | 0.121 ± 0.005 |
| 40 % Ethanol | 0.61 | 1.26 | 1.85 | 2.51 | 0.128 ± 0.003 |
| 10 % t-Butyl alcohol | 0.57 | 1.08 | 1.69 | 2.22 | 0.110 ± 0.002 |
| 20 % t-Butyl alcohol | 0.67 | 1.28 | 2.01 | 2.61 | 0.130 ± 0.004 |
| 30 % t-Butyl alcohol | 0.80 | 1.68 | 2.41 | 3.31 | 0.163 ± 0.003 |
| 40 % t-Butyl alcohol | 0.99 | 2.04 | 2.88 | 4.05 | 0.203 ± 0.002 |
| 10 % Ethylene glycol | 0.43 | 0.89 | 1.29 | 1.75 | 0.087 ± 0.002 |
| 20 % Ethylene glycol | 0.46 | 0.85 | 1.40 | 1.71 | 0.090 ± 0.001 |
| 30 % Ethylene glycol | 0.45 | 0.92 | 1.41 | 1.82 | 0.092 ± 0.002 |
| 40 % Ethylene glycol | 0.47 | 0.99 | 1.47 | 2.06 | 0.098 ± 0.001 |
| 10 % Glycerol | 0.40 | 0.85 | 1.17 | 1.66 | 0.082 ± 0.003 |
| 20 % Glycerol | 0.39 | 0.73 | 1.22 | 1.51 | 0.077 ± 0.002 |
| 30 % Glycerol | 0.42 | 0.73 | 1.23 | 1.42 | 0.075 ± 0.003 |
| 40 % Glycerol | 0.40 | 0.79 | 1.26 | 1.63 | 0.081 ± 0.002 |
| 10 % Acetonitrile | 0.41 | 0.78 | 1.20 | 1.53 | 0.080 ± 0.003 |
| 20 % Acetonitrile | 0.35 | 0.73 | 1.02 | 1.37 | 0.070 ± 0.003 |
| 30 % Acetonitrile | 0.32 | 0.65 | 0.95 | 1.31 | 0.064 ± 0.001 |
| 40 % Acetonitrile | 0.25 | 0.58 | 0.80 | 1.12 | 0.055 ± 0.003 |

Figure 5.06 Dependence of the observed first-order rate constants, k_{obs} , for the mercury(II)-catalysed aquation of the $[\text{Co}(\text{NH}_3)_5\text{Cl}]^{2+}$ cation on mercury(II) ion concentration, in several binary aqueous mixtures (40 % cosolvent), at 298.2 K. Symbols as in Figure 5.01; ● = solvent water.

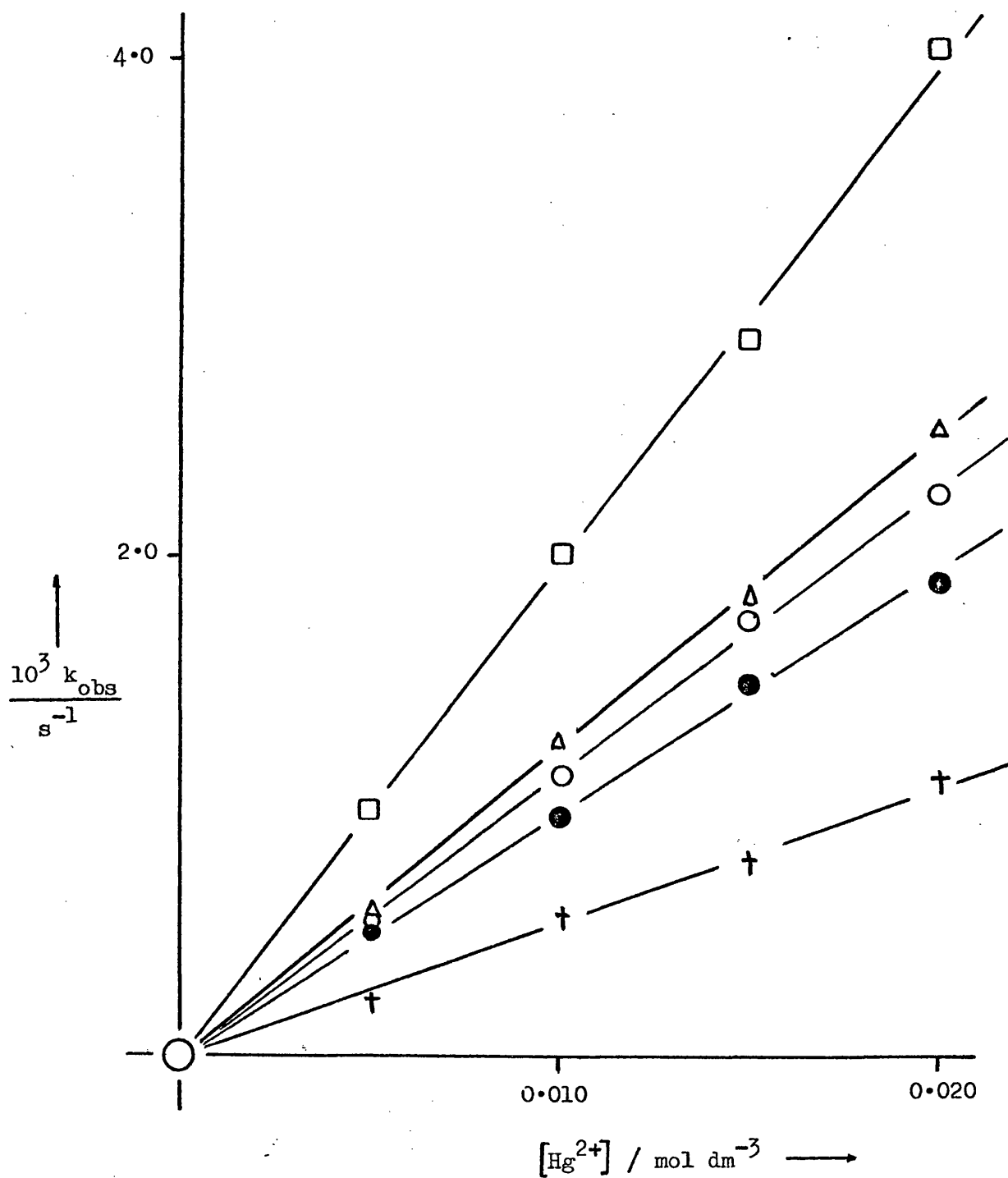
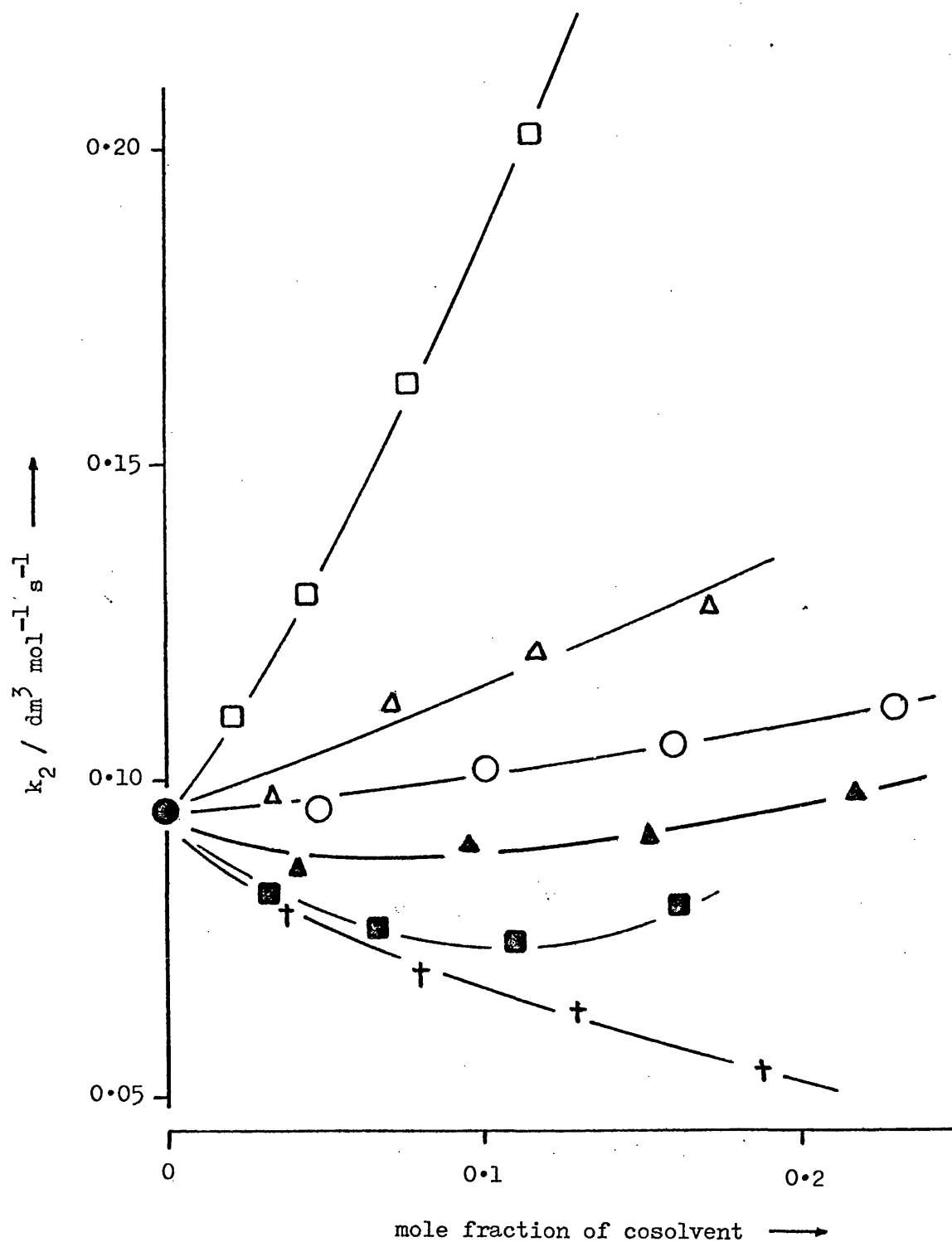


Figure 5.07 Correlation of the second-order rate constant, k_2 , for the mercury(II)-catalysed aqutation of the $[\text{Co}(\text{NH}_3)_5\text{Cl}]^{2+}$ cation with solvent composition, at 298.2 K. Symbols as in Figure 5.01; \blacksquare = cosolvent glycerol, \bullet = solvent water.



fraction of co-solvent. In this case we see that the rate and hence $\delta_m \Delta G^\ddagger$ does increase slightly, indicating that the solvation of the transition state is very similar to that of the initial state. From the slight rate enhancement on addition of co-solvent to the system, for the T.A. mixtures at least, the de-stabilisation of the initial state must be a little less than that of the transition state, thus providing an overall increase in the driving force for the reaction. Diagram 5.02 shows a schematic free energy profile of the mercury(II)-catalysed aquation of the $[\text{Co}(\text{NH}_3)_5\text{Cl}]^{2+}$ cation.

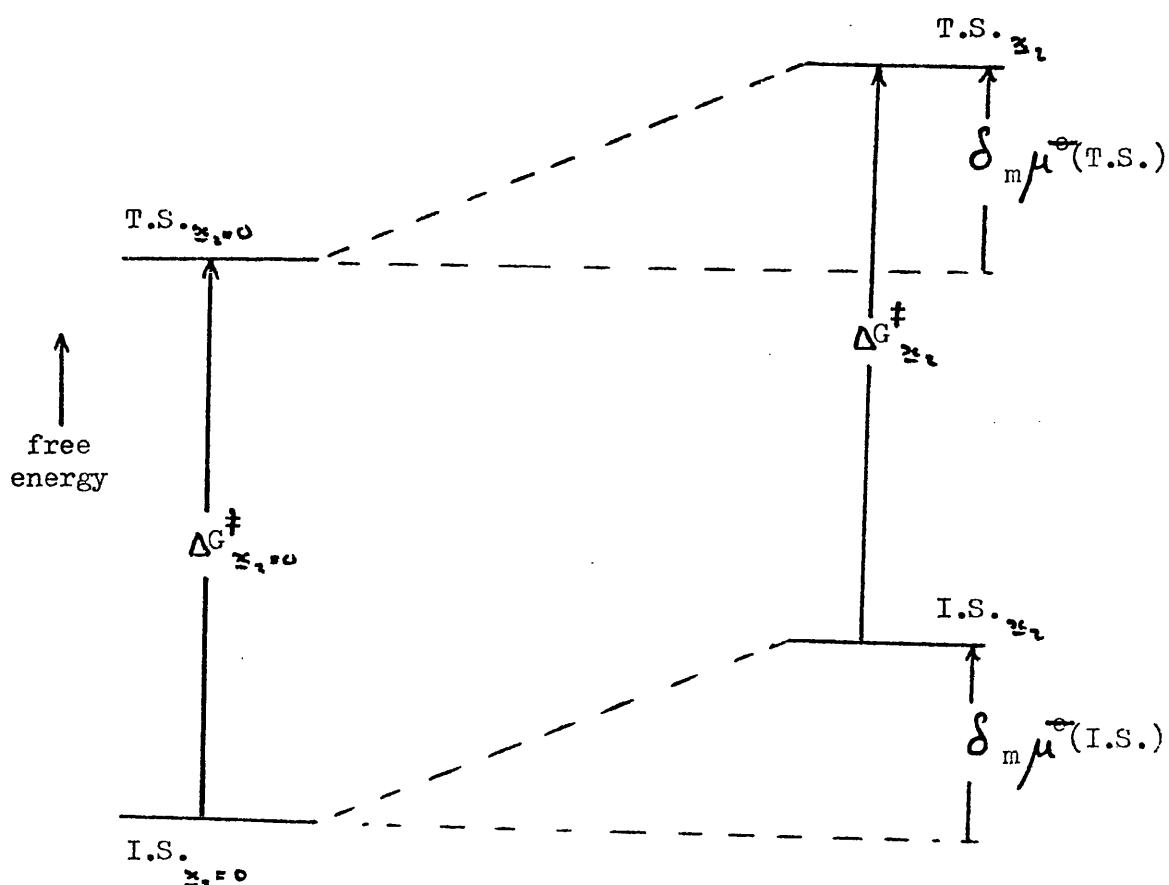


Diagram 5.02

A third complex chosen for a solvent study of the mercury(II)-catalysed aquation of transition metal complexes was the $\text{trans-}[\text{Co(en)}_2\text{Cl}_2]^+$ cation, which again has a charged transition state.

(c) Mercury(II)-Catalysed Aquation of the $\text{trans-}[\text{Co(en)}_2\text{Cl}_2]^+$ Cation

Due to the occurrence of experimental difficulties in this system, as outlined in section 5.2(ii), observed first-order rate constants for the mercury(II)-catalysed aquation of the $\text{trans-}[\text{Co(en)}_2\text{Cl}_2]^+$ cation were measured at 298.2 K for one mercury(II)-ion concentration, for 10 to 40% by volume mixtures of the co-solvents used. These results are listed in Table 5.04, together with the apparent second-order rate constants, and the consequent values of $\delta_m\Delta G^\ddagger$. The reaction was studied over a range of mercury(II)-ion concentrations in 40% by volume of selected co-solvents, as listed in Table 5.05. The derived k_2 values showed this reaction to be bimolecular under these extreme solvent conditions, as illustrated by Figure 5.08, and so in more richly aqueous media, the values of k_{app} , listed in Table 5.04 were considered to accurately convey the character of the true k_2 term. Figure 5.08 describes the dependence of the k_2 values for this reaction graphically as a function of mole fraction of co-solvent. For this system of a singly charged cation plus a doubly charged one reacting to form a triply charged cationic transition state, it seemed reasonable to expect a similar kinetic pattern to arise as was observed for the chloropentamine cobalt(III) cation case above. However, from Figure 5.09 we can see that the k_2 values at first increase with increase in mole fraction as expected, but then are seen to decrease on further increase in mole fraction. From published solubility data on the $\text{trans-}[\text{Co(en)}_2\text{Cl}_2]\text{ClO}_4$ salt in binary aqueous mixtures [5.28], and literature values of $\delta_m\mu^\ominus(\text{ClO}_4^-)$ [5.27], the free energy of transfer of the $\text{trans-}[\text{Co(en)}_2\text{Cl}_2]^+$

TABLE 5.04 Observed first-order rate constants, k_{obs} , and derived second-order rate constants, k_2 , for the mercury(II)-catalysed aquation of the $\text{trans}[\text{Co}(\text{en})_2\text{Cl}_2]^+$ cation in a range of binary aqueous mixtures, at 298.2 K. $[\text{Hg}^{2+}] = 0.10 \text{ mol dm}^{-3}$.

| Solvent Mixture | $10^3 k_{\text{obs}}$ s^{-1} | k_2 $\text{dm}^3 \text{mol}^{-1} \text{s}^{-1}$ | $\delta_m \Delta G^\ddagger$ kJ mol^{-1} |
|----------------------|--|--|--|
| Water | 3.50 | 0.035 | 0 |
| 10 | 3.85 | 0.038 ₅ | - 0.24 |
| 20 % Methanol | 4.05 | 0.040 ₅ | - 0.36 |
| 30 | 3.61 | 0.036 | - 0.075 |
| 10 | 4.14 | 0.041 | - 0.42 |
| 20 % Ethanol | 4.40 | 0.044 | - 0.57 |
| 30 | 3.99 | 0.040 | - 0.34 |
| 40 | 3.57 | 0.036 | - 0.050 |
| 10 | 3.60 | 0.036 | - 0.069 |
| 20 % Ethylene glycol | 3.26 | 0.033 | - 0.17 ₈ |
| 30 | 2.94 | 0.029 | - 0.43 |
| 40 | 2.42 | 0.024 | - 0.92 |
| 10 | 3.37 | 0.034 | - 0.099 |
| 20 % Glycerol | 3.12 | 0.031 | - 0.28 |
| 30 | 2.54 | 0.025 | - 0.80 |
| 40 | 2.06 | 0.021 | - 1.39 |
| 10 | 3.56 | 0.036 | - 0.041 |
| 20 % Acetonitrile | 2.55 | 0.025 ₅ | - 0.79 |
| 30 | 1.99 | 0.020 | - 1.40 |
| 40 | 1.31 | 0.013 | - 2.44 |

TABLE 5.05 Observed first-order rate constants, k_{obs} , for the mercury(II) -catalysed aquation of the $\text{trans-}[\text{Co(en)}_2\text{Cl}_2]^+$ cation for various mercury(II) ion concentrations, in several binary aqueous mixtures, at 298.2 K.

| Solvent Mixture | $\frac{[\text{Hg}^{2+}]}{\text{mol dm}^{-3}}$ | $10^3 k_{\text{obs}} / \text{s}^{-1}$ |
|----------------------|---|---------------------------------------|
| Water | 0.004 | 1.13 |
| | 0.008 | 2.06 |
| | 0.012 | 3.25 |
| | 0.016 | 4.56 |
| | 0.020 | 5.50 |
| 40 % t Butyl alcohol | 0.004 | 1.63 |
| | 0.008 | 3.38 |
| | 0.012 | 5.56 |
| | 0.016 | 7.44 |
| 40 % Acetonitrile | 0.004 | 0.75 |
| | 0.008 | 1.48 |
| | 0.012 | 2.50 |
| | 0.016 | 3.63 |
| | 0.020 | 4.38 |

Figure 5.08 Dependence of k_{obs} on $[\text{Hg}^{2+}]$ in 40 % aqueous t-butyl alcohol (\square), acetonitrile (\dagger), and in water (\bullet) at 298.2 K; ionic strength = $0.002 \text{ mol dm}^{-3}$ (maintained with magnesium perchlorate), for the mercury(II)-catalysed aquation of the $\text{trans-}[\text{Co(en)}_2\text{Cl}_2]^+$ cation.

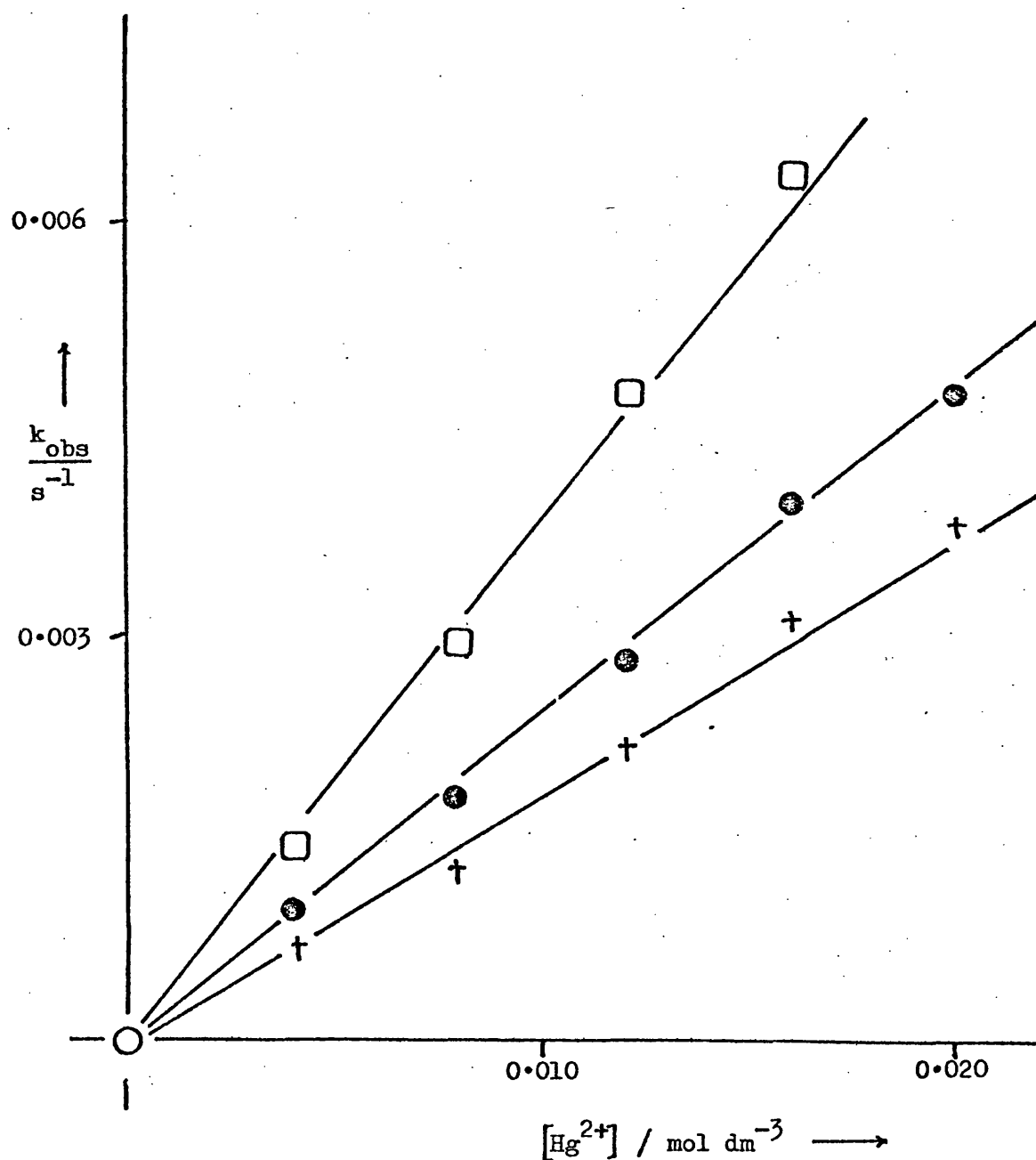


Figure 5.09 Variation of k_2 with mole fraction of cosolvent at 298.2 K for the $\text{trans-}[\text{Co(en)}_2\text{Cl}_2]^+/\text{Hg}^{2+}$ system; for the cosolvents methanol(\circ), ethanol(Δ), ethylene glycol(\blacktriangle), glycerol(\blacksquare) and acetonitrile(\dagger).

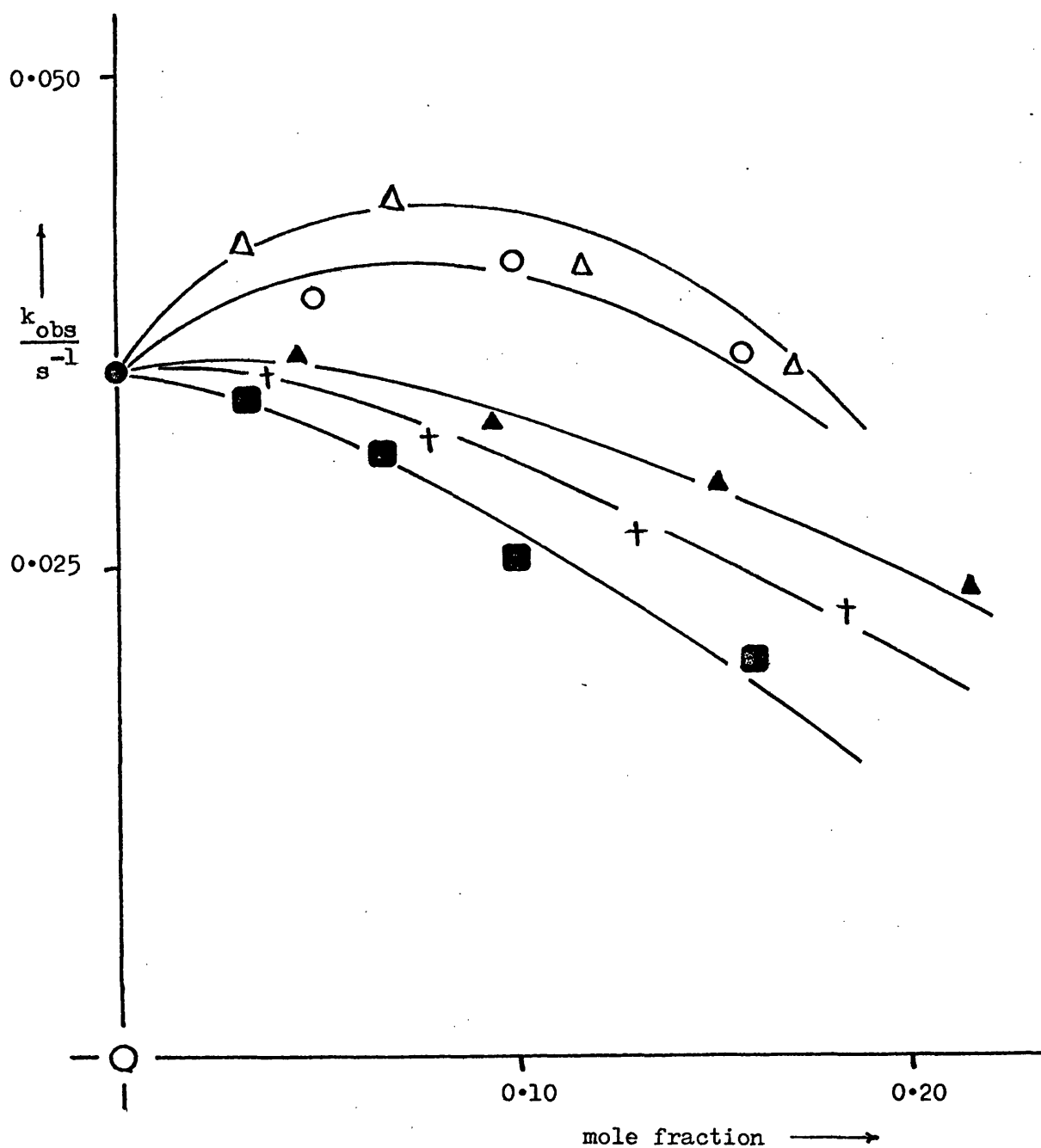
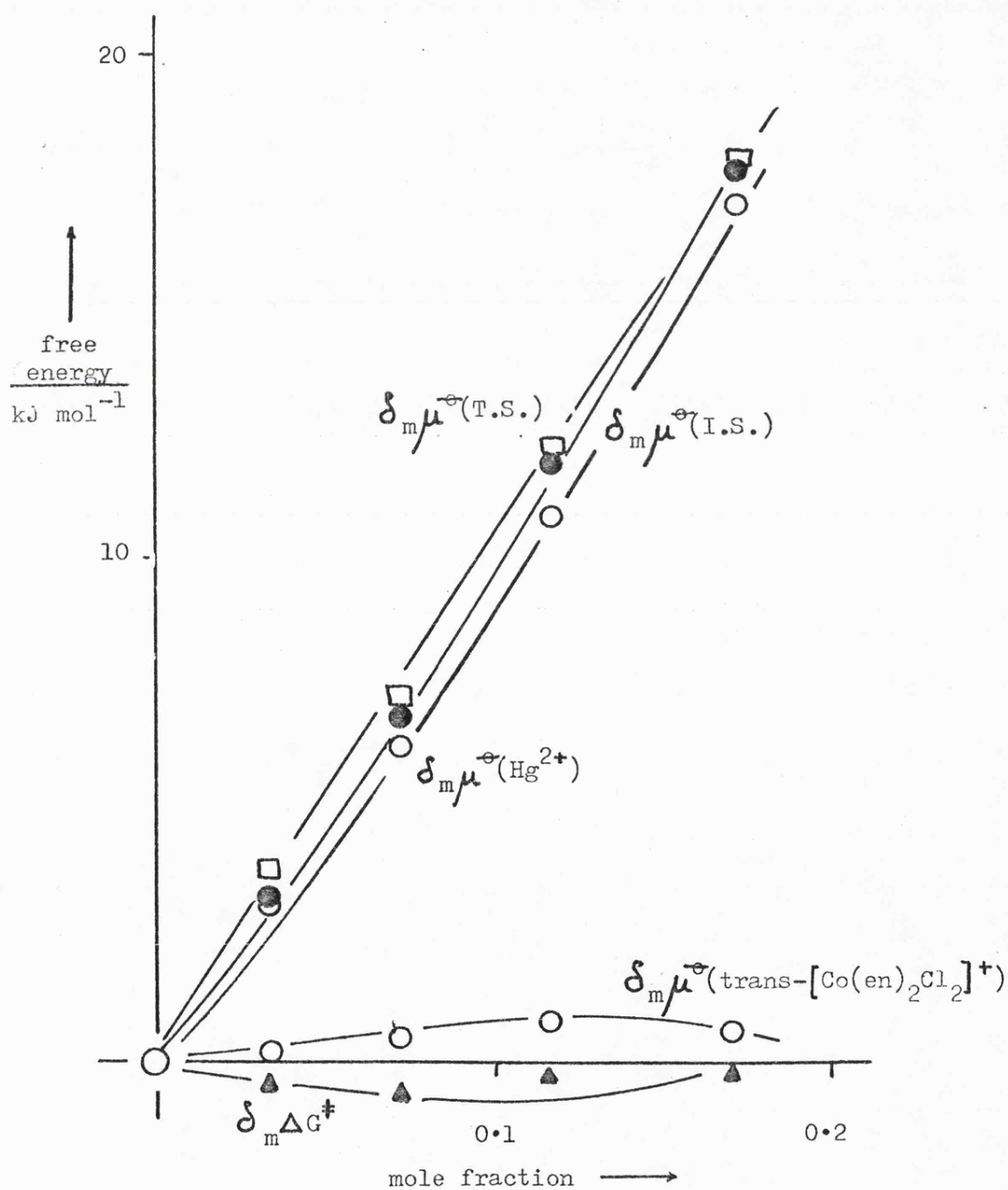


Figure 5.10 Correlation of the various transfer parameters for the trans-[Co(en)₂Cl₂]⁺/Hg²⁺ system with solvent composition, at 298.2 K.



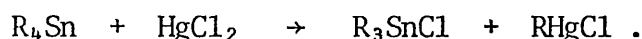
cation has been calculated. Hence we have the value of $\delta_{\text{m}\mu}^{\ominus}$ (I.S.) for this reaction. These values are reported in Table 5.02. From the combination of $\delta_{\text{m}\mu}^{\ominus}$ (IS) and $\delta_{\text{m}}\Delta G^{\ddagger}$ for appropriate solvent mixtures, an estimate of $\delta_{\text{m}\mu}^{\ominus}$ (T.S.) has been made. Fitzgerald *et al.* [5.29] have measured $\delta_{\text{m}\mu}^{\ominus}$ (cis-[Co(en)₂Cl₂]⁺) from N,N'-dimethylformamide to water, methanol and dimethylsulphoxide as +14.8, +27.3 and -5.1 kJ mol⁻¹ respectively. From these values we find that $\delta_{\text{m}\mu}^{\ominus}$ (cis-[Co(en)₂Cl₂]⁺) from water to pure methanol is +12.5 kJ mol⁻¹. We might expect somewhat similar values for the cis- and trans- isomers of this cation, and the positive value for the cis-isomer from ref. [5.29] is reasonable when compared with the positive trend in $\delta_{\text{m}\mu}^{\ominus}$ for the trans-isomer in aqueous ethanol mixtures from this work. Figure 5.10 shows the variation of the various transfer parameters for the reaction with solvent composition. From the overall trends we can see that at low mole fraction, the initial state is more de-stabilised than the transition state on going from water to aqueous-co-solvent mixtures. As the mole fraction of co-solvent increases, this trend is reversed, with the transition state becoming the more destabilised.

Although values of $\delta_{\text{m}\mu}^{\ominus}$ (IS) have been calculated from published data and from solubility measurements, some reservation must be made concerning their absolute validity. As has been pointed out in chapter 4, a necessary complication in the estimation of the single-ion free energies of transfer for the various ions from water to binary aqueous mixtures is that the values obtained are dependent upon the type of assumption used to split the value of $\delta_{\text{m}\mu}^{\ominus}$ for a parent salt into the single-ion values of its constituent ions. In chapter 4 it was seen just how variable such parameters are with the type of assumption made. However, provided the assumption which is chosen is reasonable, and is constant throughout the

work, then fairly good relative values of $\delta_{\text{m}\mu}^{\ominus}$ may be estimated. Thus we have seen in the present work that the trends in $\delta_{\text{m}\mu}^{\ominus}$ (TS) for the systems studied which have been calculated from measurements of $\delta_{\text{m}\mu}^{\ominus}$ (IS) and $\delta_{\text{m}}\Delta G^{\ddagger}$ compare very favourably with the trends predicted by comparison with similar stable species such as HgCl_2 and $\text{Fe}(\text{LL})_2(\text{CN})_2$.

A similar study of a reaction possessing a bimolecular rate-determining step in binary aqueous mixtures is that of the reaction of cyanide ion or hydroxide ion with the tris-(2,2'-bipyridyl)iron(II) cation [5.01-04]. Here, $\delta_{\text{m}\mu}^{\ominus}(\text{CN}^-)$ assumed to be equal to $\delta_{\text{m}\mu}^{\ominus}(\text{Cl}^-)$, from the close similarity of ionic radii ($r(\text{CN}^-) = 1.82 \text{ \AA}$ [5.30(a)], cf. $r(\text{Cl}^-) = 1.81 \text{ \AA}$ [5.30(b)]) and of the single-ion hydration enthalpies, -347 kJ mol^{-1} [5.30(c)] for CN^- ion and -351 kJ mol^{-1} [5.30(c)] for Cl^- ion. For this reaction it was found that $\delta_{\text{m}\mu}^{\ominus}(\text{CN}^-)$ was dominant because the ratio of $k_2[\text{CN}^-]$ in aqueous solution and in binary aqueous mixtures observed was similar to the ratio predicted from $\delta_{\text{m}\mu}^{\ominus}(\text{CN}^-)$, considering only the transfer of the CN^- ion between solvents, and assuming that $\delta_{\text{m}\mu}^{\ominus}(\text{Fe}^{\text{II}} \text{ complex}) \approx \delta_{\text{m}\mu}^{\ominus}(\text{TS})$. Again, there are broad assumptions necessary in order to interpret the experimental results. Ideally, one would prefer to be able to measure $\delta_{\text{m}\mu}^{\ominus}$ (IS) precisely, as one can do with $\delta_{\text{m}}\Delta G^{\ddagger}$. This would be possible if the reactants were neutrally charged, where the 'single-ion split' approximation is avoided. In the reaction of iodo-pentacarbonyl rhenium(I) with cyanide ion [5.31], $\delta_{\text{m}\mu}^{\ominus}(\text{Re}(\text{CO})_5\text{I})$ has been accurately determined from solubility measurements in a few aqueous-methanol mixtures. However, single-ion free energies of transfer are still required for the CN^- ion. Several reactions which have been studied, where the reactants are all neutral species include the reaction of (2,2'-bipyridyl)dichloro-platinum(II) with thiourea [5.32]. Here, $\delta_{\text{m}\mu}^{\ominus}$ (IS) values were calculated for aqueous-dioxan and aqueous-tetra-

hydrofuran mixtures. In both cases, $\delta_m \mu^\ominus$ (IS) was found to resemble $\delta_m \Delta G^\ddagger$ very closely indeed, indicating that the solvation characteristics of the reactants dominate the rôle of the reaction, the transition state having little or no effect. This type of behaviour has also been observed previously for the reactions of tetra-alkyl tin compounds with mercury(II) chloride in aqueous-methanol mixtures [5.33], i.e.:-



This reaction proceeds by way of a bimolecular substitution [5.34,35], wherein it was discovered that while the entropy of activation, ΔS^\ddagger is equally concerned with both the initial and the transition states, the enthalpy of activation, ΔH^\ddagger is mainly concerned with the solvent stabilisation effects in the initial state. An analogous result has also been found for the Menshutkin reaction of trimethylamine with methyl iodide [5.36], i.e.:-



The increased rate produced by addition of co-solvent to the reaction is entirely due to a large increase in the free energy of the reactants. A similar reaction involving trimethylamine with p-nitrobenzyl chloride could only be understood in terms of the opposite effect, i.e. the solvation of the transition state being dominant. Other examples of reactions where the transition state solvation effects are of major importance are typified by the demetallation of tetra-alkyl lead compounds with iodine [5.37] where again both initial and transition state effects are of comparable importance to reactivity trends.

In this work, we have found that the solvation characteristics of the transition states play a very important rôle in determining the

solvent sensitivity of the reactions. This fact has been made clear in spite of the obstacles of the presence of ionic species in the systems studied.

In order to extend the range of complex ions studied in this work, the $\text{trans-}[\text{Rh}(\text{en})_2\text{Cl}_2]^+$ cation was studied. The mercury(II)-catalysed aquation of this cation was expected to behave in a similar fashion to the analogous cobalt(III) complex cation above.

(iv) Mercury(II)-Catalysed Aquation of the $\text{trans-}[\text{Rh}(\text{en})_2\text{Cl}_2]^+$ Cation

This reaction was studied in aqueous solution at 308.2 K, at a constant ionic strength of 4.35 mol dm^{-3} , the maximum concentration of mercury(II) used being 1.45 mol dm^{-3} . The initial complex concentration in all runs was $1.8 \times 10^{-3} \text{ mol dm}^{-3}$, there being a large excess of mercury(II) ion in all runs. Under these conditions, good first-order kinetics were observed over at least four half-lives. The observed first-order rate constants, k_{obs} , measured over a range of mercury(II) ion concentrations, $[\text{Hg}^{2+}]$, are listed in Table 5.06, together with the apparent second-order rate constants, $k_{\text{app}} (= k_{\text{obs}}/[\text{Hg}^{2+}])$. These k_{app} values were found to decrease with increase in $[\text{Hg}^{2+}]$, thus this system deviates drastically from simple second-order kinetic behaviour, as depicted by a plot of k_{obs} versus $[\text{Hg}^{2+}]$ in Figure 5.11. This behaviour is very different from that of the $\text{trans-}[\text{Co}(\text{en})_2\text{Cl}_2]^+$ cation studied earlier in this chapter (section 5.3(iii)). This difference between the two analogous complexes of cobalt(III) and rhodium(III) is readily explained by differences in the M-X bond strengths. Both metal ions are d^6 low-spin moieties. Thus the only difference between the complexes is that cobalt is a first-row transition metal, whereas rhodium is a second-row one. This fact accounts for a 50% or so larger crystal field

TABLE 5.06 Observed first-order rate constants, k_{obs} , and apparent second-order rate constants, k_{app} , for the mercury(II)-catalysed aquation of the trans- $[\text{Rh}(\text{en})_2\text{Cl}_2]^+$ cation in aqueous solution at 308.2 K; ionic strength = $\frac{1}{2} \times 4.35 \text{ mol dm}^{-3}$ (maintained with magnesium nitrate).

| $[\text{Hg}^{2+}] / \text{mol dm}^{-3}$ | $10^3 k_{\text{obs}} / \text{s}^{-1}$ | $\frac{10^3 k_{\text{app}}}{\text{dm}^3 \text{ mol}^{-1} \text{ s}^{-1}}$ |
|---|---------------------------------------|---|
| 0.0363 | 0.236 | 6.50 |
| 0.0727 | 0.466 | 6.41 |
| 0.109 | 0.695 | 6.38 |
| 0.145 | 0.872 | 6.01 |
| 0.218 | 1.23 | 5.63 |
| 0.291 | 1.46 | 5.01 |
| 0.363 | 1.71 | 4.71 |
| 0.436 | 1.88 | 4.31 |
| 0.509 | 2.04 | 4.01 |
| 0.581 | 2.08 | 3.59 |
| 0.654 | 2.23 | 3.41 |
| 0.727 | 2.23 | 3.07 |

Figure 5.11 Dependence of the observed first-order rate constants, k_{obs} , on the mercury(II) ion concentration for the mercury(II)-catalysed aquation of the $\text{trans-}[\text{Rh(en)}_2\text{Cl}_2]^+$ cation, in aqueous solution at 308.2 K.

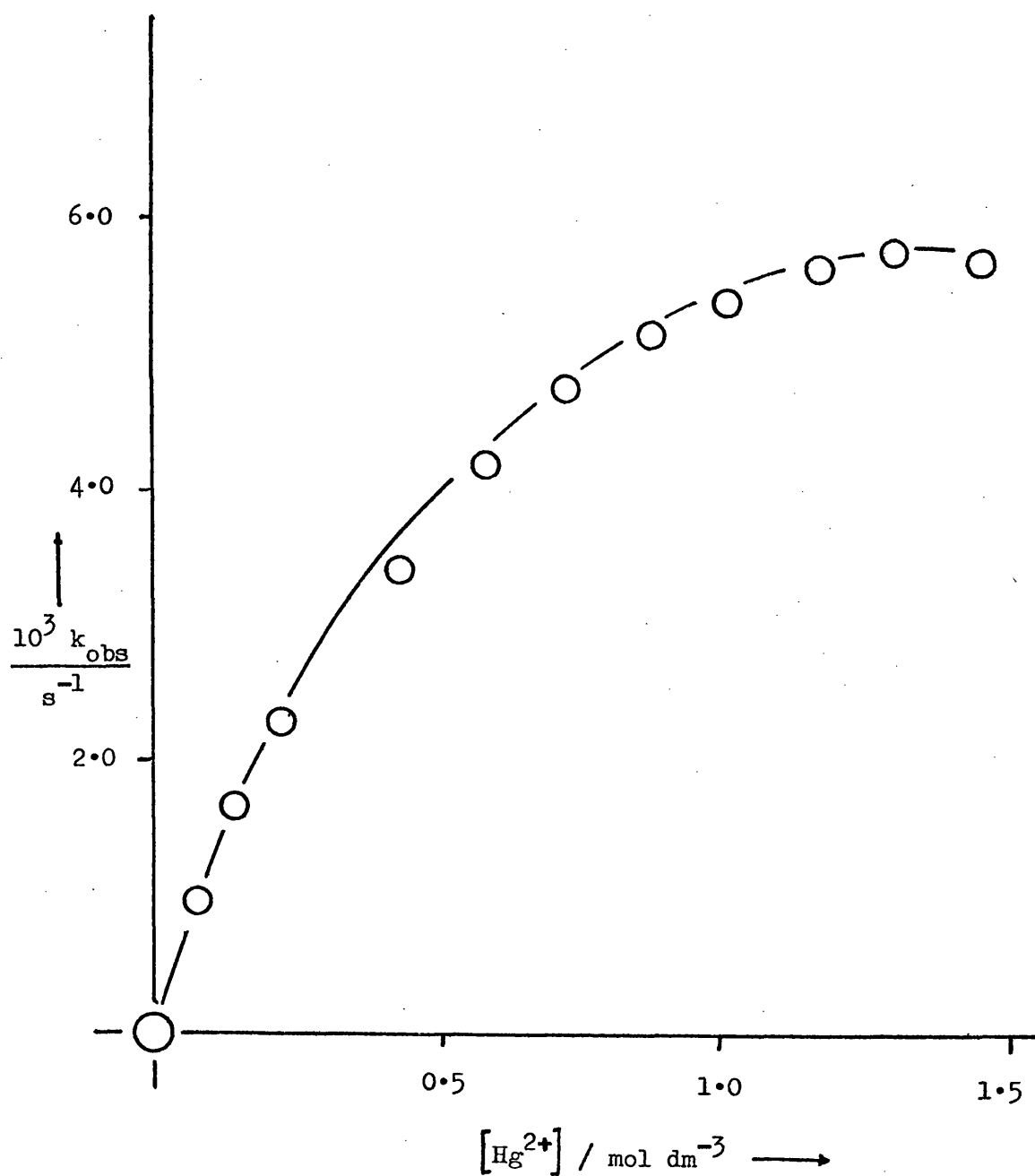
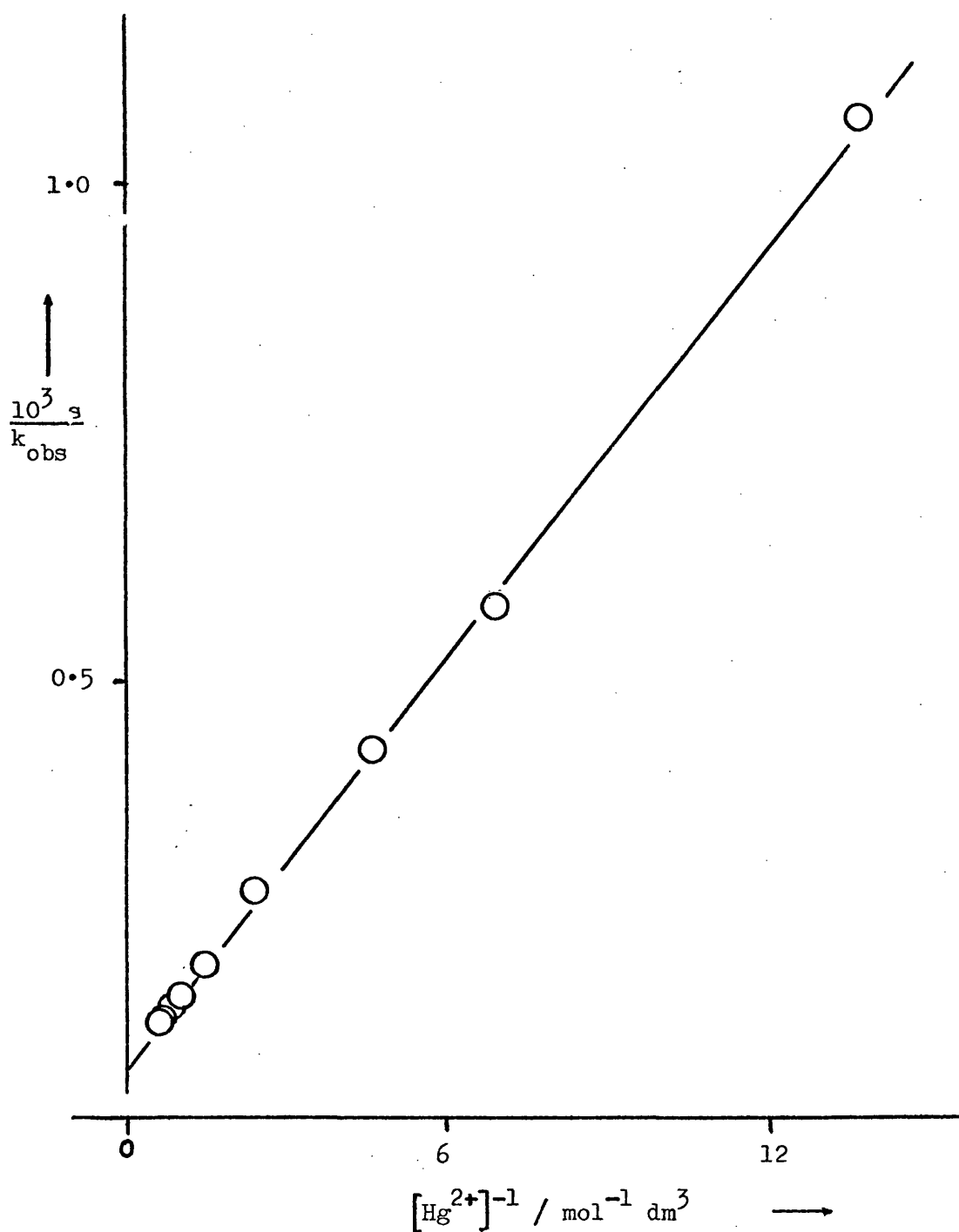
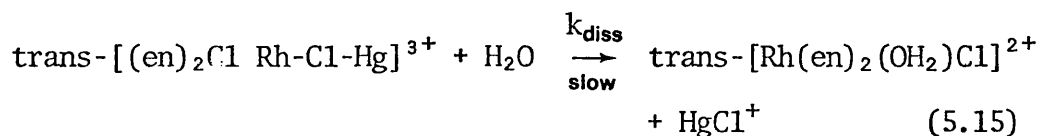
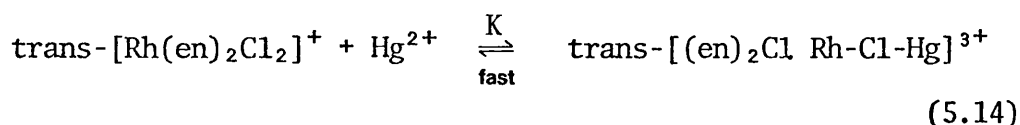


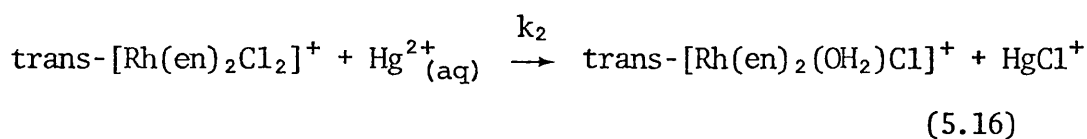
Figure 5.12 Correlation between the reciprocals of the observed first-order rate constant, and the mercury(II) ion concentration for the mercury(II) ion-catalysed aquation of the trans- $[\text{Rh}(\text{en})_2\text{Cl}_2]^+$ cation, in aqueous solution at 308.2 K.



stabilization energy, C.F.S.E., for Rh(III) than Co(III) [5.38]. Examples of the relative bond strengths of halo-complexes of these metal ions include the acid aquation of the $[\text{M}(\text{NH}_3)_5\text{Br}]^{2+}$ cations, where $k_{\text{aq}}(\text{M} = \text{Co}) = 6.3 \times 10^{-6} \text{ s}^{-1}$, and $k_{\text{aq}}(\text{M} = \text{Rh}) \approx 10^{-8} \text{ s}^{-1}$ [5.38]. Consequently, the rate of fissure of the Rh-Cl bond in the "Rh-Cl-Hg" moiety will be considerably slower than that in the cobalt system, thus producing a more stable transition state, which may possibly be stable enough to have a finite lifetime, and so become an intermediate in the reaction. From the experimental results, it appears that the mercury(II)-catalysed aquation of the $\text{trans}-[\text{Rh}(\text{en})_2\text{Cl}_2]^+$ cation exhibits a kinetic behaviour similar to, for example the $\text{cis}-[\text{Co}(\text{en})_2\text{Cl}_2]^+$ analogue [5.08], the reaction proceeding by way of a prior equilibrium association of the reactants which is being saturated at higher concentrations of mercury(II) ions. The reaction may continue via dissociative decomposition of the bimolecular intermediate, $\text{trans}-[(\text{en})_2\text{Cl Rh-Cl-Hg}]^{3+}$, to form aquation product and HgCl^+ according to equation (5.14):-



or second-order reaction of $\text{Hg}^{2+}_{(\text{aq})}$ with the remaining, uncomplexed $\text{trans}-[\text{Rh}(\text{en})_2\text{Cl}_2]^+$



As we saw for the analogous reaction of $\text{cis}-[\text{Co}(\text{en})_2(\text{RNH}_2)\text{Cl}]^{2+}$, the

observed first-order rate constant is related to the mechanistically derived rate constants by the relationship:-

$$k_{\text{obs}} = \frac{k_{\text{diss}} K[\text{Hg}^{2+}]}{1 + K[\text{Hg}^{2+}]} \quad (5.17)$$

or

$$k_{\text{obs}} = \frac{k_2 [\text{Hg}^{2+}]}{1 + K[\text{Hg}^{2+}]} \quad (5.18)$$

Both mechanisms predict that a plot of the reciprocal of k_{obs} versus the reciprocal of $[\text{Hg}^{2+}]$ should yield a straight line, the slope and intercept of which give the rate parameters. Figure 5.12 depicts such a plot, from which, via a BASIC least-mean-squares program (Appendix 2, Program No. 3) we find the slope to be 144.7 ± 1.8 and the intercept to be 193.8 ± 2.4 . Hence $k_1 K$ (or k_2)[†] = $6.91 \pm .08 \times 10^{-3}$ and $k_1 = 5.16 \pm .07 \times 10^{-3}$, $K = 1.34$. The uncatalysed acid aquation of the $\text{trans-}[\text{Rh}(\text{en})_2\text{Cl}_2]^+$ cation was measured at $3.29 \pm 0.02 \times 10^{-5} \text{ s}^{-1}$ at mol dm^{-3} ionic strength at 308.2 K. This reaction was found to be independent of acid concentration. The results are listed in Table 5.07. Hence the catalytic activity of Hg^{2+} for this reaction is found to be:

$$\frac{k_1(\text{Hg}^{2+}_{\text{cat}})}{k_1(\text{uncat})} = \frac{5.16 \times 10^{-3}}{3.29 \times 10^{-5}} = 157$$

This compares with a value of 1.06×10^5 for the mercury(II)-catalysed aquation of $\text{trans-}[\text{Co}(\text{en})_2\text{Cl}_2]^+$.

Obviously an analysis of solvent effects on this system cannot be performed as for the simpler second-order ones studied earlier. It would be interesting, however, to study the variation in the association constant, K , of equation (5.17) with solvent composition, which might give insight into the variations of the mechanism with solvent composition.

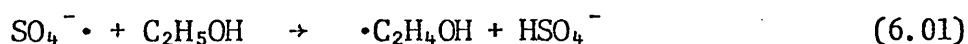
[†] Units are $\text{mol}^{-1} \text{ dm}^3 \text{ s}^{-1}$ for $k_1 K$ (or k_2); s^{-1} for k_1 ; $k_1 = k_{\text{diss}}$ (eqn (5.15))

CHAPTER 6

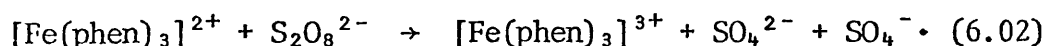
Solvent Effects on the Peroxodisulphate Oxidation
of the $[\text{Fe}(\text{phen})_3]^{2+}$ and Related Cations.

6.1 INTRODUCTION

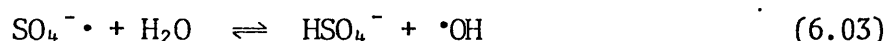
There have been several investigations of the reaction of peroxodisulphate with the tris(1,10-phenanthroline)iron(II) and tris(2,2'-bipyridyl)iron(II) cations and their ligand-substituted derivatives in aqueous solution [6.01-03]. In most cases the reaction seems to be simple oxidation [6.01], though later reports [6.03] suggested that ion-pairs may play a significant role in the reaction mechanism. However, further studies on the reaction involving neutral [6.04] and anionic [6.05] iron(II)-1,10-phenanthroline complexes have indicated a common mechanism between these [6.04,05] and other [6.01,02] reactions, the apparent differences in the observed rate laws being explicable from a knowledge of the other chemical properties of the iron(II) complexes involved [6.02,06]. Similar observations have been made for the closely related Schiff's base complexes of iron(II) [6.07]. When the reaction involving the tris(1,10-phenanthroline)iron(II) cation was studied in aqueous ethanol, [6.03] a serious retardation of the reaction was observed, which was ascribed to the reaction of sulphate radicals, $\text{SO}_4^{\cdot -}$ with the alcohol [6.08] thus:-



the $\text{SO}_4^{\cdot -}$ radical having been formed as a product of the reaction of peroxodisulphate, $\text{S}_2\text{O}_8^{2-}$, with the iron(II) complex:-



These conclusions were reached by Raman & Brubaker [6.03] from comparisons of a study by Koithoff, Medalia & Raaen [6.09] on the $S_2O_8^{2-}$ -iron (II) system and of the work of Merz & Waters [6.10] on the relative rates of reaction of $SO_4^{\cdot -}$ and $\cdot OH$ radicals with iron(II) and ethanol, with their work on the $[Fe(phen)_3]^{2+}/S_2O_8^{2-}$ system. Thus they eliminated the previous suggestion [6.01] that the second stage of this reaction was due to $\cdot OH$ radicals, formed by the rapid equilibration



Studies of the effect of added non-aqueous co-solvents [6.11,12] on the first-stage of the reaction of peroxodisulphate with the tris-(1,10-phenanthroline)iron(II) cation and its ligand-substituted derivatives have been made, including the analogous reactions of iodide ion and the hexacyanoferrate(II) anion. Here, the reactions have also found to be greatly retarded, a phenomenon which was described in terms of the relative charges of the reactants [6.12]. Thus for the $[Fe(CN)_6]^{4-}/S_2O_8^{2-}$ system, the product of the charges is +8, and the solvent sensitivity was found to be very low; in the case of the $[Fe(phen)_3]^{2+}/S_2O_8^{2-}$ system, the product of the charges is -4, and the solvent sensitivity was found to be very great.

The aim of this work is to collect data for the reaction of the $[Fe(phen)_3]^{2+}$ cation with $S_2O_8^{2-}$ ion in a wide range of binary aqueous mixtures. From these data, the reaction will be discussed both in terms of classical theories concerning reactions in mixed solvents, involving changes in dielectric constant [6.13], and in terms of the dependence of the rate of the reaction on the solvation of the initial and transition states. Classical theories, for example that of Grunwald & Winstein [6.14], which work extremely well for organic

reactions have been found to be rather less effective in interpreting inorganic reaction mechanisms (see chapter 2, and references therein). The 'component solvation' analysis of inorganic reactions, which has been used most successfully for the mercury(II)-catalysed aquation of transition metal-halo complexes (chapter 5) has been applied to the peroxodisulphate oxidation of the $[\text{Fe}(\text{phen})_3]^{2+}$ cation in this work. From the results, the solvation of the transition state has been estimated, and consequently conclusions as to the nature of the reaction mechanism have been made. The analogous reaction of the related low-spin hexadentate Schiff's base-iron(II) cation, $[\text{Fe}(\text{HXSb})]^{2+\dagger}$ has been studied in a range of binary aqueous mixtures also, and compared with its 1,10-phenanthroline predecessor.

The aforementioned oxidation reactions of $[\text{Fe}(\text{phen})_3]^{2+}$ and related complexes were all studied in neutral solution. Here, the postulated [6.01] iron(III) product is unstable [6.15] and spontaneously dissociates into $\text{Fe}^{3+}(\text{aq})$ and free ligand. However, the $[\text{Fe}(\text{phen})_3]^{3+}$ cation is stable in concentrated acid solution. In the second part of this chapter, the kinetics of aquation of the tris(1,10-phenanthroline)-iron(III) cation, and its ligand substituted derivatives have been studied in aqueous solution, and discussed in terms of the observed substituent effects.

[†] [The hexadentate Schiff's base ligand is that derived from one molecule of triethylenetetramine and two molecules of quinolyl-2-aldehyde (see chapter 9).]

6.2 EXPERIMENTAL

REAGENTS

(i) Complex Solutions and Oxidants

Stock solutions of the tris-(1,10-phenanthroline)iron(II) cation and its substituted derivatives were prepared in aqueous solution by the method described for the 5-nitro-substituted analogue in chapter 3. The hexadentate Schiff's base complex cation of iron(II), $[\text{Fe}(\text{HXSb})]^{2+}$, was prepared as described in chapter 9. Aqueous solutions of the chloride were used in this work.

Fresh aqueous solutions of AnalaR potassium peroxodisulphate were prepared daily, as solutions of this salt are not indefinitely stable. Their concentrations were checked against standard solutions of ammonium hexanitratocerate(IV) and ammonium iron(II) sulphate [6.16].

Solutions of the tris-iron(III) complexes of phen, 4,7-Me₂phen, 5-Clphen and 5-NO₂phen were prepared in situ for the study of the acid aquations of these complexes by two methods. The first entailed oxidation of the appropriate iron(II) complex by lead dioxide in known concentrations of sulphuric acid, a method which has been used for the production of the $[\text{Fe}(\text{phen})_3]^{3+}$ [6.17] and the $[\text{Fe}(5,6\text{-Me}_2\text{phen})_3]^{3+}$ [6.18] cations. The second method of generating the iron(III) complexes, which has been used more extensively in this work than the previous method, was by oxidation of the iron(II) complexes by cerium (IV), a method which has been recommended for the generation of the $[\text{Fe}(\text{phen})_3]^{3+}$ [6.15] and the $[\text{Fe}(\text{bipy})_3]^{3+}$ [6.19] cations.

(ii) Solvents and other Reagents

All solvents used in this work were of the same quality as those solvents used in chapter 2. Potassium sulphate, ammonium hexanitratocerate(IV) and sulphuric acid (98% w/v) were all AnalaR grade chemicals, received from B.D.H., and were used as received. A stock solution of 4.20 mol dm^{-3} sulphuric acid was prepared from dilution of 98% w/v acid, and standardised using sodium tetraborate decahydrate [6.20].

KINETICS

(i) Peroxodisulphate Oxidations

Due to known deviations of the reaction of peroxodisulphate oxidation of $[\text{Fe}(\text{LL})_3]^{2+}$ type cations from simple first-order kinetics after the first 50% of reaction [6.01], rate constants for such reactions in water and in binary aqueous mixtures have been computed from optical density changes for the first half-life only. Such rate constants were calculated both graphically and by use of the usual least-mean-squares program (Appendix 2, Program No. 2). These two sets of results were found to be equivalent, indicating that no significant deviation from first-order kinetics had occurred.

All kinetic runs were performed at 298.2 K in 1 cm path length silica cells in the thermostatted cell compartment of a Pye Unicam SP 800A recording spectrophotometer, at the wavelength of maximum absorption in the visible region for each complex.

The solvent compositions of the reaction solutions were varied from aqueous solution to extremes of 60% by volume of methanol and acetone for the oxidation of the $[\text{Fe}(\text{phen})_3]^{2+}$ cation. These and intermediary mixtures were produced by the method fully described in chapter 2. For the oxidation of the $[\text{Fe}(\text{phen})_3]^{2+}$ cation, a maximum peroxodisulphate concentration of 0.01 mol dm^{-3} was used, the minimum being $0.004 \text{ mol dm}^{-3}$. In the case of the Schiff's base complex cation, $[\text{Fe}(\text{HXSb})]^{2+}$, a maximum concentration of $0.001 \text{ mol dm}^{-3}$ of peroxodisulphate was used, due to the relatively high reactivity of this complex. Initial concentrations of the $[\text{Fe}(\text{phen})_3]^{2+}$ and $[\text{Fe}(\text{HXSb})]^{2+}$ cations in all kinetic runs were $10^{-4} \text{ mol dm}^{-3}$ and $3 \times 10^{-5} \text{ mol dm}^{-3}$ respectively; thus ensuring a sufficiently large excess of peroxodisulphate

to produce pseudo-first-order conditions. Ionic strength was kept constant throughout by addition of suitable amounts of AnalaR potassium sulphate.

(ii) Acid Aquation of $[\text{Fe}(\text{X-phen})_3]^{3+}$ Cations

(—for X = H, 5-Cl, 5-NO₂ or 4,7-Me₂)

The acid aquations of these cations were performed at 307.5 K in aqueous acidic media, for a range of sulphuric acid concentrations; and over a range of temperatures and acid concentrations for the 5-NO₂-phen case. All reactions exhibited good first-order kinetics for at least four half-lives.

For the measurements of rate constants for the complexes which had been generated using lead dioxide, a large excess of solid lead dioxide was shaken with a suitably acidic solution of the appropriate iron(II) complex. The resulting blue iron(III) complex solution was filtered rapidly, and its optical density-decay was monitored in the usual way. Hence rate constants were computed from these optical density changes with time.

When cerium(IV) was used as oxidant, a four-fold excess of oxidant over iron(II) complex was added to the latter in acid solution, producing the required iron(III) complex in situ in the reaction cell. The decay in optical density was then measured, whence rate constants for the acid aquation of the iron(III) complex were computed.

The above methods both used sulphuric acid in the reaction media. Attempts to use hydrochloric acid produced an evolution of chlorine gas from the solution, which has been previously reported [6.15]. Hence the use of this acid was terminated. Nitric acid and orthophosphoric

acid both produced precipitation of presumably Ce(IV) species under the above experimental conditions, and so these acids also were not used.

The extinction coefficient of the $[\text{Fe}(4,7\text{-Me}_2\text{phen})_3]^{3+}$ cation was determined by measurement of the optical density of a known concentration of the complex cation, generated by the oxidation of a solution of a known concentration of the corresponding iron(II) complex cation ($\lambda_{\text{max}} = 14,000$ [6.21]) by cerium(IV) in strong sulphuric acid.

6.3 RESULTS AND DISCUSSION

(i) Peroxodisulphate Oxidation of the $[\text{Fe}(\text{phen})_3]^{2+}$ Cation in Binary Aqueous Mixtures

The kinetics of the oxidation of the $[\text{Fe}(\text{phen})_3]^{2+}$ cation by peroxodisulphate ion were studied in a range of binary aqueous mixtures at 298.2 K. During all runs, the oxidant was present in large excess; good first-order kinetics were observed over the first 40% of the complete reaction. Considerable deviation from this first-order behaviour was seen to occur during the remainder of the reaction. Such deviations are often observed in peroxodisulphate oxidations, and are generally attributed to side reactions of intermediates ([6.01,22], see also section 6.1). The extent of the observed deviations appeared to increase with the proportions of co-solvents added, for the aqueous alcohol mixtures.

Consequently, observed first-order rate constants, k_{obs} , for the initial reaction between the $[\text{Fe}(\text{phen})_3]^{2+}$ and $\text{S}_2\text{O}_8^{2-}$ ions were calculated from plots of the natural logarithms of the optical densities at specific times, versus time. The values of k_{obs} were obtained from these plots using a BASIC least-mean-squares program (Appendix 2, Program 3). The optical density measurements were limited to 20-30% of complete reaction for all solvent mixtures, where no significant deviations from the first-order behaviour were observed. Table 6.01 lists the calculated values of k_{obs} , for the oxidation of the $[\text{Fe}(\text{phen})_3]^{2+}$ cation by peroxodisulphate ion in a range of binary aqueous mixtures at 298.2 K, and a constant ionic strength[†] of 0.03

[†] [Ionic strength maintained by potassium sulphate.]

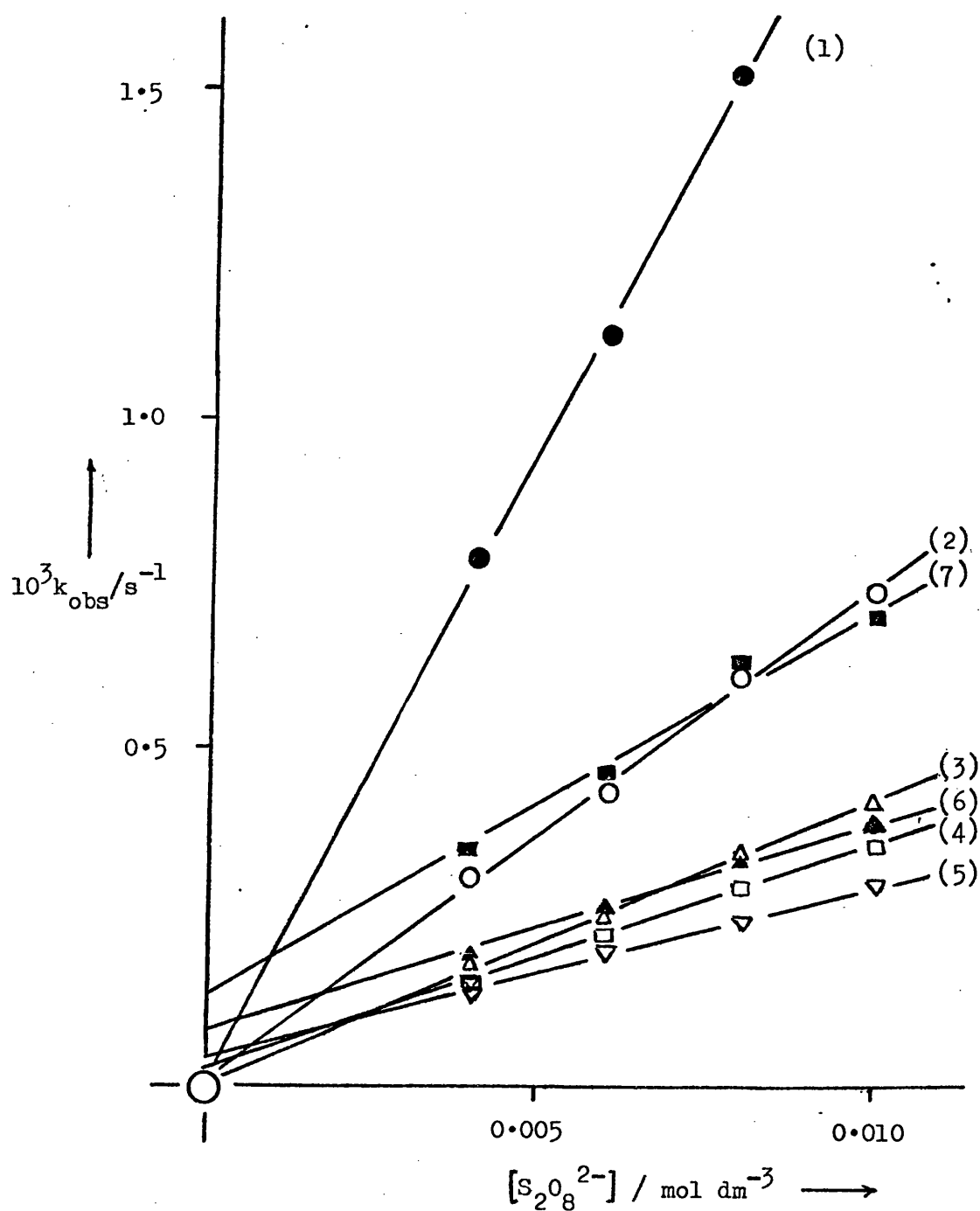
TABLE 6.01 Observed first-order rate constants, k_{obs} , for the reaction of the $[\text{Fe}(\text{phen})_3]^{2+}$ cation with peroxodisulphate (in large excess) in binary aqueous mixtures at 298.2 K. Values of k_1 and k_2 (cf. equation(6.04)) are also included.

| Solvent Mixture | $\text{---} [\text{K}_2\text{S}_2\text{O}_8] / \text{mol dm}^{-3} \text{---}$ | | | | $10^5 k_1$ s^{-1} | k_2 $\text{mol}^{-1} \text{dm}^3 \text{s}^{-1}$ |
|--------------------|---|-------|-------|-------|-------------------------------|--|
| | 0.004 | 0.006 | 0.008 | 0.010 | | |
| | $\text{---} 10^4 k_{\text{obs}} / \text{s}^{-1} \text{---}$ | | | | | |
| Water | 8.0 | 11.4 | 15.3 | 19.2 | | 0.197 |
| 10 | 3.2 | 4.5 | 6.2 | 7.5 | | 0.073 |
| 20 | 1.8 | 2.5 | 3.5 | 4.2 | | 0.043 |
| 30 | 1.5 | 2.3 | 3.0 | 3.6 | 2 | 0.036 |
| 40 | 1.4 | 2.0 | 2.5 | 3.1 | 3 | 0.028 |
| 50 | 1.8 | 2.6 | 3.5 | 3.7 | 8 | 0.031 |
| 60 | 3.6 | 4.7 | 6.3 | 7.1 | 13 | 0.061 |
| 10 | 1.6 | 2.2 | 2.5 | 3.0 | | 0.023 |
| 20 | 0.74 | 0.75 | 1.3 | 1.3 | | 0.011 |
| 30 | 0.51 | 0.64 | 0.74 | 0.82 | 3 | 0.005 |
| 40 | 0.54 | 0.62 | 0.70 | 0.73 | 3 | 0.003 |
| 60 | 0.81 | 0.82 | 0.84 | 0.85 | 7 | 0.0007 |
| 5 | 3.0 | 4.9 | 6.5 | 7.8 | | 0.080 |
| 10 | 1.7 | 3.0 | 3.6 | 4.8 | | 0.050 |
| 15 | 0.90 | 1.3 | 1.8 | 2.2 | | 0.022 |
| 20 | 0.70 | 1.1 | 1.4 | 1.6 | | 0.015 |
| 30 | 0.53 | 0.76 | 0.96 | 1.13 | 1.5 | 0.010 |
| 40 | 0.60 | 0.84 | 0.96 | 1.11 | 3 | 0.008 |
| 50 | 0.86 | 1.00 | 1.07 | 1.20 | 7 | 0.005 |
| 60 | 1.15 | 1.11 | 1.25 | 1.30 | 10 | 0.003 |
| 10 | 3.0 | 4.5 | 6.3 | 7.2 | | 0.072 |
| 20 | 0.9 | 1.3 | 1.5 | 2.1 | | 0.019 |
| 30 | 0.9 | 1.3 | 1.5 | 1.9 | | 0.015 |
| 40 | 0.37 | 0.58 | 0.83 | 1.04 | | 0.011 |
| 10 | | | | | 1.7 | 0.018 |
| 20 | | | | | 2.9 | 0.008 |
| 30 | | | | | 3.3 | 0.003 |
| 40 | | | | | 3.5 | 0.001 |

^a Values taken from ref. 6.12, at 308.2 K.

^b Where no k_1 values given, k_1 = zero, within expl. error.

Figure 6.01 Dependence of the observed first-order rate constants, k_{obs} , on peroxodisulphate concentration, $[\text{S}_2\text{O}_8^{2-}]$, in the oxidation reaction of the $[\text{Fe}(\text{phen})_3]^{2+}$ cation by peroxodisulphate, at 298.2 K. Solvent mixtures depicted are (1) water, (2) 10 (3) 20 (4) 30 (5) 40 (6) 50 and (7) 60 % by volume aqueous methanol.



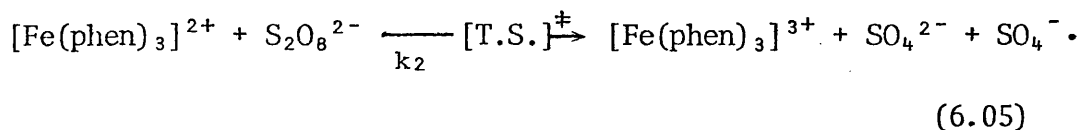
mol dm⁻³. Figure 6.01 shows the variations in the observed first-order rate constants with peroxodisulphate concentration, [S₂O₈²⁻], for the aqueous methanol mixtures used. This plot indicates the rate law to be:-

$$\frac{-d[\text{complex}]}{dt} = k_1 [\text{complex}] + k_2 [\text{complex}][\text{S}_2\text{O}_8^{2-}] \quad (6.04)$$

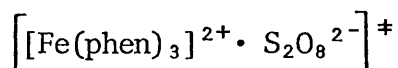
Thus parallel dissociation and oxidation of the complex appear to occur. At low mole fractions of co-solvent, the dissociative (k_1) term in equation (6.04) is negligible, but becomes increasingly important with increasing proportions of co-solvent. This behaviour of k_1 is consistent with the known trends in the rates of aquation of iron(II) complexes with solvent composition (for example, see chapter 3).

This observation of parallel reactions occurring in such a system has been found previously for closely related systems. For example, the peroxodisulphate oxidation of [Fe(X-phen)₃]ⁿ⁺, for X = 5-NO₂, 5- or 3-SO₃⁻ was found to have a rate law analogous to that shown in equation (6.04) in aqueous solution [6.05]. Here, because of the electronic effects of the substituents, the rates of dissociation are very much faster than that of the unsubstituted complex. Conversely, the analogous reaction involving the neutral iron(II) complexes of the type Fe(LL)₂(CN)₂, where LL = bipy, phen and substituted derivatives, was found [6.04] to have no dissociative term in the rate law. These complexes are known to aquate very slowly [6.23], and ^{aquation}would certainly not be observed in the presence of a second-order term like that observed for the oxidation reaction. Indeed, the same rate law was found to hold even in aqueous methanol mixtures. These published results, together with those of this work, strongly support a simple

bimolecular oxidation step,



where the transition state, T.S., is an outer-sphere complex of the form



An alternative mechanism has been postulated by Raman & Brubaker [6.03], involving the formation of a stable ion-pair. They base their hypothesis on the fact that ion-pairs of the type $[\text{M}^{n+} \cdot \text{S}_2\text{O}_8^{2-}]$ have been confirmed, e.g., for the catalytic oxidation of iodide ion by $\text{S}_2\text{O}_8^{2-}$, where M^{n+} is a metal ion [6.24]; and that a stable diamagnetic intermediate has been observed for the iron(II) iodide-peroxodisulphate reaction [6.25]. However, although the $[\text{Fe}(\text{phen})_3]^{3+}$ cation has been shown spectroscopically to form ion-pairs with dianionic species [6.15], there is no such evidence for the more lowly charged $[\text{Fe}(\text{phen})_3]^{2+}$ cation. Also, Jackmann & Lister [6.26] have shown that the alkaline earth metals cations, Mg^{2+} , Cu^{2+} , Sr^{2+} and Ba^{2+} do not form ion-pairs with the $\text{S}_2\text{O}_8^{2-}$ anion. Hence it seems very unlikely that a significant amount of ion-pairs would be formed between $[\text{Fe}(\text{phen})_3]^{2+}$ cations and $\text{S}_2\text{O}_8^{2-}$ anions. The fact that the $[\text{Co}(\text{bipy})_3]^{3+}$ cation does form ion-pairs with $\text{S}_2\text{O}_8^{2-}$ [6.27] is understandable for the higher (3+) charge of this cation (cf. $[\text{Fe}(\text{phen})_3]^{3+}$ ion-pairs also (above)). These facts tend to rule out the ion-pairing mechanism, but the transition state must be similar to one, in order that electron transfer might occur.

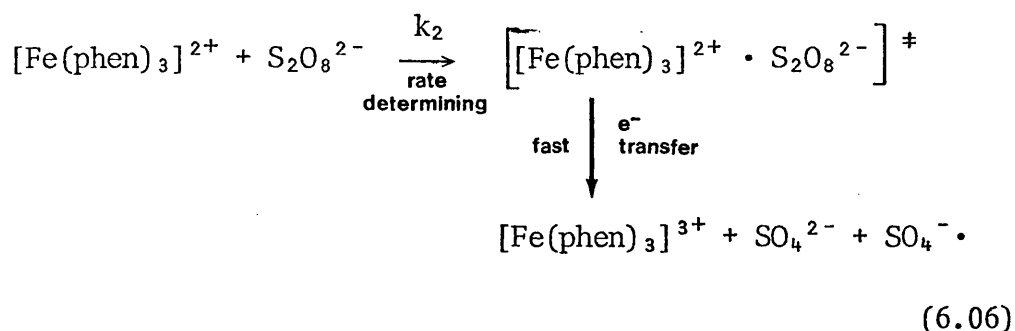
The fact that the reaction is first-order in both reactants implies that the transition state for the oxidation consists of a complex cation

linked to a peroxodisulphate anion. There are three possible paths for electron transfer from complex to peroxodisulphate; from the periphery of the aquated complex, directly from the iron atom, or from some position on one of the ligands. In the last case, if the site of transfer was a substituent, then the order of reactivity for a series of substituents would be $\text{NO}_2 > \text{Cl} > \text{H} > \text{Me}$. However the opposite trend has been observed [6.02]. Alternatively, if the transfer was from some other site on a ligand, then the 5- NO_2 substituent should not be able to deactivate all positions possible for inner-sphere bonding and electron transfer.

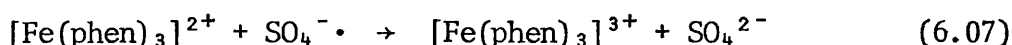
For the second inner-sphere mechanism the peroxodisulphate anion would need to approach the iron atom at the centre of the complex sufficiently closely for considerable orbital overlap to give transient $\text{Fe}^{\text{II}}-\text{S}_2\text{O}_8^{2-}$ bonding in the transition state. It is sterically possible to accommodate a peroxodisulphate anion between the phen ligands of the complex [6.02], although this is unattractive since there is only just enough room, and would necessitate the removal of occluded water molecules.

The first of the three above possible mechanisms is an outer-sphere one in which the transition state involves minimal orbital overlap between the reactants. According to Marcus [6.28,29], for a series of reactions proceeding by a similar electron transfer, a plot of the free energy of activation, ΔG^\ddagger , against the standard free-energy change of the redox step, ΔG^\ominus , should be linear. Such a linear plot has been produced by Raman & Brubaker [6.03] for the peroxodisulphate oxidations of the tris-2,2'-bipyridyl, -4,4'-dimethyl 2,2'-bipyridyl, -1,10-phenanthroline and -5-methyl 1,10-phenanthroline complexes of iron(II) for these complexes.

Hence we conclude the mechanism for these reactions to be outer-sphere, of the form:



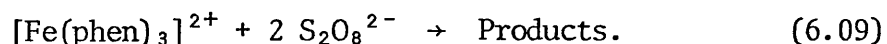
with the neutral solution dissociation of the complex occurring in parallel with the above. The secondary reaction shown in equation (6.07) is responsible for the later deviations from second-order behaviour in the reaction:



The observed first-order rate constant, k_{obs} , measured for this reaction is that defined by:-

$$\frac{-d[\text{complex}]}{dt} = k_{\text{obs}}[\text{complex}] \quad (6.08)$$

there being a large excess of peroxodisulphate present in all kinetic runs. Hence any complications arising from stoichiometries other than 1:1 for the reactants is avoided. This is necessary since Irvine [6.02] showed the stoichiometry to be:



Values for the second-order rate constants, k_2 , for this outer-sphere reaction are listed in Table 6.01. They were computed (Appendix 2, Program 3) from plots of k_{obs} versus $[\text{S}_2\text{O}_8^{2-}]$. These k_2 values are

seen to decrease rapidly on increasing the proportion of non-aqueous co-solvents. This behaviour is similar to the previously reported results in aqueous t-butyl alcohol [6.11] and aqueous acetonitrile [6.12] mixtures.

An attempt to correlate the observed trends in the rate constants with solvent composition with classical theories of solvent effects on ion-ion reactions is outlined below.

Correlations of Rates with Dielectric Constant (D)

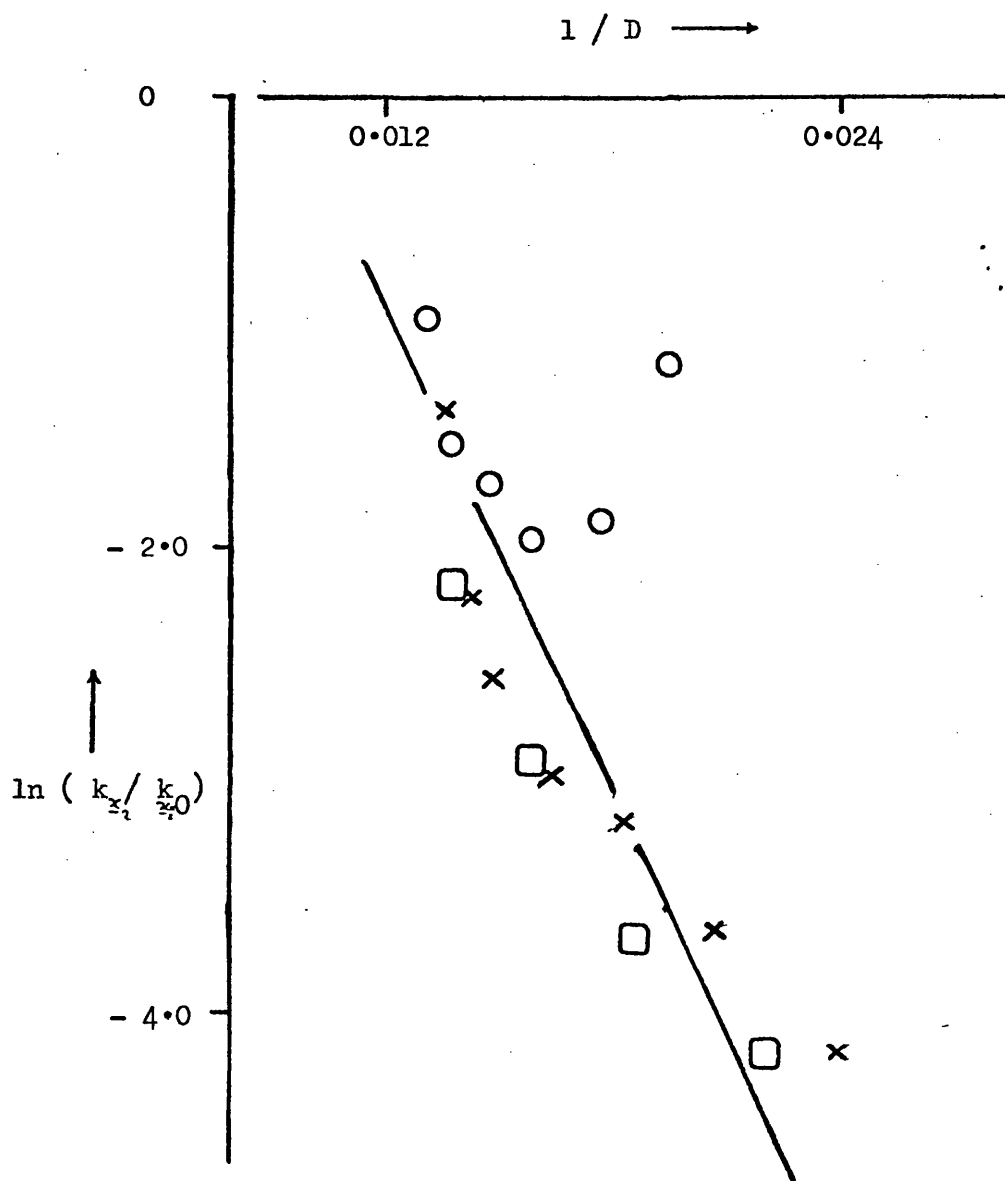
For the reaction between the two negatively charged ions tetrabromophenolsulphonphthalein and hydroxide in water-methanol and water-ethanol mixtures at 298.2 K, Amis & La Mer [6.30] showed that plots of $\ln k$ versus $1/D$ were straight lines of negative slope. Such correlations were consistent with the Rates-Scatchard equation [6.13], i.e:

$$\ln k = \ln k_{D = \infty} - \frac{Z_A Z_B \epsilon^2}{k T r D} \quad (6.10)$$

where Z_A and Z_B are the valences of the ions A and B; ϵ is the electronic charge; D the dielectric constant of the medium; k is the Boltzmann gas constant and T is the absolute temperature. The standard reference state of dielectric constant is taken as infinity [6.30,31]. The parameter r used in equation (6.10) is the distance to which two ionic reactants must approach in order to react.

Hence, for a reaction between two anions (or two cations), equation (6.10) predicts a negative slope for the plot of $\ln k$ versus $1/D$. Amis & Price [6.32] plotted these parameters for the ammonium ion-cyanate ion reaction in water-methanol and water-glycol at 303.2 K. As predicted

Figure 6.02 Correlation of the natural logarithm of the ratios of the second-order rate constants in binary aqueous mixtures to that in water, $\ln(k_{x_1}/k_{x_0})$, for the peroxodisulphate oxidation of the $[\text{Fe}(\text{phen})_3]^{2+}$ cation with the reciprocal of the dielectric constant, $1/D$, for the solvent mixture, at 298.2 K. Cosolvents used are methanol(O), t-butyl alcohol(\square) and acetone(X).



for reaction between an anion and a cation (equation (6.10)) the lines were, for the most part, linear with positive slopes.

For the peroxodisulphate oxidation of the $[\text{Fe}(\text{phen})_3]^{2+}$ cation, we have plotted $\ln (k_{\underline{x}2}/k_{\underline{x}2=0})$ versus $1/D$ (Figure 6.02) for the range of binary aqueous mixtures studied. Equation (6.10) predicts a positive slope for this plot, for reaction between an anion and a cation. We find from Figure 6.02 that there is a negative slope, with some deviation from linearity at low dielectric constant. Thus it appears that the above classical method of scrutinising solvent effects or reactions of charged species does not hold for this system.

Consequently, we have attempted to correlate the effects of variable solvent composition on reaction rates with the solvation characteristics of the participant species. Such an analysis for reactions of $2+/2-$, $2+/+$ and $2+/2+$ ions proved most informative in chapter 5, where it clarified what outwardly appeared to be some most complicated trends.

Table 6.02 lists the Gibbs free energy of transfer of the initial state, $\delta_m \mu^\ominus(\text{I.S.})$ from water into the binary aqueous mixtures used for this reaction. The values of $\delta_m \mu^\ominus(\text{I.S.})$ were calculated as the sum of the single-ion free energies of transfer of the reactants, as determined in chapter 4, for the appropriate solvent mixtures. Also listed in Table 6.02 are the activation free energies of transfer, $\delta_m \Delta G^\ddagger$ for the appropriate solvent mixtures, as calculated from the expression:-

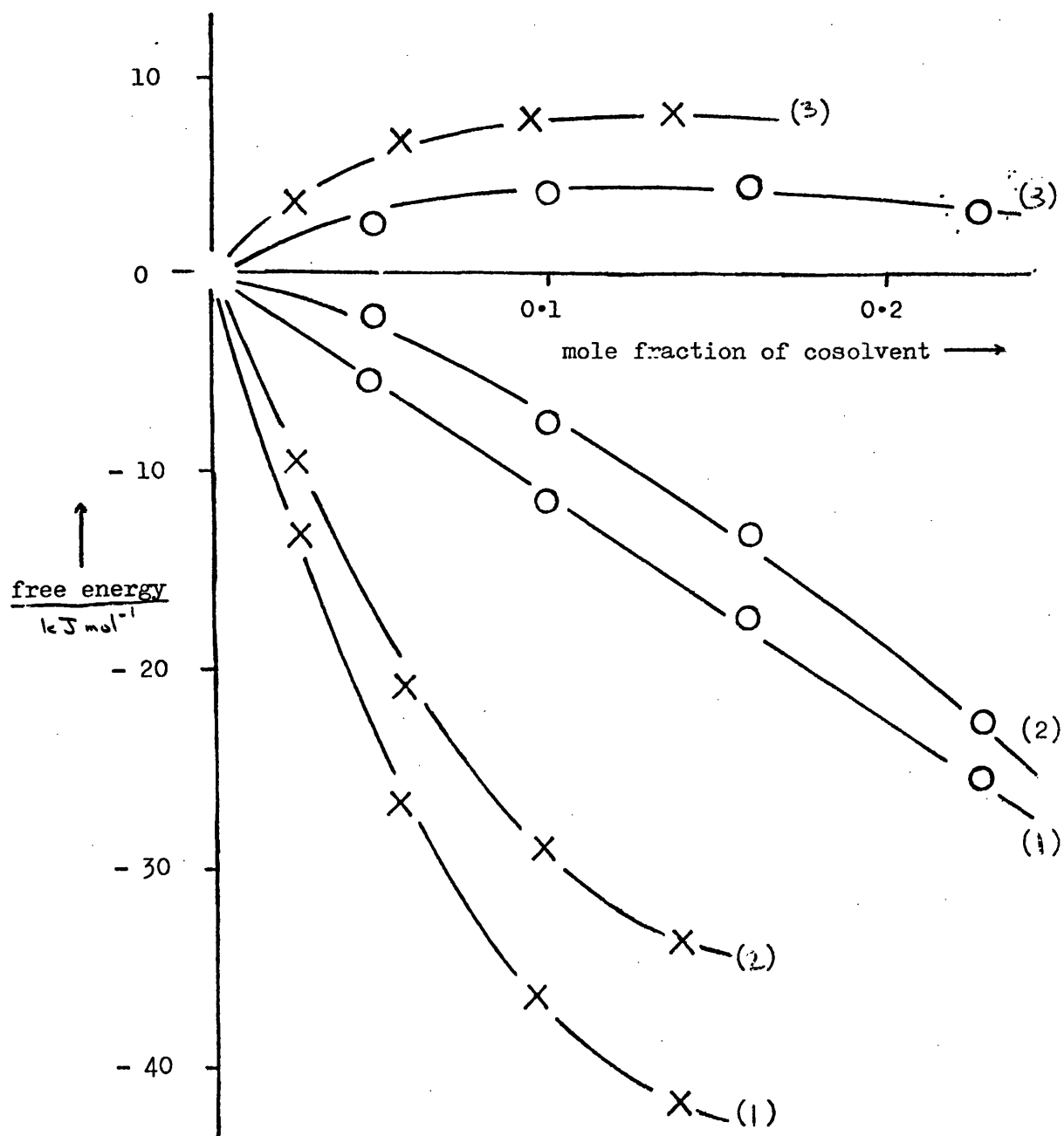
$$\delta_m \Delta G^\ddagger = \Delta G^\ddagger_{\underline{x}2} - \Delta G^\ddagger_{\underline{x}2=0} \quad (6.11)$$

as defined in chapter 1. Figure 6.03 depicts the trend of $\delta_m \mu^\ominus(\text{I.S.})$ with solvent composition relative to that of $\delta_m \Delta G^\ddagger$. The strong affinity of the $[\text{Fe}(\text{phen})_3]^{2+}$ cation for binary aqueous mixtures, relative to

TABLE 6.02 Transfer parameters $\delta_m \mu^\ominus(\text{I.S.})$, $\delta_m \Delta G^\ddagger$, and the consequently estimated values of $\delta_m \mu^\ominus(\text{T.S.})$ for the peroxodisulphate oxidation of the $[\text{Fe}(\text{phen})_3]^{2+}$ cation, from water into several binary aqueous mixtures, at 298.2 K.

| Solvent Mixture | $\delta_m \mu^\ominus(\text{I.S.})$ kJ mol ⁻¹ | $\delta_m \Delta G^\ddagger$ kJ mol ⁻¹ | $\delta_m \mu^\ominus(\text{T.S.})$ kJ mol ⁻¹ |
|-----------------|---|--|---|
| Water | 0 | 0 | 0 |
| 10 | - 5.4 | + 2.4 ₆ | - 2.9 |
| 20 | -11.7 | + 3.8 | - 7.9 |
| % Methanol | | | |
| 30 | -17.6 | + 4.2 | -13.6 |
| 40 | -25.7 | + 2.9 | -23 |
| 10 | -13.2 | + 3.4 | - 9.8 |
| 20 | -26.8 | + 6.4 | -21 |
| % Acetone | | | |
| 30 | -35.6 | + 7.4 | -29 |
| 40 | -41.8 | + 7.9 | -34 |

Figure 6.03 Dependence of the Gibbs free energies of transfer of (1) the initial state & (2) the transition state; and of (3) $\delta_m \Delta G^\ddagger$ of the peroxodisulphate oxidation of the $[\text{Fe}(\text{phen})_3]^{2+}$ cation on solvent composition, at 298.2 K. Cosolvents used are methanol(O) and acetone(X).



water, tends to swamp the solvation characteristics of the $S_2O_8^{2-}$ anion. This is evidenced by the strongly negative values of $\delta_{m\mu}^\ominus$ ($[Fe(phen)_3]^{2+}$) in such mixtures, despite the dipositive charge on the cation. Consequently, the free energy of transfer of the initial state species, $\delta_{m\mu}^\ominus(I.S.)$, which is the sum of the individual $\delta_{m\mu}^\ominus$ (reactant) values, has a negative value in binary aqueous mixtures. This becomes more negative with increase in proportion of organic co-solvent. This trend indicates a stabilisation of the initial state on going from water to binary aqueous mixtures, which will tend to retard the reaction.

The free energy of transfer of the transition state, $\delta_{m\mu}^\ominus(T.S.)$ may be expressed by the equation[†]

$$-\delta_{m\mu}^\ominus(T.S.) = \delta_m \Delta G^\ddagger - \delta_{m\mu}^\ominus(I.S.) \quad (6.12)$$

paying attention to the signs of the constituent parameters. The estimated values of $\delta_{m\mu}^\ominus(T.S.)$ have been listed in Table 6.02. From them, we see that the transition state becomes more stable on going from aqueous solution into binary aqueous mixtures. Such behaviour is consistent with the postulated transition state, since ion-pairs are known to become more stable in binary aqueous mixtures of increasing proportion of non-aqueous co-solvent (and lower dielectric constant).

Thus the oxidation of the $[Fe(phen)_3]^{2+}$ cation by peroxodisulphate in binary aqueous mixtures may be rationalised on the basis of the solvation characteristics of the participant species. Moreover, it

[†] [Equation (6.12) has been previously arrived at in chapter 5.]

suggests the nature of the transition state in terms of its solvation properties, and lends support to the postulated outer-sphere mechanism.

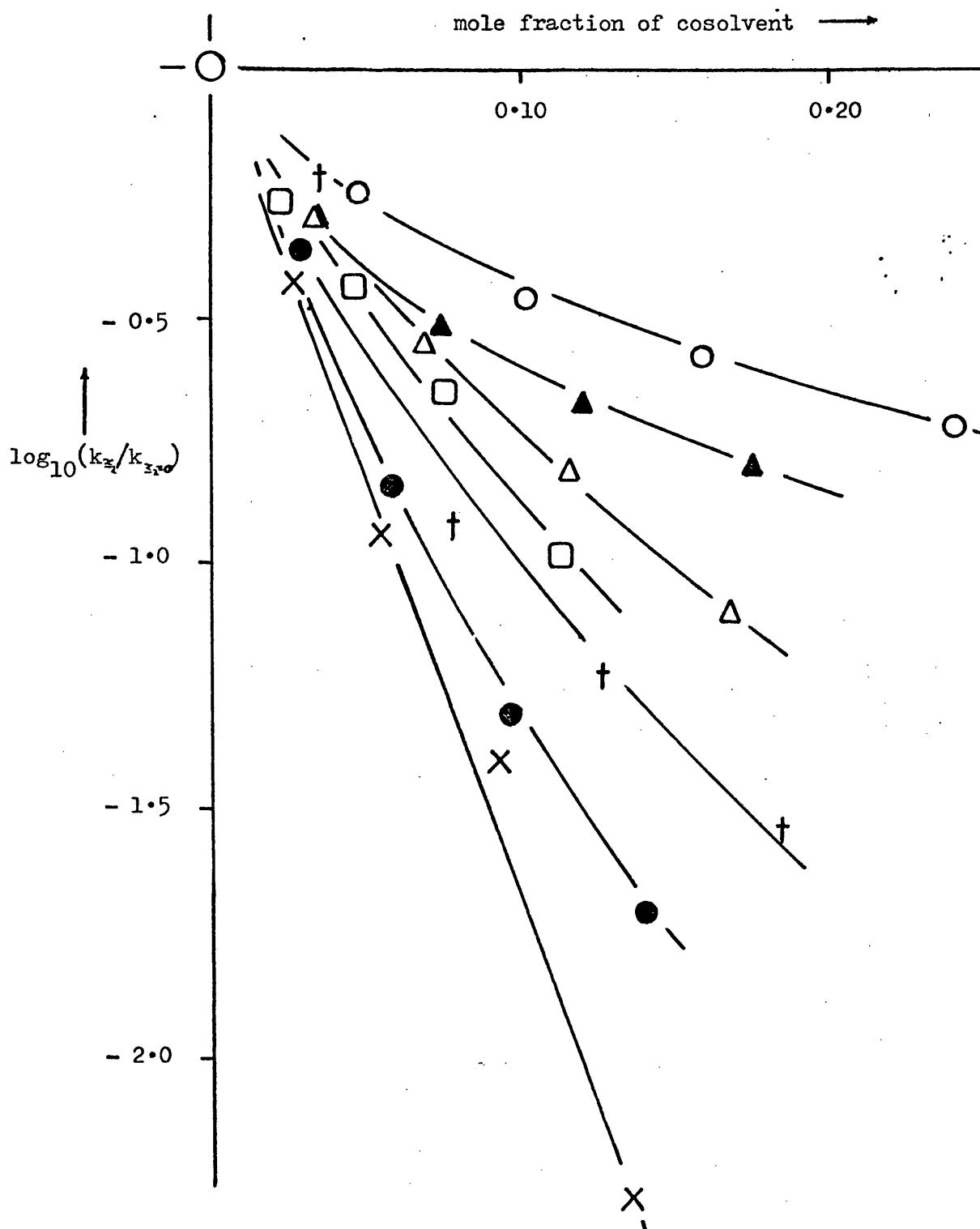
(ii) Kinetics of the Oxidation of the $[\text{Fe}(\text{HXSb})]^{2+}$ Cation by Peroxodisulphate

The blue $[\text{Fe}(\text{HXSb})]^{2+}$ cation was found to be oxidised very rapidly by peroxodisulphate ion in aqueous solution. The kinetics of this oxidation were followed in the presence of an excess of peroxodisulphate ion over the complex cation at 298.2 K in aqueous solution and in a wide range of binary aqueous mixtures. As in the case of the $[\text{Fe}(\text{phen})_3]^{2+}|\text{S}_2\text{O}_8^{2-}$ system, considerable deviation from first-order kinetics was observed after 30-40% of complete reaction had occurred. Hence, the observed first-order rate constants, k_{obs} , for the reaction were determined in the same way as for those of the analogous $[\text{Fe}(\text{phen})_3]^{2+}$ one. Due to the very rapid oxidation at 298.2 K, the maximum concentration of peroxodisulphate ion used was $0.001 \text{ mol dm}^{-3}$; the ionic strength was maintained at $0.003 \text{ mol dm}^{-3}$ by potassium sulphate while $[\text{S}_2\text{O}_8^{2-}]$ was varied between 0.25 and $1.0 \times 10^{-3} \text{ mol dm}^{-3}$. The values of k_{obs} under these conditions, together with the k_2 term of the rate law (equation (6.04)) computed (Appendix 2, Program 3) from these values of k_{obs} , are reported in Table 6.03. From plots of k_{obs} versus $[\text{S}_2\text{O}_8^{2-}]$, we find that, within experimental error, the k_1 term of the rate law is negligible for this system in the solvent mixtures used. This is consistent with the very low value of k_1 estimated in chapter 9 for the neutral solvation dissociation of $[\text{Fe}(\text{HXSb})]^{2+}$, to be $<10^{-6} \text{ s}^{-1}$, compared with the relative rates of aquation of similar cations (e.g. $[\text{Fe}(\text{5-NO}_2\text{phen})_3]^{2+}$ in chapter 3) in water-rich binary aqueous mixtures and in water [6.33].

TABLE 6.03 Observed first-order rate constants, k_{obs} , for the reaction of the $[\text{Fe}(\text{HXSb})]^{2+}$ cation with peroxodisulphate (in large excess) in binary aqueous mixtures at 298.2 K. Derived values of k_2 are also included. Ionic strength = $0.003 \text{ mol dm}^{-3}$ (maintained with potassium sulphate).

| Solvent Mixture | $\underbrace{10^4 [\text{K}_2\text{S}_2\text{O}_8] / \text{mol dm}^{-3}}_{\substack{2.5 \quad 5.0 \quad 7.5 \quad 10.0}}$ | | | | $\frac{k_2}{\text{mol}^{-1} \text{ dm}^3 \text{ s}^{-1}}$ |
|----------------------|---|------|------|------|---|
| | $\underbrace{10^3 k_{\text{obs}} / \text{s}^{-1}}_{\substack{2.5 \quad 5.0 \quad 7.5 \quad 10.0}}$ | | | | |
| Water | 4.8 | 9.7 | 15.2 | 20.0 | 20 |
| 10 | 2.9 | 5.5 | 8.7 | 11.6 | 11.6 |
| 20 % MeOH | 1.6 | 3.6 | 5.1 | 6.8 | 6.9 |
| 30 | 1.2 | 2.7 | 4.0 | 5.2 | 5.3 |
| 40 | 1.0 | 2.0 | 2.8 | 3.9 | 3.8 |
| 10 | 2.3 | 5.1 | 7.4 | 10.1 | 10.3 |
| 20 % EtOH | 1.6 | 2.9 | 4.6 | 5.9 | 5.8 |
| 30 | 0.7 | 1.5 | 2.1 | 3.1 | 3.1 |
| 40 | 0.5 | 0.7 | 1.2 | 1.7 | 1.7 |
| 10 | 2.9 | 5.4 | 8.5 | 11.0 | 11.0 |
| 20 % t -BuOH | 1.9 | 3.4 | 5.5 | 7.3 | 7.3 |
| 30 | 1.2 | 2.7 | 3.4 | 4.8 | 4.5 |
| 40 | 0.6 | 1.0 | 1.7 | 2.1 | 2.1 |
| 10 | 2.6 | 5.1 | 7.6 | 10.5 | 10.5 |
| 20 % Ethylene glycol | 1.5 | 3.4 | 4.6 | 6.2 | 6.2 |
| 30 | 1.2 | 2.2 | 3.4 | 4.4 | 4.3 |
| 40 | 0.9 | 1.6 | 2.4 | 3.2 | 3.2 |
| 10 | 1.8 | 3.6 | 5.6 | 7.4 | 7.6 |
| 20 % Acetone | 0.6 | 1.1 | 1.7 | 2.3 | 2.3 |
| 30 | 0.19 | 0.41 | 0.59 | 0.80 | 0.8 |
| 40 | 0.02 | 0.05 | 0.08 | 0.10 | 0.1 |
| 10 | 2.0 | 4.9 | 6.4 | 8.7 | 8.7 |
| 20 % DMSO | 0.7 | 1.3 | 2.2 | 2.9 | 3.0 |
| 30 | 0.3 | 0.5 | 0.8 | 1.0 | 1.0 |
| 40 | 0.1 | 0.2 | 0.3 | 0.4 | 0.4 |
| 10 | 1.7 | 3.9 | 5.5 | 7.7 | 7.9 |
| 20 % MeCN | 0.6 | 1.1 | 1.7 | 2.4 | 2.4 |
| 30 | 0.3 | 0.6 | 0.9 | 1.2 | 1.2 |
| 40 | 0.15 | 0.26 | 0.43 | 0.56 | 0.6 |

Figure 6.04 Dependence of the second-order rate constants (in terms of their logarithms relative to that in water) for the reaction of peroxodisulphate with the $[\text{Fe}(\text{HXSb})]^{2+}$ cation on solvent composition, at 298.2 K. Cosolvents used are methanol(\circ), ethanol(Δ), t-butyl alcohol(\square), ethylene glycol(\blacktriangle), acetone(\times), acetonitrile(\dagger) and dimethyl sulphoxide(\bullet).



From a plot of $\log \left(k_{x2}/k_{x2=0} \right)$ versus mole fraction of co-solvent (Figure 6.04) for the second-order oxidation of the $[\text{Fe}(\text{HXSb})]^{2+}$ cation by the $\text{S}_2\text{O}_8^{2-}$ anion, we see a very similar behaviour to that of the previously discussed (above) $[\text{Fe}(\text{phen})_3]^{2+}|\text{S}_2\text{O}_8^{2-}$ system. From these similarities in kinetic behaviour, together with the knowledge that such iron(II)-Schiff's base complexes are soluble in organic solvents (cf. $[\text{Fe}(\text{phen})_3]^{2+}$ salts dissolve in pure organic solvents (chapter 4)), it is reasonable to assume a common mechanism for the two reactions. There are no solubility data on the Schiff's base complex at present, and so a more quantitative treatment of the results is not possible.

Acid Aquation of Substituted 1,10-Phenanthroline Complexes of Iron(III) in Aqueous Solution

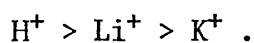
Towards the end of the last century, Blau [6.34,35] described tris-2,2'-bipyridyl and tris-1,10-phenanthroline complexes both of iron(II) and iron(III). The kinetics of substitution and of oxidation of these iron(II) complexes have been extensively studied, together with those of their ligand-substituted derivatives. However, even though the oxidations of the iron(II) complexes to their iron(III) analogues have been investigated [6.15], the kinetics of the reactions of these iron(III) complexes have been surprisingly little studied. Indeed, even the effects of ligand substitution on the aquation rates seem not yet to have been established.

The first part of this chapter dealt with solvent effects on the oxidation of selected iron(II) complexes, where the oxidation led to total dissociation of the complex, using peroxodisulphate as the oxidant. In acidic solution, strong oxidants such as cerium(IV) produce the corresponding iron(III) complex. Here, we have generated such tris-

iron(III) complex cations of substituted 1,10-phenanthrolines in aqueous acidic media, and studied the substituent effects on the rates of aquation of the participant complex cations.

Table 6.04 lists the observed first-order rate constants for aquation of the $[\text{Fe}(\text{X-phen})_3]^{3+}$ cations, where X = H, 5-Cl, 5-NO₂ and 4,7-Me₂, in aqueous sulphuric acid solutions at 307.5 K. The pattern of decreasing aquation rate with increasing acid concentration, which has been reported earlier for the unsubstituted $[\text{Fe}(\text{phen})_3]^{3+}$ [6.15,36] and $[\text{Fe}(\text{bipy})_3]^{3+}$ [6.37] cations, is also displayed by the substituted complexes. This pattern, together with the trends in reactivities of the substituted complexes is described by Figure 6.05.

This inverse dependence of rate on acid concentration has been suggested [6.36] to be due to a specific interaction between the complex and the hydrogen ion, with the resulting formation of $[\text{Fe}(\text{phen})_3\text{H}]^{4+}$. However, this theory has been discounted by Basolo et al. [6.15], since they found that the same decrease in rate constants could be achieved by replacement of the hydrogen ions by alkali metal ions. They found that the relative effectiveness of retardation of the rate was in the order:-



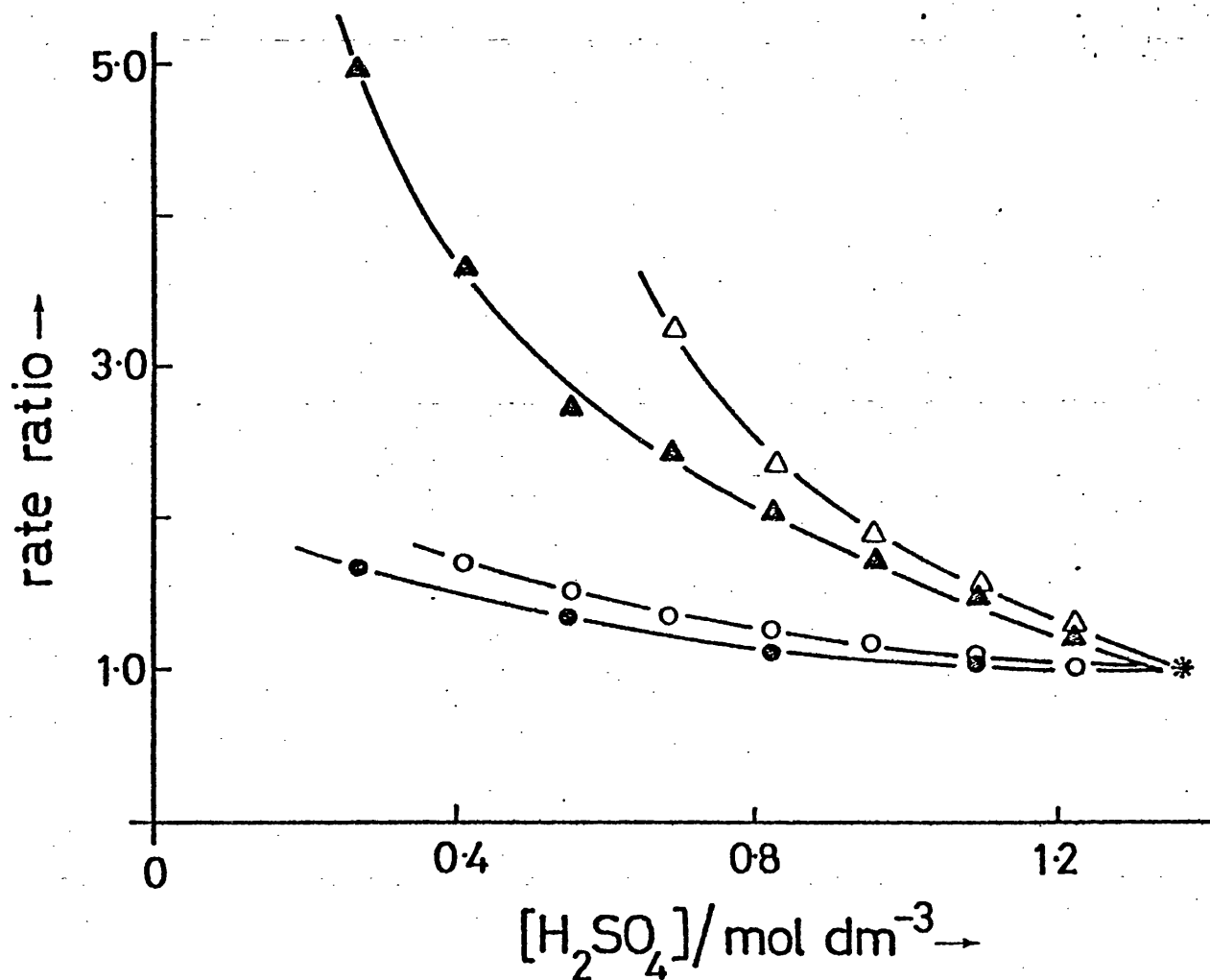
From Figure 6.05[†] we can see that the effect of substituent on reactivity is the same for the iron(III) as for the iron(II) complexes, viz:-

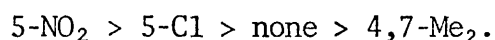
[†] [The "RATE RATIO" axis depicted in Figure 6.05 is the ratio of the aquation rates in given acid concentrations: the rate constant in 1.36 mol dm⁻³ acid.]

TABLE 6.04 Observed first-order rate constants, $10^3 k_{\text{obs}} / \text{s}^{-1}$, for the acid aquation of the $[\text{Fe}(\text{X-phen})_3]^{3+}$ cations, at 307.5 K in aqueous sulphuric acid.

| $\frac{[\text{H}_2\text{SO}_4]}{\text{mol dm}^{-3}}$ | X | | | |
|--|---------------------------------------|-------------------|------|---------------------|
| | H | 5-NO ₂ | 5-Cl | 4,7-Me ₂ |
| | $10^3 k_{\text{obs}} / \text{s}^{-1}$ | | | |
| 0.27 | | | 7.0 | 0.020 |
| 0.41 | 0.19 | | 5.1 | |
| 0.55 | 0.17 | | 3.8 | 0.017 |
| 0.68 | 0.15 | 44 | 3.5 | |
| 0.82 | 0.14 | 31 | 2.9 | 0.013 ₅ |
| 0.95 | 0.13 ₀ | 25 | 2.5 | |
| 1.09 | 0.12 ₄ | 20 | 2.2 | 0.013 ₀ |
| 1.23 | 0.11 ₅ | 16.3 | 1.8 | |
| 1.36 | 0.11 ₀ | 13.0 | 1.4 | 0.011 ₈ |
| 1.75 | | 7.3 | | |
| 2.04 | | 5.1 | | |
| 2.33 | | 3.8 | | |
| 2.62 | | 2.8 | | |

Figure 6.05 Substituent effects on the rate of aquation of the $[\text{Fe}(\text{X-phen})_3]^{3+}$ cations, at 307.5 K; X = 5- NO_2 (Δ), 5- Cl (\blacktriangle), H (\circ) and 4,7- Me_2 (\bullet), in various concentrations of sulphuric acid. 'Rate Ratio' is the ratio of the rates at a given acid concentration to that at $[\text{H}_2\text{SO}_4] = 1.36 \text{ mol dm}^{-3}$ (see text).





This comparison, a comparison of aquation and reduction rate constants, and comparisons of these kinetic parameters with other properties of the $[\text{Fe}(\text{X-phen})_3]^{3+}$ cations, are included in Table 6.05. Despite the differences in bonding, especially the π -bonding contributions, between these iron(III) and iron(II) complexes, the kinetic patterns are remarkably similar. However, the iron(III) complex aquation rates are much more sensitive to substituent variations than those for the analogous iron(II) compounds. Thus the aquation of the 5-nitro-iron(III) complex is over 1500 times faster than that of the 4,7-dimethyl-iron(III) complex, in 1.09 mol dm^{-3} of sulphuric acid at 307.5 K; the corresponding 5-nitro : 4,7-dimethyl ratio for the iron(II) complexes is only about 20 (cf. Table 6.05).

Figure 6.06 shows a plot of the logarithms of the rates of aquation of the $[\text{Fe}(\text{X-phen})_3]^{3+}$ cations in 1.09 mol dm^{-3} sulphuric acid at 307.5 K, against the values of the pK_a 's for the respective X-phen ligands, taken from Table 6.05. The linearity of this plot is an indication of the importance of the electron-withdrawing or -donating properties of the substituents of the ligands, and their influence on the reaction rates.

The rates of aquation of the $[\text{Fe}(5\text{-NO}_2\text{phen})_3]^{3+}$ cation were measured in aqueous solution for several concentrations of sulphuric acid over a range of temperatures. These rate constants are listed in Table 6.06. Figure 6.07 shows the variation of the rate of aquation with acid concentration for this cation over the range of temperatures studied. Activation parameters were calculated for the reaction for the individual acid concentrations used, the results of which are given in Table 6.06, together with the standard deviations. The activation enthalpies and

TABLE 6.05 Substituent effects on kinetic and other properties of substituted tris-(1,10-phenanthroline)iron(III) complexes, compared with those of the corresponding iron(II) ones.

| <u>Aquation</u> | | | | |
|---|-------------------|-------------------|-------------------|------------------------|
| $10^4 k / s^{-1}$ | | | | |
| <u>Fe(III)</u> (1.09 mol dm ⁻³ H ₂ SO ₄ ; at 307.5 K.) | 200 | 22 | 1.2 | 0.13 |
| <u>Fe(II)</u> ^a (1.07 mol dm ⁻³ H ₂ SO ₄ ; at 308.2 K.) | 23 | 12 | 3.8 | 1.1 |
| ^a | | | | |
| <u>Visible absorption</u> <u>of Fe(III) complexes</u> | | | | |
| $\lambda_{\max} / \text{nm}$ | 590 | 595 | 602 | 574 ^b |
| ϵ_{\max} | 950 | 760 | 870 | 1210 ^b |
| ^a | | | | |
| <u>Redox</u> | | | | |
| $10^6 k_2 / \text{mol}^{-1} \text{dm}^3 \text{s}^{-1}$ | | | | |
| Fe ²⁺ _{aq} (0.5 mol dm ⁻³ H ₂ SO ₄ ; at 298.2 K.) | 9 | 1.5 | 0.30 | ca. 0.005 ^c |
| E° / V | 1.25 ^a | 1.12 ^a | 1.06 ^a | 0.87 ^d |
| <u>Ligand pK_a</u> | 3.57 ^e | 4.26 ^e | 4.96 ^e | 5.94 ^f |

^a ref. 6.38; ^b Values determined in this work; ^c Estimated from ref.6.39 value in perchloric acid; ^d ref. 6.40; ^e ref. 6.41; ^f ref. 6.42.

Figure 6.06 Correlation between the logarithms of the rates of aquation of the $[\text{Fe}(\text{X-phen})_3]^{3+}$ cations in 1.09 mol dm^{-3} sulphuric acid and the pK_a values of the X-phen ligands, at 307.5 K .
 $\text{X} = 5\text{-NO}_2$ (1), 5-Cl (2), H (3) and $4,7\text{-Me}_2$ (4).

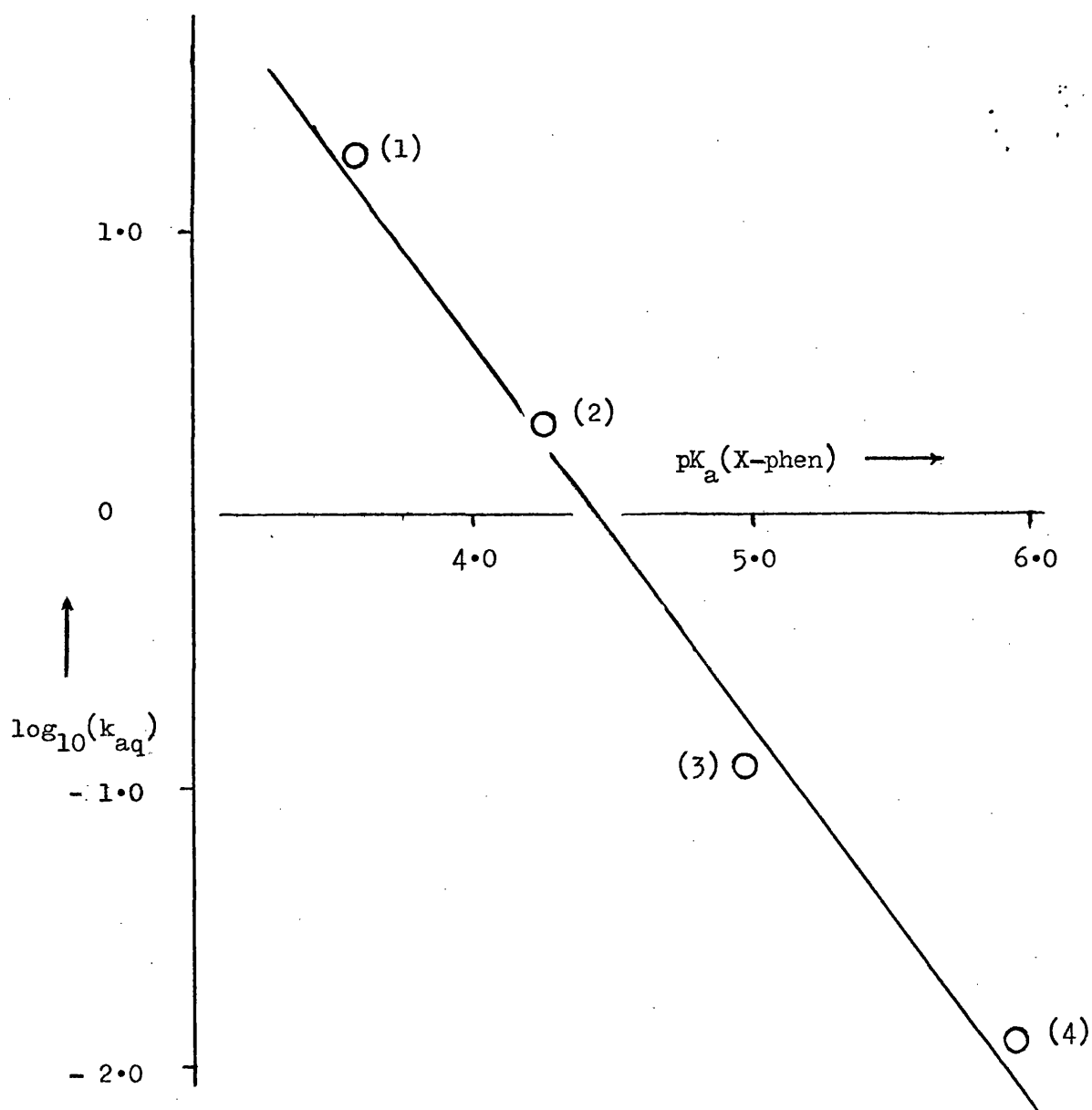
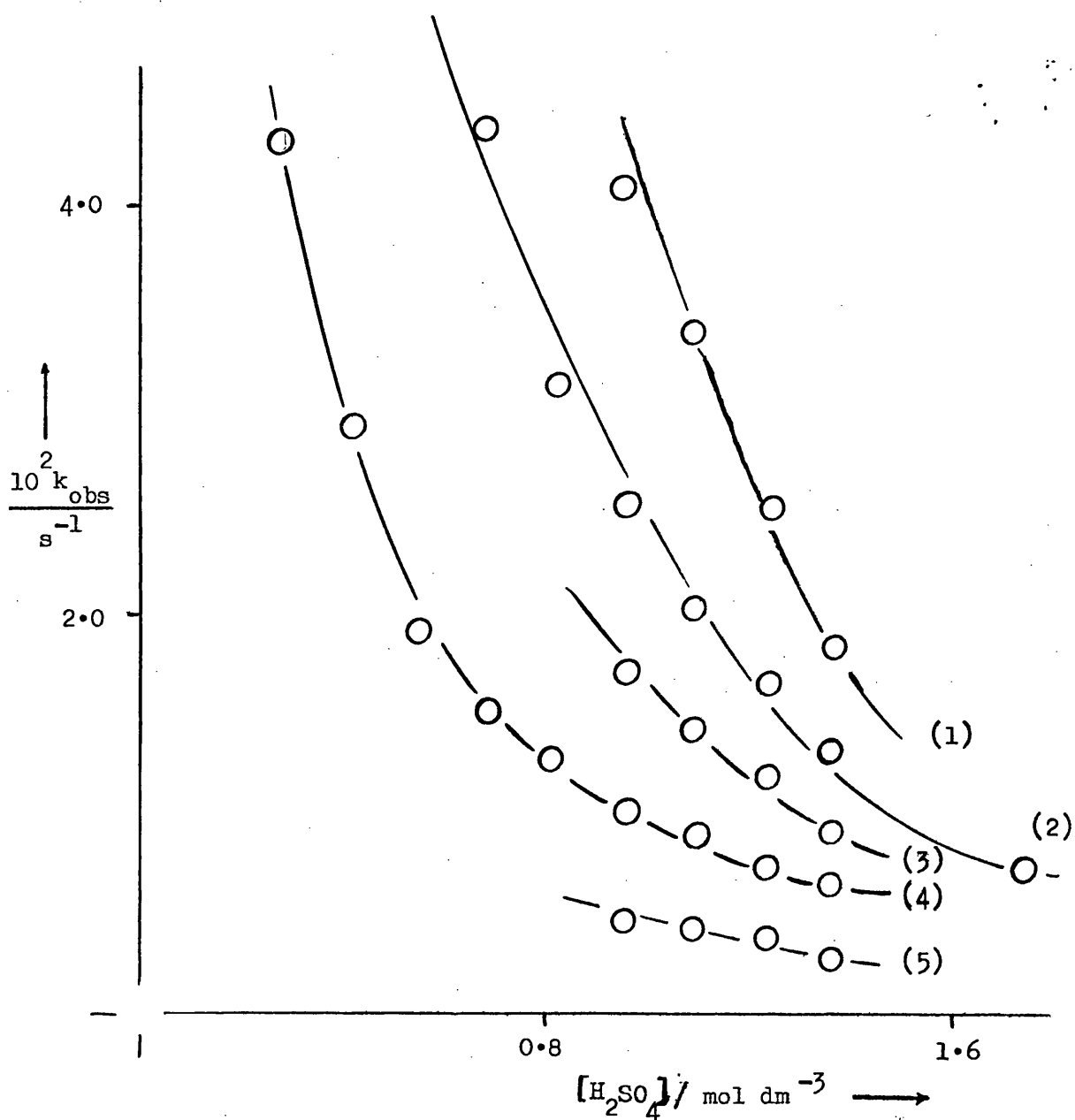


TABLE 6.06 Temperature dependence of the rates of aquation of the $[\text{Fe}(\text{5-NO}_2\text{phen})_3]^{3+}$ cation in various concentrations of sulphuric acid.

| $\frac{[\text{H}_2\text{SO}_4]}{\text{mol dm}^{-3}}$ | T / K | | | |
|--|---------------------------------------|-------|-------|-------|
| | 293.5 | 298.6 | 303.2 | 313.2 |
| | $10^3 k_{\text{obs}} / \text{s}^{-1}$ | | | |
| 0.27 | | 43 | | |
| 0.41 | | 29 | | |
| 0.55 | | 19 | | |
| 0.68 | | 15 | | |
| 0.82 | | 13 | | |
| 0.95 | 4.8 | 10.0 | 16.8 | 41 |
| 1.09 | 4.1 | 8.9 | 14.1 | 34 |
| 1.23 | 3.6 | 7.2 | 11.7 | 25 |
| 1.36 | 2.7 | 6.3 | 9.1 | 18.3 |

| | $\Delta H^\ddagger / \text{kJ mol}^{-1}$ | $\Delta S^\ddagger / \text{J K}^{-1} \text{mol}^{-1}$ |
|------|--|---|
| 0.95 | 85 ± 4 | $+ 96 \pm 11$ |
| 1.09 | 84 ± 4 | $+ 90 \pm 13$ |
| 1.23 | 77 ± 4 | $+ 67 \pm 11$ |
| 1.36 | 75 ± 4 | $+ 57 \pm 22$ |

Figure 6.07 Variation of the observed first-order rate constants, k_{obs} , for the aquation of the $[\text{Fe}(\text{5-NO}_2\text{phen})_3]^{3+}$ cation with acid concentration, at (1) 313.2, (2) 307.5, (3) 303.2, (4) 298.6 and (5) 293.5 K.



entropies are, within experimental error, constant. We can see from these results that these errors are increased for the measurements in stronger acid. We may compare these values, i.e. $\Delta H^\ddagger = 84 \text{ k J mol}^{-1}$ and $\Delta S^\ddagger = +90 \text{ J K}^{-1} \text{ mol}^{-1}$ for the aquation of $[\text{Fe}(\text{5-NO}_2\text{phen})]^{3+}$ in 1.09 mol dm^{-3} sulphuric acid (Table 6.06) with those of $\Delta H^\ddagger = 117 \text{ k J mol}^{-1}$ and $\Delta S^\ddagger = +88 \text{ J K}^{-1} \text{ mol}^{-1}$ [6.38] for the $[\text{Fe}(\text{5-NO}_2\text{phen})_3]^{2+}$ in 1.07 mol dm^{-3} sulphuric acid. The significant difference is in the ΔH^\ddagger values, which is consistent with the known differences in iron-nitrogen bond strengths between the iron(III) and iron(II) complexes, and the expected similarity of aquation mechanism.

Although this work has thrown no further light on the mechanism operating in the acid aquation of tris-(1,10-phenanthroline)iron(III) complexes, it has shown the effects of substituent variation in the system, which have shown marked similarities with the iron(II) analogues.

CHAPTER 7

X-Ray Diffraction Studies on Selected d^6 Transition
Metal Complexes; Single-Crystal and Powder
Diffraction Methods.

7.1 INTRODUCTION

This chapter is concerned with two X-ray diffraction techniques which are used to determine structural information about chemical compounds. The first involves the single crystal structure determination of trans-diisothiocyanato cyclam[†] cobalt(III) thiocyanate, trans-[Co-(cyclam)(NCS)₂]SCN. The purpose of this study was to provide absolute confirmation of the trans nature of the isothiocyanato ligands. The compound has been subjected to a solvatochromic study (see chapter 8), the results of which have been discussed partially in terms of the stereochemical nature of the participant compounds. The structure of the aforementioned compound has been successfully determined, and compared with the similar previously studied dichloro nickel(II) analogue [7.01].

The second part of this chapter deals with the X-ray powder diffraction studies of selected salts of the hexachlororhenate(IV) anion. The solubility of the tris(1,10-phenanthroline)iron(II) salt was measured in a range of binary aqueous mixtures in chapter 4, and an attempt to estimate single-ion free energies of transfer for the ReCl_6^{2-} anion, $\delta_{\text{m}\mu}^{\ominus}(\text{ReCl}_6^{2-})$, was made. The powder photograph for this salt was taken, in order to ascertain the relative nature of the ions at least in the solid state, in order to estimate the feasibility of the assumption tentatively made in chapter 4 that $\delta_{\text{m}\mu}^{\ominus}([\text{Fe}(\text{phen})_3]^{2+}) = \delta_{\text{m}\mu}^{\ominus}(\text{ReCl}_6^{2-})$. Having found this assumption to prove very poor (see chapter 4), the magnesium hexahydrate salt, $\text{Mg ReCl}_6 \cdot 6\text{H}_2\text{O}$ was prepared

[†] [cyclam = 1,4,8,11-tetraazacyclotetradecane]

and its powder photograph taken. This salt was selected due to the expected similarity in the sizes of the constituent ions (see text). From this photograph, the crystal system, lattice type and unit cell dimensions have been determined. Hence the possible assumption, $\delta_{\text{m}\mu}^{\oplus}(\text{Mg}(\text{OH}_2)_6]^{2+}) = \delta_{\text{m}\mu}^{\oplus}(\text{ReCl}_6^{2-})$ is considered to perform a 'single-ion split'.

Comprehensive accounts [7.02-05] of the theory and methods of X-ray diffraction are available in the literature and in standard texts. Therefore no attempt will be made to describe in detail the theory of X-ray diffraction and its application to the study of crystal structures. However the general principles and experimental techniques employed in this work will be outlined briefly in the text.

7.2 EXPERIMENTAL

(i) Preparations

(a) Trans-[Co(cyclam)(NCS)₂]SCN was prepared by the method of Bosnich *et al.* [7.06] from an aerated aqueous solution of cobalt(II) chloride, cyclam and an excess of sodium thiocyanate. The product was recrystallised from hot water, producing deep red crystals. All reagents were AnalaR grade. Cyclam was obtained commercially from Strem Chemicals, and was used as received.

(b) [Fe(phen)₃]ReCl₆ was prepared by adding excess of an AnalaR aqueous solution of tris(1,10-phenanthroline)iron(II) sulphate (B.D.H) to a degassed aqueous solution of potassium hexachlororhenate. The required salt immediately precipitated from solution. This was filtered, washed copiously with water to remove the excess iron(II) complex sulphate, followed by washing with ethanol, ether and drying over phosphorus pentoxide in vacuo at room temperature. The yield from this procedure is quantitative.

(c) Mg.ReCl₆.6H₂O was prepared by addition of a large excess of a strong solution of magnesium perchlorate hexahydrate to a saturated solution of potassium hexachlororhenate. The precipitated KClO₄ was filtered off, and to the filtrate, containing the required product and excess Mg.(ClO₄)₂.6H₂O was added n-propanol until precipitation of the MgReCl₆.6H₂O was complete. During this procedure, no magnesium perchlorate is precipitated. This is consistent with the fact that the solubility of this salt is 42.33 g/100g of solvent at 298.2 K [7.07]. The filtered product is recrystallised several times from aqueous n-propanol, washed with n-propanol, ether, and dried in air. The yield

TABLE 7.01 Spectrophotometric analyses of $[\text{Fe}(\text{phen})_3]\text{ReCl}_6$ and $\text{MgReCl}_6 \cdot 6\text{H}_2\text{O}$.

| | Optical Density | <u>Concentration</u> mol dm^{-3} | % $\text{Fe}(\text{phen})_3^{2+}$ | |
|---|-----------------|--|-----------------------------------|-------|
| | | | Calc. | Found |
| (i) $[\text{Fe}(\text{phen})_3]\text{ReCl}_6$ ^a | | | | |
| | 1.085 | 9.775×10^{-5} | 59.92 | 60.10 |
| (ii) $\text{MgReCl}_6 \cdot 6\text{H}_2\text{O}$ ^b | | | % ReCl_6^{2-} | |
| | 1.315 | 1.750×10^{-4} | 75.0 | 74.8 |

^a $\lambda_{\text{max}} = 510 \text{ nm}, \epsilon_{\text{max}} = 11100;$

^b $\lambda_{\text{max}} = 283 \text{ nm}, \epsilon_{\text{max}} = 13100.$

from this method is practically quantitative.

The salts of ReCl_6^{2-} were analysed spectrophotometrically, for $[\text{Fe}(\text{phen})_3]^{2+}$ content ($\epsilon_{\text{max}} = 11100$) at 510 nm in the visible spectrum [7.08] in the case of the $[\text{Fe}(\text{phen})_3]^{2+}$ salt, and for ReCl_6^{2-} content ($\epsilon_{\text{max}} = 13100$) at 283 nm in the U.V. spectrum [7.09] for the $[\text{Mg}(\text{OH}_2)_6]^{2+}$ salt. The cobalt(III) complex was characterised by comparison with published spectroscopic data [7.06]. A summary of the analysis results is given in Table 7.01.

(ii) Single-Crystal Structure Determination of $\text{trans-}[\text{Co}(\text{cyclam})(\text{NCS})_2]\text{SCN}$

Unit Cell and Space Group Determination

It is convenient to describe in this section the experimental techniques used in this study, which lead to the elucidation of the crystal structure of the compound in question.

A single-crystal of the title compound, having a parallel piped shape and uniform cross-section, and of approximate dimensions 0.01 cm x 0.01 cm x 0.03 cm was isolated under a microscope. The crystal was carefully mounted upon a glass fibre by means of 'Araldite' glue, with the longest physical axis of the crystal as near co-linear with the axis of the fibre as possible. The fibre was then attached to a small pin, which was inserted in a Unicam goniometer head. Such a head is a device having two mutually perpendicular arcs, which allow minor angular adjustment of crystal orientation with respect to the rotating shaft which carries the goniometer head. By adjustment of these arcs, the crystal was approximately aligned by viewing the crystal through an optical goniometer.

The goniometer head was then transferred to a Weissenberg camera to be aligned.

The camera was set to record an oscillation photograph of diffracted X-rays from the crystal. The principle of such photography is illustrated by Diagram 7.01.[†]

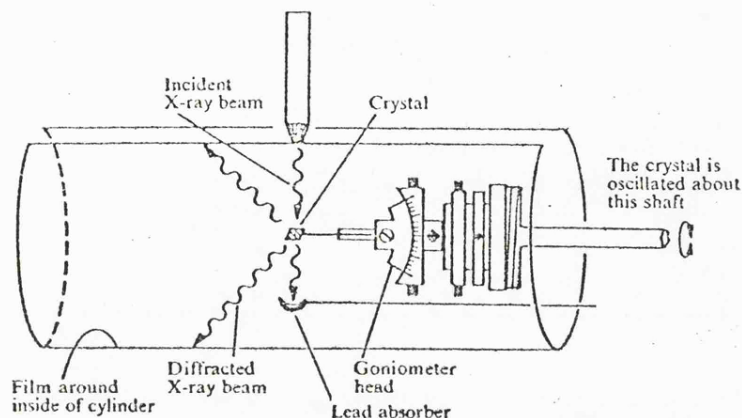


Diagram 7.01

The primary X-ray beam bathes the crystal and is then caught by a lead backstop. A cylindrical film encircles the shaft axis and intercepts and records any diffracted beams.

The shaft was oscillated through 10° , i.e. $\pm 5^\circ$ about a fixed position. The film was exposed to the diffracted beams for a period of 30 minutes, the X-ray source being Ni filtered $\text{Cu-K}\alpha$ ($\lambda = 1.5418 \text{ \AA}$) radiation. The shaft was then rotated 180° from the original fixed position, and a second oscillation photograph was superimposed upon the first, using similar conditions. The resulting developed photograph showed that the two sets of layer lines of spots were not quite superimposable, indicating slight angular misalignment of the crystal. Suitable adjustments to the goniometer arcs were made, and further "double-oscillation" photographs were taken until the crystal was

[†] [This diagram has been reproduced from J. Wormald, "Diffraction Methods", Clarendon Press, Oxford, (1973).]

accurately aligned.

Once the alignment was correct, a zero-layer Weissenberg photograph was taken using the same X-ray source. Here, the crystal was rotated about the shaft through 200° . As the diffracted beams hit the film, the camera was translated through a 10 cm distance parallel to the rotation axis in synchronization with the rotation, so that diffraction spots no longer lie on a straight line. As the direction of rotation was reversed, and the crystal rotated back through 200° , so the film was translated back through 10 cm. This cycle was repeated for a period of 48 hours, so that a sufficiently intense exposure was obtained. A slit-metal screen fitted to the camera ensures that only one layer line at a time is examined.

The crystal was mounted about its c-axis. Hence the zero-layer Weissenberg photograph represents a distorted view of the $hk\ 0$ plane in the reciprocal lattice. From this photograph recognition of the principal axes a^* and b^* ,[†] and the angle between these, γ^* , was possible. Also, from the symmetry of the photograph, the crystal class and space group were assigned.

Accurate reciprocal cell dimensions, a^* , b^* , c^* , α^* , β^* and γ^* , were measured from precession photographs. The precession camera is a moving-crystal, moving-film device for mapping one reciprocal lattice level onto one sheet of film, but unlike the Weissenberg method, it does so in such a way as to provide an undistorted record from which the angles and distances of the lattice may be measured directly. The theory and practice of the precession camera have been discussed in detail in a

[†] [Asterisks refer to reciprocal lattice parameters throughout this work.]

monograph by Buerger [7.10].

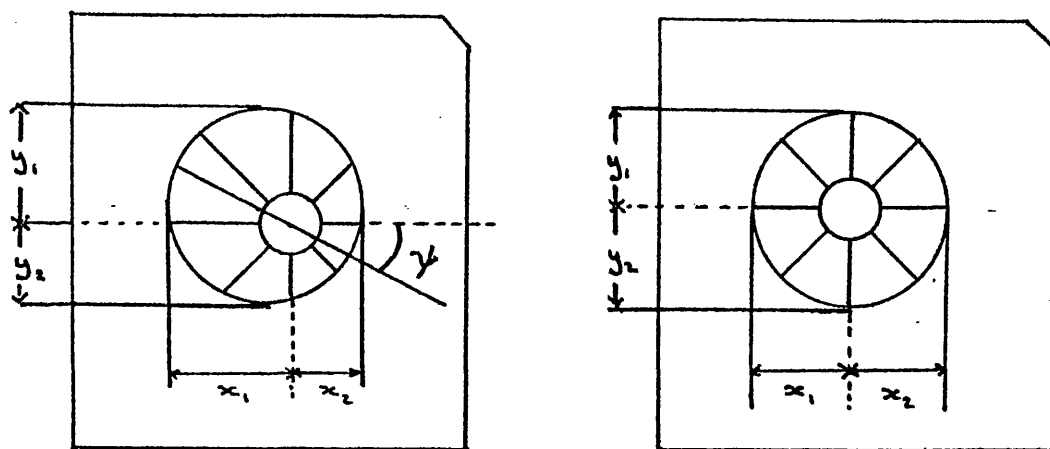
The crystal was first centred in the X-ray beam by suitable adjustment of the horizontal and vertical heights of the goniometer arcs while viewed through a microscope. Once centred, the crystal was aligned in the X-ray beam. This was accomplished by firstly taking a zero-layer precession photograph, using Cu-K α radiation (Ni filter) with a 48 hour exposure, having a screen setting of 2 cm and a $\bar{\mu}$ value of 30°. Any misalignment can be represented in terms of three errors: ϵ_H and ϵ_v , which relate to the horizontal and vertical angular separations of the direct axis from the beam; and ψ is the amount the net is rotated about the direct axis from its desired position. Provided the goniometer head is adjusted such that its arcs are reasonably close to being parallel and perpendicular to the X-ray beam, then a change in the azimuth affects ϵ_v alone, the parallel (horizontal) arc affects ϵ_H , and the perpendicular (vertical) one affects ψ . Diagram 7.02(a) shows a typical precession photograph of a misaligned crystal. If the distances from the beam to the edge of zero-level trace are measured in the two horizontal (Δx) and the two vertical (Δy) directions, the difference ($\Delta\xi$) in reciprocal lattice units between the points appearing at the edges is

$$\Delta\xi_y = \frac{||y_1| - |y_2||}{2 \times (\text{film-to-crystal distance})} \quad (7.01)$$

$$\Delta\xi_x = \frac{||x_1| - |x_2||}{2 \times (\text{film-to-crystal distance})} \quad (7.02)$$

If the arcs are properly orientated, corrections for these errors are made by changing the azimuth and the horizontal arc by $-\epsilon_v$ and $-\epsilon_H$ respectively. The sense of the correction is obtained by noting that

Diagram 7.02
Idealised Precession Photographs.



(a) Misaligned Crystal.

(b) Correctly Aligned Crystal.

the direct axis lying within the sphere of reflection is always tipped toward the short distances on the film [x_2 and y_2 in diagram 7.02(a)]. The final correction, i.e. the rotation, ψ needed to bring a reciprocal layer axis onto the spindle axis, is just the angular deviation of this axis from the beam/spindle plane. When finally aligned a precession photograph of the type illustrated in diagram 7.02(b) is obtained.

In this work, the adjustments necessary for correct alignment were:-

$$\begin{aligned}\epsilon_H &= 0^\circ 40' \\ \epsilon_V &= \text{zero} \\ \psi &= -1^\circ 10' .\end{aligned}$$

From the precession photograph of the correctly aligned crystal,

with a^* vertical, values of a^* , c^* and the angle β were computed, using the 'DRRSNAPS' program. A second such photograph, with c^* vertical was taken, from which b^* , c^* and the angle α were similarly computed. The real cell angle γ was measured as the angle between a^* and c^* , i.e. the difference in the spindle settings for the two photographs above.

Intensity Data Collection

Diffracted X-ray intensities were measured by a Stöe automatic diffractometer using $\text{Mo-K}\alpha$ ($\lambda = 0.7107 \text{ \AA}$) radiation with a graphite monochromator. This diffractometer is an adaptation of the Weissenberg film method and incorporates a counter goniometer with a Güttinger control system. Equi-inclination geometry is used, the conditions of which are satisfied when the angle (μ') between the crystal rotation axis and the incident X-ray beam is equal in magnitude to the angle (ν') between the counter and the rotation axis. In practice, however, the two angles μ and ν are set such that $\mu = 90^\circ - \mu'$ and $\nu = 90^\circ - \nu'$. These angles, which define the individual reciprocal layers, are set manually. The values of μ for various layers are calculated from the expression:-

$$\sin \mu_n = \frac{n\lambda}{2c} \quad (7.03)$$

where c = real unit cell axis length, λ = wavelength of radiation, n = number of the n th reciprocal layer.

The reflections to be recorded are located by contemporaneous movement of the counter (through 2θ degrees) and rotation of the crystal (through ω degrees). The initial measurement made on the diffractometer was to check and adjust the alignment of the crystal. This alignment is

crucial, the required condition being that the axis of rotation of the crystal is coincident with a crystal lattice vector. In this situation, reciprocal lattice planes are perpendicular to the axis, and Weissenberg geometry may be achieved.

The counter was set at a 2θ value of zero, and placed at a μ angle equal to the inclination angle (calculated from equation (7.03)) for the n^{th} layer of the reciprocal lattice, which, for in this case $n = 1$, had a value $\mu = 2.47^\circ$. With the crystal set to diffract under equi-inclination (i.e. $\nu = 2.47^\circ$) conditions, a suitable reflection was located by rotation of the crystal while keeping the counter locked in position at a value of $2\theta = 6.6^\circ$ in this case. The goniometer head was then set to zero, and the intensity of the reflection was maximised by adjustment of the horizontal arc. The head was then rotated through 180° , and the intensity was maximised again. The correct arc setting was taken as the mean of the two readings. This mean angular correction was also applied to μ in order that the reciprocal layer was fully received by the counter head. This alignment procedure was then repeated for the arc which was horizontal when the goniometer head was set at 90° and 270° . The crystal was finally centred in the X-ray beam by adjustment of its horizontal and vertical height.

The intensities of the spots of each reciprocal net were measured for the nine layers, $hk\ 0$ to $hk\ 8$ inclusively, so that the angles μ and ν , which correspond to these individual layers, were held constant for each layer. Therefore it was only necessary to measure the two angles, ω and 2θ in order to receive a particular reflection. The values of these two angles were computed from the knowledge of the reciprocal cell parameters (obtained from the earlier precession photographs) by

the FORTRAN IV program, 'STOTP'.[†] The control tape generated by this program was fed to the Guttinger control unit, which converts the setting angles for the reflections, timing information and the reflection index for a given layer into ω and 2θ values. These values were read by the diffractometer on 8-hole paper tape as absolute values, the angles being converted into the required values by two 'Slo-Syn' motors attached to the crystal shaft and counter head respectively.

The intensity measurements were undertaken with an ' ω -scanning mode', where the counter is held stationary, while the crystal is rotated. A complete profile of the reflection is recorded, consisting of a 2 minute scan with 20 second background measurements before and after the scan. For all layers measured, the rate of change of ω was 3 degrees per minute. A check reflection was recorded every 30 reflections to monitor possible decay or gradual misalignment of the crystal. The nine layers were measured in the four quadrants having positive l indices.

Solution and Refinement of the Structure

The intensities of the measured reflections were corrected for Lorentz and Polarisation effects by the 'STOWPK' program, which also produced the structure amplitudes from the initial data. The intensity of a given reflection was calculated from:-

[†] [This and all other programs in this chapter was written by Dr. D. R. Russell. As these are standard crystallographic programs, they will neither be listed nor discussed in this work.]

$$I_{(meas)} = C_p - \frac{1}{2} (C_{b1} (T_p/T_{b1}) + C_{b2} (T_p/T_{b2})) \quad (7.04)$$

where $I_{(meas)}$ is the measured intensity, C_p is the number of counts during the scan time T_p ; and C_{b1} and C_{b2} are the number of counts during the background scans of time T_{b1} and T_{b2} respectively.

The intensity of a given reflection was corrected for Lorentz and Polarisation effects by the formula:-

$$I = \frac{I_{(meas)}}{L \times P} \quad (7.05)$$

where L is the Lorentz factor for Weissenberg geometry, given by

$$L = \frac{\sin \theta}{\sin 2\theta} \times (\sin^2 \theta - \sin^2 \mu)^{-\frac{1}{2}} \quad (7.06)$$

and P is the Polarisation factor,

$$P = 1 + \cos^2 \theta \quad (7.07)$$

No correction was made for absorption since the cross-section of the crystal was uniform, and so any absorption by the crystal was expected to be uniform. This was supported by the low value for the linear absorption coefficient of 11.47.

The structure amplitude, $|F|$ and its derivative σF were calculated from the formulae:-

$$|F| = I^{\frac{1}{2}} \quad (7.08)$$

and

$$\sigma F = \frac{(I + \sigma I)^{\frac{1}{2}} - I^{\frac{1}{2}}}{L \times P^{-1}} \quad (7.09)$$

Only reflections for which $I \geq 2\sigma I$, or $F \geq 3\sigma F$ were retained by the program 'STOWPK', and consequently used in the refinement of the

structure. A statistical analysis of the periodically measured check reflection was also produced by this program, which indicated no crystal movement or decomposition during the period over which data was collected.

The output from the above program job was collected and arranged by the program 'PRFTP'. Using this condensed data, the structure was refined as outlined in section 7.3(i).

(iii) X-Ray Powder Photography of Hexachlororhenate(IV) Salts

The powder camera used was of the Straumanis-Levin⁵ type. Such a camera permits simple and accurate measurement of the diffraction angles, and is independent of uncertainties in the knowledge of the camera radius. This is because the X-ray beam enters and leaves the camera through holes in the film, so that the centres of these holes correspond to values of the Bragg angle, $\theta = 0^\circ$ and 90° respectively. These points are midway between corresponding low-angle ($2\theta < 90^\circ$) and high-angle ($2\theta > 90^\circ$) diffraction lines.

A sample of each of the salts to be photographed was finely ground with an agate mortar and pestle, and was used to fill a capillary tube to a depth of ca. 2 cm. The tube was then broken off just below the level of the sample, and the cylinder of solid finely divided sample was then mounted on the block at the centre of the camera. The sample was centralised in the camera by adjustment of the block until no horizontal or vertical movement of the sample could be observed upon rotation of the block about its axis. A film was then inserted in the camera such that it lay concentric with the camera surface. The camera was then

placed on a track on the X-ray unit. The block on which the sample was mounted was then set rotating by attachment of a connected external spindle to a motor. The sample was exposed to Cu-K α ($\lambda = 1.5418 \text{ \AA}$) for a period of 3 hours.

The developed photograph displays a series of concentric arcs, a schematic representation of a typical powder diffraction pattern being depicted in Diagram 7.03.

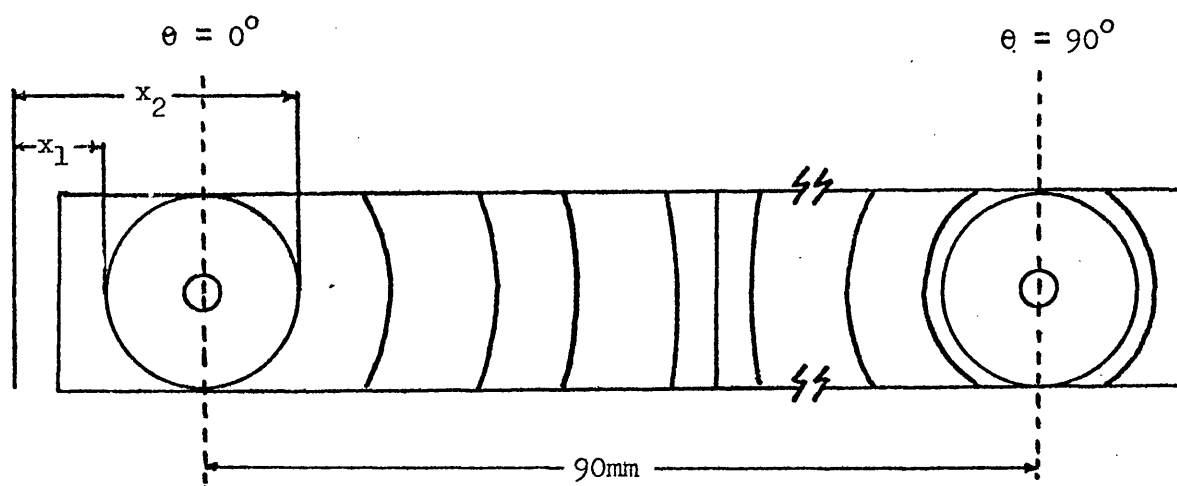


Diagram 7.03

The diameters of the rings are measured to 0.01 cm by means of a vernier scale as the distance $(x_2 - x_1)$. The radius of the camera used was 5.726 cm ($= 180^\circ/\pi$), and so the diffraction angle 2θ may be directly read in degrees from the measured radii of the rings in centimeters.

7.3 RESULTS AND DISCUSSION

(i) SINGLE CRYSTAL STUDY

Crystal Data

From the lack of symmetry in the Weissenberg photographs, the crystal was assigned a space group of $P\bar{1}$, having triclinic symmetry. The unit cell dimensions were calculated as $a = 9.573 \pm 0.019 \text{ \AA}$; $b = 12.154 \pm 0.009 \text{ \AA}$; $c = 8.262 \pm 0.011 \text{ \AA}$; $\alpha = 89.88^\circ$, $\beta = 92.42^\circ$, and $\gamma = 90.89^\circ$, the volume of the unit cell being 960.35 \AA^3 . The density of the crystalline complex was measured by the flotation method, using a mixture of iodomethane and methanol, and was found to be 1.50 g cm^{-3} . This suggests that there are two molecules of $\text{trans-[Co(cyclam)(NCS)}_2\text{]SCN}$ per unit cell. This was deduced from:-

$$\text{mass per unit cell} = \frac{\text{density} \times (\text{volume of unit cell})}{\text{molecular wt./Avogadro's No.}} \quad (7.10)$$

$$= \frac{1.5 \times 960.35 \times 10^{-24}}{433.50/6.02 \times 10^{23}} = 2.00 \text{ molecules per unit cell.}$$

I should like to express my thanks to Dr. D. R. Russell for his solution of the Phase Problem in this structure determination, and his solution of the Patterson function.

Solution of Structure

A 3-dimensional Patterson function was mapped for the asymmetric area of the unit cell. The section calculated was given by the boundaries $(0 \rightarrow x, 0 \rightarrow y/2, 0 \rightarrow z)$, the map being sectioned along the z axis. The resulting set of Patterson peaks yield the positions of two cobalt atoms as having fractional unit cell coordinates $(x/a, y/b, z/c)$ $0, 0, 0$ and

0.5, 0.5, 0.5.

A subsequent difference Fourier map (i.e. an electron density map of the unit cell with the electron density of the known cobalt atoms subtracted) yielded the positions of three sulphur atoms, i.e. one from one of the thiocyanate anions and one from each cationic molecule. A further difference Fourier map yielded the atomic positions of the carbon and nitrogen atoms of one thiocyanate anion, and only one half of each of the remainder of carbon and nitrogen atoms of the cyclam ligands and axial iso thiocyanate ligands of the complex cation. The remaining non-hydrogen atoms were found to be accessible by performing a centre of inversion symmetry operation through the cobalt atoms. This necessitates the complex cations to be centrosymmetric in their own right.

Two cycles of block-diagonal least-squares refinement reduced R^\dagger to 0.072 for 1915 reflections. The two cobalt atoms and the three sulphur atoms were made anisotropic, and a weighting scheme, with the weight given by $w = 1.9252 (\sigma^2 |F_o| + 0.002172 |F_o|^2)^{-1}$, was introduced, and two further cycles of least-squares refinement were performed. The final R factor was 0.072.

Table 7.02 lists the final atomic parameters, with standard deviations in parentheses, which were calculated from the least-squares treatment. The consequent bond lengths (\AA) and angles ($^\circ$), with estimated standard deviations, e.s.d., in parentheses, are listed in Table 7.03. Observed and calculated structure factors are listed in

$$^\dagger \left(R = \frac{\sum |F_o| - |F_c|}{\sum |F_o|} \right)$$

TABLE 7.02 Final atomic parameters and anisotropic temperature factors

for the trans-[Co(cyclam)(NCS)₂] SCN crystal structure.

Numbers in parentheses are standard deviations.

| CYCLAM NCS | | | | | | | | | | | |
|------------|-------------------|-------------------|-------------------|------------------|------------------|------------------|------------------|-------------------|-------------------|-------------------|--|
| ATOM | X/A | Y/B | Z/C | K | U11 | U22 | U33 | U23 | U13 | U12 | |
| CO1 | 0.0000 0.0000 | 0.0000 0.0000 | 0.0000 0.0000 | .5000 0.0000 | .0157 (.0012) | .0219 (.0012) | .0249 (.0013) | -.0032 (.0009) | -.0033 (.0009) | -.0005 (.0009) | |
| S1 | .3945 (.0004) | .00-0 (.0000) | .3174 (.0006) | 1.0000 0.0000 | .0285 (.0020) | .0505 (.0024) | .0699 (.0028) | -.0087 (.0021) | -.0221 (.0019) | .0203 (.0018) | |
| N1 | -.1513 (.0012) | .0164 (.0003) | -.1447 (.0013) | 1.0000 0.0000 | .0316 (.0025) | | | | | | |
| N3 | -.1228 (.0011) | -.0873 (.0003) | .1540 (.0012) | 1.0000 0.0000 | .0273 (.0024) | | | | | | |
| N4 | -.0321 (.0011) | .1413 (.0003) | .1001 (.0012) | 1.0000 0.0000 | .0262 (.0023) | | | | | | |
| C1 | -.2540 (.0014) | .0073 (.0011) | -.2192 (.0016) | 1.0000 0.0000 | .0293 (.0030) | | | | | | |
| C3 | -.2549 (.0015) | -.0411 (.0012) | .2049 (.0017) | 1.0000 0.0000 | .0357 (.0032) | | | | | | |
| C4 | .1432 (.0015) | .1973 (.0012) | -.0855 (.0017) | 1.0000 0.0000 | .0348 (.0032) | | | | | | |
| C5 | .0103 (.0015) | .2333 (.0012) | -.0178 (.0017) | 1.0000 0.0000 | .0386 (.0034) | | | | | | |
| C6 | -.1866 (.0016) | .1634 (.0012) | .1558 (.0018) | 1.0000 0.0000 | .0394 (.0034) | | | | | | |
| C7 | -.2354 (.0016) | .0651 (.0013) | .2738 (.0018) | 1.0000 0.0000 | .0413 (.0035) | | | | | | |
| CO2 | .5000 0.0000 | 0.0000 0.0000 | 0.0000 0.0000 | .5000 0.0000 | .0199 (.0013) | .0218 (.0013) | .0295 (.0013) | -.0049 (.0010) | .0053 (.0010) | .0211 (.0010) | |
| S2 | .1001 (.0004) | .0071 (.0000) | .3153 (.0006) | 1.0000 0.0000 | .0339 (.0021) | .0513 (.0025) | .0556 (.0028) | .0059 (.0020) | .0247 (.0019) | .0062 (.0015) | |
| N2 | .0520 (.0012) | .4920 (.0003) | .3526 (.0013) | 1.0000 0.0000 | .0343 (.0027) | | | | | | |
| N5 | .6075 (.0012) | .1113 (.0003) | .5590 (.0013) | 1.0000 0.0000 | .0332 (.0026) | | | | | | |
| N6 | -.4172 (.0012) | -.3577 (.0003) | -.4305 (.0014) | 1.0000 0.0000 | .0352 (.0027) | | | | | | |
| C2 | .7572 (.0013) | .4923 (.0010) | .2835 (.0015) | 1.0000 0.0000 | .0261 (.0025) | | | | | | |
| C8 | .5326 (.0017) | .4563 (.0011) | .2242 (.0020) | 1.0000 0.0000 | .0478 (.0039) | | | | | | |
| C9 | .5930 (.0019) | .5753 (.0013) | .8196 (.0022) | 1.0000 0.0000 | .0594 (.0047) | | | | | | |
| C10 | -.3535 (.0016) | -.3403 (.0013) | -.2540 (.0019) | 1.0000 0.0000 | .0441 (.0037) | | | | | | |
| C11 | .3051 (.0017) | .2560 (.0013) | .5033 (.0019) | 1.0000 0.0000 | .0473 (.0039) | | | | | | |
| C12 | .5374 (.0017) | .2993 (.0013) | .5756 (.0019) | 1.0000 0.0000 | .0461 (.0037) | | | | | | |
| S3 | .1032 (.0004) | .208- (.0000) | .4836 (.0005) | 1.0000 0.0000 | .0344 (.0021) | .0569 (.0025) | .0453 (.0022) | -.0114 (.0019) | -.0034 (.0016) | .0071 (.0019) | |
| N7 | -.1354 (.0016) | .3042 (.0012) | .5775 (.0016) | 1.0000 0.0000 | .0573 (.0037) | | | | | | |
| C13 | -.0321 (.0015) | .2564 (.0012) | -.2733 (.0017) | 1.0000 0.0000 | .0377 (.0034) | | | | | | |

RESIDUALS BEFORE CYCLE 5 FOR CYCLAM NCS

R = .0727 RA = .0764 RG = .1397 RH = .1367

N = 1915 NP = 32 MAX(NP) = 119

WEIGHT = 1.6791 / (SIGMA**2(F) + .0029-7 F*F)

TABLE 7.03 Bond lengths(\AA) and angles($^{\circ}$) for the trans-[Co(cyclam)(NCS) $_2$] SCN crystal structure. Numbering of atoms as in Figures 7.01 & 02. Atoms Co1 and Co2 refer to the cobalt atoms of the two molecules per unit cell(Figure 7.03). Numbers in parentheses are standard deviations. As the atoms N1 and N1A(Figure 7.02) are equivalent, the bonding dimensions of atoms of the latter type are not listed.

| Bond | Bond Length(\AA) | Bond Angle($^{\circ}$) | |
|-------------------|-----------------------------|--------------------------|------------|
| Co1---N1 | 1.892(0.011) | | |
| Co2---N2 | 1.902(0.011) | N3-Co1-N1 | 89.8(0.4) |
| Co1---N3 | 1.993(0.010) | N5-Co2-N2 | 88.5(0.8) |
| Co2---N5 | 1.965(0.011) | | |
| Co1---N4 | 1.977(0.010) | N4-Co1-N1 | 92.1(0.4) |
| Co2---N6 | 1.998(0.012) | N6-Co2-N2 | 87.6(0.5) |
| C1---S1 | 1.579(0.017) | N4-Co1-N3 | 93.7(0.4) |
| C2---S2 | 1.594(0.018) | N6-Co2-N5 | 93.3(0.5) |
| C1---N1 | 1.164(0.017) | C1-N1-Co1 | 166.4(1.1) |
| C2---N2 | 1.156(0.017) | C2-N2-Co2 | 169.0(1.1) |
| C3---N3 | 1.499(0.018) | C3-N3-Co1 | 119.7(0.8) |
| C8---N5 | 1.516(0.020) | C8-N5-Co2 | 118.8(0.9) |
| C4---N3 | 1.489(0.018) | C5-N4-Co1 | 107.5(0.8) |
| C9---N5 | 1.498(0.020) | C10-N6-Co2 | 109.1(0.9) |
| C5---N4 | 1.522(0.017) | C6-N4-Co1 | 118.9(0.8) |
| C10---N6 | 1.493(0.020) | C11-N6-Co2 | 119.1(0.9) |
| C6---N4 | 1.516(0.018) | C6-N4-C5 | 109.7(1.0) |
| C11---N6 | 1.511(0.018) | C11-N6-C10 | 110.4(1.3) |
| C7---C3A | 1.497(0.021) | C7-C3A-N3 | 110.7(1.1) |
| C12---C8A | 1.515(0.023) | C12-C8A-N5 | 111.3(1.2) |
| | | C4-C5-N4 | 106.3(1.1) |
| | | C9-C10-N6 | 110.4(1.3) |
| C5---C4 | 1.520(0.020) | C7-C6-N4 | 109.5(1.1) |
| C10---C9 | 1.506(0.024) | C12-C11-N6 | 116.0(1.2) |
| C7---C6 | 1.570(0.021) | C6-C7-C3A | 114.9(1.2) |
| C12---C11 | 1.528(0.023) | C11-C12-C8A | 113.1(1.4) |
| Thiocyanate Anion | | | |
| S3---C13 | 1.631(0.015) | N7-C13-S3 | 177.1(1.4) |
| N7---C13 | 1.171(0.021) | | |

Appendix 4.

Figure 7.01 depicts a $\text{trans-}[\text{Co}(\text{cyclam})(\text{NCS})_2]^+$ cation, viewed along the axial N-Co bond. This illustration clearly shows the non-co-linearity of the Co-N-C-S chain of the coordinated isothiocyanate ligands. This bending of the Co-N-C angle appears to be produced to alleviate some steric disturbance caused by both the secondary-amine protons and the protons of the end carbon atoms of the 1,3-diaminopropane linkages of the cyclam ligand. It appears that neither of these two types of proton is alone responsible for the steric effect, as the isothiocyanate ligands appear to be directed towards the ethylene-diamine residues of the cyclam ligand, a direction which is 180° away from neither of the aforementioned sets of protons.

Figure 7.02 shows a view of the cation with the cobalt atom and the apices of the 1,3-diaminopropane residues of the cyclam ligand in the plane of the page, describing the abscissa of the illustration. We may see from this figure that the 1,3-diaminopropane rings of the cyclam ligand are in a chair conformation, while the ethylenediamine residues are gauche, their carbon atoms being equatorial substituents on the nitrogens of the 1,3-diaminopropane rings. Co-planarity of the cobalt and the four coordinated nitrogens of the cyclam ligand is a necessary consequence of the fact that the cation is centro-symmetric.

Figure 7.03(a) is a view of the unit cell of the title compound, looking along the c axis. This shows the two cations, centred at the fractional coordinates (0,0,0) and (0.5,0.5,0.5), together with the corresponding thiocyanate anions. Figure 7.03(b) is a view of the unit cell shown in Figure 7.03(a) having been rotated through 90° about the a axis. This view clearly shows the relative positions of the complex cations, which appear to be almost perpendicular to one-another. This

Figure 7.02

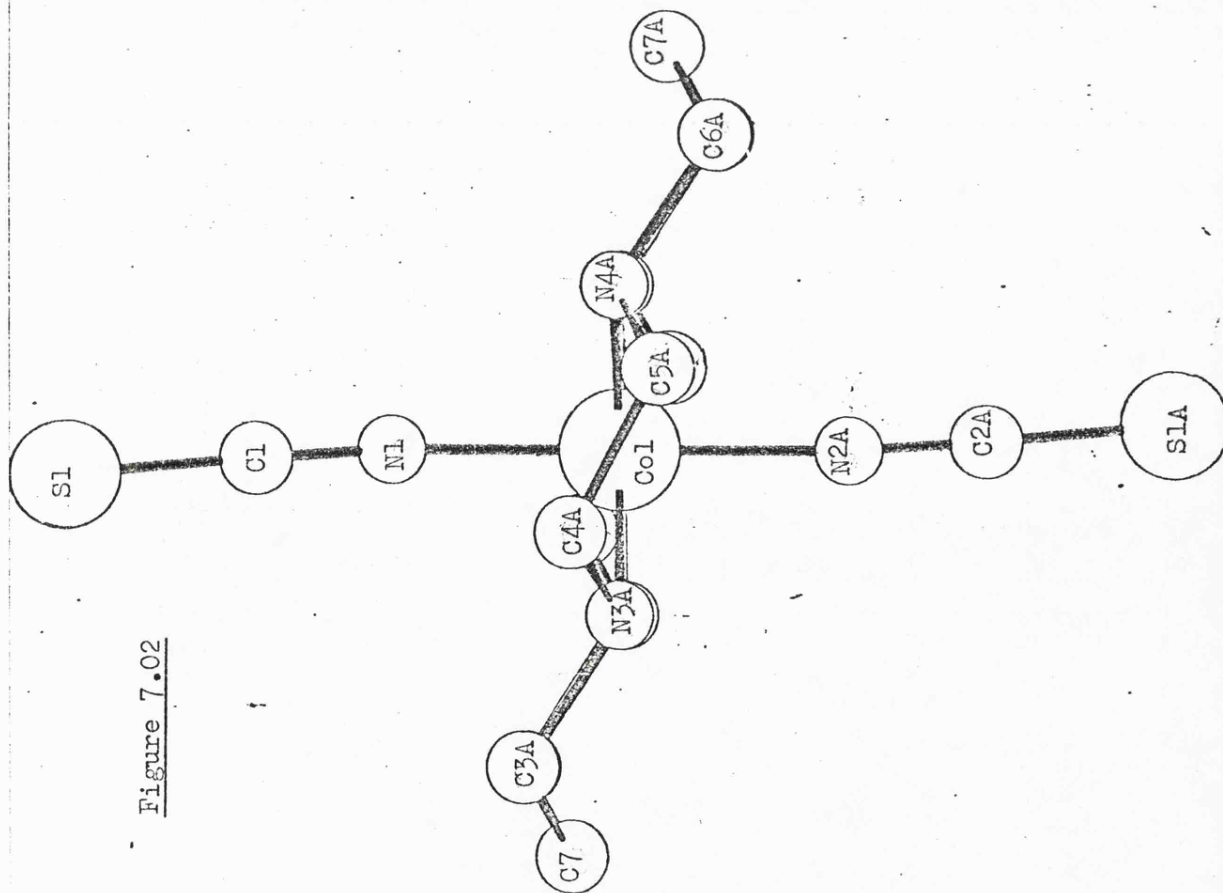


Figure 7.01

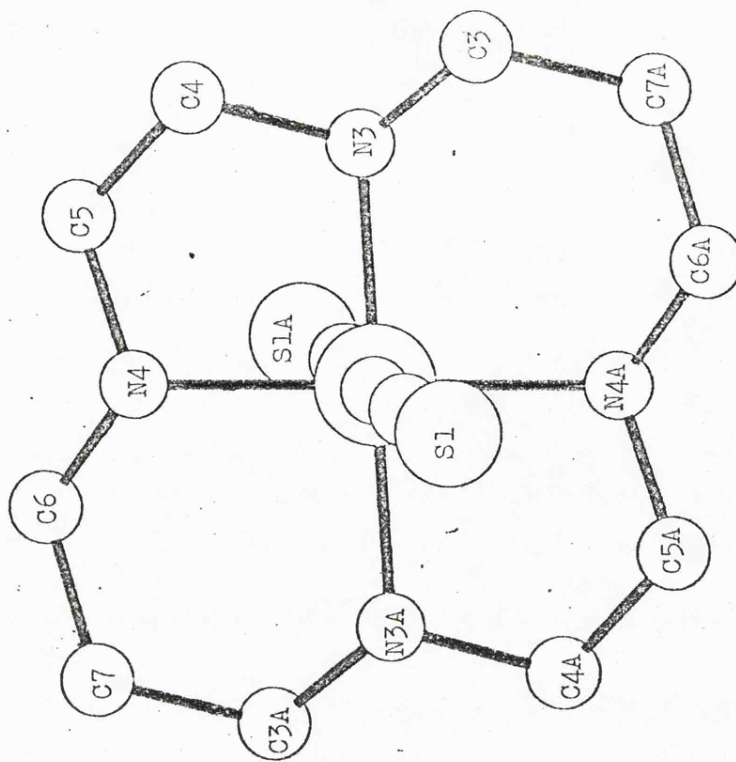


Figure 7.03(a) View of unit cell along the C-axis.

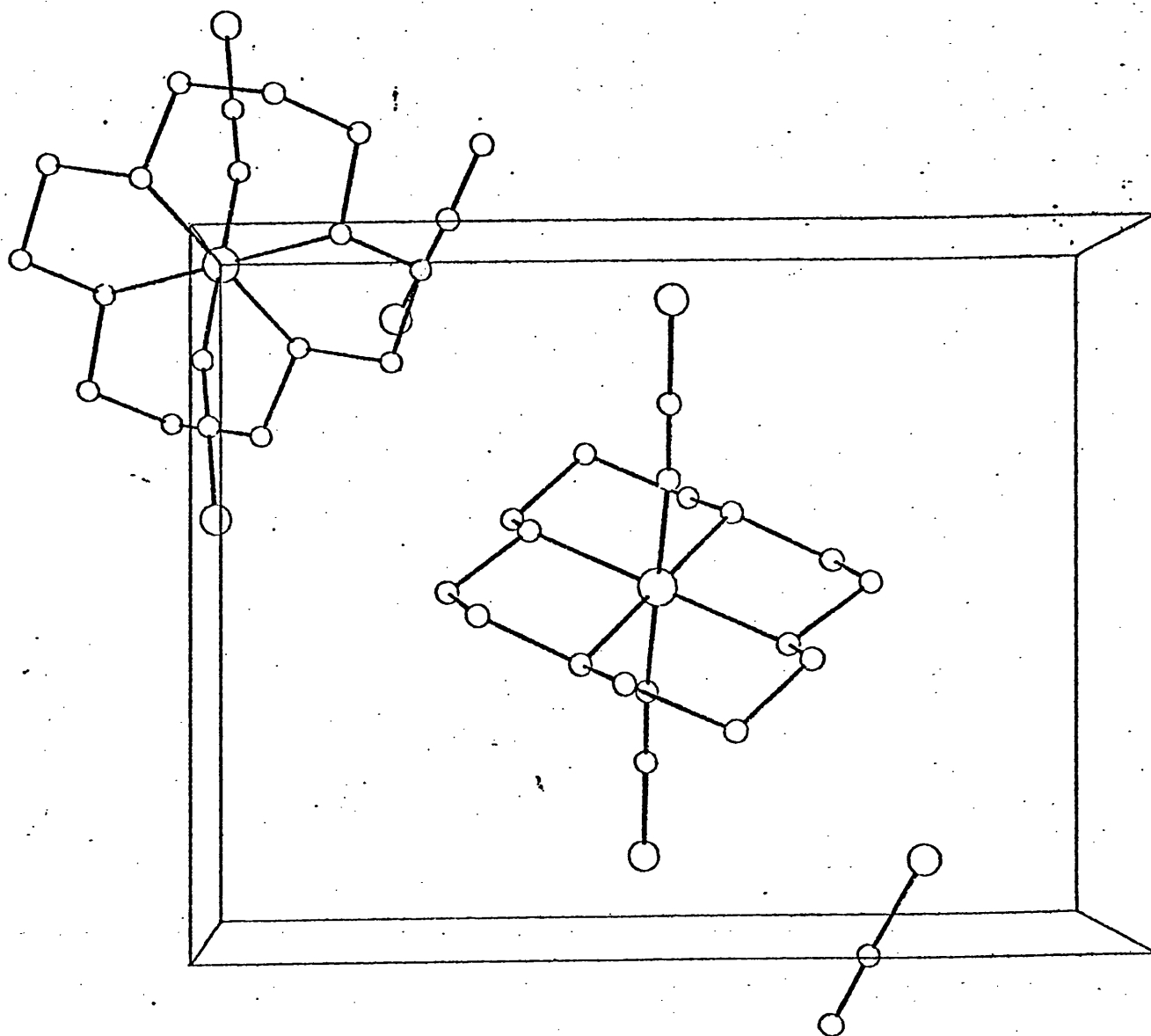


Figure 7.03(b) View of unit cell along A-axis.

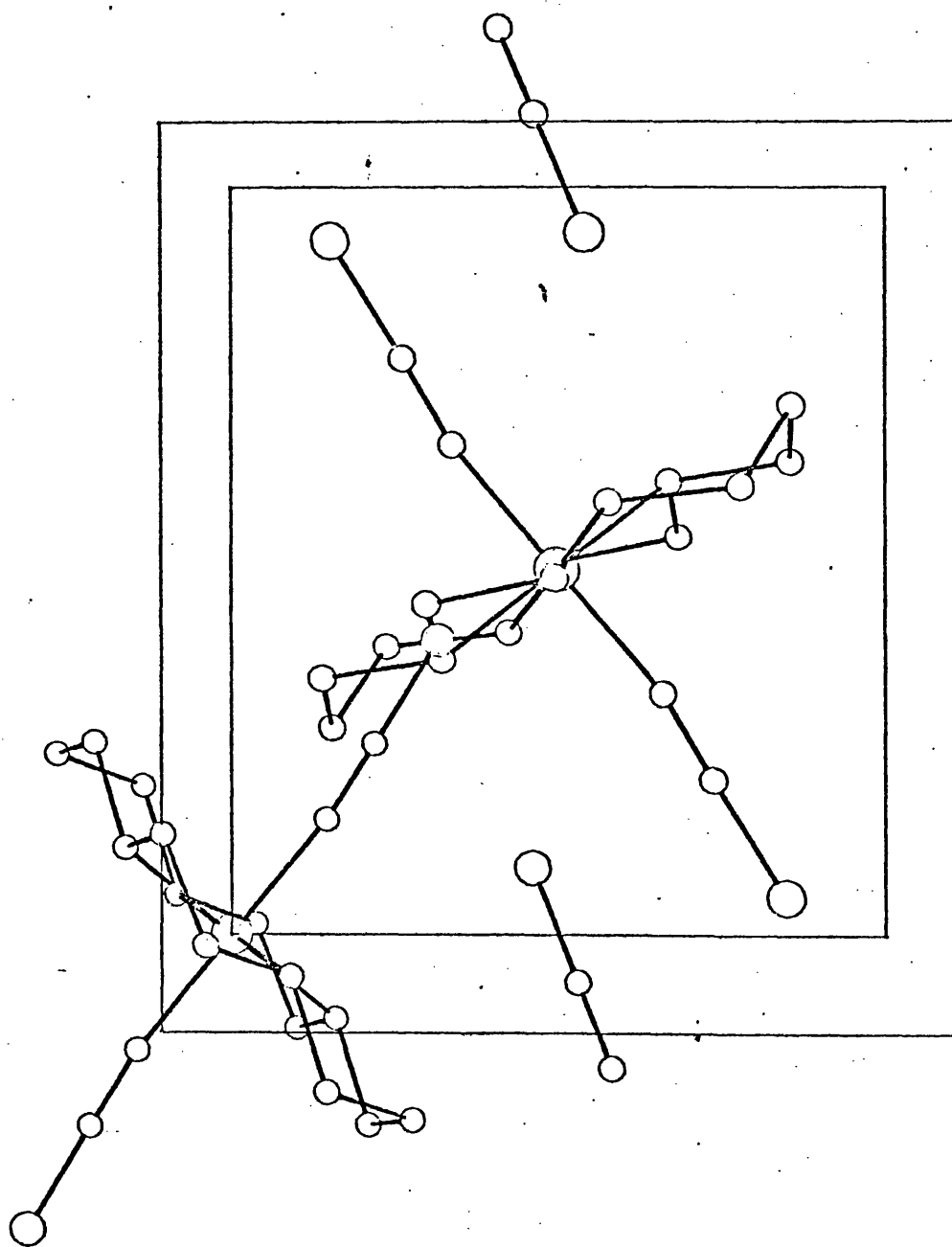
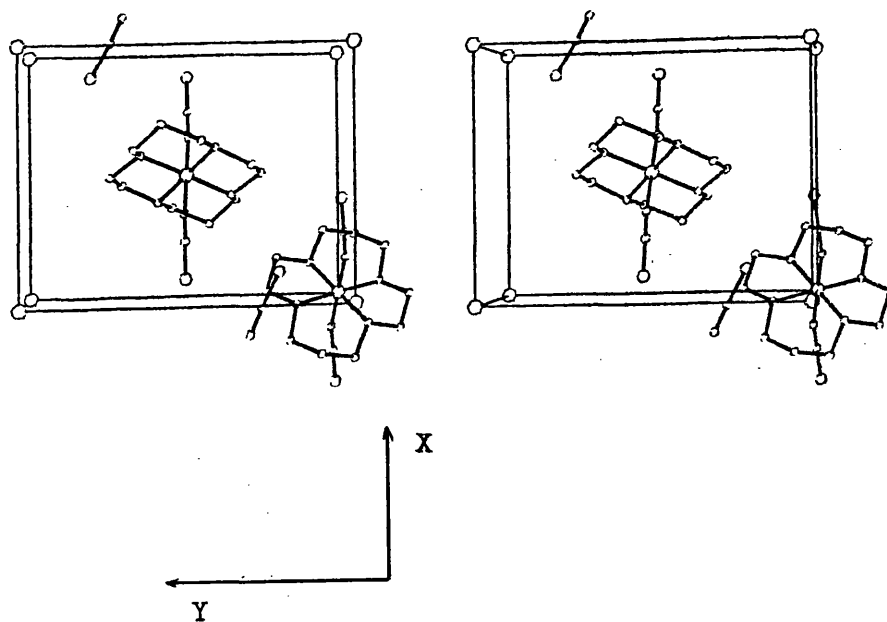


Figure 7.04 Stereoscopic view of the unit cell of trans-[Co(cyclam)(NCS)₂]SCN.



must obviously be the most efficient packing of the molecules in the crystal. Such packing may also be partly responsible for the slightly 'bent' nature of the axial thiocyanate ligands. In Figures 7.03 (a) and (b), the seven other cations which would be centred at the corners of the unit cell, together with their corresponding thiocyanate anions have been omitted for clarity. Figure 7.04 is a stereoscopic view of the unit cell shown in Figure 7.03(a), when seen through a stereo-viewer, and gives a 3-dimensional picture of the unit cell.

Other crystallographic studies of transition metal complexes containing the cyclam ligand are limited to that of the dichloro(cyclam)-nickel(II) complex [7.01]. Here the conformation of the cyclam ligand is the same as in this study. The chlorides are also sterically repelled from hydrogens attached to carbons towards those attached to nitrogen, the Cl-Co-N angles being 94.8° and 91.8° , (the two nitrogens being two adjacent 1,3-diaminopropane residue ones).

(ii) POWDER DIFFRACTION STUDIES

The X-ray powder diffraction pattern of the $\text{MgReCl}_6 \cdot 6\text{H}_2\text{O}$ salt was studied to test the criterion of size similarity, which is one of the requirements necessary in order to make an assumption that $\delta_{\text{m}\mu}^\oplus$ ($[\text{Mg}(\text{OH}_2)_6]^{2+}$) = $\delta_{\text{m}\mu}^\oplus$ (ReCl_6^{2-}). The criteria for such a situation are that (a) the sizes and the magnitudes of the charges of the ions are equal and (b) the hydrophilic natures of the peripheries of the ions are similar. A comparable assumption that $\delta_{\text{m}\mu}^\oplus$ (BPh_4^-) = $\delta_{\text{m}\mu}^\oplus$ (AsPh_4^+) has been made [7.11] (see chapter 1) where all of the above conditions hold.

From X-ray powder photographs, the relative sizes of the $[\text{Mg}(\text{OH}_2)_6]^{2+}$ and ReCl_6^{2-} ions can be determined, on condition that the crystal class is a simple one. The magnesium salt of the ReCl_6^{2-} anion was selected on the basis of certain known properties of such a compound. For example, compounds of the type MgMX_6 (where $\text{M} = \text{Pt}, \text{Pd}, \text{Sn}, \text{X} = \text{Cl}$) occur as hexahydrates, $\text{MgMX}_6 \cdot 6\text{H}_2\text{O}$ [7.12]. This number of water molecules is also confirmed for magnesium hexachlororhenate from the analysis results (Table 7.01). The radius of the ReCl_6^{2-} anion has been estimated as ca. 4.2 \AA from summations of the ionic radii of the constituent atoms, also the radii of cations $\text{M}^{2+} - \text{O} \begin{smallmatrix} \text{H} \\ \diagup \diagdown \end{smallmatrix}$ for transition metal hydrates have been estimated as ca. 4 \AA [7.13]. Hence magnesium hexachlororhenate was expected to crystallise in a cubic system, from the powder photograph of which the unit cell dimensions could be calculated, and hence the Mg—Re distance.

The measured values of 2θ are listed in Table 7.04 from the X-ray powder photograph of $\text{MgReCl}_6 \cdot 6\text{H}_2\text{O}$. An attempt at indexing this powder pattern was made by firstly assuming the system to be cubic - the simplest system. The characteristic of such a system is that the values of $\sin^2\theta$ have a common factor. This may be seen by considering the following:-

For a cubic system, the unit cell has dimensions:-

$$a = b = c; \quad \alpha = \beta = \gamma = 90^\circ.$$

And from the Bragg equation

$$n \lambda = 2 d \sin \theta \quad (7.11)$$

and the relationship

$$d = \frac{a}{\sqrt{h^2 + k^2 + l^2}} \quad (7.12)$$

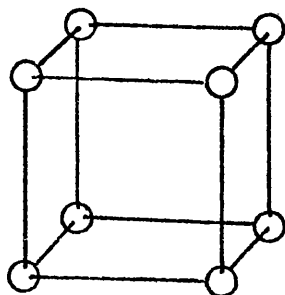
for a cubic system, we find

$$\sin^2 \theta = \frac{\lambda^2}{4a^2} (h^2 + k^2 + l^2) \quad (7.13)$$

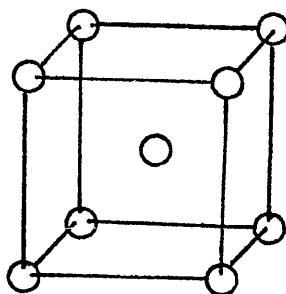
Since h , k and l are integers, then the sum of their squares must also be an integer. The term $\lambda^2/4a^2$ in equation (7.13) is a constant, hence to assign suitable indices to measured 2θ values, the $\sin^2\theta$ values may be divided by successive permissible integers. If the result is constant, the appropriate indices may be assigned to these lines.

Table 7.04 also contains $\sin^2\theta$ values, together with assigned indices and consequent values of $\lambda^2/4a^2$. The $\sin^2\theta$ values were refined by an iterative least-squares method, using a standard FORTRAN IV lattice parameter refinement program. A mean value of $a = 9.87 \pm 0.002 \text{ \AA}$ was found, with an R factor of 0.000014, indicating the compound to indeed crystallise in a cubic system.

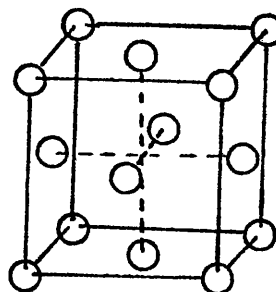
There are however several types of cubic lattice which are illustrated in Diagram 7.04. For a primitive (P) cubic unit cell, all h , k and l values are allowed. However, this structure is not possible for an ionic compound, since there would only be one ion per unit cell!



(a) Primitive (P)
Cell.



(b) Body-centred (I)
Cell.



(c) Face-centred (F)
Cell.

Diagram 7.04

TABLE 7.04 Various parameters measured from the X-ray powder photograph of magnesium hexachlororhenate hexahydrate.

| h | k | l | 2θ | $\sin^2 \theta$ | $\lambda^2 / 4a^2$ |
|---|---|---|-----------|-----------------|--------------------|
| 2 | 0 | 0 | 18.25 | 0.02515 | 0.006287 |
| 2 | 2 | 0 | 25.825 | 0.04994 | 0.006242 |
| 3 | 1 | 1 | 30.225 | 0.06797 | 0.006179 |
| 2 | 2 | 2 | 31.625 | 0.07425 | 0.006188 |
| 4 | 0 | 0 | 36.675 | 0.09898 | 0.006186 |
| 3 | 3 | 1 | 40.050 | 0.1173 | 0.006171 |
| 4 | 2 | 0 | 41.175 | 0.1236 | 0.006182 |
| 4 | 2 | 2 | 45.225 | 0.1478 | 0.006159 |
| 5 | 1 | 1 | 48.050 | 0.1658 | 0.006139 |
| 4 | 4 | 0 | 52.550 | 0.1960 | 0.006124 |
| 5 | 3 | 1 | 55.175 | 0.2145 | 0.006128 |
| 6 | 0 | 0 | 55.975 | 0.2202 | 0.006117 |
| 6 | 2 | 0 | 59.175 | 0.2438 | 0.006095 |
| 5 | 3 | 3 | 61.575 | 0.2620 | 0.006093 |
| 4 | 4 | 4 | 65.400 | 0.2919 | 0.006072 |
| 7 | 1 | 1 | 67.625 | 0.3097 | 0.006080 |
| 6 | 4 | 0 | 68.375 | 0.3157 | 0.006068 |
| 6 | 4 | 2 | 71.300 | 0.3397 | 0.006099 |
| 7 | 3 | 1 | 73.500 | 0.3580 | 0.006114 |
| 8 | 0 | 0 | 77.450 | 0.3914 | 0.006067 |
| 7 | 3 | 3 | 79.775 | 0.4112 | 0.006138 |

For a body-centred (I) cubic system (CsCl structure), only reflections for which the integer $(h+k+l)$ is even are allowed. For a face-centred (F) cubic system (NaCl structure), the restriction that the indices h , k and l must be all odd or all even occurs. From Table 7.04 we deduce that the system in the case of $\text{MgReCl}_6 \cdot 6\text{H}_2\text{O}$ must be body-centred cubic, containing 2 ions (= 1 molecule) per unit cell. Assuming that the radii of the constituent ions are equal, which is suggested by the high symmetry of the crystal lattice, we can calculate from the knowledge that the unit cell dimension, $a = 9.87 \text{ \AA}$ that the mean ionic radius is 4.27 \AA . This compares with a value of 4.2 \AA for the ReCl_6^{2-} anion [7.14].

The X-ray powder photograph of the $[\text{Fe}(\text{phen})_3]^{2+} \text{ReCl}_6^{2-}$ salt was measured. This was found to be exceedingly complicated, indicating a most inaffable crystal system, which could not be indexed without excessive labour. The indexing was not pursued, since the very complexity of the pattern indicated that the cation of the salt could not be behaving as a spherical ion. It is very possible that the ReCl_6^{2-} anions may to some extent be partially fitting in between the phen ligands of the cation. It is known [7.15] that it is possible for a peroxodisulphate ion to fit completely between two such ligands of the cation. The effective radius $[\text{Fe}(\text{phen})_3]^{2+}$ has been estimated [7.16] to be ca. 7 \AA , which is very different from the radius of the ReCl_6^{2-} anion. This fact alone is sufficient to invalidate the assumption that the free energies of transfer of these ions might be similar, regardless of the very different solvation characteristics of them (see chapter 4).

It may be concluded that the tool of X-ray diffraction is indeed a most powerful one in the elucidation of structural properties of solid state compounds. Although the subjects of study may possess different

characteristics in solution, the absolute results obtained from these solid state studies provides a firm basis for any discussion of the nature and properties of the compounds in question. This fact is fully supported by the very positive results obtained in this chapter.

CHAPTER 8

Solvatochromic Behaviour of a Series of Inorganic
Complexes.

8.1 INTRODUCTION

Much of the kinetic studies undertaken so far in this thesis has involved the question of solvation effects on the reactivities of the complexes studied. A most interesting phenomenon concerning the electronic spectra of certain inorganic complexes is the way in which the energies of the charge-transfer bonds, i.e. the wavelengths of maximum absorption vary with solvent composition [8.01]. This property is often referred to as Solvatochromism.

Solvatochromism was first described for an organic compound, in fact tetramethyldiaminofuchsonone [8.02], in 1909. Later, the topic was extended by Kiprianov [8.03] and independently by Brooker [8.04]. Brooker suggested that the variations in the electronic spectra should be used as an empirical measure of solvent sensitivity. Subsequently, several solvent-scales have been innovated, using compounds which have a very strong variation of wavelength with solvent as bases for the scales. The most noteworthy compound which was chosen was the pyridinium N-phenolbetaine shown in Diagram 8.01. The scale derived from this

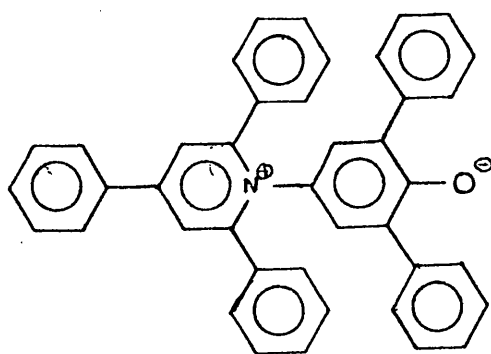


Diagram 8.01

betaine is best known as Reichardt's E_T scale [8.05]. This scale is perhaps the most extensive, both for non-aqueous solvents and for binary

aqueous mixtures [8.06]. Moreover, the solvent sensitivity of the betaine used for this scale is one of the highest known, being + 350 $\text{cm}^{-1} \text{ kcal}^{-1} \text{ mol.}$ It is considerably greater than that of the most solvatochromic inorganic complex described in this chapter. The magnitude of the solvent sensitivity of this betaine has been explained by the zwitterionic nature of the shifts in wavelength. The molecule possesses two extreme resonance forms, as indicated in Diagram 8.01. As the polarity of the solvent increases, there will be a consequent change in the electron distribution towards the polar resonance form in the ground state. Meanwhile, the structure of the excited state, by the Frank-Condon principle, will be only slightly affected. Hence the change in the wavelength of maximum absorption will be directly related to the change in energy of the ground state, produced by the variation in the solvent polarity.

Transition metal complexes of 2,2'-bipyridyl, 1,10-phenanthroline and related ligands exhibit intense charge-transfer absorptions in the visible spectrum. For tris-complexes of the type $[\text{Fe}(\text{LL})_3]^{2+}$, frequencies of maximum absorption and extinction coefficients have been found to vary extremely little with solvent composition [8.07]. However, for complexes containing both one or two of these ligands and four or two cyanide or carbonyl groups the frequencies of maximum absorption of the charge-transfer bands have been found to vary considerably with the nature of the solvent. Such behaviour has been described for complexes of the type $\text{Fe}(\text{bipy})_2(\text{CN})_2$ [8.08]. Subsequently the dependence of charge-transfer frequencies on solvent nature has been reported for a number of analogous compounds. These include a range of complexes $\text{Fe}(\text{LL})_2(\text{CN})_2$, where LL = bipy, (substituted) phen, or bidentate Schiff's base [8.09,10], and organometallic derivatives $\text{M}(\text{CO})_4(\text{LL})$, where M = Cr, Mo or W and LL =

bipy, phen [8.11,12], diazabutadiene [8.13] or substituted derivatives.

In this work, the range of inorganic complexes which exhibit solvatochromism has been extended. Several complexes of the type $\text{Fe}(\text{LL})_2(\text{CN})_2$ have been studied, and compared with previously studied analogues, mentioned above. The solvatochromic properties of the $[\text{Fe}(\text{CN})_5(\text{mpz})]^{2-}$ anion has been examined, and compared with Reichardt's betaine (Diagram 8.01), in view of the similarity in structure (see section 8.3). The methylpyrazinium complex anion has also been compared with its 4-cyanopyridine analogue. All complexes mentioned in the previous paragraph are said to have cis-geometry (see below). Although the trans-isomers of those complexes cannot be prepared,[†] a low spin iron(II) complex containing trans-cyanide ligands can be produced as the $[\text{Fe}(\text{phthalocyanine})(\text{CN})_2]^{2-}$ anion [8.14]. The visible spectra of this anion in several solvents have been studied. Unfortunately the di-isothiocyanato analogue is inaccessible (see section 8.2(i)) and so a direct cyanide-isothiocyanate comparison is not possible. However, the trans- $[\text{Co}(\text{cyclam})(\text{NCS})_2]^+$ cation has been prepared (see chapter 7), and its solvatochromic behaviour has been measured. Finally the variation in the frequencies of maximum absorption with solvent has been measured for the product of the reaction of cyanide ion with the $[\text{Fe}(\text{HXSb})]^{2+}$ cation.[‡] This variation has been correlated with similar variations for other mixed cyano-polydentate ligand complexes of iron(II),

[†] [In the trans isomers, unfavourable steric interactions, e.g. for $\text{Fe}(\text{phen})_2(\text{CN})_2$ the 2- & 9-hydrogens would interact. Hence the more stable cis isomer is preferred.]

[‡] [HXSb = Hexadentate Schiff's base derived from 1 molecule of triethylenetetrammine and 2 molecules of quinolyl-2-aldehyde.]

notably the $[\text{Fe}(\text{terpy})(\text{CN})_3]^-$ anion [8.15],[†] $\text{Fe}(\text{bipy})_2(\text{CN})_2$ [8.08] and $[\text{Fe}(\text{bipy})(\text{CN})_4]^{2-}$ [8.09]. From these correlations, an attempt has been made to deduce the structural features of the cyano-hexadentate Schiff's base complex of iron(II).

8.2 EXPERIMENTAL

(i) Preparations

Many of the compounds which have been studied in this chapter have been used in other chapters of this thesis. The details of their preparations have been outlined in those relevant chapters, and will not be repeated here. A summary of the locations of these preparative methods is given below.

(a) Complexes of the type $[\text{Fe}(\text{CN})_5\text{L}]^{n-}$, where L = the N-methyl-pyrazinium cation, mpz^+ , or 4-cyanopyridine, 4-CNpy, have been prepared as described in chapter 2.

(b) All complexes of iron(II) containing both cyanide ligands and polydentate nitrogen donor ligands[‡] have been fully discussed in chapter 9.

(c) The thiocyanate salt of the trans- $[\text{Co}(\text{cyclam})(\text{NCS})_2]^+$ cation has been described in chapter 7, the preparative method being identical to

[†] [terpy = 2,2',6',2''-terpyridyl.]

[‡] [i.e. Schiff's base ligands of bi-, quadri- and hexadenticity. The bidentate ligand 5-nitro 1,10-phenanthroline is also included.]

the literature method of Bosnich et al. [8.16].

(d) An aqueous solution of the potassium salt of the trans-biscyano-(phthalocyanine)iron(II) anion, $[\text{Fe}(\text{pc})(\text{CN})_2]^{2-}$, was prepared as suggested by Lever [8.14]. To a strong aqueous solution of AnalaR potassium cyanide (B.D.H.) was added a quantity of iron(II) phthalocyanine (Eastman). The mixture was stirred for one hour, and the undissolved portion of the iron phthalocyanine filtered. The blue solution remaining was used directly for the solvatochromic studies. The $[\text{Fe}(\text{pc})(\text{CN})_2]^{2-}$ anion could not be isolated in the solid state due to its instability [8.14] in the absence of free cyanide ions.

Attempts were made to prepare the azido, isothiocyanato and nitrito analogues of the $[\text{Fe}(\text{pc})(\text{CN})_2]^{2-}$ anion, by a similar preparative method. These attempts were unsuccessful in all cases, even after refluxing the solutions for long periods.

Solutions of $\text{K}_2[\text{Fe}(\text{pc})(\text{CN})_2]$ were prepared in the solvents methanol, ethanol, t-butyl alcohol and dimethyl sulphoxide by stirring together a quantity of $\text{Fe}(\text{pc})$ and an excess of potassium cyanide in the appropriate solvent. Undissolved materials were filtered after one hour and the resulting solutions of the complex were used for the solvatochromic study.

(e) A sample of bis-isothiocyanato-bis(1,10-phenanthroline)iron(II), $\text{Fe}(\text{phen})_2(\text{NCS})_2$ was prepared from aqueous solution according to Schilt [8.17]. Unfortunately, this compound was found to be too sparingly soluble in all solvents tried to facilitate measurement of its visible spectrum. After standing in water, in undried ethylene glycol and in undried methanol, the purple solid was found to produce a red solution which was identical to the spectrum of the $[\text{Fe}(\text{phen})_3]^{2+}$ cation, indicating disproportionation of the complex. Consequently no solvato-

chromic data were collected on this compound.

(ii) Solvents and Other Reagents

All solvents used in this study were of the best commercially available quality. Water, methanol, 1,4-dioxan and tetrahydrofuran were purified as described in chapter 2. Other solvents were used without further purification.

(iii) Spectra

The electronic spectra of all of the compounds studied were measured on a Unicam SP8000A recording spectrophotometer, using 1cm path length silica cells. The calibration of the wavelength monitor was checked periodically with standard holmium and didymium glass filters. The wavelengths of maximum absorption of the spectra for the lowest energy charge-transfer bands were taken as the intersections of the spectra with the loci of the midpoints of horizontal sections through the absorption bands.

Correlations between frequencies of maximum absorption and E_T values were computed using a BASIC least-mean-squares program (Appendix 2, Program No. 3,) on a Cyber 72 or PDP11 computer when such correlations were satisfactorily linear. The slopes of such correlation lines are reported with standard deviations.

8.3 RESULTS AND DISCUSSION

The positions of charge-transfer absorption maxima can be correlated with some success with empirical solvent parameters [8.18], especially

Reichardt's spectroscopically based solvent E_T values [8.05]. Although information concerning the solvatochromic behaviour of charge-transfer bands is available for a variety of compounds, no systematic pattern has as yet emerged. In this chapter we are concerned with the effects of several variables, the nature of the metal, the nature of the hetero-aromatic ligand and the nature of other ligands present. The results are presented and compared in terms of the slopes of plots of maximum absorption frequencies (ν_{\max}), usually of the lowest energy charge-transfer band, against solvent E_T values. As the conventional E_T values have units of kcal mol^{-1} , these solvent sensitivity slopes have units of $\text{cm}^{-1} \text{kcal}^{-1} \text{mol}$; increasing solvent sensitivity corresponds to increasing numerical values of these slopes. For some complexes it is necessary to recognise that charge-transfer frequencies in hydroxylic and in non-hydroxylic solvents give two separate correlation lines when plotted against respective solvent E_T values.

Sometimes comparisons between compounds are made directly (i.e. $\nu_{\max}(\text{I})$ vs. $\nu_{\max}(\text{II})$), rather than indirectly via E_T plots. This approach is used particularly for closely related compounds, where small solvent differences in solvent sensitivities become more readily apparent in direct comparison. It is impossible to undertake a fully systematic analysis of the effects of possible variables mentioned above, since so often a change in one variable is unavoidably accompanied by a change in one or more other variables. Hence the findings of this work have been arranged in sections according to the class of compound, with the various variables being noted as and when relevant.

(i) Complexes of the type $[\text{Fe}(\text{CN})_5\text{L}]^{n-}$

During the kinetic studies on the $[\text{Fe}(\text{CN})_5\text{L}]^{n-}$ type anions in chapter 2, a structural resemblance between the $[\text{Fe}(\text{CN})_5(\text{mpz})]^{2-}$ anion

(Diagram 8.02) and the betaine (Diagram 8.01) which is the basis of Reichardt's E_T scale, ^{was noticed.} That is, a positively charged nitrogen in the

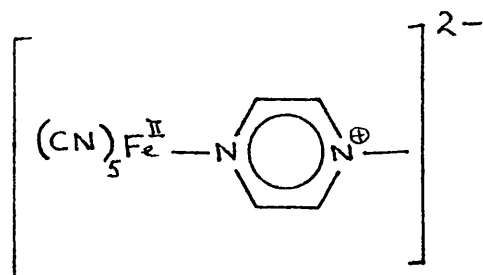


Diagram 8.02

pyrazine heterocycle is linked through a conjugated system to a negatively charged moiety - the pentacyanoferrate(II) group, $[\text{Fe}(\text{CN})_5]^{3-}$. Hence it was expected that this inorganic complex may behave in a similar manner to the organic paradigm, and might even serve as a basis for a solvent-scale for inorganic complexes. Unfortunately, the $[\text{Fe}(\text{CN})_5(\text{mpz})]^{3-}$ complex being charged, its sodium salt was found to be insoluble in pure non-aqueous solvents. However, the tetraphenylarsonium salt was found to be slightly soluble in a few non-aqueous solvents. Table 8.01 lists the observed frequencies of maximum absorption of this compound in several solvents, from which it may be seen that there is no satisfactory correlation between these frequencies and the E_T values for hydroxylic solvents.

However, from the results for the several non-hydroxylic solvents used, the slope of the ν_{max}/E_T plot is roughly $+ 370 \text{ cm}^{-1} \text{ kcal mol}^{-1}$. This value is very similar to that for the betaine (Diagram 8.01) used by Reichardt, underlining the similarities in the respective electronic and molecular structures of the two quaternary-nitrogen-containing

TABLE 8.01 Frequencies of maximum absorption, ν_{\max} , of the lowest energy charge-transfer band for the $[\text{Fe}(\text{CN})_5(\text{mpz})]^{2-}$ anion in water and in several pure non-aqueous solvents, together with the corresponding solvent E_T value.

| Solvent | E_T / kcal mol ⁻¹ | ν_{\max} / cm ⁻¹ |
|---------------------|--------------------------------|---------------------------------|
| Water | 63.1 | 15270 |
| Ethylene glycol | 56.3 | 14350 |
| Methanol | 55.5 | 13900 (13950) ^a |
| Ethanol | 51.9 | 13950 (14000) ^a |
| i-Propanol | 48.6 | 14660 (14680) ^a |
| Acetonitrile | 46.0 | 14800 |
| Dimethyl sulphoxide | 45.0 | 14000 |
| t-Butyl alcohol | 44.0 | 14370 |
| Acetone | 42.1 | 14500 |
| Tetrahydrofuran | 37.4 | 13940 |
| 1,4-Dioxan | 36.0 | 13900 |

^a Values in parentheses were obtained by extrapolation of ν_{\max} versus E_T plots of spectra in binary aqueous mixtures, taken from Table 8.02.

TABLE 8.02 Frequencies of maximum absorption, ν_{\max} , of the lowest energy charge-transfer bands for the $[\text{Fe}(\text{CN})_5(\text{mpz})]^{2-}$ and the $[\text{Fe}(\text{CN})_5(4\text{-CNpy})]^{3-}$ anions in a range of binary aqueous mixtures.

| Solvent Mixture | $E_T/\text{kcal mol}^{-1}$ | complex anion | |
|-----------------|----------------------------|--|---|
| | | $[\text{Fe}(\text{CN})_5(\text{mpz})]^{2-}$ $\nu_{\max}/\text{cm}^{-1}$ | $[\text{Fe}(\text{CN})_5(4\text{-CNpy})]^{3-}$ $\nu_{\max}/\text{cm}^{-1}$ |
| 10 | 62.2 | 15130 | |
| 20 | 61.0 | 14990 | 20490 |
| 30 | 60.0 | 14810 | |
| 40 | 59.2 | 14710 | 20080 |
| 50 | 58.3 | 14600 | |
| 60 | 57.8 | 14470 | 19610 |
| 70 | 57.2 | 14410 | |
| 80 | 56.6 | 14310 | 19190 |
| 10 | 61.7 | 15110 | |
| 30 | 58.0 | 14810 | 20160 |
| 40 | 56.6 | 14680 | 19920 |
| 50 | 55.6 | 14600 | |
| 60 | 55.0 | 14490 | 19610 |
| 70 | 54.2 | 14430 | |
| 80 | | | 19190 |
| 10 | 61.3 | 15130 | |
| 20 | 59.2 | 14990 | 20490 |
| 30 | 56.3 | 14860 | |
| 40 | 54.7 | 14810 | 20080 |
| 50 | 53.7 | 14770 | |
| 60 | 53.0 | 14750 | 19800 |
| 80 | 51.6 | 14710 | 19650 |
| 10 | 61.4 | 15060 | |
| 20 | 59.8 | 14860 | 20240 |
| 30 | 58.1 | 14750 | |
| 40 | 56.6 | 14560 | 19690 |
| 50 | 55.4 | 14490 | |
| 60 | 54.5 | 14370 | 19230 |
| 70 | 53.3 | 14330 | |
| 80 | 52.2 | 14100 | 18900 |
| 10 | 61.1 | 15060 | |
| 20 | 58.6 | 14930 | |
| 30 | 57.2 | 14710 | |
| 40 | 55.6 | 14580 | |
| 50 | 53.6 | 14530 | |
| 70 | 50.9 | 14330 | |
| 80 | 49.0 | 14270 | |

^a In aqueous solution ($E_T = 63.1 \text{ kcal mol}^{-1}$), $\nu_{\max} = 15270 \text{ cm}^{-1}$ and 20920 cm^{-1} for the mpz⁺ and the 4-CNpy complexes respectively.

Figure 8.01 Correlation between the frequencies of maximum absorption, ν_{\max} , with solvent E_T values in a range of binary aqueous mixtures, for the $[\text{Fe}(\text{CN})_5(\text{mpz})]^{2-}$ anion, at 298.2 K. Cosolvents used are methanol(\square), ethanol(Δ), i-propanol(\bullet), acetone($+$) and 1,4-dioxan(\circ).

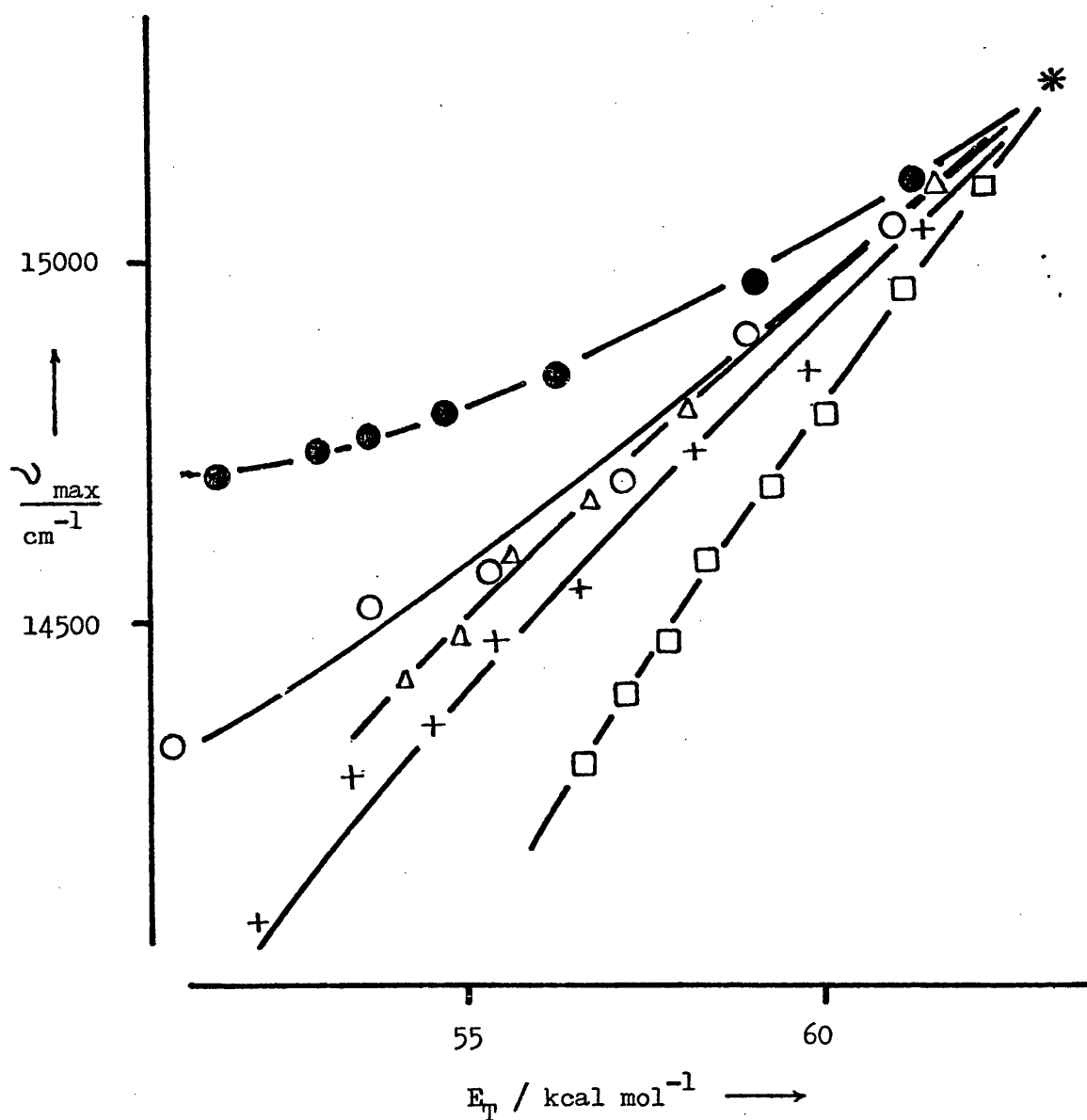
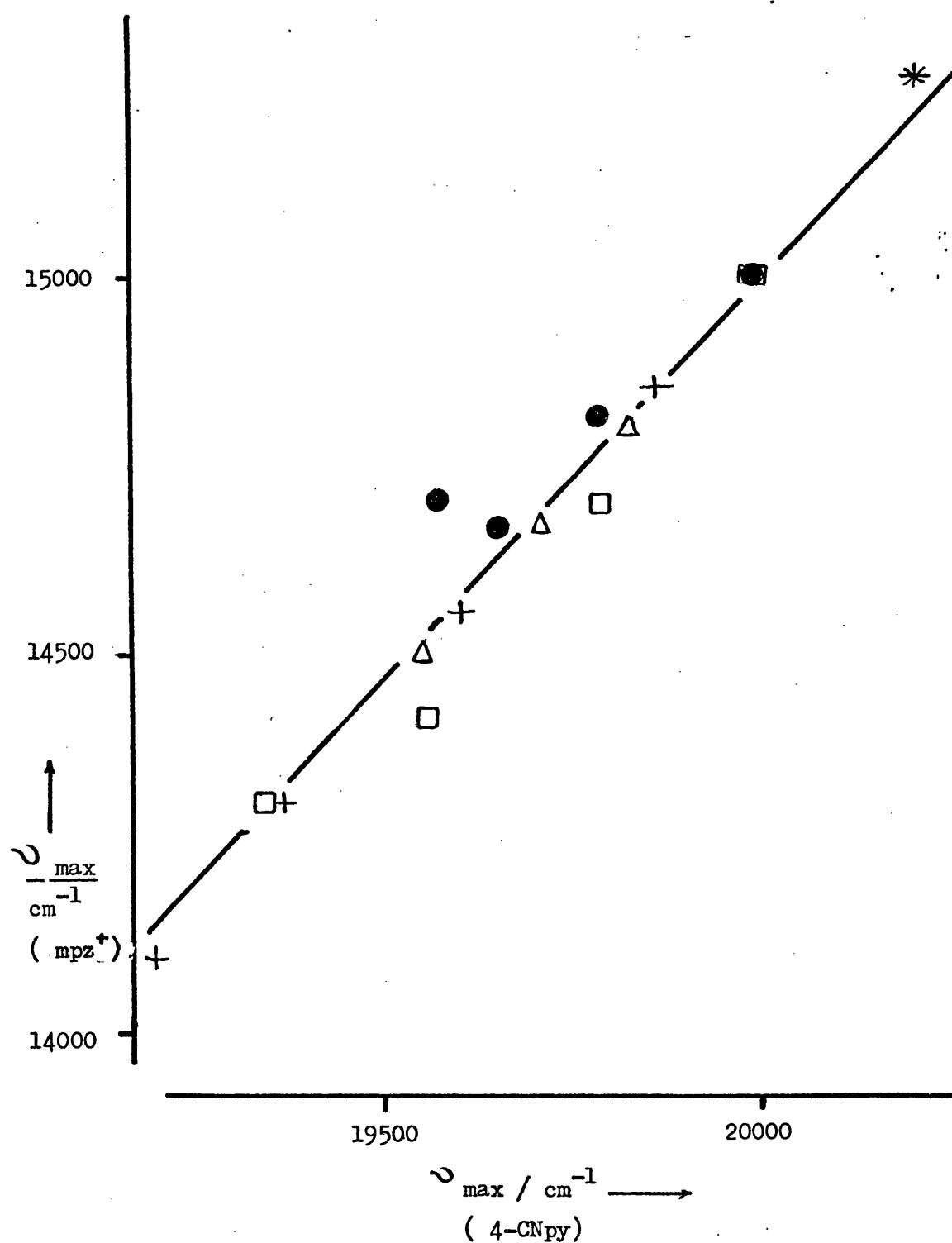


Figure 8.02 Correlation between the frequencies of maximum absorption, ν_{\max} , for the $[\text{Fe}(\text{CN})_5(\text{mpz})]^{2-}$ (ordinate) and the $[\text{Fe}(\text{CN})_5(4\text{-CNpy})]^{3-}$ (abscissa) anions, at 298.2 K. Symbols as in Figure 8.01.



compounds. Reservations must be made however on the results for the inorganic complex, due to the very few solvents used, and the consequent crudeness of the estimated solvent sensitivity.

The variation in the frequency of maximum absorption with solvent composition for the N-methylpyrazinium complex anion was also measured in a wide range of binary aqueous mixtures, for which E_T values are available [8.06]. The results of this variation are given in Table 8.02, together with similar observations for the 4-cyanopyridine analogue. For the mpz^+ case, a plot of ν_{max} against E_T , which is shown in Figure 8.01, displays a family of lines for the different solvent mixtures. In spite of the apparently good correlation between ν_{max} and E_T in these mixed solvents, there appears to be no linear dependence of ν_{max} for these pure hydroxylic solvents on E_T . The values of ν_{max} for these solvents were obtained both by extrapolation of the ν_{max}/E_T correlation lines for binary aqueous mixtures and by dissolution of the $[\text{Ph}_4\text{As}]_2[\text{Fe}(\text{CN})_5(\text{mpz})]$ salt in the pure solvents. The values obtained by both methods were found to be consistent (see Table 8.01).

The $[\text{Fe}(\text{CN})_5(4\text{-CNpy})]^{3-}$ anion was also found to be solvatochromic. The observed values of ν_{max} for this complex anion in a range of binary aqueous mixtures were plotted against corresponding values for the mpz^+ complex. This plot, which is illustrated in Figure 8.02, was found to have a slope of 1.00 ± 0.03 , using 19 points on the graph. Thus in spite of the difference in overall charge (3- for the 4-CNpy case; 2- for the mpz^+ one), and more importantly the differences in intramolecular charge separation (i.e. the dipolar nature of the mpz^+ complex as opposed to the simple negatively charged ion in the 4-CNpy one), the solvent sensitivities of these two species are identical. It must be noted that the effects of the 4-CN substituent will enhance the π -

acceptor ability of the pyridine ligand in the same way that the positive charge does in the case of the mpz^+ ligand. Hence the solvatochromic behaviours of the two complexes will be expected to be similar, but it still seems surprising that they should be equivalent.

The greater metal to ligand π back-bonding in $[\text{Fe}^{\text{II}}(\text{CN})_5\text{L}]^{n-}$ compounds than in $[\text{Co}^{\text{III}}(\text{CN})_5\text{L}]^{n-}$ ones [8.19] suggests the latter may be less solvatochromic. In fact there are no data for the latter type of complex, although there are some data for some cobalt(III) compounds of a different nature (see below, section 8.3(iv)). However, there is a little information concerning the related chromium(III) complexes, viz. $[\text{Cr}(\text{CN})_5(\text{NCS})]^{3-}$, and related mixed cyano-isothiocyanato chromium(III) complexes. These last complexes turn out to be only slightly solvatochromic, the $[\text{Cr}(\text{CN})_5(\text{NCS})]^{3-}$ anion having a solvent sensitivity of $-60 \text{ cm}^{-1} \text{ kcal}^{-1} \text{ mol}$, and the $[\text{Cr}(\text{CN})(\text{NCS})_5]^{3-}$ anion having one of $-18 \text{ cm}^{-1} \text{ kcal}^{-1} \text{ mol}$ [8.20]. Interestingly, these $\nu_{\text{max}}/E_{\text{T}}$ graphs have a negative slope. This feature is reminiscent of iron(III) compounds, e.g. the $[\text{Fe}(\text{phen})_2(\text{CN})_2]^+$ cation, which has a sensitivity of $-83 \text{ cm}^{-1} \text{ kcal}^{-1} \text{ mol}$. [8.09]. This sign reversal is probably due to reversal of the direction of the π charge-transfer, which is in the direction metal \rightarrow ligand for iron(II) compounds, but is ligand \rightarrow metal for iron(III) and chromium(III) ones [8.21]. It may also be seen that the more NCS ligands (and less CN ones) that are present, the less solvatochromic is the complex. This is as expected from the differences in the π -acceptor abilities of these two types of ligand.

(ii) Complexes of the type $\text{Fe}(\text{LL})_2(\text{CN})_2$ (where LL is a bidentate N-donor ligand).

(a) LL = 5-Nitro 1,10-phenanthroline.

The solvatochromic behaviour of a compound which was assigned the formula $\text{Fe}(\text{5-NO}_2\text{phen})_2(\text{CN})_2$ has been previously reported [8.09]. Attempts to prepare this compound by the usual method for compounds of the type $\text{Fe}(\text{LL})_2(\text{CN})_2$ (see chapter 9) produced a sparingly soluble dark red material, identical with the afore-mentioned [8.09] compound. However, this material, which is fully discussed in chapter 9, is in fact an intermediate in the reaction of cyanide ion with the $[\text{Fe}(\text{5-NO}_2\text{phen})_3]^{2+}$ cation, having a formula $[\text{Fe}(\text{5-NO}_2\text{phen.CN})_2(\text{5-NO}_2\text{phen})]$ or $[\text{Fe}(\text{5-NO}_2\text{phen.CN})(\text{5-NO}_2\text{phen})_2](\text{CN})$. This material has a wavelength of maximum absorption, λ_{max} of 515 nm in aqueous solution. This value of λ_{max} was found to remain constant when the compound was dissolved in non-aqueous solvents, i.e. the compound was not solvatochromic. In this way it resembles the $[\text{Fe}(\text{phen})_3]^{2+}$ cation, which similarly shows negligible solvatochromism [8.07]. This lack of solvent sensitivity of the charge-transfer band of the 5- NO_2phen complex suggests, in view of the properties of mixed cyano-phenanthroline iron(II) and other related complexes (see section 8.1), that there are no cyanide ligands co-ordinated directly to the iron(II) atom. This deduction is borne out by the lack of evidence for a CN-Fe bond in the infrared spectrum of the compound (see chapter 9), and the salt effects on solubility (chapter 4).

An authentic sample of $\text{Fe}(\text{5-NO}_2\text{phen})_2(\text{CN})_2$ has been prepared by a method devised in chapter 9. This blue/purple solid has $\lambda_{\text{max}} = 527$ nm in aqueous solution. The visible spectrum of this compound was measured in a range of non-aqueous solvents, the results of which are listed in Table 8.03. From these results we can see that the compound is markedly solvatochromic.

A plot of ν_{max} versus E_{T} for $\text{Fe}(\text{5-NO}_2\text{phen})_2(\text{CN})_2$ is shown in Figure 8.03. We see a linear correlation between ν_{max} and E_{T} , the slope

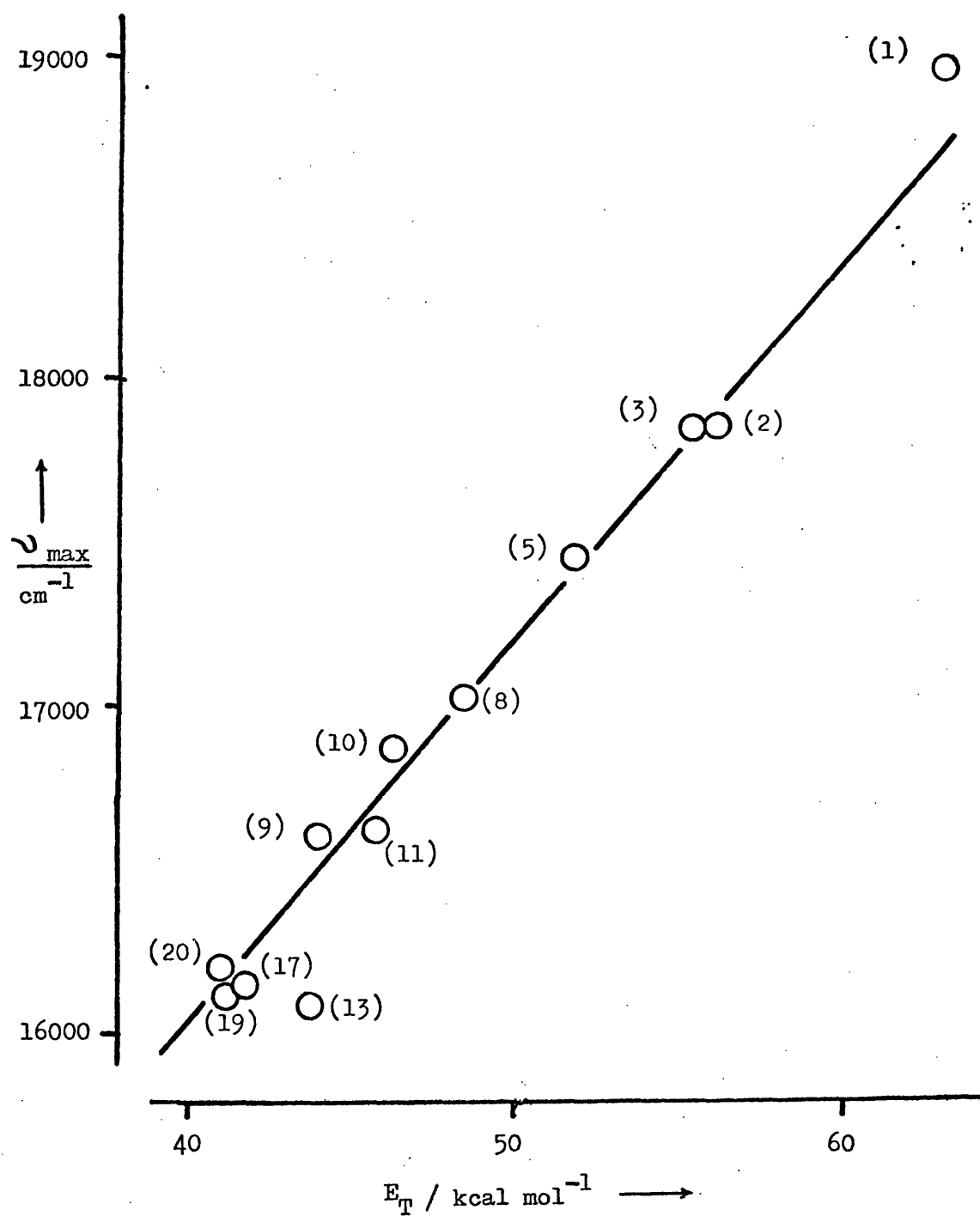
TABLE 8.03 Frequencies of maximum absorption, ν_{\max} , of compounds of the type $\text{Fe}(\text{LL})_2(\text{CN})_2$ in water and in a range of pure non-aqueous solvents.

| Solvent | E_T kcal mol ⁻¹ | LL ^a | | |
|-------------------------|---------------------------------|-----------------|--|--------|
| | | BDSB | 5-NO ₂ phen ν_{max}/cm^{-1} | QDSB/2 |
| <u>HYDROXYLIC</u> | | | | |
| 1. Water | 63.1 | 16640 | 18980 | 16890 |
| 2. Ethylene glycol | 56.3 | 16180 | 17860 | 16230 |
| 3. Methanol | 55.5 | 16130 | 17860 | |
| 4. Diethylene glycol | 53.8 | 15970 | | |
| 5. Ethanol | 51.9 | 15950 | 17480 | 15970 |
| 6. n-Propanol | 50.7 | 15800 | | 15900 |
| 7. n-Butanol | 50.2 | 15820 | | |
| 8. i-Propanol | 48.6 | 15720 | 17040 | 15770 |
| 9. t-Butyl alcohol | 43.9 | 15460 | 16610 | |
| <u>NON-HYDROXYLIC</u> | | | | |
| 10. Nitromethane | 46.3 | 15150 | 16890 | |
| 11. Acetonitrile | 46.0 | 15110 | 16640 | 15350 |
| 12. Dimethyl sulphoxide | 45.0 | 14900 | | 15200 |
| 13. Dimethylformamide | 43.8 | 14860 | 16100 | |
| 14. Nitroethane | 43.6 | 14970 | | |
| 15. Acetone | 42.2 | 14810 | | 15070 |
| 16. Nitrobenzene | 42.0 | 14790 | | |
| 17. 1,2-Dichloroethane | 41.9 | 15020 | 16160 | |
| 18. Methyl ethyl ketone | 41.3 | 15020 | | |
| 19. Acetophenone | 41.3 | 14990 | 16130 | |
| 20. Dichloromethane | 41.1 | 15060 | 16230 | |
| 21. Pyridine | 40.2 | 15020 | | |
| 22. Chloroform | 39.1 | 15240 | | |
| 23. 1,2-Dimethoxyethane | 38.2 | 15240 | | 15400 |
| 24. Ethyl acetate | 38.1 | 14730 | | |
| 25. Chlorobenzene | 37.5 | 14620 | | |
| 26. Tetrahydrofuran | 37.4 | 14370 | | 14680 |
| 27. 1,4-Dioxan | 36.0 | 15170 | | 14900 |
| 28. Piperidine | 35.5 | 14600 | | |
| 29. Diphenyl ether | 35.3 | 14640 | | |
| 30. Benzene | 34.5 | 14600 | | |

^a

See text for description of ligands.

Figure 8.03 Correlation of the frequency of maximum absorption, ν_{\max} , with the solvent E_T parameter for $\text{Fe}(\text{5-NO}_2\text{phen})_2(\text{CN})_2$ in various pure solvents. Numbering of solvents as in Table 8.03.



for the hydroxylic solvents being $+121 \pm 8 \text{ cm}^{-1} \text{ kcal}^{-1} \text{ mol}$. This value is very similar to, although statistically slightly smaller than the sensitivities of the analogues complexes of phen, 4,7-Me₂phen, 5-Cl phen, and 2,2'-bipy [8.01]. Such solvatochromic sensitivities for these and for related compounds are summarised in Table 8.07.

These relatively small differences in sensitivity between, on the one hand the complex containing the strongly electron-withdrawing nitro substituent ($+121 \text{ cm}^{-1} \text{ kcal}^{-1} \text{ mol}$) and on the other the strongly electron donating methyl substituents ($+131 \text{ cm}^{-1} \text{ kcal}^{-1} \text{ mol}$) is somewhat surprising. We can compare this trend with substituent effects on compounds of the type $\text{W}(\text{CO})_4(\text{X-phen})$ ([8.01] and Table 8.07). Here the effects of ligand variation are again very small, the ratios $\nu_{\text{max}}[\text{W}(\text{CO})_4(\text{X-phen})]/\nu_{\text{max}}[\text{W}(\text{CO})_4(\text{bipy})]$ being 0.94 ± 0.06 , 0.86 ± 0.05 and 0.96 ± 0.03 for $\text{X} = \text{phen}$, 4,7-Me₂phen and 5-Cl phen respectively. It seems odd that ligand substitution should have such a small effect. In contrast, the solvent sensitivities for the thirty or so complexes of the type shown in Diagram 8.03, estimated from their spectra in N,N-di-

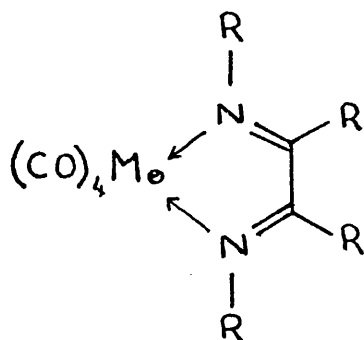


Diagram 8.03

methylformamide and in benzene [8.22], range between $+100$ and $+280 \text{ cm}^{-1} \text{ kcal}^{-1} \text{ mol}$; substituents R^1 and R^2 in Diagram 8.03 include e.g. alkyl

groups, $p\text{-XC}_6\text{H}_4$ and NH_2 . (Higher π -acceptor ability of the hetero-aromatic chelating ligand.) It is not possible to give more than an approximate indication of these solvent sensitivities, as the charge-transfer frequencies have only been reported in the two solvents mentioned.

(b) LL = Bidentate Schiff's base derived from one molecule of di-2-pyridyl ketone and one molecule of p -toluidine (Diagram 8.04).

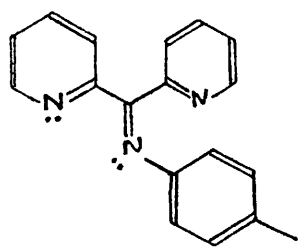
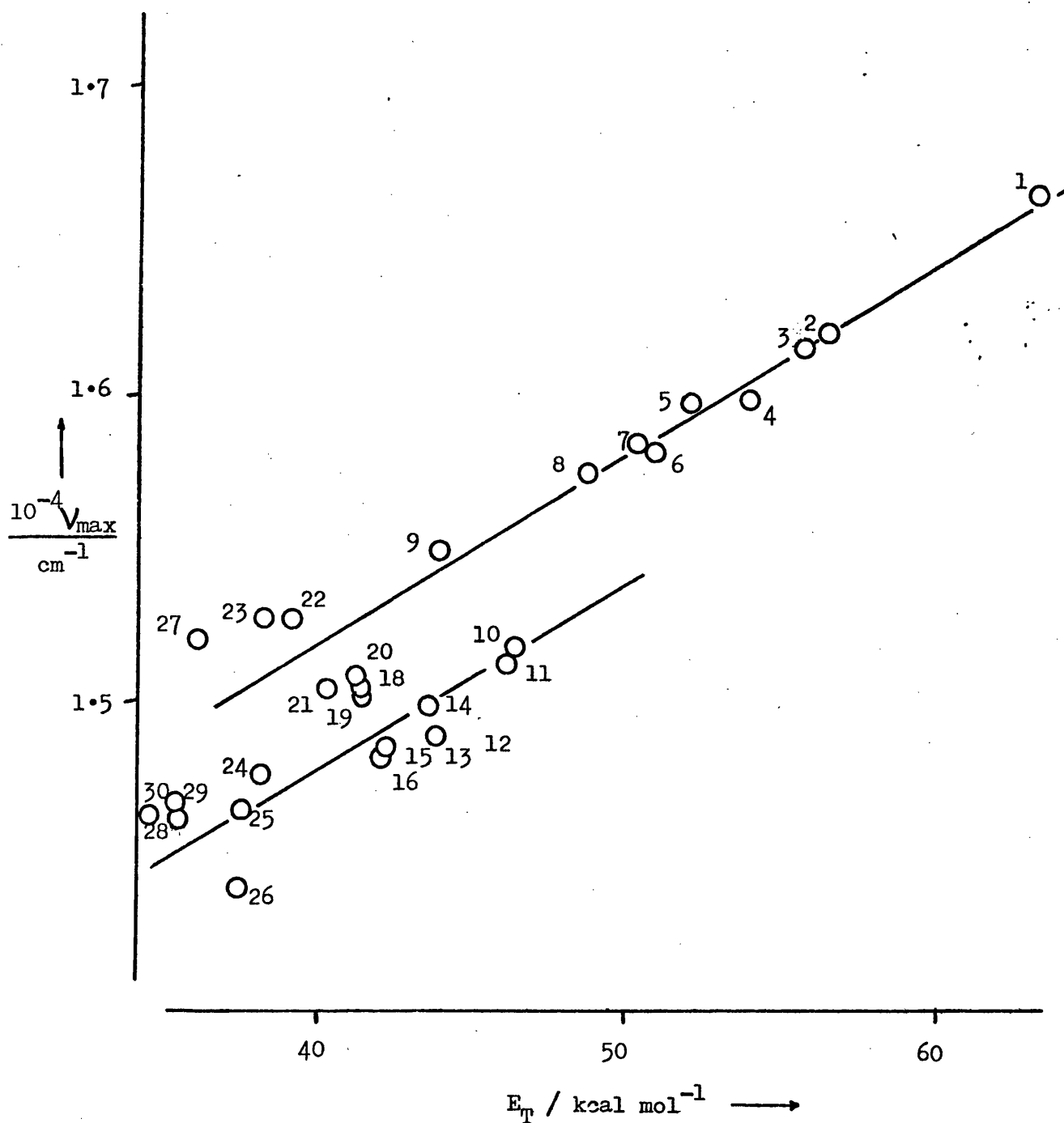


Diagram 8.04

The solvent sensitivity of this compound has been studied in a wide range of solvents, the results of which are listed in Table 8.03. We find a slope for the plot of ν_{max} against E_T , which is depicted in Figure 8.04, of $61 \pm 2 \text{ cm}^{-1} \text{ kcal}^{-1} \text{ mol}$ in hydroxylic solvents, and $58 \pm 9 \text{ cm}^{-1} \text{ kcal}^{-1} \text{ mol}$ in non-hydroxylic ones. Figure 8.04 clearly shows two distinct correlation lines for these two types of solvent, a feature which is common to such plots for compounds of the type $\text{Fe}(\text{LL})_2(\text{CN})_2$ [8.09]. Such ^aphenomenon has also been reported for a series of charge-transfer complexes of N,N -dimethylaniline, chloranil, and similar organic donors and acceptors [8.23]. Here, an extreme case is reached where the slopes of ν_{max} versus E_T have different signs for different types (hydroxylic or non-hydroxylic) solvents. Other inorganic examples of

Figure 8.04 Correlation of the frequency of maximum absorption with the solvent E_T parameter for the $\text{Fe}(\text{BDSB})_2(\text{CN})_2$ compound in a range of solvents. Numbering of solvents as in Table 8.03; solvents 1 to 9 -hydroxylic, 10 to 30(excluding 17) - non-hydroxylic.



the phenomenon, where two correlation lines occur, but of the same sense, is the series $M(CO)_4bipy$, where $M = Mo$ or W [8.12].

Chlorine-containing solvents which have been used have consistently been found to be anomalous, both for this Schiff's base-iron(II) complex and for other complexes studied. They can be regarded as intermediary between the aforementioned two types of solvent, having some degree of hydrogen-bonding. In any computed correlation slopes the points concerning these chloro-compounds have been omitted.

We find from comparisons of solvent sensitivities for complexes of the type $Fe(LL)_2(CN)_2$, for different bidentate ligands, that all complexes where LL is a Schiff's base, the sensitivities are all very similar. Comparing these with analogous observations where LL is a substituted phenanthroline, the Schiff's base complex sensitivities are consistently lower than the latter type.

Plots of ν_{max} for the lowest energy charge-transfer band against solvent E_T values are less satisfactory for the analogous quadridentate Schiff's base complex $Fe(QDSB)(CN)_2$, where QDSB is the Schiff's base (Diagram 8.05) derived from one molecule of o-phenylenediamine and two molecules of phenyl-2-pyridyl ketone. The measured ν_{max} values for a

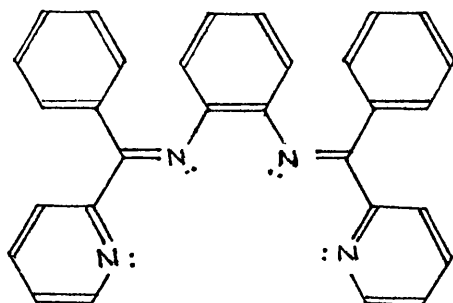
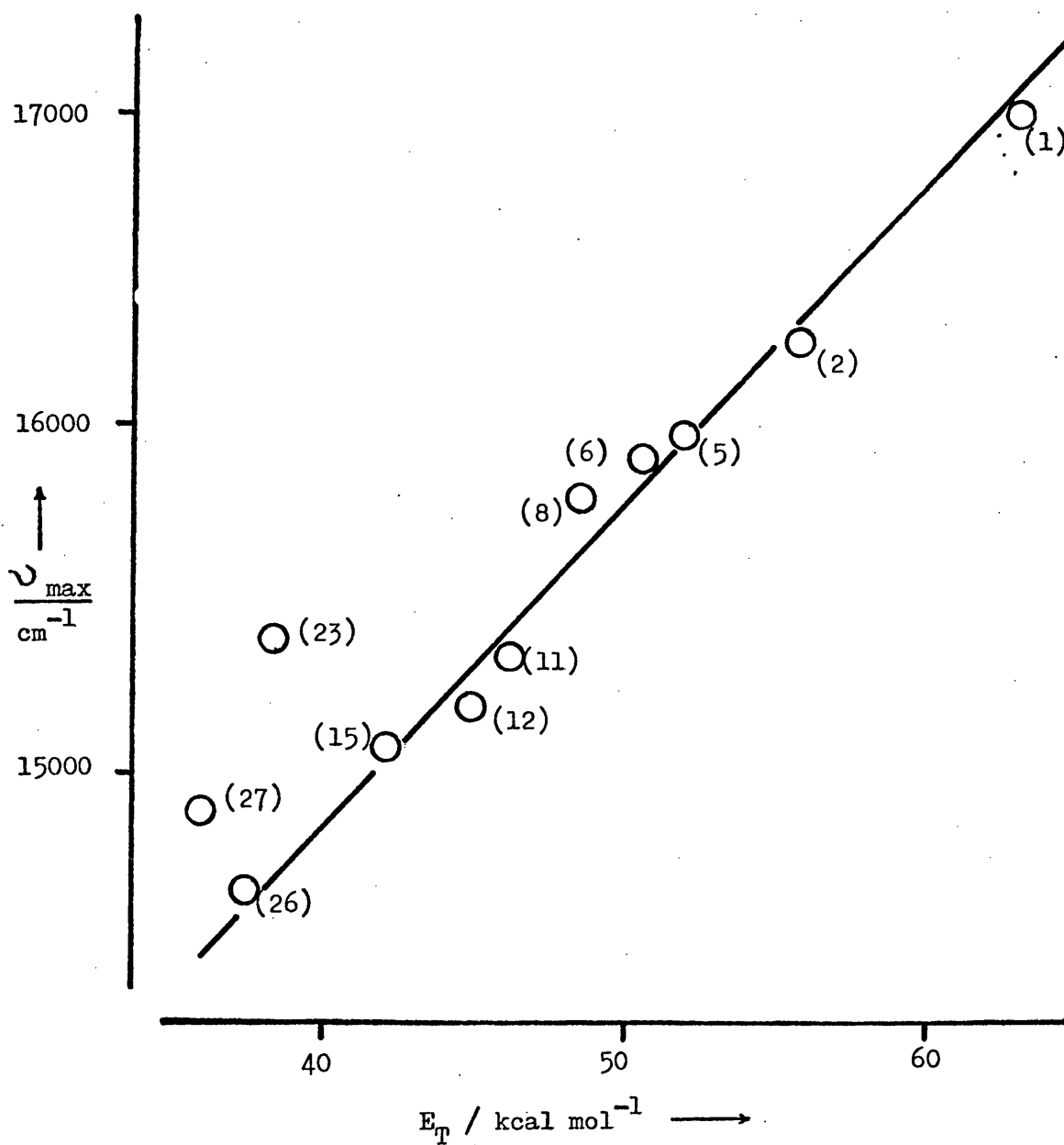


Diagram 8.05

Figure 8.05 Correlation of the frequency of maximum absorption, ν_{\max} , for the $\text{Fe}(\text{QDSB})(\text{CN})_2$ complex with solvent E_T values, at 298.2 K. Numbering of solvents as in Table 8.03.



range of solvents are reported in Table 8.03. The plot of ν_{\max} against E_T (Figure 8.05) shows the points for t-butyl alcohol, chlorinated hydrocarbons and for 1,2-dimethoxyethane to lie off the correlation lines. The remaining points give a sensitivity slope of $+80 \pm 5 \text{ cm}^{-1} \text{ kcal}^{-1} \text{ mol}$ for both hydroxylic and non-hydroxylic solvents. The separation of the two expected correlation lines is very much less well defined than that for the previously discussed complexes. The quadridentate Schiff's base might be expected to be planar, producing an octohedral complex having trans-cyanide ligands. From considerations below, we might expect such a complex to exhibit little or no solvatochromism. However, the presence of the phenyl groups in the ligand will cause distortion of the ligand from planarity, and consequently the complex may well be intermediary between cis- and trans-isomers. As will be pointed out in chapter 9, the α di-imine linkages in such ligands are susceptible to partial hydrolysis. Thus if a solvent molecule is added across the di-imine, the ligand will no longer be rigid, and the cis-conformation is accessible. Such possibilities are fully discussed in chapter 9, concerning such complexes. It would be interesting to examine such substituent effects on solvatochromism. For the diaza-butadiene complexes (Diagram 8.03) mentioned earlier, such substituent changes have a very large effect on the solvatochromic behaviour of the complexes. Unfortunately such data are not available at present.

Complexes of the type $\text{Fe}(\text{LL})_2(\text{CN})_2$ are assumed to be of cis-octohedral geometry. Such a geometry has been indicated by all the available infra-red and visible absorption spectroscopic data for both the iron(II) and the ruthenium(II) series of complexes [8.24].

Although the trends in frequencies of maximum absorption have been observed in ranges of solvents, the specific site of solvation which

effects such trends has not been discussed. In the case of $\text{Mo}(\text{CO})_4(\text{bipy})$, Adams [8.25] has shown by infra-red methods that solvent interactions occur at the carbonyl groups. For the iron(II)/2,2'-bipyridyl/cyanide systems, solvent effects on the spectrum of $[\text{Fe}(\text{bipy})_3]^{2+}$ are negligibly small [8.09], while those on the spectra of $\text{Fe}(\text{bipy})_2(\text{CN})_2$ and $[\text{Fe}(\text{bipy})(\text{CN})_4]^{2-}$ are large. This evidence suggests that direct solvent interaction with the bipy ligand is unlikely to be the cause of solvent effects on the frequencies of maximum absorption. A comparison of the solvent sensitivities of $\text{Fe}(\text{bipy})_2(\text{CN})_2$ and $\text{Ru}(\text{bipy})_2(\text{CN})_2^\dagger$ has shown [8.01] that the nature of the metal ion has no effect on the sensitivity, at least for these two species. Indeed a plot of the lowest energy charge-transfer band of $\text{Ru}(\text{bipy})_2(\text{CN})_2$ against the corresponding values for $\text{Fe}(\text{bipy})_2(\text{CN})_2$ has a slope of 1.00 ± 0.05 . Similarly there is little or no difference between the solvent sensitivities of the complexes of the type $\text{M}(\text{CO})_4(\text{bipy})$, for $\text{M} = \text{Mo}, \text{W}$ or Cr , as can be seen from the slopes of the ν_{max} against E_T plots given in Table 8.07. Consequently the source of the solvent effects on the metal to ligand charge-transfer absorptions must be indirectly through the cyanide ligands in our system.

Let us consider, for example, $\text{cis-Fe}(\text{bipy})_2(\text{CN})_2$. We have said that the charge-transfer band is metal to ligand, and this operates through the π -orbital system. Supposing the compound has a given value of ν_{max} in a given solvent, then if the solvent is changed to a more polar one, the solvation of the cyanide ligands will increase. This

[†] [Values of ν_{max} for $\text{Ru}(\text{bipy})_2(\text{CN})_2$ have been taken from D. Klassen, Ph.D. Thesis, New Mexico, (1966).]

will effectively decrease the $\text{CN} \rightarrow \text{Fe}$ π -back bonding ability of the cyanide, thus raising the ground state energy. Since, by the Frank-Condon principle the energy of the excited state will remain approximately constant, there will be a nett change in the energy of the absorption as the nature of the solvent and hence solvation of the cyanide ligands is changed. A phenomenon which has been explained by a similar argument is the protonation of $\text{Fe}(\text{bipy})_2(\text{CN})_2$ [8.26] which is believed to occur at the cyanide ligands. Here, protonation of a CN ligand produces an increase in the π -acceptor properties of the cyanide groups (i.e. now $\text{C}\equiv\text{N}^+\text{H}$) thus lowering the ground state energy, and producing a shift to higher wavelength [8.27].

We may see that such indirect cyanide-bipy π -bonding interactions can only occur when these ligands are 'trans' to one another in the compound, i.e. in the cis-isomer of the compound. In the case of the trans-isomer, such cyanide-bipy interactions cannot occur, and so no such solvatochromic behaviour would be expected. Unfortunately, compounds of the type $\text{Fe}(\text{LL})_2(\text{CN})_2$ do not occur as the trans-isomers. However, it is possible to prepare a trans-biscyano iron(II) complex which contains a rigid cyclic tetraaza ligand.

(iii) The trans- $[\text{Fe}(\text{phthalocyanine})(\text{CN})_2]^{2-}$ Anion.

This trans-biscyano iron(II) complex anion can only be prepared in solution in the presence of excess free cyanide ions [8.14]. The neutral compound phthalocyanine iron(II), $\text{Fe}(\text{pc})$, is insoluble in all solvents except those capable of acting as donor ligands, e.g. pyridine, dimethyl sulphoxide etc. [8.14]. The species in solution is then $\text{Fe}(\text{pc})(\text{solvent})_2$, the two solvent molecules occupying the axial positions. $\text{Fe}(\text{pc})$ is depicted in Diagram 8.06, the iron(II) atom lying in the plane of the

four nitrogens.

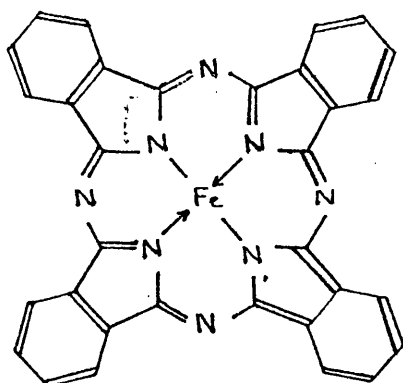


Diagram 8.06

Solutions of the $\text{trans-[Fe(pc)(CN)}_2\text{]}^{2-}$ anion were prepared as described in section 8.2(i)(d) above in several solvents, and the visible spectra were measured. The frequencies of maximum absorption for these spectra are reported in Table 8.04. A plot of ν_{max} versus E_T for these results has a slope of $-1.5 \pm 4 \text{ cm}^{-1} \text{ kcal}^{-1} \text{ mol}$. Clearly this complex anion has negligible solvent sensitivity, which is predicted for a trans-biscyano complex.

Unfortunately, it is not possible to make a direct cyanide-isothiocyanate intercomparison of solvatochromic behaviour for any of the given iron(II) complex^{es} mentioned above. As noted in the experimental section [8.2(i)(d)], although $\text{Fe(phen)}_2(\text{NCS})_2$ is low spin and stable at room temperature, it is insoluble in all solvents tried, and decomposes in aqueous solutions. It was also found impossible to prepare the isothiocyanato analogue of the $\text{trans-[Fe(pc)(CN)}_2\text{]}^{2-}$ anion.

However, a compound containing trans-isothiocyanato ligands is that of the $\text{trans-[Co(cyclam)(NCS)}_2\text{]}^+$ cation.

TABLE 8.04 Frequencies of maximum absorption, ν_{max} , of the lowest energy charge-transfer band for the $[\text{Fe}(\text{pc})(\text{CN})_2]^{2-}$ anion in water and in several non-aqueous solvents. E_{T} values for these solvents may be found in Table 8.03.

| Solvent | $\nu_{\text{max}} / \text{cm}^{-1}$ |
|---------------------|-------------------------------------|
| Water | 14750 |
| Methanol | 14810 |
| Ethanol | 14790 |
| t-Butyl alcohol | 14860 |
| Dimethyl sulphoxide | 14710 |

(iv) Solvatochromism of the trans-[Co(cyclam)(NCS)₂]⁺ Cation

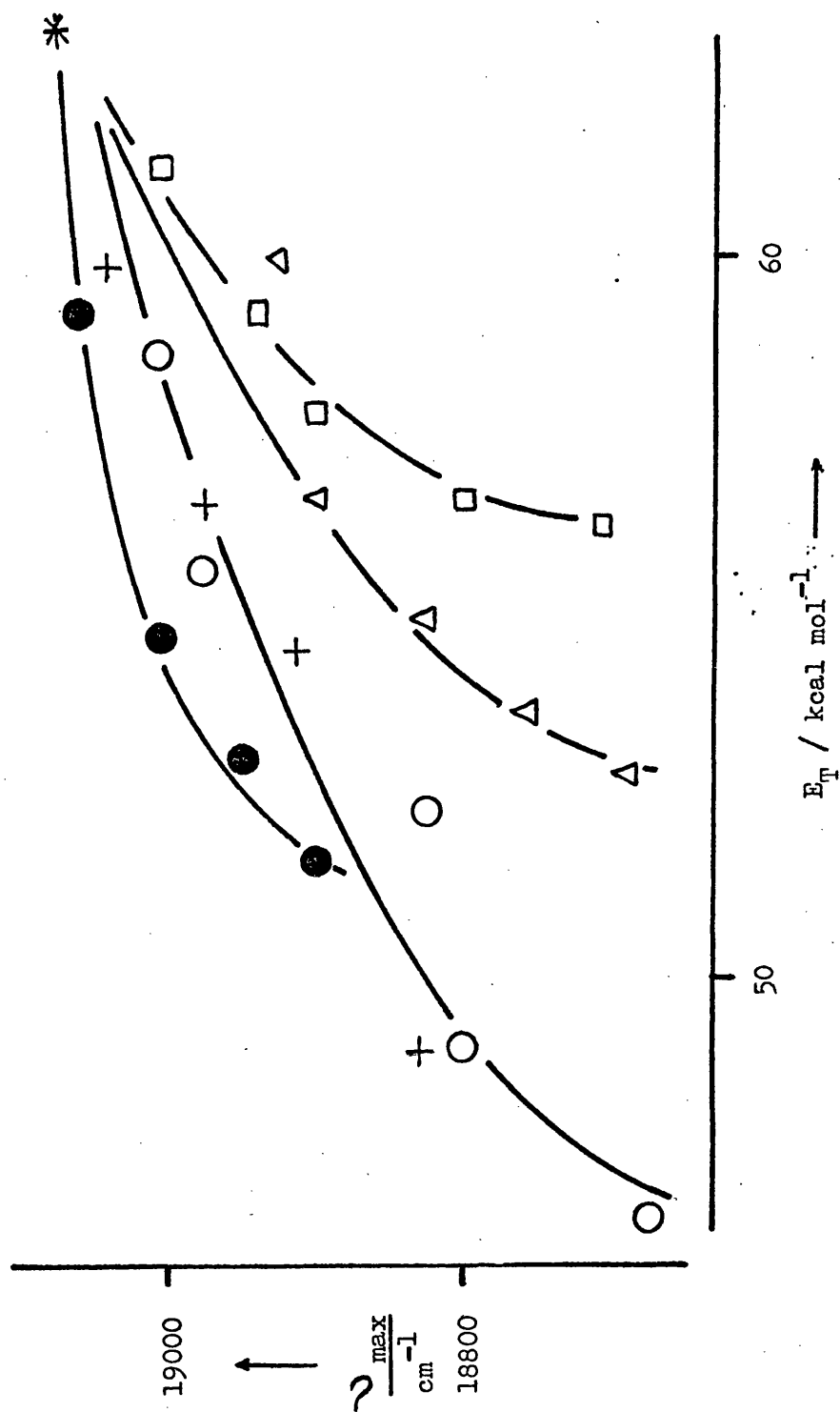
Due to the ionic nature of this species, the visible spectrum was measured in a range of binary aqueous mixtures. The ν_{\max} values for these solvent mixtures are reported in Table 8.05. Figure 8.06 represents a plot of these ν_{\max} values against the corresponding E_T values, which shows a family of correlation curves, a feature similar to that of the $[\text{Fe}(\text{CN})_5(\text{mpz})]^{2-}$ anion above. We see that the complex is only slightly solvatochromic, the most extreme shift in wavelength being 12 nm from water ($\lambda_{\max} = 536 \text{ nm}$) to 90% by volume aqueous-1,4-dioxan. The average sensitivity of these curves (obtained graphically) is ca. $+20 \text{ cm}^{-1} \text{ kcal}^{-1} \text{ mol}$. Although this value is small, it might be expected to be much smaller in the light of the above results on the $[\text{Fe}(\text{pc})(\text{CN})_2]^{2-}$ anion. However, other cobalt(III) complexes containing rigid planar ligands have been found to exhibit solvatochromic properties [8.28], with a solvent sensitivity of about $+40 \text{ cm}^{-1} \text{ kcal}^{-1} \text{ mol}$. More closely related to the $[\text{Fe}(\text{pc})(\text{CN})_2]^{2-}$ species is the trans-biscyano (corrin) cobalt(III) complex [8.29]. This has been found to be solvatochromic also, with a sensitivity of about $+18 \text{ cm}^{-1} \text{ kcal}^{-1} \text{ mol}$.

In chapter 7, the crystal structure of trans-[Co(cyclam)(NCS)₂] SCN was determined, and showed the isothiocyanato ligands to be distorted from being purely trans-in nature. This distortion may explain the occurrence of the slight solvatochromism of the compound, there being the possibility of some slight π -interaction between the NCS ligands and the tetraaza macrocycle. However, such explanations for the other cobalt(III) complexes above cannot be presumed without crystallographic evidence for the conformation of the ligands. Surprisingly the complex cations $[\text{Co}(\text{phen})_2\text{Cl}_2]^+$ and $[\text{Co}(\text{phen})_2(\text{CN})_2]^+$ are only very slightly solvatochromic [8.30] there being only a change in wavelength of 2 nm

TABLE 8.05 Frequencies of maximum absorption, ν_{\max} , of the lowest energy charge-transfer band of the trans-[Co(cyclam)(NCS)₂]⁺ cation in water and in a range of binary aqueous mixtures.

| Solvent Mixture | $\nu_{\max} / \text{cm}^{-1}$ |
|-----------------|-------------------------------|
| Water | 19080 |
| 20 | 18980 |
| 40 | 18940 |
| 60 % Methanol | 18900 |
| 80 | 18800 |
| 90 | 18690 |
| 20 | 18940 |
| 40 | 18900 |
| 60 % Ethanol | 18830 |
| 80 | 18760 |
| 90 | 18690 |
| 20 | 19060 |
| 40 | 19010 |
| 60 % i-Propanol | 18950 |
| 80 | 18900 |
| 20 | 19010 |
| 40 | 18980 |
| 60 % 1,4-Dioxan | 18850 |
| 80 | 18800 |
| 90 | 18670 |
| 20 | 19050 |
| 40 | 18980 |
| 60 % Acetone | 18910 |
| 80 | 18830 |

Figure 8.06 Correlation of the frequencies of maximum absorption, ν_{\max} , for the trans- $[\text{Co}(\text{cyclam})(\text{NCS})_2]^+$ cation and the solvent E_T values for a range of binary aqueous mixtures, at 298.2 K. Symbols as in Figure 8.01.



from water to n-propanol for the dichloro-cation, producing a sensitivity of ca. $-40 \text{ cm}^{-1} \text{ kcal}^{-1} \text{ mol}$. The dicyano analogue was found to have a sensitivity of $+20 \text{ cm}^{-1} \text{ kcal}^{-1} \text{ mol}$.

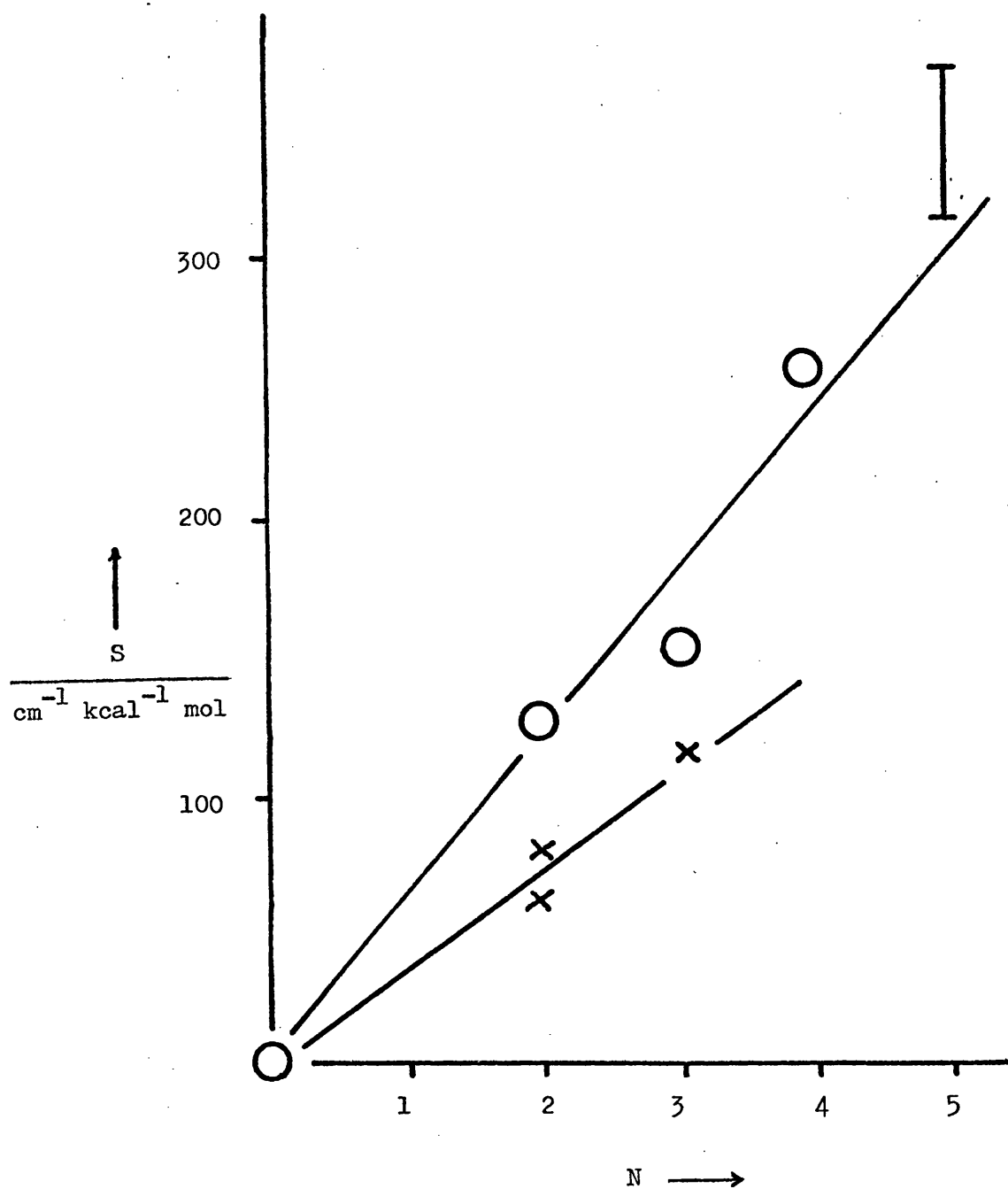
So far the solvatochromic behaviour of compounds of known structure have been examined. From consideration of the solvent sensitivities of a wide range of compounds listed in Table 8.07, we can see several striking features. The main one which shall concern us for the present is the similarity of solvent sensitivities for a given closely related series of compounds. Thus all compounds of the type $\text{Fe}(\text{X-phen})_2(\text{CN})_2$ have ν_{max}/E_T slopes of around $+130 \text{ cm}^{-1} \text{ kcal}^{-1} \text{ mol}$. Such correlations are better related by taking one specific example as a standard. Thus by plotting ν_{max} for, say $\text{Fe}(4,7\text{-Me}_2\text{phen})_2(\text{CN})_2$ against all substituted analogues, the slopes remain approximately constant at unity. Similar correlations have been made for the series $\text{W}(\text{CO})_4(\text{X-phen})$ [8.01]. Similarly, a plot of $\nu_{\text{max}}([\text{Fe}(\text{CN})_5(\text{mpz})]^{2-})$ versus $\nu_{\text{max}}([\text{Fe}(\text{CN})_5(4\text{-CNpy})]^{3-})$ has a slope of 1.00 ± 0.03 (see above). Table 8.07 also shows that the series $\text{Fe}(\text{LL})_2(\text{CN})_2$, where LL is a bidentate Schiff's base, has an almost constant sensitivity. This is noticeably lower than the corresponding 1,10-phenanthroline series.

Hence it seemed reasonable to assume (tentatively) that, at least for iron(II)-cyanide complexes, the sensitivity was related to the structure of the solvatochromic species. It is also noticeable from Table 8.07 that the solvent sensitivities of the series of compounds increase with increase in the number of, for example cyanide ligands in iron(II)-cyanide-polydentate ligand systems. If we plot sensitivity against the number of cyanides per molecule of compound for this series we find that there is an almost linear correlation between these parameters. Figure 8.07 shows such a plot for the series of species

Figure 8.07 Correlation between the solvent sensitivities (S) of ternary iron(II)-cyanide compounds and the number of cyanide ligands per molecule (N), at 298.2 K.

(\bigcirc) = polypyridyl-containing compounds;

(\times) = Schiff's base-containing compounds.



$[\text{Fe}(\text{bipy})_3]^{2+}$ (no. of $(\text{CN}) = 0$), $\text{Fe}(\text{bipy})_2(\text{CN})_2$, $[\text{Fe}(\text{terpy})(\text{CN})_3]^-$, $[\text{Fe}(\text{bipy})(\text{CN})_4]^{2-}$ and $[\text{Fe}(\text{CN})_5(\text{mpz})]^{2-}$. The sensitivity of the $[\text{Fe}(\text{bipy})_3]^{2+}$ cation is taken as zero [8.09]. Values for the other species have been taken from Table 8.07.

Hence from the previous observation that compounds of like structure have very similar sensitivities, noting that values for Schiff's base complexes are consistently lower than their 1,10-phenanthroline analogues, it is reasonable to suppose that we might use Figure 8.07 as a yardstick for the determination of certain structural properties of unknown species. Such an assumption can only at present be used for ternary iron(II) compounds of the type mentioned above. It may be argued that $\text{Ru}(\text{bipy})(\text{CN})_2$ fits in with this theory, but clearly compounds of cobalt(III) do not.

In chapter 9, the kinetics of the reaction of cyanide ion with a hexadentate Schiff's base complex of iron(II), $[\text{Fe}(\text{HXSb})]^{2+}$ (see Diagram 8.07(a)) were studied. Unfortunately the product of this reaction could not be obtained in a pure enough form for satisfactory analysis. A similar reaction had previously been studied [8.31] where again the product could not be isolated. These workers had assumed their hexadentate Schiff's base to be behaving as three linked bidentate ligands.

In our reaction, no neutral species of the type $\text{Fe}(\text{HXSb})(\text{CN})_2$, analogous to $\text{Fe}(\text{LL})_2\text{CN}_2$, could be isolated. The product behaved like an ionic compound, being insoluble in organic solvents, but soluble in water. The question was, were there three or four cyanides coordinated to the iron(II), with a ter- or bidentate residue of ligand respectively? (see Diagrams 8.07(b) and (c)).

An aqueous solution of the cyanide-Schiff's base complex was

isolated and its visible spectrum measured. The solution was also mixed with appropriate volumes of co-solvents, and the trends in ν_{\max} were measured. The results of this study are reported in Table 8.06. Figure 8.08 shows a family of curves for the plot of ν_{\max} against E_T . This feature is not uncommon for a charged species in mixed solvents, as was noted for the $[\text{Fe}(\text{CN})_5\text{L}]^{n-}$ and $\text{trans-}[\text{Co}(\text{cyclam})(\text{NCS})_2]^+$ ions earlier.

The ν_{\max} values of the 'unknown' compound were plotted against available corresponding values for the $[\text{Fe}(\text{terpy})(\text{CN})_3]^-$ anion, shown in Figure 8.09. This plot has a slope of 0.85 ± 0.03 . This lower sensitivity of the Schiff's base complex is consistent with the lower sensitivities of $\text{Fe}(\text{LL})_2(\text{CN})_2$ type Schiff's base complexes as compared with the 1,10-phenanthroline analogues (see above). The other possible structure of the complex is $[\text{Fe}(\text{HXS}^{\text{III}})(\text{CN})_4]^{2-}$ as shown in Diagram 8.07(c). However on comparing the solvent sensitivities of this with the available data for $[\text{Fe}(\text{bipy})(\text{CN})_4]^{2-}$ [8.09], we find the ratio $\text{HXS}^{\text{III}}/\text{bipy} = 0.56$. Thus the most probable structure for the cyanide-hexadentate Schiff's base iron(II) complex is $[\text{Fe}(\text{HXS}^{\text{I}})(\text{CN})_3]^-$, as shown in Diagram 8.07(b).

Conclusions

We have seen that the solvent sensitivity parameter, E_T , can be used to an extent as a measure of the solvent sensitivity of inorganic complexes as well as organic ones. However the presence of more than one correlation line in plots of ν_{\max} against E_T for various kinds of solvents is a reflection of the differing relative importance of hydrogen-bonding, lone-pair availability and other solvent molecular

TABLE 8.06 Frequencies of maximum absorption, ν_{\max} , of the lowest energy charge-transfer band for the $[\text{Fe}(\text{HXSb}')(\text{CN})_3]^-$ species in water and in a range of binary aqueous mixtures. Included in this table are analogous figures for the $[\text{Fe}(\text{terpy})(\text{CN})_3]^-$ anion, taken from ref.8.15.

| Solvent Mixture ^a | $[\text{Fe}(\text{HXSb}')(\text{CN})_3]^-$ | $[\text{Fe}(\text{terpy})(\text{CN})_3]^-$ |
|------------------------------|--|--|
| | $\nu_{\max} / \text{cm}^{-1}$ | |
| Water | 17040 | 20240 |
| 20 | 16780 | 20000 |
| 40 | 16530 | 19690 |
| 60 % Methanol | 16290 | 19420 |
| 70 | 16230 | |
| 80 | 16080 | 19190 |
| 100 | 15920 | 18940 |
| 20 | 16780 | |
| 40 | 16500 | |
| 60 % Ethanol | 16210 | |
| 80 | 16080 | |
| 100 | 15750 | 18690 |
| 20 | 16810 | |
| 40 | 16450 | |
| 60 % i-Propanol | 16260 | |
| 80 | 16130 | |
| 100 | 15870 | |
| 10 | 16890 | |
| 20 | 16720 | |
| 40 % Acetone | 16340 | |
| 60 | 16050 | |
| 80 | 15900 | |
| 100 % t-Butyl alcohol | 15920 | |

^a

E_{T} values for these solvent mixtures may be found in Table 8.02; that for t-butyl alcohol is 43.9 kcal mol⁻¹.

Figure 8.08 Correlation between the frequencies of maximum absorption, ν_{\max} , for the $[\text{Fe}(\text{HXSb})(\text{CN})_3]^-$ anion and the solvent E_{T} parameter in a range of binary aqueous mixtures, at 298.2 K. Symbols as in Figure 8.01; (∇) = pure t-butyl alcohol.

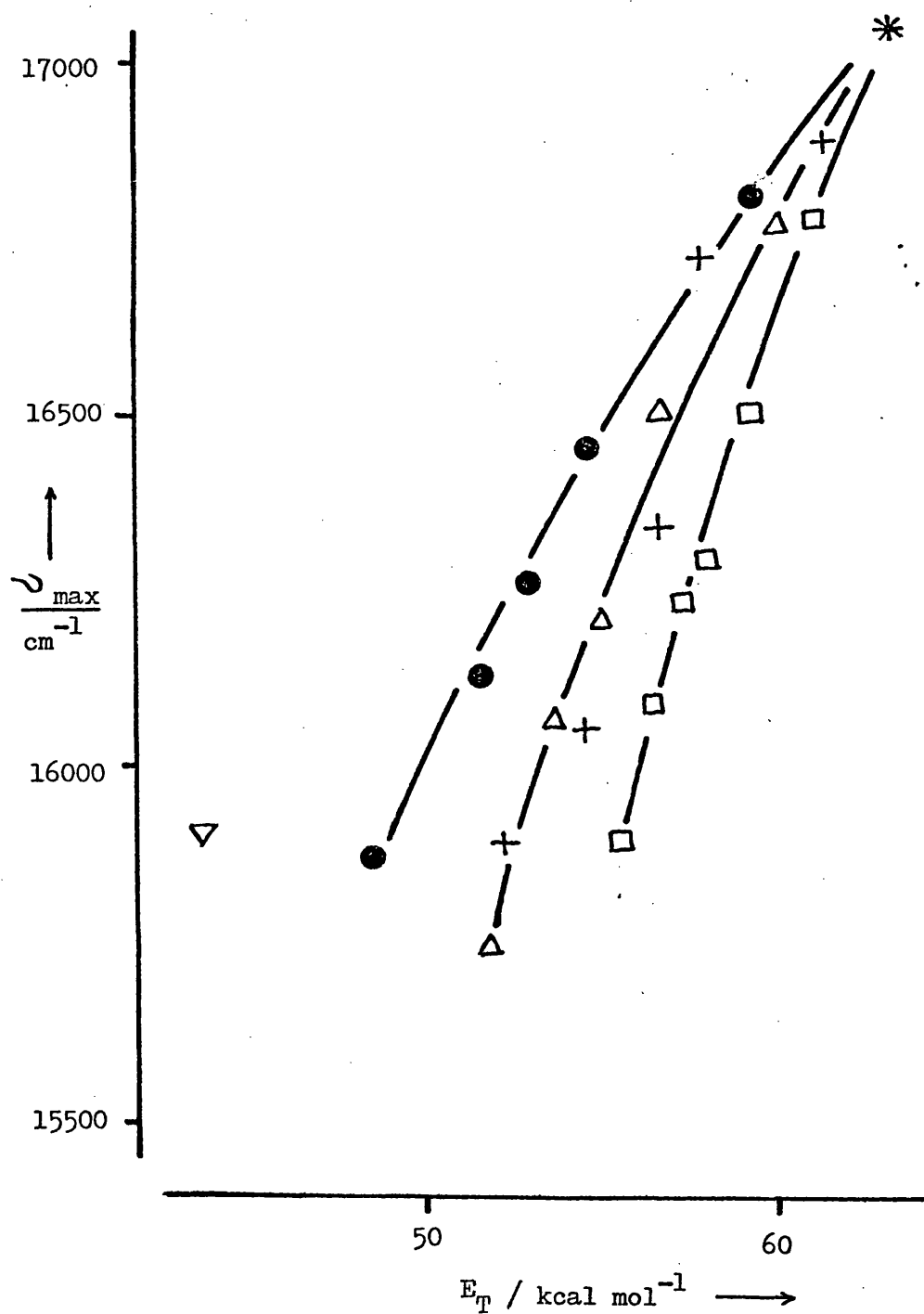


Figure 8.09 Correlation between the frequencies of maximum absorption, ν_{\max} , of the $[\text{Fe}(\text{HXSb})(\text{CN})_3]^-$ (ordinate) and the $[\text{Fe}(\text{terpy})(\text{CN})_3]^-$ (abscissa) anions, in a range of binary aqueous mixtures, at 298.2 K.

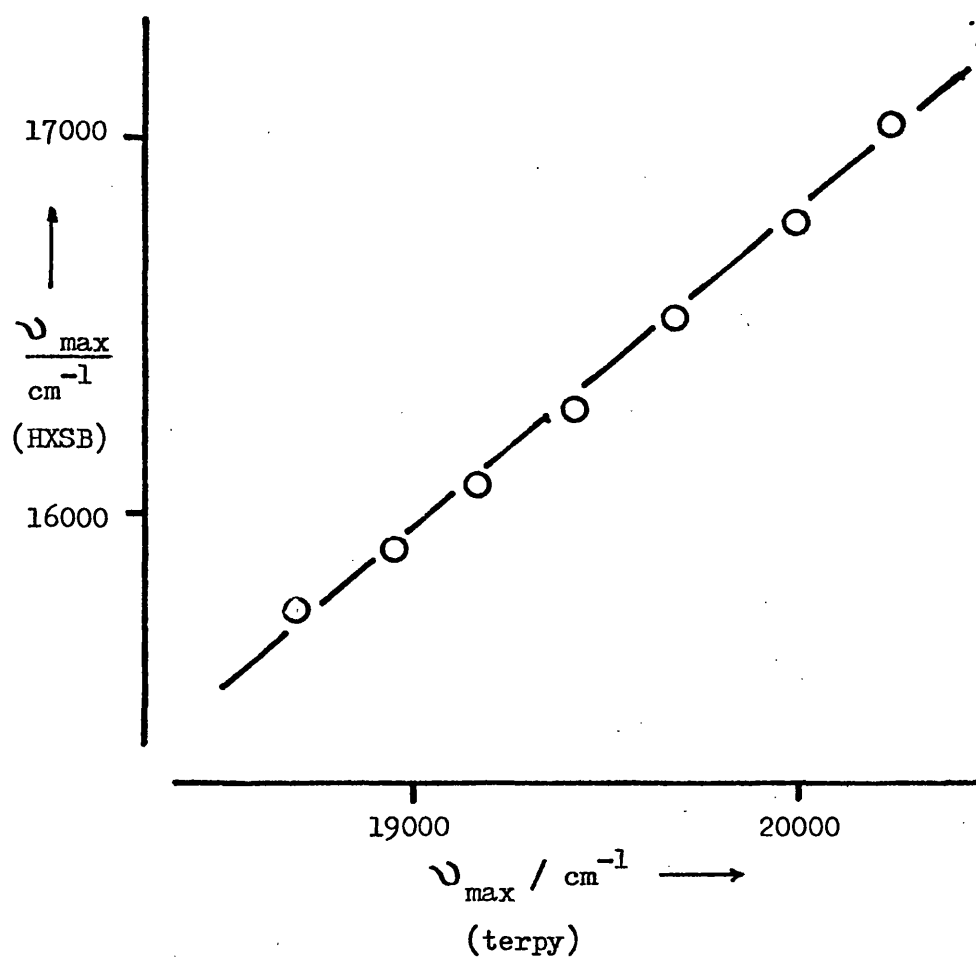


TABLE 8.07 Summary of solvent sensitivities ($\text{cm}^{-1} \text{ kcal}^{-1} \text{ mol}$) for the solvatochromic inorganic compounds mentioned in this chapter. Values in parentheses have been estimated approximately, from ν_{max} vs. E_T plots which were not good straight lines.

| Compound | ref. | Solvent Sensitivity | |
|---|-----------|---------------------|-------------------------|
| | | Hydroxylic Solvents | Non-hydroxylic Solvents |
| $[\text{Fe}(\text{CN})_5(\text{mpz})]^{2-}$ | this work | (320-370) | |
| $[\text{Fe}(\text{CN})_5(4\text{-CNpy})]^{3-}$ | this work | (320-370) | |
| $\text{Fe}(\text{bipy})_2(\text{CN})_2$ | 8.08 | 116 | 119 |
| $\text{Fe}(\text{phen})_2(\text{CN})_2$ | 8.09,10 | 121 | |
| $\text{Fe}(4,7\text{-Me}_2\text{phen})_2(\text{CN})_2$ | " " | 131 | 131 |
| $\text{Fe}(5\text{-Clphen})_2(\text{CN})_2$ | " " | 129 | |
| $\text{Fe}(5\text{-NO}_2\text{phen})_2(\text{CN})_2$ | this work | | 121 ± 8 |
| $\text{Fe}(\text{bmi})_2(\text{CN})_2^a$ | (a) | | 80 |
| $\text{Fe}(\text{BDSB})_2(\text{CN})_2$ | this work | 61 ± 2 | 58 ± 9 |
| $\text{Fe}(\text{QDSB})(\text{CN})_2$ | this work | | 80 ± 5 |
| $[\text{Fe}(\text{terpy})(\text{CN})_3]^-$ | 8.15 | 137 | |
| $[\text{Fe}(\text{HXSb})(\text{CN})_3]^-$ | this work | (116) | |
| $[\text{Fe}(\text{bipy})(\text{CN})_4]^{2-}$ | 8.09 | 260 | |
| $[\text{Fe}(\text{phen})_2(\text{CN})_2]^+$ | 8.09 | - 83 | |
| $\text{Ru}(\text{bipy})_2(\text{CN})_2$ | (b) | | 166 |
| $\text{Ru}(\text{bipy})_2(\text{ox})$ | | | (110) |
| $\text{Cr}(\text{CO})_4(\text{bipy})$ | 8.11,12 | | 199 |
| $\text{Mo}(\text{CO})_4(\text{bipy})$ | " " | 179 | 220 |
| $\text{W}(\text{CO})_4(\text{bipy})$ | " " | 196 | 228 |
| $\text{Mo}(\text{CO})_4(\text{subs.1,4-diazabutadienes})$ | 8.13 | | 100 to 280 |
| $[\text{Cr}(\text{NCS})_{6-x}(\text{CN})_x]^{3-}$ | 8.20 | (- 20 to - 60) | |
| $\text{trans-}[\text{Co}(\text{cyclam})(\text{NCS})_2]^+$ | this work | (20) | |

(a) bmi = biacetylbismethylimine, P. Krumholz, O.A. Serra and M.A. de Paoli, J. Inorg. Nuclear Chem., (1975), 37, 1820.

(b) D. Klassen, Ph.D. Thesis, New Mexico, (1966).

properties on the charge-transfer energies of the systems studied. Consequently, it is impossible to define a single solvent parameter to embrace all possible variables [8.32]. The sensitivity of a particular type of compound appears to be independent of the nature of the metal ion present. For example we saw that there was little or no difference between the sensitivities of $\text{Fe}(\text{bipy})_2(\text{CN})_2$ and $\text{Ru}(\text{bipy})_2(\text{CN})_2$; likewise the series $\text{M}(\text{CO})_4(\text{bipy})$ (where $\text{M} = \text{Mo}, \text{W}$ or Cr) has a more or less constant value for its sensitivity. It has also been noted that there is little substituent effect for compounds of the type $[\text{Fe}(\text{CN})_5\text{L}]^{n-}$ and $\text{Fe}(\text{LL})_2(\text{CN})_2$.

An interesting feature also is the sensitivities of the various systems relative to the solvated ligands. For the iron(II)-cyanide-polydentate ligand system, we have said that the solvation of the cyanide ligands is the main factor in deciding the nature of the solvatochromic behaviour. It appears that from a plot of sensitivities (Figure 8.07) against the number of cyanide ligands present, there is an almost linear correlation between these two parameters. Naturally, $[\text{Fe}(\text{CN})_6]^{4-}$ is excluded as the $\text{Fe} \rightarrow (\text{polydentate ligand})$ charge-transfer band is under examination. (Indeed, this latter trend has suggested that solvatochromism may in some circumstances be used as a tool to probe the structural properties of certain species by comparisons with species of known structure.) Thus this phenomenon indicated the nature of the product of the reaction of the $[\text{Fe}(\text{HXSb})]^{2+}$ cation with cyanide ion; it also suggested the lack of cyanide coordinated directly to iron in the $[\text{Fe}(5\text{-NO}_2\text{phen.CN})_2(5\text{-NO}_2\text{phen})]$ -type complex.

A final feature of this work, for iron(II) compounds at least, is that solvatochromism is strongest when a solvated ligand (e.g. cyanide or carbonyl) is 'trans' to the ligand involved in the charge-transfer

absorption; and least when this criterion does not hold, e.g. as in the case of the $\text{trans-}[\text{Fe}(\text{pc})(\text{CN})_2]^{2-}$ anion.

It would be interesting to be able to study relative solvation effects of, say cyanide and isothiocyanate from studies of analogous compounds. So far, this has been shown not to be possible, in the case of $\text{Fe}(\text{phen})_2\text{X}_2$ (where $\text{X} = \text{CN}, \text{NCS}$). It would also be desirable to have a true cis-trans comparison of solvatochromic effects. Unfortunately this is not possible at present.

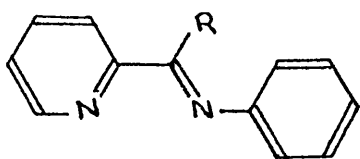
CHAPTER 9

Nucleophilic Substitution Reactions at Ternary

Iron(II) and Related Complexes.

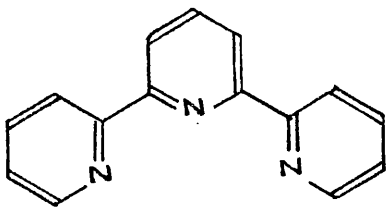
9.1 INTRODUCTION

There have been extensive studies of the kinetics of a variety of reactions of low-spin iron(II) complexes of such bidentate ligands as 2,2'-bipyridyl (bipy), 1,10-phenanthroline (phen), related Schiff's bases (I), and their substituted derivatives [9.01].

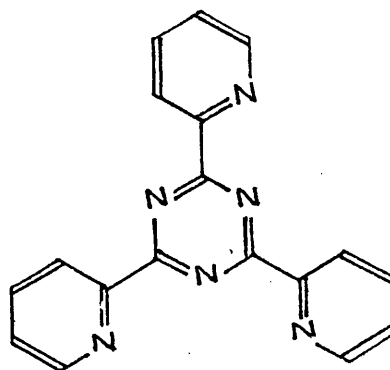


(I)

The kinetics of reactions of iron(II) complexes containing ligands of different denticities have also been reported, for example that of 2,2',6',2''-terpyridyl (terpy) [9.02] and of 2,4,6-tri(2-pyridyl)-1,3,5-triazine (tptz) [9.03], and of a hexadentate Schiff's base complex



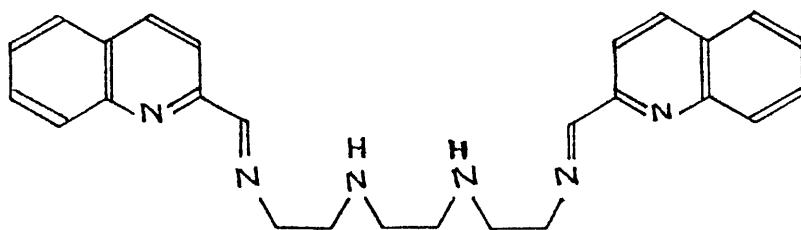
terpy



tptz

[9.04], the ligand (II) being derived from one molecule of triethylene-tetramine (trien) and two molecules of phenyl-2-pyridyl ketone.

The nucleophilic substitution reactions of all these complexes exhibit simple second-order kinetics, having in the rate law a dominant



(II)

term in [iron(II) complex][nucleophile], e.g. for the nucleophiles CN^- [9.05] and OH^- [9.06] reacting with the $[\text{Fe}(\text{bipy})_3]^{2+}$ cation. Such bimolecular behaviour had been ascribed [9.07] to direct attack of the nucleophile at the iron atom of the complex, despite the t_{2g} [9.06] electronic configuration which gives high electron density in just those regions through which the incoming nucleophile must approach the metal.

Recently, a general reaction mechanism for the above systems has been put forward [9.08], involving initial attack of the incoming nucleophile at the heterocyclic ligands. Here, an analogy has been made between the complexing of such bidentate ligands as bipy with metals and the quaternisation of pyridines (by protons, alkyl and aryl groups etc.). In particular, the idea of nucleophilic attack in such quaternised pyridines at the 2- positions has been extended to corresponding attacks at metal derivatives (Diagram 9.01).

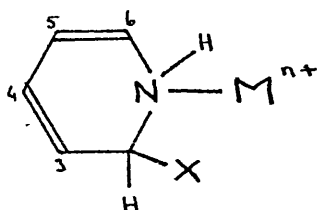
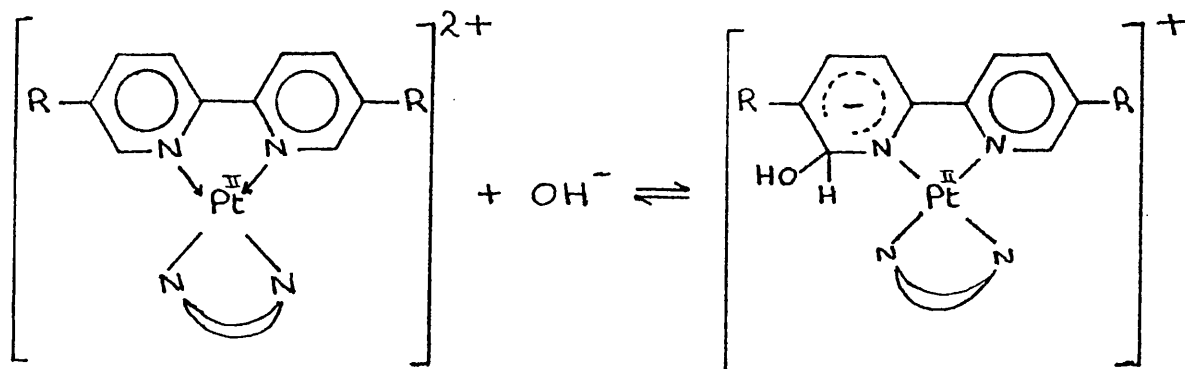


Diagram 9.01

Many anomalous properties of complexes of the type $[M(LL)_3]^{n+}$ have been rationalised on this basis. For example, the redox potentials of $[M(LL)_3]^{n+}$ cations (where $M = Fe, Ru$ or Os) vary strongly with acidity [9.09]. This has been explained [9.10] in terms of extensive formation of very stable ion-pairs. It has been said [9.11] that very marked changes in the participant species is indicated by such a pH-dependent behaviour.

The electronic spectra of 5-nitro 1,10-phenanthroline [9.07(b)] and of $[M(5-NO_2phen)_3]^{2+}$ ($M = Fe$ [9.07(b)] or Ru [9.12]) have been found to show a reversible change with pH. The circular dichroism for the π exciton region of the resolved ruthenium complex [9.12] shows a concomitant reversible decrease, suggesting that the ligand is being altered. However, no conjugate base is involved, since there is no exchange of C-H in alkaline deuterium oxide [9.13]. Cyanide ion reacts reversibly with aqueous solutions of $[Ru(5-NO_2phen)_3]^{2+}$ [9.14], the reaction having been shown to involve addition of a cyanide to either the 2- or 9- position of a ligand molecule. In the presence of excess cyanide, a neutral species of the type $Ru(5-NO_2phen.CN)_2(5-NO_2phen)$ is formed. This provides conclusive evidence for nucleophilic attack at the ligand for this ruthenium complex. Gillard has also produced n.m.r. evidence for a similar cyanide adduct of the $[Pt(bipy)_2]^{2+}$ cation [9.13], where large changes in the spectrum occur on addition of base, and have been attributed to the equilibrium:-



The $[\text{Pd}(5,5'\text{-Me}_2\text{bipy})]^{2+}$ species also exhibits this behaviour [9.13].

Although there is emerging a large amount of data concerning such reactions [9.12-15], there is at present no direct evidence for such intermediates in the corresponding reactions of iron(II) complexes, other than the aforementioned spectral data [9.07(b)]. In the reaction of, for example cyanide ion with the $[\text{Fe}(\text{bipy})_3]^{2+}$ cation, the only product isolated is the $\text{Fe}(\text{bipy})_2(\text{CN})_2$ species [9.16], with no hint, spectroscopic or otherwise, of a $[\text{Fe}(\text{LL}.\text{CN})_2(\text{LL})]$ -type intermediate. It may well be that such a species, for the bipy complex at least, is too short-lived to be detectable using spectroscopic or preparative means.

Consequently, this work is concerned with the study of nucleophilic substitution at the relatively inert $\text{Fe}(\text{LL})_2(\text{CN})_2$ type complexes primarily, where LL = bipy, phen and 5-Cl phen. Here it was hoped to observe possible "nucleophile-on-ligand" intermediates of the reactions, which should be more stable than those from the tris-ligand complexes because of the stabilising effect of the two cyanide ligands.

The reaction of $\text{Fe}(\text{bipy})_2(\text{CN})_2$ with cyanide ion, producing ultimately $[\text{Fe}(\text{bipy})(\text{CN})_4]^{2-}$ has been studied over a range of temperatures, whence activation parameters have been determined; in a few binary aqueous mixtures, to compare with previously studied reactions in mixed solvents; and for several different ligands, to compare substituent effects with such effects in other substitution reactions.

The reaction of cyanide ion with the $[\text{Fe}(5\text{-NO}_2\text{phen})_3]^{2+}$ cation has also been studied, and some kinetic studies have been performed on the products of this reaction.

In the second part of this chapter, a series of polydentate Schiff's base-iron(II) complexes have been prepared and the kinetics of their

reactions with cyanide ion and in some cases acid have been observed. Where possible, reaction products have been isolated and characterised. The mechanisms of these reactions have been discussed in broad terms in relation to those of the nucleophilic substitution reactions of the polypyridyl-iron(II) complex analogues.

9.2 EXPERIMENTAL

(i) PREPARATIONS

(a) Cationic Schiff's Base Complexes of Iron(II)

All such iron(II) complex cations containing Schiff's base ligands of various denticities were prepared by a general method, which is outlined below.

Stoichiometric proportions of methanolic solutions of the appropriate precursors of the required Schiff's base were mixed at room temperature. To this 'in situ' Schiff's base was then added the stoichiometric amount of iron(II) chloride tetrahydrate dissolved in methanol containing 1 cm³ of glacial acetic acid.[†] Depending on the stability and/or the rate of formation of the required complex, the reaction solution was allowed to age at room temperature for a suitable length of time. The resulting (deep blue) solution was then filtered

[†] [This constituent has been shown [9.17] to reduce the extent of oxidation of the iron(II) ions in the presence of the basic Schiff's base ligands.]

through 'Celite' filter-aid, and rotary-evaporated to dryness at room temperature.[†] The crude product was then ground to a powder and thoroughly washed with toluene and then diethyl ether, to remove any unreacted organic materials. The iron(II) complex was then taken up in water and filtered through 'Celite'. The complex was isolated by precipitation of its perchlorate salt, by addition to the above complex solution of a strong aqueous solution of AnalaR sodium perchlorate. The filtered product was washed thoroughly with water, ethanol and ether, and dried in vacuo at room temperature over phosphorus pentoxide. The types of iron(II) complexes formed, the quantities and natures of their precursors and the conditions required for their individual preparations have been tabulated in summary form below:-

| Complex Cation | Organic Precursors ^a | | Aging Period |
|--|---------------------------------|-------------------------|--------------|
| | Ketone | Amine | |
| [Fe(BDSB) ₃] ²⁺ | di-2-pyridyl ketone(3) | p-toluidine(3) | 60 mins |
| [Fe(TDSB) ₂] ²⁺ | 2,6-diacetylpyridine(2) | p-toluidine(4) | 30 mins |
| [Fe(QDSB)(OH ₂) ₂] ²⁺ | | | |
| ligand (I) | phenyl-2-pyridyl ketone(2) | o-phenylenediamine(1) | 10 mins |
| " (II) | pyridyl-2-aldehyde(2) | " (1) | " |
| " (III) | phenyl-2-pyridyl ketone(2) | ethylenediamine(1) | " |
| " (IV) | pyridyl-2-aldehyde(2) | " (1) | " |
| [Fe(HXSB)] ²⁺ | quinolyl-2-aldehyde(2) | triethylenetetramine(1) | 0.5 hours |

^a Numbers in parentheses are the number of moles of precursor used per mole of FeCl₂.4H₂O in the preparations.

The perchlorate salts of these cations were analysed for C, H and

[†] [It had previously been found that these iron(II)-Schiff's base complexes decomposed on heating to temperatures exceeding ca. 313 K.]

N by the 'Butterworth Micro Analytical Company', the results being listed in Table 9.01.

(b) Neutral Complexes of the type $\text{Fe}(\text{LL})_2(\text{CN})_2$

Compounds of this type, where the bidentate ligand, LL is 2,2'-bipyridyl, 1,10-phenanthroline or 5-chloro 1,10-phenanthroline, were prepared by the method of Schilt [9.16]. They were characterised by their known electronic spectra.

Similar compounds where $(\text{LL})_2 \equiv (\text{BDSB})_2$ or (QDSB) were also prepared by this method.

$\text{Fe}(\text{5-NO}_2\text{phen})_3(\text{CN})_2$

This compound could not be prepared in the same way as the analogous compounds above. The outcome of such an attempt is related below. In order to isolate a pure sample of the required compound, the following method was found to be successful.

To 20 cm³ of a methanolic solution of 0.4 g (0.002 mol) iron(II) chloride tetrahydrate was added 1.35 g (0.006 mol) of solid 5-nitro 1,10-phenanthroline. The mixture was refluxed for 30 minutes, to ensure complete formation of the $[\text{Fe}(\text{5-NO}_2\text{phen})_3]^{2+}$ cation. To the hot deep red solution was added 0.63 g (0.004 mol) of tetraethylammonium cyanide. The resulting blue/purple solution was refluxed for 10 minutes, and then evaporated to dryness. The residue was washed thoroughly with toluene and then ether to remove any liberated 5-nitro 1,10-phenanthroline. The required product was then extracted with dichloromethane, and recrystallised from a dichloromethane/n-hexane mixture several times.

TABLE 9.01 Microanalysis results for the various iron(II) compounds prepared in this work. Results are in % by weight of element.

| Compound | | Element | | |
|--|-------|---------|------|---------|
| | | C | H | N |
| (i) <u>Cationic iron(II) compounds</u> | | | | |
| $[\text{Fe}(\text{BDSB})_3](\text{ClO}_4)_2$ | Calc. | 60.3 | 4.22 | 11.7 |
| | Found | 59.7 | 4.10 | 12.0 |
| $[\text{Fe}(\text{QDSB})(\text{OH}_2)_2](\text{ClO}_4)_2$ Ligand I | Calc. | 49.4 | 3.59 | 7.7 |
| | Found | 49.8 | 3.62 | 8.1 |
| II | Calc. | 35.3 | 2.96 | 9.1 |
| | Found | 36.1 | 2.92 | 8.6 |
| III | Calc. | 45.8 | 3.85 | 8.2 |
| | Found | 45.9 | 4.04 | 8.2 |
| IV | Calc. | 30.8 | 3.33 | 10.3 |
| | Found | 31.3 | 3.20 | 9.6 |
| $[\text{Fe}(\text{HXSb})](\text{ClO}_4)_2$ | Calc. | 45.9 | 4.30 | 12.3 |
| | Found | 45.9 | 4.20 | 11.9 |
| (ii) <u>Neutral iron(II) compounds</u> | | | | |
| $\text{Fe}(5\text{-NO}_2\text{phen})_2(\text{CN})_2 \cdot 2\text{H}_2\text{O}$ | Calc. | 52.5 | 3.05 | 18.9 |
| | Found | 51.7 | 3.16 | 17.9 |
| $\text{Fe}(5\text{-NO}_2\text{phen.CN})_2(5\text{-NO}_2\text{phen})$ | Calc. | 54.5 | 3.25 | 18.4 |
| | Found | 53.7 | 3.20 | 17.8 |
| $\text{Fe}(\text{HDSB})_2(\text{CN})_2 \cdot 0.5\text{H}_2\text{O}$ | Calc. | 68.8 | 4.71 | 16.9 |
| | Found | 68.0 | 4.80 | 16.4 |
| $\text{Fe}(\text{QDSB})(\text{CN})_2 \cdot 0.5\text{H}_2\text{O}$ | Calc. | 69.2 | 4.17 | 15.1 |
| | Found | 68.5 | 3.82 | 14.1 |
| | | | | O Fe |
| | | | | 1.3 9.1 |
| | | | | 3.8 8.8 |

A Compound of the type $\text{Fe}(\text{5-NO}_2\text{phen.CN})_2(\text{5-NO}_2\text{phen})^\dagger$

This compound was produced when the preparation of $\text{Fe}(\text{5-NO}_2\text{phen})_2(\text{CN})_2$ was attempted by the method used for the unsubstituted analogue.

On addition of an aqueous solution of potassium cyanide to one of the $[\text{Fe}(\text{5-NO}_2\text{phen})_3]^{2+}$ cation, there was an immediate precipitation of a dark red material. This was filtered, washed thoroughly with water to remove any unreacted precursors. It was then washed with ethanol, ether and dried in vacuo over phosphorus pentoxide at room temperature.

The products of the reactions of cyanide ion with the ter- and hexadentate Schiff's base complexes of iron(II) could not be isolated in a pure state. The latter product has been deduced to be a species of the form $[\text{Fe}(\text{HXSb}')(\text{CN})_3]^-$, where HXSb' is a terdentate residue of the hexadentate ligand, the remainder of the ligand being uncoordinated (see chapter 8).

(ii) KINETICS

All kinetic runs were performed in the thermostatted cell compartment of a Pye Unicam SP800A recording spectrophotometer. For studies at ambient temperatures, the cell compartment was thermostatted to within $\pm 0.05^\circ$ using a flow of water from a constant temperature water bath. For high temperature kinetics, an electrical thermostating system was employed, which was calibrated over the range 323-375 K, within $\pm 0.5^\circ$. Optical density values were monitored at positions of maximum difference between reactant and product spectra for the

[†] [See section 9.3(iii).]

appropriate complexes. All such wavelengths were in the visible region, where none of the components of the reaction mixtures except the iron(II) complexes showed any significant absorption. All kinetic runs were at least duplicated, the reported results being the mean results of at least two measurements. Observed first-order rate constants were computed in the usual way (see chapter 2).

Due to differences in the properties, e.g. solubilities, reactivities, of the complexes studied in this chapter, the conditions (temperature, ionic strength, solvent composition) under which the kinetic studies were made vary somewhat between these complexes. Hence, such conditions used in the kinetic studies of the various complexes are summarised below:-

(i) Schiff's base complexes

| Complex Cation | Solvent | Temperature/K | Reagent | Ionic Strength ^a /mol dm ⁻³ |
|--|------------|---------------|-----------------|--|
| [Fe(BDSB) ₃] ²⁺ | Water | Several | CN ⁻ | 0.40 |
| | " | 298.2 | H ⁺ | |
| [Fe(TDSB) ₂] ²⁺ | 30% % MeOH | " | CN ⁻ | 0.40 |
| [Fe(QDSB)(OH ₂) ₂] ²⁺ | | | | |
| ligand (I) | 30% % MeOH | " | CN ⁻ | 1.33 |
| " (II) | " " | " | " | 1.33 |
| " (III) | " " | " | " | 1.33 |
| " (IV) | " " | " | " | 1.33 |
| [Fe(HXSB)] ²⁺ | Water | 281.2 | CN ⁻ | 0.40 |
| | " | " | H ⁺ | |

^a Ionic strength was maintained with potassium nitrate.

(ii) Fe(LL)₂(CN)₂ Complexes

| LL | Solvent | Temperature/K | Reagent | Ionic Strength ^a /mol dm ⁻³ |
|-----------|-----------------------|-----------------------|-----------------|--|
| phen | Water | 373.5 | CN ⁻ | 0.100 |
| 5-Cl phen | " | " | " | " |
| bipy | " | various (343.9-356.7) | " | 0.667 |
| | 30% Glycol | 356.7 | " | " |
| | " n ^o PrOH | " | " | " |
| | " DMSO | " | " | " |

^a Ionic strength was maintained with potassium nitrate.

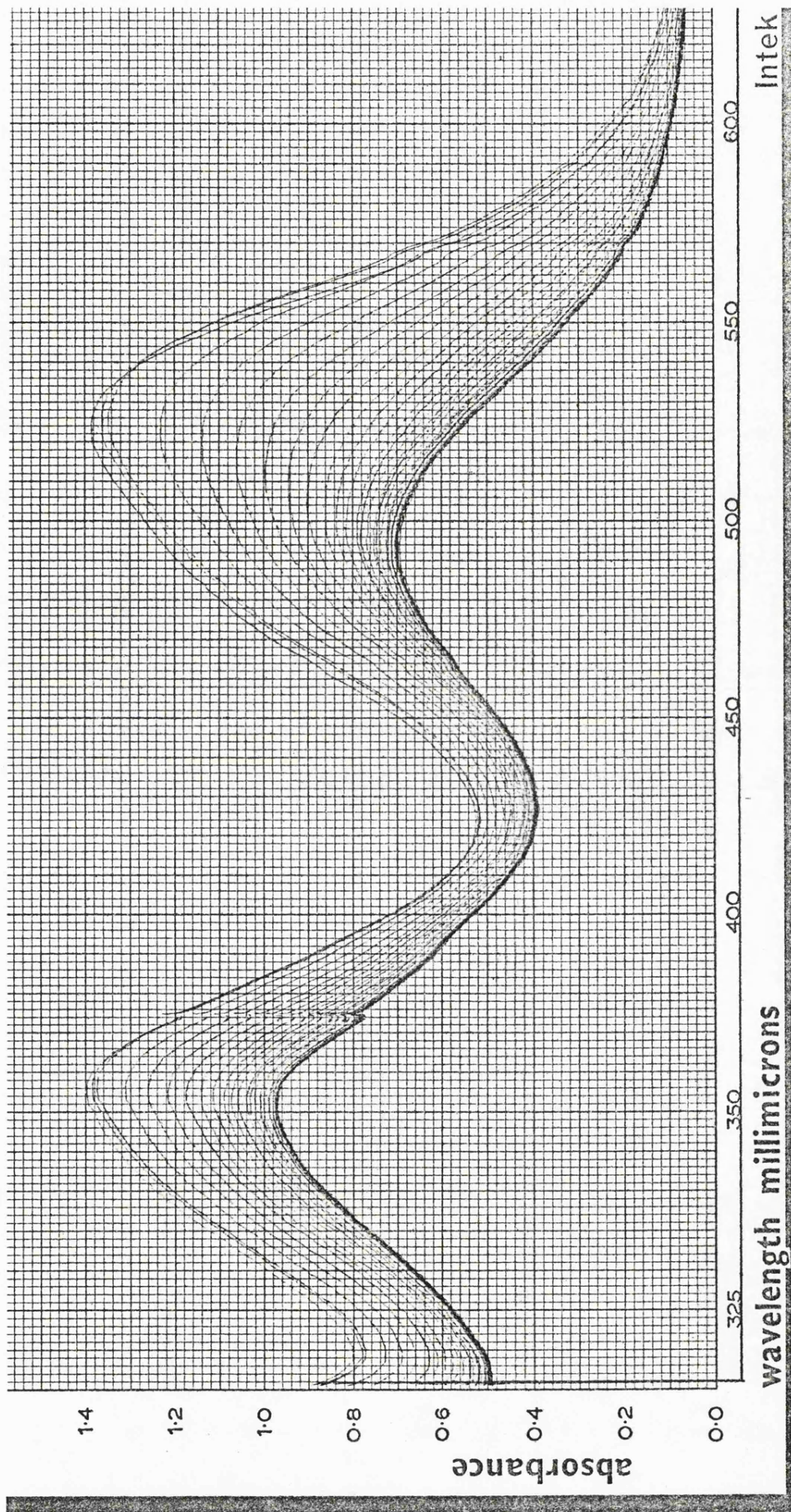
9.3 RESULTS AND DISCUSSION

(i) Kinetics of Reactions of Fe(LL)₂(CN)₂-Type Complexes

At ambient temperatures, substitution reactions of compounds of the type Fe(LL)₂(CN)₂ are extremely slow, for example 1,10-phenanthroline reacts with Fe(bipy)₂(CN)₂ at 308.2 K with a first-order rate constant of $2.8 \times 10^{-6} \text{ s}^{-1}$ in aqueous solution [9.18]. Hence for convenience the kinetics of the reactions of such compounds have been measured at elevated temperatures.

Figure 9.01 shows a variable wavelength repeat scan of the visible spectrum (700-450 nm) of a reaction mixture of Fe(bipy)₂(CN)₂ and a large excess of cyanide ion in aqueous solution at 356.7 K. From this there appear to be two distinct stages in the reaction, the first relatively fast stage produces a slight change in the wavelength of maximum

Figure 9.01 Variable wavelength repeat-scan of the UV / visible spectrum of a mixture of an excess of cyanide ion and 3×10^{-4} mol dm $^{-3}$ of $\text{Fe}(\text{bipy})_2(\text{CN})_2$, in aqueous solution at 356.7 K.



absorption (from 524 nm to 526 nm) of the complex, with the corresponding production of an isosbestic point at 538 nm; the second slower stage of the reaction results in a decrease in absorbance by 50% (from 1.38 to 0.69 absorbance units). This is consistent[†] with the loss of one of the two chromophoric units in the compound, i.e. a bipy ligand, producing the tetracyano(2,2'-bipyridyl)iron(II) anion, $[\text{Fe}(\text{bipy})(\text{CN})_4]^{2-}$. This has previously been shown to be the product of the reaction, and has been thoroughly characterised [9.16].

The rate constant for the first stage of the reaction could not be measured accurately, due to the very small difference in optical densities between the visible spectra of $\text{Fe}(\text{bipy})_2(\text{CN})_2$ and the product of the first stage of the reaction. The 1,10-phenanthroline and 5-chloro 1,10-phenanthroline analogues of $\text{Fe}(\text{bipy})_2(\text{CN})_2$, $\text{Fe}(\text{phen})_2(\text{CN})_2$ and $\text{Fe}(5\text{-Clphen})_2(\text{CN})_2$ were also found to react with cyanide ion in aqueous solution at high temperatures in two distinct stages, although at much slower rates than in the bipy case. The first stages of these systems was found to proceed with sufficient optical density change for the first-order rate constants to be observed, in the presence of large excesses of cyanide ion. Table 9.02 lists these rate constants for the reactions of $\text{Fe}(\text{phen})_2(\text{CN})_2$ and $\text{Fe}(5\text{-Clphen})_2(\text{CN})_2$ with cyanide ion in aqueous solution at 373.5 K. The amounts of solute in these reaction mixtures proved to be sufficient to elevate the boiling points of the solutions beyond this temperature.

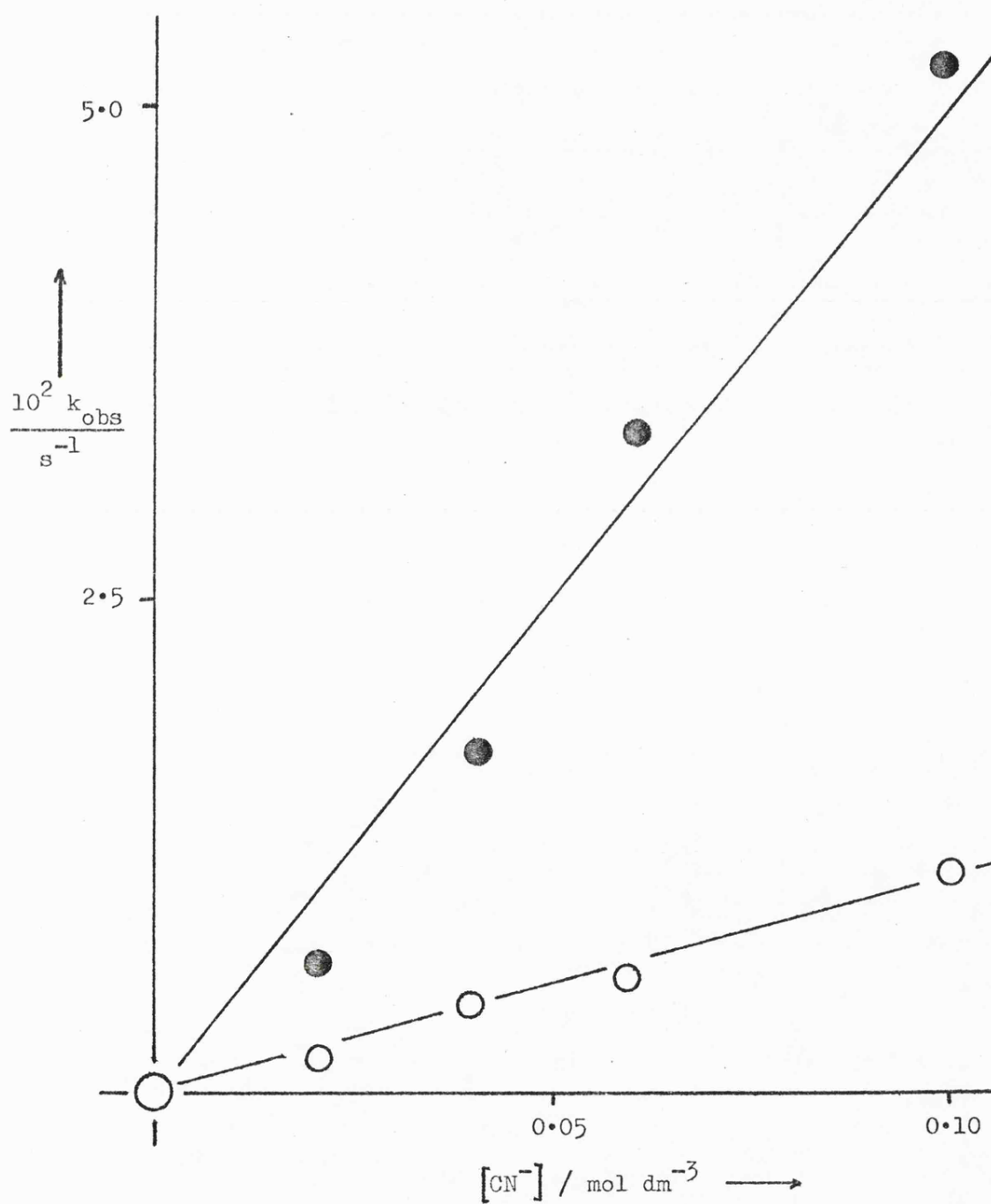
Due to the limited optical density changes for these reactions, the measured rate constants are not as accurate as would be desired,

[†] $\epsilon_{\max}([\text{Fe}(\text{LL})_3]^{2+}) : \epsilon_{\max}(\text{Fe}(\text{LL})_2(\text{CN})_2) : \epsilon_{\max}([\text{Fe}(\text{LL})(\text{CN})_4]^{2-}) \simeq 3:2:1$ [9.04]

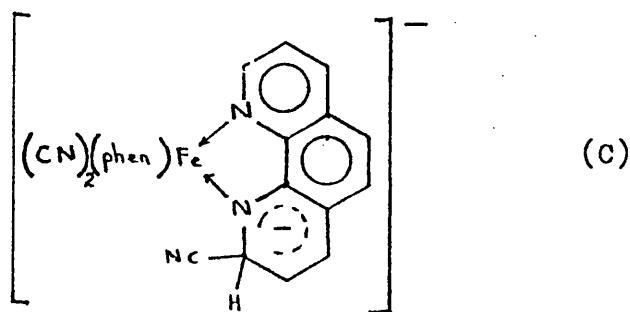
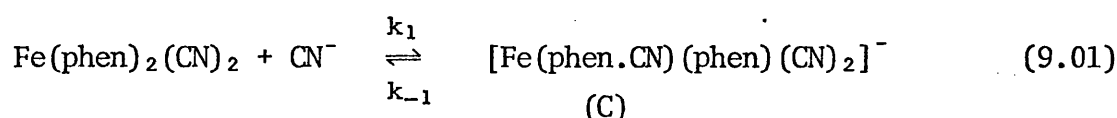
TABLE 9.02 Observed first-order rate constants, k_{obs} , for both stages of the reactions of cyanide ion with the compounds $\text{Fe}(\text{X-phen})_2(\text{CN})_2$, where $\text{X} = \text{H}$ or 5-Cl , over a range of cyanide ion concentrations, in aqueous solution at 373.5 K . Ionic strength = 0.10 mol dm^{-3} (maintained with potassium nitrate).

| <u>1st Stage</u> | $\frac{[\text{CN}^-]}{\text{mol dm}^{-3}}$ | X | |
|------------------|--|---------------------------------------|------|
| | | H | 5-Cl |
| | | $10^2 k_{\text{obs}} / \text{s}^{-1}$ | |
| | 0.02 | 0.143 | 0.65 |
| | 0.04 | 0.446 | 1.71 |
| | 0.06 | 0.554 | 3.32 |
| | 0.10 | 1.10 | 5.21 |
| | | | |
| <u>2nd Stage</u> | | $10^4 k_{\text{obs}} / \text{s}^{-1}$ | |
| | 0.02 | 3.03 | 5.29 |
| | 0.04 | 3.10 | 5.35 |
| | 0.06 | 2.96 | 5.38 |
| | 0.10 | 2.81 | 5.30 |

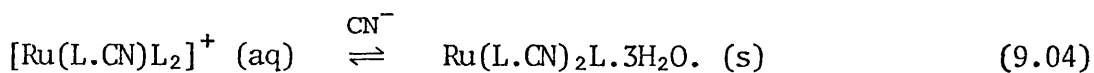
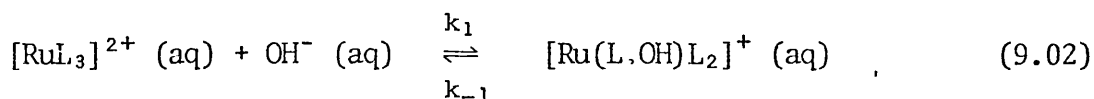
Figure 9.02 Dependence of the observed first-order rate constants, k_{obs} , on cyanide ion concentration, for the reaction of cyanide ion with $\text{Fe}(\text{phen})_2(\text{CN})_2$ (\bigcirc) and with $\text{Fe}(5\text{-Clphen})_2(\text{CN})_2$ (\bullet), in aqueous solution, at 373.5 K.



but repeated determinations have produced tolerable results. These results suggest a first-order dependence on $[\text{CN}^-]$, the correlation line between k_{obs} and $[\text{CN}^-]$ passing through the origin, within experimental error. The second-order rate constants measured from the slope of the plot (Figure 9.02) of k_{obs} vs $[\text{CN}^-]$, are 1.0 & $5.2 \times 10^{-4} \text{ dm}^3 \text{ mol}^{-1} \text{ s}^{-1}$ for the reactions involving $\text{Fe}(\text{phen})_2(\text{CN})_2$ and $\text{Fe}(5\text{-Clphen})_2(\text{CN})_2$ respectively. Such a first-order dependence on $[\text{CN}^-]$ is commonplace in the reactions of this nucleophile with iron(II) complexes containing N-heterocyclic ligands (see section 9.1). This behaviour is consistent with the formation of a dicyano(phen.CN)(phen)iron(II) species (C), for the reaction of $\text{Fe}(\text{phen})_2(\text{CN})_2$ with cyanide ion:-

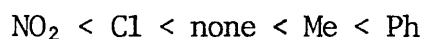


An analogous addition of a nucleophile to a ligand of the $[\text{Ru}(5\text{-NO}_2\text{phen})_3]^{2+}$ cation, for the nucleophiles CN^- [9.14], OH^- [9.19], MeO^- [9.15] and EtO^- [9.15] has been well documented. The kinetics of, for example the reaction of cyanide ion with $[\text{Ru}(5\text{-NO}_2\text{phen})_3]^{2+}$ have been shown [9.14] to be consistent with the formation of the cation $[\text{Ru}(5\text{-NO}_2\text{phen.CN})(5\text{-NO}_2\text{phen})_2]^+$ in competition with a dead-end equilibrium involving $[\text{Ru}(5\text{-NO}_2\text{phen})_3]^{2+}$ and hydroxide ion, as shown by equations (9.02-04):



(where L = 5-NO₂phen)

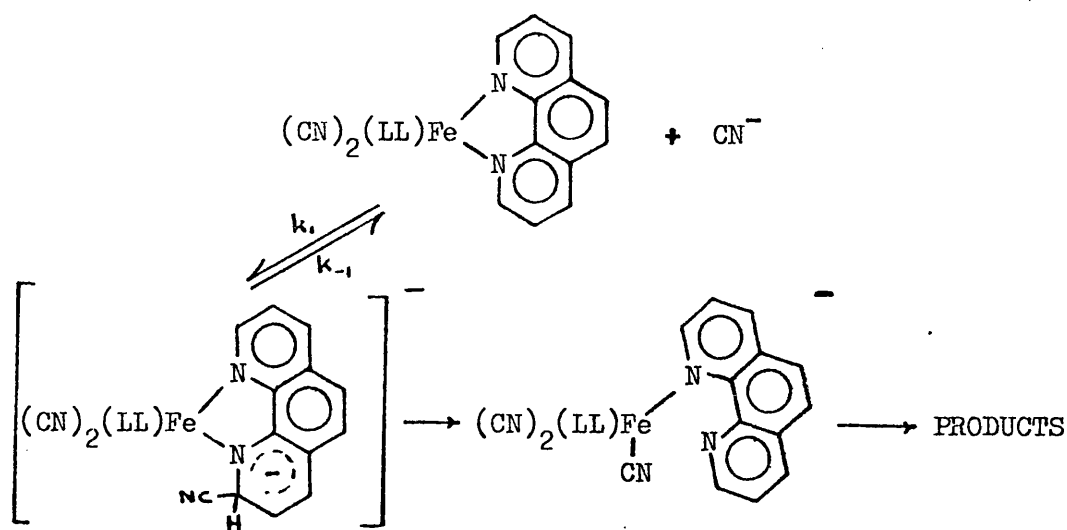
Hence we may assume similar reactions to be occurring in the Fe(LL)₂(CN)₂ + CN⁻ systems, but without precipitation of a final product. The kinetics of the second stage of these reactions have also been studied at 373.5 K in aqueous solution for the Fe(phen)₂(CN)₂ compound and its 5-Clphen analogue. The observed first-order rate constants for this reaction, i.e. the production of [Fe(LL)(CN)₄]²⁻ from [Fe(LL.CN)(LL)(CN)₂]⁻ (where LL = phen or 5-Cl phen), are reported in Table 9.02, for a range of cyanide ion concentrations. It appears that these rate constants are independent of [CN⁻], within experimental error. The first-order rate constants, k₁, are 2.98 x 10⁻⁴ and 5.34 x 10⁻⁴ s⁻¹ for the reactions involving the phen and 5-Cl phen compounds respectively. That the rate of reaction of the 5-Cl phen complex is faster than the unsubstituted analogue is consistent with known differences in ligand basicities, and hence reactivities, where the trend in reactivities for 5-substituted phenanthrolines is:-



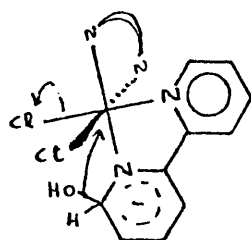
(see, e.g. chapter 6 and refs. therein).

The fact that these second-stage reactions have rates which are independent of [CN⁻] indicate that the rate-determining step is an intramole-

cular shift of cyanide from the ligand to the iron(II) centre followed by rapid loss of a ligand:-



A similar shift of a nucleophile from a ligand to a metal ion has been envisaged [9.20] to explain the observed promotion by base of hydrolysis of the first chloride ion from $[\text{M}(\text{LL})_2\text{Cl}_2]^+$ (where LL = bipy or phen; M = Co or Cr) thus:-



The second stage of the reaction between $\text{Fe}(\text{bipy})_2(\text{CN})_2$ and cyanide ion has been studied in aqueous solution over the temperature range 343.9 - 356.7 K for a variety of cyanide ion concentrations. Table 9.03 reports the observed first-order rate constants for this study, which indicate this reaction, like those of $\text{Fe}(\text{phen})_2(\text{CN})_2$ and

TABLE 9.03 Observed first-order rate constants, k_{obs} , for the second-stage of the reaction of cyanide ion with $\text{Fe}(\text{bipy})_2(\text{CN})_2$ over a range of cyanide ion concentrations and temperatures, in aqueous solution.

| $\frac{[\text{CN}^-]}{\text{mol dm}^{-3}}$ | T / K | $10^5 k_{\text{obs}} / \text{s}^{-1}$ |
|--|-------|---------------------------------------|
| 0.167 | 343.9 | 2.61 |
| 0.333 | " | 2.63 |
| 0.500 | " | 2.43 |
| 0.667 | " | 2.55 |
| 0.167 | 348.7 | 6.90 |
| 0.333 | " | 6.48 |
| 0.500 | " | 6.53 |
| 0.667 | " | 6.70 |
| 0.167 | 350.6 | 10.1 |
| 0.333 | " | 9.66 |
| 0.500 | " | 10.2 |
| 0.667 | " | 9.83 |
| 0.167 | 352.1 | 12.9 |
| 0.333 | " | 12.8 |
| 0.500 | " | 11.6 |
| 0.667 | " | 12.8 |
| 0.167 | 356.7 | 30.7 |
| 0.333 | " | 30.8 |
| 0.500 | " | 29.4 |
| 0.667 | " | 31.3 |

$\text{Fe}(\text{5-Clphen})_2(\text{CN})_2$ with cyanide ion, to be independent of $[\text{CN}^-]$. From the variable temperature study, an activation energy of $47 \pm 2 \text{ kJ mol}^{-1}$ was computed (Appendix 2, Program 4), with an A factor of $\text{antilog}_{10}(25.3 \pm 1.0)$. Hence, the activation enthalpy and entropy of the reaction are 194 kJ mol^{-1} and $+228 \text{ J K}^{-1} \text{ mol}^{-1}$ respectively at 348.7 K .

The rate constants for the reaction of $\text{Fe}(\text{bipy})_2(\text{CN})_2$ with cyanide ion were also measured in several binary aqueous mixtures at 356.6 K . The observed first-order rate constants for these mixtures are tabulated below:-

| Solvent Mixture | $10^4 k_{\text{obs}}/\text{s}^{-1}$ | |
|---------------------------|-------------------------------------|---|
| Water | 3.08 | $[\text{CN}^-] = 0.667 \text{ mol dm}^{-3}$ |
| 30% ⁿ Propanol | 3.15 | Temp. = 356.6 K . |
| 30% Ethylene Glycol | 2.97 | |
| 30% Dimethyl Sulphoxide | 3.44 | |

The kinetics of the above reaction were studied at 356.6 K in several binary aqueous mixtures, for $[\text{CN}^-] = 0.667 \text{ mol dm}^{-3}$. There appears to be very little solvent sensitivity for this reaction, which suggests very similar solvation properties of the initial state and transition state. This favours the transfer of cyanide ligand to the iron(II) centre as the rate-determining step, where there would be very little peripheral change from the initial state to the transition state.

The solvent sensitivity of this reaction is very similar in magnitude to those for the nucleophilic substitution reactions of the $[\text{Fe}(\text{CN})_5\text{L}]^{n-}$ anion (chapter 2) and the acid aquation of the $[\text{Fe}(\text{5-NO}_2\text{phen})_3]^{2+}$ cation (chapter 3); it is very different from the highly solvent sensitive second-order reaction of cyanide ion with the

$[\text{Fe}(\text{bipy})_3]^{2+}$ cation [9.21].

The fact that this first-order reaction is one of a species other than $\text{Fe}(\text{bipy})_2(\text{CN})_2$ is supported by a kinetic study of substitution by 1,10-phenanthroline at the authentic $\text{Fe}(\text{bipy})_2(\text{CN})_2$ [9.18]. This reaction was also found to be independent of both the substitution and the concentration of added phen, and was found to have a rate constant of $2.8 \times 10^{-6} \text{ s}^{-1}$ for unsubstituted phen, and $3.0 \times 10^{-6} \text{ s}^{-1}$ for $(5\text{-SO}_3\text{phen})^-$, at 308.2 K in aqueous solution. These values are very different from the one for the second stage of the reaction of cyanide ion with $\text{Fe}(\text{bipy})_2(\text{CN})_2$ under the same conditions (found by extrapolation of an Arrhenius plot back to 308.2 K), of $3.0 \times 10^{-8} \text{ s}^{-1}$. Similarly, the value for the rate of acid aquation [9.22] of $\text{Fe}(\text{bipy})_2(\text{CN})_2$ in aqueous solution at 333.2 K is $1.6 \times 10^{-6} \text{ s}^{-1}$, as compared with a value of $2.5 \times 10^{-6} \text{ s}^{-1}$ for the second-stage of the reaction of cyanide ion with this complex. Such differences would be expected if the rate determining step in the cyanide reaction was the dissociation of an Fe-N bond to a 6-cyano-2,2'-bipyridyl ligand, since this Fe-N bond should be slightly weaker than a normal bipy one since there is some disruption of the aromaticity of the ligand.

(ii) Reaction of Cyanide Ion with the $[\text{Fe}(5\text{-NO}_2\text{phen})_3]^{2+}$ Cation

A red compound, sparingly soluble in most common solvents, was isolated from the reaction of cyanide ion with the $[\text{Fe}(5\text{-NO}_2\text{phen})_3]^{2+}$ cation in aqueous solution. The results of a C, H and N microanalysis (Table 9.01) suggested the presence of three 5- NO_2phen ligands and two cyanide ligands in this iron(II) complex. Figure 9.03 shows the electronic spectrum of this complex ($\lambda_{\text{max}} = 532 \text{ nm}$) compared with that of the $[\text{Fe}(5\text{-NO}_2\text{phen})_3]^{2+}$ cation ($\lambda_{\text{max}} = 510 \text{ nm}$). We can see that

Figure 9.03 Visible spectra of (i) the $[\text{Fe}(\text{5-NO}_2\text{phen})_3]^{2+}$ cation and (ii) its cyanide adduct in aqueous solution at 298.2 K; Concentration of each species = $1.1 \times 10^{-4} \text{ mol dm}^{-3}$.

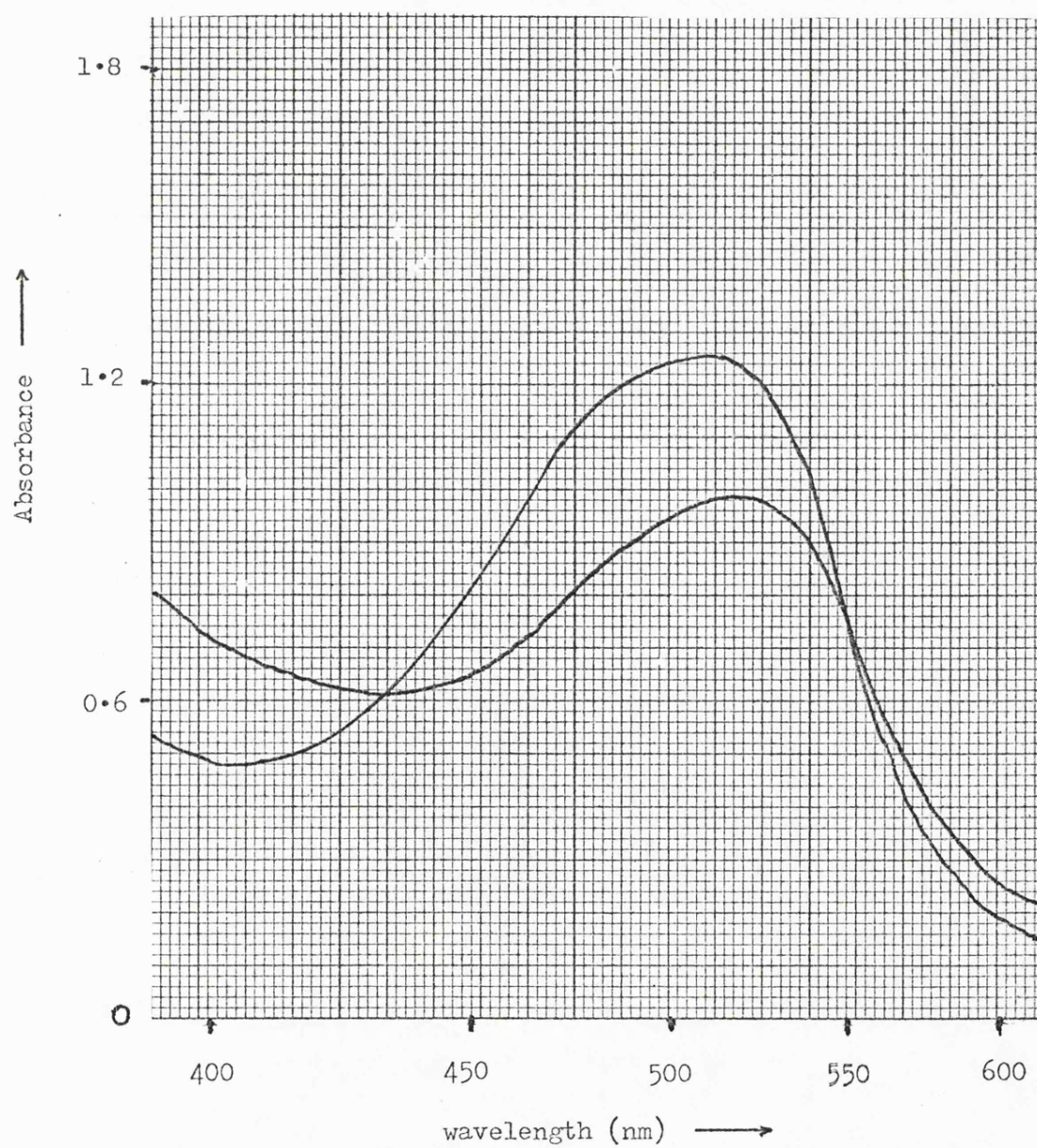
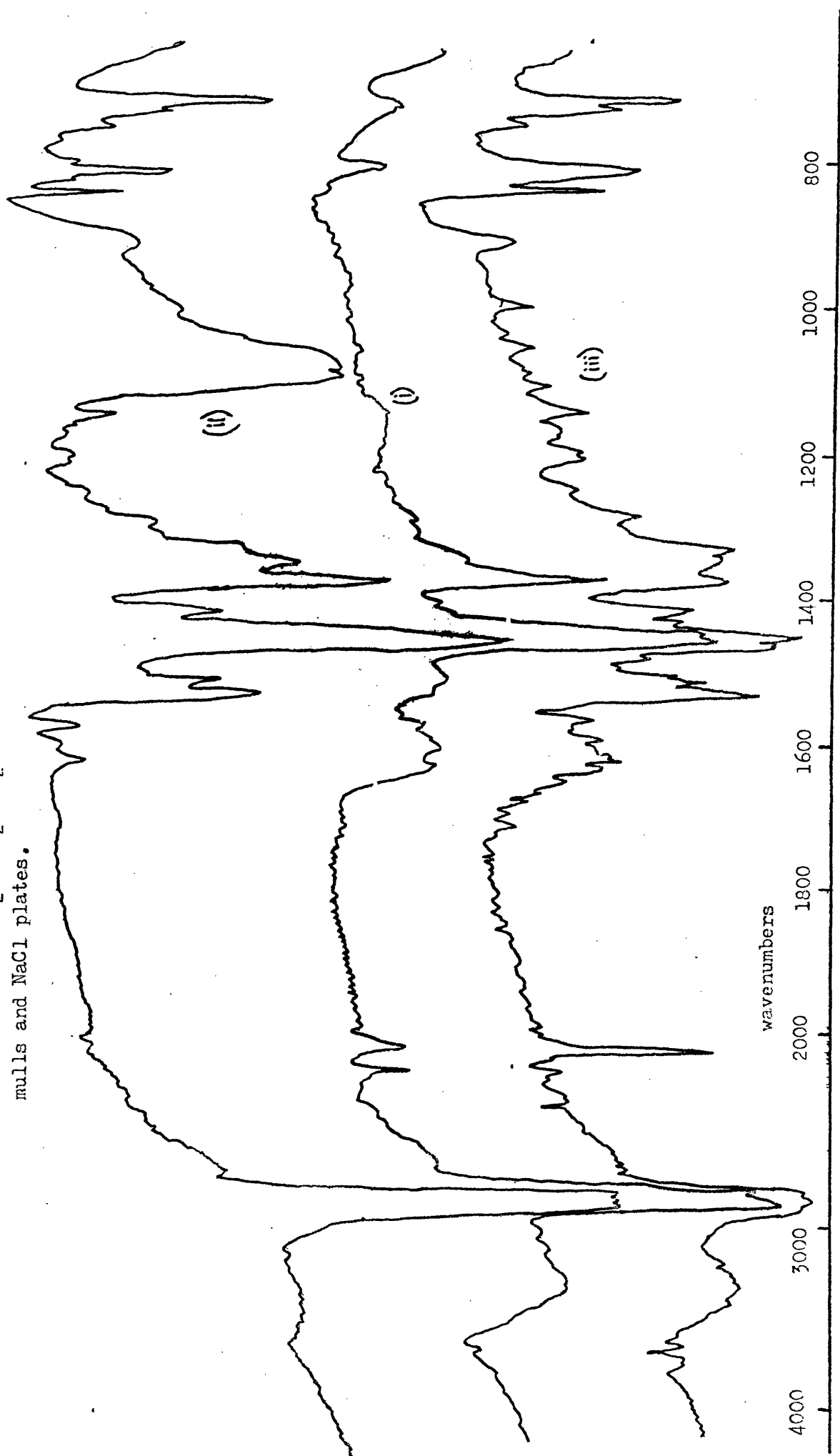


Figure 9.04 Infrared spectra of (i) $\text{Fe}(\text{5-NO}_2\text{phen.CN})_2$, (ii) $\text{Fe}(\text{5-NO}_2\text{phen})_2$ (ClO₄)⁻ and (iii) $\text{Fe}(\text{5-NO}_2\text{phen})_2(\text{CN})_2$; scans over 4000 - 650 wavenumbers, using nujol mulls and NaCl plates.



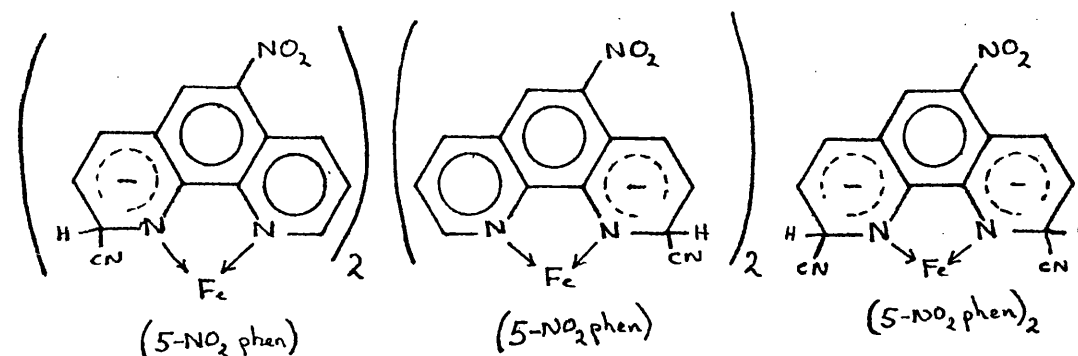
there are significant differences between these spectra. These differences suggest that the complex in question is not simply the cyanide salt of the tris-(5-nitro 1,10-phenanthroline)iron(II) cation. Such an insoluble salt is formed for the thiocyanate anion [9.23], the electronic spectrum of which is identical with that of the tris-complex cation.

Figure 9.04 shows a comparison of the infra-red spectra of (i) the red cyano-adduct of $[\text{Fe}(\text{5-NO}_2\text{phen})_3]^{2+}$, (ii) a sample of $[\text{Fe}(\text{5-NO}_2\text{phen})_3](\text{ClO}_4)_2$ and (iii) an authentic sample of $\text{Fe}(\text{5-NO}_2\text{phen})_2(\text{CN})_2$. Here, we see several noteworthy features which differ between these spectra. In spectrum (i), the CN stretch at $2190\text{--}2200\text{ cm}^{-1}$ is higher than that expected for ionic cyanide (ca. 2080 cm^{-1}), and greater than any absorption tabulated [9.24] for cyanide coordinated to metal ions ($2000\text{--}2163\text{ cm}^{-1}$; $\text{Hg}(\text{CN})_2$ has an anomalous value of 2194 cm^{-1}). The frequency is rather in the region of nitrile absorptions. The absorption at 2060 cm^{-1} is also present in the spectrum of $\text{Fe}(\text{5-NO}_2\text{phen})_2(\text{CN})_2$, and in that of $\text{Fe}(\text{phen})_2(\text{CN})_2$. Thus it is the absorption due to the CN stretch of cyanide coordinated to iron(II). A second striking feature is the large number of new bands in (i) in the region $1650\text{--}1150\text{ cm}^{-1}$ as compared with (ii), and also the changes in the aromatic 'fingerprint' region at ca. 665 and 805 cm^{-1} from (ii) to (i). This indicates that there has been a reaction between the cyanide ion and the ligand of $[\text{Fe}(\text{5-NO}_2\text{phen})_3]^{2+}$.

Such variations in spectra are analogous to those observed [9.14] in the reaction of cyanide ion with the $[\text{Ru}(\text{5-NO}_2\text{phen})_3]^{2+}$ cation, where a dicyano product was isolated, and deduced to be of the form

$\text{Ru}(\text{L}.\text{CN})_2\text{L}^{\dagger}$ or $\text{Ru}(\text{L}(\text{CN})_2)_2\text{L}_2$ (where $\text{L} = 5\text{-NO}_2\text{phen}$).

Hence, by comparison, we can deduce the red material isolated from the reaction of cyanide ion with the $[\text{Fe}(5\text{-NO}_2\text{phen})_3]^{2+}$ cation to be of the form $\text{Fe}(5\text{-NO}_2\text{phen}.\text{CN})_2(5\text{-NO}_2\text{phen})$, where the cyanide groups have attacked the 2- or 9-positions. Diagram 9.02 shows these various



bis (9- isomer)

bis (2- isomer)

2,9- isomer

Diagram 9.02

possible isomers of the compound of general formula $\text{Fe}(5\text{-NO}_2\text{phen})_3.(\text{CN})_2$.

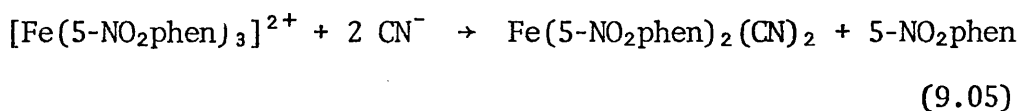
Unfortunately, the compound was insufficiently soluble in any solvent tried to permit the measurement of its ^1H n.m.r. spectrum. Hence the exact site at which the cyanides attack could not be elucidated. Reaction of methoxide with the $[\text{Ru}(5\text{-NO}_2\text{phen})_3]^{2+}$ cation in methanolic solution has been shown [9.15] to proceed via addition of $[\text{OMe}]^-$ to the 2-position of each of the three heterocyclic ligands. However, we cannot assume the reaction of such cations with cyanide ion to be analogous, since hydroxide ion has been shown [9.25] to add to the 9-position in its reaction with the same $[\text{Ru}(5\text{-NO}_2\text{phen})_3]^{2+}$ cation.

[†][The two possible sites of attack, the 2- or 9-positions were not differentiated between, and so the true nature of the isomer isolated was not determined.]

It has been noted [9.15] that the 2-position is less (although slightly) electrophilic than the 9-position. Hence, although it is at present impossible to differentiate between the 2- and 9- isomers, we can by analogy with the corresponding ruthenium(II)-methoxide species conclude that the red material isolated from the reaction of cyanide ion with $[\text{Fe}(\text{5-NO}_2\text{phen})_3]^{2+}$ cation is of the form $\text{Fe}(\text{5-NO}_2\text{phen.CN})_2(\text{5-NO}_2\text{phen})$.

The presence of a band at 2060 cm^{-1} in spectrum (ii), which indicates the presence of cyanide coordinated to iron(II), is consistent with there being a mixture of $\text{Fe}(\text{L.CN})_2\text{L}$ and $\text{FeL}_2(\text{CN})_2$ present ($\text{L} = \text{5-NO}_2\text{phen}$). During the preparations of the dicyano adducts of the $[\text{Fe}(\text{5-NO}_2\text{phen})_3]^{2+}$ cation, it was found that the lower the reaction temperature, and the faster the speed with which the preparation was performed, the greater the proportion of the band at $2190\text{--}2200\text{ cm}^{-1}$ relative to that at 2060 cm^{-1} was obtained, in the i.r. spectrum of the isolated product of the reaction.

This suggests that the $\text{Fe}(\text{5-NO}_2\text{phen.CN})_2(\text{5-NO}_2\text{phen})$ species is an intermediate in the reaction:-



where there must follow rearrangement of the intermediate to form the final product. At higher reaction temperatures, the rearrangement of the intermediate will be accelerated, thus lowering the yield of intermediate, and increasing that of the bis-cyano bis(ligand) product. In the preparation of pure $\text{Fe}(\text{5-NO}_2\text{phen})_2(\text{CN})_2$, refluxing of the reaction mixture in methanol produced the required product which gave the i.r. spectrum shown in Figure 9.04 (ii). Here there is no appreciable band due to cyanide coordinated to the heterocyclic ligand, but a strong band

due to the CN stretch of a cyanide coordinated to iron(II).

Such a course in the reaction of the $[\text{Fe}(\text{5-NO}_2\text{phen})_3]^{2+}$ cation with cyanide ion (and hydroxide ion) clearly explains the bimolecular nature of the kinetics of such reactions [9.26], the rate determining step being attack of the nucleophile at the heterocyclic ligand.

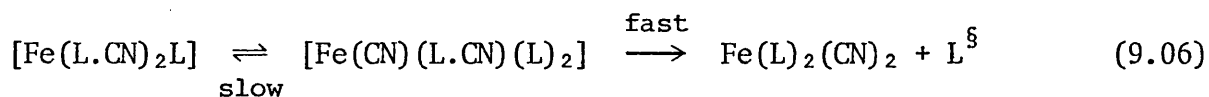
In nucleophilic substitution reactions of other substituted 1,10-phenanthroline analogues of the $[\text{Fe}(\text{5-NO}_2\text{phen})_3]^{2+}$ cation, no anomalous spectral changes have been observed like those of the 5-nitro case. However, the kinetic behaviour of these analogues has been of the same bimolecular nature, having rate laws with dominant terms in $[\text{Fe}(\text{X-phen})_3]^{2+}[\text{Nu}^-]$ (where $\text{Nu} = \text{CN}^-$ or OH^-). However, such intermediates as those discussed above for the 5- NO_2phen complexes do not appear to be stable for other substituted derivatives, and complete dissociation in basic solution occurs where, for reactions of cyanide and hydroxide ions with iron(II) complexes of aromatic diimine ligands, a ligand is ultimately lost [9.03,04,07,26,27]. Such hypothetical intermediates for these complexes may be expected to be very much less stable than those of the 5- NO_2phen case, since the 2- (and 9-) positions are not activated to the extent of the latter, where the NO_2 group is strongly electron withdrawing. Thus such intermediates may be expected to be transient intermediates only, which are not recognisable from conventional electronic spectra.

(iii) Kinetics of Reactions of $\text{Fe}(\text{5-NO}_2\text{phen.CN})_2(\text{5-NO}_2\text{phen})$ with Nucleophiles

The compound isolated from the reaction between cyanide ion and the $[\text{Fe}(\text{5-NO}_2\text{phen})_3]^{2+}$ cation was in turn found to react with cyanide and with hydroxide rapidly at ambient temperatures in aqueous solution.

Observed first-order rate constants for the reaction of this compound with cyanide and with hydroxide at 317.7 K in 30% by volume aqueous methanol solution are reported in Table 9.04. From a plot of k_{obs} versus $[\text{Nu}^-]$ (where $\text{Nu} = \text{CN}$ or OH), we see a first-order dependence of k_{obs} on both $[\text{CN}^-]$ and $[\text{OH}^-]$, with a value of k_{obs} at $[\text{Nu}^-] = \text{zero}$ common to both nucleophile. The second-order rate constants, calculated from the slopes of k_{obs} versus $[\text{Nu}^-]$ plots for cyanide ion and hydroxide ion were found to be 0.26 ± 0.02 and $0.033 \pm 0.001 \text{ dm}^3 \text{ mol}^{-1} \text{ s}^{-1}$ respectively. The first-order rate constants, i.e. the intercepts of these plots with the ordinate were 0.0027 ± 0.0004 and $0.0024 \pm 0.0001 \text{ s}^{-1}$ for $\text{Nu}^- = \text{CN}^-$ and OH^- respectively.

The rate of acid aquation of this complex in 0.05 mol dm^{-3} and 0.10 mol dm^{-3} sulphuric acid was measured as 0.69×10^{-3} and $0.76 \times 10^{-3} \text{ s}^{-1}$ respectively under the same conditions as for the reactions of the compound with CN^- and OH^- . Similarly, the rate of neutral solution dissociation of the complex, in 1×10^{-2} and $5 \times 10^{-3} \text{ mol dm}^{-3}$ EDTA^\dagger was found to be $0.53 \times 10^{-3} \text{ s}^{-1}$, being independent of $[\text{EDTA}]$. Hence we find that, as in the case of $\text{Fe}(\text{bipy})_2(\text{CN})_2$ above, the k_1 term in the reaction of $[\text{Fe}(5\text{-NO}_2\text{phen.CN})_2(5\text{-NO}_2\text{phen})]$ is not simply the dissociation of the complex. By analogy with the $\text{Fe}(\text{bipy})_2(\text{CN})_2$ system above, we can assign this k_1 term with the intramolecular transfer of cyanide from a ligand to the iron(II) centre:-



[†] [EDTA = Ethylenediaminetetraacetic acid, disodium salt.]

[§] [L = 5-NO₂phen.]

TABLE 9.04 Observed first-order rate constants, k_{obs} , for the reaction of the $[\text{Fe}(5\text{-NO}_2\text{phen.CN})_2(5\text{-NO}_2\text{phen})]$ species with cyanide and with hydroxide ions in 30 % by volume aqueous methanol, at 317.7 K; ionic strength = 0.21 mol dm^{-3} (maintained with sodium chloride).

| $\frac{[\text{Nu}]}{\text{mol dm}^{-3}}$ | Nu | |
|--|---------------------------------------|---------------|
| | CN^- | OH^- |
| | $10^2 k_{\text{obs}} / \text{s}^{-1}$ | |
| 0.002 | 0.298 | 0.273 |
| 0.004 | 0.349 | |
| 0.006 | 0.436 | |
| 0.008 | 0.491 | 0.289 |
| 0.010 | | 0.297 |
| 0.020 | 0.770 | |
| 0.040 | 1.31 | |
| 0.050 | | 0.412 |
| 0.100 | | 0.581 |
| 0.150 | | 0.753 |
| 0.180 | | 0.859 |

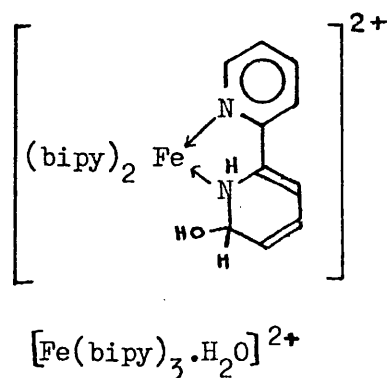
The second-order term involving $[\text{Nu}^-]$ in the rate law:-

$$\frac{-d [\text{complex}]}{dt} = (k_1 + k_2 [\text{Nu}^-]) [\text{complex}] \quad (9.07)$$

is consistent with further attack by Nu^- at a ligand of the complex.

Further attack at the ligand is feasible since the NO_2 -group is strongly electron-withdrawing, and makes the 2- (and 9-) positions of the ligand more susceptible to nucleophilic attack. Such activation was not present for the $\text{Fe}(\text{bipy})_2(\text{CN})_2$ and $\text{Fe}(\text{phen})_2(\text{CN})_2$ compounds, and no such first-order dependence on $[\text{Nu}^-]$ was observed for these systems. It is however, somewhat surprising that the second stage of the reaction of cyanide ion with $\text{Fe}(5\text{-Cl phen})_2(\text{CN})_2$ should be independent of $[\text{CN}^-]$, since the Cl - group is also electron-withdrawing, although to a lesser extent than NO_2 -.

The second-order rate constants [9.03, 26] for the loss of ligand on reaction with OH^- and CN^- from the $[\text{Fe}(5\text{-NO}_2\text{phen})_3]^{2+}$ cation in aqueous solution are 0.29 and $0.51 \text{ dm}^3 \text{ mol}^{-1} \text{ s}^{-1}$ respectively. The greater reactivity here of CN^- over OH^- is also observed in the reaction of these nucleophiles with $[\text{Fe}(5\text{-NO}_2\text{phen.CN})_2(5\text{-NO}_2\text{phen})]$. A complication to the above systems is the possibility of the presence of 'covalent hydrates', i.e. for $[\text{Fe}(\text{bipy})_3]^{2+}$ say, a covalent hydrate would be:-



Schilt [9.16] has shown the hydrates of $\text{Fe(LL)}_2(\text{CN})_2$ compounds and $[\text{Fe(LL)}(\text{CN})_4]^{2-}$ salts (below) for example to have anomalous magnetic behaviour.

Compound

| | |
|--|--|
| $\text{Fe(phen)}_2(\text{CN})_2 \cdot 2\text{H}_2\text{O}$ | $\text{K}_2[\text{Fe(bipy)}(\text{CN})_4] \cdot 3\text{H}_2\text{O}$ |
| $\text{Fe(bipy)}_2(\text{CN})_2 \cdot 3\text{H}_2\text{O}$ | $\text{K}_2[\text{Fe(phen)}(\text{CN})_4] \cdot 4\text{H}_2\text{O}$ |

However, for simplicity, this possible complication has been ignored. In the work involving reactions of Schiff's base complexes of iron(II) (below), this phenomenon of covalent hydration crops up again, and is dealt with in the relevant section.

In this work, a series of iron(II)-Schiff's base complexes have been prepared, having a variety of ligand denticities. The kinetics of their reactions with cyanide ion, and in one or two cases acid, have been measured and are discussed. Due to the variations in the types of complexes prepared, the complexes will be discussed according to the denticity of the Schiff's base ligand.

(iv) A tris-Bidentate Schiff's Base Complex of Iron(II)

The ligand synthesised in this work is that derived from the condensation of di-2-pyridyl ketone with p-toluidine (Diagram 9.03(a)). The structure of the tris-iron(II) cation is analogous to that of the tris-(2,2'-bipyridyl)iron(II) one, and is represented in Diagram 9.04. The visible spectrum contains a strong band at $\lambda_{\text{max}} = 597 \text{ nm}$, with a shoulder at 570 nm. Such a spectrum is characteristic of tris-(α, α' -diimine)iron(II) species [9.28], and is attributed to the intense iron-to-ligand charge-transfer band.

Diagram 9.03(a)

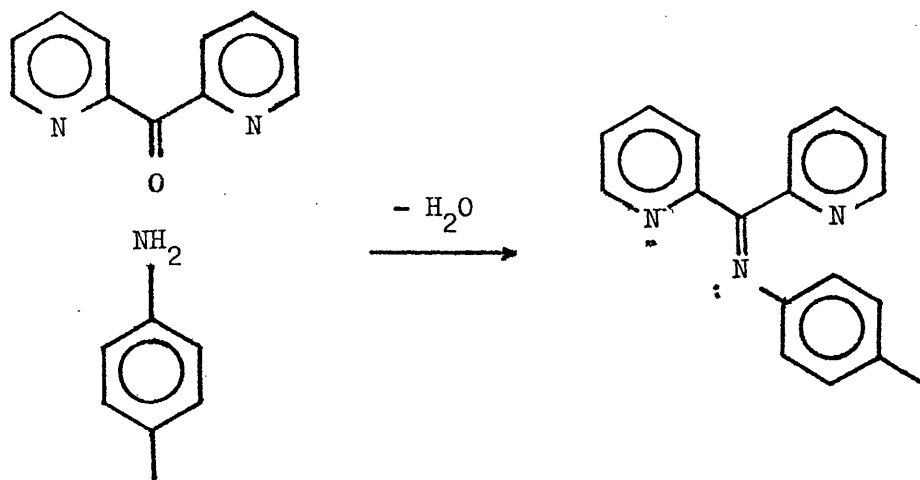


Diagram 9.03(b)

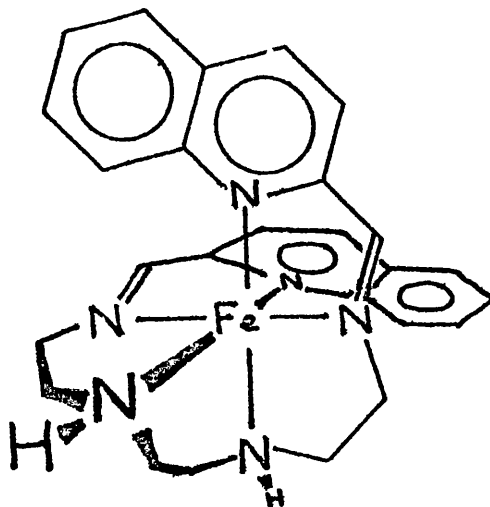
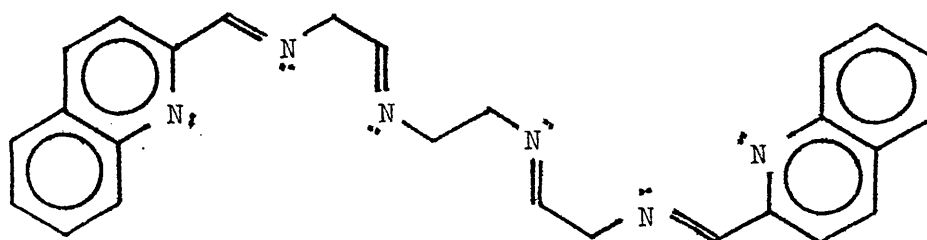


Diagram 9.03(c)



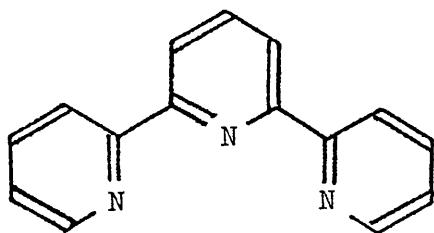
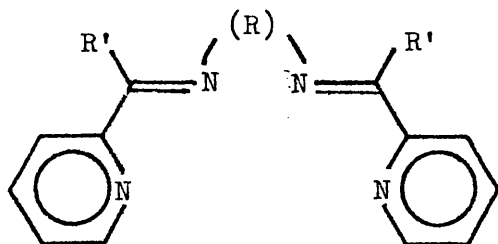


Diagram 9.03(d)



Substituent

Ligand

$R = C_6H_4$ (phenylene),

$R' = C_6H_5$

I

$R' = H$

II

$R = C_2H_4$,

$R' = C_6H_5$

III

$R' = H$

IV

Diagram 9.03(e)

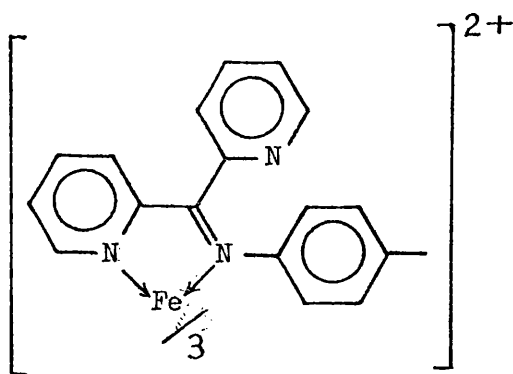


Diagram 9.04

Kinetics of Reaction with Cyanide Ion

The $[\text{Fe}(\text{PDSB})_3]^{2+}$ cation reacts with cyanide ion in aqueous solution, with a decrease in optical density of ca. 33%, producing a species having $\lambda_{\text{max}} = 601 \text{ nm.}$ in aqueous solution. The observed first-order rate constants, k_{obs} for the reaction of cyanide ion with the $[\text{Fe}(\text{BDSB})]^{2+}$ cation have been measured, for various concentrations of cyanide ion, in 30% by volume aqueous methanol solution[†] over a range of temperatures. A large excess of cyanide ion over complex was maintained in all kinetic runs, and good first-order conditions were observed over at least four half-lives of the reaction. These observations are reported in Table 9.05. Figure 9.05 is a representation of these results as a plot of k_{obs} against $[\text{CN}^-]$ for the various temperatures. We can see that the reaction is first-order in $[\text{CN}^-]$, a feature which is analogous to similar reactions of tris-(α, α' -diimine)iron(II)

[†][This solvent mixture was necessary because of the low solubility of the perchlorate salt of the iron(II) complex used in aqueous solution.]

TABLE 9.05 Observed first-order rate constants, k_{obs} , and derived second-order rate constants, k_2 , for the reaction of cyanide ion with the $[\text{Fe}(\text{BDSB})_3]^{2+}$ cation, for a range of cyanide ion concentrations and temperatures, in 30 % by volume aqueous methanol; ionic strength = 0.20 mol dm^{-3} (maintained with potassium nitrate).

| $\frac{[\text{CN}^-]}{\text{mol dm}^{-3}}$ | T / K | | | |
|--|--|-------|-------------------|-------|
| | 294.3 | 298.6 | 302.8 | 307.5 |
| | $10^3 k_{\text{obs}} / \text{s}^{-1}$ | | | |
| 0.010 | | | | 1.18 |
| 0.020 | | | | 1.81 |
| 0.025 | 0.646 | 0.916 | 1.83 | |
| 0.030 | | | | 2.77 |
| 0.040 | | | | 3.17 |
| 0.050 | 1.41 | 1.65 | 2.52 | 4.60 |
| 0.060 | | | | 5.11 |
| 0.075 | 2.10 | 2.68 | 5.42 | |
| 0.080 | | | | 7.85 |
| 0.100 | 2.67 | 3.84 | 6.72 | 8.99 |
| 0.125 | 3.28 | 4.52 | 8.48 | |
| 0.150 | 3.99 | 5.47 | 9.81 | |
| 0.175 | 4.62 | 6.69 | 11.3 ₆ | |
| 0.200 | 5.53 | 7.03 | 13.4 ₃ | |
| | $10^2 k_2 / \text{mol}^{-1} \text{ dm}^3 \text{ s}^{-1}$ | | | |
| | 2.69 | 3.62 | 6.60 | 9.31 |

Figure 9.05 Dependence of the observed first-order rate constants on cyanide ion concentration for the reaction of cyanide ion with the $[\text{Fe}(\text{BDSB})_3]^{2+}$ cation, over a range of temperatures in 30% aqueous methanol. Temperatures (1) 294.3, (2) 298.6, (3) 302.8 and (4) 307.5 K.

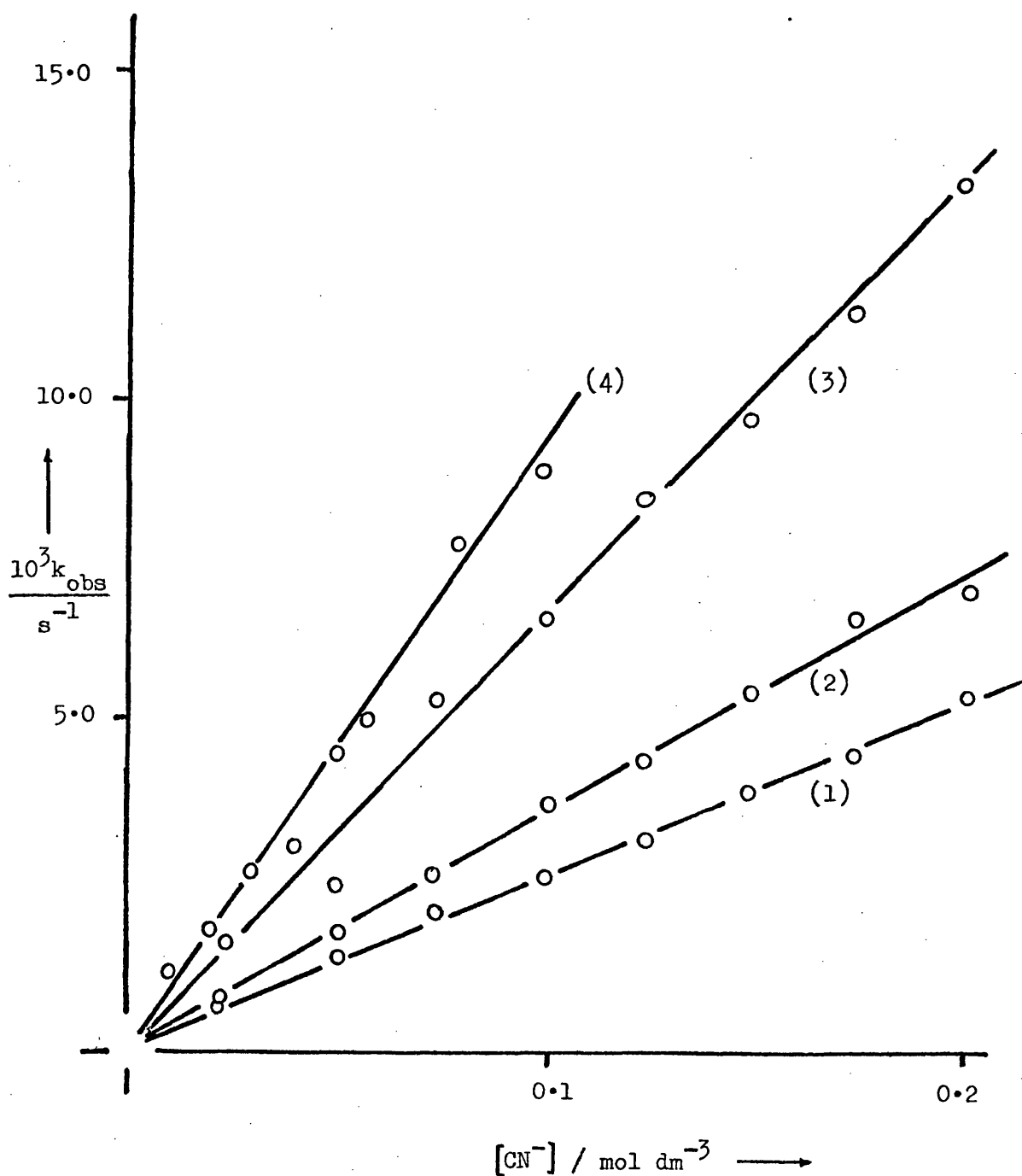
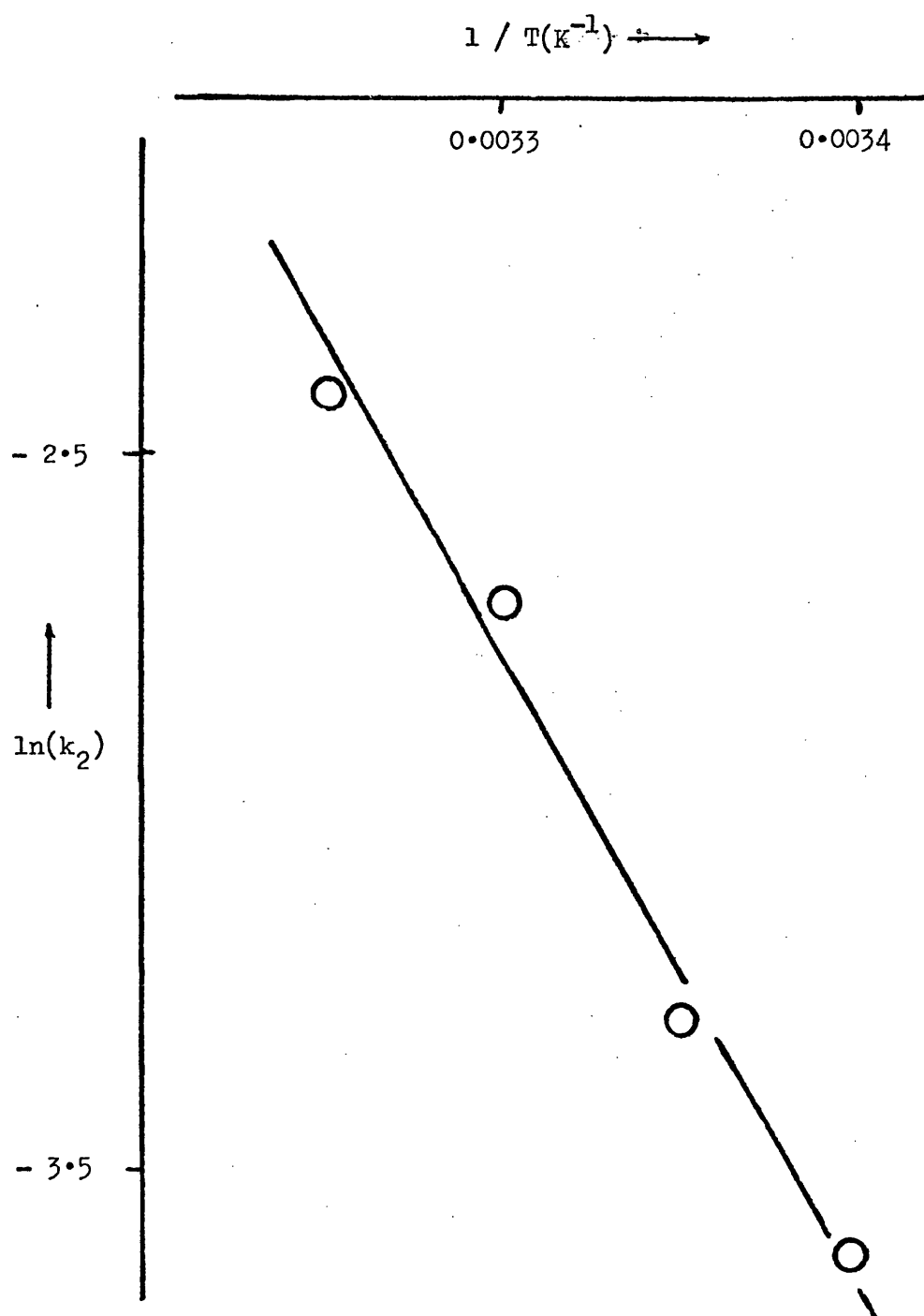


Figure 9.06 Plot of $\ln(k_2)$ versus $1/T$ for the reaction of cyanide ion with the $[\text{Fe}(\text{BDSB})_3]^{2+}$ cation, in 30 % by volume aqueous methanol.



cations [9.27]. Such kinetic behaviour has been interpreted as nucleophilic attack at the ligand for reactions of $\text{Fe}(\text{LL})_2(\text{CN})_2$ -type compounds above. Thus we may envisage a rate-determining bimolecular attack of CN^- at the Schiff's base ligand, followed by very rapid intramolecular rearrangement and ligand loss to form the cyanide-Schiff's base-iron(II) product. In this reaction, only one stage was observed, indicating that the 'cyanide-on-ligand' intermediate can only be a transient species. The products of this reaction are discussed below.

Figure 9.06 shows a plot of the natural logarithm of the second-order rate constants ($=k_{\text{obs}}/[\text{CN}^-]$) derived from the observed first-order rate constants listed in Table 9.05, against the reciprocal of the absolute temperature.

From the slope of this plot, the enthalpy and entropy of activation have been calculated, having the values $83.7 \text{ k J mol}^{-1}$ and $-42 \text{ J K}^{-1} \text{ mol}^{-1}$ respectively at 298.2 K. The negative entropy of activation supports the bimolecularity of the reaction mechanism. These activation parameters, together with the second-order rate constant at 298.2 K are compared with similar parameters for the reaction of cyanide ion with complex cations of the type $[\text{Fe}(\text{LL})_3]^{2+}$, for LL = bipy, phen and substituted derivatives, in Table 9.06. From such comparisons we find that the Schiff's base complex is more reactive (i.e. less stable) than its phenanthroline-type analogues, a fact which is consistent with previous observations on similar Schiff's base complexes [9.27].

From Figure 9.05 we see that, within experimental error, there is no dissociative term in the rate law. The neutral solution dissociation of the complex is hence suggested to be very slow. This is supported by the fact that the $[\text{Fe}(\text{BDSB})_3]^{2+}$ cation was found to react with 1,10-phenanthroline in 50% by volume aqueous methanol, where complete forma-

TABLE 9.06 Comparison of rates and activation parameters for the reactions of cyanide ion with various iron(II)-multidentate ligand complexes, in aqueous solution at 308.2 K.

| Ligand | k_2 $\text{mol}^{-1} \text{dm}^3 \text{s}^{-1}$ | ΔH^\ddagger kJ mol^{-1} | ΔS^\ddagger $\text{J K}^{-1} \text{mol}^{-1}$ | Ionic Strength mol dm^{-3} | Ref. |
|--------------------|--|---|--|---|-----------|
| terpy | 0.019 | 91 | -17 | 0.10 | 9.02 |
| phen | 0.025 | 86 | -42 | 2.0 | 9.07 |
| 5-Mephen | 0.016 | 83 | 0 | 0.33 | (a) |
| bipy | 0.028 | 96 | -3.8 | 0.10 | 9.05 |
| ppsa ^a | 0.0034 | 105 | -50 | 0.33 | (b) |
| ppadd ^b | 0.000039 | 102 | 0 | 0.33 | 9.04 |
| padd ^c | 0.0072 | 82 | 0 | 0.33 | (c) |
| pma ^d | 5.6 | 73 | -8.4 | 0.004 | 9.27 |
| BDSB | 0.093 | 84 | -42 | 0.20 | This Work |

Refs. (a) J. Burgess and J.G. Chambers, personal communication;
 (b) E.R. Gardner, F.M. Mekhail, J. Burgess and J.M. Rankin, J. Chem. Soc.(Dalton), (1973), 1340;
 (c) J. Burgess and G.M. Burton, personal communication.

^a ppsa = 3-(2-Pyridyl)-5,6-bis(4-phenylsulphonato)-1,2,4-triazine;

^b ppadd = 1,12-diphenyl-1,12-di(2-pyridyl)-2,5,8,11-tetraazadodeca-1,11-diene;

^c padd = 1,12- " " " " " ;

^d pma = N-(2-pyridylmethylene)aniline, parameters measured in 95 % by volume methanol.

tion of $[\text{Fe}(\text{phen})_3]^{2+}$ took four days at 298.2 K. Hence $k_{\text{diss}} \leq 10^{-5} \text{ s}^{-1}$ under these conditions.

Acid Aquation of the $[\text{Fe}(\text{BDSB})_3]^{2+}$ Cation

In acidic solution, rapid decay of optical density of the complex was observed. The kinetics of this aquation in aqueous solution were monitored for various acid concentrations, over a range of temperatures. The first-order rate constants observed under these conditions are reported in Table 9.07. Figure 9.07, which is a plot of k_{obs} versus $[\text{H}^+]$ for these results, shows the aquation of the $[\text{Fe}(\text{BDSB})_3]^{2+}$ cation to be catalysed by acid, the rate law being of the form

$$\text{rate} = k_1 + k_2 [\text{Fe}(\text{BDSB})_3^{2+}] [\text{H}^+] \quad (9.08)$$

where k_1 , the neutral solution dissociative rate constant, is negligible, the plot of k_{obs} versus $[\text{H}^+]$ (Figure 9.07) passing through the origin, within experimental error. In general, rates of aquation of low-spin iron(II) complexes vary with acid concentration when the leaving ligand is flexible, for example 2,2'-bipyridyl [9.29] or 2,2',6',2''-terpyridyl [9.30,31], but are independent of acid concentration when the leaving ligand is rigid, for example 1,10-phenanthroline[†] [9.32]. The bidentate Schiff's base of this work not only is flexible with the possibility of protonation of dissociated nitrogen donor atom, but also has a pyridyl substituent, which can also be protonated.

Figure 9.08 is a plot of $\ln k_2$ versus $1/T$ for the acid aquation of

[†] [When the phen ligand has a protonatable substituent, like $-\text{NH}_2$, a dependence of aquation rate on acid concentration is observed [9.33].]

TABLE 9.07 Observed first-order rate constants, k_{obs} , for the acid aquation of the $[\text{Fe}(\text{EDSB})_3]^{2+}$ cation in aqueous solution, over a range of acid concentrations and of temperatures.

| $\frac{[\text{H}^+]}{\text{mol dm}^{-3}}$ | T / K | | | | |
|---|---------------------------------------|-------|-------|-------|-------|
| | 291.4 | 294.2 | 298.2 | 303.2 | 309.2 |
| | $10^3 k_{\text{obs}} / \text{s}^{-1}$ | | | | |
| 0.0137 | | | 0.128 | | |
| 0.0342 | | | 0.180 | | |
| 0.0685 | | 0.147 | 0.228 | | 1.17 |
| 0.137 | 0.101 | 0.191 | 0.506 | 1.03 | 1.90 |
| 0.205 | 0.175 | | 0.721 | | 2.55 |
| 0.274 | 0.248 | 0.464 | 0.902 | | 3.71 |
| 0.342 | | | | 2.10 | 4.88 |
| 0.411 | 0.307 | 0.741 | 1.60 | 4.10 | 5.42 |
| 0.548 | 0.404 | 1.06 | 2.15 | 4.58 | 7.91 |
| 0.685 | 0.551 | 1.13 | 2.93 | | 9.53 |
| 0.822 | | 1.47 | | 6.25 | |
| 0.890 | 0.768 | | 3.73 | | |
| 0.959 | | 1.87 | | 7.31 | |
| 1.03 | | | | | |
| 1.10 | 1.13 | 2.33 | 4.38 | | |
| 1.23 | | | | 8.99 | |
| 1.37 | 1.19 | 2.81 | 5.47 | 9.76 | |

Figure 9.07 Dependence of the observed first-order rate constants on acid concentration for the aquation of the $[\text{Fe}(\text{BDSB})_3]^{2+}$ cation in aqueous solution, for the temperatures (1) 291.4, (2) 294.2, (3) 298.2, (4) 303.2 and (5) 309.2 K.

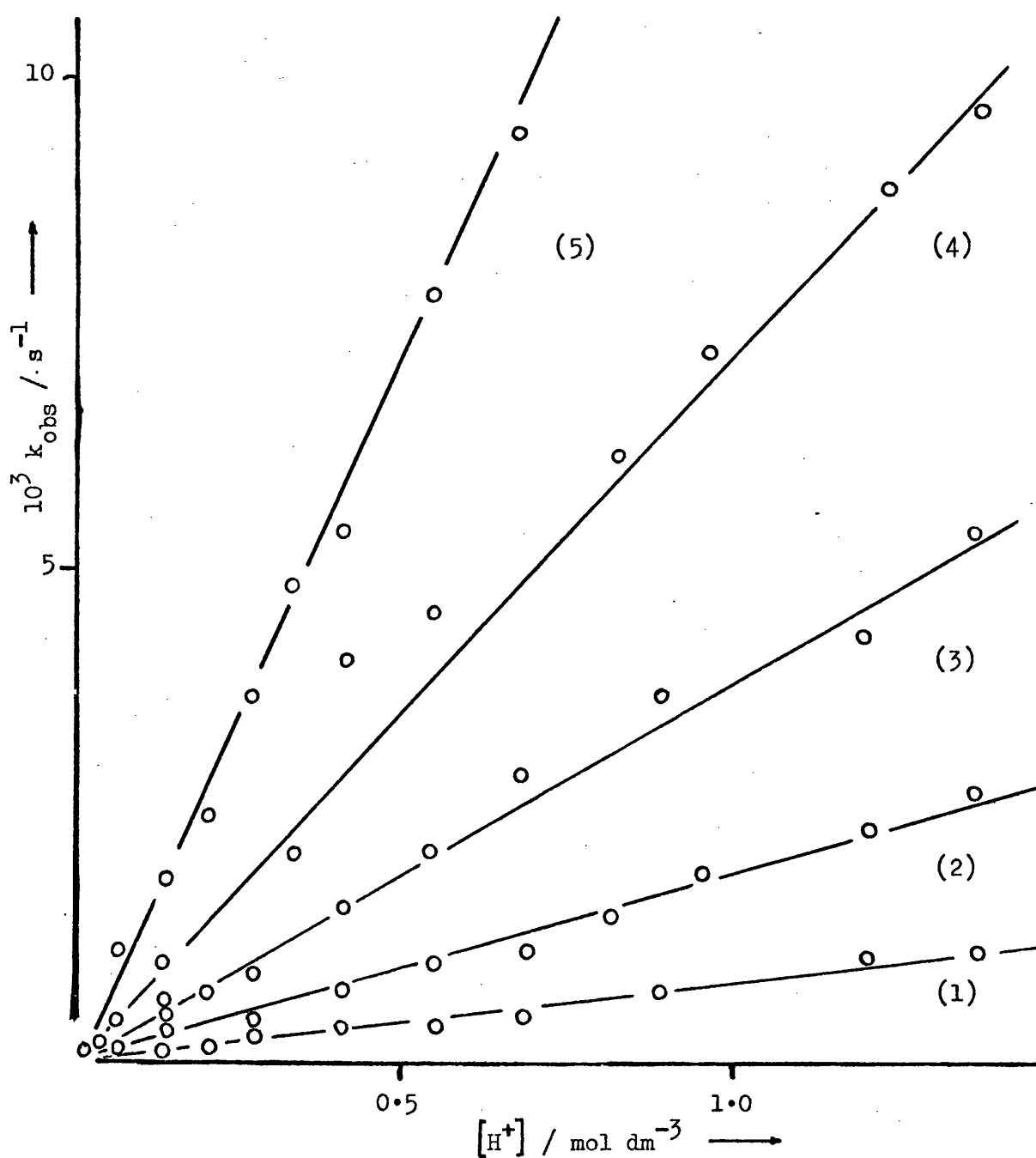
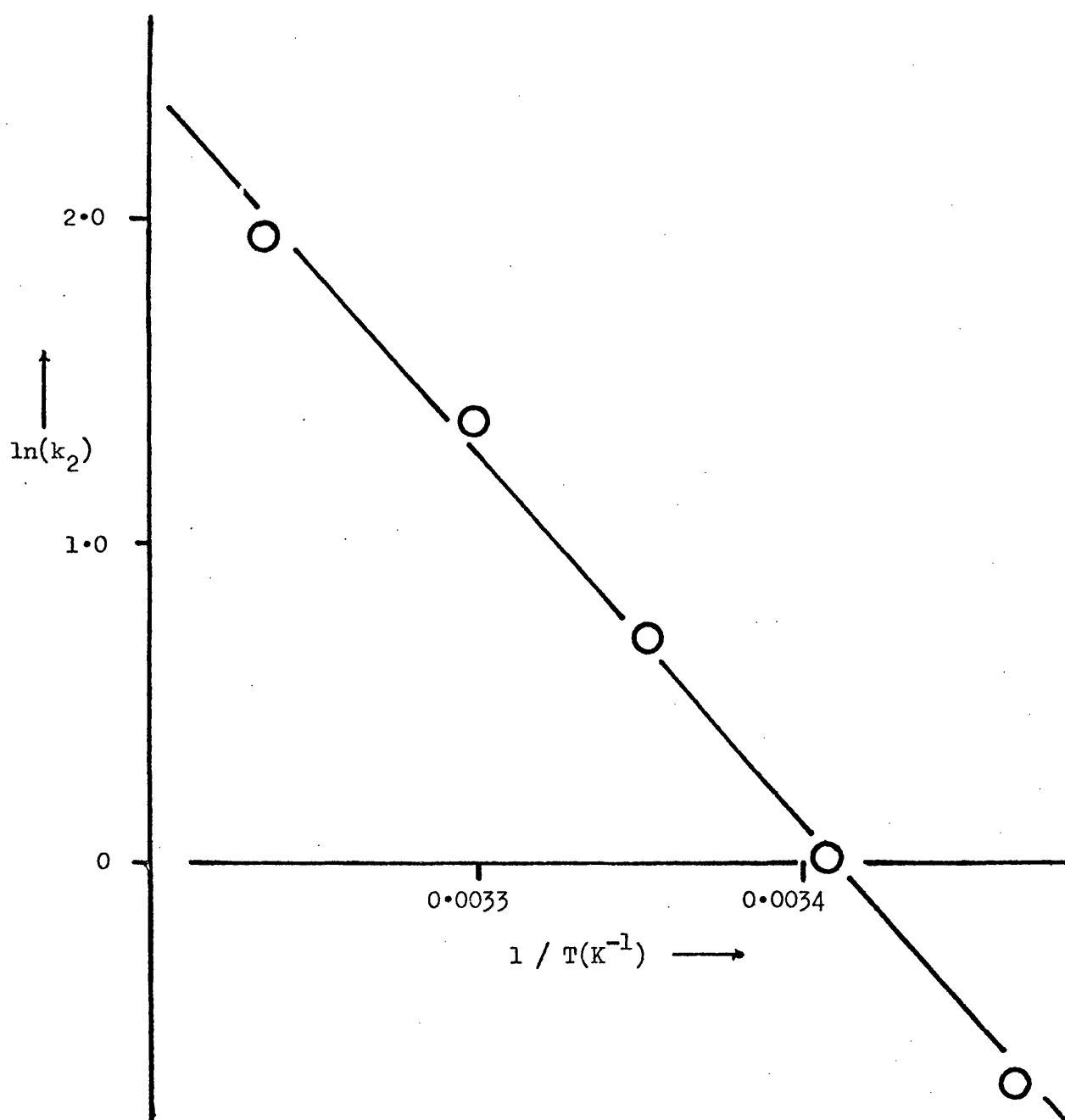


Figure 9.08 Plot of $\ln(k_2)$ versus $1/T$ for the acid aqutation of the $[\text{Fe}(\text{BDSB})_3]^{2+}$ cation, in aqueous solution.



the $[\text{Fe}(\text{BDSB})_3]^{2+}$ cation, from which the activation parameters for the reaction have been calculated. These parameters, $\Delta H^\ddagger = 84 \pm 8 \text{ k J mol}^{-1}$ and $\Delta S^\ddagger = -9.4 \pm 2.4 \text{ J K}^{-1} \text{ mol}^{-1}$ may be compared with those for the acid aquation of the $[\text{Fe}(\text{bipy})_3]^{2+}$ cation, which have values of $96 \pm 3 \text{ k J mol}^{-1}$ and $+38 \text{ J K}^{-1} \text{ mol}^{-1}$ respectively. As expected, $\Delta H^\ddagger(\text{BDSB}) < \Delta H^\ddagger(\text{bipy})$, evidencing the greater lability of the Schiff's base complex.

Products of Reaction of Cyanide ion with the $[\text{Fe}(\text{BDSB})_3]^{2+}$ Cation

Under preparative conditions, when a large excess of potassium cyanide in water was added to an aqueous solution of the iron(II) complex cation, a blue solid was precipitated from solution. This product was found to behave as a neutral species, having a low solubility in water, but being readily soluble in a wide range of organic solvents. By analogy with the similar reactions of, for example $[\text{Fe}(\text{LL})_3]^{2+}$ cations (where LL = bipy, phen or substituted derivatives) with cyanide ion, which produce compounds of the type " $\text{Fe}(\text{LL})_2(\text{CN})_2$ " [9.16], we can conclude that the primary product of our reaction is $\text{Fe}(\text{BDSB})_2(\text{CN})_2$. This assumption is borne out by the similarity in behaviour of the product with such compounds as $\text{Fe}(\text{phen})_2(\text{CN})_2$ and $\text{Fe}(\text{bipy})_2(\text{CN})_2$ with respect to their solvatochromic properties (see chapter 8). The extinction coefficient of the product is ca. two-thirds of the $[\text{Fe}(\text{BDSB})_3]^{2+}$ precursor. This suggests that one of the three chromophoric ligands has been displaced.[†] The product of the reaction was analysed for C, H and N content. The results, given in Table 9.01,

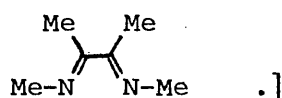
[†][See section 9.3(i), footnote concerning relative ϵ_{max} values.]

indicate that there is ca. $\frac{1}{2}$ molecule of water (solvent) per molecule of $\text{Fe}(\text{LL})_2(\text{CN})_2$ product. This may be interpreted in terms of a mixture of products, $\text{Fe}(\text{LL})_2(\text{CN})_2$ and $\text{Fe}(\text{LL})(\text{LL} \cdot \text{H}_2\text{O})(\text{CN})_2$, in roughly equal proportions. A similar phenomenon has been observed by Krumholz [9.34] in the reaction of the $[\text{Fe}(\text{bmi})_3]^{2+}$ cation with cyanide ion. A mixture of products was isolated, and the components separated and analysed. Both components were found to be solvatochromic, so this behaviour could not be used to distinguish between them. In this work, the products have not been subjected to any treatment other than a solvatochromic study (in chapter 8), and so no attempt to separate them has been made.

The $\text{Fe}(\text{LL})(\text{LL} \cdot \text{H}_2\text{O})(\text{CN})_2$ product is analogous to, for example the $\text{Fe}(\text{5-NO}_2\text{phen} \cdot \text{CN})_2(\text{5-NO}_2\text{phen})$ -type compound isolated in the reaction of the $[\text{Fe}(\text{5-NO}_2\text{phen})_3]^{2+}$ cation with cyanide ion (see above). Although there is no evidence, such as n.m.r. studies, as to the true nature of this 'solvate' of $\text{Fe}(\text{LL})_2(\text{CN})_2$, it seems reasonable to assume that this solvent molecule has added to the Schiff's base ligand, by analogy to the above iron(II)-5- NO_2phen complex, and the ruthenium(II) analogue [9.14]. However, the actual site of addition of the solvent molecule is unknown; the addition of CN^- , OH^- , OMe^- and OEt^- have been found to attack the $[\text{Ru}(\text{5-NO}_2\text{phen})_3]^{2+}$ cation at different sites on the ligand, depending upon which nucleophile is used [9.15].

It is interesting that no such partial solvolysis appears to occur for the tris-bidentate ligand complex (as evidenced by the analysis

[†] [bmi = biacetyl methylimine,



results in Table 9.01), but only in the dicyano-adducts. This is to be expected however, since the cyanide ligands will add extra stability to the low spin iron(II) species, whereas covalent solvation of the tris-ligand complex would result in destabilisation, resulting in a high spin state, which would be unstable.[†]

(v) A Hexadentate Schiff's Base Complex of Iron(II)

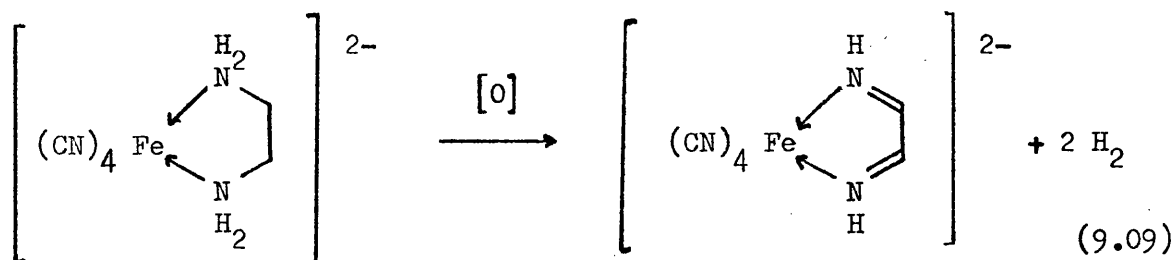
A stable, low spin iron(II) complex cation of the hexadentate Schiff's base ligand, HXSB, derived from the condensation of two molecules of quinolyl-2-aldehyde with one of triethylenetetramine (Diagram 9.03(d)) was isolated as the perchlorate salt. That a complex of such a ligand, having apparently only two α, α' -diimine groups and effectively an ethylenediamine residue, is low spin is surprising. Complexes of the formula $\text{Fe}(\text{LL})_2\text{X}_2$ are only low spin at room temperature for $\text{X}^{\text{§}} = \text{CN}$ or NCO [9.35], or S-bonded sulphinate [9.36] when $\text{LL} = \text{bipy}$, and for $\text{X} = \text{CN}$, NCO or NO_2 [9.35] when LL is phen. No stable complexes of the type $[\text{Fe}(\text{phen})_2(\text{NH}_3)_2]^{2+}$ or $[\text{Fe}(\text{phen})_2(\text{en})]^{2+}$ are known. We have shown (above) that bidentate Schiff's base ligands form complexes $[\text{Fe}(\text{BDSB})_3]^{2+}$ which are slightly less stable than $[\text{Fe}(\text{phen})_3]^{2+}$. Hence a low spin complex $[\text{Fe}(\text{SB})_2\text{L}_2]^{2+}$ with $\text{L} =$ an aliphatic nitrogen ligand, seems unlikely.

Goedken [9.37] has shown that for the $[\text{Fe}(\text{CN})_4(\text{en})]^{2-}$ anion, a

[†] [N.B. $[\text{Fe}(\text{en})_3]^{2+}$ is high spin, but $[\text{Fe}(\text{CN})_4(\text{en})]^{2-}$ is low spin [9.37]; (en = ethylenediamine).]

[§] [When $\text{X} = \text{NCS}$, $\text{Fe}(\text{LL})_2(\text{NCS})_2$ complexes are low spin at low temperatures [9.23].]

spontaneous intramolecular redox reaction occurs in air with formation of the tetracyano(α,α' -diimine)iron(II) anion, thus:-



via an iron(III) intermediate. The tetracyano-complex was chosen as it was found to be the first low-spin iron(II)-cyano-ethylenediamine complex which was isolable. It is feasible that a similar intramolecular redox process could have occurred in the preparation of the $[\text{Fe}(\text{HXSb})]^{2+}$ species. From consideration of molecular models, we find that the most stable conformation of the partially aliphatic (original Schiff's base) ligand-iron(II) cation is an octahedral complex consisting of two terdentate portions linked by a flexible ethylenediamine residue (Diagram 9.03(b)). This is a result of the co-planarity of the units shown in Diagram 9.05, which terminate both ends of the ligand. Such a conformation induces an unfavourable eclipsing of the

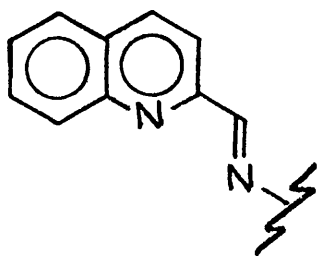
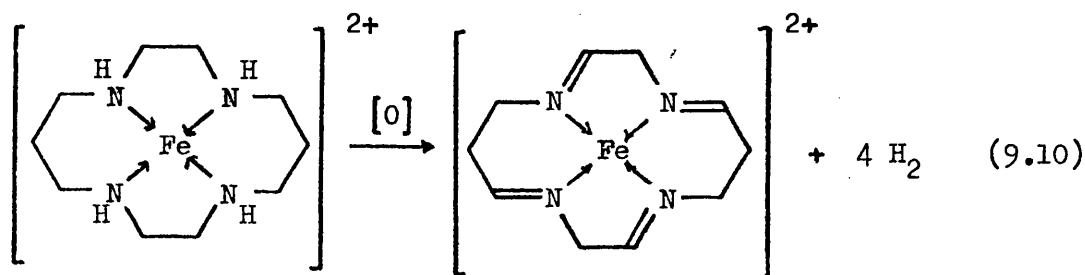


Diagram 9.05

aliphatic protons of the ligand. The occurrence of an intramolecular redox process would alleviate such steric clashes, and also some bond angle strain (i.e. $\text{sp}^3(109.5^\circ) \rightarrow \text{sp}^2(120^\circ)$). The resulting complex would be of the form shown in Diagram 9.03(c). The π -systems thus

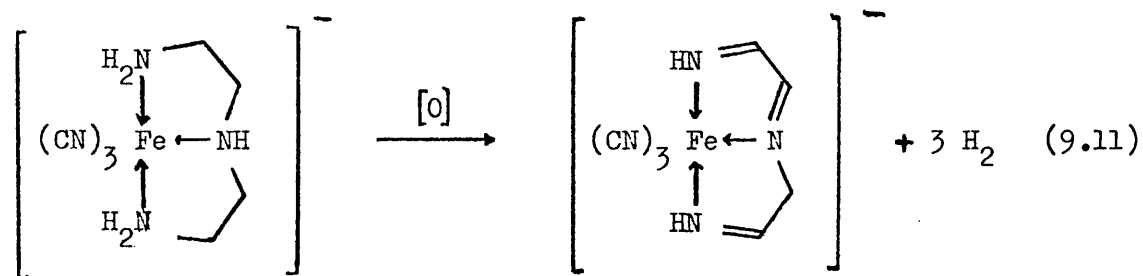
formed are similar to those of the $[\text{Fe}(\text{terpy})_2]^{2+}$ cation (Diagram 9.04(d)). It seems surprising that two separate π -systems, for the two terdentate units should be preferred to three sets of α, α' -diimine groups, connected by two ethylenediamine linkages. However, apart from the fact that there will be some extra strain in the additional ethylene link in the latter form, there is also the possibility of some hyperconjugation in the former bis-terdentate form. That such an intramolecular redox process should produce non-conjugated poly-imine groups is not unknown. Busch *et al.* [9.38] have shown that the macrocyclic complex (X) can be oxidised to the tetra-imine (XI) via successive intramolecular redox reactions; in preference to, for example, a bis(α, α' -diimine) isomer.



For the $[\text{Fe}(\text{HXSb})]^{2+}$ cation, the microanalysis results are unfortunately insufficiently accurate to distinguish between the aliphatic and olefinic forms, the difference in the molecular weights of which is only 4 in 681. N.m.r. spectroscopy should be able to distinguish between the two structures, but unfortunately the perchlorate salt isolated is insufficiently soluble to produce such a spectrum.

Attempts to prepare the $[\text{Fe}(\text{dien})(\text{CN})_3]^-$ anion by Goedken's method for the $[\text{Fe}(\text{en})(\text{CN})_4]^{2-}$, resulted in a yellow material which was oxidised in air in the solid form, or in aqueous solution to a purple species. This reaction appears to be analogous to the above intramole-

cular redox processes, of the form:-



These observations are at present only qualitative, but there remains the opportunity for much work to be carried out on these and related systems.

Reaction with Cyanide Ion

The complex reacts rapidly with cyanide ion in aqueous solution, the visible spectrum having two clean isosbestic points at 557 and 598 nm. The final product ($\lambda_{\text{max}} = 632 \text{ nm}$) has an optical density ca. 50% of the starting material. This suggests a terdentate residue in the product, with presumably three cyanide ligands, i.e. a species of the form $[\text{Fe}(\text{HXSb}')(\text{CN})_3]^-$. This product could not be isolated in a sufficiently pure state to produce satisfactory analysis results, due to its very similar solubility behaviour to potassium cyanide, from which it was formed. Using tetraethylammonium cyanide in the preparation in non-aqueous solvents, only tarry products could be obtained. The product was found, like potassium cyanide, to be very soluble in water, moderately so in methanol, and insoluble in a variety of other organic solvents.

However, it was shown in chapter 8 that the solvatochromic behaviour of the product relative to the $[\text{Fe}(\text{terpy})(\text{CN})_3]^-$ anion was

parallel to that of the $\text{Fe}(\text{BDSB})_2(\text{CN})_2$ species relative to $\text{Fe}(\text{bipy})_2(\text{CN})_2$. From this consideration, and from comparisons with the behaviours of, for example, the $[\text{Fe}(\text{bipy})(\text{CN})_4]^{2-}$ anion, it was concluded that the compound in question was almost certainly of the form $[\text{Fe}(\text{HXSb}')(\text{CN})_3]^-$.

Kinetics

Observed first-order rate constants, k_{obs} , for the reaction of cyanide ion with the $[\text{Fe}(\text{HXSb})]^{2+}$ cation for a range of cyanide ion concentrations, at 281.2 K in aqueous solution are reported in Table 9.08. These show a first-order dependence of k_{obs} on $[\text{CN}^-]$, a feature which has emerged as characteristic of low-spin iron(II)- α, α' -diimine complexes. Thus we might reasonably invoke a mechanism for this reaction involving nucleophilic attack at the ligand, analogous to those previously mentioned. We may compare the value of k_2 of $1.6 \times 10^{-3} \text{ mol}^{-1} \text{ dm}^3 \text{ s}^{-1}$ at 281.2 K with that of $0.94 \times 10^{-3} \text{ mol}^{-1} \text{ dm}^3 \text{ s}^{-1}$ for the analogous HXSb, derived from phenyl-2-pyridyl ketone and triethylenetetramine [9.04], at 298.5 K in aqueous solution. Such a difference is to be expected, since quinolyl complexes are much less stable than the corresponding pyridyl ones.[†] In addition, substituent effects are in the order:-



for reactions of $[\text{Fe}(\text{LL})_3]^{2+}$ -type and related species [9.27].

[†][In fact, low spin tris(Sb)iron(II) complexes from quinolyl-2-aldehyde are not formed, due to steric interaction of the 8-protons.]

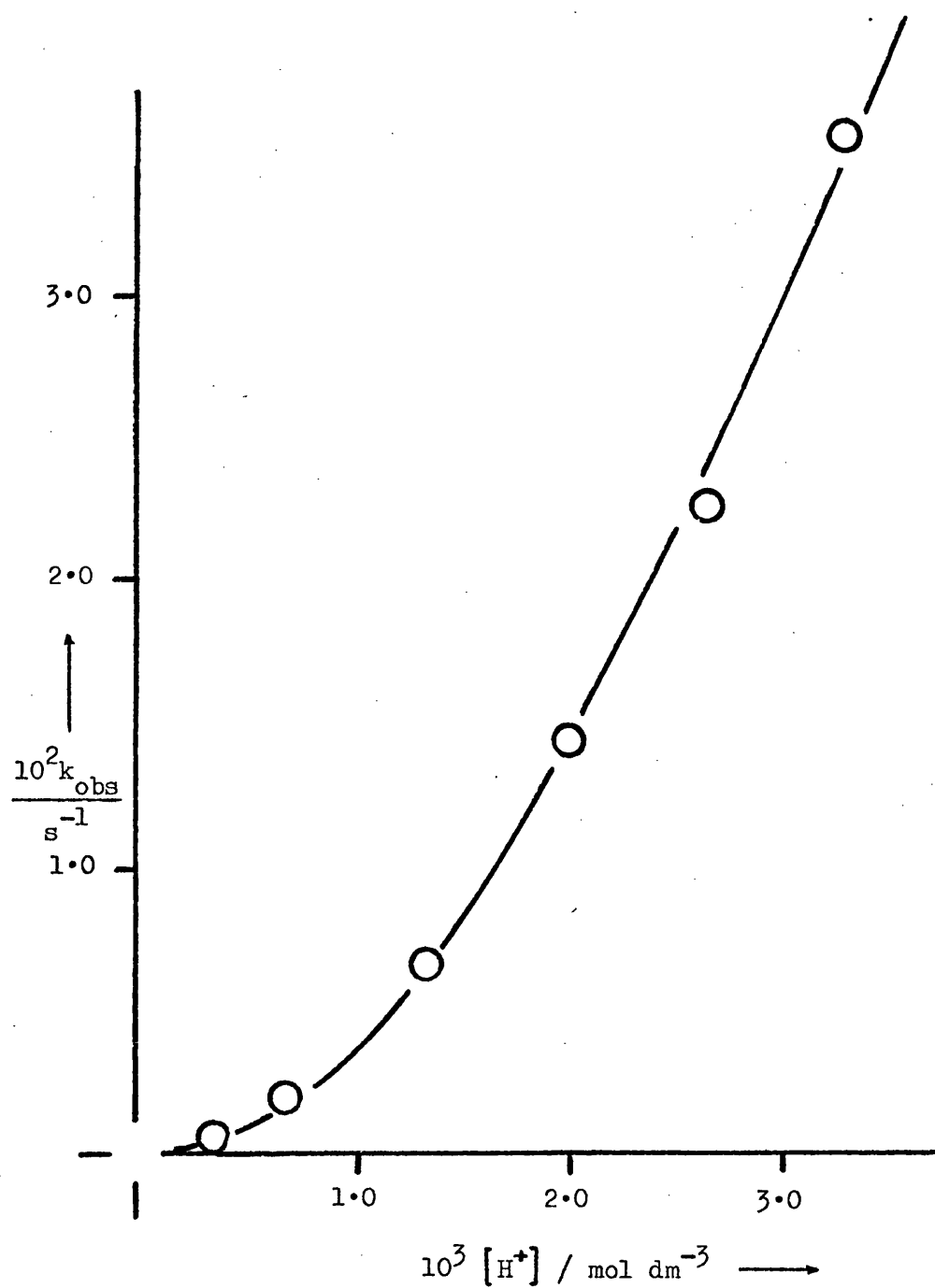
TABLE 9.08 Observed first-order rate constants, k_{obs} , for the reaction of cyanide ion with the $[\text{Fe}(\text{HXSb})]^{2+}$ cation in aqueous solution, at 281.2 K.

| $\frac{[\text{CN}^-]}{\text{mol dm}^{-3}}$ | $\frac{10^2 k_{\text{obs}}}{\text{s}^{-1}}$ |
|--|---|
| 0.02 | 0.34 |
| 0.05 | 1.03 |
| 0.10 | 1.69 |
| 0.20 | 3.29 |
| 0.30 | 5.14 |

TABLE 9.09 Observed first-order rate constants, k_{obs} , for the acid aquation of the $[\text{Fe}(\text{HXSb})]^{2+}$ cation in aqueous solution, at 298.2 K.

| $\frac{[\text{H}^+]}{\text{mol dm}^{-3}}$ | $\frac{10^2 k_{\text{obs}}}{\text{s}^{-1}}$ |
|---|---|
| 0.00033 | 0.040 |
| 0.00067 | 0.208 |
| 0.00133 | 0.674 |
| 0.00200 | 1.42 |
| 0.00267 | 2.26 |
| 0.00333 | 3.57 |

Figure 9.09 Dependence of the observed first-order rate constants, k_{obs} , on acid concentration for the aquation of the $[\text{Fe}(\text{HXSb})]^{2+}$ cation, in aqueous solution at 298.2 K.



Acid Aquation

In neutral solution, the $[\text{Fe}(\text{HXSb})]^{2+}$ cation is stable for long periods (several months). In acidic solution, the complex rapidly dissociates:-

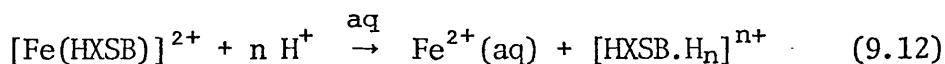


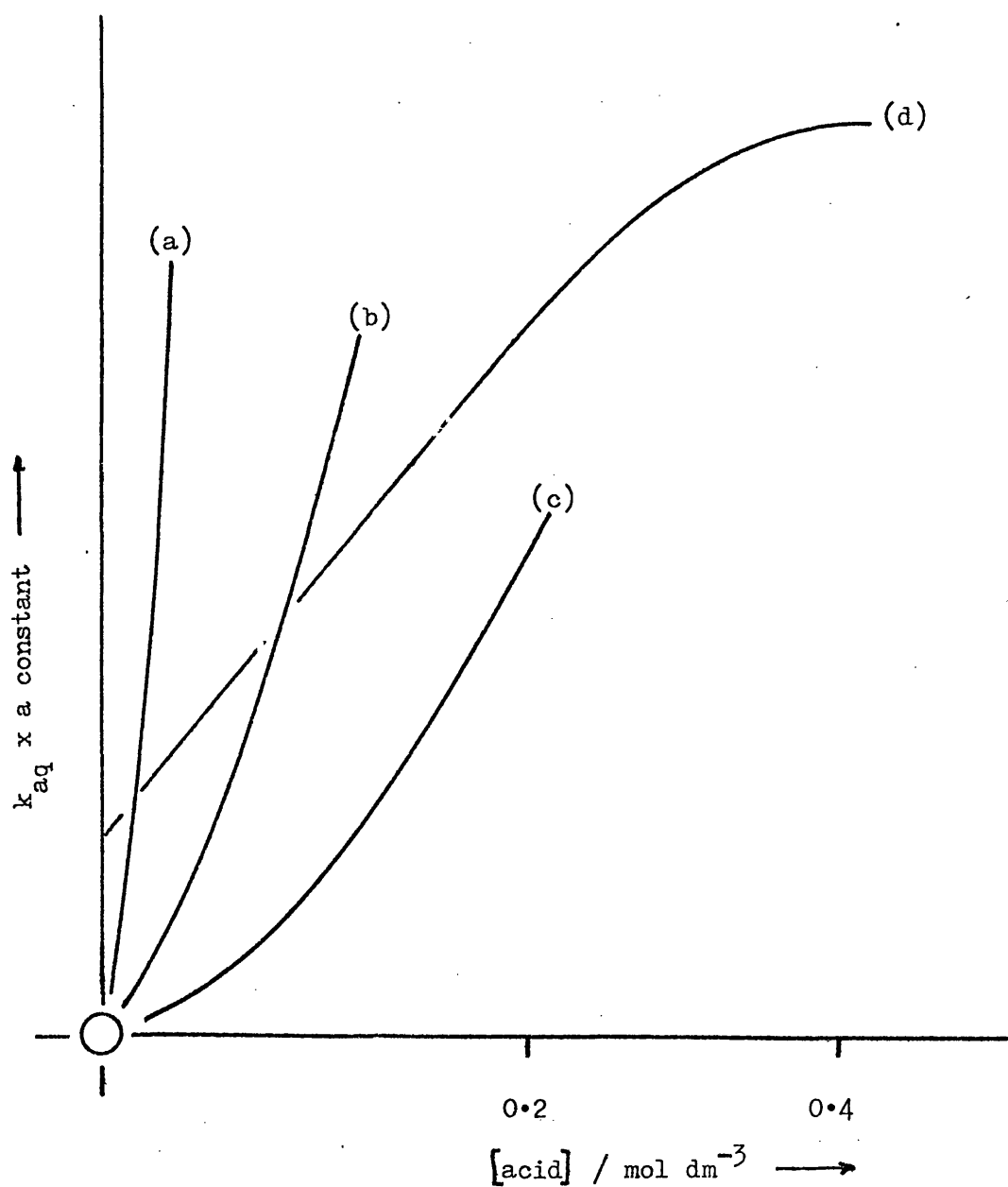
Table 9.09 lists the observed first-order rate constants for this aquation reaction at 298.2 K in aqueous solution, for several acid concentrations. The range of concentrations usable was greatly restricted by the rapid rates, which were just followable using the conventional technique available. The plot of k_{obs} vs $[\text{H}^+]$ (Figure 9.09) shows a curvature, indicating a complicated rate law, with terms in $[\text{H}^+]$ of order higher than one.

The form of the dependence of the aquation rates on acid concentration for the $[\text{Fe}(\text{HXSb})]^{2+}$ cation is compared diagrammatically with those for the $[\text{Fe}(\text{bipy})_3]^{2+}$, $[\text{Fe}(\text{terpy})_2]^{2+}$ and the $[\text{Fe}(\text{HXSb})]^{2+\dagger}$ cations, in Figure 9.10. From this we see the behaviours of all these species except that of the $[\text{Fe}(\text{bipy})_3]^{2+}$ cation to be similar, possibly indicating similar aquation mechanisms for similar species. The actual rate law for the acid aquation of the $[\text{Fe}(\text{terpy})_2]^{2+}$ cation has been shown [9.02] to be exceedingly complicated. Thus we can expect those for the hexadentate Schiff's base complexes to be at least as complicated, since there are six protonatable nitrogens in the ligand molecule.

[†] [This complex is that from ref. 9.04.]

Figure 9.10 Comparison of the dependences of aquation rates, k_{aq} , on acid concentration for flexible multidentate ligand complexes of iron(II). Ligands: (a) HXSB^a; (b) terpy; (c) HXSB^b; (d) bipy.

^a Ligand prepared & studied in this work; ^b ligand studied in ref. 9.04.



Other Reactions

The peroxodisulphate oxidation of the $[\text{Fe}(\text{HXSb})]^{2+}$ cation has also been studied in aqueous solution and in a range of binary aqueous mixtures. This study has been fully discussed in chapter 6, together with a similar but more rigorous study involving the $[\text{Fe}(\text{phen})_3]^{2+}$ cation.

(vi) Quadridentate Schiff's Base Complexes of Iron(II)

A series of complexes of this type have been synthesised, having the quadridentate ligands, QDSB, I-IV, shown in Diagram 9.03(e). The perchlorate salts of these complexes have been analysed for C, H and N, the results of which are given in Table 9.01. These results suggest the general formula $[\text{Fe}(\text{QDSB})(\text{OH}_2)_2](\text{ClO}_4)_2$.

Reaction with Cyanide

Of the four Schiff's base ligands studied here, there are two general types:-

- (a) 'Rigid' - i.e. those (I & II) prepared from o-phenylenediamine and a ketone, producing in the free ligand at least, a rigid planar conjugated system.
- (b) 'Flexible' - i.e. those prepared [(III) & (IV)] using ethylenediamine as one of the precursors. This produces a Schiff's base containing two α, α' -diimine moieties linked by a flexible aliphatic $=\text{N}-(\text{CH}_2)_2-\text{N}=\text{group}$.

(a) Kinetics of Complexes containing 'Rigid' ligands,

Cyanide ion was found to react rapidly with the $[\text{Fe}(\text{QDSB})(\text{OH}_2)_2]^{2+}$ cations, containing ligands I and II in a single step. Observed first-order rate constants for the reaction of cyanide ion with these cations are reported in Table 9.10. A plot of k_{obs} vs $[\text{CN}^-]$ for both complexes is illustrated in Figure 9.11 showing the reaction to be first-order in $[\text{CN}^-]$, there being a negligible dissociative term in the rate law, as evidenced by the passage of the plot of Figure 9.11 through the origin, within experimental error. The second-order rate constants, k_2 , for the reaction of the two 'rigid'-ligand complexes, are $0.068 \pm 0.004 \text{ mol}^{-1} \text{ dm}^3 \text{ s}^{-1}$ and $0.072 \pm 0.003 \text{ mol}^{-1} \text{ dm}^3 \text{ s}^{-1}$ for ligands I and II respectively. This close similarity, in spite of the differences in the substituents of ligands suggests that this reaction does not involve the ligand directly. This may be contrasted, with for example the relative reactivities of the $[\text{Fe}(\text{HXSb})]^{2+}$ type complexes, for the ligands derived from quinolyl-2-aldehyde (above) and from phenyl-2-pyridyl ketone [9.04].

The product of the reaction is a species behaving like ones of the form $\text{Fe}(\text{LL})_2(\text{CN})_2$. It is soluble in a range of organic solvents, and has low solubility in water. The cyanide product containing ligand I has been analysed for C, H, N and O (Table 9.01). The results indicate that the compound has a formula $\text{Fe}(\text{QDSB})(\text{CN})_2 \cdot \text{H}_2\text{O}$ in spite of prolonged desiccation in vacuo over phosphorus pentoxide. It exhibits solvatochromism, having a sensitivity of $+61 \text{ cm}^{-1} \text{ kcal}^{-1} \text{ mol}$ which is very similar to that (ca. $59 \text{ cm}^{-1} \text{ kcal}^{-1} \text{ mol}$) for the $\text{Fe}(\text{BDSB})_2(\text{CN})_2$ species (see chapter 8). This behaviour, in spite of the predicted planarity of the ligand, and hence trans-nature of the cyanide ligands, indicates that the cyanide ligands are of cis-geometry. This is apparent in the light of the discussion concerning the solvatochromic properties of cis-

TABLE 9.10 Observed first-order rate constants, k_{obs} , for the first stage of the reaction of cyanide ion with the cations $[\text{Fe}(\text{QDSB})(\text{OH}_2)]^{2+}$, for QDSB = I to IV (see text). Reaction studied in 30 % by volume aqueous methanol, at 298.2 K; ionic strength = 1.33 mol dm^{-3} (maintained with potassium nitrate).

| $\frac{[\text{CN}^-]}{\text{mol dm}^{-3}}$ | QDSB | | | |
|--|---------------------------------------|----------|-------|----------|
| | I | II | III | IV |
| | $10^2 k_{\text{obs}} / \text{s}^{-1}$ | | | |
| 0.083 | 0.550 | 0.614 | 0.334 | 0.650 |
| 0.167 | 1.10 | 1.22 | 0.745 | 1.33 |
| 0.333 | 2.17 | 2.49 | 1.40 | 2.40 |
| 0.500 | 3.58 | 3.74 | 2.05 | 4.11 |
| 0.667 | 4.65 | too fast | 2.61 | too fast |
| $10^2 k_2 / \text{mol}^{-1} \text{ dm}^3 \text{ s}^{-1}$ | 6.77 | 7.4 | 4.14 | 7.8 |

TABLE 9.11 Observed first-order rate constants, k_{obs} , for the second stage of the reaction of cyanide ion with the cations $[\text{Fe}(\text{QDSB})(\text{OH}_2)]^{2+}$, for QDSB = III & IV. Conditions of study as in Table 9.10.

| $\frac{[\text{CN}^-]}{\text{mol dm}^{-3}}$ | QDSB | |
|--|---------------------------------------|------|
| | III | IV |
| | $10^4 k_{\text{obs}} / \text{s}^{-1}$ | |
| 0.083 | 0.017 | 10.0 |
| 0.167 | 0.036 | 18.6 |
| 0.333 | 0.075 | 27.2 |
| 0.500 | 0.113 | 55.3 |
| 0.667 | 0.149 | 73.9 |
| $10^2 k_2 / \text{mol}^{-1} \text{ dm}^3 \text{ s}^{-1}$ | 0.022 | 1.07 |

Figure 9.11 Dependence of the observed first-order rate constants, k_{obs} , on cyanide ion concentration for the first stage of the reaction of cyanide ion with the $[\text{Fe}(\text{QDSB})(\text{OH}_2)_2]^{2+}$ cations, for QDSB = (a) I, (b) II, (c) III and (d) IV; reaction medium is 30 % by volume aqueous methanol, ionic strength of 1.33 mol dm^{-3} (maintained with potassium nitrate), at 298.2 K .

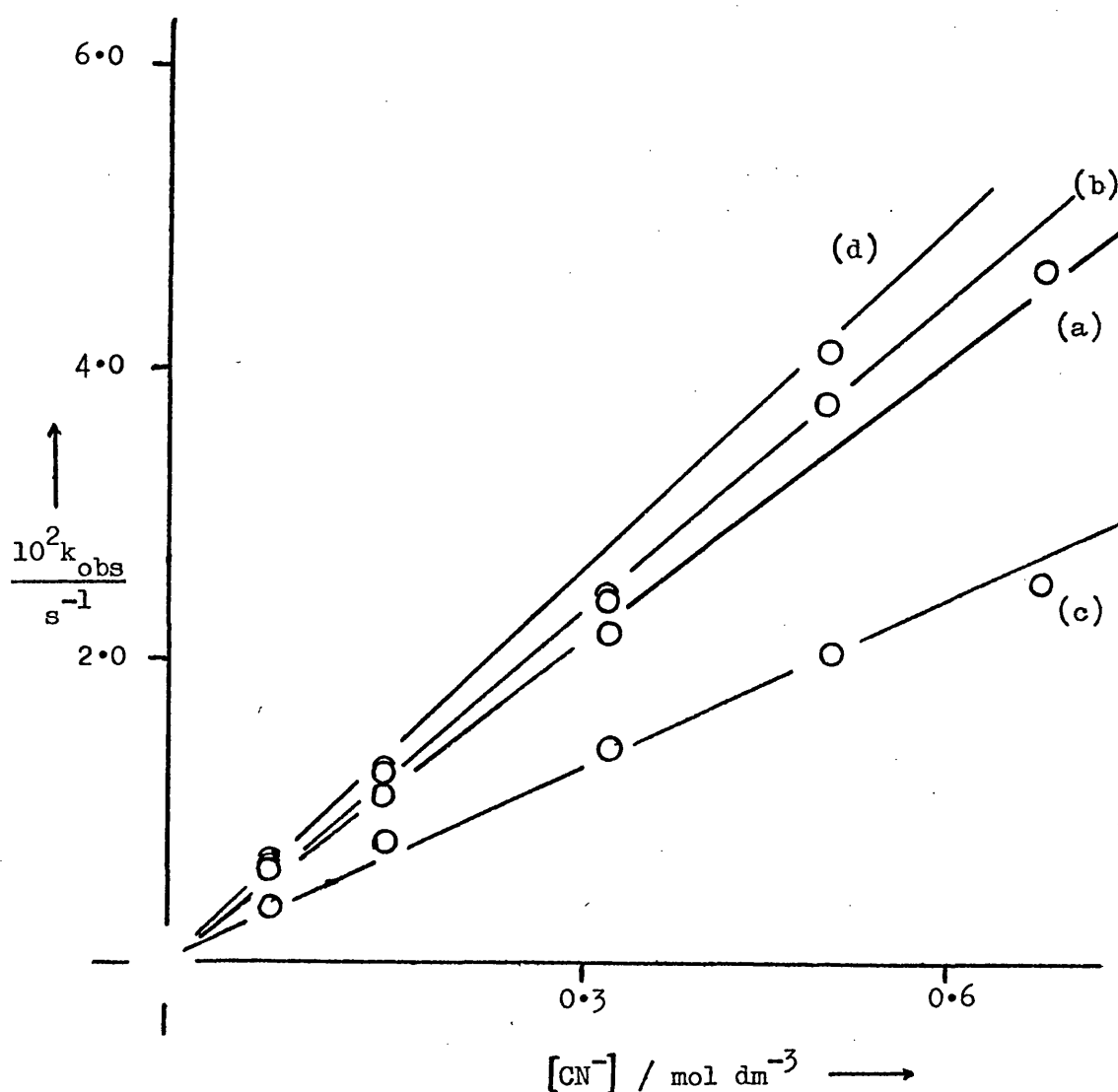
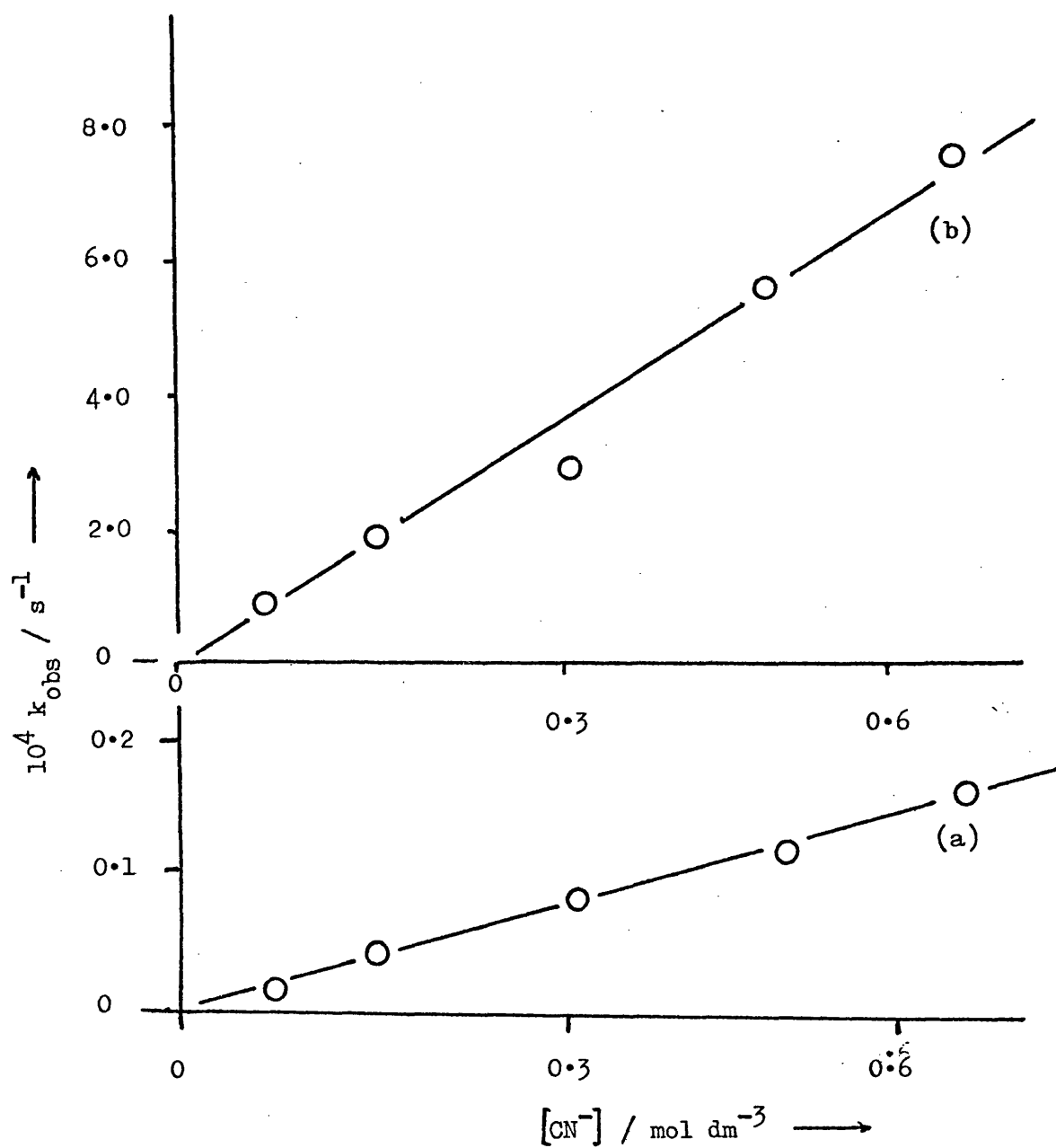


Figure 9.12 Dependence of the observed first-order rate constants, k_{obs} , on cyanide ion concentration for the second stage of the reaction of cyanide ion with the $[\text{Fe}(\text{QDSB})(\text{OH}_2)_2]^{2+}$ cations, for QDSB = (a) III and (b) IV. Conditions as in Figure 9.11.



$\text{Fe}(\text{LL})_2(\text{CN})_2$ compounds relative to $\text{trans-}[\text{Fe}(\text{LLLL})(\text{CN})_2]^{2-}$ ones, where LL = bipy or phen, and LLLL = phthalocyanine, in chapter 8.

Harris & McKenzie [9.39], in attempting to prepare the copper(II) complex of ligand (III), isolated a complex of the partially hydrolysed ligand shown in Diagram 9.06 where a molecule of solvent (ROH) had added

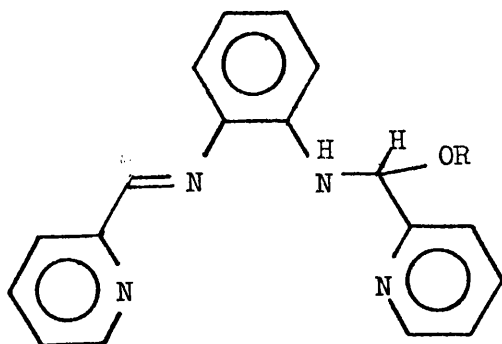


Diagram 9.06

across one of the imine linkages. Reasons put forward to explain such a phenomenon suggested that the increased flexibility of this partially solvolysed ligand enabled alleviation of steric clashes that would occur on coordination of its more rigid diimine precursor (Diagram 9.03(c)). Related examples of addition to strained coordinated imine functions in other M^{n+} complexes are known [9.40].

From the knowledge of the microanalysis of the dicyano adduct of $[\text{Fe}(\text{QDSB})(\text{OH}_2)_2]^{2+}$, coupled with that of the above situation for copper complexes, we might intuitively suggest that in the reaction of cyanide ion with the $[\text{Fe}(\text{QDSB})(\text{OH}_2)_2]^{2+}$ cation, a neutral dicyano species is produced which contains a partially solvolysed ligand, analogous to that shown in Diagram 9.06. This is reasonable when it is considered that the quadridentate ligands III and IV are very similar to that in the copper(II) complex, and the ligand I with the phenyl substituents

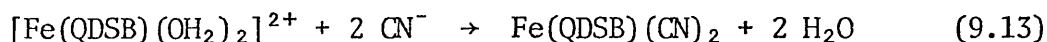
will be under considerable steric strain in its own right, from clashes between the 2- and 6-protons of the phenyl groups with the 3-protons of the pyridyl groups and the 3- and 6-protons of the phenylene group.

(b) Kinetics of Complexes containing 'Flexible' ligands

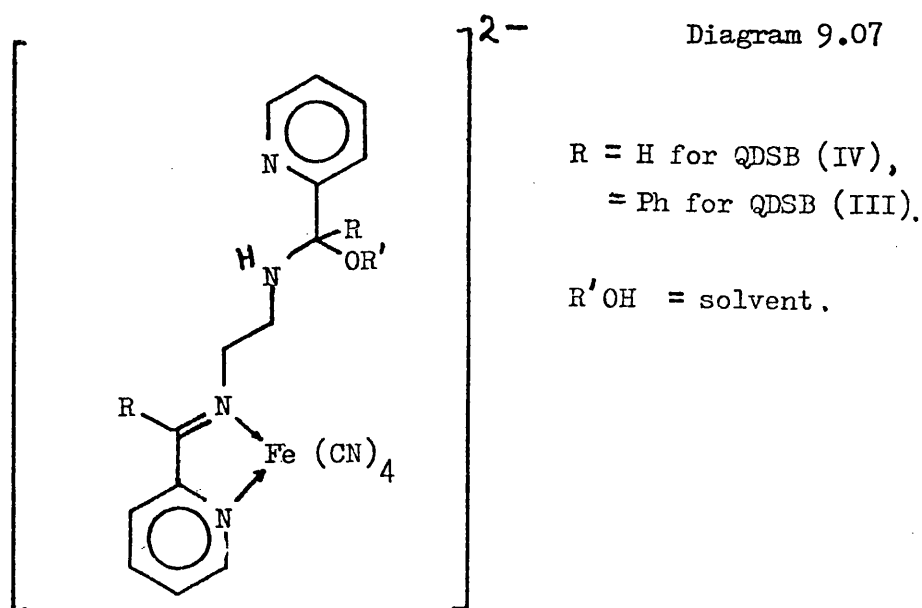
In the reactions of these complexes with cyanide ion, two distinctly separate stages in the reaction were observable, the first stage being ca. 2^{00} times faster than the second for the complexes containing both quadridentate ligand III. Observed first-order rate constants for the first stage of the reaction of cyanide ion with the $[\text{Fe}(\text{QDSB})(\text{OH}_2)_2]^{2+}$ cations, for the ligands III and IV are reported in Table 9.10. The rate constants were measured from optical density changes at optimum wavelengths (ascertained from variable wavelength repeat scans) for the first 60% of the first stage of the reaction. Over this extent of reaction good first-order conditions were observed for a large excess of cyanide over complex, with no observable interference from the second stage of the reaction. For the measurement of the second stage first-order rate constants, the first 20% of this stage in the reaction was ignored, good first-order conditions being observed for the next 70% or so of the reaction. These rate constants are reported in Table 9.11 for the complexes containing the quadridentate ligands III and IV.

Both the first and second stages of these reactions, from plots of k_{obs} against $[\text{CN}^-]$ (Figures 9.11 and 9.12), are first-order in $[\text{CN}^-]$, the correlation lines passing through the origin, within experimental error. The first stage second-order rate constants for the complexes containing ligands III and IV are 0.050 ± 0.004 and $0.057 \pm 0.003 \text{ mol}^{-1} \text{ dm}^3 \text{ s}^{-1}$ respectively. These are very similar to the second-order rate

constants for the complexes containing ligands I and II. This suggests that the first stage of the reaction is analogous to that for the previous 'rigid'-ligand complexes, i.e.:-



Considering the flexibility of ligands III and IV, it is conceivable that further reaction of $\text{Fe}(\text{QDSB})(\text{CN})_2$ with cyanide ion may occur, with initial attack by the CN^- at the ligand followed by rapid rearrangement via rotation of the C-C bond in the ethylenediamine residue,



producing a species of the type $[\text{Fe}(\text{QDSB}')(\text{CN})_4]^{2-}$, as shown in Diagram 9.07. Unfortunately, the cyanide products of these reactions could not be isolated in a sufficiently pure state for microanalysis. They exhibited ionic behaviour, being extremely soluble in water, and insoluble in organic solvents. Consequently the true nature of the cyanide products concerned is only conjectured at present as a tetracyano species.

The rates of the second stages for the reactions of cyanide ion with the $[\text{Fe}(\text{QDSB})(\text{OH}_2)_2]^{2+}$ cations were measured in 30% by volume methanol at 298.2 K as 1.13 ± 0.02 and $80 \pm 1.5 \times 10^{-5} \text{ dm}^3 \text{ mol}^{-1} \text{ s}^{-1}$ for the ligands (III) and (IV) respectively. This difference clearly indicates that a substituent effect by the ligands is operating in this system. The presence of the extra phenyl groups in (IV) as compared with (III) will lend extra stability to the Fe-N bonds by way of their π -electron-acceptor properties. Hence the observation that the complex containing ligand (IV) reacts ca. 70 times more slowly than that containing (III) suggests that the rate-determining step of the reaction with cyanide ion could involve the rupture of a Fe-N band. Similarly, attack of cyanide at the ligand may also be retarded by the presence of the phenyl groups, both on the grounds of steric hindrance to the approach of the nucleophile, and the electronic effect of the phenyl groups, altering the nucleophilicity of the possible sites of attack of the cyanide ion.

Thus this difference in reactivity may be explained by both possible mechanisms, and so adds no further enlightenment to the situation.

(vii) Other Complexes

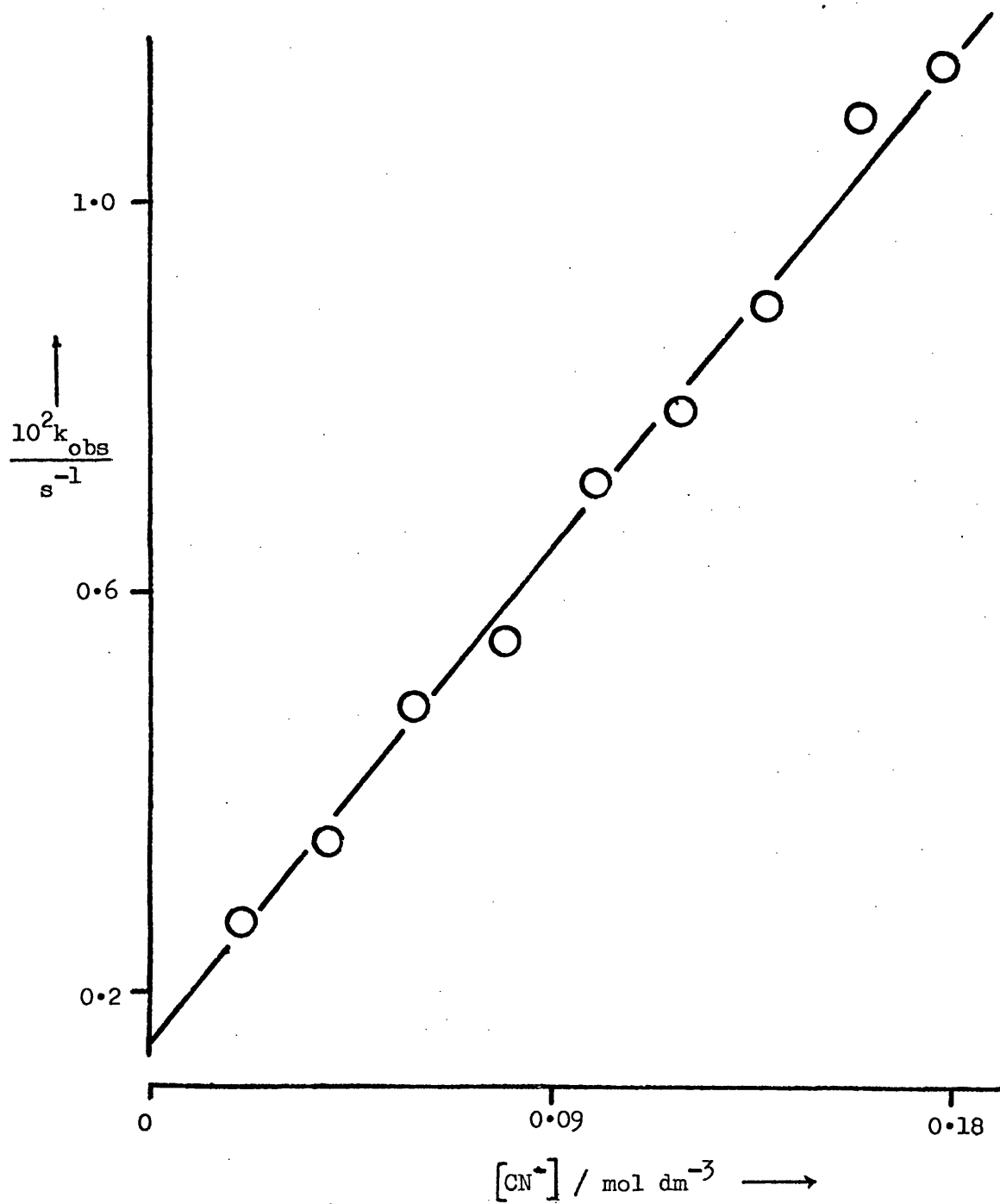
The $[\text{Fe}(\text{TDSB})_2]^{2+}$ Cation

A bis-terdentate Schiff's base complex was prepared, and found to react with cyanide ion, the optical density of the initial complex solution falling to 50% of its original value after the reaction, indicating the loss of one terdentate ligand with the formation of a ter-cyano adduct. The first-order rate constants for the reaction of cyanide ion with the $[\text{Fe}(\text{TDSB})_2]^{2+}$ cation were measured at 298.2 K in

TABLE 9.12 Observed first-order rate constants, k_{obs} , for the reaction of cyanide ion with the $[\text{Fe}(\text{TDSB})_2]^{2+}$ cation, in aqueous solution at 298.2 K; ionic strength = 0.40 mol dm⁻³ (maintained with potassium nitrate).

| $\frac{[\text{CN}^-]}{\text{mol dm}^{-3}}$ | $\frac{10^2 k_{\text{obs}}}{\text{s}^{-1}}$ |
|--|---|
| 0.02 | 0.268 |
| 0.04 | 0.352 |
| 0.06 | 0.486 |
| 0.08 | 0.552 |
| 0.10 | 0.713 |
| 0.12 | 0.788 |
| 0.14 | 0.892 |
| 0.16 | 1.09 |
| 0.18 | 1.14 |

Figure 9.13 Dependence of the observed first-order rate constant on cyanide ion concentration for the reaction of the $[\text{Fe}(\text{TDSB})_2]^{2+}$ cation with cyanide ion in aqueous solution, at 298.2 K.



aqueous solution. This solvent mixture was necessary due to the low solubility of the complex perchlorate. These results are listed in Table 9.12. From a plot of k_{obs} vs $[\text{CN}^-]$ (Figure 9.13), we see that the rate law is of the form:-

$$\frac{-d[\text{complex}]}{dt} = (k_1 + k_2[\text{CN}^-]) [\text{complex}] \quad (9.14)$$

with values of k_1 and k_2 being $1.5 \pm 0.1 \times 10^{-3} \text{ s}^{-1}$ and $5.4 \pm 0.1 \text{ dm}^3 \text{ mol}^{-1} \text{ s}^{-1}$ respectively.

This is consistent with parallel dissociation and nucleophilic attack by cyanide ion. The second-order term may be thought of as analogous with previously discussed reactions of a nucleophile attacking the ligand (above). The complex was seen to dissociate rapidly in neutral solution, as evidenced by relatively rapid fading of the colour. Because of the rapidity of the kinetics of this reaction, even at 281.2 K, no further studies were made on it.

CONCLUSIONS

We have seen that in correlating the kinetic parameter $\delta_m \Delta G^\ddagger$ with physical parameters of solvent mixtures such as G_E , a definite pattern emerges. Thus typically aqueous mixtures (T.A.) always (in the systems studied in this work) have similar effects on the reaction rate. Also, T.N.A.P. mixtures such as aqueous acetonitrile appear to be close in behaviour to the T.A. ones. T.N.A.N. mixtures appear in all cases to be anomalous, but are consistently so. These general observations have been observed to hold no matter what mechanism is operating in the system, be it dissociative (chapters 2 and 3) or associative (chapter 5) in nature.

Mechanistically, the effects of various solvent mixtures on reaction rates have been explained satisfactorily in terms of the relative solvation characteristics of the initial and transition states. This analysis has proved fruitful in elucidating the seemingly large differences between the kinetic behaviours of, for example the mercury(II)-catalysed aquations of the several complexes studied in chapter 5. It has also explained the somewhat surprising effects of solvent on the bimolecular-like oxidation of the $[\text{Fe}(\text{phen})_3]^{2+}$ cation by peroxodisulphate in chapter 6.

The solvatochromic properties of inorganic compounds studied in this work have led to a very useful method, although limited at present to ternary iron(II)-cyanide complexes, of analysis of the constitution and stereochemistry of these complexes.

Finally, the study of nucleophilic attack on bis-cyano bis-(bidentate ligand)iron(II) has led to firm proof of intermediates in these reactions, which were not observable for the related tris(bidentate ligand)iron(II) complexes.

APPENDIX

1. Solvent Parameters.

| Solvent Mixture ^a | mole fraction | $\frac{G^E}{\text{kJ mol}^{-1}}$ | γ ^b | D ^c |
|------------------------------|------------------|----------------------------------|-----------------------|----------------|
| Water | 0 | 0 | 3.49 | |
| 10 | 0.047 | 116 | 3.28 | 76.6 |
| 20 | 0.100 | 211 | 3.03 | 72.1 |
| 30 % Methanol | 0.160 | 284 | 2.75 | 68.1 |
| 40 | 0.229 | 335 | 2.39 | 63.3 |
| 50 | 0.308 | | | 56.8 |
| 60 | 0.400 | | | 51.2 |
| 10 | 0.033 | 107 | 3.31 | |
| 20 % Ethanol | 0.072 | 224 | 3.05 | |
| 30 | 0.117 | 349 | 2.72 | |
| 40 | 0.171 | 479 | 2.20 | |
| 10 | 0.021 | 129 | 3.32 | 71.8 |
| 20 % t-Butyl | 0.046 | 269 | 2.90 | 62.9 |
| 30 % alcohol | 0.076 | 419 | 1.87 | 54.2 |
| 40 | 0.113 | 576 | 0.94 | 45.4 |
| 60 | 0.222 | | | 28.9 |
| 10 | 0.041 | -101 | 3.25 | |
| 20 % Ethylene | 0.094 | -197 | 3.04 | |
| 30 % glycol | 0.151 | -288 | 2.81 | |
| 40 | 0.217 | -371 | 2.68 | |
| 10 | 0.031 | -84 | | |
| 20 % Glycerol | 0.067 | -123 | | |
| 30 | 0.110 | -274 | | |
| 40 | 0.161 | -367 | | |
| 10 | 0.037 | 191 | | |
| 20 % Acetonitrile | 0.079 | 386 | | |
| 30 | 0.129 | 586 | | |
| 40 | 0.187 | 789 | | |
| 5 | 0.013 | | | |
| 10 | 0.027 | 87 | | 73.0 |
| 15 | 0.041 | | | |
| 20 % Acetone | 0.058 | 184 | | 67.0 |
| 30 | 0.095 | 294 | | 61.0 |
| 40 | 0.140 | 417 | | 54.6 |
| 50 | 0.196 | | | 48.2 |
| 60 | 0.268 | | | 41.8 |
| 10 | 0.027 | -75 | | |
| 20 % Dimethyl- | 0.059 | -165 | | |
| 30 % sulphoxide | 0.098 | -277 | | |
| 40 | 0.144 | -428 | | |
| 10 | 0.024 | 165 | | |
| 20 % Tetrahydro- | 0.053 | 343 | | |
| 30 % furan | 0.087 | 532 | | |
| 40 | 0.129 | 728 | | |
| 10 | 0.023 | 121 | | |
| 20 % 1,4-Dioxan | 0.050 | 207 | | |
| 30 | 0.083 | 290 | | |
| 40 | 0.124 | 400 | | |

a

All solvent mixtures are expressed in % by volume before mixing;

b

Solvent Y values were calculated from the expression:-

$$\log \frac{k}{k_o} = 1.00 \underline{Y}$$

where k is the rate of solvolysis of *t*-butyl chloride in a given solvent mixture; and k_o is that in 80 % ethanol. Values of k and k_o were taken from R.E. Robertson and S.E. Sugamori, J. Amer. Chem. Soc., (1969), 91, 7254.

c

Values of the dielectric constant, D , of the various solvent mixtures were taken from J. Timmermans, 'Physico-chemical Constants of Binary Systems', Interscience Publishers, Inc., New York, (1950), Vol. 4.

2. Computer Programs.

PROGRAM No. 1

```
5 CLOSE 3
6 OPEN "KB:" AS FILE 3
8 DIM X(30),Y(30),A(30),E(30),W(30)
10 LET S1=0:LET S2=0:LET S3=0:LET S4=0:LET L=0
11 PRINT "T=";
12 INPUT #3,Q
18 PRINT "NO. PTS.=";
19 INPUT #3,N
20 FOR I=1 TO N: LET X(I)=I: NEXT I
24 FOR I=1 TO N
25 PRINT "Y(;;I;)"=;
26 INPUT #3,Y(I)
27 NEXT I
28 GOSUB 200
29 GOTO 34
30 PRINT "?";
33 STOP
34 LET L=0
35 PRINT "P,R,0=";
36 INPUT #3,P,R,0
40 FOR W=P TO R STEP 0
45 FOR I=Z TO V
47 LET X=X(I): LET Y=Y(I)
49 LET Y=LOG(Y-W)
55 LET S1=S1+X: LET S2=S2+Y
56 LET S3=S3+X*Y: LET S4=S4+X*X
59 NEXT I
61 LET G=(V-(Z-1))
62 LET C=1/(G*S4-S1*S1)
63 LET A=(G*S3-S1*S2)*C
64 LET B=(S4*S2-S1*S3)*C
68 FOR I=Z TO V
70 LET D2=A*X(I)+B-LOG(Y(I)-W)
75 LET D=D+D2*D2
80 NEXT I
85 LET D=D*C/(G-2)
88 LET E=(SQR(G*D))/(-1*A)*100
90 LET L=L+1
91 LET E(L)=E: LET A(L)=A: LET W(L)=W
100 LET S1=0:LET S2=0:LET S3=0:LET S4=0:LET D=0
102 NEXT W
103 LET H=L
104 GOSUB 250
110 GOTO 30
200 PRINT "1ST I VALUE =";
205 INPUT #3,Z
210 PRINT "LAST I VALUE =";
215 INPUT #3,V
220 RETURN
250 PRINT "H=";H
252 FOR L=2 TO H
255 IF E(L)<E(L-1) THEN 305
256 PRINT E(L),E(L-1)
258 NEXT L
259 PRINT "NO MIN."
303 GOTO 34
305 IF E(L)<E(L+1) THEN 350
307 PRINT E(L),E(L+1)
310 GOTO 258
355 PRINT "K=";-A(L)/Q,"ERR.=";E(L),"Z"
357 PRINT "INF=";W(L)
360 RETURN
365 STOP
```

PROGRAM No. 2

```

00100 REM**** INSTRUCTIONS FOR USE****
00110 REM..PUT IN TIME INT.,NO. OF POINTS,THEN
00120 REM.. O.D. VALUES AT LINES 00810 TO 01000
00130 DIMX(30),Y(30),E(400),A(400),W(400)
00140 LETS1=S2=S3=S4=D=0
00150 READ Q,N
00160 FORI=1TON
00170 LETX(I)=I
00180 NEXTI
00190 FORI=1TON
00200 READY(I)
00210 NEXTI
00220 GOSUB 00770
00230 LET Z=2
00240 PRINT"INPUT INFINITY RANGE + STEP,(P,R,0)";
00250 INPUTP,R,0
00260 LETL=0
00270 FORW=PTOR STEPO
00280 FOR I=Z TO V
00290 LET X=X(I)
00300 LETY2=ABS(Y(I)-W)
00310 LETY=LOG(Y2)
00320 LETS1=S1+X
00330 LETS2=S2+Y
00340 LETS3=S3+X*Y
00350 LETS4=S4+X*X
00360 NEXT I
00370 LETG=(V-(Z-1))
00380 LETC=1/(G*S4-S1*S1)
00390 LETA=(G*S3-S1*S2)*C
00400 LETB=(S4*S2-S1*S3)*C
00410 FORI=ZTOV
00420 LETY2=ABS(Y(I)-W)
00430 LETD2=A*X(I)+B-LOG(Y2)
00440 LETD=D+D2*D2
00450 NEXTI
00460 LETD=D*C/(G-2)
00470 LETE=(SQR(G*D))/(-1*A)*100
00480 LETL=L+1
00490 LET E(L)=E
00500 LETA(L)=A
00510 LETW(L)=W
00520 LETS1=S2=S3=S4=D=0
00530 NEXT W
00540 LET H=L
00550 PRINT"H=";H
00560 LET H1=H-1
00570 FORL=2TOH1
00580 IF E(L)<E(L-1) THEN 00610
00590 NEXTL
00600 GOTO 00630
00610 IFE(L)<E(L+1) THEN 00650
00620 GOTO 00590
00630 PRINT"NO SOLN"
00640 GOTO 00720
00650 PRINT USING 00660,-A(L)/Q
00660 :***RATE CONSTANT IS #.###^
00670 PRINT USING 00680,E(L)
00680 : % ERROR IS #.###
00690 PRINT USING 00700,W(L)
00700 : INFINITY IS #.###
00710 PRINT
00720 PRINT"DO YOU WISH TO HAVE ANOTHER GO";
00730 INPUTT$
00740 IF T$="NO" THEN 01000
00750 IFT$="YES" THEN 00760
00760 GOTO 00220
00770 PRINT"INPUT RANGE OF POINTS,(Z,V) ";
00780 INPUTZ,V
00790 RETURN
00800 REM.....DATA UP TO 1000
01000 END

```

[illegible]

```

5 CLOSE3
6 OPEN"KB:"ASFILE3
10 DIMX(20),Y(20)
21 LET S1=0:LETS2=0:LETS3=0:LETS4=0
23 LETD=0
29 PRINT "NO.OF POINTS=";
30 INPUT #3,N
40 FORI=1TON
45 PRINT"X(";I;")=";
50 INPUT#3,X
53 PRINT"Y(";I;")=";
54 INPUT#3,Y
55 LET X(I)=X
56 LET Y(I)=Y
60 LETS1=S1+X
70 LETS2=S2+Y
80 LETS3=S3+X*Y
90 LET S4=S4+X*X
100 NEXT I
110 LETC=1/(N*S4-S1*S1)
120 LETA=(N*S3-S1*S2)*C
130 LETB=(S4*S2-S1*S3)*C
140 FOR I=1 TO N
150 LET D2=A*X(I)+B-Y( I):LET D=D+D2*D2
160 NEXT I
165 LETD=D*C/(N-2)
170 PRINT"Y=((";A;"#";SQR(N*D);")X+";B;"#";SQR(S4*D)
178 PRINT"% ERROR="(SQR(N*D)/A)*100
180 STOP

```

PROGRAM No. 4

```

5 CLOSE3
6 OPEN**KB:**ASFILE3
10 DIMX(20),Y(20)
21 LET S1=0:LETS2=0:LETS3=0:LETS4=0
23 LETD=0
29 PRINT "NO.OF POINTS=";
30 INPUT #3,N
35 PRINT "X IS TEMP. INCENTIGRADE, Y IS K"
40 FOR I=1 TO N
45 PRINT"X(";I;")=";
52 INPUT#3,X
53 PRINT"Y(";I;")=";
54 INPUT#3,Y
55 LET X=1000/(X+273.16)
56 LET X(I)=X
57 LET Y=LOG(Y)/2.302585
58 LET Y(I)=Y
60 LETS1=S1+X
70 LETS2=S2+Y
80 LETS3=S3+X*Y
90 LETS4=S4+X*X
100 NEXT I
110 LETC=1/(N*S4-S1*S1)
120 LETA=(N*S3-S1*S2)*C
130 LETB=(S4*S2-S1*S3)*C
140 FOR I=1TON
150 LET D2=A*X(I)+B-Y(I):LET D=D+D2*D2
160 NEXT I
165 LETD=D*C/(N-2)
170 PRINT"Y=(";A;"#";SQR(N*D);")X+";B;"#";SQR(S4*D)
171 PRINT"E-ACT=";-4.57563*A;
172 PRINT"#4.57563*SQR(N*D);"KCAL"
173 PRINT"A FACTOR IS 10^";B;"#";SQR(S4*D)
180 STOP

```

3. The Arrhenius Law.

The dependence of reaction rate upon temperature, was initially explained by Arrhenius, using arguments similar to those on which transition state theory was later based. He arrived at equation(A3.01), which, when combined with the Maxwell-Boltzmann theory of the distribution of energy among molecules produced equation(A3.02), which is now known as the Arrhenius equation.

$$k_R = A \times (\text{fraction of the number of molecules with the necessary activation energy}) \quad (\text{A3.01})$$

where k_R is the rate constant; and A is a proportionality constant.

$$k_R = A \times e^{-E/RT} \quad (\text{A3.02})$$

(The quantity $-E/RT$ is known as the Boltzmann factor, E being the activation energy, i.e. the minimum amount of energy necessary for a reactant molecule to reach the transition state energy.)

Hence the activation energy may be determined from several measurements of k_R at different temperatures. A plot of $\ln(k_R)$ against $1/T$ gives a linear correlation, of slope equal to $-E/R$. The enthalpy of activation, ΔH^\ddagger , is related to E by the expression:-

$$E = \Delta H^\ddagger - RT \quad (\text{A3.03})$$

The entropy of activation, ΔS^\ddagger , is contained in the Arrhenius equation as part of the A factor. Using the expression

$$k_R = \frac{R.T.K^\ddagger}{N.h} \quad (\text{A3.04})$$

(where K^\ddagger is the pseudo-equilibrium constant for formation of the transition state, N is the Avogadro number, and h is Planck's constant.)

then the Arrhenius equation becomes:-

$$k_R = \frac{RT}{Nh} \cdot \exp \frac{\Delta S^\ddagger}{R} \cdot \exp \frac{-\Delta H^\ddagger}{RT} \quad (\text{A3.05})$$

whence, knowing k_R and ΔH^\ddagger , ΔS^\ddagger may be calculated.

4. Structure Factors for the trans-[Co(cyclam)(NCS)₂]SCN
Single Crystal Study.

[illegible]

[illegible]

[illegible]

[illegible]

[illegible]

[illegible][illegible][illegible][illegible][illegible]

[illegible]

[illegible][illegible]

```
L      TTTTTTTTTTTTTTTTTTTTTTTTTTTTTTTTTTTTTTTTTTTTTTTTTTTTTTTT
K      T1000000TTTTTTTTTTTTTTTTNNNNNNNNNNNNNNNNNNMMMMf444444ffff5555
H      07-5M5A71-06-fMNMNMF07-06NHNHNM7FENONONNMN07-fM-fO-HN-f-f-MN
```

[illegible][illegible]

REFERENCES

CHAPTER 1

- 1.01 S. Glasstone, K.J. Laidler and H. Eyring, 'The Theory of Rate Processes', McGraw-Hill, New York, (1941).
- 1.02 F. Basolo and R.G. Pearson, 'Mechanisms in Inorganic Chemistry', 2nd. Edn., J. Wiley, New York, (1967), pp.141-142.
- 1.03 J.E. Leffler and E. Grunwald, 'Rates and Equilibria of Organic Reactions', J. Wiley, New York, (1963), p.156.
- 1.04 T.W. Swaddle, Coord. Chem. Rev., (1974), 14, 217.
- 1.05 T.W. Swaddle and G. Guastalla, Inorg. Chem., (1968), 7, 1915.
- 1.06 M.J. Blandamer and J. Burgess, Chem. Soc. Rev., (1975), 4, 55.
- 1.07 E.M. Moelwyn-Hughes, 'The Chemical Statics and Kinetics of Solutions', Academic Press, London, (1971).
- 1.08 R.E. Robertson, Progr. Phys. Org. Chem., (1967), 4, 213.
- 1.09 E.F. Caldin and H.P. Bennetto, J. Soln. Chem., (1973), 2, 217.
- 1.10 See, for example, 'Inorganic Reaction Mechanisms', ed. J. Burgess, Chem. Soc. Specialist Periodical Reports, (1971), 1, pp.163-166, 172-173, 201-204; (1972), 2, pp.150-151, 162-163, 168-169; (1974), 3, pp.182-184, 201-203, 318-324; C.H. Langford and V.S. Sastri, 'Reaction Mechanisms in Inorganic Chemistry', ed. M.L. Tobe, M.T.P. Internat. Rev. Sci., Butterworths, London, (1971), 2, series 1, chapter 6.
- 1.11 J. Burgess, 'Inorganic Reaction Mechanisms', ed. A. McAuley, Chem. Soc. Specialist Periodical Reports, in press.
- 1.12 See, for example, E.S. Amis, 'Solvent Effects on Reaction Rates and Mechanisms', Academic Press, New York, (1966), p.169.
- 1.13 E. Grunwald and S. Winstein, J. Amer. Chem. Soc., (1948), 70, 846.
- 1.14 H.P. Bennetto and E.F. Caldin, J. Chem. Soc.(A), (1971), 2190,2198, 2207.
- 1.15 E.F. Caldin and M.W. Grant, J. Chem. Soc.(Faraday I), (1973), 1648.

- 1.16 'Hydrogen-Bonded Solvent Systems', Ed. A. Covington and P. Jones, Taylor and Francis, London, (1968), (a) F. Franks, p.31, (b) J.B. Hyne, p.99.
- 1.17 R.S. Rowlinson, 'Liquids and Liquid Mixtures', Butterworths, (1969), p.111.
- 1.18 E.A. Guggenheim, Trans. Faraday Soc., (1937), 33, 151.
- 1.19 G. Scatchard, Chem. Rev., (1949), 44, 7.
- 1.20 J.A. Barker, Austral. J. Chem., (1953), 6, 207.
- 1.21 J.E. Leffler and E. Grunwald, 'Rates and Equilibria of Organic Reactions', Wiley, New York, (1963).
- 1.22 D. Feakins and P. Watson, J. Chem. Soc., (1963), 4734; A.L. Andrews, H.P. Bennetto, D. Feakins, K.G. Lawrence and R.P.T. Tomkins, J. Chem. Soc.(A), (1968), 1486; D. Feakins, 'Physico-Chemical Processes in Mixed Aqueous Solvents', Ed. F. Franks, Elsevier, New York, (1967), pp.71-90.
- 1.23 B. Case and R. Parsons, Trans Faraday Soc., (1967), 63, 1224.
- 1.24 J.E.B. Randles, Trans. Faraday Soc., (1956), 52, 1573.
- 1.25 C.F. Wells, J. Chem. Soc.(Faraday I), (1973), 69, 984; *ibid.*, (1974), 70, 694; *ibid.*, (1975), 71, 1868.
- 1.26 M. Alfenaar^{A.G. Remijnse} and C.L. de Ligny, Rec. Trav. Chim., (1967), 86, 929; C.L. de Ligny, H.J.M. Denessen and M. Alfenaar, *ibid.*, (1971), 90, 1265; D. Bax, C.L. de Ligny and M. Alfenaar, *ibid.*, (1972), 91, 452; D. Bax, C.L. de Ligny and A.G. Remijnse, *ibid.*, (1972), 91, 965, 1225.
- 1.27 B.G. Cox, G.R. Hedwig, A.J. Parker and D.W. Watts, Austral. J. Chem., (1974), 27, 477.
- 1.28 M.H. Abraham, J. Chem. Soc.(Faraday I), (1973), 69, 1375.

CHAPTER 2

- 2.01 C.H. Langford and H.B. Gray, 'Ligand Substitution Processes', W.A. Benjamin, Inc., New York, (1965).
- 2.02 J.E. Byrd and W.K. Wilmarth, *Inorg. Chim. Acta Rev.*, (1971), 5, 7.
- 2.03 A. Haim and W.K. Wilmarth, *Inorg. Chem.*, (1962), 1, 573, 583;
R. Grassi, A. Haim and W.K. Wilmarth, *ibid.*, (1967), 6, 273.
- 2.04 D.R. Stranks and J.K. Yandell, *Inorg. Chem.*, (1970), 9, 751.
- 2.05 (a) A.M. Sargeson, *Pure Applied Chem.*, (1973), 33, 527; (b) C.K. Poon, *Coord. Chem. Rev.*, (1973), 10, 1.
- 2.06 H.E. Toma and J.M. Malin, *Inorg. Chem.*, (1973), 12, 1039.
- 2.07 H.E. Toma and J.M. Malin, *Inorg. Chem.*, (1973), 12, 2080.
- 2.08 H.E. Toma, J.M. Malin and E. Giesbrecht, *Inorg. Chem.*, (1973), 12, 2084.
- 2.09 D. Pavlović, I. Murati and S. Ašperger, *J. Chem. Soc.(Dalton)*, (1973), 602.
- 2.10 Z. Bradić, D. Pavlović, I. Murati and S. Ašperger, *J. Chem. Soc.(Dalton)*, (1974), 344.
- 2.11 Z. Bradić, M. Pribanić and S. Ašperger, *J. Chem. Soc.(Dalton)*, (1975), 353.
- 2.12 D. Pavlović, D. Šutić and S. Ašperger, *J. Chem. Soc.(Dalton)*, (1976), 2406.
- 2.13 C. Reichardt, 'Lösungsmittelleffekte in der organischen Chemie', Verlag Chemie, Weinheim, (1968).
- 2.14 D.J. Kenney, T.P. Flynn and J.B. Gallini, *J. Inorg. Nuclear Chem.*, (1961), 20, 75.
- 2.15 C.T. Bahner and L.L. Norton, *J. Amer. Chem. Soc.*, (1950), 72, 2881.
- 2.16 I. Dézsi, B. Molnar, T. Szalay and I. Jaszberényi, *Chem. Phys. Lett.*, (1973), 18, 598.

- 2.17 A.J. Gordon and R.A. Ford, 'The Chemist's Companion', Wiley, New York, (1972), pp.429-437.
- 2.18 D.P. Biddiscombe and E.F.G. Herington, *Analyst*, (1956), 81, 711.
- 2.19 R.P. Mitra, B.K. Sharma and S.P. Mittal, *J. Inorg. Nuclear Chem.*, (1972), 34, 3919.
- 2.20 L. Dozsa, I. Szilassy and M.T. Beck, *Magyar Kém. Folyóirat*, (1973), 79, 45.
- 2.21 B. Jezowska-Trzebiatowska, A. Keller and J. Ziolkowski, *Bull. Acad. Sci. chim. polon.*, (1972), 20, 649; A.D. James and R.S. Murray, *J. Chem. Soc.(Dalton)*, (1975), 1530.
- 2.22 F. Basolo and R.G. Pearson, 'Mechanisms of Inorganic Reactions', 2nd. Edn., Wiley, New York, (1967), p.129.
- 2.23 J.E. Leffler, *J. Org. Chem.*, (1955), 20, 1202.
- 2.24 J.E. Leffler and E. Grunwald, 'Rates and Equilibria of Organic Reactions', J. Wiley & Sons, Inc., New York, (1963).
- 2.25 B. Raistrick, R.H. Sapiro and O.M. Newitt, *J. Chem. Soc.*, (1939), 1761.
- 2.26 E.A. Braude, L.M. Jackmann and R.P. Linstead, *J. Chem. Soc.*, (1954), 3548.
- 2.27 R.A. Orr and H.L. Williams, *J. Phys. Chem.*, (1953), 57, 925.
- 2.28 R.T.M. Frazer and H. Taube, *J. Amer. Chem. Soc.*, (1961), 83, 2242.
- 2.29 R. Barca, J. Ellis, Tsao-Maah-Sang and W.K. Wilmarth, *Inorg. Chem.*, (1967), 6, 243.
- 2.30 J. Halpern, R.A. Palmer and L.M. Blackley, *J. Amer. Chem. Soc.*, (1966), 88, 2877.
- 2.31 P.H. Tewari, R.W. Saver, H.K. Wilcox and W.K. Wilmarth, *Inorg. Chem.*, (1967), 6, 611.
- 2.32 W. Robb, M.M. De V. Steyn and H. Krüger, *Inorg. Chim. Acta*, (1967), 3, 383.

- 2.33 J. Burgess, R.I. Haines, D.R. Stranks and T.R. Sullivan, J. Chem. Soc.(Dalton), in press.
- 2.34 D.R. Stranks, Pure Applied Chem., (1974), 38, 303.
- 2.35 H.S. Golinkin, W.G. Laidlow and J.B. Hyne, Canad. J. Chem., (1966), 44, 2193.
- 2.36 See, for example, E. Whalley, Adv. Phys. Org. Chem., (1964), 2, 93; Ann. Rev. Phys. Chem., (1967), 18, 205; W.J. le Noble, Progr. Phys. Org. Chem., (1967), 5, 207.
- 2.37 D.R. Stranks and T.W. Swaddle, J. Amer. Chem. Soc., (1971), 93, 2783.
- 2.38 D.R. Stranks and T.W. Swaddle, J. Amer. Chem. Soc., (1972), 94, 8357.
- 2.39 H.R. Hunt and H. Taube, J. Amer. Chem. Soc., (1958), 80, 2642.
- 2.40 See, for example, 'Inorganic Reaction Mechanisms', ed. J. Burgess, Chem. Soc. Specialist Periodical Reports, London, (1971), 1, pp.176-177, 186-187; (1972), 2, pp.168-169, 173, 182; (1974), 3, pp.214-217, 243-244; C.H. Langford and V.S. Sastri, 'Reaction Mechanisms in Inorganic Chemistry', ed. M.L. Tobe, M.T.P. Internat. Rev. Sci., 2, Butterworths, London, series 1, (1971), p.252.
- 2.41 Reference 2.22, pp.218-219.
- 2.42 J. Burgess, J. Chem. Soc.(A), (1968), 1085.
- 2.43 J. Burgess, J. Chem. Soc.(A), (1969), 1899.
- 2.44 J.-M. Lucie, D.R. Stranks and J. Burgess, J. Chem. Soc.(Dalton), (1975), 245.
- 2.45 L. Pauling, 'Nature of the Chemical Bond', Cornell University Press, Ithaca, New York, 3rd. Edn., chapter 7.
- 2.46 K.R. Brower and J.S. Chan, J. Amer. Chem. Soc., (1965), 87, 3396.
- 2.47 K.R. Brower and T. Chan, Inorg. Chem., (1973), 12, 2198.
- 2.48 K.R. Brower, J. Amer. Chem. Soc., (1963), 85, 1401.
- 2.49 E. Whalley, Ann. Rev. Phys. Chem., (1967), 18, 205.

- 2.50 E. Grunwald and S. Winstein, J. Amer. Chem. Soc., (1948), 70, 846; E.M. Kosower, 'Introduction to Physical Organic Chemistry', Wiley, New York, (1968), chapters 2.6 & 2.7.
- 2.51 H.P. Bennetto and E.F. Caldin, J. Chem. Soc.(A), (1971), 2190, 2198,2207.
- 2.52 E.F. Caldin and M.W. Grant, J. Chem. Soc.(Faraday I), (1973), 1648.
- 2.53 M.J. Blandamer and J. Burgess, Chem. Soc. Rev., (1975), 4, 55.
- 2.54 See, for example, J. Chatt, L.A. Duncanson and L.M. Venanzi, J. Chem. Soc., (1955), 4456.
- 2.55 J. Burgess, J. Chem. Soc. Chem. Comm., (1969), 1422; J. Chem. Soc. (Dalton), (1972), 203.
- 2.56 M.J. Blandamer, J. Burgess and J.G. Chambers, J. Chem. Soc.(Dalton), (1976), 606.
- 2.57 J. Burgess and M.G. Price, J. Chem. Soc.(A), (1971),3108; G. Thomas and L.A.P. Kane-Maguire, J. Chem. Soc.(Dalton), (1974), 1688.
- 2.58 J. Burgess, R.D. Peacock and A.M. Petric, J. Chem. Soc.(Dalton), (1973), 902.
- 2.59 J. Burgess, J. Chem. Soc.(Dalton), (1973), 825.
- 2.60 O. Baudich, Ber., (1921), 54, 413.
- 2.61 P. Debye, Trans. Electrochem. Soc., (1942), 82, 265; M. Eigen, Z. Elektrochem. Ber. Bunsengesellschaft Phys. Chem., (1960), 64, 115; D.N. Hague, 'Fast Reactions', Wiley-Interscience, New York, (1971), pp.12-14.

CHAPTER 3

- 3.01 T.S. Lee, I.M. Kolthoff and D.L. Leussing, J. Amer. Chem. Soc., (1948), 70, 2348; W.W. Brandt and D.K. Gullstrom, *ibid.*, (1952), 74, 3532.
- 3.02 J.M. Lucie, D.R. Stranks and J. Burgess, J. Chem. Soc.(Dalton), (1975), 245.
- 3.03 J. Burgess, J. Chem. Soc.(A), (1969), 1899.
- 3.04 J. Burgess, J. Chem. Soc.(A), (1968), 1085.
- 3.05 J. Burgess, J. Chem. Soc.(A), (1970), 2351.
- 3.06 J. Burgess, F.M. Mekhail and E.R. Gardner, J. Chem. Soc.(Dalton), (1973), 1335.
- 3.07 M.J. Blandamer, J. Burgess and R.I. Haines, J. Chem. Soc.(Dalton), (1976), 385.
- 3.08 A.I. Vogel, 'Quantitative Inorganic Analysis', 3rd. Edn., Longmans, (1961), p.238.
- 3.09 M.J. Blandamer, J. Burgess and S.H. Morris, J. Chem. Soc.(Dalton), (1974), 1717.
- 3.10 S. Winstein and A.H. Fainberg, J. Amer. Chem. Soc., (1956), 78, 2770.
- 3.11 R.H. Schuster and I.A. Schneider, Rev. Roumaine Chim., (1973), 18, 1841.
- 3.12 R.E. Robertson and S.E. Sugamori, J. Amer. Chem. Soc., (1969), 91, 7254.
- 3.13 R.E. Robertson and S.E. Sugamori, Canad. J. Chem., (1972), 50, 1353.
- 3.14 E. Tommila, M. Tiilikainen and A. Voipo, Ann. Acad. Sci. Fennicae, (1955), A2, 65.
- 3.15 K. Heinonen and E. Tommila, Suomen Kem., (1965), B38, 9.
- 3.16 M.J. Blandamer and J.R. Membrey, personal communication.
- 3.17 M.J. Blandamer and J.R. Membrey, J. Chem. Soc. Chem. Comm., (1973), 614.

- 3.18 M.J. Blandamer, J. Burgess and S. Hamshire, J. Chem. Research, in press.
- 3.19 R.C. Weast(ed.), 'Handbook of Chemistry and Physics', 53rd. Edn., Chemical Rubber Co., p.C287.
- 3.20 C.K. Poon and M.L. Tobe, J. Chem. Soc.(A), (1968), 1549.
- 3.21 C.F. Wells, J. Chem. Soc.(Faraday I), (1973), 69, 985.
- 3.22 F.M. Van Meter and H.M. Neumann, J. Amer. Chem. Soc., (1976), 98, 1382.

CHAPTER 4

, A.G. Remijnse

- 4.01 M. Alfenaar and C.L. de Ligny, Rec. Trav. Chim., (1967), 86, 929;
C. L. de Ligny, H.J.M. Denessen and M. Alfenaar, ibid., (1971), 90,
1265; D. Bax, C.L. de Ligny and M. Alfenaar, ibid., (1972), 91, 452;
D. Bax, C.L. de Ligny and A.G. Remijnse, ibid., (1972), 91, 965, 1225;
C.F. Wells, J. Chem. Soc.(Faraday I), (1973), 69, 984; C.F. Wells,
ibid., (1974), 70, 694; C.F. Wells, ibid., (1975), 71, 1868.
- 4.02 M.H. Abraham, J. Chem. Soc.(Faraday I), (1973), 69, 1375.
- 4.03 J. Burgess, N. Morton and J.C. McGowan, J. Chem. Soc.(Dalton),
in press.
- 4.04 F.M. Van Meter and H.M. Neumann, J. Amer. Chem. Soc., (1976), 98, 1382.
- 4.05 H.P. Bennetto and J.W. Letcher, Chem. Ind.(London), (1972), 847.
- 4.06 A.J. Dill and O. Popovych, J. Chem. Eng. Data, (1969), 14, 240.
- 4.07 M.L. Moss, M.G. Mellon and G.F. Smith, Anal. Chem.,
(1942), 14, 931.
- 4.08 'Solubilities of Inorganic and Organic Compounds', Ed. H. Stephen
and T. Stephen, 1, part 1, Pergamon Press, Oxford, (1963), p.164.
- 4.09 V. Rothmund, Z. phys. Chem., (1910), 69, 523.
- 4.10 J. Setschenow, Z. phys. Chem., (1889), 4, 117; Ann. Chim. phys.,
(1891), 25, 226.
- 4.11 J.C. McGowan, Nature, (1974), 252, 296.
- 4.12 E.M. Strel'tsova, N.K. Markova and G.A. Krestov, Izvest. Vyssh.
Ucheb. Zaved. Khim. i Tekhnol., (1973), 16, 694; Russ. J. Phys. Chem.,
(1974), 48, 2244.
- 4.13 E.M. Strel'tsova, N.K. Markova and G.A. Krestov, Russ. J. Phys. Chem.,
(1974), 48, 992; Zhur. Fiz. Khim., (1976), 50, 264.
- 4.14 B.G. Cox, G.R. Hedwig, A.J. Parker and D.W. Watts, Austral. J. Chem.,
(1974), 27, 477.

- 4.15 N.N. Greenwood, 'Ionic Crystals, Lattice Defects and Non-Stoichiometry', Butterworths, (1965), pp.40-41.
- 4.16 J.E. Dickens, F. Basolo and H.M. Neumann, J. Amer. Chem. Soc., (1957), 79, 1286.
- 4.17 C.W. Davies, J. Chem. Soc., (1938), 2093.
- 4.18 L. Burlamacchi, G. Martini and M. Romanelli, J. Chem. Phys., (1973), 59, 3008.
- 4.19 F.A. Long and W.F. McDevitt, Chem. Rev., (1952), 51, 119.
- 4.20 R.D. Gillard, C.T. Hughes, L.A.P. Kane-Maguire and P.A. Williams, Transit. Met. Chem., (1976), 1, 226.
- 4.21 G.F. Smith and F.P. Richter, 'Phenanthroline and Substituted Phenanthroline Indicators', G.F. Smith Chem. Co., Columbus, Ohio, (1944).
- 4.22 J.S. Fritz, F.Wm. Cagle Jr. and G.F. Smith, J. Amer. Chem. Soc., (1949), 71, 2480.
- 4.23 A. Seidell, 'Solubilities of Organic Compounds', 3rd. Edn., 2, (1941), D. Van Nostrand Co. Inc., p. 742.
- 4.24 J.G. Chambers, Ph.D. Thesis, Leicester University, (1976).
- 4.25 J.C. McGowan, J. Chem. Soc. Chem. Comm., (1971), 514, and references therein.
- 4.26 J.C. McGowan, Rec. Trav. Chim., (1956), 75, 193.
- 4.27 E.C.M. Grigg, J.R. Hall and R.A. Plowman, Austral. J. Chem., (1962), 15, 864.
- 4.28 N.P. Komar and G.S. Zaslavskaya, Russ. J. Phys. Chem., (1973), 47, 1642.

CHAPTER 5

- 5.01 J. Burgess, J. Chem. Soc.(Dalton), (1972), 1061.
- 5.02 J. Burgess and R.H. Prince, J. Chem. Soc., (1965), 6061.
- 5.03 M.J. Blandamer, J. Burgess and J.G. Chambers, J. Chem. Soc. (Dalton), (1976), 606.
- 5.04 M.J. Blandamer, J. Burgess, J.G. Chambers, R.I. Haines and H.E. Marshall, J. Chem. Soc.(Dalton), (1977), 165.
- 5.05 B.E. Fleischfresser and I. Lauder, Austral. J. Chem., (1962), 15, 251.
- 5.06 I.G. Ryss and L.P. Bogdanova, Russ. J. Inorg. Chem., (1963), 8, 11;
I.G. Ryss, L.P. Bogdanova, S.L. Idel's and T.N. Kotlyar, *ibid.*, (1969), 4, 1577; L.P. Bogdanova and T.N. Kotlyar, Kinetika i Kataliz, (1973), 14, 245; M.D. Bentley, S.E. Bowie and R.D. Limoges, J. Phys. Chem., (1971), 75, 1763.
- 5.07 M.J. Blandamer, J. Burgess and S.H. Morris, J. Chem. Soc.(Dalton), (1975), 2118.
- 5.08 H. Morawetz and B. Vogel, J. Amer. Chem. Soc., (1969), 91, 563.
- 5.09 S.W. Foong, B. Kipling and A.G. Sykes, J. Chem. Soc.(A), (1971), 118.
- 5.10 J.H. Espenson and S.R. Hubbard, Inorg. Chem., (1966), 5, 686.
- 5.11 A.B. Venediktov and A.V. Belyaev, Russ. J. Inorg. Chem., (1972), 17, 1158; S.C. Chan and S.F. Chan, J. Inorg. Nuclear Chem., (1972), 34, 2311.
- 5.12 C. Bifano and R.G. Linck, Inorg. Chem., (1968), 7, 908.
- 5.13 G.G. Schlessinger, Inorg. Syntheses, (1967), 9, 160.
- 5.14 J.C. Bailar Jr., Inorg. Syntheses, (1946), 2, 222.
- 5.15 S.N. Anderson and F. Basalo, Inorg. Syntheses, (1963), 7, 217.

- 5.16 Y.K. Sze and D.E. Irish, *Canad. J. Chem.*, (1975), 53, 427.
- 5.17 J. Burgess, R.D. Peacock and A.M. Petric, *J. Chem. Soc.(Dalton)*, (1973), 902.
- 5.18 S.C. Chan and S.F. Chan, *J. Chem. Soc.(A)*, (1969), 202.
- 5.19 J. Burgess and S.J. Cartwright, *J. Chem. Soc.(Dalton)*, (1976), 1561.
- 5.20 I.V. Kozhevnikov and E.S. Rudakov, *Inorg. Nuclear Chem. Lett.*, (1972), 8, 571.
- 5.21 F. Basolo and R.G. Pearson, 'Mechanisms of Inorganic Reactions', Wiley, New York, p.64.
- 5.22 S.F. Chan and S.L. Tan, *Austral. J. Chem.*, (1975), 28, 1133.
- 5.23 J. Burgess N. Morton and J.C. McGowan, *J. Chem. Soc.(Dalton)*, in press.
- 5.24 M.H. Abraham, J.F.C. Oliver and J.A. Richards, *J. Chem. Soc.(A)*, (1970), 203.
- 5.25 J.G. Chambers, Ph.D. Thesis, Leicester, (1976).
- 5.26 E.M. Strel'tsova, N.K. Markova and G.A. Krestov, *Izvest. Vyssh. Ucheb. Zaved. Khim. i Tekhnol.*, (1973), 16, 694; *Russ. J. Phys. Chem.*, (1974), 48, 2244.
- 5.27 C.F. Wells, *J. Chem. Soc.(Faraday I)*, (1974), 70, 694.
- 5.28 E.M. Strel'tsova, N.K. Markova and G.A. Krestov, *Russ. J. Phys. Chem.*, (1974), 48, 992; *Zhur. Fiz. Khim.*, (1976), 50, 264.
- 5.29 W.R. Fitzgerald, A.J. Parker and D.W. Watts, *J. Amer. Chem. Soc.*, (1968), 90, 5744.
- 5.30 N.N. Greenwood, 'Ionic Crystals, Lattice Defects and Non-Stoichiometry', Butterworths, London, (1968), pp.(a)40-41, (b) 35, (c) 27.
- 5.31 J. Burgess and S.J. Cartwright, *J. Chem. Soc.(Dalton)*, (1976), 1158.

- 5.32 M.J. Blandamer, J. Burgess and J.G. Chambers, J. Chem. Soc. (Dalton), (1977), 60.
- 5.33 M.H. Abraham, J. Chem. Soc.(A), (1971), 1061, and references therein.
- 5.34 M.H. Abraham and G.F. Johnston, J. Chem. Soc.(A), (1970), 188.
- 5.35 M.H. Abraham and G.F. Johnston, J. Chem. Soc.(A), (1970), 193.
- 5.36 M.H. Abraham, J. Chem. Soc. Chem. Comm., (1969), 1307.
- 5.37 M.H. Abraham, J. Chem. Soc.(Perkin II), (1972), 1343.
- 5.38 Ref. 5.21, p.164, 169.

CHAPTER 6

- 6.01 See, for example, D.H. Irvine, J. Chem. Soc., (1959), 2977; D.A. House, Chem. Rev., (1962), 62, 185.
- 6.02 J. Burgess and R.H. Prince, J. Chem. Soc.(A), (1966), 1772.
- 6.03 S. Raman and C.H. Brubaker, J. Inorg. Nuclear Chem., (1969), 31, 1091.
- 6.04 J. Burgess, J. Chem. Soc.(A), (1970), 2114.
- 6.05 J. Burgess, J. Chem. Soc.(A), (1970), 2111.
- 6.06 J. Burgess, J. Chem. Soc.(A), (1967), 431.
- 6.07 J. Burgess, J. Chem. Soc.(A), (1968), 497.
- 6.08 W.C. Vasudeva and S. Wasif, J. Chem. Soc.(B), (1970), 960.
- 6.09 I.M. Kolthoff, A.L. Medalia and H.P. Raaen, J. Amer. Chem. Soc., (1951), 75, 1733.
- 6.10 J.H. Merz and W.A. Waters, Disc. Faraday Soc., (1949), 2, 179.
- 6.11 J. Burgess, J. Chem. Soc.(A), (1968), 2571.
- 6.12 J. Burgess, J. Chem. Soc.(A), (1970), 2351.
- 6.13 See, for example, E.S. Amis, 'Solvent Effects on Reaction Rates and Mechanisms', Academic Press, London, (1966), chapter 1.
- 6.14 E. Grunwald and S. Winstein, J. Amer. Chem. Soc., (1948), 70, 846; E.M. Kosower, 'Introduction to Physical Organic Chemistry', Wiley, New York, (1968), chapters 2.6 & 2.7.
- 6.15 J.E. Dickens, F. Basolo and H.M. Neumann, J. Amer. Chem. Soc., (1957), 79, 1286.
- 6.16 A.I. Vogel, 'Quantitative Inorganic Analysis', Longmans, London, (1961), p.325.
- 6.17 E. Eichler and A.C. Wahl, J. Amer. Chem. Soc., (1958), 80, 4145.
- 6.18 L. Eimer and A.I. Medalia, J. Amer. Chem. Soc., (1952), 74, 1592.

- 6.19 F.P. Dwyer and E.C. Gyarfas, J. Amer. Chem. Soc., (1952), 74, 4699.
- 6.20 See reference 6.16, p.238.
- 6.21 J. Halpern, R.J. Legare and R. Lumry, J. Amer. Chem. Soc., (1963), 85, 680.
- 6.22 D. Benson, 'Mechanisms of Inorganic Reactions in Solution, An Introduction', McGraw-Hill, London, (1968), chapter 5.
- 6.23 V. Balzani, V. Carassiti and L. Moggi, Inorg. Chem., (1964), 3, 1252.
- 6.24 H. Galiba, L.J. Csanyi and Z.G. Sobazo, Z. anorg. allgem Chem., (1956), 287, 169.
- 6.25 S.S. Bhatnager, B. Prakash and J. Singh, J. Indian Chem. Soc., (1940), 17, 133.
- 6.26 F.A. Jackmann and M.W. Lister, J. Solution Chem., (1976), 5, 417.
- 6.27 K. Ohashi, M. Matsuzawa, E. Hamano and K. Yamamoto, Bull. Chem. Soc. Japan, (1976), 49, 2440.
- 6.28 R.A. Marcus, J. Chem. Phys., (1956), 24, 966.
- 6.29 G. Dulz and N. Sutin, Inorg. Chem., (1963), 2, 917.
- 6.30 E.S. Amis and V.K. Lather, J. Amer. Chem. Soc., (1939), 61, 905.
- 6.31 E.S. Amis, 'Kinetics of Chemical Change in Solution', Macmillan, New York, (1949), chapter IV.
- 6.32 E.S. Amis and J.B. Price, J. Phys. Chem., (1943), 47, 338.
- 6.33 M.J. Blandamer, J. Burgess and R.I. Haines, J. Chem. Soc.(Dalton), (1976), 385.
- 6.34 F. Blau, Chem. Ber., (1888), 21, 1077.
- 6.35 F. Blau, Monatsh, (1898), 19, 647.
- 6.36 T.S. Lee, I.M. Kolthoff and D.L. Leussing, J. Amer. Chem. Soc., (1948), 70, 3596.
- 6.37 D.L. Egan¹⁴_K and D.T. Sawyer, Inorg. Chem., (1969), 8, 900.
- 6.38 J. Burgess and R.H. Prince, J. Chem. Soc., (1963), 5752.

- 6.39 M.H. Ford-Smith and N Sutin, J. Amer. Chem. Soc., (1961), 83, 1830;
and references therein.
- 6.40 W.W. Brandt and G.F. Smith, Anal. Chem., (1949), 21, 1313.
- 6.41 C.J. Hawkins, H. Duewell and W.F. Pickering, Anal. Chim. Acta, (1961),
25, 257.
- 6.42 M. Yasada, K. Sone and K. Yamasaki, J. Phys. Chem., (1956), 60, 1667.

CHAPTER 7

- 7.01 B. Bosnich, M.L. Tobe and G.A. Webb, *Inorg. Chem.*, (1965), 4, 1109.
- 7.02 C.W. Bunn, 'Chemical Crystallography', Pergamon Press, Oxford, (1961).
- 7.03 M.J. Buerger, 'Crystal Structure Analysis', Wiley, New York, (1960).
- 7.04 'Internat. Tables for X-Ray Crystallography', I-IV, Birmingham, (1952-1968).
- 7.05 G.H. Stout and L.H. Jensen, 'X-Ray Structure Determinations', New York, (1968).
- 7.06 B. Bosnich, C.K. Poon and M.L. Tobe, *Inorg. Chem.*, (1965), 4, 1102.
- 7.07 'Solubilities of Inorganic and Organic Compounds', 1, part 1, Ed. H. Stephen and T. Stephen, Pergamon, Oxford, (1963), p.774.
- 7.08 M.L. Moss, M.G. Mellon and G.F. Smith, *Anal. Chem.*, (1942), 14, 931.
- 7.09 J. Burgess and S.J. Cartwright, *J. Chem. Soc.(Dalton)*, (1975), 100.
- 7.10 M.J. Buerger, 'The Precession Method', Wiley, New York, (1964).
- 7.11 B.G. Cox, G.R. Hedwig, A.J. Parker and D.W. Watts, *Austral. J. Chem.*, (1974), 27, 477.
- 7.12 'Handbook of Chemistry and Physics', 53rd.Edn., C.R.C. Press, Chemical Rubber Co., Ed. R.C. Weast, (1972-1973), p. B106.
- 7.13 J.N. Albright, *J. Phys. Chem.*, (1972), 56, 3783; D.L. Wertz and R.F. Kruh, *J. Phys. Chem.*, (1969), 50, 4313.
- 7.14 N.N. Greenwood, 'Ionic Crystals, Lattice Defects and Non-Stoichiometry', Butterworths, (1965), pp.40-41.
- 7.15 J. Burgess and R.H. Prince, *J. Chem. Soc.(A)*, (1966), 1772.
- 7.16 J.E. Dickens, F. Basolo and H.M. Neumann, *J. Amer. Chem. Soc.*, (1957), 79, 1286.

CHAPTER 8

- 8.01 J. Burgess, J.G. Chambers and R.I. Haines, J. Chem. Research, in press, and references therein.
- 8.02 W. Schlenk, Annalen., (1909), 368, 294.
- 8.03 A.I. Kiprianov and V.E. Petrunkin, Zhur. Obshch. Khim., (1940), 10, 600.
- 8.04 L.G.S. Brooker, G.H. Keyes and D.W. Heseltine, J. Amer. Chem. Soc., (1951), 73, 5350.
- 8.05 K. Dimroth, C. Reichardt, T. Siepmann and F. Bohlmann, Annalen, (1963), 661, 1.
- 8.06 C. Reichardt, 'Lösungsmittelleffekte in der organischen Chemie', Verlag Chemie, Weinheim, (1968).
- 8.07 For example, D.K. Hazra and S.C. Lahiri, Z. phys. Chem., (Leipzig), (1976), 257, 497.
- 8.08 J. Bjerrum, A.W. Adamson and O. Bostrup, Acta Chem. Scand., (1956), 10, 329.
- 8.09 J. Burgess, Spectrochim. Acta, (1970), A26, 1369, 1957.
- 8.10 H. Kobayashi, B.V. Agarwala and Y. Kaizu, Bull. Chem. Soc. Japan, (1975), 48, 465.
- 8.11 H. Saito, J. Fujita and K. Saito, Bull. Chem. Soc. Japan, (1968), 41, 863.
- 8.12 J. Burgess, J. Organometallic Chem., (1969), 19, 218.
- 8.13 H. Bock and H. tom Dieck, Angew. Chem. Internat. Edn., (1966), 5, 520; Chem. Ber., (1967), 100, 228; H. tom Dieck and I.W. Renk, Angew. Chem. Internat. Edn., (1970), 9, 793; D. Walther, Z. anorg. Chem., (1973), 46, 396.
- 8.14 A.B.P. Lever, 'Advances in Inorganic and Radiochemistry', (1965), 7, 27.

- 8.15 J. Burgess and M.V. Twigg, J. Chem. Soc.(Dalton), (1974), 2032.
- 8.16 B. Bosnich, C.K. Poon and M.L. Tobe, Inorg. Chem., (1965), 4, 1102.
- 8.17 A.A. Schilt, and K. Fritsch, J. Inorg. Nuclear Chem., (1966), 28, 2677.
- 8.18 C. Reichardt, Angew. Chem. Internat. Edn., (1965), 4, 29.
- 8.19 J.A. Olabe and P.J. Aymonino, J. Inorg. Nuclear Chem., (1976), 38, 225.
- 8.20 E. Blasius and H. Augustin, Z. anorg. allgem. Chem., (1975), 417, 55.
- 8.21 H. tom Dieck and I.W. Renk, Chem. Ber., (1971), 104, 110.
- 8.22 P.H. Emslie and R. Foster, Rec. Trav. Chim., (1965), 84, 255.
- 8.23 See, for example, N.K. Hamer and L.E. Orgel, Nature, (1961), 190, 439; A.A. Schilt, Inorg. Chem., (1964), 3, 1323; J.N. Demas, T.F. Turner and G.A. Crosby, Inorg. Chem., (1969), 8, 674; G.M. Bancroft, M.J. Mays and B.E. Prater, J. Chem. Soc. Chem. Comm., (1968), 1374.
- 8.24 D.M. Adams, J. Chem. Soc.(A), (1969), 87.
- 8.25 P.C. Ford, J.R. Kuempel and H. Taube, Inorg. Chem., (1968), 7, 1976.
- 8.26 A.A. Schilt, J. Amer. Chem. Soc., (1960), 82, 3000.
- 8.27 M.J. Barcelona and G. Davies, J. Chem. Soc.(Dalton), (1975), 1906.
- 8.28 Y. Murakami, Y. Aoyama and S. Nakanishi, Inorg. Nuclear Chem. Lett., (1976), 12, 809.
- 8.29 J. Burgess and S.F.N. Morton, personal communication, and ref. 8.01.
- 8.30 J. Burgess, E.R. Gardner and F.M. Mekhail, Internat. J. Chem. Kinetics, (1974), IV, 133.
- 8.31 W. Liptay, Angew Chem. Internat. Edn., (1969), 8, 177.

CHAPTER 9

- 9.01 See, for example, 'Inorganic Reaction Mechanisms', ed, J. Burgess. Chem. Soc. Specialist Periodical Reports, London, (1971), 1, p.177; (1972), 2, pp.168-169, 182; C.H. Langford and V.S. Sastri, 'Reaction Mechanisms in Inorganic Chemistry', ed. M.L. Tobe, M.T.P. Internat. Rev. Sci., 2, Butterworths, London, (1971), series 1, p.252, and references therein.
- 9.02 J. Burgess and M.V. Twigg, J. Chem. Soc.(Dalton), (1974), 2032.
- 9.03 G.K. Pagenkopf and D.W. Margerum, Inorg. Chem., (1968), 7, 2514.
- 9.04 J. Burgess, E.R. Gardner and F.M. Mekhail, Internat. J. Chem. Kinetics, (1974), IV, 133.
- 9.05 J. Burgess, J. Chem. Soc.(Dalton), (1972), 1061, and references therein.
- 9.06 D.W. Margerum, J. Amer. Chem. Soc., (1957), 79, 2728.
- 9.07 D.W. Margerum and L.P. Morgenthaler, J. Amer. Chem. Soc., (1962), 84, 706; J. Burgess and R.H. Prince, J. Chem. Soc., (1965), 4679.
- 9.08 R.D. Gillard, Coord. Chem. Rev., (1975), 16, 67.
- 9.09 W.W. Brandt and G.F. Smith, Anal. Chem., (1949), 21, 1313.
- 9.10 F.P. Dwyer and E.C. Gyarfas, J. Amer. Chem. Soc., (1954), 76, 6320.
- 9.11 A.A. Schilt, Anal. Chem., (1963), 35, 1599.
- 9.12 R.D. Gillard and R.E.E. Hill, J. Chem. Soc.(Dalton), (1974), 1217.
- 9.13 R.D. Gillard and J.R. Lyons, J. Chem. Soc. Chem. Comm., (1973), 585.
- 9.14 R.D. Gillard, C.T. Hughes, L.A.P. Kane-Maguire and P.A. Williams, Transit. Met. Chem., (1976), 1, 226.
- 9.15 R.D. Gillard, L.A.P. Kane-Maguire and P.A. Williams, Transit. Met. Chem., (1977), 1, 1039, and references therein.
- 9.16 A.A. Schilt, J. Amer. Chem. Soc., (1960), 82, 3000.

- 9.17 L.F. Lindoy, *Quart. Rev.*, (1971), 25, 379.
- 9.18 J. Burgess, *J. Chem. Soc.(Dalton)*, (1972), 203.
- 9.19 R.D. Gillard, C.T. Hughes and P.A. Williams, *Transit. Met. Chem.*, (1976), 1, 51.
- 9.20 J. Josephsen and C.E. Schäffer, *J. Chem. Soc. Chem. Comm.*, (1970), 61.
- 9.21 M.J. Blandamer, J. Burgess and J.G. Chambers, *J. Chem. Soc.(Dalton)*, (1976), 606.
- 9.22 V. Balzani, V. Carassiti and L. Moggi, *Inorg. Chem.*, (1964), 3, 1252.
- 9.23 K. Madeja and M. König, *J. Inorg. Nuclear Chem.*, (1963), 25, 377.
- 9.24 K. Nakamoto, 'Infrared Spectra of Inorganic and Coordination Compounds', Wiley, New York, (1963).
- 9.25 R.D. Gillard, C.T. Hughes, L.A.P. Kane-Maguire and P.A. Williams, *Proc. XVII Internat. Conf. Coord. Chem.*, (1976), Hamburg, p.171.
- 9.26 J. Burgess, *Inorg. Chim. Acta*, (1971), 5, 133.
- 9.27 J. Burgess, G.E. Ellis, D.J. Evans, A. Porter, R. Wane and R.D. Wyvill, *J. Chem. Soc.(A)*, (1971), 44.
- 9.28 P. Krumholz, *J. Amer. Chem. Soc.*, (1953), 75, 2163.
- 9.29 F. Basolo and R.G. Pearson, 'Mechanisms of Inorganic Reactions', 1st.Edn., Wiley, New York, (1958), pp.152-155.
- 9.30 R. Farina, R. Hogg, and R.G. Wilkins, *Inorg. Chem.*, (1968), 7, 170.
- 9.31 J. Burgess and R.H. Prince, *J. Chem. Soc.*, (1965), 6061.
- 9.32 T.S. Lee, I.M. Kolthoff and D.L. Leussing, *J. Amer. Chem. Soc.*, (1948), 70, 2348.
- 9.33 J. Burgess, *J. Chem. Soc.(A)*, (1967), 431.
- 9.34 P. Krumholz, O.A. Sera and M.A. De Paoli, *J. Inorg. Nuclear Chem.*, (1975), 37, 1820.
- 9.35 E. König, *Coord. Chem. Rev.*, (1968), 3, 471.

- 9.36 E. König, E. Lindner, I.P. Lorenz and G. Ritter, *Inorg. Chim. Acta*, (1972), 6, 123.
- 9.37 V.L. Goedken, *J. Chem. Soc. Chem. Comm.*, (1972), 207.
- 9.38 E.K. Barefield, and D.H. Busch, *Inorg. Chem.*, (1971), 10, 108.
- 9.39 C.M. Harris and E.D. McKenzie, *J. Chem. Soc.(A)*, (1969), 746;
- 9.40 D.H. Busch and J.C. Bailar, *J. Amer. Chem. Soc.*, (1956), 80, 1137; *ibid.*, (1969), 91, 1072; *ibid.*, (1969), 91, 2122.